UNIVERSAL
LIBRARY

OU_160022

UNIVERSAL
LIBRARY

OSMANIA UNIVERSITY LIBRARY

Call No. Accession No.

Author

Title

This book should be returned on or before the date last marked below.

MECHANICAL VIBRATIONS

MECHANICAL VIBRATIONS

By

J. P. DEN HARTOG

PROFESSOR OF MECHANICAL ENGINEERING
MASSACHUSETTS INSTITUTE OF TECHNOLOGY

Third Edition

New York and London
McGRAW-HILL BOOK COMPANY, INC.
1947

MECHANICAL VIBRATIONS

COPYRIGHT, 1934, 1940, 1947, BY THE
McGRAW-HILL BOOK COMPANY, INC.
PRINTED IN THE UNITED STATES OF AMERICA

All rights reserved. This book, or parts thereof, may not be reproduced in any form without permission of the publishers

V

THE MAPLE PRESS COMPANY, YORK, PA.

PREFACE

This book grew from a course of lectures given to students in the Design School of the Westinghouse Company in Pittsburgh, Pa., in the period from 1926 to 1932, when the subject had not yet been introduced into the curriculum of our technical schools. From 1932 until the beginning of the war, it became a regular course at the Harvard Engineering School, and the book was written for the purpose of facilitating that course, being first published in 1934. In its first edition, it was influenced entirely by the author's industrial experience at Westinghouse; the later editions have brought modifications and additions suggested by actual problems published in the literature, by private consulting practice, and by service during the war in the Bureau of Ships of the U.S. Navy.

The book aims to be as simple as is compatible with a reasonably complete treatment of the subject. Mathematics has not been avoided, but in all cases the mathematical approach used is the simplest one available.

In the third edition the number of problems has again been increased, while the principal changes in the text concern subjects in which recent advances have been made, such as airplane wing flutter, helicopter ground vibration, torsional pendulum dampers, singing ships' propellers, and electronic instruments.

The author expresses his gratitude to the many readers who have written him calling attention to errors and making suggestions for improvements and hopes that readers of this third edition will also offer suggestions.

J. P. Den Hartog.

Cambridge, Mass.,
January, 1947.

CONTENTS

PREFACE v

LIST OF SYMBOLS x

CHAPTER I

KINEMATICS OF VIBRATION

1. Definitions 1
2. The Vector Method of Representing Vibrations 3
3. Beats 6
4. A Case of Hydraulic-turbine Penstock Vibration 8
5. Representation by Complex Numbers 11
6. Work Done on Harmonic Motions 14
7. Non-harmonic Periodic Motions 19

CHAPTER II

THE SINGLE DEGREE OF FREEDOM SYSTEM

8. Degrees of Freedom 34
9. Derivation of the Differential Equation 36
10. Other Cases 38
11. Free Vibrations without Damping 43
12. Examples 47
13. Free Vibrations with Viscous Damping 51
14. Forced Vibrations without Damping 57
15. Forced Vibrations with Viscous Damping 63
16. Frequency Measuring Instruments 72
17. Seismic Instruments 75
18. Electrical Measuring Instruments 80
19. Theory of Vibration Isolation 89
20. Application to Single-phase Electrical Machinery 92
21. Application to Automobiles; Floating Power 96

CHAPTER III

TWO DEGREES OF FREEDOM

22. Free Vibrations; Natural Modes 103
23. The Undamped Dynamic Vibration Absorber 112
24. The Damped Vibration Absorber 119

25. Ship Stabilization by Means of Frahm's Tanks 133
26. Gyroscopic Ship Stabilizers 139
26a. Activated Ship Stabilizers 142
27. Automobile Shock Absorbers 145

CHAPTER IV

Many Degrees of Freedom

28. Free Vibrations without Damping 155
29. Forced Vibrations without Damping 160
30. Free and Forced Vibration with Damping 165
31. Strings and Organ Pipes; Longitudinal and Torsional Vibrations of Uniform Bars 170
32. Rayleigh's Method 178
33. Bending Vibrations of Uniform Beams 185
34. Beams of Variable Cross Section 194
35. Normal Functions and Their Applications 198
35a. Stodola's Method for Higher Modes 202
36. Rings, Membranes, and Plates 205

CHAPTER V

Multicylinder Engines

37. Troubles Peculiar to Reciprocating Engines 213
38. Dynamics of the Crank Mechanism 217
39. Inertia Balance of Multicylinder Engines 225
40. Natural Frequencies of Torsional Vibration 232
41. Numerical Calculation of Diesel Ship Drive 236
42. Torque Analysis 248
43. Work Done by Torque on Crank-shaft Oscillation 254
44. Damping of Torsional Vibration 260
45. Dampers and Other Means of Mitigating Torsional Vibration 266

CHAPTER VI

Rotating Machinery

46. Critical Speeds 285
46a. Holzer's Method for Flexural Critical Speeds 290
47. Balancing of Solid Rotors 292
48. Simultaneous Balancing in Two Planes 300
49. Balancing of Flexible Rotors; Field Balancing 305
50. Secondary Critical Speeds 309
50a. Critical Speeds of Helicopter Rotors 312
51. Gyroscopic Effects 317

52. Frame Vibration in Electrical Machines 323
53. Vibration of Propellers 328
54. Vibration of Steam-turbine Wheels and Blades 337

CHAPTER VII

Self-excited Vibrations

55. General 346
56. Mathematical Criterion of Stability 350
57. Instability Caused by Friction 354
58. Internal Hysteresis of Shafts and Oil-film Lubrication in Bearings as Causes of Instability 361
59. Galloping of Electric Transmission Lines 366
60. Autorotation; Instability Caused by Finite Speed of Formation of Turbulence 375
61. Hunting of Steam-engine Governors 377
62. Diesel-engine Fuel-injection Valves 382
63. Axial Oscillation of Turbine Caused by Steam Leakage . . . 386
64. Airplane-wing Flutter 392
65. Automobile Shimmy 399

CHAPTER VIII

Systems with Variable or Non-linear Characteristics

66. The Principle of Superposition 406
67. Examples of Systems with Variable Elasticity 408
68. Solution of the Equation 415
69. Interpretation of the Result 420
70. Examples of Non-linear Systems 424
71. Free Vibrations with Non-linear Elasticity or Damping . . . 427
72. Forced Vibrations with Non-linear Springs 431
73. Forced Vibrations with Non-linear Damping 435
74. Relaxation Oscillations 439
75. Subharmonic Resonance 448

APPENDICES

I. The Gyroscope 453

II. A Collection of Formulas 457

Bibliography 461

Answers to Problems 466

Index 475

LIST OF SYMBOLS

a, A = cross-sectional area.
a_0 = amplitude of support.
a_n = Fourier coefficient of sin $n\omega t$.
b_n = Fourier coefficient of cos $n\omega t$.
c = damping constant, either linear (lb. in.$^{-1}$ sec.) or torsional (lb. in. rad.$^{-1}$).
C = condenser capacity.
c_c = criticial damping constant, Eq. (22), page 52.
C_1, C_2 = constants.
d, D = diameters.
D = aerodynamic drag.
e = eccentricity.
e = amplitude of pendulum support (Sec. 69 only).
E = modulus of elasticity.
E_0 = maximum voltage, E_0 sin ωt.
f = frequency = $\omega/2\pi$.
f_n = natural frequency.
f and **g** = numerical factors used in the same sense in one section only as follows: Sec. 24 as defined by Eq. (56), page 122. Sec. 30 as defined by Eq. (92), page 168. Sec. 45 as defined on page 266.
F = force in general or dry friction force in particular.
F = frequency function [Eq. (80), page 158]
g = acceleration of gravity.
g = See **f**.
G = modulus of shear.
h = height in general; metacentric height in particular (page 134).
i = electric current.
I = moment of inertia.
j = $\sqrt{-1}$ = imaginary unit.
k, K = spring constants.
Kin = kinetic energy.
Δk = variation in spring constant (page 408).
l = length in general; length of connecting rod in Chap. V.
l_n = distance from nth crank to first crank (Sec. 39).
L = inductance.
L = aerodynamic lift.
m, M = mass.
M = moment or torque.
$\vec{\mathfrak{M}}$ = angular momentum vector.
$\mathfrak{M}$ = magnitude of angular momentum.
n = a number in general; a gear ratio in particular (page 41).
p = real part of complex frequency s (page 166).
p = pressure.
p_1, p_2 = (in Sec. 68 only) defined by Eqs. (212) and (213), page 417.
P_0 = maximum force, P_0 sin ωt.
Pot = potential energy.
q = natural frequency of damped vibration (pages 53 and 168).

$\mathbf{q}$ = load per unit length on beam (page 185).
Q = condenser charge.
r, R = radius of circle.
R = electrical resistance.
s = complex frequency = $\pm p \pm jq$ (page 188).
$\mathbf{s}$ = (in Sec. 68 only) multiplication factor.
t = time.
T = period of vibration = $1/f$.
T_0 = maximum torque $T_0 \sin \omega t$.
$\mathbf{T}$ = tension in string.
v, V = velocity.
$\mathbf{v}$, $\mathbf{V}$ = volume.
W = work or work per cycle.
$\mathbf{W}$ = weight.
x = displacement.
x_0 = maximum amplitude.
x_{st} = static deflection, usually = P_0/k.
y = $y_0 \sin \omega t$ = amplitude of relative motion.
y = lateral deflection of string or bar.

α = angle in general; angle of attack of airfoil.
α_n = n^{th} crank angle in reciprocating engine.
α_{mn} = influence number, deflection at m caused by unit force at n.
β_n = angular amplitude of vibration of nth crank (Chap. V).
$\bar{\beta}_n$ = vector representing β_n.
δ = small length or small quantity in general.
δ_{st} = static deflection.
ϵ = parameter defined in Eq. (230), page 441.
λ = a length.
μ = mass ratio m/M (Secs. 23 and 24).
μ_1 = mass per unit length of strings, bars, etc.
ξ = longitudinal displacement of particle along beam (page 172).
ρ = radius of gyration.
φ = phase angle or some other angle.
φ_n = phase angle between vibration of nth crank and first crank (Chap. V).
ψ = an angle.
ω = circular frequency = $2\pi f$.
ω = angular velocity.
Ω = large angular velocity.
ω_n, Ω_n = natural circular frequencies.

Vector quantities are letters with superposed bar, $\bar{a}$, $\bar{V}$, $\bar{\mathbf{M}}$, etc.

Scalar quantities are letters without bar, a, T, $\mathbf{T}$, $\mathbf{M}$, etc. Note especially that **boldface** type does not denote a vector, but is used merely for avoiding confusion. For example, $\mathbf{V}$ denotes volume and V velocity.

Subscripts used are the following: a = absorber; c = critical, e = engine, f = friction, g = governor or gyroscope, k = variation in spring constant k, p = propeller, s = ship, st = statical, w = water.

MECHANICAL VIBRATIONS

CHAPTER I

KINEMATICS OF VIBRATION

1. Definitions.—A vibration in its general sense is a periodic motion, *i.e.*, a motion which repeats itself in all its particulars after a certain interval of time, called the *period* of the vibration and usually designated by the symbol T. A plot of the displacement x against the time t may be a curve of considerable

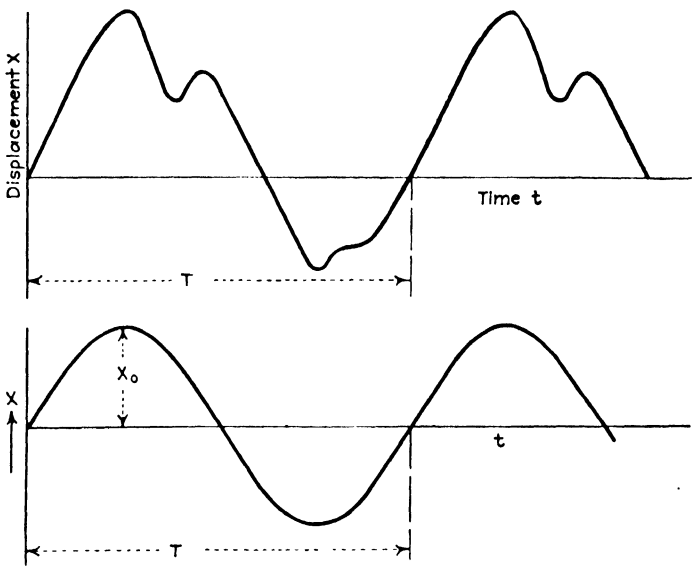


FIG. 1.—A periodic and a harmonic function, showing the period T and the amplitude x_0.

complication. As an example, Fig. 1*a* shows the motion curve observed on the bearing pedestal of a steam turbine.

The simplest kind of periodic motion is a *harmonic motion;* in it the relation between x and t may be expressed by

$$x = x_0 \sin \omega t \tag{1}$$

as shown in Fig. 1*b*, representing the small oscillations of a simple pendulum. The maximum value of the displacement is x_0, called the *amplitude* of the vibration.

The period T usually is measured in seconds; its reciprocal $f = 1/T$ is the *frequency* of the vibration, measured in *cycles per second.* In some publications this is abbreviated as *cyps* and pronounced as it is written. In the German literature cycles per second are generally called *Hertz* in honor of the first experimenter with radio waves (which are electric vibrations).

In Eq. (1) there appears the symbol ω, which is known as the *circular frequency* and is measured in radians per second. This rather unfortunate name has become familiar on account of the properties of the vector representation, which will be discussed in the next section. The relations between ω, f, and T are as follows. From Eq. (1) and Fig. 1*b* it is clear that a full cycle of the vibration takes place when ωt has passed through 360 deg. or 2π radians. Then the sine function resumes its previous values. Thus, when $\omega t = 2\pi$, the time interval t is equal to the period T or

$$T = \frac{2\pi}{\omega} \text{ sec.} \tag{2}$$

Since f is the reciprocal of T,

$$f = \frac{\omega}{2\pi} \text{ cycles per second} \tag{3}$$

For rotating machinery the frequency is often expressed in vibrations per minute, denoted as v.p.m. $= 30\omega/\pi$.

In a harmonic motion for which the displacement is given by $x = x_0 \sin \omega t$, the velocity is found by differentiating the displacement with respect to time,

$$\frac{dx}{dt} = \dot{x} = x_0\omega \cdot \cos \omega t \tag{4}$$

so that the velocity is also harmonic and has a maximum value ωx_0.

The acceleration is

$$\frac{d^2x}{dt^2} = \ddot{x} = -x_0\omega^2 \sin \omega t \tag{5}$$

also harmonic and with the maximum value $\omega^2 x_0$.

Consider two vibrations given by the expressions $x_1 = a \sin \omega t$ and $x_2 = b \sin (\omega t + \varphi)$ which are shown in Fig. 2, plotted against ωt as abscissa. Owing to the presence of the quantity φ, the two vibrations do not attain their maximum displacements at the same time, but the one is φ/ω sec. behind the other. The quantity φ is known as the *phase angle* or *phase difference* between the two vibrations. It is seen that the two motions have the

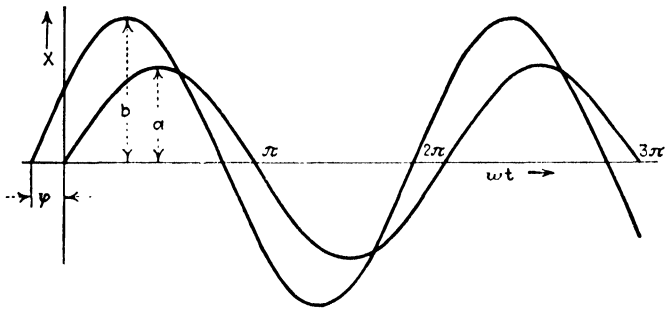


FIG. 2.—Two harmonic motions including the phase angle φ.

same ω and consequently the same frequency f. A phase angle has meaning only for two motions of the same frequency; if the frequencies are different, phase angle is meaningless.

Example: A body, suspended from a spring, vibrates vertically up and down between two positions 1 and 1½ in. above the ground. During each second it reaches the top position (1½ in. above ground) twenty times. What are T, f, ω, and x_0?

Solution: $x_0 = \frac{1}{4}$ in., $T = \frac{1}{20}$ sec., $f = 20$ cycles per second, and $\omega = 2\pi f = 126$ radians per second.

2. The Vector Method of Representing Vibrations.—The motion of a vibrating particle can be conveniently represented by means of a rotating vector. Let the vector $\bar{a}$ (Fig. 3) rotate with uniform angular velocity ω in a counterclockwise direction. When time is reckoned from the horizontal position of the vector as a starting point, the horizontal projection of the vector can be written as

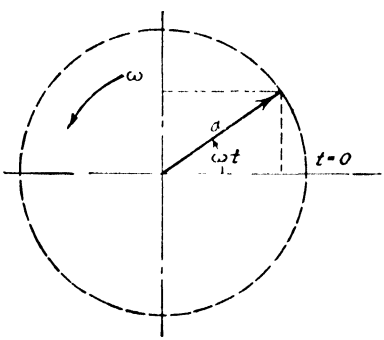


FIG. 3.—A harmonic vibration represented by the horizontal projection of a rotating vector.

$$a \cos \omega t$$

and the vertical projection as

$$a \sin \omega t$$

Either projection can be taken to represent a reciprocating motion; in the following discussion, however, we shall consider only the *horizontal* projection.

This representation has given rise to the name *circular frequency* for ω. The quantity ω, being the angular speed of the vector, is measured in *radians per second;* the frequency f in this case is measured in *revolutions per second.* Thus it can be seen immediately that $\omega = 2\pi f$.

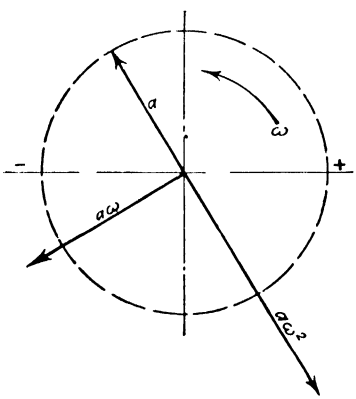


FIG. 4.—Displacement, velocity, and acceleration are perpendicular vectors.

The *velocity* of the motion $x = a \cos \omega t$ is

$$\dot{x} = -a\omega \sin \omega t$$

and can be represented by (the horizontal projection of) a vector of length $a\omega$, rotating with the same angular velocity ω as the displacement vector but situated always 90 deg. ahead of that vector. The *acceleration* is $-a\omega^2 \cos \omega t$ and is represented by (the horizontal projection of) a vector of length $a\omega^2$ rotating with the same angular speed ω and 180 deg. ahead of the position or displacement vector or 90 deg. ahead of the velocity vector (Fig. 4). The truth of these statements can be easily verified by following the various vectors through one complete revolution.

This vector method of visualizing reciprocating motions is very convenient. For example, if a point is simultaneously subjected to two motions of the same frequency which differ by the phase angle φ, namely, $a \cos \omega t$ and $b \cos (\omega t - \varphi)$, the addition of these two expressions by the methods of trigonometry is wearisome. However, the two vectors are easily drawn up, and the total motion is represented by the geometric sum of the two vectors as shown in the upper part of Fig. 5. Again the entire parallelogram $\bar{a}$, $\bar{b}$ is considered to rotate in a counterclockwise direction with the uniform angular velocity ω, and the horizontal projections of the various vectors represent the

displacements as a function of time. This is shown in the lower part of Fig. 5. The line a-a represents the particular instant of time for which the vector diagram is drawn. It is readily seen that the displacement of the sum (dotted line) is actually the sum of the two ordinates for $\bar{a}$ and $\bar{b}$.

That this vector addition gives correct results is evident, because $a \cos \omega t$ is the horizontal projection of the $\bar{a}$-vector and

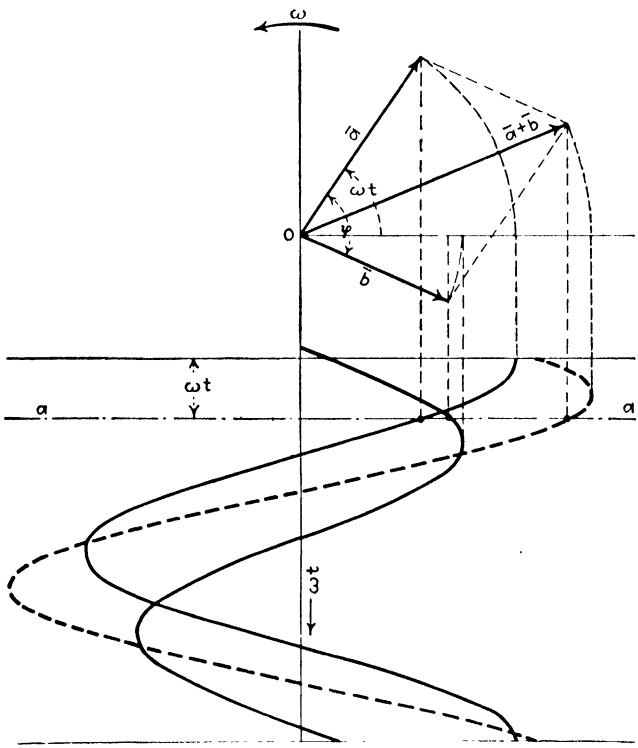


FIG. 5.—Two vibrations are added by adding their vectors geometrically.

$b \cos (\omega t - \varphi)$ is the horizontal projection of the $\bar{b}$-vector. The horizontal projection of the geometric sum of these two vectors is evidently equal to the sum of the horizontal projections of the two component vectors, which is exactly what is wanted.

Addition of two vectors is permissible only if the vibrations are of the same frequency. The motions $a \sin \omega t$ and $a \sin 2\omega t$ can be represented by two vectors, the first of which rotates with an angular speed ω and the second with twice this speed, *i.e.*, with 2ω. The relative position of these two vectors in the

diagram is changing continuously, and consequently a geometric addition of them has no meaning.

A special case of the vector addition of Fig. 5, which occurs rather often in the subsequent chapters, is the addition of a sine and a cosine wave of different amplitudes: $a \sin \omega t$ and $b \cos \omega t$. For this case the two vectors are perpendicular, so that from the diagram of Fig. 6 it is seen at once that

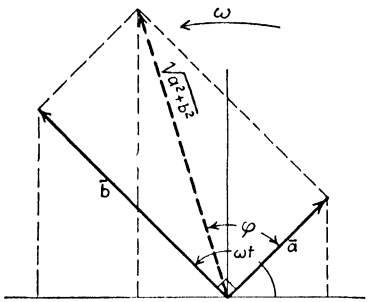


FIG. 6.—Addition of a sine and cosine wave of different amplitudes.

$$a \sin \omega t + b \cos \omega t = \sqrt{a^2 + b^2} \sin (\omega t + \varphi) \quad (6)$$

where $\tan \varphi = b/a$.

Example: What is the maximum amplitude of the sum of the two motions

$x_1 = 5 \sin 25t$ in. and $x_2 = 10 \sin (25t + 1)$ in.?

Solution: The first motion is represented by a vector 5 in. long which may be drawn vertically and pointing downward. Since in this position the vector has no horizontal projection, it represents the first motion at the instant $t = 0$. At that instant the second motion is $x_2 = 10 \sin 1$, which is represented by a vector of 10 in. length turned 1 radian (57 deg.) in a counterclockwise direction with respect to the first vector. The graphical vector addition shows the sum vector to be 13.4 in. long.

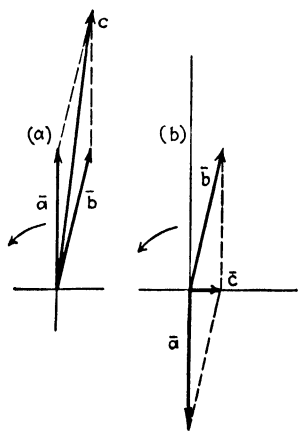


FIG. 7.—Vector diagrams illustrating the mechanism of beats.

3. Beats.—If the displacement of a point moving back and forth along a straight line can be expressed as the sum of two terms, $a \sin \omega_1 t + b \sin \omega_2 t$, where $\omega_1 \neq \omega_2$, the motion is said to be the "superposition" of two vibrations of different frequencies. It is clear that such a motion is not itself sinusoidal. An interesting special case occurs when the two frequencies ω_1 and ω_2 are nearly equal to each other. The first vibration can be represented by a vector $\bar{a}$ rotating at a speed ω_1, while the $\bar{b}$-vector rotates with ω_2. If ω_1 is nearly equal to ω_2, the two vectors will retain sensibly the same relative position during one revolution,

i.e., the angle included between them will change only slightly. Thus the vectors can be added geometrically, and during one revolution of the two vectors the motion will be practically a sine wave of frequency $\omega_1 \approx \omega_2$ and amplitude $\bar{c}$ (Fig. 7). During a large number of cycles, however, the relative position of $\bar{a}$ and $\bar{b}$ varies, because ω_1 is not exactly equal to ω_2, so that the magnitude of the sum vector $\bar{c}$ changes. Therefore the resulting motion can be described approximately as a sine wave with a frequency ω_1 and an amplitude varying slowly between $(b + a)$ and $(b - a)$, or, if $b = a$, between $2a$ and 0 (Figs. 7 and 8).

This phenomenon is known as *beats*. The beat frequency is the number of times per second the amplitude passes from a

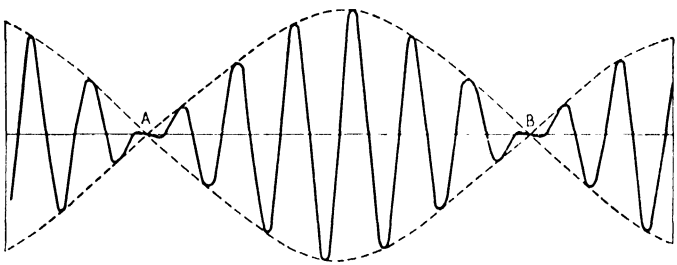


FIG. 8.—Beats.

minimum through a maximum to the next minimum (A to B in Fig. 8). The period of one beat evidently corresponds to the time required for a full revolution of the $\bar{b}$-vector with respect to the $\bar{a}$-vector. Thus the beat frequency is seen to be $\omega_1 - \omega_2$.

Example: A body describes simultaneously two vibrations, $x_1 = 3 \sin 40t$ and $x_2 = 4 \sin 41t$, the units being inches and seconds. What is the maximum and minimum amplitude of the combined motion and what is the beat frequency?

Solution: The maximum amplitude is $3 + 4 = 7$ in.; the minimum is $4 - 3 = 1$ in. The circular frequency of the beats $\omega_b = 41 - 40 = 1$ radian per second. Thus $f_b = \omega_b/2\pi = 1/2\pi$ cycles per second. The period T_b or duration of one full beat is $T_b = 1/f_b = 6.28$ sec.

The phenomenon can be observed in a great many cases (pages 109, 402). For audio or sound vibrations it is especially notable. Two tones of slightly different pitch and of approximately the same intensity cause fluctuations in the total intensity with a frequency equal to the difference of the frequencies of the two tones. For example, beats can be heard in electric power houses when a generator is started. An electric machine has a

"magnetic hum," of which the main pitch is equal to twice the frequency of the current or voltage, usually 120 cycles per second. Just before a generator is connected to the line the electric frequency of the generator is slightly different from the line frequency. Thus the hum of the generator and the hum of the line (other generators or transformers) are of different pitch, and beats can be heard.

The existence of beats can be shown also by trigonometry. Let the two vibrations be $a \sin \omega_1 t$ and $b \sin \omega_2 t$, where ω_1 and ω_2 are nearly equal and $\omega_2 - \omega_1 = \Delta\omega$.

Then

$$\begin{aligned} & a \sin \omega_1 t + b \sin \omega_2 t \\ &= a \sin \omega_1 t + b (\sin \omega_1 t \cos \Delta\omega t + \cos \omega_1 t \sin \Delta\omega t) \\ &= (a + b \cos \Delta\omega t) \sin \omega_1 t + b \sin \Delta\omega t \cos \omega_1 t \end{aligned}$$

Applying formula (6) the resultant vibration is

$$\sqrt{(a + b \cos \Delta\omega t)^2 + b^2 \sin^2 \Delta\omega t} \cdot \sin (\omega_1 t + \varphi)$$

where the phase angle φ can be calculated but is of no interest in this case. The amplitude, given by the radical, can be written

$$\begin{aligned} & \sqrt{a^2 + b^2(\cos^2 \Delta\omega t + \sin^2 \Delta\omega t) + 2ab \cos \Delta\omega t} \\ &= \sqrt{a^2 + b^2 + 2ab \cos \Delta\omega t} \end{aligned}$$

which expression is seen to vary between $(a + b)$ and $(a - b)$ with a frequency $\Delta\omega$.

4. A Case of Hydraulic-turbine Penstock Vibration.—A direct application of the vector concept of vibration to the solution of an actual problem is the following.

In a water-power generating station the penstocks, *i.e.*, the pipe lines conducting the water to the hydraulic turbines, were found to be vibrating so violently that the safety of the brick building structure was questioned. The frequency of the vibration was found to be 113⅓ cycles per second, coinciding with the product of the speed (400 r.p.m.) and the number of buckets (17) in the rotating part of the (Francis) turbine. The penstocks emitted a loud hum which could be heard several miles away. Incidentally, when standing close to the electric transformers of the station, the 6⅔ cyps. beat between the penstock and transformer hums could be plainly heard. The essential parts of the turbine are shown schematically in Fig. 9, which is drawn in a horizontal plane, the turbine shaft being vertical. The water enters from the penstock I into the "spiral case"

II; there the main stream splits into 18 partial streams on account of the 18 stationary, non-rotating guide vanes. The water then enters the 17 buckets of the runner and finally turns through an angle of 90 deg. to disappear into the vertical draft tube III.

Two of the 18 partial streams into which the main stream divides are shown in the figure. Fixing our attention on one of these, we see that for each revolution of the runner, 17 buckets pass by the stream, which thus is subjected to 17 impulses. In

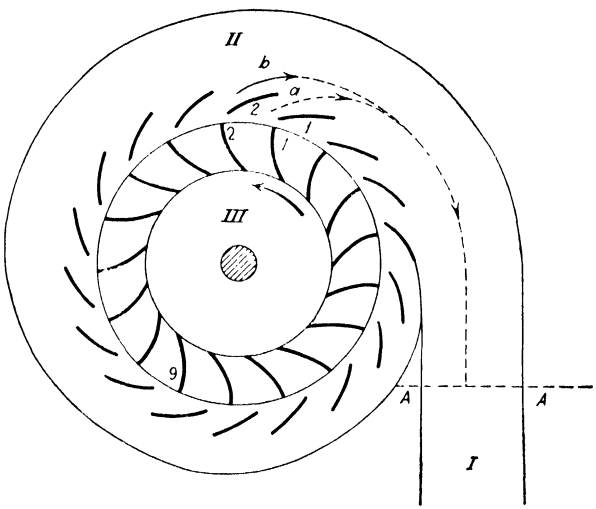


FIG. 9.—Explains the vibration in the penstock of a Francis hydraulic turbine.

total, 113⅓ buckets are passing per second, giving as many impulses per second, which are transmitted back through the water into the penstock. This happens not only in stream *a* but in each of the other partial streams as well, so that there arrive into the penstock 18 impulses of different origins, all having the same frequency of 113⅓ cycles per second. If all these impulses had the same *phase*, they would all add up arithmetically and give a very strong disturbance in the penstock.

Assume that stream *a* experiences the maximum value of its impulse when the two vanes 1 and 1 line up. Then the maximum value of the impulse in stream *b* takes place somewhat *earlier* (to be exact, 1/(17 × 18)th revolution earlier, at the instant that the two vanes 2 and 2 are lined up).

The impulse of stream *a* travels back into the penstock with the velocity of sound in water (about 4,000 ft./sec.)* and the same is true for the impulse of stream *b*. However, the path traveled by the impulse of *b* is somewhat longer than the path for *a*, the difference being approximately one-eighteenth part of the circumference of the spiral case. Because of this fact, the impulse *b* will arrive in the penstock *later* than the impulse *a*.

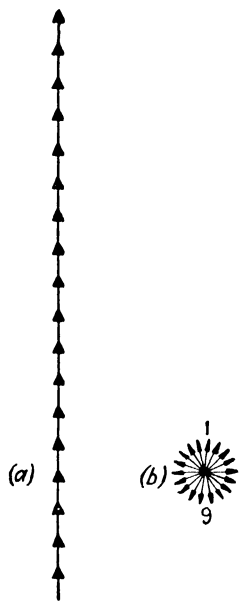


Fig. 10.—The 18 partial impulses at the section AA of Fig. 9 for a 17-bucket runner (*a*) and for a 16-bucket runner (*b*).

In the machine in question it happened that these two effects just canceled each other so that the two impulses *a* and *b* arrived at the cross section AA of the penstock simultaneously, *i.e.*, in the same phase. This of course is true not only for *a* and *b* but for all the 18 partial streams. In the vector representation the impulses behave as shown in Fig. 10*a*, the total impulse at AA being very large.

In order to eliminate the trouble, the existing 17-bucket runner was removed from the turbine and replaced by a 16-bucket runner. This does not affect the time difference caused by the different lengths of the paths *a*, *b*, etc., but it does change the interval of time between the impulses of two adjacent guide vanes. In particular, the circumferential distance between the bucket 2 and guide vane 2 becomes twice as large after the change. In fact, at the instant that rotating bucket 1 gives its impulse, bucket 9 also gives its impulse, whereas in the old construction bucket 9 was midway between two stationary vanes (Fig. 9).

It was a fortunate coincidence that half the circumference of the spiral case was traversed by a sound wave in about $\frac{1}{2} \times \frac{1}{113}$ sec., so that the two impulses due to buckets 1 and 9 arrived in the cross section AA in phase opposition (Fig. 10*b*). The phase angle between the impulses at section AA of two adjacent partial streams is thus one-ninth of 180 degrees, and the 18 partial

* The general streaming velocity of the water is small in comparison to the velocity of sound, so that its effect can be neglected.

impulses arrange themselves in a circular diagram with a zero resultant.

The analysis as given would indicate that after the change in the runner had been made the vibration would be totally absent. However, this is not to be expected, since the reasoning given is only approximate, and many effects have not been considered (the spiral case has been replaced by a narrow channel, thus neglecting curvature of the wave front, reflection of the waves against the various obstacles, and effect of damping). In the actual case the amplitude of the vibration on the penstock was reduced to one-third of its previous value, which constituted a satisfactory solution of the problem.

5. Representation by Complex Numbers.—It was shown in the previous sections that rotating vectors can represent harmonic motions, that the geometric addition of two vectors corresponds to the addition of two harmonic motions of the same frequency, and that a differentiation of such a motion with respect to time can be understood as a multiplication by ω and a forward turning through 90 deg. of the representative vector. These vectors, after a little practice, afford a method of visualizing harmonic motions which is much simpler than the consideration of the sine waves themselves.

For *numerical* calculations, however, the vector method is not well adapted, since it becomes necessary to resolve the vectors into their horizontal and vertical components. For instance, if two motions have to be added as in Fig. 5, we write

$$\bar{c} = \bar{a} + \bar{b}$$

meaning *geometric* addition. To calculate the length of $\bar{c}$, *i.e.*, the amplitude of the sum motion, we write

$$\bar{a} = a_x + a_y$$

which means that $\bar{a}$ is the geometric sum of a_x in the x-direction and a_y in the y-direction. Then

$$\bar{c} = a_x + a_y + b_x + b_y = (a_x + b_x) + (a_y + b_y)$$

and the *length* of $\bar{c}$ is consequently

$$c = \sqrt{(a_x + b_x)^2 + (a_y + b_y)^2}$$

This method is rather lengthy and loses most of the advantage due to the introduction of vectors.

There exists, however, a simpler method of handling the vectors numerically, employing imaginary numbers. A complex number can be represented graphically by a point in a plane where the *real* numbers 1, 2, 3, etc., are plotted horizontally and the *imaginary* numbers are plotted vertically. With the notation

$$j = \sqrt{-1}$$

these imaginary numbers are j, $2j$, $3j$, etc. In Fig. 11, for example, the point $3 + 2j$ is shown. In joining that point with the origin, the complex number can be made to represent a vector. If the angle of the vector with the horizontal axis is α and the length of the vector is a, it can be written as

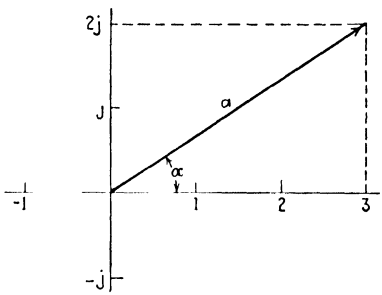


FIG. 11. A vector represented by a point in the complex plane.

$$a(\cos \alpha + j \sin \alpha)$$

Harmonic motions are represented by *rotating* vectors. A substitution of the variable angle ωt for the fixed angle α in the last equation leads to

$$a(\cos \omega t + j \sin \omega t) \tag{7}$$

representing a rotating vector, the horizontal projection of which is a harmonic motion. But this horizontal projection is also the real part of (7). Thus if we say that a "vector represents a harmonic motion," we mean that the *horizontal projection of the rotating* vector represents that motion. Similarly if we state that a "complex number represents a harmonic motion," we imply that the *real part of such a number, written in the form* (7) represents that motion.

Example: Solve the example of page 6 by means of the complex method. *Solution:* The first vector is represented by $-5j$ and the second one by $-10j \cos 57° + 10 \sin 57° = -5.4j + 8.4$. The sum of the two is $8.4 - 10.4j$, which represents a vector of the length $\sqrt{(8.4)^2 + (10.4)^2} = 13.4$ in.

Differentiate (7) which gives the result

$$a(-\omega \sin \omega t + j\omega \cos \omega t) = j\omega \cdot a(\cos \omega t + j \sin \omega t)$$

since by definition of j we have $j^2 = -1$. It is thus seen that *differentiation of the complex number* (7) *is equivalent to multiplication by* $j\omega$.

In vector representation, differentiation multiplies the length of the vector by ω and turns it ahead by 90 deg. Thus we are led to the conclusion that multiplying a complex number by j is equivalent to moving it a quarter turn ahead without changing its absolute value. That this is so can be easily verified:

$$j(a + jb) = -b + ja$$

which Fig. 12 actually shows in the required position.

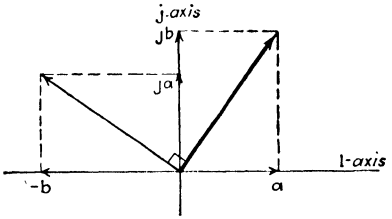


Fig. 12.—Multiplying a complex number by j amounts to turning its vector ahead through 90 deg.

In making extended calculations with these complex numbers the ordinary rules of algebra are followed. With every step we may remember that the motion is represented by only the *real* part of what we are writing down. Usually, however, this is not done: the algebraic manipulations are performed without much recourse to their physical meaning and only the final answer is interpreted by considering its real part.

For simple problems it is hardly worth while to study the complex method, since the solution can be obtained just as easily without it. However, for more complicated problems, such as are treated in Sec. 24, for example, the labor-saving brought about by the use of the complex notation is substantial.

The expression (7) is sometimes written in a different form:

$$a(\cos \omega t + j \sin \omega t) = ae^{j\omega t} \tag{8}$$

or, if for simplicity $a = 1$ and $\omega t = \alpha$,

$$e^{j\alpha} = \cos \alpha + j \sin \alpha \tag{8a}$$

The right-hand side of this equation is an ordinary complex number, but the left-hand side needs to be interpreted, as follows. The Maclaurin series development of e^x is

$$e^x = 1 + x + \frac{x^2}{2!} + \frac{x^3}{3!} + \cdots$$

Substituting $x = j\alpha$ this becomes

$$e^{j\alpha} = 1 + j\alpha - \frac{\alpha^2}{2!} - j\frac{\alpha^3}{3!} + \frac{\alpha^4}{4!} + j\frac{\alpha^5}{5!} - \cdots$$

$$= (1 - \frac{\alpha^2}{2!} + \frac{\alpha^4}{4!} - \cdots) + j(\alpha - \frac{\alpha^3}{3!} + \frac{\alpha^5}{5!} - \cdots)$$

The right-hand side is a complex number, which by definition is the meaning of $e^{j\alpha}$. But we recognize the brackets to be the Maclaurin developments of cos α and sin α, so that formula (8*a*) follows.

A simple graphical representation of the result can be made in the complex plane of Fig. 11 or 12. Consider the circle with unit radius in this plane. Each point on the circle has a horizontal projection cos α and a vertical projection sin α and thus represents the number, cos $\alpha + j$ sin $\alpha = e^{j\alpha}$. Consequently the number $e^{j\alpha}$ is represented by a point on the unit circle, α radians away from the point +1. If α is now made equal to ωt, it is seen that $e^{j\omega t}$ represents the rotating unit vector of which the horizontal projection is a harmonic vibration of unit amplitude and frequency ω.

On page 52 we shall have occasion to make use of Eq. (8*a*).

6. Work Done on Harmonic Motions.—A concept of importance for many applications is that of the work done by a harmonically varying force upon a harmonic motion of the same frequency.

Let the force $P = P_0 \sin(\omega t + \varphi)$ be acting upon a body for which the motion is given by $x = x_0 \sin \omega t$. The work done by the force during a small displacement dx is $P dx$, which can be written as $P\frac{dx}{dt} \cdot dt$.

During one cycle of the vibration, ωt varies from 0 to 2π and consequently t varies from 0 to $2\pi/\omega$. The work done during one cycle is:

$$\int_0^{\frac{2\pi}{\omega}} P\frac{dx}{dt}dt = \frac{1}{\omega}\int_0^{2\pi} P\frac{dx}{dt}d(\omega t) = P_0x_0\int_0^{2\pi} \sin(\omega t + \varphi)\cos\omega t\, d(\omega t)$$

$$= P_0x_0\int_0^{2\pi} \cos\omega t[\sin\omega t\cos\varphi + \cos\omega t\sin\varphi]d(\omega t)$$

$$= P_0x_0\cos\varphi\int_0^{2\pi} \sin\omega t\cos\omega t\, d(\omega t) + P_0x_0\sin\varphi\int_0^{2\pi} \cos^2\omega t\, d(\omega t)$$

A table of integrals will show that the first integral is zero and that the second one is π, so that the work per cycle is

$$W = \pi P_0 x_0 \sin\varphi \tag{9}$$

This result can also be obtained by a graphical method, which interprets the above calculations step by step, as follows.

The force and motion can be represented by the vectors $\bar{P}_0$ and $\bar{x}_0$ (Fig. 13). Now resolve the force into its components

$P_0 \cos \varphi$ in phase with the motion, and $P_0 \sin \varphi$, 90 deg. ahead of the motion $\bar{x}_0$. This is permissible for the same reason that geometric addition of vectors is allowed, as explained in Sec. 2. Thus the work done splits up into two parts, one part due to a force in phase with the motion and another part due to a force 90 deg. ahead of the motion.

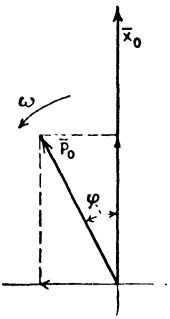


FIG. 13.—A force and a motion of the same frequency.

Consider the first part as shown in Fig. 14*a*, in which the ordinates are the displacement x and the "in phase" component of the force. Between A and B the force is positive, say upward, and the body is moving in an upward direction also; positive work is done. Between B and C, on the other hand, the body moves downward toward the equilibrium point while the force is still positive (upward, though of gradually diminishing intensity), so that negative work is done. The work between A and B cancels that between B and C, and over a whole cycle the work done is zero. *If a harmonic force acts on a body subjected to a harmonic motion of the same frequency, the component of the force in phase with the displacement does no work.*

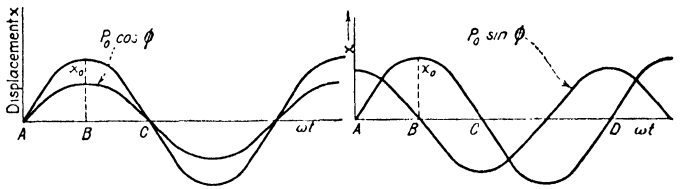


FIG. 14.—A force in phase with a displacement does no work over a full cycle; a force 90 deg. out of phase with a displacement does a maximum amount of work.

It was shown in Sec. 2 that the velocity is represented by a vector 90 deg. ahead of the displacement, so that the statement can also be worded as follows:

A force does work only with that component which is in phase with the velocity.

Next we consider the other component of the force, which is shown in Fig. 14*b*. During the interval AB the displacement increases so that the motion is directed upward, the force is positive, and consequently upward also, so that positive work is done. In the interval BC the motion is directed downward, but

the force points downward also, so that the work done is again positive. Since the whole diagram is symmetrical about a vertical line through B, it is clear that the work done during AB equals that done during BC. The work done during the whole cycle AD is four times that done during AB.

To calculate that amount it is necessary to turn to the definition of work:

$$W = \int P dx = \int P \frac{dx}{dt} dt = \int Pv \cdot dt$$

This shows that the work done during a cycle is the time integral of the product of *force* and *velocity*. The force is (Fig. 14*b*)

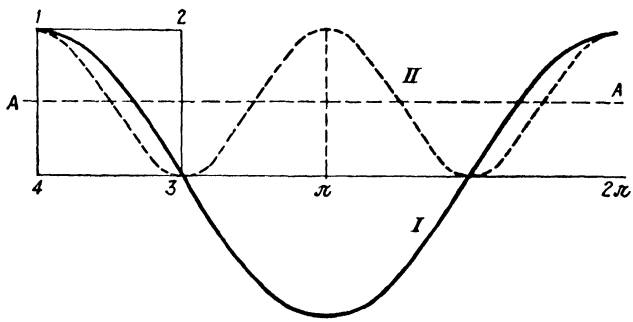


FIG. 15.—Showing that $\int_0^{2\pi} \cos^2 \alpha d\alpha = \pi$.

$P = (P_0 \sin \varphi) \cdot \cos \omega t$ and the velocity is $v = x_0 \omega \cos \omega t$, so that the work per cycle is

$$\int_0^T P_0 \sin \varphi \cos \omega t \, x_0 \omega \cos \omega t \, dt = P_0 x_0 \sin \varphi \int_0^{2\pi} \cos^2 \omega t \, d(\omega t)$$

The value of the definite integral on the right-hand side can be deduced from Fig. 15, in which curve I represents $\cos \omega t$ and curve II represents $\cos^2 \omega t$. The curve $\cos^2 \omega t$ is sinusoidal about the dotted line AA as center line and has twice the frequency of $\cos \omega t$, which can be easily verified by trigonometry:

$$\cos^2 \alpha = \tfrac{1}{2}(1 + \cos 2\alpha)$$

Consider the quadrangle 1-2-3-4 as cut in two pieces by the curve II and note that these two pieces have the same shape and the same area. The distance 1-4 is unity, while the distance 3-4 is $\pi/2$ radians or 90 deg. Thus the area of the entire quadrangle is $\pi/2$ and the area of the part under curve II is half of that.

Consequently the value of our definite integral taken between the limits 0 and $T/4$ is $\pi/4$, and taken between the limits 0 and T it is π. Thus the work during a cycle is

$$W = \pi P_0 x_0 \sin \varphi \tag{9}$$

It will be seen in the next section that a periodic force as well as a periodic motion may be "impure," *i.e.*, it may contain "higher harmonics" in addition to the "fundamental harmonic." In this connection it is of importance to determine the work done by a harmonic force on a harmonic motion of a frequency *different* from that of the force. Let the force vary with a frequency which is an integer multiple of ω, say $n\omega$, and let the frequency of the motion be another integer multiple of ω, say $m\omega$. It will now be proved that the work done by such a force on such a motion during a full cycle of ω is zero.

Let the force be $P = P_0 \sin n\omega t$ and let the corresponding motion be $x = x_0 \sin (m\omega t + \varphi)$. Then the work per cycle is

$$\int P dx = \int_0^T P \frac{dx}{dt} dt = \int_0^T P_0 \sin n\omega t \cdot x_0 m\omega \cdot \cos (m\omega t + \varphi) dt$$

Since

$$\cos (m\omega t + \varphi) = \cos m\omega t \cos \varphi - \sin m\omega t \sin \varphi$$

and since φ is independent of the time and can be brought in front of the integral sign, the integral splits up into two parts of the form

$$\int_0^T \sin n\omega t \sin m\omega t \, dt \qquad \text{and} \qquad \int_0^T \sin n\omega t \cos m\omega t \, dt$$

Both these integrals are zero if n is different from m, which can be easily verified by transforming the integrands as follows:

$$\sin n\omega t \sin m\omega t = \tfrac{1}{2} \cos (n - m)\omega t - \tfrac{1}{2} \cos (n + m)\omega t$$
$$\sin n\omega t \cos m\omega t = \tfrac{1}{2} \sin (n + m)\omega t + \tfrac{1}{2} \sin (n - m)\omega t$$

Since the interval of integration is $T = 2\pi/\omega$, the sine and cosine functions are integrated over multiples of 2π, giving a zero result. In order to gain a physical understanding of this fact let us consider the first of the above two integrals with $n = 4$ and $m = 5$. This case is represented in Fig. 16, where the amplitudes of the two waves are drawn to different vertical scales in order to distinguish them more easily. The time interval over which the integration extends is the interval AB. The ordinates of the two curves have to be multiplied together and then integrated.

Consider two points, one somewhat to the right of A and another at the same distance to the left of C. Near A both waves are positive; near C one is positive and the other is negative, but the absolute *values* of the ordinates are the same as near A. Therefore the contribution to the integral of an element near A cancels the contribution of the corresponding element near C. This canceling holds true not only for elements very *near* to A and C but generally for two elements at equal distances to the left from C and to the right from A. Thus the integral over the region AD cancels that over CD. In the same way it can be shown that the integral over CB is zero.

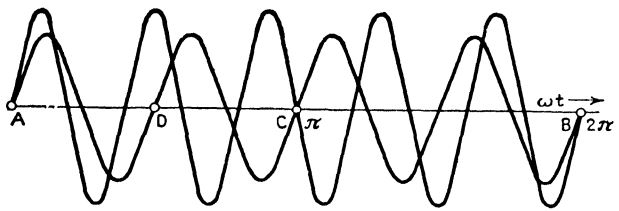


FIG. 16.—Showing that $\int_0^{2\pi} \sin n\alpha \sin m\alpha \, d\alpha = 0$.

It should be understood that the work is zero only over a *whole cycle.* Starting at A, both waves (the force and the velocity) are positive, so that positive work is done. This work, however, is returned later on (so that in the meantime it must have been stored in the form of potential or kinetic energy).

This graphical process can be repeated for any combination of integral values of m and n and also for integrals containing a cosine in the integrand. When m becomes equal to n, we have the case of equal frequencies as already considered. Even then there is no work done when the force and displacement are in phase. In case $m = n$ and the force and displacement are 90 deg. out of phase, the work per cycle of the nth harmonic is $\pi P_0 x_0$ as before, and since there are n of these cycles in *one* cycle of the fundamental frequency ω, the work per fundamental cycle is $n\pi P_0 x_0$.

The results thus obtained can be briefly summarized as follows:

1. *The work done by a harmonic force acting upon a harmonic displacement or velocity of a different frequency from that of the force is zero during a time interval comprising both an integer number of force cycles and a (different) integer number of velocity cycles.*

2. *The work done by a harmonic force* 90 *deg. out of phase with a harmonic velocity of the same frequency is zero during a whole cycle.*

3. *The work done by a harmonic force of amplitude* P_0 *and frequency* ω, *in phase with a harmonic velocity* $v_0 = x_0\omega$ *of the same frequency, is* $\pi P_0 v_0/\omega = \pi P_0 x_0$ *over a whole cycle.*

Example: A force 10 sin $2\pi 60t$ (units are pounds and seconds) is acting on a displacement of $\frac{1}{10}$ sin $[2\pi 60t - 45°]$ (units are inches and seconds). What is the work done during the first second, and also during the first one-thousandth of a second?

Solution: The force is 45 deg. out of phase with the displacement and can be resolved into two components, each of amplitude $10/\sqrt{2}$ lb., being in phase and 90 deg. out of phase with the displacement. The component in phase with the displacement does no work. That 90 deg. out of phase with the displacement does per cycle $\pi P_0 x_0 = \pi \cdot \frac{10}{\sqrt{2}} \cdot \frac{1}{10} = 2.22$ in. lb. of work. During the first second there are 60 cycles so that the work performed is $60 \times 2.22 = 133$ in. lb.

During the first one-thousandth of a second there are 60/1,000 = 0.06 cycle, so that the vectors in the diagram turn through only 0.06×360 deg. = 21.6 deg. Formula (9) holds only for a full cycle. For part of a cycle the integration has to be performed in full:

$$
\begin{aligned}
W &= \int P dx = \int P_0 \sin \omega t \cdot x_0 \omega \cos(\omega t - \varphi) dt \\
&= P_0 x_0 \int_0^{21.6°} \sin(\omega t) \cos(\omega t - \varphi) d(\omega t) \\
&= 10 \cdot \tfrac{1}{10} \int_0^{21.6°} \sin(\omega t)[\cos(\omega t)\cos\varphi + \sin(\omega t)\sin\varphi] d(\omega t) \\
&= \cos\varphi \int_0^{21.6°} \sin(\omega t)\cos(\omega t) d(\omega t) + \sin\varphi \int_0^{21.6°} \sin^2(\omega t) d(\omega t) \\
&= \tfrac{1}{2}\cos\varphi \sin^2(\omega t) + \sin\varphi[\tfrac{1}{2}\omega t - \tfrac{1}{4}\sin 2\omega t]\Big|_0^{21.6°}. \\
&= \frac{1}{2}\cos 45° \sin^2 21.6° + \frac{1}{2}\frac{21.6}{57.3}\sin 45° - \frac{1}{4}\sin 45° \sin 43.2° \\
&= \frac{1}{2} \times 0.707 \times 0.368^2 + \frac{1}{2}\frac{21.6}{57.3} \times 0.707 - \frac{1}{4} \times 0.707 \times 0.685 \\
&= 0.048 + 0.133 - 0.121 = +0.060 \text{ in. lb.}
\end{aligned}
$$

This is considerably less than one-thousandth part of the work performed in a whole second, because during this particular 1/1,000 sec. the force is very small, varying between 0 and $0.368P_0$.

7. Non-harmonic, Periodic Motions.—A "periodic" motion has the property of repeating itself in all details after a certain time interval, the "period" of the motion. All harmonic

motions are periodic, but not every periodic motion is harmonic. For example, Fig. 17 represents the motion

$$x = a \sin \omega t + \frac{a}{2} \sin 2\omega t,$$

the superposition of two sine waves of different frequency. It is periodic but not harmonic. The mathematical theory shows

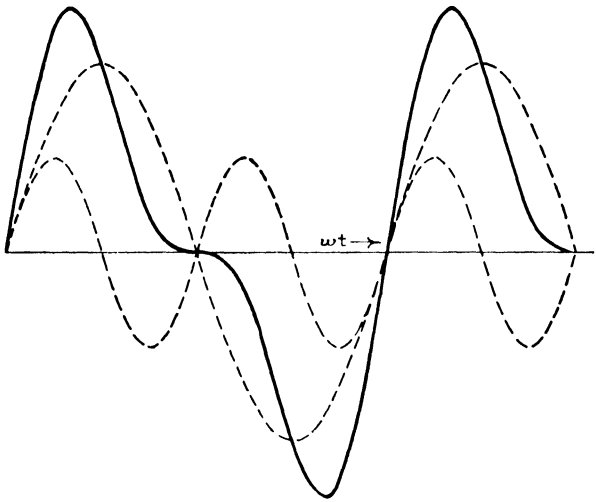


FIG. 17.—The sum of two harmonic motions of different frequencies is not a harmonic motion.

that *any periodic curve* $f(t)$ of frequency ω can be split up into a series of sine curves of frequencies ω, 2ω, 3ω, 4ω, etc. Or

$$f(t) = A_0 + A_1 \sin (\omega t + \varphi_1) + A_2 \sin (2\omega t + \varphi_2) + A_3 \sin (3\omega t + \varphi_3) + \cdots \quad (10)$$

provided that $f(t)$ repeats itself after each interval $T = 2\pi/\omega$. The amplitudes of the various waves A_1, A_2, . . . , and their phase angles φ_1, φ_2, . . . , can be determined analytically when $f(t)$ is given. The series (10) is known as a *Fourier series.*

The second term is called the fundamental or first harmonic of $f(t)$ and in general the $(n + 1)$st term of frequency $n\omega$ is known as the nth harmonic of $f(t)$. Since

$$\sin (n\omega t + \varphi_n) = \sin n\omega t \cos \varphi_n + \cos n\omega t \sin \varphi_n$$

the series can also be written as

$$f(t) = a_1 \sin \omega t + a_2 \sin 2\omega t + \cdots + a_n \sin n\omega t + \cdots + b_0 + b_1 \cos \omega t + b_2 \cos 2\omega t + \cdots + b_n \cos n\omega t + \cdots \quad (10a)$$

The constant term b_0 represents the "average" height of the curve $f(t)$ during a cycle. For a curve which is as much above the zero line during a cycle as it is below, the term b_0 is zero. The amplitudes $a_1 \ldots a_n \ldots, b_1 \ldots b_n \ldots$ can be determined by applying the three energy theorems of pages 18 and 19.

Consider for that purpose $f(t)$ to be a *force*, and let this non-harmonic force act on a point having the harmonic velocity $\sin n\omega t$. Now consider the force $f(t)$ as the sum of all the terms of its Fourier series and determine the work done by each harmonic term separately. All terms of the force except $a_n \sin n\omega t$ and $b_n \cos n\omega t$ are of a frequency different from that of the velocity $\sin n\omega t$, so that no work per cycle is done by them. Moreover, $b_n \cos n\omega t$ is 90 deg. out of phase with the velocity so that this term does not do any work either. Thus the total work done is that of the force $a_n \sin n\omega t$ on the velocity $\sin n\omega t$, and is $\frac{\pi \cdot a_n \cdot 1}{n\omega}$ per cycle of the $n\omega$-frequency. Per cycle of the fundamental frequency (which is n times as long), the work is $\pi a_n/\omega$.

Thus the amplitude a_n is found to be ω/π times as large as the work done by the complete non-harmonic force $f(t)$ on a velocity $\sin n\omega t$ during one cycle of the force. Or, mathematically

$$a_n = \frac{\omega}{\pi}\int_0^{\frac{2\pi}{\omega}} f(t) \sin n\omega t \, dt \qquad (11a)$$

By assuming a velocity $\cos n\omega t$ instead of $\sin n\omega t$ and repeating the argument, the meaning of b_n is disclosed as

$$b_n = \frac{\omega}{\pi}\int_0^{\frac{2\pi}{\omega}} f(t) \cos n\omega t \, dt \qquad (11b)$$

The relations between a_n, b_n and the quantities A_n, φ_n of Eq. (10) are as shown in Eq. (6), page 6, so that

$$A_n^2 = a_n^2 + b_n^2 \qquad \text{and} \qquad \tan \varphi_n = \frac{b_n}{a_n}.$$

Thus the work done by a non-harmonic force of frequency ω upon a harmonic velocity of frequency $n\omega$ is merely the work of the component of the nth harmonic of that force in phase with the velocity; the work of all other harmonics of the force is zero when integrated over a complete force cycle.

With the aid of the formulas (11) it is possible to find the a_n and b_n for any periodic curve which may be given. The branch

of mathematics which is concerned with this problem is known as *harmonic analysis.*

Example: The curve c of Fig. 254 (page 426) shows approximately the damping force caused by turbulent air on a body in harmonic motion. If the origin of coordinates of Fig. 254 is displaced one-quarter cycle to the left, the mathematical expression for the curve is

$$f(\omega t) = \sin^2 \omega t \qquad \text{for } 0 < \omega t < \pi$$
$$f(\omega t) = -\sin^2 \omega t \qquad \text{for } \pi < \omega t < 2\pi$$

Find the amplitudes of the various harmonics of this curve.

Solution: The curve to be analyzed is an "antisymmetric" one, *i.e.*, the values of $f(\omega t)$ are equal and opposite at two points $\pm \omega t$ at equal distances on both sides of the origin. Sine waves are antisymmetric and cosine waves are symmetric. An antisymmetric curve cannot have cosine components. Hence, all b_n are zero. This can be further verified by sketching the integrand of Eq. (11*b*) in the manner of Fig. 16 and showing that the various contributions to the integral cancel each other. The constant term $b_0 = 0$, because the curve has no average height. For the sine components we find

$$a_n = \frac{\omega}{\pi}\int_0^{\frac{2\pi}{\omega}} f(\omega t) \sin n\omega t \, dt$$
$$= \frac{1}{\pi}\left[\int_0^{\pi} \sin^2 \omega t \sin n\omega t \, d(\omega t) - \int_{\pi}^{2\pi} \sin^2 \omega t \sin n\omega t \, d\omega t\right]$$

The integrands can be transformed by means of the last formula on page 17,

$$\sin^2 \omega t \sin n\omega t = (\tfrac{1}{2} - \tfrac{1}{2} \cos 2\omega t) \sin n\omega t$$
$$= \tfrac{1}{2} \sin n\omega t - \tfrac{1}{4} \sin (n + 2)\omega t - \tfrac{1}{4} \sin (n - 2)\omega t$$

The indefinite integral of this is

$$F(\omega t) = \frac{-1}{2n} \cos n\omega t + \frac{1}{4(n + 2)} \cos (n + 2)\omega t + \frac{1}{4(n - 2)} \cos (n - 2)\omega t$$

The harmonic a_n is $1/\pi$ times the definite integrals.
Since $F(2\pi) = F(0)$, we have

$$a_n = \frac{1}{\pi}\left[F(\pi) - F(0) - F(2\pi) + F(\pi)\right] = \frac{2}{\pi}\left[F(\pi) - F(0)\right]$$
$$= \frac{2}{\pi}(\cos n\pi - 1) \cdot \left[-\frac{1}{2n} + \frac{1}{4(n + 2)} + \frac{1}{4(n - 2)}\right] = \frac{4}{\pi} \frac{\cos n\pi - 1}{n(n^2 - 4)}$$

For even values for n the a_n thus is zero, while only for odd values of n the harmonic exists. In particular for $n = 1$, we have for the fundamental harmonic

$$a_1 = \frac{8}{3\pi} = 0.85$$

Thus the amplitude of the fundamental harmonic is 85 per cent of the maximum amplitude of the curve itself.

The evaluation of the integrals (11) by calculation can be done only for a few simple shapes of $f(t)$. If $f(t)$ is a curve taken from an actual vibration record or from an indicator diagram, we do not even possess a mathematical expression for it. However, with the aid of the curve so obtained the integrals can be determined either graphically or numerically or by means of a machine, known as a *harmonic analyzer*.

Such a harmonic analyzer operates on the same principle as Watt's steam-engine indicator. The indicator traces a closed curve of which the ordinate is the steam pressure (or piston

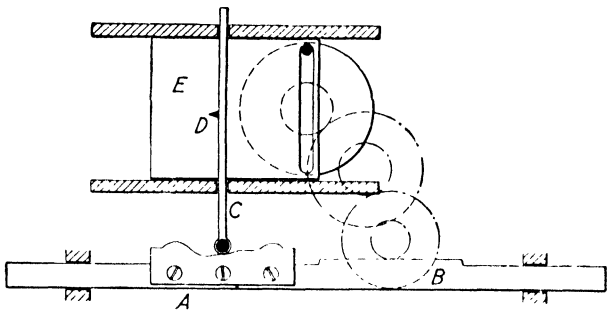


FIG. 18.—The harmonic analyzer, an instrument operating on the same principle as Watt's steam-engine indicator.

force) and the abscissa is the piston displacement. The area of this closed curve is the work done by the piston force per cycle. The formulas (11) state that the coefficients a_n or b_n are ω/π times the work done per cycle by the force $f(t)$ on a certain displacement of which the velocity is expressed by $\sin n\omega t$. To obtain complete correspondence between the two cases, we note that $\sin n\omega t$ is the velocity of $\frac{-1}{n\omega}\cos n\omega t$, so that (11$a$) can be written in the modified form

$$a_n = \frac{-1}{n\pi}\int f(t)d(\cos n\omega t) = \frac{-1}{n\pi}\oint Pds$$

The symbol $\oint$ indicates that the integration extends over the closed curve described during one cycle of the force $f(t)$.

The machine is shown schematically in Fig. 18. A is a cardboard template representing one cycle of the curve $f(t)$ which is to be analyzed. The template A is fastened to a rack and a pinion B, which is rotated by an electric motor. The arm C

is guided so that it can move in its longitudinal direction only and is pressed lightly against the template by a spring. Thus the vertical motion of the pen D on the arm C is expressed by $f(t)$. The table, or "platen," E moves horizontally and is driven by a scotch crank and gear which is connected by suitable intermediate gears to B so that E oscillates n times, while A moves through the length of the diagram. The machine has with it a box of spare gears so that any gear ratio n from 1 to 30 can be obtained by replacing one gear in the train by another.

The horizontal motion of the platen E is expressed by $\sin n\omega t$ or by $\cos n\omega t$, depending on the manner in which the gears are interlocked. The point D will thus trace a closed curve on the platen, for which the area equals a_n or b_n (multiplied by a constant $1/n\pi$). Instead of actually tracing this curve, the instrument usually carries a planimeter of which one point is attached to E and the other end to D, so that the area is given directly by the planimeter reading.

Harmonic analyzers have been built on other principles as well. An interesting optical method using the sound tracks of motion picture films was invented by Wente and constructed by Montgomery, both of the Bell Telephone Laboratories. The reference to this paper is given in the Bibliography.

Electrical harmonic analyzers giving an extremely rapid analysis of the total harmonics $A_n = \sqrt{a_n^2 + b_n^2}$ [Eqs. (10) and (10a)], without giving information on the phase angles φ_n [or the ratios a_n/b_n, Eq. (10)], are available on the market. They have been developed by the Western Electric Company (model RA-277 to be used in conjunction with model RA-246) for sound or noise analysis and require the original curve to be available in the form of an electric voltage, varying with the time, such as results from an electric vibration pickup (page 81) or a microphone. This voltage, after proper amplification, is fed into an electric network known as a "band-pass filter," which suppresses all frequencies except those in a narrow band of a width equal to 5 cycles per second. This passing band of frequencies can be laid anywhere in the range from 10 to 10,000 cycles per second.

When a periodic (steady-state) vibration or noise is to be Fourier-analyzed, a small motor automatically moves the pass band across the entire spectrum and the resulting analysis is drawn graphically by a stylus on a strip of waxed paper, giving the harmonic amplitudes *vs.* the frequency from 10 to 10,000 cycles per second, all in a few minutes. The record is immediately readable.

Another electrical analyzer, operating on about the same principle but without graphic recording, is marketed by the General Radio Company, Cambridge, Mass.

There are several methods for calculating the Fourier coefficients numerically, *i.e.*, methods to evaluate the integrals (11) in cases where the function $f(t)$ is given only in the form of a curve. For convenience we rewrite Eq. (11), by taking as the abscissa not the time t, but rather the combination $\varphi = \omega t$, which is an angle. With the latter, Eqs. (11*a* and *b*) become

$$a_n = \frac{1}{\pi}\int_0^{2\pi} f(\varphi) \sin n\varphi \, d\varphi \qquad b_n = \frac{1}{\pi}\int_0^{2\pi} (f\varphi) \cos n\varphi \, d\varphi$$

In order to calculate these integrals numerically, we divide the base length 2π of the curve in a number N of equal parts, each of which is $2\pi/N = \Delta$. (In the particular example that follows, $N = 48$ and $\Delta = 7.5$ deg.) The ordinates of the curve $f(\varphi)$ at these N points are designated as y_0, y_1, y_2 . . . , etc., so that $y_2 = f(k\Delta)$. With this notation we can replace the above continuous integrals by finite sums, which are approximately equal to these integrals:

$$\left.\begin{aligned} a_n &\approx \frac{1}{\pi}\sum_{k=0}^{k=N-1} y_k(\sin nk\Delta)\cdot\Delta \\ b_n &\approx \frac{1}{\pi}\sum_{k=0}^{k=N-1} y_k(\cos nk\Delta)\cdot\Delta \end{aligned}\right\} \qquad (11c)$$

In case the subdivision of the base of the curve becomes finer and finer, *i.e.*, N becomes greater and Δ smaller, these sums gradually approach the integrals in value. In order to find, say, the fifth sine harmonic of a curve, the expressions (11*c*) instruct us to subdivide the base in a number, say, 48 equal pieces of 7.5 deg.; to measure the ordinates y_0, y_1, y_2, . . . , y_{22}; to calculate the products $y_1 \sin (5 \times 7\frac{1}{2})$, $y_2 \sin (10 \times 7\frac{1}{2})$, etc.; to add these 48 products, and to multiply the sum by Δ/π which is $\frac{1}{24}$. The sines appearing in these 48 products show certain regularities. For instance, taking the following four terms out of the 48,

$y_1 \sin (5 \times 7\frac{1}{2})°$, $y_{47} \sin (47 \times 5 \times 7\frac{1}{2})°$, $y_{23} \sin (23 \times 5 \times 7\frac{1}{2})°$, $y_{25} \sin (25 \times 5 \times 7\frac{1}{2})°$

we can write

$$y_1 \sin 37\tfrac{1}{2}^\circ,\ y_{47} \sin (5 \times 360 - 37\tfrac{1}{2})^\circ,\ y_{23} \sin (5 \times 180 - 37\tfrac{1}{2})^\circ,\ y_{25} \sin (5 \times 180 + 37\tfrac{1}{2})^\circ$$

and the sum of these four terms is

$$(y_1 + y_{23} - y_{25} - y_{47}) \sin 37\tfrac{1}{2}^\circ$$

In order to take full advantage of the simplifications arising from these regularities, Runge devised the scheme of pages 28 and 29. In this schedule the full-size numbers are always the same, while the small-type numbers refer to a specific example. The example taken in this case is the squared sine function of page 22. The 48 ordinates of this function are first entered in the top two rows. For example, $y_9 = \sin^2 (9 \times 7\tfrac{1}{2})^\circ = \sin^2 (82\tfrac{1}{2}) = 0.924^2 = 0.854$ is shown in the space provided for it, while immediately below appears $y_{39} = -0.854$. Since we picked an antisymmetric curve, the values $y_{24\text{-}48}$ are equal and opposite to $y_{24\text{-}0}$. The third and fourth line of small numbers are the sum **c** and difference **d**, respectively, of the two numbers above them. The third line is entirely made up of zeros, because our curve is antisymmetric. The **c**-values of the third line are entered into the second square to the left, while the **d**-values are copied at the right. In copying the numbers they are "folded about the center" in order to take advantage of the regularities in the sine and cosine functions. The same operation of addition and subtraction is performed on the **c**'s and **d**'s, and continuing in this manner the entire sheet is filled in. The **A**-values appearing in the bottom center are the sines of $7\tfrac{1}{2}$, 15, $22\tfrac{1}{2}$ deg., etc.

Now any harmonic can be calculated by referring to pages 30 and 31. The formulas shown there are the same as Eqs. (11c), taking advantage of the various symmetries. Consider for example the third sine harmonic. By Eqs. (11c) we have

$$\frac{\pi}{\Delta} a_3 = 24 a_3 = y_0 \sin 0 + y_1 \sin 3\Delta + y_2 \sin 6\Delta + \cdots + y_{46} \sin 138\Delta + y_{47} \sin 141\Delta = (y_1 - y_{47}) \sin 3\Delta + (y_2 - y_{46}) \sin 6\Delta \cdots + (y_{23} - y_{25}) \sin 69\Delta + (y_{24}) \sin 72\Delta.$$

Now $\sin 72\Delta = \sin 540^\circ = 0$, and using the notation of pages 28 and 29 this can be written as

$$\begin{aligned} 24 a_3 &= d_1 \sin 3\Delta + d_2 \sin 6\Delta + \cdots + d_{23} \sin 69\Delta \\ &= (d_1 + d_{23}) \sin 3\Delta + (d_2 + d_{22}) \sin 6\Delta + \cdots \\ &\qquad \cdots + (d_{11} + d_{13}) \sin 33\Delta + d_{12} \sin 36\Delta \\ &= g_1 \sin 3\Delta + g_2 \sin 6\Delta + \cdots + g_{11} \sin 33\Delta - d_{12} = \end{aligned}$$

$$= (g_1 \sin 3\Delta) + g_7 \sin 21\Delta + g_9 \sin 27\Delta) + (g_2 \sin 6\Delta + g_6 \sin 18\Delta + g_{10} \sin 30\Delta) + (g_3 \sin 9\Delta) + g_5 \sin 15\Delta + g_{11} \sin 33\Delta) + (g_4 \sin 12\Delta + g_8 \sin 24\Delta) - d_{12}$$
$$= j_1 \sin 3\Delta + j_2 \sin 6\Delta + j_3 \sin 9\Delta + g_4 - d_{12}$$
$$= g_4 - d_{12} + A_3 j_1 + A_6 j_2 + A_9 j_3$$

In a similar manner the other entries on pages 30 and 31 can be verified.

The numerical calculation of the various harmonics of our sine squared curve by substituting the figures of pages 28 and 29 in the formulas of pages 30 and 31 leads to the results below. The exact answers from page 22 are listed for comparison.

	By Runge's scheme	Exact
a_1	0.846	0.848
a_3	−0.170	−0.170
a_5	−0.0246	−0.0243
a_7	−0.0073	−0.0081
a_9	−0.0033	−0.0037

The higher odd sine harmonics up to a_{22} become too small to be of any importance; *i.e.*, $a_{21} = -0.0005$ by Runge's method and $a_{21} = -0.0003$ by the exact formula.

In this exposition of the method the formulas (11*c*) have been considered merely as approximations of the integrals (11*a*) and (11*b*). However, they have an additional significance. Suppose we write not an infinite Fourier series, but a finite one containing 23 *a*- or sine terms and 25 *b*- or cosine terms, 48 in all. Let the coefficients *a* and *b* of this finite series be indeterminate to start with. Consider next the 48 points $y_0, y_1, y_2 \ldots y_{47}$ of our curve. Now by algebra it will be possible to solve for the 48 *a*'s and *b*'s, so that the curve determined by the finite Fourier series passes *exactly* through the 48 points of the given curve. To find the *a*- and *b*-values that do just this requires writing the 48 conditions that the series curve passes through the designated points and then solving the 48 unknown *a*'s and *b*'s from the 48 algebraic equations. This has been done, and the result, surprisingly, is just Eqs. (11*c*). For a proof of this interesting property, the reader is referred to the books of Runge or Scarborough, quoted in the Bibliography.

Problems

1. A force $P_0 \sin \omega t$ acts on a displacement $x = x_0 \sin (\omega t + 30°)$, where $P_0 = 5$ lb., $x_0 = 2$ in., and $\omega = 62.8$ rad./sec.

a. What is the work done during the first second?

b. What is the work done during the first $\frac{1}{40}$ sec.?

(*Continued on page* 32)

y	0 (24)	1 (47)	2 (46)	3 (45)	4 (44)	5 (43)	6 (42)	7 (41)	8 (40)	9 (39)	10 (38)
	0 000	0.017	0.068	0 146	0.250	0.370	0.500	0.630	0.750	0.854	0.932
	0 000	−0.017	−0.068	−0.146	−0.250	−0.370	−0.500	−0.630	−0.750	−0.854	−0.932
Sum: c	0 0	0	0	0	0	0	0	0	0	0	0
Diff.: d	0 000	0.034	0.136	0.292	0.500	0.740	1.000	1.260	1.500	1.708	1.864

c	0 (12)	1 (23)	2 (22)	3 (21)	4 (20)	5 (19)	6 (18)	7 (17)	8 (16)	9 (15)	10 (14)	11 (13)
	0	0	0	0	0	0	0	0	0	0	0	0
	0	0	0	0	0	0	0	0	0	0	0	0
Sum: e	0	0	0	0	0	0	0	0	0	0	0	0
Diff.: f	0	0	0	0	0	0	0	0	0	0	0	0

e	0 (6)	1 (11)	2 (10)	3 (9)	4 (8)	5 (7)
	0	0	0	0	0	0
	0	0	0	0	0	0
Sum: k	0	0	0	0	0	0
Diff.: l	0	0	0	0	0	0

$$f_1 - f_7 - f_9 = i_1 = 0$$
$$f_2 - f_8 - f_{10} = i_2 = 0$$
$$f_3 - f_5 - f_{11} = i_3 = 0$$

k	0 (3)	1 (5)	2 (4)
	0	0	0
	0	0	0
Sum: p	0	0	0
Diff.: q	0	0	0

l	0 (3)	1 (5)	2 (4)
	0	0	0
	0	0	0
Sum: r	0	0	0
Diff.: s	0	0	0

$A_1 = 0.131$
$A_2 = 0.259$
$A_3 = 0.383$
$A_4 = 0.500$
$A_5 = 0.609$
$A_6 = 0.707$

11 (37)	12 (36)	13 (35)	14 (34)	15 (33)	16 (32)	17 (31)	18 (30)	19 (29)	20 (28)	21 (27)	22 (26)	23 (25)
0.983	1.000	0.983	0 932	0.854	0.750	0 630	0.500	0.370	0 250	0.146	0 068	0 017
−0.983	−1.000	−0.983	−0 932	−0.854	−0 750	−0.630	−0 500	−0 370	−0 250	−0.146	−0 068	−0 017
0	0	0	0	0	0	0	0	0	0	0	0	0
1 966	2 000	1 966	1.864	1.708	1 500	1 260	1 000	0 740	0 500	0 292	0 136	0 034

d	0 (12)	1 (23)	2 (22)	3 (21)	4 (20)	5 (19)	6 (18)	7 (17)	8 (16)	9 (15)	10 (14)	11 (13)
	0 000	0 034	0 136	0 292	0.500	0 740	1 000	1.260	1.500	1 708	1 864	1 966
	2 000	0 034	0 136	0 292	0 500	0 740	1 000	1 260	1 500	1 708	1 864	1 966
Sum: **g**	2 000	0.068	0 272	0 584	1 000	1 480	2 000	2 520	3 000	3 416	3 728	3 932
Diff.: **h**	−2 000	0	0	0	0	0	0	0	0	0	0	0

$g_1 + g_7 - g_9 = j_1 = -0\ 828$

$g_2 + g_6 - g_{10} = j_2 = -1\ 456$

$g_3 + g_6 - g_{11} = j_3 = -1\ 868$

h	0 (6)	1 (11)	2 (10)	3 (9)	4 (8)	5 (7)
	−2 000	0	0	0	0	0
	0	0	0	0	0	0
Sum: **m**	−2 000	0	0	0	0	0
Diff.: **n**	−2.000	0	0	0	0	0

$A_7 = 0.793$
$A_8 = 0.866$
$A_9 = 0.924$
$A_{10} = 0.966$
$A_{11} = 0.991$

m	0 (3)	1 (5)	2 (4)
	−2 0	0	0
	0	0	0
Sum: **t**	−2 0	0	0
Diff.: **u**	−2.0	0	0

n	0 (3)	1 (5)	2 (4)
	−2.0	0	0
	0	0	0
Sum: **v**	−2.0	0	0
Diff.: **w**	−2.0	0	0

Sine Terms

(For Fourier Analysis with 48 Ordinates)

$$24\ a_1 = +d_{12} + A_1g_1 + A_2g_2 + A_3g_3 + A_4g_4 + A_5g_5 + A_6g_6 + A_7g_7 + A_8g_8 + A_9g_9 + A_{10}g_{10} + A_{11}g_{11}$$

$$24\ a_2 = +h_6 + A_2m_1 + A_4m_2 + A_6m_3 + A_8m_4 + A_{10}m_5$$

$$24\ a_3 = +(g_4 - d_{12}) + A_3j_1 + A_6j_2 + A_9j_3$$

$$24\ a_4 = +n_3 + A_4v_1 + A_5v_2$$

$$24\ a_5 = +d_{12} - A_1g_5 + A_2g_{10} - A_3g_9 + A_4g_4 + A_5g_1 - A_6g_6 + A_7g_{11} - A_8g_8 + A_9g_3 + A_{10}g_2 - A_{11}g_7$$

$$24\ a_6 = +(m_2 - h_6) + A_6(u_1 + m_3)$$

$$24\ a_7 = -d_{12} + A_1g_7 + A_2g_{10} + A_3g_3 - A_4g_4 - A_5g_{11} - A_6g_6 + A_7g_1 + A_8g_8 + A_9g_9 + A_{10}g_2 - A_{11}g_5$$

$$24\ a_8 = +A_8(w_1 + w_2)$$

$$24\ a_9 = -(g_4 - d_{12}) - A_3j_3 + A_6j_2 + A_9j_1$$

$$24\ a_{10} = +h_6 + A_2m_5 + A_4m_2 - A_6m_3 - A_8m_4 + A_{10}m_1$$

$$24\ a_{11} = -d_{12} - A_1g_{11} + A_2g_2 + A_3g_9 - A_4g_4 - A_5g_7 + A_6g_6 + A_7g_5 - A_8g_8 - A_9g_3 + A_{10}g_{10} + A_{11}g_1$$

$$24\ a_{12} = +v_1 - n_3$$

$$24\ a_{13} = +d_{12} - A_1g_{11} - A_2g_2 + A_3g_9 + A_4g_4 - A_5g_7 - A_6g_6 + A_7g_5 + A_8g_8 - A_9g_3 - A_{10}g_{10} + A_{11}g_1$$

$$24\ a_{14} = -h_6 + A_2m_5 - A_4m_2 - A_6m_3 + A_8m_4 + A_{10}m_1$$

$$24\ a_{15} = +(g_4 - d_{12}) - A_3j_3 - A_6j_2 + A_9j_1$$

$$24\ a_{16} = +A_8(w_1 - w_2)$$

$$24\ a_{17} = +d_{12} + A_1g_7 - A_2g_{10} + A_3g_3 + A_4g_4 - A_5g_{11} + A_6g_6 + A_7g_1 - A_8g_8 + A_9g_9 - A_{10}g_2 - A_{11}g_5$$

$$24\ a_{18} = -(m_2 - h_6) + A_6(u_1 + m_3)$$

$$24\ a_{19} = -d_{12} - A_1g_5 - A_2g_{10} - A_3g_9 - A_4g_4 + A_5g_1 + A_6g_6 + A_7g_{11} + A_8g_8 + A_9g_3 - A_{10}g_2 - A_{11}g_7$$

$$24\ a_{20} = +n_3 + A_4v_1 - A_8v_2$$

$$24\ a_{21} = -(g_4 - d_{12}) + A_3j_1 - A_6j_2 + A_9j_3$$

$$24\ a_{22} = -h_6 + A_2m_1 - A_4m_2 + A_6m_3 - A_8m_4 + A_{10}m_5$$

$$24\ a_{23} = -d_{12} + A_1g_1 - A_2g_2 + A_3g_3 - A_4g_4 + A_5g_5 - A_6g_6 + A_7g_7 - A_8g_8 + A_9g_9 - A_{10}g_{10} + A_{11}g_{11}$$

Cosine Terms
(For Fourier Analysis with 48 Ordinates)

$$48\ b_0 = +p_0 + p_1 + p_2$$
$$24\ b_1 = +d_0 + A_1f_{11} + A_2f_{10} + A_3f_9 + A_4f_8 + A_5f_7 + A_6f_6 + A_7f_5 + A_8f_4 + A_9f_3 + A_{10}f_2 + A_{11}f_1$$
$$24\ b_2 = +f_0 + A_2l_5 + A_4l_4 + A_6l_3 + A_8l_2 + A_{10}l_1$$
$$24\ b_3 = +(d_0 - f_8) + A_3i_3 + A_6i_2 + A_9i_1$$
$$24\ b_4 = +l_0 + A_4q_2 + A_8q_1$$
$$24\ b_5 = +d_0 - A_1f_7 + A_2f_2 - A_3f_3 + A_4f_8 + A_5f_{11} - A_6f_6 + A_7f_1 - A_8f_4 + A_9f_9 + A_{10}f_{10} - A_{11}f_5$$
$$24\ b_6 = +(f_0 - l_4) + A_6(s_1 - l_3)$$
$$24\ b_7 = +d_0 - A_1f_5 - A_2f_2 - A_3f_9 + A_4f_8 + A_5f_1 + A_6f_6 - A_7f_{11} - A_8f_4 - A_9f_3 - A_{10}f_{10} + A_{11}f_7$$
$$24\ b_8 = +q_0 + A_4(p_1 - p_2)$$
$$24\ b_9 = +(d_0 - f_8) + A_3i_1 - A_6i_2 - A_9i_3$$
$$24\ b_{10} = +f_0 + A_2l_1 + A_4l_4 - A_6l_3 - A_8l_2 + A_{10}l_5$$
$$24\ b_{11} = +d_0 + A_1f_1 - A_2f_{10} - A_3f_3 + A_4f_8 + A_5f_5 - A_6f_6 - A_7f_7 + A_8f_4 + A_9f_9 - A_{10}f_2 - A_{11}f_{11}$$
$$24\ b_{12} = +l_0 - q_2$$
$$24\ b_{13} = +d_0 - A_1f_1 - A_2f_{10} + A_3f_3 + A_4f_8 - A_5f_5 - A_6f_6 + A_7f_7 + A_8f_4 - A_9f_9 - A_{10}f_2 + A_{11}f_{11}$$
$$24\ b_{14} = +f_0 - A_2l_1 + A_4l_4 + A_6l_3 - A_8l_2 - A_{10}l_5$$
$$24\ b_{15} = +(d_0 - f_8) - A_3i_1 - A_6i_2 + A_9i_3$$
$$24\ b_{16} = +p_0 - A_4(p_1 + p_2)$$
$$24\ b_{17} = +d_0 + A_1f_5 - A_2f_2 + A_3f_9 + A_4f_8 - A_5f_1 + A_6f_6 + A_7f_{11} - A_8f_4 + A_9f_3 - A_{10}f_{10} - A_{11}f_7$$
$$24\ b_{18} = +(f_0 - l_4) - A_6(s_1 - l_3)$$
$$24\ b_{19} = +d_0 + A_1f_7 + A_2f_2 + A_3f_3 + A_4f_8 - A_5f_{11} - A_6f_6 - A_7f_1 - A_8f_4 - A_9f_9 + A_{10}f_{10} + A_{11}f_5$$
$$24\ b_{20} = +l_0 + A_4q_2 - A_8q_1$$
$$24\ b_{21} = +(d_0 - f_8) - A_3i_3 + A_6i_2 - A_9i_1$$
$$24\ b_{22} = +f_0 - A_2l_5 + A_4l_4 - A_6l_3 + A_8l_2 - A_{10}l_1$$
$$24\ b_{23} = +d_0 - A_1f_{11} + A_2f_{10} - A_3f_9 + A_4f_8 - A_5f_7 + A_6f_6 - A_7f_5 + A_8f_4 - A_9f_3 + A_{10}f_2 - A_{11}f_1$$
$$24\ b_{24} = +q_0 - p_1 + p_2$$

2. If a body is vibrating harmonically back and forth on a table with dry friction between the two so that the friction force is independent of the velocity, that force can be expressed as

$$f(t) = F \quad \text{for } 0 < \omega t < \pi \quad \text{and} \quad f(t) = -F \quad \text{for } \pi < \omega t < 2\pi$$

Calculate the harmonic coefficients of this force by means of (11) and show that

$$f(t) = \frac{4}{\pi}F\left(\sin \omega t + \frac{1}{3}\sin 3\omega t + \frac{1}{5}\sin 5\omega t + \cdots\right)$$

3. Let a periodic curve $f(t)$ be as shown in Fig. 19.
Prove that

$$f(t) = \frac{8}{\pi^2}\left(\sin \omega t - \frac{1}{3^2}\sin 3\omega t + \frac{1}{5^2}\sin 5\omega t - \cdots\right)$$

4. Referring to Fig. 18, let the curve to be analyzed consist of a pure sine wave, so that $a_1 = 1$ and all other a's and b's are zero. Sketch the

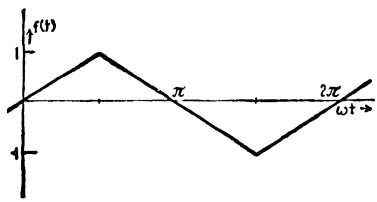


FIG. 19.—Curve represented by the series of Problem 3.

shape of the curve traced on the platen E of Fig. 18, if the gear B and the scotch crank rotate at equal speeds. The closed curve on E depends on how the two gears are coupled. Show that by displacing them 90 deg. with respect to each other, the platen curve varies from a circle to a straight line at 45 deg. Find the area of the circular E-curve and show that $a_1 = 1$ and $b_1 = 0$.

5. Sketch the E-curves of Problem 4 for the case where the scotch crank turns 2, 3, . . . times as fast as B, and show that the area registered by the planimeter is zero in all these cases.

6. Deduce Eq. (6) on page 6 by trigonometry.

7. A rectangular curve has the value $+a$ during three-eighths of the time and the value $-a$ during five-eighths of the time, as shown in Fig. 20. Find the Fourier coefficients.

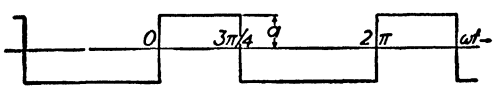


FIG. 20.

8. A curve is made up of parabolic arcs as follows. Between $x = -l/2$ and $x = +l/2$ the equation is $y = a(2x/l)^2$. Farther the curve repeats itself by mirroring about the vertical lines $x = -l/2$ and $x = +l/2$. Calculate the Fourier coefficients.

m

9. The torque-angle relation of a two-cycle Diesel engine, of the type discussed on page 248, has the following ordinates:

$y_0 = 0$, $y_1 = 0.500$, $y_2 = 0.980$, $y_3 = 1.120$, $y_4 = 1.060$
$y_5 = 0.940$, $y_6 = 0.810$, $y_7 = 0.675$, $y_8 = 0.575$, $y_9 = 0.450$
$y_{10} = 0.375$, $y_{11} = 0.310$, $y_{12} = 0.260$, $y_{13} = 0.210$, $y_{14} = 0\ 160$
$y_{15} = 0.115$, $y_{16} = 0.080$, $y_{17} = 0.045$, $y_{18} = 0.020$, $y_{19} = 0\ 005$
y_{20} to $y_{34} = 0$, $y_{35} = -0.005$, $y_{36} = -0.020$, $y_{37} = -0.040$
$y_{38} = -0.075$, $y_{39} = -0.115$, $y_{40} = -0.155$, $y_{41} = -0.190$, $y_{42} = -0.270$
$y_{43} = -0.350$, $y_{44} = -0\ 430$, $y_{45} = -0\ 475$, $y_{46} = -0\ 495$, $y_{47} = -0.315$

Find the various harmonics by means of Runge's method.

CHAPTER II

THE SINGLE-DEGREE-OF-FREEDOM SYSTEM

8. Degrees of Freedom.—A mechanical system is said to have one degree of freedom if its geometrical position can be expressed at any instant by one number only. Take, for example, a piston moving in a cylinder; its position can be specified at any time by giving the distance from the cylinder end, and thus we have a system of one degree of freedom. A crank shaft in rigid bearings is another example. Here the position of the system is completely specified by the angle between any one crank and the vertical plane. A weight suspended from a spring in such a manner that it is constrained in guides to move in the up-and-down direction only is the classical single-degree-of-freedom vibrational system (Fig. 23).

Generally if it takes n numbers to specify the position of a mechanical system, that system is said to have n degrees of freedom. A disk moving in its plane without restraint has three degrees of freedom: the x- and y-displacements of the center of gravity and the angle of rotation about the center of gravity. A cylinder *rolling* down an inclined plane has one degree of freedom; if, on the other hand, it descends partly rolling and partly sliding, it has two degrees of freedom, the translation and the rotation.

A rigid body moving freely through space has six degrees of freedom, three translations and three rotations. Consequently it takes six numbers or "coordinates" to express its position. These coordinates are usually denoted as x, y, z, φ, ψ, χ. A system of two rigid bodies connected by springs or other ties in such a manner that each body can move only along a straight line and cannot rotate has two degrees of freedom (Fig. 21). The two quantities determining the position of such a system can be chosen rather arbitrarily. For instance, we may call the distance from a fixed point O to the first body x_1, and the distance from O to the second body x_2. Then x_1 and x_2 are the coordinates. However, we might also choose the distance from O to

the center of gravity of the two bodies for one of the coordinates and call that y_1. For the other coordinate we might choose the distance between the two bodies, $y_2 = x_2 - x_1$. The pair of numbers x_1, x_2 describes the position completely, but the pair y_1, y_2 does it equally well. The latter choice has a certain practical advantage in this case, since usually we are not interested so much in the location of the system as a whole as in the stresses inside it. The stress in the spring of Fig. 21 is completely determined by y_2, so that for its calculation a knowledge of y_1 is not required. A suitable choice of the coordinates of a system of several degrees of freedom may simplify the calculations considerably.

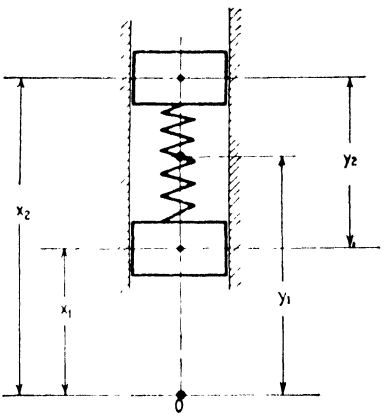


FIG. 21. - Two degrees of freedom.

It should not be supposed that a system of a single degree of freedom is always very simple. For example, a 12-cylinder gas engine, with a rigid crank shaft and a rigidly mounted cylinder block, has only one degree of freedom with all its moving pistons, rods, valves, cam shaft, etc. This is so because a single number (for instance, the angle through which the crank shaft has turned) determines completely the location of every moving part of the engine. However, if the cylinder block is mounted on flexible springs so that it can freely move in every direction (as is the case in many modern automobiles), the system has seven degrees of freedom, namely the six pertaining to the block as a rigid body in free space and the crank angle as the seventh coordinate.

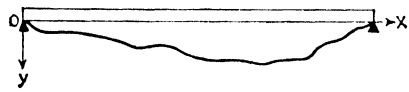


FIG. 22.—A beam has an infinite number of degrees of freedom.

A completely flexible system has an infinite number of degrees of freedom. Consider, for example, a flexible beam on two supports. By a suitable loading it is possible to bend this beam into a curve of any shape (Fig. 22). The description of this curve requires a function $y = f(x)$, which is equivalent to an infinite number of numbers. To each location x along the beam, any

deflection y can be given independent of the position of the other particles of the beam (within the limits of strength of the beam) and thus complete determination of the position requires as many values of y as there are points along the beam. As was the case in Fig. 21, the $y = f(x)$ is not the only set of numbers that can be taken to define the position. Another possible way of determining the deflection curve is by specifying the values of all its Fourier coefficients a_n and b_n [Eq. (11), page 21], which again are infinite in number.

9. Derivation of the Differential Equation.—Consider a mass m suspended from a rigid ceiling by means of a spring, as shown in Fig. 23. The "stiffness" of the spring is denoted by its "spring constant" k, which by definition is *the number of pounds tension necessary to extend the spring* 1 *in.* Between the mass and the rigid wall there is also an oil or air dashpot mechanism. This is not supposed to transmit any force to the mass as long as it is at rest, but as soon as the mass moves, the "damping force" of the dashpot is $c\dot{x}$ or cdx/dt, *i.e.*, proportional to the velocity and directed opposite to it. The quantity c is known as the *damping constant* or more at length as the *coefficient of viscous damping.*

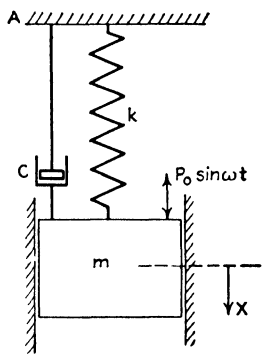


FIG. 23.—The fundamental single-degree-of-freedom system.

The damping occurring in actual mechanical systems does not always follow a law so simple as this $c\dot{x}$-relation; more complicated cases often arise. Then, however, the mathematical theory becomes very involved (see Chap. VIII, pages 430 and 435), whereas with "viscous" damping the analysis is comparatively simple.

Let an external alternating force $P_0 \sin \omega t$ be acting on the mass, produced by some mechanism which we need not specify in detail. For a mental picture assume that this force is brought about by somebody pushing and pulling on the mass by hand.

The problem consists in calculating the motions of the mass m, due to this external force. Or, in other words, if x be the distance between any instantaneous position of the mass during its motion and the equilibrium position, we have to find x as a function of time. The "equation of motion," which we are about to derive,

is nothing but a mathematical expression of Newton's second law,

$$\text{Force} = \text{mass} \times \text{acceleration}$$

All forces acting on the mass will be considered positive when acting downward and negative when acting upward.

The spring force has the *magnitude* kx, since it is zero when there is no extension x. When $x = 1$ in., the spring force is k lb. by definition, and consequently the spring force for any other value of x (in inches) is kx (in pounds), because the spring follows Hooke's law of proportionality between force and extension.

The *sign* of the spring force is negative, because the spring pulls *upward* on the mass when the displacement is *downward*, or the spring force is negative when x is positive. Thus the spring force is expressed by $-kx$.

The damping force acting on the mass is also negative, being $-c\dot{x}$, because, since it is directed *against* the velocity $\dot{x}$, it acts *upward* (negative) while $\dot{x}$ is directed *downward* (positive). The three downward forces acting on the mass are

$$-kx - c\dot{x} + P_0 \sin \omega t$$

Newton's law gives

$$m\frac{d^2x}{dt^2} = m\ddot{x} = -kx - c\dot{x} + P_0 \sin \omega t,$$

or

$$m\ddot{x} + c\dot{x} + kx = P_0 \sin \omega t \tag{12}$$

This very important equation* is known as the *differential equation of motion of a single-degree-of-freedom system.* The four terms in Eq. (12) are the inertia force, the damping force, the spring force, and the external force.

Before proceeding to a calculation of x from Eq. (12), *i.e.*, to a solution of the differential equation, it is well to consider some other problems that will lead to the same equation.

* In the derivation, the effect of gravity has been omitted. The amplitude x was measured from the "equilibrium position," *i.e.*, from the position where the downward force mg is held in equilibrium by an upward spring force $k\delta$ (δ being the deflection of the spring due to gravity). It would have been possible to measure x_1 from the position of the *unstressed* spring, so that $x_1 = x + \delta$. In Eq. (12), then, x must be replaced by x_1, and on the right-hand side a force mg must be added. This leads to the same result (12).

10. Other Cases.—Figure 24 represents a disk of moment of inertia I attached to a shaft of torsional stiffness k, defined as *the torque in inch-pounds necessary to produce* 1 *radian twist at the disk.* Consider the twisting motion of the disk under the influence of an externally applied torque $T_0 \sin \omega t$. This again is a one-degree-of-freedom problem since the torsional displacement of the disk from its equilibrium position can be expressed by a single quantity, the angle φ. Newton's law for a rotating body states that

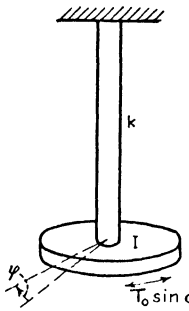


FIG. 24.—The torsional one-degree-of-freedom system.

$$\text{Torque} = \text{moment of inertia} \times \text{angular acceleration} = I\frac{d^2\varphi}{dt^2} = I\ddot{\varphi}$$

As in the previous problem there are *three* torques acting on the disk: the spring torque, damping torque, and external torque. The spring torque is $-k\varphi$, where φ is measured in radians. The negative sign is evident for the same reason that the spring force in the previous case was $-kx$. The damping torque is $-c\dot{\varphi}$, caused by a dashpot mechanism not shown in the figure. The "damping constant" c in this problem is the *torque on the disk caused by an angular speed of rotation of* 1 *radian per second.* The external torque is $T_0 \sin \omega t$, so that Newton's law leads to the differential equation

$$I\ddot{\varphi} + c\dot{\varphi} + k\varphi = T_0 \sin \omega t \quad (12a)$$

which has the same form as Eq. (12).

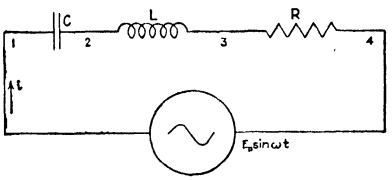


FIG. 25.—The electrical single-degree-of-freedom circuit.

As a third example, consider an electric circuit with an alternating-current generator, a condenser C, resistance R, and inductance L all in series. Instead of Newton's law, use the relation that the instantaneous voltage of the generator $e = E_0 \sin \omega t$ is equal to the sum of the three voltages across C, R, and L. Let i be the instantaneous value of the current in the circuit in the direction indicated in Fig. 25. According to Ohm's law, the voltage across the resistance is $V_3 - V_4 = Ri$. The voltage across the inductance is $V_2 - V_3 = L\frac{di}{dt}$. For the condenser, the

relation $Q = CV$ holds, where Q is the charge, C the capacitance, and V the voltage. The charge Q can be expressed in terms of i, as follows. If the current i flows during a time element dt, the quantity of electricity transported through the circuit is idt. This does not flow *through* the condenser but merely increases its charge so that

$$dQ = idt.*$$

Hence

$$i = \frac{dQ}{dt} = \dot{Q} \qquad \text{or} \qquad Q = \int i dt$$

To show that this electric circuit behaves in the same manner as the vibrating mass of Fig. 23 it is better to work with the charge Q rather than with the more familiar current i. The various voltage drops can be written

$$V_1 - V_2 = \frac{Q}{C}$$

$$V_2 - V_3 = L\frac{di}{dt} = L\frac{d^2Q}{dt^2} = L\ddot{Q}$$

$$V_3 - V_4 = Ri = R\frac{dQ}{dt} = R\dot{Q}$$

As the sum of these three voltage drops must equal the generator voltage, the differential equation is

$$L\ddot{Q} + R\dot{Q} + \frac{1}{C}Q = E_0 \sin \omega t \qquad (12b)$$

which is of exactly the same form as Eq. (12).

Therefore, the linear, torsional, and electrical cases thus far discussed all lead to the same differential equation. The translation from one case to another follows directly from the table shown on page 40.

All the mechanical statements made have their electrical analogues and *vice versa*. For example, it was stated that "the voltage across the inductance L is $L\frac{di}{dt}$." In mechanical language this would be expressed as "the force of the mass m is $m\frac{dv}{dt}$." A mechanical statement would be "The energy stored in the

* The letter i unfortunately is dotted. To avoid confusion it is agreed that i shall mean the current itself and that for its differential coefficient the Leibnitz notation di/dt will be used.

mass is $\frac{1}{2}mv^2$." The electrical analogue is "The energy stored in the inductance is $\frac{1}{2}Li^2$."

Linear		Torsional		Electrical	
Mass	m	Moment of inertia	I	Inductance	L
Stiffness	k	Torsional stiffness	k	1/capacitance	$1/C$
Damping	c	Torsional damping	c	Resistance	R
Impressed force	$P_0 \sin \omega t$	Impressed torque	$T_0 \sin \omega t$	Impressed voltage	$E_0 \sin \omega t$
Displacement	x	Angular displacement	φ	Condenser charge	Q
Velocity	$\dot{x} = v$	Angular velocity	$\dot{\varphi} = \omega$	Current	$\dot{Q} = i$

Nor are these three cases the only ones that are determined by Eq. (12). Any system with inertia, elasticity, and damping proportional to the velocity, for which the displacements can be described by a single quantity, belongs to this class. For example, consider two disks of moment of inertia I_1 and I_2, joined by a shaft of torsional stiffness k in.-lb./radian (Fig. 26). On the first disk the torque $T_0 \sin \omega t$ is made to act, while there is a damping with constant c, proportional to the twist in the shaft. What will be the motion? There are two disks, each of which can assume an angular position independent of the other by twisting the shaft. Apparently, therefore, this is a "two-degree-of-freedom" system. However, the quantity in which the engineer is most interested is the angle of twist of the shaft, and it is possible to express the motion in terms of this quantity only. Let φ_1 and φ_2 be the angular displacements of the two disks, then $\varphi_1 - \varphi_2$ is the shaft twist, $k(\varphi_1 - \varphi_2)$ is the shaft torque, and $c(\dot{\varphi}_1 - \dot{\varphi}_2)$ is the damping torque. Apply Newton's law to the first disk,

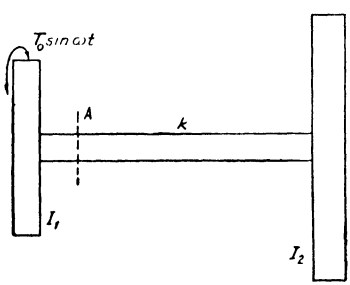


FIG. 26.—Torsional vibrations of two disks on an elastic shaft.

$$T_0 \sin \omega t = I_1\ddot{\varphi}_1 + k(\varphi_1 - \varphi_2) + c(\dot{\varphi}_1 - \dot{\varphi}_2)$$

and to the second disk,

$$0 = I_2\ddot{\varphi}_2 + k(\varphi_2 - \varphi_1) + c(\dot{\varphi}_2 - \dot{\varphi}_1)$$

Divide the first equation by I_1, the second by I_2, and subtract the results from each other:

$$\frac{T_0}{I_1} \sin \omega t = (\ddot{\varphi}_1 - \ddot{\varphi}_2) + \left(\frac{k}{I_1} + \frac{k}{I_2}\right)(\varphi_1 - \varphi_2) + \left(\frac{c}{I_1} + \frac{c}{I_2}\right)(\dot{\varphi}_1 - \dot{\varphi}_2)$$

Call the twist angle $\varphi_1 - \varphi_2 = \psi$, and multiply the whole equation by $I_1I_2/(I_1 + I_2)$,

$$\frac{I_1I_2}{I_1 + I_2}\ddot{\psi} + c\dot{\psi} + k\psi = \frac{I_2T_0}{I_1 + I_2} \cdot \sin \omega t \qquad (12c)$$

giving again an equation of the form (12). Of course, this equation, when solved, tells us only about the twist in the shaft or about the *relative* motion of the two disks with respect to each other. No information can be gained from it as to the motions of the disks individually.

A variant of Fig. 26 is shown in Fig. 27, in the shaft of which is inserted a gear-and-pinion system. Let the disks again have the moments of inertia I_1 and I_2, and assume the gears G and P to be without any inertia whatsoever. Also assume the gear teeth to be stiff, so that the torsional flexibility is limited to the shafts k_1 and k_2. The gear ratio is n.

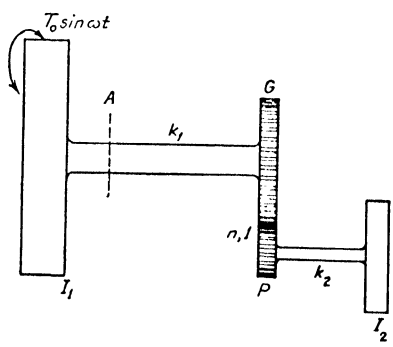


FIG. 27.—Geared system which can be reduced to the system of Fig. 26.

The differential equation for Fig. 27 could be derived from Newton's law directly, but suppose we reduce Fig. 27 to Fig. 26 by omitting the gears and replacing k_2, I_2, and ψ by other "equivalent quantities" so that the differential equation (12c) can be applied.

In Fig. 26 the elasticity k can be determined experimentally by clamping I_2 and applying a constant torque T_0 to I_1. This causes I_1 to deflect through an angle φ_0, so that $k = T_0/\varphi_0$.

Repeat this experiment with Fig. 27, *i.e.*, clamp I_2 and apply T_0 to I_1. On account of the gears the torque in the shaft k_2 is T_0/n, and the angle of twist of k_2 is therefore T_0/nk_2. Since I_2 is clamped, this is the angle of rotation of the pinion P. The angle of the gear G is n times smaller or T_0/n^2k_2. Add to this the angle T_0/k_1 for the shaft k_1 and we have the angular displacement of I_1. Thus the equivalent k is

$$\frac{1}{k} = \frac{\varphi}{T_0} = \frac{1}{k_1} + \frac{1}{n^2k_2}$$

Now consider the inertia. The inertia I_2 in Fig. 26 could be determined by the following hypothetical experiment. Give I_1 (or the whole shaft k) a *constant* angular acceleration α. Then the shaft at the section A would experience a torque $T_0 = \alpha I_2$ coming from the right. Thus, $I_2 = T_0/\alpha$. Repeat this experiment in Fig. 27. The acceleration α in k_1 and G becomes $n\alpha$ in k_2. Hence, the torque in k_2 is $n\alpha I_2$. This is also the torque at the pinion P. The gear G makes it n times larger, so that the torque at A is $n^2\alpha I_2$ and the equivalent of I_2 in the gearless system is n^2I_2. In general, therefore, a geared system (such as shown in Fig. 27) can be reduced to an equivalent non-geared system (Fig. 26) by the following rule:

Divide the system into separate parts each of which has the same speed within itself. (In Fig. 27 there are two such parts but in general there may be several.) Choose one of these parts as the base and assign numbers n to each of the other parts so that n is the speed ratio with respect to the base. ($n > 1$ for speeds higher than the base speed; the n of the base is unity.) Then, *remove all gears and multiply all spring constants k and all inertias I by the factors* n^2. The differential equation of the reduced gearless system is then the same as that of the original geared construction.

The last example to be considered resembles the first one in many respects and yet is different. Instead of having the force $P_0 \sin \omega t$ acting on the mass of Fig. 23, the upper end or ceiling A of the spring is made to move up and down with an amplitude a_0, the motion of A being determined by $a_0 \sin \omega t$. It will be shown that this *motion* of the top of the spring is completely equivalent to a *force* on the suspended mass.

Again let the downward displacement of the mass be x; then, since the top of the spring moves as $a_0 \sin \omega t$, the spring extension

at any time will be $x - a_0 \sin \omega t$. The spring force is thus $-k(x - a_0 \sin \omega t)$ and the damping force is $-c(\dot{x} - a_0\omega \cos \omega t)$. Newton's law gives

$$m\ddot{x} + k(x - a_0 \sin \omega t) + c(\dot{x} - a_0\omega \cos \omega t) = 0$$

or

$$m\ddot{x} + c\dot{x} + kx = ka_0 \sin \omega t + ca_0\omega \cos \omega t$$

By Eq. (6), page 6, the sum of a sine and a cosine wave of the same frequency is again a harmonic function, so that

$$m\ddot{x} + c\dot{x} + kx = \sqrt{(ka_0)^2 + (ca_0\omega)^2} \sin (\omega t + \varphi) \quad (12d)$$

Therefore, a motion of the top of the spring with amplitude a_0 is equivalent to a force on the mass with amplitude $\sqrt{(ka_0)^2 + (ca_0\omega)^2}$. The expressions ka_0 and $c\omega a_0$ in the radical are the maxima of the spring force and damping force, while the entire radical is the maximum value of the total force for the case where the mass is clamped, *i.e.*, where the x-motion is prevented.

Example: Find the differential equation of the *relative* motion y between the mass and the ceiling of Fig. 23, in which $P_0 = 0$ and in which the ceiling is moved harmonically up and down.

$$y = x - a_0 \sin \omega t$$

Solution: We have by differentiation:

$$\begin{aligned} x &= y + a_0 \sin \omega t \\ \dot{x} &= \dot{y} + a_0\omega \cos \omega t \\ \ddot{x} &= \ddot{y} - a_0\omega^2 \sin \omega t \end{aligned}$$

Substitute these into Eq. (12*d*):

$$\begin{aligned} m\ddot{y} - ma_0\omega^2 \sin \omega t + c\dot{y} + ca_0\omega \cos \omega t + ky + ka_0 \sin \omega t \\ = ka_0 \sin \omega t + ca_0\omega \cos \omega t \end{aligned}$$

or

$$m\ddot{y} + c\dot{y} + ky = ma_0\omega^2 \sin \omega t \quad (12e)$$

Thus the relative motion between the mass and the moving ceiling acts in the same manner as the absolute motion of the mass with a ceiling at rest and with a force of amplitude $ma_0\omega^2$ acting on the mass. The right-hand side of (12*e*) is the inertia force of the mass if it were moving at amplitude a_0; hence, it can be considered as the force that has to be exerted at the top of the spring if the spring is made stiff, *i.e.*, if the y-motion is prevented.

11. Free Vibrations without Damping.—Before developing a solution of the general equation (12), it is useful to consider first some important simplified cases. If there is no external or impressed force $P_0 \sin \omega t$ and no damping ($c = 0$), the expression (12) reduces to

$$m\ddot{x} + kx = 0 \tag{13}$$

or

$$\ddot{x} = -\frac{k}{m}x$$

or, in words: *The deflection x is such a function of the time that when it is differentiated twice, the same function is again obtained, multiplied by a negative constant.* Even without a knowledge of differential equations, we may remember that such functions exist, *viz.*, sines and cosines, and a trial reveals that $\sin t\sqrt{k/m}$ and $\cos t\sqrt{k/m}$ are actually solutions of (13). The most general form in which the solution of (13) can be written is

$$x = C_1 \sin t\sqrt{\frac{k}{m}} + C_2 \cos t\sqrt{\frac{k}{m}} \tag{14}$$

where C_1 and C_2 are arbitrary constants. That (14) is a solution of (13) can be verified easily by differentiating (14) twice and then substituting in (13); that there are no solutions of (13) other than (14) need not be proved here: it is true and may be taken for granted.

Let us now interpret (14) physically. First, it is seen that the result as it stands is very indefinite; the constants C_1 and C_2 may have any value we care to assign to them. But the problem itself was never fully stated. The result (14) describes *all* the motions the system of mass and spring is capable of executing. One among others is the case for which $C_1 = C_2 = 0$, giving $x = 0$, which means that the mass remains permanently at rest.

We now specify more definitely that the mass is pulled out of its equilibrium position to $x = x_0$ and then released without initial velocity. Measuring the time from the instant of release, the two conditions are

At $t = 0$, $\qquad x = x_0 \qquad$ and $\qquad \dot{x} = 0$

The first condition substituted into (14) gives

$$x_0 = C_1 \cdot 0 + C_2 \cdot 1 \qquad \text{or} \qquad C_2 = x_0$$

For the second condition, Eq. (14) must be differentiated first and then we get

$$0 = C_1\sqrt{\frac{k}{m}} \cdot 1 - C_2 \cdot \sqrt{\frac{k}{m}} \cdot 0 \qquad \text{or} \qquad C_1 = 0$$

Substitution of these results in (14) leads to the specific solution

$$x = x_0 \cos t\sqrt{\frac{k}{m}} \tag{14a}$$

This represents an *undamped vibration*, one cycle of which occurs when $t\sqrt{k/m}$ varies through 360 deg. or 2π radians (Fig. 28). Denoting the time of a cycle or the *period* by T, we thus have

$$\sqrt{\frac{k}{m}} \cdot T = 2\pi \qquad \text{or} \qquad T = 2\pi\sqrt{\frac{m}{k}} \tag{15}$$

It is customary to denote $\sqrt{k/m}$ by ω_n, called the "natural circular frequency." This value $\sqrt{k/m} = \omega_n$ is the angular

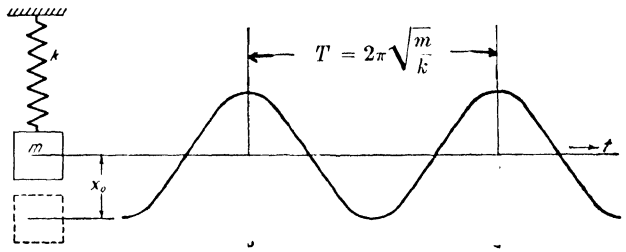


FIG. 28.—Undamped free vibration starting from an initial displacement.

velocity of the rotating vector which represents the vibrating motion (see page 4).

The reciprocal of T or the *natural frequency* f_n is

$$f_n = \frac{1}{T} = \frac{1}{2\pi}\sqrt{\frac{k}{m}} = \frac{\omega_n}{2\pi} \tag{16}$$

measured in cycles per second. Hence it follows that if m is replaced by a mass twice as heavy, the vibration will be $\sqrt{2}$ times as slow as before. Also, if the spring is made twice as weak, other things being equal, the vibration will be $\sqrt{2}$ times as slow. On account of the absence of the impressed force $P_0 \sin \omega t$, this vibration is called a *free vibration.*

If we start with the assumption that the motion is harmonic, the frequency can be calculated in a very simple manner from an *energy consideration.* In the middle of a swing the mass has considerable kinetic energy, whereas in either extreme position it stands still for a moment and has no kinetic energy left. But

then the spring is in a state of tension (or compression) and thus has elastic energy stored in it. At any position between the middle and the extreme, there is both elastic and kinetic energy, the sum of which is constant since external forces do no work on the system. Consequently, the kinetic energy in the middle of a stroke must be equal to the elastic energy in an extreme position.

We now proceed to calculate these energies. The spring force is kx, and the work done on increasing the displacement by dx is $kx \cdot dx$. The potential or elastic energy in the spring when stretched over a distance x is $\int_0^x kx \cdot dx = \frac{1}{2}kx^2$. The kinetic energy at any instant is $\frac{1}{2}mv^2$. Assume the motion to be $x = x_0 \sin \omega t$, then $v = x_0\omega \cos \omega t$. The potential energy in the extreme position is $\frac{1}{2}kx_0^2$, and the kinetic energy in the neutral position, where the velocity is maximum, is $\frac{1}{2}mv_{\max}^2 = \frac{1}{2}m\omega^2x_0^2$.

Therefore,

$$\tfrac{1}{2}kx_0^2 = \tfrac{1}{2}m\omega^2x_0^2$$

from which $\omega^2 = k/m$, independent of the amplitude x_0. This "energy method" of calculating the frequency is of importance. In Chaps. IV and VI, dealing with systems of greater complexity, it will be seen that a frequency determination from the differential equation often becomes so complicated as to be practically impossible. In such cases a generalized energy method, known as the method of *Rayleigh*, will lead to a result (see pages 178–194).

The formula $\omega_n = \sqrt{k/m}$ may be written in a somewhat different form. The weight of the mass m is mg, and the deflection of the spring caused by this weight is mg/k. It is called the static deflection δ_{st} or static sag of the spring under the weight.

$$\delta_{st} = \frac{mg}{k}$$

Hence,

$$\frac{k}{m} = \frac{g}{\delta_{st}}$$

or

$$\omega_n = \sqrt{\frac{g}{\delta_{st}}} \tag{17}$$

If δ_{st} is expressed in inches, $g = 386$ in./sec.^{2}, and the frequency is

$$f_n = \frac{\sqrt{386}}{2\pi}\sqrt{\frac{1}{\delta_{st}}} = 3.14\sqrt{\frac{1}{\delta_{st}}} \text{ cycles per second}$$

$$f_n = 188\sqrt{\frac{1}{\delta_{st}}} \text{ cycles per minute} \qquad (17a)$$

This relationship, which is very useful for quickly estimating natural frequencies or critical speeds, is shown graphically in Fig. 29.

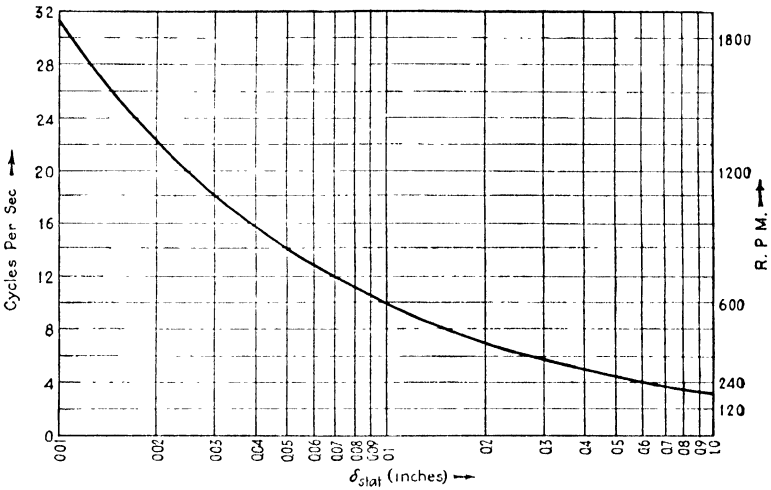


FIG. 29.—Curve representing Eq. (17*a*) for the natural frequency of an undamped, single-degree system.

12. Examples.—Consider some numerical examples of the application of the fundamental formula (16).

1. A steel bar of 1 by ½ in. cross section is clamped solidly in a vise at one end and carries a weight of 20 lb. at the other end (Fig. 30). (*a*) What is the frequency of the vibration if the distance between the weight and the vise is 30 in.? (*b*) What percentage change is made in the frequency by shortening the rod ¼ in.?

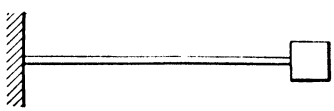


FIG. 30.

a. The weight of the bar itself is ½ by 1 by 30 cu. in. × 0.28 lb. per cubic inch or roughly 4 lb. The particles of the bar near the 20-lb. weight at its end vibrate with practically the same amplitude as that weight, whereas the particles near the clamped end vibrate hardly at all. This is taken account of by adding a

fraction of the weight of the bar to the weight at its end. On page 194 it is shown that approximately one-quarter of the weight of the bar has to be thus added. Therefore the mass m in Eq. (16) is $21/g = 21/386$ lb. in.$^{-1}$ sec.^{2}.

A force P at the end of a cantilever gives a deflection $\delta = Pl^3/3EI$. The spring constant by definition is

$$k = P/\delta = 3EI/l^3.$$

The moment of inertia of the section is $I = \frac{1}{12}bh^3 = \frac{1}{24}$ (or $\frac{1}{96}$, depending upon whether the vibrations take place in the stiff or in the limber plane). The circular frequency is

$$\omega_n = \sqrt{\frac{k}{m}} = \sqrt{\frac{3 \cdot 30 \cdot 10^6 \cdot 386}{24 \cdot 30^3 \cdot 21}} = 50.4 \text{ radians per second}$$

The frequency $f_n = \omega_n/2\pi = 8.0$ cycles per second.

In case the bar vibrates in the direction of the weak side of the section, $I = \frac{1}{96}$, and f_n becomes one-half its former value, 4.0 cycles per second.

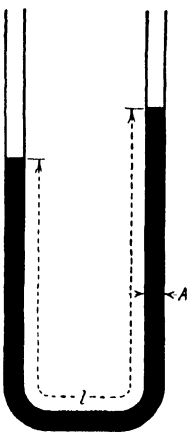


FIG. 31.—Oscillations of a liquid column in a U-tube.

b. The question regarding the change in frequency due to a change in length can be answered as follows. The spring constant k is proportional to $1/l^3$, and the frequency consequently is proportional to $\sqrt{1/l^3} = l^{-3/2}$. Shortening the bar by 1 per cent will raise the frequency by $1\frac{1}{2}$ per cent. Thus the shortening of $\frac{1}{4}$ in. will increase f_n by $1\frac{1}{4}$ per cent.

2. As a second example consider a U-tube filled with water (Fig. 31). Let the total length of the water column be l, the tube cross section be A, and the mass of water per cubic inch be m_1. If the water oscillates back and forth, the mass in motion is $m_1 \cdot A \cdot l$. In this problem there is no specific "spring," but still the force of gravity tends to restore the water level to an equilibrium position. Thus we have a "gravity spring," of which the spring constant by definition is the force per unit deflection. Raise the level in one arm of the tube by 1 in., then it will fall in the other arm 1 in. This gives an unbalanced weight of 2 in. water column, causing a force of

$(2m_1A) \cdot g$, which is the spring constant. Therefore the frequency is

$$\omega_n = \sqrt{\frac{k}{m}} = \sqrt{\frac{2g}{l}}$$

3. Consider the systems shown in Fig. 32, where a mass m is suspended from two springs k_1 and k_2 in three apparently different ways. However, the cases 32*a* and 32*b* are dynamically identical, because a downward deflection of 1 in. creates an upward force of $(k_1 + k_2)$ lb. in both cases. Thus the natural frequency of such systems is

$$\omega_n = \sqrt{\frac{k_1 + k_2}{m}}$$

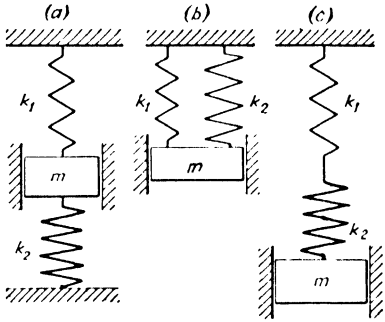


Fig. 32.—Three systems with compound springs, which are equivalent to the system of Fig. 28. (*a*) and (*b*) have "parallel" springs; (*c*) has its springs "in series."

For Fig. 32*c* the situation is different. Let us pull downward on the mass with a force of 1 lb. This force will be transmitted through *both* springs in full strength. Their respective elongations are $1/k_1$ and $1/k_2$, the total elongation per pound being $\frac{1}{k_1} + \frac{1}{k_2}$. But, by definition, this is $1/k$, the reciprocal of the combined spring constant. Hence,

$$k = \frac{1}{\frac{1}{k_1} + \frac{1}{k_2}}$$

Rule: The combined spring constant of several "parallel" springs is $k = \Sigma k_n$; for n *springs "in series" the spring constant is found from* $1/k = \Sigma 1/k_n$.

For example, if a given coil spring of stiffness k is cut in two equal parts, each piece will have the stiffness $2k$. (It takes twice as much load to give to half the spring the same deflection as to the whole spring.) Putting the two half springs in series, we find, indeed, $\frac{1}{k} = \frac{1}{2k} + \frac{1}{2k}$.

It is of interest to note that this rule for compounding spring constants is exactly the same as that for finding the total conductance of series and parallel circuits in electrical engineering.

4. The last example to be discussed in this section is illustrated in Fig. 33. A massless, inflexible beam is hinged at one end and carries a mass m at the other end. At a distance a from the hinge there is a spring of stiffness k. What is the natural frequency of vibration of this system?

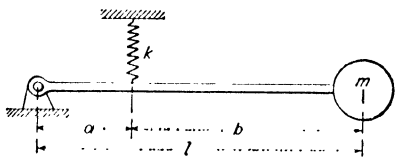


FIG. 33.—The spring k as shown is equivalent to a fictitious spring of stiffness $k(a/l)^2$ placed at the mass m.

We shall consider the vibrations to be so small that the mass moves sensibly up and down only. In deriving the equation of motion on page 35, the spring force *on the mass* was equated to $m\ddot{x}$. In this case also we have to ask: What force has to be exerted *on the mass* in order to deflect it 1 in? Let that force be F. Then from static equilibrium the force in the spring is $\frac{l}{a} \cdot F$. Since the deflection at the mass is 1 in., it is a/l in. at the spring. This leads to a spring force $\frac{a}{l} \cdot k$. Hence

$$\frac{l}{a} \cdot F = \frac{a}{l} \cdot k \qquad \text{or} \qquad F = \left(\frac{a}{l}\right)^2 \cdot k$$

Therefore, the effective spring constant at the mass is $k \cdot (a/l)^2$. The effect of the stiffness of the spring is thus seen to diminish very fast when it is shifted to the left.

The frequency is

$$\omega_n = \frac{a}{l}\sqrt{\frac{k}{m}}$$

With the energy method of page 46 the calculation is as follows: Let the motion of the mass be $x = x_0 \sin \omega_n t$, where ω_n is as yet unknown. The amplitude of motion at the spring then is $x_0 a/l$ and the potential energy in the spring is $\frac{1}{2}k\delta^2 = \frac{1}{2}k(x_0 a/l)^2$. The kinetic energy of the mass is $\frac{1}{2}mv^2 = \frac{1}{2}m\omega_n^2 x_0^2$. Equating these two, the amplitude x_0 drops out and

$$\omega_n^2 = \frac{k}{m}\frac{a^2}{l^2}$$

Some of the problems at the end of this chapter can be solved more easily with the energy method than by a direct application of the formula involving $\sqrt{k/m}$.

13. Free Vibrations with Viscous Damping.—It was seen that an undamped free vibration persists forever [Eq. (14) or (14*a*)]. Evidently this never occurs in nature; all free vibrations die down after a time. Therefore consider Eq. (12) with the damping term $c\dot{x}$ included, *viz.*:

$$m\ddot{x} + c\dot{x} + kx = 0 \tag{18}$$

The term "viscous damping" is usually associated with the expression $c\dot{x}$ since it represents fairly well the conditions of damping due to the viscosity of the oil in a dashpot. Other types of damping exist and will be discussed later (page 436). The solution of (18) cannot be found as simply as that of (13). However, if we consider the function $x = e^{st}$, where t is the time and s an unknown constant, it is seen that upon differentiation the same function results, but multiplied by a constant. This function, substituted in (18) permits us to divide by e^{st} and leads to an *algebraic* equation instead of a *differential* equation, which is a great simplification. Thus we assume that the solution is e^{st}. With this assumption, Eq. (18) becomes

$$(ms^2 + cs + k)e^{st} = 0 \tag{19}$$

If (19) can be satisfied, our assumption $x = e^{st}$ for the solution is correct. Since Eq. (19) is a quadratic in s, there are two values s_1 and s_2 that will make the left side of (19) equal to zero

$$s_{1,2} = -\frac{c}{2m} \pm \sqrt{\left(\frac{c}{2m}\right)^2 - \frac{k}{m}} \tag{20}$$

so that $e^{s_1 t}$ and $e^{s_2 t}$ are both solutions of Eq. (18). The most general solution is

$$x = C_1 e^{s_1 t} + C_2 e^{s_2 t} \tag{21}$$

where C_1 and C_2 are arbitrary constants.

In discussing the physical significance of this equation two cases have to be distinguished, depending upon whether the expressions for s in Eq. (20) are real or complex. Clearly for $(c/2m)^2 > k/m$, the expression under the radical is positive so that both values for s are real. Moreover, they are both negative because the square root is smaller than the first term $c/2m$.

Thus (21) describes a solution consisting of the sum of two decreasing exponential curves, as shown in Fig. 34. As a representative example, the case $C_1 = 1$, $C_2 = -2$ is drawn as a dashed line.

Without analyzing any special cases by determining their values for C_1 and C_2, the figure shows that the motion is no "vibration" but rather a creeping back to the equilibrium position. This is due to the fact that for $(c/2m)^2 > k/m$ the damping c is extremely large. For smaller values of c, which pertain to more practical cases, (20) gives complex values for s,

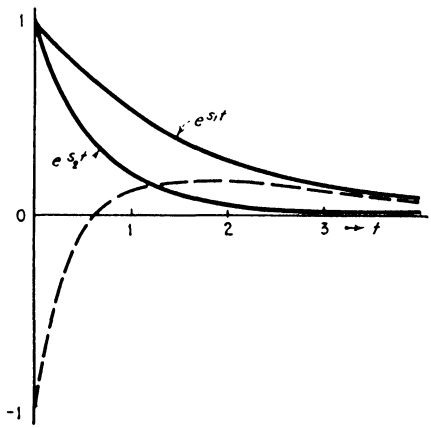


FIG. 34.—Motions of a single-degree system with damping greater than the critical damping c_c.

and the solution (21), as written, becomes meaningless. The damping c at which this transition occurs is called the *critical* damping c_c:

$$c_c = 2m\sqrt{\frac{k}{m}} = 2\sqrt{mk} = 2m\omega_n \tag{22}$$

In case the damping is less than this, (20) can better be written as

$$s_{1,2} = -\frac{c}{2m} \pm j\sqrt{\frac{k}{m} - \left(\frac{c}{2m}\right)^2} \tag{20a}$$

where $j = \sqrt{-1}$. Though the radical is now a real number both values of s contain j and consequently the solution (21) contains terms of the form $e^{j\omega t}$, which have to be interpreted by means of Eq. (8*a*), page 13.

With (20*a*) and (8*a*), the solution (21) becomes

$$x = e^{-\frac{c}{2m}t}[C_1(\cos qt + j \sin qt) + C_2(\cos qt - j \sin qt)]$$

$$= e^{-\frac{c}{2m}t}[(C_1 + C_2) \cos qt + (jC_1 - jC_2) \sin qt] \qquad (23)$$

Since C_1 and C_2 were arbitrary constants, $(C_1 + C_2)$ and $(jC_1 - jC_2)$ are also arbitrary, so that for simplicity we may write them C_1' and C_2'. Thus

$$\left.\begin{aligned} x &= e^{-\frac{c}{2m}t}(C_1' \cos qt + C_2' \sin qt) \\ \text{where} \qquad q &= \sqrt{\frac{k}{m} - \frac{c^2}{4m^2}} \end{aligned}\right\} \qquad (24a, b)$$

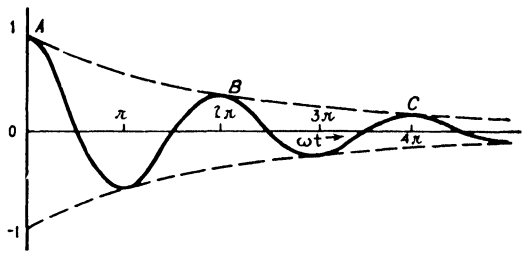


FIG. 35.—Free vibration of a system with damping less than the critical damping of Eq. (22).

This is the solution for a damping smaller than c_c. It consists of two factors, the first a decreasing exponential (Fig. 34) and the second a sine wave. The combined result is a "damped sine wave," lying in the space between the exponential curve and its mirrored image (Fig. 35). The smaller the damping constant c, the flatter will be the exponential curve and the more cycles it will take for the vibrations to die down.

The *rate* of this dying down is of interest and can be calculated in a simple manner by considering any two consecutive maxima of the curve: *A*-*B*, *B*-*C*, etc. During the time interval between two such maxima, *i.e.*, during $2\pi/q$ sec., the amplitude of the vibration (which at these maxima practically coincides with $e^{-\frac{c}{2m}t}$) diminishes from $e^{-\frac{c}{2m}t}$ to $e^{-\frac{c}{2m}\left(t+\frac{2\pi}{q}\right)}$. The latter of these two expressions is seen to be equal to the first one multiplied by the constant factor $e^{-\frac{\pi c}{mq}}$, which factor naturally is smaller than unity. It is seen that this factor is the same for *any* two

consecutive maxima, independent of the amplitude of vibration or of the time. The ratio between two consecutive maxima is constant; the amplitudes decrease in a geometric series.

If x_n is the nth maximum amplitude during a vibration and x_{n+1} is the next maximum, then we have seen that $x_{n+1} = x_n e^{-\pi c/mq}$ or also $\log (x_n/x_{n+1}) = \pi c/mq = \delta$. This quantity δ is known as the logarithmic decrement. For small damping we have

$$\delta = \frac{\pi c}{mq} = 2\pi \frac{c}{c_c} \Big/ \sqrt{1 - \left(\frac{c}{c_c}\right)^2} \approx \frac{2\pi c}{c_c} \tag{25}$$

and also $x_{n+1}/x_n = e^{-\delta} \approx 1 - \delta$, so that

$$\frac{x_n - x_{n+1}}{x_n} = \delta = \frac{2\pi c}{c_c} \tag{25a}$$

The *frequency* of the vibration is seen to diminish with increasing damping according to (24*b*), which if written in a dimensionless form with the aid of (22) becomes

$$\frac{q}{\omega_n} = \sqrt{1 - \left(\frac{c}{c_c}\right)^2}$$

This relation is plotted in Fig. 36 where the ordinate q/ω_n is the ratio of the damped to the undamped natural frequency, while the abscissa is the ratio of the actual to the critical damping constant. The figure is a circle; naturally for critical damping ($c = c_c$) the natural frequency q is zero. The diagram is drawn for negative values of c as well, the meaning of which will be explained later in Chap. VII (page 347). On account of the horizontal tangent of the circle at $c = 0$, the natural frequency is practically constant and equal to $\sqrt{k/m}$ for all technical values of the damping ($c/c_c < 0.2$).

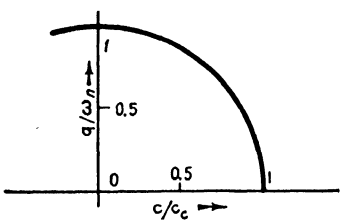


FIG. 36.—The natural frequency of a damped single-degree-of-freedom system as a function of the damping; Eq. (24*b*).

The *undamped* free vibration, being a harmonic motion, can be represented by a rotating vector, the end point of which describes a circle. With the present case of *damped* motion this graphical picture still holds, with the exception that the amplitude decreases with time. Thus, while revolving, the vector shrinks at a rate proportional to its length, giving a geometric series diminution. The end point of this vector describes a

"logarithmic spiral" (Fig. 37). The amplitudes of a diagram like Fig. 35 can be derived from Fig. 37 by taking the horizontal projection of the vector, of which the end point lies on the spiral and which rotates with the uniform angular velocity q [Eq. (24)].

A special case of the foregoing occurs when the mass or inertia of the system is negligibly small, so that there remain only a spring and a dashpot. We want to know the motion of the

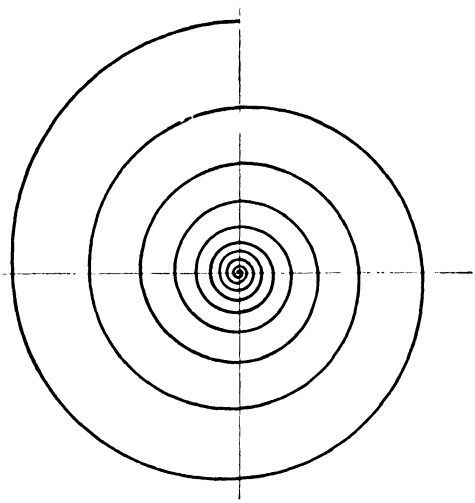


FIG. 37.—Vector diagram of a damped free vibration.

(massless) dashpot piston when it is released from an initial deflection x_0. The differential equation is

$$c\frac{dx}{dt} + kx = 0$$

which can be solved directly by writing

$$\frac{c}{k}\frac{dx}{x} = -dt$$

$$t = -\frac{c}{k}\int\frac{dx}{x} = -\frac{c}{k}(\log x + \text{const.})$$

At $t = 0$ the deflection $x = x_0$, so that the constant is $-\log x_0$. Hence

$$t = -\frac{c}{k}\log\frac{x}{x_0} \qquad \text{and} \qquad x = x_0 e^{-\frac{k}{c}t}, \tag{26}$$

a relation represented by one of the solid curves of Fig. 34. Evidently the exponent of the e-function is a dimensionless quantity, so that c/k must have the dimension of a time. It is known as the *relaxation time*, which, by definition, is the time in which the deflection x_0 of the system "relaxes" to $1/e$th part of its original value. On page 444 we shall have occasion to use this concept.

Example: In the system shown in Fig. 33, page 50, the mass weighs 1 oz.; the spring has a stiffness of 10 lb. per inch; $l = 4$ in.; $a = b = 2$ in. Moreover, a dashpot mechanism is attached to the mid-point of the beam, *i.e.*, to the same point where the spring is fastened to it. The dashpot produces a force of 0.01 lb. for a velocity of 1 in. per second.

a. What is the rate of decay of the free vibrations?

b. What would be the critical damping in the dashpot?

c. Find the relaxation time in the case of critical damping.

Solution: Let us first answer question (*b*) by means of Eq. (22). The undamped natural frequency is $\omega_n = \sqrt{k/m}$. On page 50 we found that the equivalent spring constant of Fig. 33 is ka^2/l^2 or $k/4 = 2.5$ lb. per inch. Thus

$$\omega_n = \sqrt{2.5 \times 16 \times 386} = 124 \text{ radians per second}$$

The critical damping constant of the system (*i.e.*, the critical damping of an imaginary dashpot *at the mass*) is, by Eq. (22),

$$2 \times \frac{1}{16 \times 386} \times 124 = 0.041 \text{ lb./in./sec.}$$

Since the dashpot is actually located at the mid-point of the beam, the dashpot must have a constant which is four times as great, for the same reason that the spring there must be taken four times as stiff as the "equivalent" spring (see page 50). Thus we find for the answer to question (*b*)

$$c_c = 0.164 \text{ lb./in./sec.}$$

a. The rate of decay is to be found from Eq. (24). First it is noted that the actual damping is one-sixteenth of critical, so that by Fig. 36 the difference between q and ω_n is negligible. The vibrations decrease as $e^{-\frac{c}{2m}t}$ and for a full cycle (two consecutive deviations to the same side)

$$t = T = \frac{1}{f} = \frac{2\pi}{q} \approx \frac{2\pi}{\omega_n} = \frac{2\pi}{124} = \frac{1}{20} \text{ sec.}$$

The damping constant c is that at the mass, which is four times smaller than that at the dashpot: $c = 0.01/4$. Thus the ratio between consecutive amplitudes is

$$\frac{x_{n+1}}{x_n} = e^{-\frac{c}{2m}t} = e^{-\frac{0.01 \times 16 \times 386}{4 \times 2 \times 20}} = e^{-0.386} = 0.68$$

Question (*c*) requires the calculation of the "relaxation time," which was defined only for a system without mass. Assuming the mass absent, the interaction of the spring and the dashpot alone gives a relaxation time

$$t_{\text{relax}} = \frac{c}{k} = \frac{0.164}{10} = 0.0164 \text{ sec.}$$

The mass in the system will cause the motion to slow down somewhat. For this case it is noted that the two roots, Eq. (20*a*), are equal, which makes the solution of the differential equation too difficult to be treated here. Readers familiar with this theory may calculate the relaxation time with the mass present and find the answer 0.017 sec., slightly larger than without the mass.

14. Forced Vibrations without Damping.—Another important particular case of Eq. (12) is the one where the damping term $c\dot{x}$ is made zero, while everything else is retained:

$$m\ddot{x} + kx = P_0 \sin \omega t \tag{27}$$

It is reasonable to suspect that a function $x = x_0 \sin \omega t$ may satisfy this equation. Indeed, on substitution of this function Eq. (27) becomes

$$-m\omega^2 x_0 \sin \omega t + kx_0 \sin \omega t = P_0 \sin \omega t$$

which can be divided throughout by $\sin \omega t$, so that

$$x_0(k - m\omega^2) = P_0$$

or

$$x_0 = \frac{P_0}{k - m\omega^2} = \frac{P_0/k}{1 - m\omega^2/k} = \frac{P_0/k}{1 - (\omega/\omega_n)^2}$$

and

$$x = \frac{P_0/k}{1 - (\omega/\omega_n)^2} \cdot \sin \omega t \tag{28}$$

is a solution of (27). The expression P_0/k in the numerator has a simple physical significance: it is the static deflection of the spring under the (constant) load P_0. We therefore write

$$\frac{P_0}{k} = x_{st}$$

and with this the solution becomes

$$\frac{x}{x_{st}} = \frac{1}{1 - (\omega/\omega_n)^2} \cdot \sin \omega t \tag{28a}$$

Although it is true that this is "a" solution of (27), it cannot be the most general solution, which must contain two integration constants. It can be easily verified, by substitution, that

$$x = C_1 \sin \omega_n t + C_2 \cos \omega_n t + \frac{x_{st}}{1 - (\omega/\omega_n)^2} \cdot \sin \omega t \qquad (29)$$

satisfies (27). The first two terms are the undamped *free* vibration; the third term is the undamped *forced* vibration. This is a manifestation of a general mathematical property of differential equations of this type, as stated in the following theorem:

Theorem: "The general solution (29) of the complete differential equation (27) is the sum of the general solution (14) of the equation with zero right-hand member (13), *and* a particular solution (28) of the complete equation (27)."

It is seen that the first two terms of (29) (the free vibration) form a sine wave having the free or natural frequency ω_n, whereas the forced vibration (the third term) is a wave having the forced frequency ω. Since we are at liberty to make ω what we please, it is clear that ω and ω_n are entirely independent of each other. The solution (29), being the sum of two sine waves of different frequencies, is itself *not* a harmonic motion (see Fig. 44*c*, page 71).

It is of interest now to examine more closely the implications of the result (28*a*). Evidently x/x_{st} is a sine wave with an amplitude $1/[1 - (\omega/\omega_n)^2]$, depending on the frequency ratio ω/ω_n. Figure 38 represents this relation.

From formula (28*a*) it follows immediately that for $\omega/\omega_n < 1$ the amplitudes or ordinates are positive, while for $\omega/\omega_n > 1$ they are negative. In order to understand the meaning of these negative amplitudes we return to Eq. (27) and the assumption $x_0 \sin \omega t$ for the solution made immediately thereafter. It appears that in the region $\omega/\omega_n > 1$ the results for x_0 are negative. But we can write

$$-x_0 \sin \omega t = +x_0 \sin (\omega t + 180 \text{ deg.})$$

which shows that a "negative amplitude" is equivalent to a positive amplitude of a wave which is merely 180 deg. out of phase with (in opposition to) the original wave. Physically this means that, while for $\omega/\omega_n < 1$ force and motion are in phase, they are in opposition for $\omega/\omega_n > 1$. Whereas for $\omega/\omega_n < 1$ the mass is below the equilibrium position when the force pushes downward, we find that for $\omega/\omega_n > 1$ the mass is above the equilibrium position while the force is pushing downward.

Usually this phase relation is considered as of slight interest, while the amplitude is vitally important; therefore, the negative sign may be disregarded and the dashed line in Fig. 38 appears.

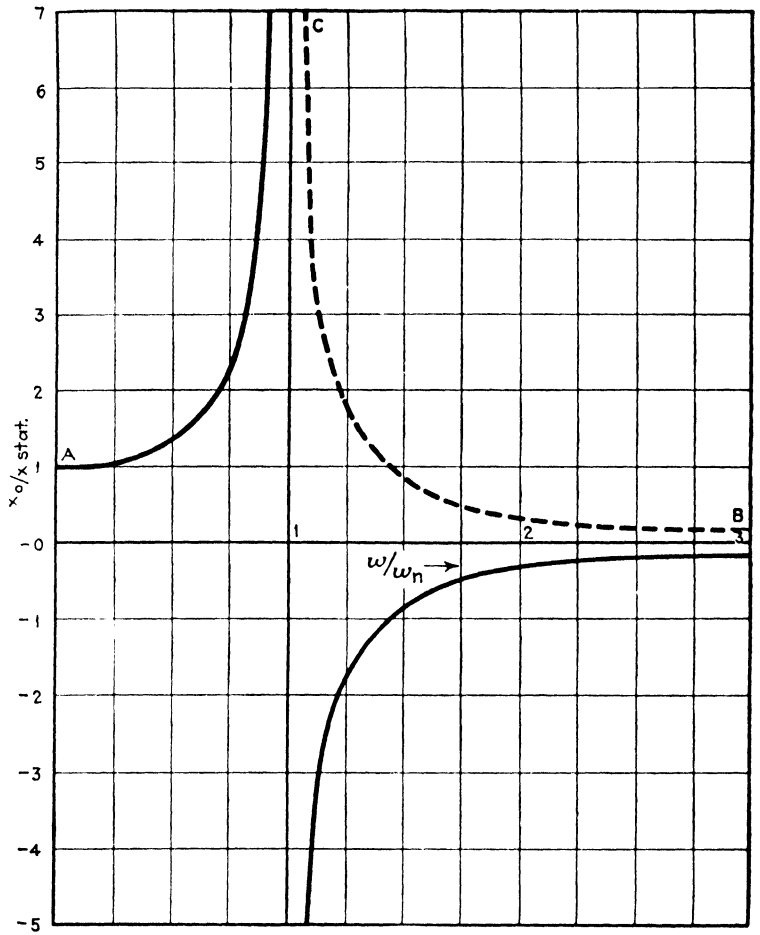


FIG. 38.—Resonance diagram for the absolute motion of a system of which the mass is subjected to a force of constant amplitude and variable frequency; Eq. (28). This diagram is different from Fig. 40.

There are three important points, A, B, and C in Fig. 38, at which it is possible to deduce the value of the ordinate from purely physical reasoning. First consider the point A, very close to $\omega = 0$; the forced frequency is extremely slow, and the mass will be deflected by the force to the amount of its static

deflection only. This is physically clear, and thus the amplitudes of the curve near the point A must be nearly equal to unity. On the other hand, for very high frequencies $\omega/\omega_n \gg 1$, the force moves up and down so fast that the mass simply has no time to follow, and the amplitude is very small (point B).

But the most interesting thing happens at point C, where the amplitude becomes infinitely large. This can also be understood physically. At $\omega/\omega_n = 1$, the forced frequency coincides exactly with the natural frequency. The force then can push the mass always at the right time in the right direction, and the amplitude can increase indefinitely. It is the case of a pendulum which is pushed slightly in the direction of its motion every time it swings: a comparatively small force can make the amplitude very large. This important phenomenon is known as "resonance," and the natural frequency is sometimes called also the "resonant frequency."

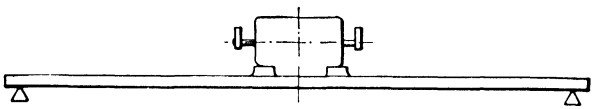


FIG. 39.—Unbalanced motor giving a force $m\omega^2 a_0$ leading to the resonance diagram of Fig. 40.

Thus far the theory has dealt with an impressed force of which the amplitude P_0 is *independent* of the frequency ω. Another technically important case is where P_0 is proportional to ω^2. For example, Fig. 39 represents a beam on two supports and carrying an unbalanced motor in the middle. While running, the motor axle experiences a rotating centrifugal force $m_1\omega^2 r$, where m_1 is the mass of the unbalance and r its distance from the center of the shaft. This rotating force can be resolved into a vertical component $m_1\omega^2 r \sin \omega t$ and a horizontal component $m_1\omega^2 r \cos \omega t$. Assume that the beam is very stiff against horizontal displacements but not so stiff against vertical ones. Then we have a single-degree-of-freedom system with a mass m (the motor), and a spring $k = 48EI/l^3$ (the beam), acted upon by a vertical disturbing force of amplitude $m_1\omega^2 r$, which is *dependent* on the frequency.

Another example of this type was discussed on page 43. There it was seen that the "relative motion" y between the mass and the support of Fig. 23 (where the support moves as $a_0 \sin \omega t$ and the force P_0 is absent) acts as if a force $ma_0\omega^2$ were acting

on the mass. Incidentally, this case is of great importance since most vibration-recording instruments (vibrographs) are built on this principle (see page 75).

The resonance curve for the two cases just mentioned can be found directly from Eq. (28) by substituting $m\omega^2 a_0$ for P_0. Then

$$y_0 = \frac{m\omega^2 a_0/k}{1 - (\omega/\omega_n)^2} = a_0 \frac{(\omega/\omega_n)^2}{1 - (\omega/\omega_n)^2}$$

or

$$\frac{y_0}{a_0} = \frac{(\omega/\omega_n)^2}{1 - (\omega/\omega_n)^2} \tag{30}$$

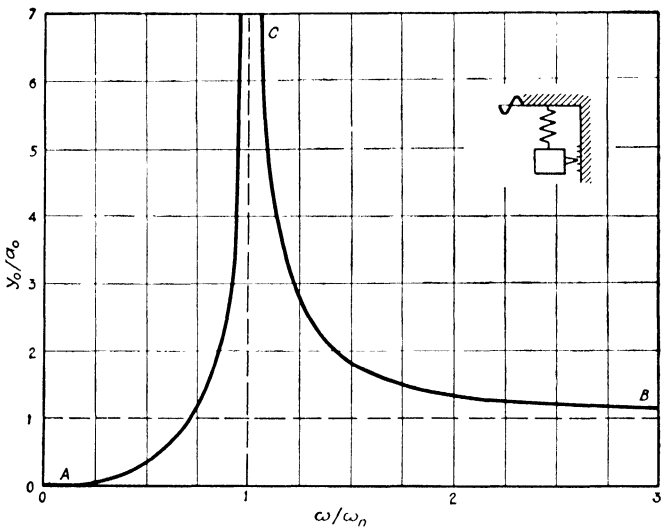


FIG. 40.—Resonance diagram of Eq. (30) showing (*a*) the relative motion of a system in which the end of the spring is subjected to an alternating motion of constant amplitude a_0, and (*b*) the absolute motion of a system in which the mass experiences a force of variable amplitude $m\omega^2 a_0$.

It is to be remembered that a_0 is the amplitude of motion at the top of the spring, while y_0 is the relative motion between the mass and the top of the spring, or the extension of the spring, which is the same thing. The ordinates of the three points *A*, *B*, and *C* of Fig. 40, representing (30), can again be understood physically. At *A* the frequency ω is nearly zero; the top of the spring is moved up and down at a very slow rate; the mass follows this motion and the spring does not extend: $y_0 = 0$. At *B* the motion of the top of the spring is very rapid, so that the mass cannot follow and stands still in space. Then the relative motion

is equal to the motion of the top and $y_0/a_0 = 1$. At the point C there is resonance, as before, so that the extensions of the spring become theoretically infinitely large.

This last result is obviously not in agreement with actual observations, and it is necessary therefore to consider damping, which is done in Sec. 15.

Example: A motor generator set consists of a 25-cycle induction motor coupled to a direct-current generator. The set is rated at 200 hp. and 725 r.p.m. The connecting shaft has a diameter of $3\frac{5}{16}$ in. and a length of 14 in. The moment of inertia of the motor rotor is 150 lb. in. sec.^{2} and that of the generator is 600 lb. in. sec.^{2}. The driving torque of the induction motor is not constant (see page 90) but varies between zero and twice the full-load torque T_0 at twice the frequency of the current, *i.e.*, 50 cycles per second, thus

$$T_0 + T_0 \sin (2\pi \cdot 50t)$$

while the counter torque of the direct-current generator is constant in time. Find the maximum stress in the shaft at full load.

Solution: First find the torsional spring constant of the shaft.

$$k = \frac{\text{torque}}{\text{angle}} = \frac{GI_p}{l} = \frac{G \cdot \frac{\pi}{32} d^4}{l} = \frac{12 \cdot 10^6 \frac{\pi}{32} (3\frac{5}{16})^4}{14} = 10.20 \times 10^6 \text{ in. lb./rad.}$$

The system is idealized in Fig. 26 (page 40) and its differential equation is (12c). The natural circular frequency is

$$\omega_n = \sqrt{\frac{k}{\frac{I_1 I_2}{I_1 + I_2}}} = \sqrt{\frac{10.2 \times 10^6 \times 750}{150 \times 600}} = 290 \text{ radians per second}$$

The forced frequency is 50 cycles per second, or

$$\omega = 2\pi f = 314 \text{ radians per second}$$

Apparently the system is excited at $\frac{314}{290} = 1.08$ times resonance, so that by Fig. 38 or Eq. (28) the effect of the torque is magnified by a factor

$$\frac{1}{1 - (1.08)^2} = 6.0$$

From Eq. (12c) we see that the torque in question is $\frac{600}{750} T_0$, or four-fifths of the amplitude of the alternating component of the torque. As stated, the torque consists of a steady part T_0 and an alternating part of the same amplitude T_0. The maximum torque in the shaft thus is

$$T_0 + 6.0 \times \tfrac{4}{5} T_0 = 5.80 T_0$$

The steady torque T_0 can be found from the speed and horse power thus:

$$T_0 = \frac{\text{hp.}}{\omega} = \frac{200 \times 33{,}000}{725 \times 2\pi} = 1{,}450 \text{ ft. lb.} = 17{,}400 \text{ in. lb.}$$

The shear stress in the shaft due to this steady torque is

$$S_s = \frac{T_0 r}{I_p} = \frac{T_0 d/2}{\pi d^4/32} = 5\frac{T_0}{d^3} = \frac{5 \times 17{,}400}{(3\frac{5}{16})^3} = 2{,}500 \text{ lb./in.}^2$$

On account of the proximity to resonance, this stress is multiplied by 5.80, so that the total maximum *shear* stress is 14,500 lb./in.^{2}. The "fatigue strength" of a steel, as listed, is derived from a tensile test, where the tensile stress is twice the shear stress. The fatigue limit of usual shaft steels is lower than 29,000 lb./in.^{2}, so that the shaft is expected to fail. The design can be improved by reducing the shaft diameter to $2\frac{1}{2}$ in. Then the natural frequency becomes 171 radians per second and the magnification factor 0.42. The new maximum tensile stress becomes 6,200 lb./in.^{2}, which is safe.

15. Forced Vibrations with Viscous Damping.—Finally, the complete Eq. (12),

$$m\ddot{x} + c\dot{x} + kx = P_0 \sin \omega t \tag{12}$$

will be considered. It can be verified that the theorem of page 58 holds here also. According to that theorem, the complete solution of (12) consists of the sum of the complete solution of the Eq. (18), which is (12) with the right-hand side zero, *and* a particular solution of the whole Eq. (12). But the solution of the equation with the zero right-hand side has already been obtained (Eq. 24), so that

$$x = e^{-\frac{c}{2m}t}(C_1 \sin qt + C_2 \cos qt) + \text{particular solution} \tag{31}$$

It is therefore necessary merely to find the particular solution. Analogous to the case of Sec. 14, we might assume $x = x_0 \sin \omega t$, but then the term $c\dot{x}$ would give $\cos \omega t$, so that this assumption is evidently incorrect. It is possible to assume

$$x = A \sin \omega t + B \cos \omega t$$

and to substitute this in (12). In this case, only terms with $\sin \omega t$ and $\cos \omega t$ occur, but there are *two* constants A and B at our disposal. By solving for A and B algebraically, a particular solution can be obtained. Here we shall derive the result in a somewhat different manner, in order to give a clearer physical understanding of the phenomenon.

Let it be assumed that the solution is a sine wave with the forced frequency ω. Then all the four forces of Eq. (12) are sine waves of this frequency and can be represented by vectors.

A differentiation is equivalent to a multiplication of the length of the vector with ω and a forward rotation through 90 deg., as explained on page 4.

Let the displacement be represented by $x = x_0 \sin(\omega t - \varphi)$, where x_0 and φ are as yet unknown, and draw this displacement as a vertical upward vector (dotted) in the diagram of Fig. 41. The spring force $-kx$ has an amplitude kx_0 and is directed downward in the diagram. The damping force $-c\dot{x}$ has an amplitude $c\omega x_0$ and is 90 deg. ahead of the spring force. The inertia force $-m\ddot{x}$ is 90 deg. ahead of the damping force and has an amplitude $m\omega^2 x_0$. The external force $P_0 \sin \omega t$ is φ deg. ahead of the displacement $x_0 \sin(\omega t - \varphi)$. Thus the complete diagram in Fig. 41 is obtained (x_0 and φ being unknown).

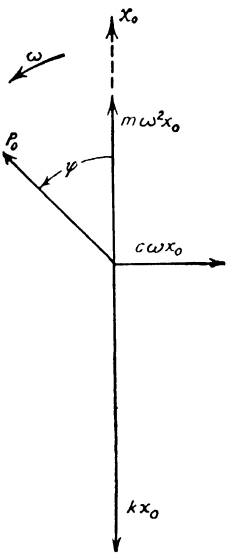


FIG. 41.—Vector diagram from which Fig. 42 can be deduced.

Newton's law [or Eq. (12), which is the same thing] requires that the sum of the four forces be zero at all times. This means that the geometric sum of the four vectors in Fig. 41 must be zero, which again implies that the horizontal as well as the vertical component of this resultant must be zero. Expressed mathematically:

$$\text{Vertical component: } kx_0 - m\omega^2 x_0 - P_0 \cos \varphi = 0$$
$$\text{Horizontal component: } c\omega x_0 - P_0 \sin \varphi = 0$$

From these two equations the unknowns x_0 and φ are solved, with the result that

$$x_0 = \frac{P_0}{\sqrt{(c\omega)^2 + (k - m\omega^2)^2}} = \frac{\frac{P_0}{k}}{\sqrt{\left(1 - \frac{\omega^2}{\omega_n^2}\right)^2 + \left(2\frac{c}{c_c} \cdot \frac{\omega}{\omega_n}\right)^2}} \tag{32a}$$

$$\tan \varphi = \frac{c\omega}{k - m\omega^2} = \frac{2\frac{c}{c_c} \cdot \frac{\omega}{\omega_n}}{1 - (\omega^2/\omega_n^2)}. \tag{32b}$$

With the aid of the mechanical-electrical glossary of page 40, this can be translated into

$$Q_0 = \frac{E_0}{\sqrt{(R\omega)^2 + \left(\frac{1}{C} - L\omega^2\right)^2}}$$

or

$$Q_0\omega = \frac{E_0}{\sqrt{R^2 + \left(L\omega - \frac{1}{\omega C}\right)^2}} \tag{33}$$

Since $i = dQ/dt$, and $Q = Q_0 \sin \omega t$, the current is $i = Q_0\omega \cos \omega t$. The left-hand side of Eq. (33) is the maximum value of the current. The square root in the denominator to the right is known as the "impedance," a familiar element in electrical engineering.

The expressions (32*a*, *b*) for the amplitude x_0 and for the phase angle φ are in terms of "dimensionless quantities" or ratios only. There appear the frequency ratio ω/ω_n and the damping ratio c/c_c, where c_c is the "critical damping" of formula (22). P_0/k can be interpreted as the deflection of the spring under a load P_0; it is sometimes called the "static deflection" x_{st}.

These relations are plotted in Figs. 42*a* and *b*. The amplitude diagram contains a family of curves, one for each value of the damping c. All curves lie below the one for zero damping, which is of course the same curve as that of Fig. 38. Thus we see that the amplitude of forced vibration is diminished by damping. Another interesting property of the figure is that the maxima of the various curves do not occur any longer at $\omega/\omega_n = 1$ but at a somewhat smaller frequency. In fact, in the case of damped vibrations *three* different frequencies have to be distinguished, all of which coincide for $c = 0$, *viz.*,

(1) $\omega_n = \sqrt{\frac{k}{m}}$ = the "undamped natural frequency"

(2) $q = \sqrt{\frac{k}{m} - \left(\frac{c}{2m}\right)^2}$ = the "damped natural frequency"

(3) The "frequency of maximum forced amplitude," sometimes referred to as the "resonant frequency."

For small values of the damping these three frequencies are very close together.

The phase-angle diagram 42*b* also is of considerable interest. For no damping, it was seen that below resonance the force and the displacement are in phase ($\varphi = 0$), while above resonance

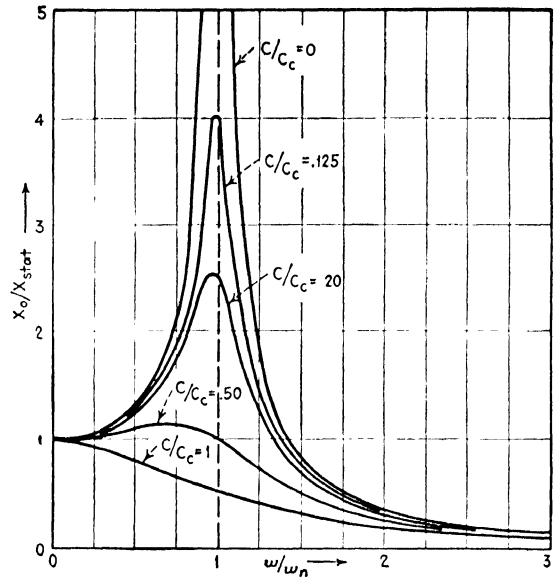


FIG. 42*a*.—Amplitudes of forced vibration of any of Figs. 23 to 27 for various degrees of damping.

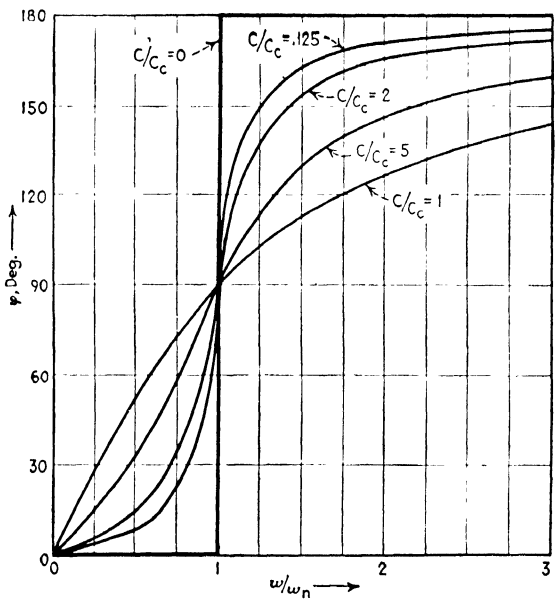


FIG. 42*b*.—The phase angle between force and displacement as a function of the frequency for various values of the damping.

they are 180 deg. out of phase. The phase-angle curve therefore shows a discontinuous jump at the resonance point. This can also be seen from Eq. (32*b*) by imagining the damping c very small. Below resonance, the denominator is positive so that $\tan \varphi$ is a very small positive number. Above resonance, $\tan \varphi$ is a very small negative number. Thus the angle φ itself is either close to 0 deg. or slightly smaller than 180 deg. Make the damping *equal* to zero, and φ becomes exactly 0 deg. or exactly 180 deg.

For dampings different from zero the other curves of Fig. 42*b* represent the phase angle. It is seen that in general the damping tends to smooth out the sharpness of the undamped diagrams for the amplitude as well as for the phase.

It is instructive to go back to the vector diagram of Fig. 41 and visualize how the amplitude and phase angle vary with the frequency. For very slow vibrations ($\omega \approx 0$) the damping and inertia forces are negligible and $P_0 = kx_0$, with $\varphi = 0$. With increasing frequency the damping vector grows, but the inertia force grows still faster. The phase angle cannot be zero any longer since P_0 must have a horizontal component to the left to balance $c\omega x_0$. The inertia-force vector will grow till it becomes as large as the spring force. Then φ must be 90 deg. and $P_0 = c\omega x_0$. This happens at resonance, because $m\omega^2 x_0 = kx_0$ or $\omega^2 = k/m$. Thus at resonance the phase angle is 90 deg., independent of damping. Above this frequency $m\omega^2 x_0$ will grow larger than kx_0, so that P_0 dips downward and φ is larger than 90 deg. For very high frequencies kx_0 is insignificant with respect to $m\omega^2 x_0$, so that P_0 is used up to balance the inertia force and $\varphi = 180$ deg.

At slow speeds the external force overcomes the spring force; at high speeds the external force overcomes inertia, while at resonance it balances the damping force.

The *energy relations* involved in this process also serve to give a better physical understanding. For *very slow* motions $\varphi = 0$, and it was shown on page 15 that no work is done over a whole cycle. In other words, no mechanical energy is transformed into heat during a cycle. Starting from the equilibrium position, the external force moves through a certain distance before reaching the extreme position. It certainly does work then. But that work is merely converted into potential or elastic energy stored in the spring. During the next quarter cycle the motion goes *against* the external force and the spring gives up its stored energy. At slow speeds, therefore, the work of the external

force is thrown into elastic energy and nothing is converted into heat. At the resonant frequency, $\varphi = 90$ deg. and the work dissipated per cycle is $\pi P_0 x_0$ (page 17). The external force is equal and opposite to the damping force in this case, so that the work is dissipated in damping. The spring force and the inertia force are equal and opposite, and also in phase with the displacement. Each of these forces *does* perform work during a quarter cycle, but stores the energy, which is returned during the next quarter cycle. The work of the spring force is stored periodically as elastic energy in the spring and the work of the inertia force as kinetic energy of motion of the mass.

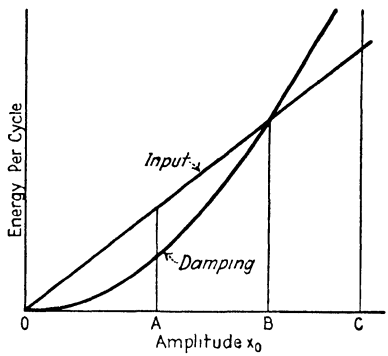


FIG. 43.—Work per cycle performed by a harmonic force and by a viscous damping force for various amplitudes.

Incidentally these energy relations can be used for calculating the "resonant amplitude." The damping force has the amplitude $c(\dot{x})_{\max} = c\omega x_0$ and is 90 deg. out of phase with the displacement x_0. Consequently the work dissipated in damping per cycle is $\pi c\omega x_0^2$. The work done per cycle by the external force is $\pi P_0 x_0$ which must equal the dissipation of damping:

$$\pi P_0 x_0 = \pi c\omega x_0^2 \tag{34}$$

This relation is illustrated by Fig. 43 in which the work per cycle done by the force P_0 at resonance and also that by the damping force are plotted against the amplitude of motion. Where the two curves intersect, we have energy equilibrium and *this* amplitude x_0 is the one that will establish itself. If at some instant the amplitude were greater, the energy dissipation would be greater than the input, which would gradually diminish the kinetic energy of the system until the equilibrium amplitude is reached.

Solving (34) for x_0, we obtain

$$(x_0)_{\text{resonance}} = \frac{P_0}{c\omega} \tag{34a}$$

Strictly speaking, this is the amplitude at the frequency where the phase angle is 90 deg., which is not exactly the frequency of

maximum amplitude. However, these two frequencies are so close together that a very good approximation of the maximum amplitude can be obtained by equating the work done by the external force to the work dissipated by damping. For the single-degree-of-freedom system this method of calculating the resonant amplitude is of no great interest, but later we shall consider more complicated cases where an exact calculation is too laborious and where the approximate method of Eq. (34) and Fig. 43 gives acceptable results (page 256).

Equations (32*a*) and (32*b*) are the most important ones of this book. They have been derived from the differential equation (12) in two ways: first by algebra and second by the vector diagram of Fig. 41. We shall now deduce them in a third manner, by means of the complex-number method (page 11).

This is done with two purposes in mind: not only will it serve to make the results better understood, but it will also be an introduction to more complicated cases (page 120), where the complex method affords a great saving in effort.

Each of the four vectors of Fig. 41 can be replaced by a complex number. If the displacement be denoted by the complex number x, the first derivative $\dot{x}$ can be written $j\omega x$ and the second derivative $\ddot{x} = -\omega^2 x$ as was shown earlier (page 13). Let the external-force vector, written as a complex number, be denoted by P'. Then (12) becomes

$$-m\omega^2 x + j\omega c x + kx = P'$$

or

$$(-m\omega^2 + j\omega c + k)x = P'$$

Solving for x by the rules of ordinary algebra,

$$x = \frac{P'}{-m\omega^2 + j\omega c + k}$$

In this expression P' is still a complex quantity. It can be made real by turning the complete diagram Fig. 41 clockwise through about 135 deg. (Fig. 41*a*). After this has been done, $P' = P_0$ is real and the expression for x can be brought to the form $a + jb$ as follows:

$$x = \frac{P_0}{(-m\omega^2 + k) + j\omega c} = P_0 \frac{1}{(-m\omega^2 + k) + j\omega c} \times \frac{(-m\omega^2 + k) - j\omega c}{(-m\omega^2 + k) - j\omega c}$$

$$= P_0 \frac{(-m\omega^2 + k) - j\omega c}{(-m\omega^2 + k)^2 - (j\omega c)^2} = \frac{P_0}{[(-m\omega^2 + k)^2 + \omega^2 c^2]} \cdot \{(-m\omega^2 + k) - j\omega c\}$$

This is a complex number, the real part of which represents the length OA in Fig. 41*a* and the (negative) imaginary part represents OB. It follows that

$$\tan \varphi = \frac{\text{imaginary part}}{\text{real part}} = \frac{\omega c}{k - m\omega^2} \qquad (32b)$$

and

$$x_0 = \text{length of vector} = \sqrt{(\text{real})^2 + (\text{imag.})^2}$$
$$= \frac{P_0}{[(-m\omega^2 + k)^2 + \omega^2 c^2]} \cdot \sqrt{(-m\omega^2 + k)^2 + \omega^2 c^2}$$
$$= \frac{P_0}{\sqrt{(-m\omega^2 + k)^2 + \omega^2 c^2}}, \qquad (32a)$$

the same results as obtained before (page 62).

Finally we return to the expression (31) on page 63 and remember that everything stated in the 7 previous pages pertains to the "particular solution" or "forced vibration" only. The general solution consists of the damped free vibration superposed on the forced vibration. After a short time the damped free vibration disappears and the forced vibration alone persists. Therefore, the forced vibration is also called the "sustained

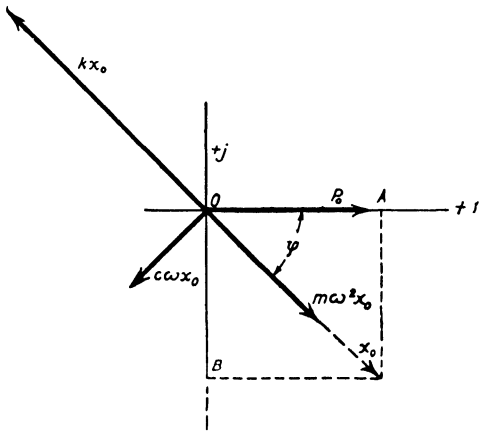


FIG. 41a.—The diagram of Fig. 41 turned around so as to make the disturbing force P_0 a real quantity.

vibration," while the free vibration is known as the "transient." The values of the constants C_1 and C_2 depend on the conditions at the start and can be calculated from these conditions by an analytical process similar to that performed on page 44. However, it is possible to construct the whole motion by physical reasoning only. As an example, consider the following problem:

A spring-suspended mass is acted on by an external harmonic force having a frequency eight times as slow as the natural frequency of the system. The mass is held tight with a clamp, while the external force is acting. Suddenly the clamp is removed. What is the ensuing motion if the damping in the system is such that the free vibration decreases by 10 per cent for each cycle?

In solving this problem, it is first to be noted that its statement is ambiguous, since it was not mentioned at what instant during the force cycle the mass was released. To make the

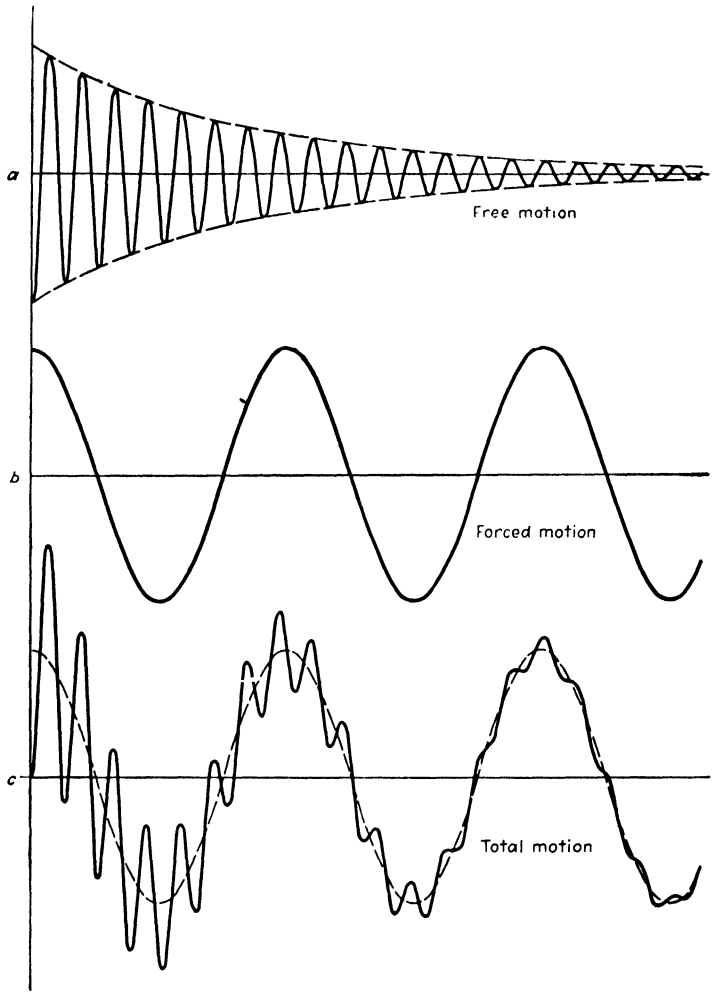


FIG. 44.—Starting transient.

problem definite, assume the release to occur at the moment that the forced vibration would just have its maximum amplitude. From the initial conditions of the problem it follows that at the instant of release the mass has no deflection and no velocity. We have prescribed the *forced* vibration to start with

$x = x_0$ and $\dot{x} = 0$. These two conditions can be satisfied only by starting a *free* vibration with $x = -x_0$ and $\dot{x} = 0$. Then the *combined* or *total* motion will start at zero with zero velocity. Figure 44*a* shows the free vibration, 44*b* the forced vibration, and 44*c* the combined motion.

It is seen that the transient disappears quickly and that the maximum amplitude at the start is nearly twice as great as the sustained final amplitude. If the difference between the free and forced frequencies is small and if the damping is also small, the diagram shows "beats" between the two frequencies (see page 7). Because of damping such beats will disappear after some time. In order to have sustained beats it is necessary to have two sustained or forced vibrations.

Example: An automobile has a body weighing 3,000 lb. mounted on four equal springs which sag 9 in. under the weight of the body. Each one of the four shock absorbers has a damping coefficient of 7 lb. for a velocity of 1 in. per second. The car is placed with all four wheels on a test platform which is moved up and down at resonant speed with an amplitude of 1 in. Find the amplitude of the car body on its springs, assuming the center of gravity to be in the center of the wheel base.

Solution: From Eq. (17*a*) the natural frequency is

$$\omega_n = 2\pi f_n = \sqrt{386/\delta_{st}} = \sqrt{386/9} = 6.6 \text{ radians per second}$$

The damping of the system (four shock absorbers) is

$$c = 4 \times 7 = 28 \text{ lb./in./sec.}$$

The differential equation governing the motion is (12*d*) of page 43. At resonance the disturbing force is

$$\sqrt{(ka_0)^2 + (ca_0\omega)^2}$$

Here $k = \dfrac{3{,}000 \text{ lb.}}{9 \text{ in.}} = 333$ lb./in.; $a_0 = 1$ in.; $c = 28$ lb./in./sec., and $\omega = \omega_n = 6.6$ radians per second.

$$\sqrt{(ka_0)^2 + (ca_0\omega)^2} = \sqrt{(333)^2 + (185)^2} = 380 \text{ lb.}$$

From Eq. (34*a*) the amplitude of the car body is found:

$$x_0 = \frac{P_0}{c\omega} = \frac{380}{28 \times 6.6} = 2.06 \text{ in.}$$

16. Frequency-measuring Instruments.—Figure 40 is the key to the understanding of most vibration-measuring instruments. A vibration is sometimes a wave of rather complicated shape. When this wave has been traced on paper, everything regarding the vibration is known, but in many cases such complete knowl-

edge is not necessary. We may want to know only the frequency or the amplitude of the motion or its acceleration. For such partial requirements, instruments can be made very much simpler and cheaper than if a record of the complete wave shape were demanded.

First, consider the methods of measuring *frequency* only. In many cases the vibration is fairly pure, *i.e.*, the fundamental harmonic has a much greater amplitude than any of the higher harmonics. In such cases a measurement of the frequency is usually easily made, and the result may give a hint of the cause of the vibration. Frequency meters are based nearly always on the resonance principle. For frequencies below about 100 cycles per second, *reed tachometers* are useful. There are two types of these: with a single reed and with a great many reeds.

The *single-reed frequency meter* consists of a cantilever strip of spring steel held in a clamp at one end, the other end being free. The length of the free portion of the strip can be adjusted by turning a knob, operating a screw mechanism in the clamp. Thus the natural frequency of the strip can be adjusted at will, and for each length the natural frequency in cycles per second is marked on the reed (see Fig. 120*a* on page 192). In use, the clamped end is pressed firmly against the vibrating object, so that the base of the reed partakes of the vibration to be measured. The screw is then turned slowly, varying the free length of the reed, until at one particular length it is in resonance with the impressed vibration and shows a large amplitude at the free end. The frequency is then read. Such an instrument is made and marketed by the Westinghouse Corporation. (Type JC-1 Vibrometer.)

Example: A variable-length, single-reed frequency meter consists of a strip of spring steel of cross section 0.200 by 0.020 in. and carries a weight of ¼ oz. at its end. What should be the maximum free length of the cantilever if the instrument is to be designed for measuring frequencies from 6 cycles per second to 60 cycles per second?

Solution: The spring constant of a cantilever beam is $3EI/l^3$. The moment of inertia of the cross section is $I = \frac{1}{12}bh^3 = \frac{1}{12} \times 0.2 \times (0.02)^3 = \frac{2}{3} \cdot 10^{-7}$ in.^{4}. The bending stiffness EI thus is $30 \cdot 10^6 \times \frac{2}{3} \cdot 10^{-7} = 4$ lb. in.^{2}, and the spring constant $k = 12/l^3$. The mass at the end is $m = 1/(4 \times 16 \times 386) = 4.05 \cdot 10^{-5}$ lb. in.$^{-1}$ sec.^{2} The mass per inch of strip is $\mu_1 = 0.004 \times 0.28/386 = 0.29 \cdot 10^{-5}$ lb. in.$^{-2}$ sec.^{2} Since about one-quarter of the strip length is effective as mass (see page 188), we have in total

$$m + \frac{\mu_1 l}{4} = (4.05 + 0.07l)10^{-5}$$

The frequency of maximum length is 6 cycles per second, or $\omega^2 = (2\pi \cdot 6)^2 = 1{,}420$ rad.^{2}/sec.^{2}

Applying Eq. (16),

$$1{,}420 = \frac{12 \cdot 10^5}{l^3(4.05 + 0.07l)}$$

or

$$l^3(1 + 0.017l) = 206$$

This equation can be solved by trial and error. Since the second term in the parentheses (due to the mass of the strip) is small with respect to the first term (due to the ¼-oz. mass), we neglect the second term as a first guess.

$$l^3 = 206 \quad \text{or} \quad l = 5.9$$

With this, the parentheses becomes $1 + 5.9 \times 0.017 = 1.10$, so that

$$l^3 = \frac{206}{1.10} = 187 \text{ in.}^3$$

and

$$l = 5.72 \text{ in.},$$

which is sufficiently accurate.

The other type of frequency meter employs a great number of reeds and is known as *Frahm's* tachometer. It consists of a

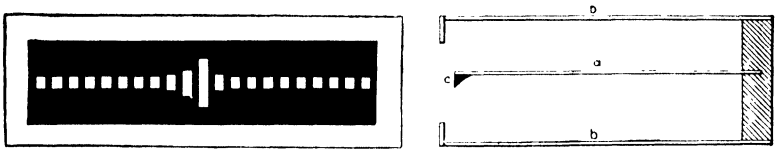


FIG. 45.—Frahm's tachometer.

light box *b* containing many small cantilever spring-steel strips *a* placed in one or more rows. Each reed has a slightly higher natural frequency than its left-hand neighbor, so that a whole range of natural frequencies is covered. In use, the box is placed on the vibrating machine with the result that most of the reeds hardly move at all. However, one or two of them for which the natural frequency is very close to that of the impressed vibration will swing with considerable amplitude. This is made clearly visible by painting the inside of the box dull black and giving white tips *c* to the free ends of the reeds (Fig. 45). Tachometers of this type are widely used.

The same instrument is also used for indicating the frequency of an alternating electric current. The mechanical excitation of an impressed force is replaced by an electric excitation. To this end one or more coils are placed

in the box under the reeds. The current flowing through these coils produces an alternating magnetic force on the reeds.

17. Seismic Instruments.—For measurement of the *amplitude* of the vibration a "seismic" instrument is ordinarily used, consisting of a mass mounted on springs inside a box. The box is then placed on the vibrating machine, and the amplitude of the relative motion between the box and the mass follows the diagram of Fig. 40 for the various frequencies of the motion to be recorded. It is seen that, when the disturbing frequency is large with respect to the natural frequency of the instrument, the recorded amplitude y_0 is practically the same as that of the motion a_0. Thus *to get a displacement-measuring device or "vibrometer" it is necessary to give the instrument a natural frequency at least twice as slow as the slowest vibration to be recorded.* In case the motion is impure, *e.g.*, contains higher harmonics, this does not present any difficulty, since any higher harmonic has a higher frequency than the fundamental and will be recorded still more precisely.

A seismic mass on springs is capable of recording *accelerations* also. If the motion be $a_0 \sin \omega t$, the corresponding acceleration is $-a_0\omega^2 \sin \omega t$, with the amplitude $a_0\omega^2$. Now, the left-hand branch of Fig. 40 (from $\omega/\omega_n = 0$ to $\omega/\omega_n = \frac{1}{2}$) has practically this $a_0\omega^2$ characteristic. The equation of Fig. 40 is (page 61)

$$\frac{y_0}{a_0} = \frac{\left(\frac{\omega}{\omega_n}\right)^2}{1 - \left(\frac{\omega}{\omega_n}\right)^2} \tag{30}$$

For small values of ω/ω_n, the denominator differs only slightly from unity, so that the equation becomes approximately

$$\frac{y_0}{a_0} = \left(\frac{\omega}{\omega_n}\right)^2 \qquad \text{or} \qquad y_0 = \frac{1}{\omega_n^2} \cdot a_0\omega^2$$

Here $1/\omega_n^2$ is a constant of the instrument, independent of the frequency of the external vibration. Hence the extreme left-hand part of Fig. 40 actually represents the accelerations at various frequencies.

An accelerometer is a seismic instrument with a natural frequency at least twice as high as the highest frequency of the accelerations to be recorded. This statement carries the possibility of a real difficulty, because an impure motion contains harmonics of frequen-

cies higher than the fundamental and it may well be that one of these frequencies is very close to the natural frequency of the instrument. This trouble is peculiar to the accelerometer. A vibrometer is free from it since the harmonics in a wave are always *higher* in frequency than the main or fundamental wave, so that there is danger of resonance only when the recorded main frequency is *lower* than the natural frequency of the instrument. In order to avoid this particular difficulty, it is necessary to introduce damping in the accelerometer. Besides the original curve of Fig. 40 (for $c/c_c = 0$) and the desired parabola of acceleration,

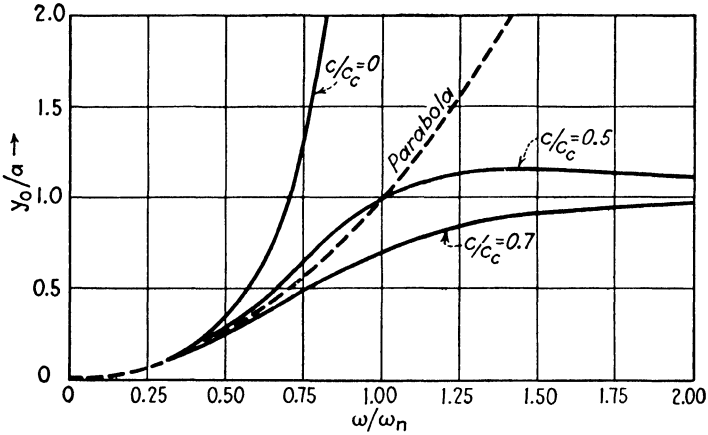


FIG. 46.—Resonance curves with various amounts of damping compared with the parabolic curve of an ideal accelerometer.

Fig. 46 shows two other curves, namely those for 0.5 and for 0.7 critical damping. Both these lie even closer to the desired parabola than does the undamped characteristic. Moreover, no resonance is to be feared. An accelerometer, therefore, with damping between half and 0.7 critical value will record accelerations up to three-quarters of the instrument frequency without appreciable error, while higher harmonics in the acceleration are diminished or, if their frequency is sufficiently high, they are practically suppressed.

The calculation of the curves of Fig. 46 is as follows: The differential equation (12*e*), page 41, applies. Its solution [Eq. (32*a*), page 62] can be used immediately, after replacing P_0 by $m\omega^2 a_0$. Thus

$$\frac{y_0}{a_0} = \frac{\omega^2/\omega_n^2}{\sqrt{\left(1 - \frac{\omega^2}{\omega_n^2}\right)^2 + \left(2\frac{c}{c_c}\frac{\omega}{\omega_n}\right)^2}}$$

is the equation of Fig. 46. The reader would do well to check the formula with the figure for a few points.

The phase-angle formula (32*b*) and the corresponding figure 42*b* can be applied to this case without any change at all. It is interesting to note that for a damping between 0.5 and 0.7 critical the phase characteristic Fig. 42*b* differs but slightly from a straight diagonal line in the region below resonance. This has the advantage of avoiding an error known as "phase distortion." For each harmonic of an impure wave the damped instrument shows a different phase angle between the actual wave and its record. If this angle is proportional to the frequency, all the recorded waves form the same combined pattern as the actual waves.

Historically, the oldest seismic instruments are the *seismographs* for the recording of earthquake vibrations. The elastically suspended mass in these devices is sometimes very large, weighing a ton or more. The natural frequency is very low, of the order of a single vibration per 10 sec.

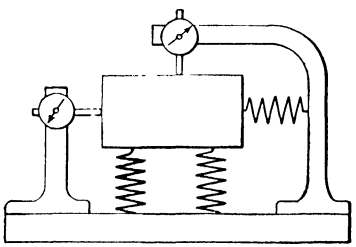


FIG. 47.—Vibrometer for horizontal and vertical motions.

For *technical* applications a great variety of portable instruments are on the market, weighing from about 20 lb. for general use to a few ounces for airplane work. The main difference among the various instruments lies in the manner of recording. In the most simple ones a dial gage is attached to the frame of the instrument and rests with its foot on the seismic mass. Figure 47 shows such an arrangement with one gage for horizontal and one for vertical vibrations. The vibratory motion is usually so rapid that the pointer of the gage is seen as two pointers with a blurred region between them; twice the amplitude of the vibration is then the distance between the two positions of the pointer. A very simple and light instrument of this type is made by the American Instrument Company, Silver Spring, Md., under the name of "Cordero Vibrometer."

In a variation of this scheme the dial gage is replaced by a tiny mirror which is given a rocking motion by the vibration. The light of a small automobile headlight passes through a slit and is then reflected from the rocking mirror on a strip of ground glass. With the mirror standing still the image is a line, which broadens into a band due to the vibration. All instruments of these types, where no permanent record is made, are called *vibrometers*. The more elaborate *vibrographs* contain a recording mechanism, which usually is larger than the seismic part of the instrument. Some

have a pen recording on a band of paper, which is moved by clockwork; some scratch the record on celluloid or glass, which is examined subsequently under the microscope, and some throw a light beam on a moving photographic film. Vibrographs sometimes are built without special damping devices. These devices *do* appear in accelerometers, sometimes as dashpots with either air or oil, but usually in the form of magnetic damping, where the seismic mass carries a tongue or thin copper plate moving parallel to its own plane in the narrow slit between the two poles of a powerful electromagnet. The motion of the tongue induces eddy currents in itself, and these currents develop a damping force proportional to the velocity.

Example: The vibrograph is sometimes used without the seismic part at all, *i.e.*, as a mere recording device. In that case the instrument is mounted in a place free from vibration, for example it is placed on a mass which is suspended from a crane in the factory. The only connection with the vibrating object is a needle which is pressed against the object with a spring; the other end of the needle operates the recording mechanism. Find the spring pressure on the needle which is necessary to hold it down on an object vibrating as $a_0 \sin \omega t$. The mass of the needle and the connected moving parts of the recording device is m.

Solution: If there were no spring at all, the vibrating object would lose contact with the needle point as soon as the object would have a receding acceleration. If there is no contact, the acceleration of the needle toward the object is P/m, where P is the spring pressure. This acceleration must be at least equal to the maximum receding acceleration of the vibrating object, so that

$$\frac{P}{m} = a_0\omega^2$$

or

$$P = ma_0\omega^2$$

For recording *torsional* vibrations, a seismic instrument is used which is a modification of a vibrograph. Instead of a mass on linear springs the *torsiograph* contains a flywheel on torsional springs. A very light aluminum pulley a (Fig. 48) is keyed to the shaft b. The heavy flywheel c can turn freely on the shaft but is coupled to it by a soft torsional spring d. When the pulley is held, the flywheel can perform free torsional vibrations about the shaft with a low natural frequency. When an alternating angular motion is given to the pulley, the relative motion between flywheel and pulley is again governed by the diagram of Fig. 40 (on account of the equivalence of the Figs. 23 and 24). Torsiographs of this type are widely used for measuring the torsional

vibrations of crank shafts of slow- and medium-speed internal-combustion engines. Besides the vibration to be measured, such a shaft has also a uniform rotation. In use, the pulley *a* is driven from the crank shaft by means of a small canvas belt. When the crank shaft rotates uniformly, the flywheel follows and no relative motion between *a* and *c* occurs. When the shaft rotates non-uniformly (*i.e.*, has a torsional vibration superimposed on its rotation), the light pulley *a* will follow the shaft motion faithfully. The flywheel *c*, however, has so much inertia that it can rotate only at uniform speed. Thus the vibration appears as a relative motion between *a* and *c*, which is transmitted through a system of small bell cranks and a thin rod located along the center line of the hollow shaft *b*. The rod

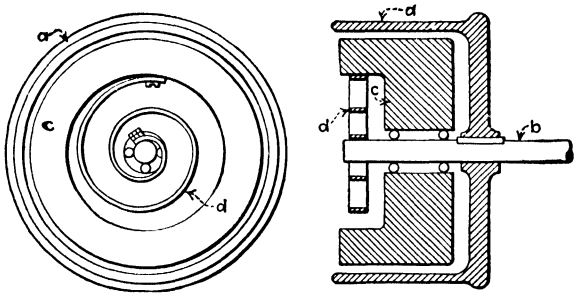


FIG. 48.—Seismic part of a torsiograph.

in turn operates a pen which scribes the record on a strip of paper, moved under the pen by clockwork. This instrument, known as the *Geiger* vibro- and torsiograph dating back to 1916, is marketed by the Commercial Engineering Laboratories, Detroit, Mich. It is still suitable for slow-speed machines, such as ship drives. However, for modern high-speed Diesel engines the recording-pen system comes to local resonance and, moreover, the magnification of the record obtainable (up to 24) is not sufficient. Then the *Summers* mechanical torsiograph, made by the General Motors Research Laboratories, Detroit, Mich., can be used to advantage. It is good up to 10,000 cycles per minute and gives a record in the form of a polar diagram.

Example: Let the flywheel *c* of the torsiograph of Fig. 48 be represented approximately by a solid steel disk of 4½ in. diameter and 2 in. thickness. The outside diameter of the pulley is 5 in. If the flywheel *c* is held clamped, a string is wrapped round the pulley, and a ¾-lb. weight is suspended from

one end of the string, the pulley circumference turns ½ in. (*i.e.*, the weight descends ½ in.).

If, with this instrument, a record is taken of a torsional vibration of 3 cycles per second, what is the error in the reading? What is the error in the recorded amplitude of the third harmonic of this curve?

Solution: First we have to find the natural frequency of the instrument. The torsional stiffness k in inch pounds per radian follows from the fact that a torque of ¾ lb. × 2½ in. causes an angular deflection of $\frac{\frac{1}{2}\text{ in.}}{2\frac{1}{2}\text{ in.}} \times 1$ radian. Thus

$$k = \frac{\frac{3}{4} \times 2\frac{1}{2}}{\frac{1}{5}} = 9.37 \text{ in.-lb./rad.}$$

The weight of the flywheel is

$$\frac{\pi}{4} \cdot \left(4\frac{1}{2}\right)^2 \times 2 \times 0.28 \text{ lb.} = 8.9 \text{ lb.}$$

Its moment of inertia is

$$I = \frac{1}{2}mr^2 = \frac{1}{2} \cdot \frac{8.9}{386}\left(2\frac{1}{4}\right)^2 = 0.059 \text{ lb. in sec.}^2$$

The natural frequency thus is

$$\omega_n = \sqrt{\frac{k}{I}} = \sqrt{\frac{9.37}{0.059}} = \sqrt{159} = 12.6 \text{ radians per second}$$

$$f_n = \frac{\omega_n}{2\pi} = \frac{12.6}{2\pi} = 2.0 \text{ cycles per second}$$

The frequency to be recorded is 50 per cent higher. Thus by Eq. (30) the ratio of the recorded to the actual amplitudes is

$$\frac{(1.5)^2}{1 - (1.5)^2} = \frac{2.25}{1.25} = 1.80$$

The third harmonic is 4½ times as fast as the natural vibration of the instrument, so that its magnification factor is

$$\frac{(4\frac{1}{2})^2}{1 - (4\frac{1}{2})^2} = \frac{20.25}{19.25} = 1.05$$

18. Electrical Measuring Instruments.—The rapid development in radio technique during the last decade has made possible a number of instruments that are generally much smaller and more sensitive than the older mechanical types discussed in the previous section. Most of these electrical "pickups" are still *seismic* instruments, for either linear or torsional vibrations, which operate on the same principle as the devices described in the previous section but have electrical windings in them that convert the mechanical vibration into an electrical voltage which

can then be amplified and recorded by means of an oscillograph. Figure 49*a* shows schematically a pickup for linear vibrations, developed by Draper and Bentley, made and marketed under the name "Sperry-M.I.T." by the Sperry Gyroscope Company, Brooklyn, N.Y. and by the Consolidated Engineering Corporation, Pasadena, Calif. The electrical apparatus inside this unit, which has over-all dimensions of about 1 in. and a weight not exceeding 2 oz., is practically the same as that found in a dynamic type of radio loud-speaker. The instrument is a body of revolution which can be conceived of as generated by a rotation about its vertical center line. The part *a* is a piece of steel which is seismically supported on springs *c*. An important item, not

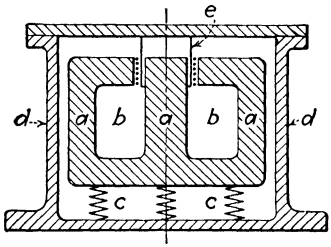


FIG. 49*a*.—Seismo-electric pickup, being essentially a loud-speaker element.

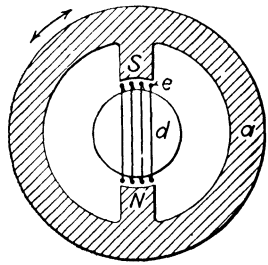


FIG. 49*b*.—Torsiograph-seismo-electric pickup.

shown in the figure, is the guiding of the mass *a*, the motion of which is restricted to the vertical direction entirely. No lateral motion of *a* can be allowed. In the hollow interior of *a*, a coil *b* is mounted around the central cylindrical core. This coil is energized by direct current so as to make a magnet out of *a*. Sometimes, for simplicity, the coil *b* is omitted and the part *a* is fashioned as a permanent magnet of some special alloy steel. The magnet *a*, being a body of revolution, has a ring-shaped air gap with a radial magnetic field, into which is inserted a thin paper cylinder *e* carrying a coil around it of extremely thin wire. The paper cylinder *e* is attached to the cover of the housing *d* and the entire apparatus is supposed to be attached to the machine of which the vibration is to be measured. Any motion of the magnet *a* in a vertical direction will cause a relative motion between the magnet and the "voice coil" *e* and will set up an electrical alternating voltage in *e*. This voltage, which is proportional to the *velocity* of relative motion, is now fed into

an amplifier and after sufficient magnification is recorded on an oscillograph film. Oscillographs suitable for this work have been developed in the last decade primarily in connection with applications of oil prospecting and are now readily available on the market.

A torsiograph pickup of a similar type is illustrated in Fig. 49*b* where *a* is the torsionally seismic element comparable to the part *c* in Fig. 48. This seismic element is made to be a permanent magnet with a north and a south pole as indicated. It can revolve freely on a soft torsional spring around the core *d* which is rigidly attached to the shaft of which the torsional vibration is to be measured. The core *d* carries a voice coil *e*. The magnetic field travels from the north pole to the south pole across

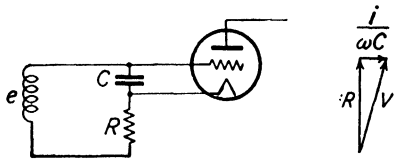


FIG. 49*c*.—Integrating circuit to transform a velocity record into an amplitude record.

the core *d* and any relative torsional motion between *a* and *d* will cause voltage variations in the voice coil *e*, the intensity of which is proportional to the angular *velocity* of the relative motion.

The records obtained on the oscillograph from either of these two instruments therefore indicate velocity rather than amplitude. This in itself is no particular disadvantage, but for certain applications it is more convenient to have a direct record of the amplitude instead of performing the necessary integration numerically or graphically on the record. This can be done electrically by means of the so-called "integrating circuit" illustrated in Fig. 49*c*. In this figure, *e* is again the "voice coil," carrying a voltage proportional to the velocity. This voltage is fed into a *C*-*R*-series circuit so proportioned that the voltage across the resistance is many times, say ten times, greater than the voltage across the condenser. The voltage across the resistance is iR and the voltage across the condenser is $\frac{1}{C}\int i\,dt$, and if the first voltage is very much greater than the second, it is permissible to say that the voltage iR is practically equal to the total voltage V of the voice coil. Since, therefore, V is directly

proportional to i (or to the velocity), the voltage across the condenser is directly proportional to $\int i\,dt$ (or to the integral of the velocity) which is exactly the quantity we are looking for. These relations are illustrated for harmonic variations in the vector diagram of Fig. 49*c*. The integrated voltage is then put on the grid of the first tube of the amplifier. Since the voltage across the condenser is about one-tenth part of the total voltage, the sensitivity of the scheme is cut down by a factor 10, which means that an additional stage of amplification is necessary.

Amplifiers of a sensitivity independent of the frequency can be easily built for frequencies higher than 10 cycles per second and

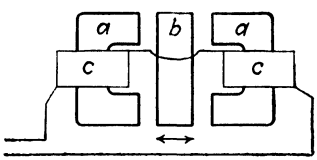


FIG. 49*d*.—Instrument operating on the principle of variation of reluctance, employing a carrier current of a frequency substantially higher than that of the vibration to be measured.

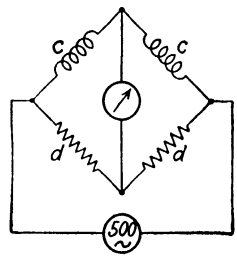


FIG. 49*e*.—Wheatstone-bridge circuit for the instrument of Fig. 49*d*.

recently have been made even down to ¾ cycle per second, and up to 8,000 cycles per second, thus covering the entire practical frequency range for mechanical work.

For vibrations of very slow frequency another electrical principle known as the "variation of reluctance" has been employed, which is illustrated in Figs. 49*d*, *e*, and *f*. In Fig. 49*d*, the two pieces *a* are rigidly attached to each other and they carry coils *c* which are energized by a constant voltage of a frequency that is high with respect to the frequencies that are to be measured. Usually, ordinary 60-cycle current will suffice for vibrations slower than 15 cycles per second; however, if vibrations considerably faster than this are to be recorded, a special alternator of say 500 cycles per second is used to energize the coils *c*. The voltage of the alternator is fed through the two coils *c* in series. A core *b*, made of laminated steel sheets like the U-pieces *a*, is mounted between these U-pieces so that the air gaps between them are as narrow as practicable. The central piece *b* vibrates

back and forth between the two pieces *a*, thus varying the air gaps with the frequency of the vibration. If the two air gaps on the two sides of *b* are exactly alike, the voltage of the alternator is equally divided between the coils *c*; but if the air gaps of one of the pieces *a* are wider than those of the other piece *a*, then the voltages of the two coils *c* differ. The instrument is connected in a Wheatstone-bridge circuit as shown in Fig. 49*e* in which the coils are balanced by two equal impedances *d*. For equal air gaps and consequently equal voltages across *c*, the instrument in the Wheatstone bridge will show a zero reading, and the reading of that instrument will be proportional to the difference between the two air gaps. Naturally, the meter is

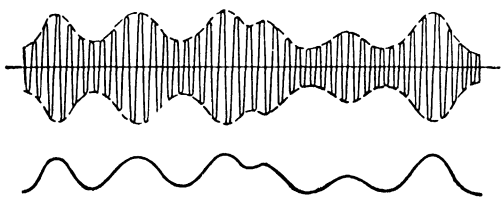


FIG. 49*f*.—Record obtained from the Wheatstone bridge.

affected by a current of a frequency equal to that of the exciting source; and if the instrument is replaced by an oscillograph, a record such as the upper one in Fig. 49*f* results. The fast variations in this record are those of the exciting alternator and the slow variation of the envelope is the effect we are looking for. For greater ease of reading, sometimes an electrical rectifier is inserted in the instrument branch of a Wheatstone bridge which transforms the upper record of Fig. 49*f* into the lower one. The apparatus of Fig. 49*d* can be used as a seismic instrument where the two pieces *a* are mounted seismically, whereas *b* is directly attached to the object to be measured. It has also been used as a strain meter where the two pieces *a* are attached to one part of the structure to be measured, while the central piece *b* is attached to some other part of that structure.

The device under the name "Siemens-McNab Electric Torsion Meter" has been used for measuring the horse power of ships' shafts while under way. The part *a* of Fig. 49*d* is attached to a sleeve clamped on one section of the propeller shaft. The part *b* is attached to another sleeve, clamped to a section of the shaft some 3 ft. away from the first. If this length of 3 ft. of shafting twists with the strain, the parts *b* and *a* change position relative

to each other, while rotating with the shaft. Turning to Fig. 49*e*, the parts *c*, *c* rotate with the shaft, and the current is supplied the shaft through three slip rings. But the non-rotating instrument contains not just dead resistances *d*, but again a complete set-up like Fig. 49*d*. The relative position of the (non-rotating) pieces *b* and *a* is varied with an accurate micrometer screw until the ammeter reads zero. Then the rotating and non-rotating air gaps must be alike; their position, and hence the shaft torque, is read off the non-rotating micrometer screw.

A device which has become very important in recent years is the resistance-strain-sensitive wire gage, first used by Simmons and Datwyler, further developed by Ruge and De Forest, marketed under the trade name "SR-4 gage" by the Baldwin Locomotive Works, Philadelphia, Pa., and now in universal use, particularly in the aircraft industry. The gage is made of very thin (0.001 in.) wire of high electric resistance (nichrome) arranged as shown in Fig. 49*g* and mounted between two thin sheets of paper. The total length is about an inch; the total electric resistance is about 500 ohms. The gage is glued to the metal object under test, and if the metal (and consequently the nichrome wire) is strained, its electric resistance changes. The strain-sensitivity factor, which is the percentage change in resistance divided by the percentage change in length, is about 3. This means that for a stress of 30,000 lb./in.^{2} in steel, where the strain is 0.001, the resistance changes by 0.003, so that in a gage of 500 ohms resistance the change in resistance is 1.5 ohms. Figure 49*h* shows how the gage may be connected in a circuit. The battery voltage is divided between the gage *a* and a steady resistance *b*. If the strain and hence the resistance of *a* varies with time, so will the voltage across its terminals, and this varying voltage is put on the grid of the first vacuum tube in an amplifier, and from there passed on to an oscillograph.

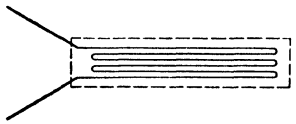


FIG. 49*g*.—Wire-strain gage.

Figure 49*i* shows the adaptation of this method to the measurement of twist in a shaft. It is well known that in a shaft in torsion the maximum strains have directions of 45 deg. with respect to the longitudinal axis of the shaft. Therefore, if two strain gages are glued on as shown, and the shaft is twisted, one of the gages will be elongated and the other one will be shortened. The voltage of the direct-current battery, therefore, will be

unequally divided between the two strain gages and the variations in voltage will follow the strain and consequently the torque in the shaft.

The particular advantage of the strain gages just described lies in their extreme lightness. For the measurement of stresses in airplane propellers or turbine blades, where the centrifugal field is as high as 9,000 g, only a pickup of practically no weight is at all feasible. The introduction of electric-resistance-strain gages has made possible for the first time the reliable measurement of vibrational phenomena in airplane propellers.

For variations of very slow frequency, the ordinary amplifier does not work, and the gages are energized by a high-frequency current, much as in Fig. 49*e*. The Foxboro Company, Foxboro, Mass., is marketing an instrument under the trade name "Dyna-

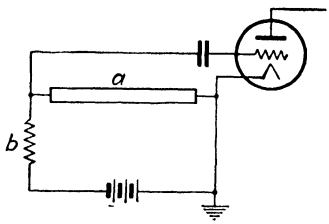


FIG. 49*h*.—Circuit for electric-resistance-strain gage.

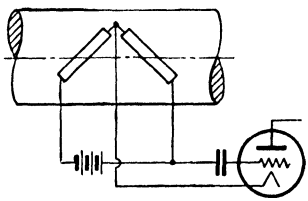


FIG. 49*i*.—Two strain gages mounted at 45 deg. on a shaft to form a torsion-sensitive unit.

log" with a 1,000-cycle carrier current generated by a vacuum tube oscillator built in the instrument. The wiring diagram is somewhat like Fig. 49*e*, where *c*, *c* are the two gages, one in tension, the other in compression, and *d*, *d* are condensers, one fixed, the other variable. The unbalance current of the bridge, instead of passing through the ammeter of Fig. 49*e* passes through a small motor which turns the shaft changing the capacity of the variable condenser *d*, until new balance is obtained and the motor current is zero. The position of the condenser shaft indicates the strain, which can be read easily to 1 per cent of full scale, the full scale commonly being a strain of 0.001 in./in.

In conjunction with this Dynalog there are available a number of "pickups" for the measurement of various quantities, such as strain, stress, and pressure. The pressure pickups have the appearance and size of spark plugs and can be screwed into the pipe line. They contain a member which is strained proportionally

to the fluid or gas pressure, and to which an SR-4 gage is attached. They come in various sensitivities, the most sensitive being 0 to 600 lb./in.^{2} full scale, while the least sensitive ranges from 0 to 20,000 lb./in.^{2} full scale. Also there are spark-pluglike differential pressure gages, the most sensitive of which registers from 0 to 100 in. of water head full scale, superposed on a basic pressure of 500 lb./in.^{2} or higher.

The *stroboscope* is a device for producing intermittent flashes of light by means of which rapid vibratory motions can be made to appear to stand still or to move very slowly. In a good stroboscope the flashes of light are of extremely short duration. Imagine a vibrating object illuminated with this kind of light which is adjusted to the same frequency as the vibration. The object will be seen in a certain position; then it will be dark, and consequently the object is invisible while traveling through its cycle. When it returns to the first position after one cycle, another flash of light occurs. Thus the object appears to stand still. If the frequency of the flashes differs slightly from the frequency of the motion, the vibration will apparently take place very slowly. There have to be at least 15 flashes per second in order to create a good, non-flickering illusion of standstill, just as in a moving-picture projector. The sharpness of the picture obtained depends on the fact that during the time of the flash the object moves very little. A flash of long duration will blur the picture. The modern developments in vacuum and gas-filled tubes have made it possible to construct stroboscopes giving flashes of great intensity and of very short duration. The frequency of the flashes can be read on a calibrated dial as in a radio receiver. Thus for rather large amplitudes the instrument can be used as frequency and amplitude meter combined.

For smaller amplitudes, the stroboscope in conjunction with a seismically mounted microscope is useful. Take a seismic mass of very low frequency, carrying a microscope. Paste a very small piece of emery cloth to the vibrating object and focus the microscope on the emery, which is illuminated by stroboscopic light. The individual emery particles will appear as sharp points, which, on account of the stroboscope, run through closed curves. Thus the frequency and the amplitude can be determined.

Some stroboscopes have two or more lamps available which are operated from the same circuit and thus flash simultaneously.

This is very useful for finding phase relations. Suppose that two parts of a machine are vibrating at the same frequency and that it is desired to know whether the vibrations are in phase or in opposition. Each of two observers takes a lamp, the flash frequency being regulated so that the vibration appears very slow. They now observe the two spots and the first observer signals each time his vibration is in one of the two extreme positions. The other observer can then easily check whether his motion is in phase or in opposition. A very convenient instrument, developed by Edgerton, is marketed by the General Radio Company, Cambridge, Mass., under the trade name "Strobotac."

Example: We wish to observe stroboscopically a point located 4 in. from the axis of a machine rotating at 10,000 r.p.m. If we desire a blurring of less than $\frac{1}{32}$ in., what should be the duration of the light flashes?

Solution: The point in question travels per second

$$\frac{10{,}000}{60} \cdot 2\pi \cdot 4 = 4{,}200 \text{ in.} = 135{,}000 \times \tfrac{1}{32} \text{ in.}$$

Thus the flash should last 1/135,000 sec. or less.

An interesting torsiograph, based on an entirely different principle, was developed by the General Motors Research Laboratories. It is called the "phase-shift torsiograph" and consists of a thin (say $\frac{1}{16}$ in.) wheel with a large number of equally spaced teeth (say 300) mounted on the rotating shaft. Two small electromagnets with windings are brought close to the toothed wheel, which operates somewhat like an inverted electric clock. The teeth passing by set up an alternating voltage of tooth-passing frequency in the two coils. This frequency is constant only if the shaft rotates uniformly; if the shaft executes a torsional vibration the record of the current shows alternate sine waves bunched close together and further apart. This variable frequency output current is fed into a box and mixed with a constant frequency current of average frequency generated by a vacuum tube oscillator. Thus the two currents will have a constantly varying phase angle between them, and by a clever trick it is possible to take an oscillograph record in which the torsional vibration amplitude shows directly against time. The advantages of this method are the absence of slip rings, the possibility of installing it on engines so compactly built that there is no space for any other instrument, and that the record is

independent of the amplification ratio of the electronic apparatus, since it depends on phase angles only. It is interesting to note that the "seismic" element in this method is no longer a mechanical flywheel running at constant speed, but rather the vacuum tube oscillator producing a current of constant frequency.

Finally, for electric wave analyzers, see page 24 in the section on Fourier series.

19. Theory of Vibration Isolation.—An unbalanced machine has to be installed in a structure where vibration is undesirable. Such a situation is not uncommon. An alternating-current elevator motor in a hospital or hotel and the engine in an automobile are examples. The problem consists in mounting the machine in such a manner that no vibrations will appear in the structure to which it is attached.

Its universal solution consists in properly mounting the machine on springs, and again Figs. 38 and 40 contain the information for the correct design of such mountings. In Fig. 50 the machine is represented as a mass m with a force $P_0 \sin \omega t$ acting on it. In Fig. 50*a* it is attached solidly to its substructure, while in 50*b* it is mounted on springs with a combined vertical flexibility k (the k of Fig. 50*a* is infinitely large). For simplicity the substructure is assumed to be rigid. If now P_0 is held constant and the frequency is varied, the amplitude of motion of m varies according to the diagram of Fig. 38.

Our problem consists in finding the magnitude of the *force* transmitted to the substructure by the machine. Since only the springs k are in contact with the foundation, the only transmitted force can be the spring force, which has the amplitude kx (damping being considered absent). The ordinates of Fig. 38 represent the ratio of the maximum displacement x_0 of the mass to the static displacement $x_{st} = P_0/k$. Thus

$$\text{Ordinate} = \frac{x_0}{x_{st}} = \frac{x_0}{P_0/k} = \frac{kx_0}{P_0} = \frac{\text{spring force}}{\text{impressed force}}$$
$$= \frac{\text{transmitted force}}{\text{impressed force}} = \text{"transmissibility"}$$

The ideal is to have this ratio zero; the practical aim is to make it rather small. In Fig. 50*a* the spring constant $k = \infty$ and hence the natural or resonant frequency is infinite. Therefore, the operating frequency ω of the force is very slow with respect to the natural frequency; *i.e.*, we are at the point A of Fig. 38,

so that the transmitted force equals the impressed force. Physically this is obvious, since a rigid foundation was assumed and thus the mass m cannot move: the whole force P_0 must be transmitted to the foundation. The diagram of Fig. 38 shows immediately that *it is necessary to design the supporting springs so as to make the natural frequency of the whole machine very slow compared*

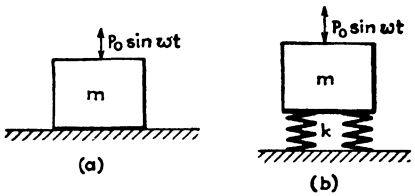


FIG. 50.—A support of very flexible springs prevents vibrations from being transmitted to the foundation.

with the frequency of the disturbance; in other words, the springs should be very soft.

An inspection of this diagram and its formula (28*a*) reveals that if ω is smaller than $\omega_n\sqrt{2} = \sqrt{2K/m}$, the springs actually make matters *worse:* the transmissibility is greater than one. If the natural frequency is one-fifth of the disturbing frequency, the transmissibility is 1 part in 24. This is fairly good, but in many cases it is better to make the springs softer yet.

Thus far, the support has been considered to be entirely without damping, which is practically the condition existing in steel springs. Sometimes, however, rubber or cork padding is used for this purpose, and then the damping is not negligible. The system can then be symbolized by Fig. 51; the amplitude of the motion of m being shown by one of the curves of Fig. 42. In this case the displacement curve is *not* directly proportional to the amplitude of the transmissibility curve, as was the case with no damping. Now the transmitted force is made up not only of the spring force kx_0 but of the damping force $c\omega x_0$ as well. It was shown on page 64 that these two forces (being in phase with the displacement and the velocity respectively) have a 90-deg. phase angle between them. Consequently their sum, being the total transmitted force, is [Eq. (6), page 6]

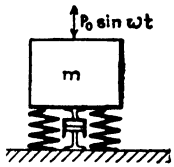


FIG. 51.—A spring support with damping.

$$x_0\sqrt{k^2 + (c\omega)^2} \tag{35}$$

The amplitude x_0 is given by formula (32*a*) on page 64 so that (35) becomes

$$\text{Transmitted force} = P_0 \frac{\sqrt{1 + \left(\frac{c\omega}{k}\right)^2}}{\sqrt{\left(1 - \frac{\omega^2}{\omega_n^2}\right)^2 + \left(2\frac{c}{c_c}\frac{\omega}{\omega_n}\right)^2}}$$

or, since P_0 is the impressed force,

$$\text{Transmissibility} = \sqrt{\frac{1 + \left(2\frac{c}{c_c}\frac{\omega}{\omega_n}\right)^2}{\left(1 - \frac{\omega^2}{\omega_n^2}\right)^2 + \left(2\frac{c}{c_c}\frac{\omega}{\omega_n}\right)^2}} \tag{36}$$

which actually reduces to formula (28*a*) on page 57 for the case of zero damping, $c/c_c = 0$. This relation is shown graphically

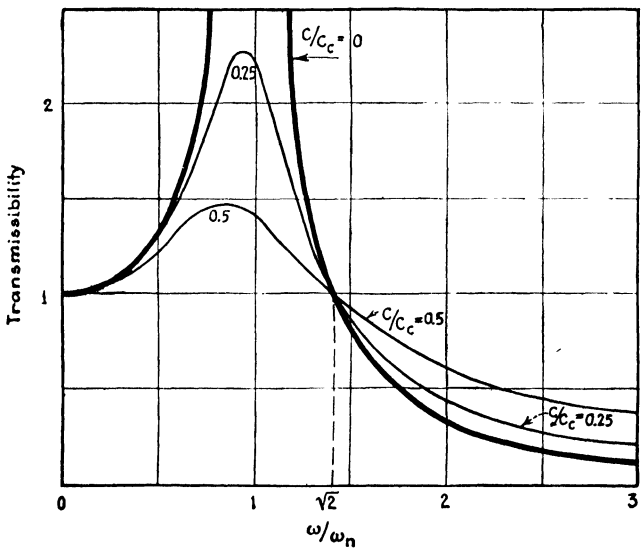


FIG. 52.—Showing that damping in the spring support is advantageous for $\omega < \omega_n \sqrt{2}$, but is detrimental for $\omega > \omega_n \sqrt{2}$.

in Fig. 52. *Damping is seen to be advantageous only in the region* $\omega/\omega_n < 1.41$ (*where spring mounting makes matters worse*); *for all values of* ω/ω_n *where spring mounting helps, the presence of damping makes the transmissibility worse.*

This rather paradoxical statement is not quite so important as it sounds. In the first place, the bad effect of damping is not great and can be easily offset by making the springs some-

what weaker, *i.e.*, by moving somewhat more to the right in Fig. 52. On the other hand, though it is not our *intention* to run at the resonance point $\omega/\omega_n = 1$, this unfortunately may sometimes occur, and *then* the presence of damping is highly desirable. Thus in spite of the dictum of Fig. 52, some damping in the springs generally is of advantage.

20. Application to Single-phase Electrical Machinery.—Practical cases of isolation by means of springs occur in many machines. The main field of application, however, lies in apparatus which is inherently unbalanced or inherently has a non-uniform torque. Among the latter, single-phase electric generators or motors and internal-combustion engines are the most important.

First, single-phase machines are to be discussed. As is well known, the torque in any electric machine is caused by the pull of the magnetic field on current-carrying conductors. The magnetic field itself is caused by a current flowing through the field coils. If the machine is operated by single-phase alternating current of say 60 cycles per second, it is clear that the current flowing into the machine (and through the field coils) must become zero 120 times per second. But at zero current there is zero magnetic field and hence zero torque. Without knowing anything about the mechanism of such a machine we may suspect the torque to be some alternating periodic function of 120 cycles per second.

A more exact analysis is as follows: In any electric machine the instantaneous power in watts (which is of the dimension of work per second) equals the product of voltage and current, or

$$\text{Watts} = ei$$

If the voltage on the machine is $e = e_{\max} \sin \omega t$ (where $\omega = 60 \times 2\pi$ radians per second), and $i = i_{\max} \sin (\omega t - \varphi)$,

$$\begin{aligned}
\text{Watts} &= e_{\max} i_{\max} \sin \omega t \sin (\omega t - \varphi) \\
&= e_{\max} i_{\max} \sin \omega t (\sin \omega t \cos \varphi - \cos \omega t \sin \varphi) \\
&= e_{\max} i_{\max} (\sin^2 \omega t \cos \varphi - \sin \omega t \cos \omega t \sin \varphi) \\
&= \frac{e_{\max} i_{\max}}{2} [\cos \varphi (1 - \cos 2\omega t) - \sin \varphi \sin 2\omega t] \\
&= \frac{e_{\max} i_{\max}}{2} [\cos \varphi - \cos (2\omega t - \varphi)]
\end{aligned}$$

This is seen to consist of two terms, one independent of the time, representing a steady flow of power (which is the purpose for which the machine is built), and another harmonically alternating with frequency 2ω. This latter term does not deliver power during a long period of time, because its positive

parts are neutralized by corresponding negative parts. The *torque* is found from the power as follows:

$$\text{Power} = \frac{\text{work}}{\text{second}} = \frac{\text{torque} \times \text{angle}}{\text{second}} = \text{torque} \times \text{angular velocity}$$

Thus all conclusions drawn for the power hold also for the torque when the angular velocity is constant, which is practically the case for a running machine.

The torque-time relation is given in Fig. 53, showing in this particular case that the amplitude of torque variation a is 30 per cent larger than the steady rated torque b of the machine. Though this represents a bad condition, the best that can possibly

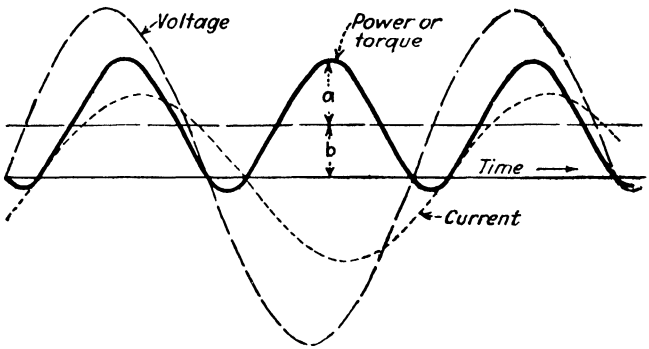


FIG. 53.—The torque of a single-phase a.c. motor is a periodic function having twice the frequency of the line voltage.

occur is that $a = b$. Then the torque merely becomes zero 120 times per second but does *not* become negative.

The machine consists of two parts, a *rotor* and a *stator*. Though it is the object of the machine to deliver torque to the rotor, Newton's law that action equals reaction requires that an equal and opposite torque act on the stator. If this stator is solidly bolted to its foundation, we have the torsional equivalent of the case of Fig. 50*a*. The torque reaction is fully transmitted to the foundation and from there can travel far and wide. Though the vibratory motion thus broadcast is usually very small, it may be that at quite a distance from the source there is a beam or other structure having for its natural frequency the same 120 cycles. That structure will pick up the motion and magnify it by resonance. A case is on record concerning a number of large single-phase generators installed in a basement in New York City. Complaints of a bad humming noise came from the occupants of

an apartment house several blocks from where the generators were located, while the neighbors much closer to the source did *not* complain. The obvious explanation was that the complainers were unfortunate enough to have a floor or ceiling just tuned to 120 cycles per second. The cure for the trouble was found in mounting the generators on springs, as shown in Fig. 54.

Since the disturbance is a pure *torque* and not an up-and-down *force*, the springs have to be arranged in such a fashion that the stator can twist (*i.e.*, yield to the torque). The stiffness of the

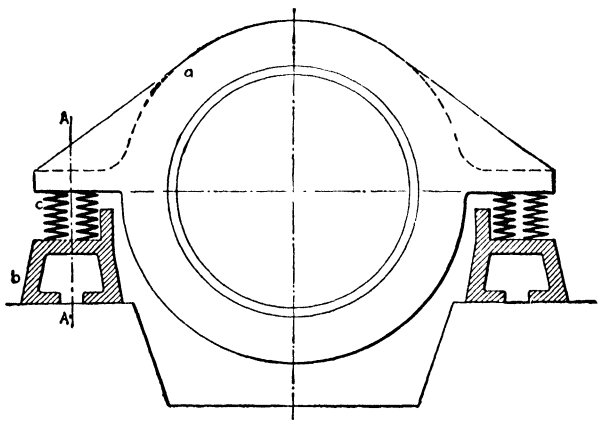


FIG. 54.—Spring support for large single-phase generators to take the torque reaction.

springs has to be so chosen that the torsional natural frequency of the stator on the springs is about one-seventh of 120 cycles per second.

In an actual construction for a large machine the springs of Fig. 54 are usually not coil springs as shown but rather beams of spring-steel loaded in bending, arranged with their length direction parallel to the axis of rotation of the generator. Figure 55 is a sketch of such a construction (cross section AA of Fig. 54); a denotes the stator, b the supporting foot, and c the beam spring, which carries its load on four points.

Small single-phase motors are used extensively in domestic appliances like refrigerators, washing machines, etc. Sometimes such motors have a pinion on the shaft, driving a gear, and then it becomes imperative to support the rotor bearings so that they are very stiff against either vertical or lateral displacements in order to secure good operation of the gears. On the other

hand, the stator should be mounted very flexibly in the rotational mode of motion.

There are several constructions on the market whereby both these requirements are satisfied. Two of them will be described here. Their common feature is that the rotor bearings are built solidly into the stator (which constitutes a difference from Fig. 54

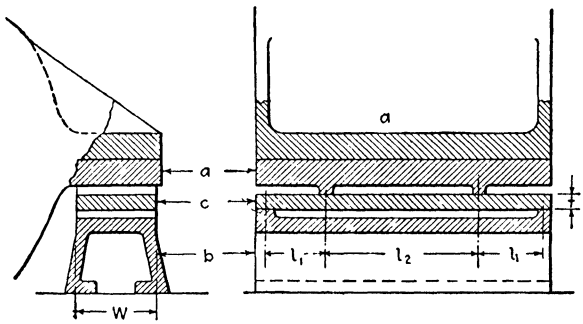


FIG. 55.—Detail of beam spring for machine of Fig. 54.

where the bearings are mounted solidly on the floor so that the springs are between the rotor bearings and the stator). This solid rotor-stator unit is mounted on springs to the base or floor. The manner in which this is done, however, varies considerably. In the first construction (Fig. 56) each end of the stator is mounted in a heavy rubber ring *a* which is held in the foot *b* bolted to the floor. Rubber is a material which can be stretched

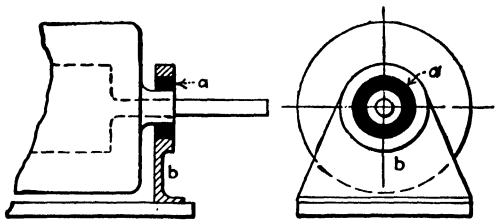


FIG. 56.—Support of small single-phase motor in a rubber ring *a*, which is flexible in torsion and stiff against vertical or lateral displacements.

enormously within the elastic limit, but at the same time it is extremely resistant to changes in volume: if a band of rubber is stretched to twice its length, its average cross section becomes half as small. (Another way of stating this is that rubber has a Poisson's ratio of one-half.) Owing to this property, the bearing inside the rubber ring can hardly move sidewise with respect to the foot, because that would mean thinning of the ring on one side, which can occur only if rubber escapes vertically. This,

however, is prevented by friction, so that the ring forms a stiff link between the bearing and the foot as far as lateral (or vertical) motions are concerned. Against rotation of the bearing in the foot, however, the rubber opposes only a shearing reaction, which can take place without a change in volume, making the ring flexible with respect to that motion.

The second method of accomplishing the same result is equally ingenious and is shown in Fig. 57. The bearing is supported on a strip of steel, bent so as to have two 45-deg. sections and three horizontal sections (being the spring and supporting foot in one). This amounts to having two 45-deg. beams between the floor and the bearing, *built in* at each end. The design is

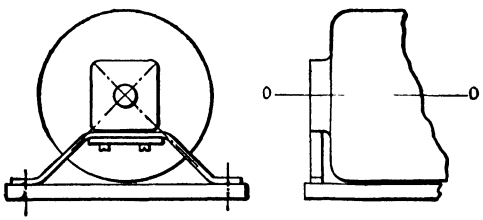


FIG. 57.—Small-motor spring support consisting of two 45-deg. sections passing through the center of the machine.

such that the center lines of the beams pass through the bearing center. Any vertical or horizontal displacement of the bearing is associated with either *tension* or *compression* in the beams, whereas a turning of the bearing only *bends* the beams. Since thin strips are flexible in bending but very much stiffer in direct tension or compression, the desired result is obtained.

21. Application to Automobiles; "Floating Power."—Internal-combustion engines have a torque-time diagram which does not differ appreciably from that of Fig. 53. For a four-cycle engine its frequency is $\frac{n}{2} \times$ (r.p.m.) cycles per minute where n is the number of cylinders. This will be explained in detail on page 248; here it is of interest only to know that the non-uniformity in torque exists. With the engine mounted rigidly on the frame, these torque variations have reactions on the car which may make themselves felt very uncomfortably. The obvious remedy is to mount the engine so that the free rotary vibration about the torque axis takes place very slowly, or, more precisely, so that the natural frequency of such a vibration is appreciably lower than $n/2$ times the running speed.

This can be accomplished conveniently by mounting the whole engine block on two journals, fore and aft, supported in bearings attached to the chassis, enabling the block to rotate about an axis practically parallel to the torque axis and passing through the center of gravity (shown as AA in Fig. 58). Without anything other than the construction just described, the block would be free to rotate about the A-axis. This is prevented by a cantilever leaf spring B between the block and the frame, of which the stiffness is so chosen as to make the natural frequency sufficiently low.

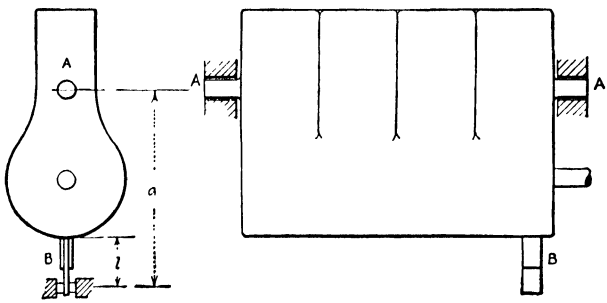


FIG. 58.—Scheme of "floating-power" automobile engine.

Besides having an unbalanced *torque*, a four-cylinder engine also experiences some horizontal and vertical inertia *forces* (see page 221), which naturally have reactions at A and B. For this reason the bearings A as well as the end of the spring B are embedded in rubber.

In the actual construction, the axis AA is *not* quite parallel to the torque axis. This is correct procedure, for generally the torque axis is not a principal axis of inertia and consequently does not coincide with the corresponding axis of rotation.

Any rigid body has three "principal axes of inertia." Consider, for instance, an elongated solid piece of rectangular steel (Fig. 59) and attach to it a (weightless) shaft passing through the center of gravity but *not* coinciding with one of the principal axes (here axes of symmetry). The bar and shaft lie in the plane of the drawing. Apply a sudden torque to the shaft, and consider the acceleration caused by it. The upper part of the bar is accelerated *into* the paper, the lower part comes *out of* the paper (as indicated by dots and crosses in the figure). Multiplied by the mass of the respective elements these accelerations become "inertia forces." It is clear from the figure that these inertia forces multiplied by their distances from the shaft form a torque, which is equal and opposite to the impressed torque. *Moreover*, these forces multiplied by their distances to the vertical

dotted line have a torque about that line as an axis. This will have its reaction in the bearings; the right-hand bearing will feel a force pushing it toward the reader out of the paper, and the left-hand bearing is pushed into the paper. Now if the bearings were absent, it is clear that under the influence of the torque the body would *not* rotate about the torque axis (since forces at the bearings are required in order to make it do so). Thus, in general, a body under the influence of a torque will rotate about an axis *not* coinciding with the torque axis (if the torque axis is not a principal axis).

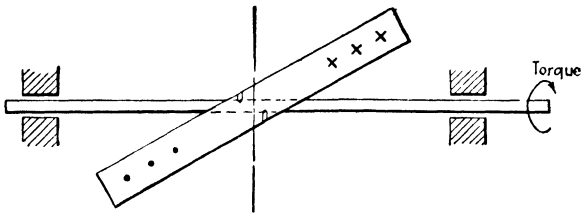


FIG. 59.—Rotation about an axis different from a principal axis of inertia results in rotating reaction forces at the bearings.

The axis, about which the "floating-power" engine has to be suspended, therefore should not be the torque axis itself but rather the axis of rotation belonging to the torque axis. Only when the torque axis is a principal axis do the two coincide.

There are several other constructions of spring-supported automobiles on the market, most of which are similar in principle to the scheme of Fig. 58. Some have one rubber support at the rear of the engine and two rubber supports close together at the same height in the front. These two are virtually a combination of the single bearing A and the restoring spring B of Fig. 58.

Example: A four-cylinder automobile engine weighing 400 lb. is supported as indicated in Fig. 58. The radius of gyration of the engine about the axis AA is 6 in., the distance a is 18 in., and the length l of the cantilever is 4 in. The diameter of the rear wheels is 30 in. and in high gear the engine makes three revolutions per revolution of the rear wheels. It is desired that the engine be in resonance at a speed corresponding to 3½ m.p.h. in high gear.

a. What should be the spring constant of the centilever?

b. If one of the four cylinders does not spark properly, at what other speed is trouble to be expected?

Solution: a. 3½ m.p.h. = 61 in. per second. The circumference of the wheel is $30\pi = 94.2$. At the critical speed the wheel makes $61/94.2 = 0.65$ r.p.s. and the engine therefore runs at $3 \times 0.65 = 1.95$ r.p.s. The torque curve of the engine goes through a full cycle for every firing. Since there are two firings per revolution in a four-cylinder, four-cycle engine, there are 3.9 firings per second. The natural frequency of the engine is desired to be $f_n = 3.9$ cycles per second or $\omega_n^2 = 4\pi^2(3.9)^2 = 600$ rad.^{2}/sec.^{2} $= k/I$. Here k is the torque caused by the cantilever per radian twist.

The deflection at the end of the cantilever for a twist of φ radians is 18φ in.

If k_1 be the linear stiffness of the cantilever in lb./in., the spring force is $18k_1\varphi$ lb., acting on a moment arm of 18 in., so that the torque is $18 \times 18k_1\varphi$. Thus

$$k = 324k_1$$

Further

$$I = \frac{400}{386} \cdot (6)^2 = 37 \text{ lb. in. sec.}^2$$

so that

$$\omega_n^2 = 600 = \frac{324k_1}{37}$$

and

$$k_1 = \frac{37 \times 600}{324} = 69 \text{ lb. per inch}$$

b. If one cylinder fires inadequately, there is another periodicity in the torque curve for each two revolutions of the engine. Since this disturbance is four times as slow as the one discussed, it comes to resonance with the natural frequency of the engine at a speed of $4 \times 3.5 = 14$ m.p.h.

Problems

10. Derive the results (32*a*) and (32*b*) in the manner indicated directly below Eq. (31).

11. Derive Eq. (28) by an energy method.

12. A rotor of weight **W** and of moment of inertia I about its axis of symmetry is laid with its journals on two guides with radius of curvature R (Fig. 60). The radius of the journals is r. When the rotor rolls without sliding, it executes small harmonic vibrations about the deepest point of the track. Find the frequency (energy method, see pages 46 and 50).

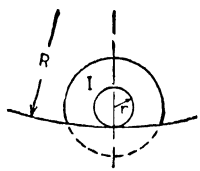


FIG. 60.

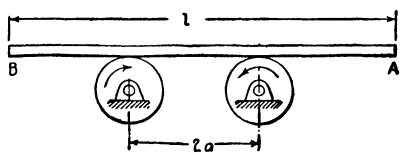


FIG. 61.

13. The same problem as 12, except that the track is straight ($R = \infty$) and the rotor is unbalanced by a small weight **w** attached to it at a distance r_1 from the axis.

14. Two cylindrical rolls are located at a distance $2a$ apart; their bearings are anchored and they rotate with a great speed ω in opposite directions (Fig. 61). On their tops rests a bar of length l and weight **W**. Assuming dry friction of coefficient f between the rolls and the bar, the bar will oscillate back and forth longitudinally. (*a*) Calculate its frequency. (*b*) If one end of the bar A is pushed into the paper somewhat and B is pulled out, is the equilibrium stable or unstable?

15. A pendulum consists of a stiff weightless bar of length l carrying a mass m on its end (Fig. 62). At a distance a from the upper end two springs k are attached to the bar. Calculate the frequency of the vibrations with small amplitude.

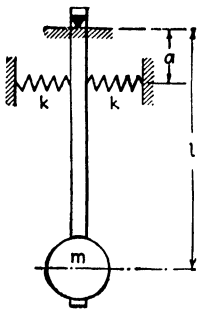


FIG. 62.

16. Turn Fig. 62 upside down. (*a*) Find the relation between a, m, and l for which the equilibrium is stable. (*b*) Find the frequency.

17. Calculate the frequency of the stator of Fig. 54. The linear stiffness of each of the four springs is k, their average distance from the center of the rotor is a, and the moment of inertia of the stator is I.

18. Calculate the frequency of Problem 17 for the spring system of Fig. 55. The beams c are made of steel with a modulus of elasticity E; their dimensions are l_1, l_2, w, and t as indicated in the figure.

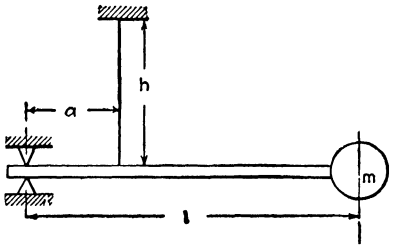


FIG. 63.

19. A stiff weightless horizontal bar of length l is pivoted at one end and carries a mass m at its other end (Fig. 63). It is held by an inextensible string of length h. If the mass is pulled perpendicularly out of the paper and then released, it will oscillate. Calculate the frequency.

20. A mass m is attached to the center of a thin wire of cross section A and total length l which is stretched with a large tension of T lb. between two immovable supports. The modulus of elasticity of the wire is E. Calculate the frequency of the vibrations of the mass in a plane perpendicular to the wire.

21. A heavy solid cylinder of diameter D, length l, and mass m can roll over a horizontal surface. Two springs k are attached to the middle of l at a distance a above the center (Fig. 64). Calculate the frequency.

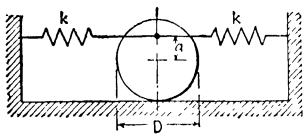


FIG. 64.

22. Find an expression for the linear spring constant k of a steel coil spring of wire diameter d, coil diameter D, and having n turns. Calculate k numerically for $d = 0.1$ in., $D = 1\frac{1}{2}$ in., and $n = 10$.

23. Find the torsional-spring constant of a coil spring, *i.e.*, a coil spring of which the ends are subjected to torques about the longitudinal axis of the spring. Calculate this k numerically for the spring of Problem 22.

24. Find the spring constant k in bending of a coil spring, *i.e.*, the bending moment to be applied to the ends of the spring divided by the angle through which the two ends turn with respect to each other. Calculate this k numerically for the spring of Problem 22.

25. What are the expressions for the linear-spring constants of

a. A cantilever beam of bending stiffness EI with the mass attached to the end l?

b. A beam of total length l on two supports with the mass in the center?

c. A beam of total length l built in at both ends with the mass in the center?

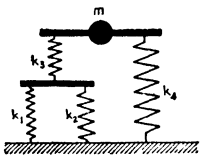


FIG. 65.

26. Calculate the frequency of the small vertical vibrations of the mass m of Fig. 65. The two bars are supposed to be stiff and weightless. The mass is in the center between k_3

and k_4, and k_3 is midway between k_1 and k_2. The mass is guided so that it can move up and down only. It can rotate freely and has no moment of inertia.

27. A point on a machine executes simultaneously a horizontal and a vertical vibration of the same frequency. Viewed with the seismic microscope described on page 87 the point will be seen as an ellipse (Fig. 66). By observation, the lengths h and AB are found. (*a*) Calculate from these the phase angle between the horizontal and vertical motions. What shapes does the ellipse assume for (*b*) φ = zero, and (*c*) φ = 90 deg.?

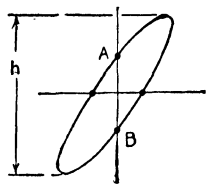


FIG. 66.

28. A damped vibrating system consists of a spring of k = 20 lb. per inch and a weight of 10 lb. It is damped so that each amplitude is 99 per cent of its previous one (*i.e.*, 1 per cent loss in amplitude per *full* cycle).

a. Find the frequency by formula and from Fig. 29.

b. Find the damping constant.

c. Find the amplitude of the force of resonant frequency necessary to keep the system vibrating at 1 in. amplitude.

d. What is the rate of increase in amplitude if at 1 in. amplitude the exciting force (at resonant frequency) is doubled?

e. What is the final amplitude to which the system tends under the influence of this doubled force?

f. Find the amplitude-time relation of this growing vibration.

29. Find the expression for the steady-state torque, assuming no damping,

a. In shaft k of Fig. 26, page 40.

b. In shaft k_2 of Fig. 27.

30. A "static balancing machine" (page 293) consists of a bearing B inclined at an angle α with the vertical (Fig. 67). A rotor placed in this bearing has a moment of inertia I and an unbalance m at a distance r from the center. Write the differential equation of the vibrations of the rotor in terms of its angle of rotation φ. Find the natural frequency for small vibrations φ.

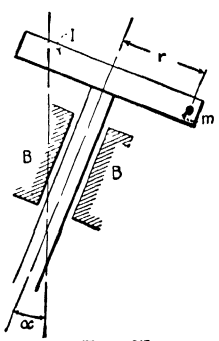


FIG. 67.

31. Find the natural frequency of the small oscillations of a solid half cylinder (the contour consisting of a half circle and a diameter), which rolls without sliding on a horizontal plane.

32. A simple k-m system is at rest. A constant force P is applied to the mass during a stated time interval t_0, after which the force is removed. Find the motion of the mass after removal.

33. Set up the differential equations of motion of the system of Fig. 27; then, by elimination, reduce them to a single differential equation in terms of the variable $\psi = \varphi_1 - \varphi_2/n$, which is an angle that becomes zero if the shafts are not twisted. In this manner verify the statements made on page 42.

34. A weightless, stiff bar is hinged at one end. At a distance l from the hinge there is a mass m, at a distance $2l$ there is a dashpot c, and at a distance $3l$ there is a spring k and an alternating force $P \sin \omega t$. Set up the

differential equation. Assuming small damping c (but *not* zero damping), calculate the natural frequency; the amplitude of forced vibration at the spring at the natural frequency and at half natural frequency.

35. A circular solid disk of mass M and radius r is suspended in a horizontal plane from a fixed ceiling by three vertical wires of length l, attached to three equally spaced points on the periphery of the disk.

a. The disk is turned through a small angle about its vertical center line and let go. Calculate the frequency of rotational vibration.

b. The disk is displaced sidewise through a small distance without rotation and let go. Calculate the frequency of the ensuing swinging motion.

36. Prove the statement made on page 77 that there is no phase distortion in a seismographic instrument if the phase-angle diagram Fig. 42*b* is a straight diagonal line passing through the origin.

37. A mass m is suspended from a ceiling by a spring k and a dashpot c. The ceiling has a forced motion $a_0 \sin \omega t$. Calculate the work done by the ceiling on the system per cycle of vibration in the steady state. Write the answer in dimensionless form.

38. In the system of Fig. 23 and Fig. 42*a*, the maximum *work* input by the force as a function of frequency is only approximately equal to $\pi P_0 x_0$, where x_0 is the amplitude at $\omega/\omega_n = 1$. The actual maximum work is at a slightly different frequency. Prove that this maximum work can be computed from $\pi P_0 x_0$ by multiplying that quantity by the correction factor

$$\frac{\sqrt{1 - 2(c/c_c)^2}}{1 - (c/c_c)^2}$$

and show that this error is less than 0.1 per cent for a damping as high as $c/c_c = 20$ per cent.

39. In 1940 a large two-bladed windmill, capable of generating 1,250 kw. of electric power was built on Grandpa's Knob near Rutland, Vt. The diameter of the blade circle is 175 ft, the blades rotate at 30 r.p.m. in a plane which is considered vertical for our purpose. The blades are mounted on the "pintle" or cap, which itself can rotate slowly about a vertical axis in order to make the blades face the wind. Since there are only two blades in the rotor, the moment of inertia of the rotor about the vertical pintle axis is very much greater when the blades are pointing horizontally than when they are vertical, 90 deg. further. Let Ω be the constant angular speed of the rotor, ω the very much smaller angular speed of the pintle, and I_{max} and I_{min} the extreme values of inertia about the vertical axis.

a. Assuming the driving mechanism of the pintle motion to be extremely soft torsionally, so that no torque acts on the pintle (except friction, which is to be neglected), find the ratio between the maximum and mimimum values of ω.

b. Assuming the pintle drive to be extremely stiff torsionally, so that the pintle motion ω is forcibly uniform, find an expression for the torque in the pintle drive.

CHAPTER III

TWO DEGREES OF FREEDOM

22. Free Vibrations, Natural Modes.—In the preceding chapter there was discussed the theory of the vibrations of a system with a single degree of freedom with viscous damping. Though the exact idealized system with which the theory dealt occurs rarely, it was seen that a number of actual cases are sufficiently close to the ideal to permit conclusions of practical importance. The theory of the single-degree-of-freedom system enabled us to explain the resonance phenomenon in many machines, to calculate natural frequencies of a number of structures, to explain the action of most vibration-measuring instruments, and to discuss spring suspension and vibration isolation.

This exhausts the possibilities of application pretty thoroughly, and in order to explain additional phenomena it is necessary to develop the theory of more complicated systems. As a first step consider two degrees of freedom, which will yield the explanation of most "vibration dampers," of the action of a number of contrivances for stabilizing ships against rolling motions in a rough sea, and of the operation of automobile shock absorbers.

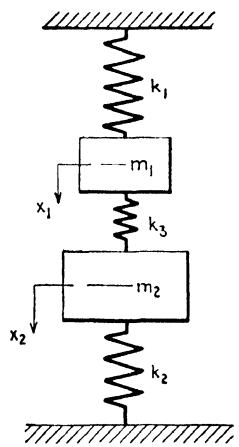


FIG. 68.—Undamped two-degree-of-freedom system with spring coupling.

The most general undamped two-degree-of-freedom system can be reduced to that of Fig. 68 and consists of two masses m_1 and m_2 suspended from springs k_1 and k_2 and tied together by a "coupling spring" k_3. Assuming that the masses are guided so as to be capable of purely vertical motions only, there are evidently two degrees of freedom, since the two masses can move independently of each other. By specifying their vertical positions x_1 and x_2 the configuration is entirely determined.

As in the single-degree-of-freedom case, there are a number of torsional, electrical, etc., two-degree-of-freedom systems which are completely equivalent to Fig. 68.

Proceeding now to a calculation of the *free* vibrations, we notice that there are two distinct forces acting on the mass m_1, namely the force of the main spring k_1 and that of the coupling spring k_3. The main force is $-k_1x_1$ acting downward (in the $+x_1$-direction). The shortening of the coupling spring is $x_1 - x_2$, so that its compressive force is $k_3(x_1 - x_2)$. A compressed coupling spring pushes m_1 upward, so that the force has to be taken with the negative sign. These two are the only tangible forces acting on m_1, so that its equation of motion is

$$m_1\ddot{x}_1 = -k_1x_1 - k_3(x_1 - x_2)$$

or

$$m_1\ddot{x}_1 + (k_1 + k_3)x_1 - k_3x_2 = 0 \tag{37}$$

The equation of motion for the second mass can be derived in the same manner. But by turning Fig. 68 upside down and reversing the directions of x_1 and x_2, m_2 and k_2 assume the positions of m_1 and k_1 and

$$m_2\ddot{x}_2 + (k_2 + k_3)x_2 - k_3x_1 = 0 \tag{38}$$

Assume now that the masses m_1 and m_2 execute harmonic motions with the same frequency ω (as yet unknown) and different amplitudes a_1 and a_2 (also unknown).

$$\left.\begin{aligned} x_1 &= a_1 \sin \omega t \\ x_2 &= a_2 \sin \omega t \end{aligned}\right\} \tag{39}$$

This is a mere guess; we do not know whether such a motion is possible. By substituting in the differential equations we shall soon find out if it is possible.

$$\begin{aligned} [-m_1a_1\omega^2 + (k_1 + k_3)a_1 - k_3a_2] \sin \omega t &= 0 \\ [-m_2a_2\omega^2 + (k_2 + k_3)a_2 - k_3a_1] \sin \omega t &= 0 \end{aligned}$$

These equations must be satisfied at any instant of time. They represent sine waves, so that in order to make them zero *at all times* the amplitudes in the brackets have to be zero.

$$\left.\begin{aligned} a_1(-m_1\omega^2 + k_1 + k_3) - k_3a_2 &= 0 \\ -k_3a_1 + a_2(-m_2\omega^2 + k_2 + k_3) &= 0 \end{aligned}\right\} \tag{40}$$

If the assumption (39) is correct, it is necessary that Eqs. (40) be satisfied. In general this is not true, but we must remember that in (39) nothing was specified about the amplitudes a_1 and a_2 or about the frequency ω. It will be possible to choose a_1/a_2 and ω so that (40) is satisfied, and with these values of a_1/a_2 and ω Eq. (39) becomes a solution. In order to find the correct values we have only to solve them from (40). Thus from (40*a*)

$$\frac{a_1}{a_2} = \frac{-k_3}{m_1\omega^2 - k_1 - k_3} \tag{41}$$

From (40*b*), also, the amplitude ratio can be solved:

$$\frac{a_1}{a_2} = \frac{m_2\omega^2 - k_2 - k_3}{-k_3} \tag{42}$$

In order to have agreement, it is necessary that

$$\frac{-k_3}{m_1\omega^2 - k_1 - k_3} = \frac{m_2\omega^2 - k_2 - k_3}{-k_3}$$

or

$$\omega^4 - \omega^2\left\{\frac{k_1 + k_3}{m_1} + \frac{k_2 + k_3}{m_2}\right\} + \frac{k_1k_2 + k_2k_3 + k_1k_3}{m_1m_2} = 0 \tag{43}$$

This equation, known as the "frequency equation," leads to two values for ω^2. Each one of these, when substituted in either (41) or (42), gives a definite value for a_1/a_2. This means that (39) can be a solution of the problem and that there are *two* such solutions.

For readers familiar with *Mohr's* circle diagram in two-dimensional elasticity, the following construction is of interest. Let in Fig. 68

$$\omega_a^2 = \frac{k_1 + k_3}{m_1}, \qquad \omega_b^2 = \frac{k_2 + k_3}{m_2}, \qquad \omega_{ab}^2 = \frac{k_3}{\sqrt{m_1m_2}}$$

The quantities ω_a and ω_b are the frequencies of the system in which one of the masses is held clamped, while ω_{ab} expresses the strength of the coupling. With this notation, Eq. (43) can be written as

$$\omega^4 - \omega^2(\omega_a^2 + \omega_b^2) + (\omega_a^2\omega_b^2 - \omega_{ab}^4) = 0$$

Lay off in the diagram of Fig. 69 the following distances:

$$OA = \omega_a^2 \qquad OB = \omega_b^2 \qquad BC = \omega_{ab}^2$$

Then draw a circle through C about the mid-point between A and B as center. The new points D and E thus found determine the natural frequencies of the system:

$$\omega_1^2 = OD \qquad \text{and} \qquad \omega_2^2 = OE$$

which can be verified from the equation. In particular, when there is no coupling ($BC = 0$), the points D and E coincide with A and B, so that then ω_a and ω_b are the natural frequencies.

For further discussion, let us simplify the system somewhat by making it symmetrical. Let $k_1 = k_2 = k$ and $m_1 = m_2 = m$.

The frequency equation then reduces to

$$\omega^4 - 2\omega^2\frac{k + k_3}{m} + \frac{k(k + 2k_3)}{m^2} = 0 \qquad (43a)$$

with the solutions

$$\omega^2 = \frac{k + k_3}{m} \pm \sqrt{\left(\frac{k + k_3}{m}\right)^2 - \frac{k(k + 2k_3)}{m^2}}$$

or

$$\omega_1^2 = \frac{k}{m} \qquad \text{and} \qquad \omega_2^2 = \frac{k + 2k_3}{m}$$

which are the *two natural frequencies* of the system. Substituting these frequencies in (41) or (42),

$$\frac{a_1}{a_2} = +1 \qquad \text{and} \qquad \frac{a_1}{a_2} = -1$$

The physical significance of these results is obvious. The fact that $a_1/a_2 = +1$ means (Eq. 39) that the two masses move in the same direction through the same distance. The coupling spring is not stretched or compressed in this process. Naturally the frequency of this motion is $\omega^2 = k/m$, since the system reduces to two independent single-degree-of-freedom systems. The fact that $a_1/a_2 = -1$ means that the two masses move through the same distance but in opposition to each other. This motion is wholly symmetrical, so that the mid-point of the coupling spring k_3 does not move. If this mid-point were held clamped, no change in the motion would take place. Thus the system is again split up into two independent single-degree-of-freedom systems. This time, however, the mass is connected to ground

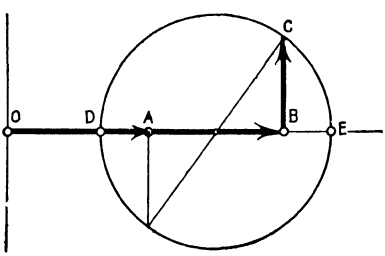


FIG. 69.—Mohr's circle for determining the natural frequencies of Fig. 68.

by *two* springs, one of stiffness k and another of stiffness $2k_3$ (see page 47), so the frequency is $\omega^2 = (k + 2k_3)/m$.

Thus there are *two "natural modes of motion,"* each with its corresponding natural frequency. The solution shows that if the system is given an initial disturbance of $x_1 = +1$ and $x_2 = +1$ (Fig. 68) and then released, the ensuing motion will be purely sinusoidal with the frequency $\omega_1^2 = k/m$; it swings in the first natural mode. On the other hand, if the initial displacement is $x_1 = +1$ and $x_2 = -1$, again a purely sinusoidal motion follows with the frequency $\omega_2^2 = (k + 2k_3)/m$, the second mode.

Assume next that the initial displacement is $x_1 = 1$ and $x_2 = 0$, from which position the system is released. As yet we have no solution for this case. But this initial displacement can be considered as the sum of two parts: first $x_1 = \frac{1}{2}$, $x_2 = \frac{1}{2}$ and second $x_1 = \frac{1}{2}$, $x_2 = -\frac{1}{2}$, for each of which a solution is known.

Assume now that the ensuing motion is the "superposition" of these two partial motions as follows:

$$\left.\begin{aligned} x_1 &= \tfrac{1}{2}\cos\omega_1 t + \tfrac{1}{2}\cos\omega_2 t \\ x_2 &= \tfrac{1}{2}\cos\omega_1 t - \tfrac{1}{2}\cos\omega_2 t \end{aligned}\right\} \qquad (44)$$

That this is the correct solution can be concluded from the fact that on substitution in (37) and (38) the differential equations are satisfied. Moreover at $t = 0$, the initial conditions are satisfied.

Equation (44) shows that the ensuing motion will be one in the first mode with amplitude $\frac{1}{2}$ and frequency ω_1, superposed on a motion with amplitude $\frac{1}{2}$ and frequency ω_2. As long as there is a coupling spring k_3, it is seen that ω_1 and ω_2 are different. Thus the combined motion of either mass can *not* be sinusoidal but must be composed of two frequencies. Naturally "beats" will occur if the two frequencies are close together (Fig. 8). This happens if $k_3 \ll k$, or, in words, if the coupling spring is very soft in comparison to the main springs. With an initial displacement $x_1 = 1$, $x_2 = 0$, first m_1 will vibrate with amplitude 1 and m_2 will stand practically still. After a time, however, the difference in the two frequencies will have changed the phase between the two vibrations by 180 deg. (see Fig. 7). Then instead of

$x_1 = \frac{1}{2}$, $x_2 = \frac{1}{2}$ (first mode) and $x_1 = \frac{1}{2}$, $x_2 = -\frac{1}{2}$ (second mode)

we have

$x_1 = \frac{1}{2}, x_2 = \frac{1}{2}$ (first mode) and
$x_1 = -\frac{1}{2}, x_2 = +\frac{1}{2}$ (second mode)

Thus the first mass stands still and the second one executes vibrations of amplitude 1. The phenomenon is periodic so that all motion travels from one mass to the other continuously.

This very interesting experiment can be shown in a number of variations, of which Fig. 70 gives five possibilities. The first case consists of two pendulums capable of swinging in the plane

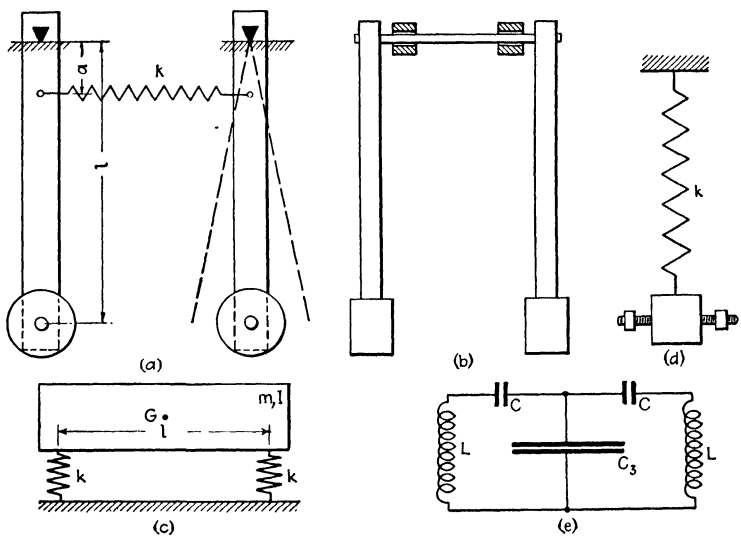


FIG. 70.—Five experiments in which we can observe a periodic wandering of the energy from one part to another.

of the paper. The main springs have been replaced here by gravity, but the coupling spring exists in the form of a very soft coil spring. For "small" vibrations (say below 30-deg. amplitude) a gravity pendulum behaves like the fundamental mass-spring system. The spring constant k, which is the restoring force for unit displacement, is mg/l, so that for a simple pendulum $\omega^2 = k/m = g/l$. In further reducing Fig. 70*a* to Fig. 68, it is seen that the coupling-spring constant k_3 in Fig. 68 is the force at the masses caused by the coupling spring if the masses are pulled one unit apart. Applying this experimental definition to Fig. 70*a*, we find that, in the absence of gravity, a force of $k\frac{a^2}{l^2}$ at

one of the masses pulls those masses 1 in. apart (see also page 48). Thus the equivalent of k_3 is ka^2/l^2.

The two natural modes of motion are easily recognized. The pendulums swing either with each other or against each other, the frequencies being $\omega_1 = \sqrt{\frac{g}{l}}$ and $\omega_2 = \sqrt{\frac{g}{l} + 2\frac{k}{m} \cdot \frac{a^2}{l^2}}$.

Pulling the left pendulum 1 in. to the left and keeping the right pendulum in its place is equivalent to the sum of the two displacements shown in Fig. 71*b* and *c*. Upon releasing the left pendulum, it will perform vibrations as indicated by Fig. 71*a* (the right-hand pendulum stands still). This motion can be

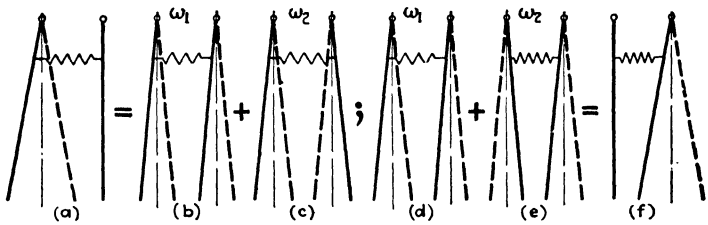


FIG. 71.—Any motion can be broken up into the sum of two natural motions having the two different natural frequencies ω_1 and ω_2.

regarded as the sum of two others with frequencies ω_1 and ω_2 as shown in the diagram. For the first few cycles this motion of one pendulum only will persist, because the two natural frequencies are sufficiently close together to keep in step for a short time. However, the second mode actually goes somewhat faster than the first one and gains on it since $\omega_2 > \omega_1$. After a sufficient time interval (say 20 cycles), it will be 180 deg. in advance of the first mode, which is indicated in Fig. 71*d* and *e*. Performing the addition shown in the figure, it is seen that the left pendulum now stands still, while the right pendulum swings with the full amplitude. Then the phenomenon repeats itself; the amplitude wanders from one pendulum to the other continuously, until the inevitable damping brings everything to rest.

In Fig. 70*b* the pendulums swing perpendicular to the plane of the paper. Two natural motions are possible: (1) the pendulums swing together, or (2) they swing against each other, thereby twisting the very slender connecting shaft, which causes some increase in the frequency. Pulling out *one* of the pendulums while keeping the other in place (thereby slightly twisting the coupling rod) and then releasing leads to the same phenomenon

of continuous transfer of all motion from one pendulum to the other.

Figure 70*c* shows a system resembling in some respects an automobile chassis on its springs. Two natural motions of the mass are possible: (1) a bobbing up and down parallel to itself with the frequency $\omega_1^2 = 2k/m$ and (2) a rocking about the center of gravity G in the plane of the drawing with a frequency $\omega^2 = kl^2/2I$. The derivation of these frequency formulas is left to the reader. Now suppose the left-hand end of the chassis is pulled up 1 in. while the right-hand end is kept in place. From this position the system is released. Again the motion is split up into two parts (Fig. 72*a* reading from left to right).

If the quantities m, I, k, and l are such that ω_1 and ω_2 are nearly the same, the motion of Fig. 72*a* will keep on for the first few

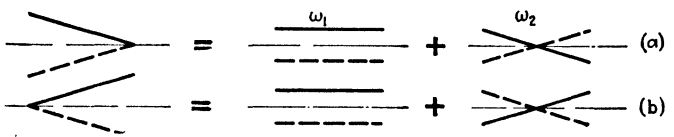


FIG. 72.—Illustrates the energy transfer of the experiment of Fig. 70*c*.

cycles without marked change. But after a larger number of cycles one of the motions (say the rocking one) gains 180 deg. on the other. Read now Fig. 72*b* from right to left and it is seen that the body vibrates with the *left*-hand end stationary. Of course, after an equal interval of time the first motion occurs again and so on until everything dies out on account of damping.

While in Fig. 70*a* and *b* the coupling spring could be easily seen as a separate part of the system, this is not the case in 70*c*. But the essential requirement for the experiment is that the system have two degrees of freedom with slightly different natural frequencies, and it does not matter whether the "coupling spring" can be recognized or not.

A striking experiment is shown in Fig. 70*d* known as *Wilberforce's spring*. A mass, suspended from a coil spring, has two protruding screws with adjustable nuts. The two degrees of freedom consist of an up-and-down motion and of a twisting motion. The "coupling" exists due to the fact that a coil spring when pulled out causes a slight torque and when twisted gives a slight pull. By changing the position of the nuts the moment of inertia I is changed while the mass m remains constant. Thus by a proper adjustment of the nuts the two natural

frequencies can be brought to nearly the same value. Then by pulling down and releasing, an up-and-down motion of the mass without twist is initiated. After a while only twisting occurs without vertical motion, and so on.

The last case, illustrated in Fig. 70*e*, is the electrical analogue of this phenomenon (see pages 39, 40). Two equal masses (inductances) L connected to equal main springs (condensers) C are coupled with a *weak* coupling spring (*large* coupling condenser C_3 since k is equivalent to $1/C$). A current initiated in one mesh will after a time be completely transferred to the other mesh, and so on. Electrically minded readers may reason out how the currents flow in each of the two "natural modes" and what the frequencies are, and may also construct a figure similar to 71 or 72 for this case.

Example: A uniform bar of mass m and length $2l$ is supported by two springs, one on each end (Fig. 70*c*). The springs are *not* equally stiff, their constants being k (left) and $2k$ (right), respectively. Find the two natural frequencies and the shapes of the corresponding modes of vibration.

Solution: Let x be the upward displacement of the center of the bar and φ its (clockwise) angle of rotation. Then the displacement of the left end is $x + l\varphi$ and that of the right end $x - l\varphi$. The spring forces are $k(x + l\varphi)$ and $2k(x - l\varphi)$, respectively. Thus

$$m\ddot{x} + k(x + l\varphi) + 2k(x - l\varphi) = 0$$

and

$$(\tfrac{1}{12}ml^2)\ddot{\varphi} + kl(x + l\varphi) - 2kl(x - l\varphi) = 0$$

are the differential equations. With the assumption of Eq. (39) we obtain

$$\begin{aligned}(-m\omega^2 + 3k)x_0 - kl\varphi_0 &= 0\\ -klx_0 + (-\tfrac{1}{3}m\omega^2l^2 + 3kl^2)\varphi_0 &= 0\end{aligned}$$

from which follows the frequency equation

$$(-m\omega^2 + 3k)(-\tfrac{1}{3}m\omega^2l^2 + 3kl^2) - k^2l^2 = 0$$

or

$$\omega^4 - 12\frac{k}{m}\omega^2 + 24\left(\frac{k}{m}\right)^2 = 0.$$

with the solutions

$$\omega_1^2 = 2.54\frac{k}{m} \qquad \text{and} \qquad \omega_2^2 = 9.46\frac{k}{m}$$

The shapes of the motion corresponding to these frequencies are found from the second differential equation, which can be written as

$$\frac{x_0}{l\varphi_0} = -\frac{1}{3}\frac{m}{k}\omega^2 + 3$$

Substituting the values for ω^2 just found, this becomes

$$\left(\frac{x_0}{l\varphi_0}\right)_1 = +2.16 \qquad \left(\frac{x_0}{l\varphi_0}\right)_2 = -0.15$$

This means a rotary vibration of the bar about a point which lies at a distance of $2.16l$ to the right of the center of the bar for the first natural frequency and about a point at $0.15l$ to the left of the center for the second natural frequency.

23. The Undamped Dynamic Vibration Absorber.—A machine or machine part on which a steady alternating force of *constant* frequency is acting may take up obnoxious vibrations, especially when it is close to resonance. In order to improve such a situation, we might first attempt to eliminate the force. Quite often this is not practical or even possible. Then we may change the mass or the spring constant of the system in an attempt to get away from the resonance condition, but in some cases this also is impractical. A third possibility lies in the application of the *dynamic vibration absorber*, invented by Frahm in 1909.

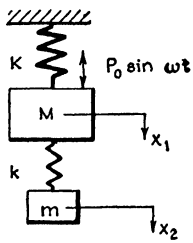


FIG. 73.—The addition of a small k-m-system to a large machine K-M prevents vibration of that machine in spite of the alternating force $P_0 \sin \omega t$.

In Fig. 73 let the combination K, M be the schematic representation of the machine under consideration, with the force $P_0 \sin \omega t$ acting on it. The vibration absorber consists of a comparatively small vibratory system k, m attached to the main mass M. *The natural frequency* $\sqrt{k/m}$ *of the attached absorber is chosen to be equal to the frequency* ω *of the disturbing force. It will be shown that then the main mass* M *does not vibrate at all,* and that the small system k, m vibrates in such a way that its spring force is at all instants equal and opposite to $P_0 \sin \omega t$. Thus there is no net force acting on M and therefore that mass does not vibrate.

To prove this statement, write down the equations of motion. This is a simple matter since Fig. 73 is a special case of Fig. 68 in which k_2 is made zero. Moreover, there is the external force $P_0 \sin \omega t$ on the first mass M. Equations (37) and (38) are thus modified to

$$\left.\begin{aligned} M\ddot{x}_1 + (K + k)x_1 - kx_2 &= P_0 \sin \omega t \\ m\ddot{x}_2 + k(x_2 - x_1) &= 0 \end{aligned}\right\} \tag{45}$$

The *forced* vibration of this system will be of the form

$$\left.\begin{aligned} x_1 &= a_1 \sin \omega t \\ x_2 &= a_2 \sin \omega t \end{aligned}\right\} \tag{46}$$

This is evident since (45) contains only x_1, $\ddot{x}_1$ and x_2, $\ddot{x}_2$, but *not* the first derivatives $\dot{x}_1$ and $\dot{x}_2$. A sine function remains a sine function after two differentiations, and consequently, with the assumption (46), all terms in (45) will be proportional to sin ωt. Division by sin ωt transforms the *differential* equations into *algebraic* equations as was seen before with Eqs. (37) to (40). The result is that

$$\left.\begin{aligned} a_1(-M\omega^2 + K + k) - ka_2 &= P_0 \\ -ka_1 + a_2(-m\omega^2 + k) &= 0 \end{aligned}\right\} \tag{47}$$

For simplification we want to bring these into a dimensionless form and for that purpose we introduce the following symbols:

$x_{st} = P_0/K$ = static deflection of main system
$\omega_a^2 = k/m$ = natural frequency of absorber
$\Omega_n^2 = K/M$ = natural frequency of main system
$\mu = m/M$ = mass ratio = absorber mass/main mass

Then Eq. (47) becomes

$$\left.\begin{aligned} a_1\left(1 + \frac{k}{K} - \frac{\omega^2}{\Omega_n^2}\right) - a_2\frac{k}{K} &= x_{st} \\ a_1 &= a_2\left(1 - \frac{\omega^2}{\omega_a^2}\right) \end{aligned}\right\} \tag{47a}$$

or, solving for a_1 and a_2,

$$\left.\begin{aligned} \frac{a_1}{x_{st}} &= \frac{1 - \dfrac{\omega^2}{\omega_a^2}}{\left(1 - \dfrac{\omega^2}{\omega_a^2}\right)\left(1 + \dfrac{k}{K} - \dfrac{\omega^2}{\Omega_n^2}\right) - \dfrac{k}{K}} \\ \frac{a_2}{x_{st}} &= \frac{1}{\left(1 - \dfrac{\omega^2}{\omega_a^2}\right)\left(1 + \dfrac{k}{K} - \dfrac{\omega^2}{\Omega_n^2}\right) - \dfrac{k}{K}} \end{aligned}\right\} \tag{48}$$

From the first of these equations the truth of our contention can be seen immediately. The amplitude a_1 of the main mass is zero when the numerator $1 - \dfrac{\omega^2}{\omega_a^2}$ is zero, and this occurs when the frequency of the force is the same as the natural frequency of the absorber.

Let us now examine the second equation (48) for the case that $\omega = \omega_a$. The first factor of the denominator is then zero, so that this equation reduces to

$$a_2 = -\frac{K}{k}x_{st} = -\frac{P_0}{k}$$

With the main mass standing still and the damper mass having a motion $-P_0/k \cdot \sin \omega t$ the force in the damper spring varies as $-P_0 \sin \omega t$, which is actually equal and opposite to the external force.

These relations are true for any value of the ratio ω/Ω_n. It was seen, however, that the addition of an absorber has not much reason unless the original system is in resonance or at least near it. We therefore consider, in what follows, the case for which

$$\omega_a = \Omega_n \qquad \text{or} \qquad \frac{k}{m} = \frac{K}{M} \qquad \text{or} \qquad \frac{k}{K} = \frac{m}{M}$$

The ratio

$$\mu = \frac{m}{M}$$

then defines the size of the damper as compared to the size of the main system. For this special case, (48) becomes

$$\left.\begin{aligned} \frac{x_1}{x_{st}} &= \frac{1 - \dfrac{\omega^2}{\omega_a^2}}{\left(1 - \dfrac{\omega^2}{\omega_a^2}\right)\left(1 + \mu - \dfrac{\omega^2}{\omega_a^2}\right) - \mu} \sin \omega t \\ \frac{x_2}{x_{st}} &= \frac{1}{\left(1 - \dfrac{\omega^2}{\omega_a^2}\right)\left(1 + \mu - \dfrac{\omega^2}{\omega_a^2}\right) - \mu} \sin \omega t \end{aligned}\right\} \tag{49}$$

A striking peculiarity of this result and of Eq. (48) is that the two denominators are equal. This is no coincidence but has a definite physical reason. When multiplied out, it is seen that the denominator contains a term proportional to $(\omega^2/\omega_a^2)^2$, a term proportional to $(\omega^2/\omega_a^2)^1$ and a term independent of this ratio. When equated to zero, the denominator is a quadratic equation in ω^2/ω_a^2 which necessarily has two roots. Thus for two values of the external frequency ω both denominators of (49) become zero, and consequently x_1 as well as x_2 becomes infinitely large. These two frequencies are the *resonant* or *natural* frequencies of

the system. If the two denominators of (49) were *not* equal to each other, it could occur that one of them was zero at a certain ω and the other one not zero. This would mean that x_1 would be infinite and x_2 would not. But, if x_1 is infinite, the extensions and compressions of the damper spring k become infinite and necessarily the force in that spring also. Thus we have the impossible case that the amplitude x_2 of the damper mass m is finite while an infinite force $k(x_1 - x_2)$ is acting on it. Clearly, therefore, if one of the amplitudes becomes infinite, so must the other, and consequently the two denominators in (49) must be the same.

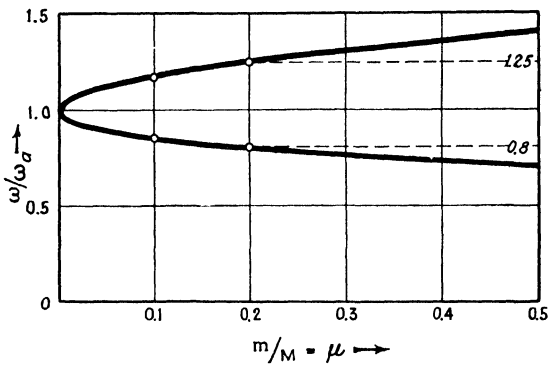


FIG. 74.—The two natural or resonant frequencies of Fig. 73 as a function of the mass ratio m/M, expressed by Eq. (50).

The natural frequencies are determined by setting the denominators equal to zero:

$$\left(1 - \frac{\omega^2}{\omega_a^2}\right)\left(1 + \mu - \frac{\omega^2}{\omega_a^2}\right) - \mu = 0$$

or

$$\left(\frac{\omega}{\omega_a}\right)^4 - \left(\frac{\omega}{\omega_a}\right)^2(2 + \mu) + 1 = 0$$

with the solutions

$$\left(\frac{\omega}{\omega_a}\right)^2 = \left(1 + \frac{\mu}{2}\right) \pm \sqrt{\mu + \frac{\mu^2}{4}} \qquad (50)$$

This relation is shown graphically in Fig. 74, from which we find, for example, that an absorber of one-tenth the mass of the main system causes two natural frequencies of the combined

system at 1.17 and 0.85 times the natural frequency of the original system.

The main result (49) is shown in Figs. 75*a* and *b* for $\mu = \frac{1}{5}$, *i.e.*, for an absorber of one-fifth the mass of the main system.

Follow the diagram 75*a* for an increasing frequency ratio $\omega/\Omega_n = \omega/\omega_a$. It is seen that $x_1/x_{st} = 1$ for $\omega = 0$, while for values somewhat larger than zero x_1 is necessarily positive, since both the numerator and the denominator of Eq. (49*a*) are posi-

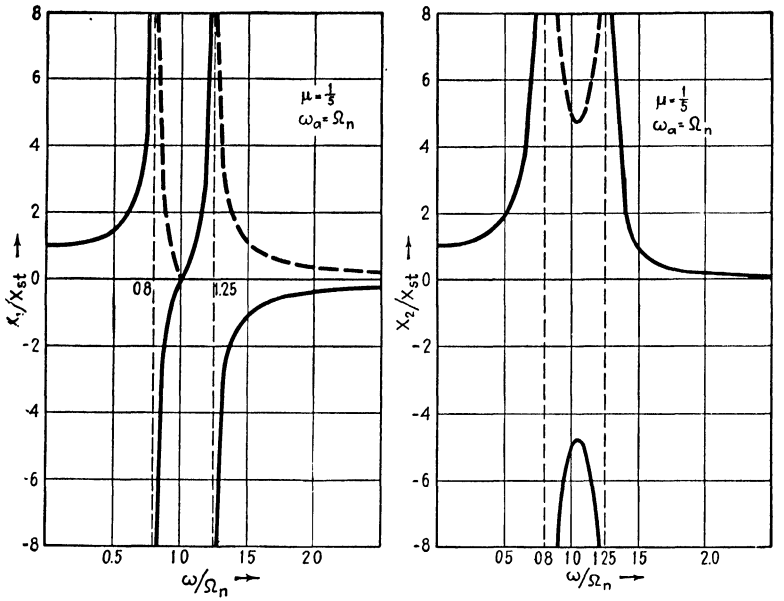


FIG. 75*a* and *b*.—Amplitudes of the main mass (x_1) and of the absorber mass (x_2) of Fig. 73 for various disturbing frequencies ω. The absorber mass is one-fifth of the main mass.

tive. At the first resonance the denominator passes through zero from positive to negative, hence x_1/x_{st} becomes negative. Still later, at $\omega = \Omega_n = \omega_a$, the numerator becomes negative and x_1/x_{st} becomes positive again, since both numerator and denominator are negative. At the second resonance the denominator changes sign once more with negative x_1 as a result.

The x_2/x_{st} diagram passes through similar changes, only here the numerator remains positive throughout, so that changes in sign occur only at the resonance points. It was seen in the discussion of Fig. 38 that such changes in sign merely mean a change of 180 deg. in the phase angle, which is of no particular impor-

tance to us. Therefore we draw the dotted lines in Figs. 75*a* and *b* and consider these lines as determining the amplitude, eliminating from further consideration the parts of the diagrams below the horizontal axes.

The results obtained thus far may be interpreted in another manner, which is useful in certain applications. In Fig. 73 let the Frahm absorber k, m be replaced by a mass m_{equiv} attached solidly to the main mass M, and let this equivalent mass be so chosen that the motion x_1 is the same as with the absorber. Since the absorber is more complicated than just a mass, it is clear that m_{equiv} cannot be constant but must be different for each disturbing frequency ω. The downward force transmitted by the absorber to the main system M is the spring force $k(x_2 - x_1)$, which, by Eq. 45, is equal to $-m\ddot{x}_2$. If a mass m_{eqviv} were solidly attached to M, its downward reaction force on M would be the pure inertia force $-m_{\text{equiv}}\ddot{x}_1$. For equivalence these two reactions must be equal, so that, by Eq. 46 and the second Eq. 47*a*, we have

$$\frac{m_{\text{equiv}}}{m} = \frac{\ddot{x}_2}{\ddot{x}_1} = \frac{x_2}{x_1} = \frac{a_2}{a_1} = \frac{1}{1 - \dfrac{\omega^2}{\omega_a^2}}$$

which is the well-known resonance relation, shown in Fig. 38, page 59. Thus it is seen that the Frahm dynamic-absorber system can be replaced by an equivalent mass attached to the main system, so that the equivalent mass is positive for slow disturbing frequencies, is infinitely large for excitation at the absorber resonant frequency, and is *negative* for high frequency excitation. This way of looking at the operation of the absorber will be found useful on page 274.

From an inspection of Fig. 75*a*, which represents the vibrations of the main mass, it is clear that the undamped dynamic absorber is useful only in cases where the frequency of the disturbing force is nearly constant. Then we can operate at $\omega/\omega_a = \omega/\Omega_n = 1$ with a very small (zero) amplitude. This is the case with all machinery directly coupled to synchronous electric motors or generators. In variable-speed machines, however, such as internal-combustion engines for automotive or aeronautical applications, the device is entirely useless, since we merely replace the original system of one resonant speed (at $\omega/\Omega_n = 1$) by another system with two resonant speeds. But even then the

absorber can be made to work to advantage by the introduction of a certain amount of damping in the absorber spring, as will be discussed in the next section.

An interesting application of the absorber is made in an electric hair clipper which was recently put on the market. It is shown in Fig. 76 and consists of a 60-cycle alternating-current magnet *a* which exerts a 120-cycle alternating force on a vibrating system *b*. System *b* is tuned to a frequency near 120 cycles but sufficiently far removed from it (20 per cent) to insure an amplitude of the cutter *d*, which is not dependent too much on damping. Thus the cutter blade *d* will vibrate at about the same amplitude independent of whether it is cutting much hair or no hair at all.

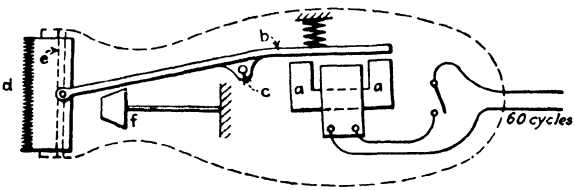


FIG. 76.—Electric hair clipper with vibration absorber. *a* = magnet, *b* = armature tongue, *c* = pivot, *d* = cutter, *e* = guide for cutter, *f* = vibration absorber.

The whole mechanism, being a free body in space without external forces, must have its center of gravity, as well as its principal axes of inertia, at rest. Since the parts *b*, *d* are in motion, the housing must move in the opposite direction to satisfy these two conditions. The housing vibration is unpleasant for the barber's hands and creates a new kind of resistance, known as sales resistance. This is overcome to a great extent by the dynamic vibration absorber *f*, tuned exactly to 120 cycles per second, since it prevents all motion of the housing at the location of the mass *f*. With stroboscopic illumination the masses *d* and *f* are clearly seen to vibrate in phase opposition.

The device as sketched is not perfect, for the mass *f* is not located correctly. At a certain instant during the vibration, the cutter *d* will have a large inertia force upward, while the overhung end *b* will have a small inertia force downward. The resultant of the inertia forces of the moving parts *b*, *d* therefore is an alternating force located to the left of the cutter *d* in Fig. 76.

The effect of the absorber is to completely eliminate 120-cycle motion of a point of the housing right under the absorber mass *f*, but it does not prevent the housing from rotating about that motionless point. Complete elimination of all 120-cycle motion of the housing can be accomplished by mounting two absorbers *f* in the device with a certain distance (perpendicular

to the direction of the cutter motion) between their two masses. The two masses will then automatically assume such amplitudes as to cause two inertia forces which will counteract the force as well as the moment of the inertia action of the cutter assembly d, b, or in different words the two masses will enforce two motionless points of the housing.

For a *torsional* system, such as the crank shaft of an internal-combustion engine, the Frahm dynamic vibration absorber takes the shape of a flywheel A that can rotate freely on the shaft on bearings B and is held to it by mechanical springs k only (Fig. 77a). Since the torsional impulses on such an engine are harmonics of the firing frequency, *i.e.*, have a frequency proportional to the engine speed, the device will work for one engine speed only, while there are two neighboring speeds at which the shaft goes to resonance (Fig. 75a). In order to overcome this, it has been proposed recently to replace the mechanical springs of Fig. 77a by the "centrifugal spring" of Fig. 77b. The pendulum in the centrifugal field of that figure acts in the same manner as an ordinary gravity pendulum in which the field g is replaced by the centrifugal field $r\omega^2$. Since the frequency of a gravity pendulum is $\sqrt{g/l}$, the frequency of a centrifugal pendulum becomes $\omega\sqrt{r/l}$, *i.e.*, proportional to the engine speed. Thus a centrifugal pendulum will act as a Frahm dynamic absorber that is tuned correctly at all engine speeds. Further details of this device are discussed on page 273.

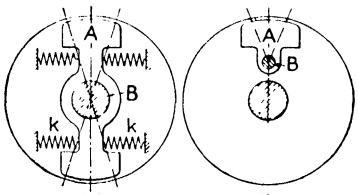


FIG. 77.—Torsional dynamic vibration absorber with mechanical springs (*a*) and with centrifugal springs (*b*).

24. The Damped Vibration Absorber.—Consider the system of Fig. 73 in which a dashpot is arranged parallel to the damper spring k, between the masses M and m. The main spring K remains without dashpot across itself. Newton's law applied to the mass M gives

$$M\ddot{x}_1 + Kx_1 + k(x_1 - x_2) + c(\dot{x}_1 - \dot{x}_2) = P_0 \sin \omega t \quad (51)$$

and applied to the small mass m

$$m\ddot{x}_2 + k(x_2 - x_1) + c(\dot{x}_2 - \dot{x}_1) = 0 \quad (52)$$

The reader should derive these equations and be perfectly clear on the various algebraic signs. The argument followed is analogous to that of page 37 and of page 104. The four terms

on the left-hand side of (51) signify the "inertia force" of M, the main-spring force, the damper-spring force, and the dashpot force. We are interested in a solution for the *forced* vibrations only and do not consider the transient free vibration. Then both x_1 and x_2 are harmonic motions of the frequency ω and can be represented by vectors. Any term in either (51) or (52) is representable by such a vector rotating with velocity ω. The easiest manner of solving these equations is by writing the vectors as complex numbers. The equations then are

$$\begin{aligned} -M\omega^2 x_1 + Kx_1 + k(x_1 - x_2) + j\omega c(x_1 - x_2) &= P_0 \\ -m\omega^2 x_2 + k(x_2 - x_1) + j\omega c(x_2 - x_1) &= 0 \end{aligned}$$

where x_1 and x_2 are (unknown) complex numbers, the other quantities being real.

Bringing the terms with x_1 and x_2 together:

$$\left.\begin{aligned} [-M\omega^2 + K + k + j\omega c]x_1 - [k + j\omega c]x_2 &= P_0 \\ -[k + j\omega c]x_1 + [-m\omega^2 + k + j\omega c]x_2 &= 0 \end{aligned}\right\} \qquad (53)$$

These can be solved for x_1 and x_2. We are primarily interested in the motion of the main mass x_1, and, in order to solve for it, we express x_2 in terms of x_1 by means of the second equation of (53) and then substitute in the first one. This gives

$$x_1 = P_0 \frac{(k - m\omega^2) + j\omega c}{\{(-M\omega^2+K)(-m\omega^2+k) - m\omega^2 k\} + j\omega c\{-M\omega^2+K-m\omega^2\}} \qquad (54)$$

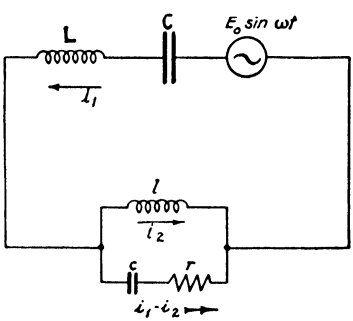


FIG. 78.—Equivalent electric circuit. The small l-c-r "wave trap" corresponds to the absorber.

For readers somewhat familiar with alternating electric currents this result will also be derived by means of the equivalent electric circuit shown in Fig. 78. The equivalence can be established by setting up the voltage equations and comparing them with (51) and (52) or directly by inspection as follows. The extension (or velocity) of the spring K, the displacement (or velocity) of M, and the displacement (or velocity) of the force P_0 are all equal to x_1 (or $\dot{x}_1$). Consequently the corresponding electrical elements $1/C$, L, and E_0 must carry the same current (i_1) and thus must be connected in series. The velocities across k or across the dashpot ($\dot{x}_1 - \dot{x}_2$) are also equal among themselves, so that $1/c$ and r electrically must be in series but must carry

a different current from that in the main elements L, C, and E_0. The velocity of m is $\dot{x}_2$, equal to the difference of the velocity of $M(\dot{x}_1)$ and the velocity across the damper spring $(\dot{x}_1 - \dot{x}_2)$. Hence the current i_2 through l must be equal to the difference of i_1 and $(i_1 - i_2)$. The equivalence of the electrical circuit and the mechanical system is thus established.

We are interested in the main current i_1. The impedance of a coil is $j\omega L$, that of a condenser is $1/j\omega C$, that of a resistance simply R. Impedances in series, when expressed in complex, add directly, and impedances in parallel add reciprocally. Thus the impedance of the c, r branch is $r + \frac{1}{j\omega c}$ and that of the l branch is $j\omega l$. The two branches in parallel have an impedance

$$\frac{1}{\frac{1}{r + 1/j\omega c} + \frac{1}{j\omega l}}$$

To this has to be added the impedance of the other elements in series, giving

$$Z = j\omega L + \frac{1}{j\omega C} + \frac{1}{\frac{1}{r + 1/j\omega c} + \frac{1}{j\omega l}} = \frac{E}{i_1}$$

By performing some algebra on this expression and translating back into mechanics, the result (54) follows.

The complex expression (54) can be reduced to the form

$$x_1 = P_0(A_1 + jB_1) \tag{54a}$$

where A_1 and B_1 are real and do not contain j. The meaning which has to be attached to (54) is then that in vector representation the displacement x_1 consists of two components, one in phase with the force P_0 and another a quarter turn ahead of it (compare Fig. 41*a* on page 70). Adding these two vectors geometrically, the magnitude of x_1 is expressed by

$$x_1 = P_0\sqrt{A_1^2 + B_1^2}.$$

But (54) is not yet in the form (54*a*); it is rather of the form

$$x_1 = P_0\frac{A + jB}{C + jD}$$

which can be transformed as follows:

$$x_1 = P_0 \cdot \frac{(A + jB)(C - jD)}{(C + jD)(C - jD)} = P_0 \cdot \frac{(AC + BD) + j(BC - AD)}{C^2 + D^2}$$

Hence the length of the x_1 vector is

$$\frac{x_1}{P_0} = \sqrt{\left(\frac{AC + BD}{C^2 + D^2}\right)^2 + \left(\frac{BC - AD}{C^2 + D^2}\right)^2}$$

$$= \sqrt{\frac{A^2C^2 + B^2D^2 + B^2C^2 + A^2D^2}{(C^2 + D^2)^2}} = \sqrt{\frac{(A^2 + B^2)(C^2 + D^2)}{(C^2 + D^2)^2}}$$

$$= \sqrt{\frac{A^2 + B^2}{C^2 + D^2}}$$

Applying this to (54), we may write

$$\frac{x_1^2}{P_0^2} = \frac{(k - m\omega^2)^2 + \omega^2c^2}{[(-M\omega^2+K)(-m\omega^2+k) - m\omega^2k]^2+\omega^2c^2(-M\omega^2+K-m\omega^2)^2} \tag{55}$$

which is the *amplitude of the motion of the main mass M*.

It is instructive to verify this result for several particular cases and see that it reduces to known results as previously obtained. The reader is advised to do this for some of the following cases:

1. $k = \infty$
2. $k = 0$; $c = 0$
3. $c = \infty$
4. $c = 0$; $\omega = \Omega_n = \sqrt{K/M} = \sqrt{k/m}$
5. $m = 0$

Thus we are in a position to calculate the amplitude in all cases. In Eq. (55) x_1 is a function of seven variables: P_0, ω, c, K, k, M, and m. However, the number of variables can be reduced, as the following consideration shows. For example, if P_0 is doubled and everything else is kept the same, we should expect to see x_1 doubled, and there are several relations of this same character. In order to reveal them, it is useful to write Eq. (55) in a dimensionless form, for which purpose the following symbols are introduced:

$$\left.\begin{aligned}
\mu &= m/M = \text{mass ratio} = \text{absorber mass/main mass} \\
\omega_a^2 &= k/m = \text{natural frequency of absorber} \\
\Omega_n^2 &= K/M = \text{natural frequency of main system} \\
\mathbf{f} &= \omega_a/\Omega_n = \text{frequency ratio (natural frequencies)} \\
\mathbf{g} &= \omega/\Omega_n = \text{forced frequency ratio} \\
x_{st} &= P_0/K = \text{static deflection of system} \\
c_c &= 2m\Omega_n = \text{"critical" damping (see page 52)}
\end{aligned}\right\} \tag{56}$$

After performing some algebra Eq. (55) is transformed into

$$\frac{x_1}{x_{st}} = \sqrt{\frac{\left(2\frac{c}{c_c}\mathbf{g}\right)^2 + (\mathbf{g}^2 - \mathbf{f}^2)^2}{\left(2\frac{c}{c_c}\mathbf{g}\right)^2(\mathbf{g}^2 - 1 + \mu\mathbf{g}^2)^2 + [\mu\mathbf{f}^2\mathbf{g}^2 - (\mathbf{g}^2 - 1)(\mathbf{g}^2 - \mathbf{f}^2)]^2}} \tag{57}$$

This is the amplitude ratio x_1/x_{st} of the main mass as a function of the four essential variables μ, c/c_c, $\mathbf{f}$, and $\mathbf{g}$. Figure 79 shows a plot of x_1/x_{st} as a function of the frequency ratio $\mathbf{g}$ for the definite

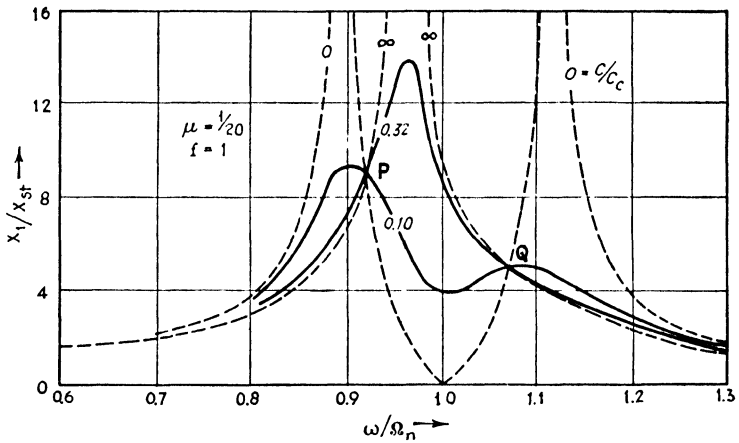


FIG. 79.—Amplitudes of the main mass of Fig. 73 for various values of absorber damping. The absorber is twenty times as small as the main machine and is tuned to the same frequency. All curves pass through the fixed points P and Q.

system: $\mathbf{f} = 1$, $\mu = 1/20$, and for various values of the damping c/c_c. In other words, the figure describes the behavior of a system in which the main mass is 20 times as great as the damper mass, while the frequency of the damper is equal to the frequency of the main system ($\mathbf{f} = 1$).

It is interesting to follow what happens for increasing damping. For $c = 0$ we have the same case as Fig. 75*a*, a known result. When the damping becomes infinite, the two masses are virtually clamped together and we have a single-degree-of-freedom system with a mass $21/20M$. Two other curves are drawn in Fig. 79, for $c/c_c = 0.10$ and 0.32.

In adding the absorber to the system, the object is to bring the resonant peak of the amplitude down to its lowest possible value. With $c = 0$ the peak is infinite; with $c = \infty$ it is again infinite. Somewhere in between there must be a value of c for which the peak becomes a minimum.

This situation also can be understood physically as follows. It was learned on page 62 that the amplitude at resonance of a single-degree-of-freedom system is limited by damping only. It was seen that damping energy is dissipated, *i.e.*, converted into heat. When the damping force does considerable work, the amplitude remains small at resonance. This is a relation that holds for more complicated systems also. The work done by the damping force is given by the force times the displacement through which it operates. In our case the displacement is the relative motion between the two masses or also the extension of the damper spring. If $c = 0$, the damping *force* is zero, no work is done, and hence the resonant amplitude is infinite. But when $c = \infty$, the two masses are locked to each other so that their relative *displacement* is zero and again no work is done. Somewhere in between 0 and ∞ there is a damping for which the product of damping force and displacement becomes a maximum, and then the resonant amplitude will be small.

Before proceeding to a calculation of this "optimum damping," we observe a remarkable peculiarity in Fig. 79, *viz.*, that all four curves intersect at the two points P and Q. (See Fig. 52, p. 91.) This, we shall presently prove, is no accident; *all curves pass through these two points independent of the damping.* If we can calculate their location, our problem is practically solved, because *the most favorable curve is the one which passes with a horizontal tangent through the highest of the two fixed points P or Q.* The best obtainable "resonant amplitude" (at optimum damping) is the ordinate of that point.

Even this is not all that can be done. By changing the relative "tuning" $\mathbf{f} = \omega_a/\Omega_n$ of the damper with respect to the main system, the two fixed points P and Q can be shifted up and down the curve for $c = 0$. By changing **f**, one point goes up and the other down. Clearly the most favorable case is such that *first* by a proper choice of **f** the two fixed points are adjusted to equal heights, and *second* by a proper choice of c/c_c the curve is adjusted to pass with a horizontal tangent through *one* of them. It will be seen later (Fig. 80) that it makes practically no difference which one of the two (P or Q) we choose.

Now return to Eq. (57) to see if there are any values of **g** for which x_1/x_{st} becomes independent of c/c_c. The formula is of the form

$$\frac{x_1}{x_{st}} = \sqrt{\frac{A\left(\frac{c}{c_c}\right)^2 + B}{C\left(\frac{c}{c_c}\right)^2 + D}}$$

This is independent of damping if $A/C = B/D$, or written out fully, if

$$\left(\frac{1}{\mathbf{g}^2 - 1 + \mu\mathbf{g}^2}\right)^2 = \left(\frac{\mathbf{g}^2 - \mathbf{f}^2}{\mu\mathbf{f}^2\mathbf{g}^2 - (\mathbf{g}^2 - 1)(\mathbf{g}^2 - \mathbf{f}^2)}\right)^2$$

We can obliterate the square sign on both sides but then have to add a $\pm$ in front of the right-hand side. With the minus sign, after cross-multiplication,

$$\mu\mathbf{f}^2\mathbf{g}^2 - (\mathbf{g}^2 - 1)(\mathbf{g}^2 - \mathbf{f}^2) = -(\mathbf{g}^2 - \mathbf{f}^2)(\mathbf{g}^2 - 1 + \mu\mathbf{g}^2) \quad (58)$$

It is seen that the whole of the second term on the left-hand side cancels a part of the right-hand side, so that

$$\mu\mathbf{f}^2\mathbf{g}^2 = -\mu\mathbf{g}^2(\mathbf{g}^2 - \mathbf{f}^2)$$

or

$$\mathbf{f}^2 = -\mathbf{g}^2 + \mathbf{f}^2 \qquad \text{so that} \qquad \mathbf{g}^2 = 0$$

This is a trivial (but true) result. At $\mathbf{g} = 0$ or $\omega = 0$ the amplitude is x_{st}, independent of the damping, simply because things move so slowly that there is no chance for a damping force to build up (damping is proportional to velocity).

The other alternative is the plus sign before the right-hand side of (58). After a short calculation the equation then becomes

$$\mathbf{g}^4 - 2\mathbf{g}^2\frac{1 + \mathbf{f}^2 + \mu\mathbf{f}^2}{2 + \mu} + \frac{2\mathbf{f}^2}{2 + \mu} = 0 \quad (59)$$

This is a quadratic equation in $\mathbf{g}^2$, giving *two values*, the "fixed points" we are seeking. Let the two roots of this equation be $\mathbf{g}_1^2$ and $\mathbf{g}_2^2$. It is seen that $\mathbf{g}_1$ and $\mathbf{g}_2$ (*i.e.*, the horizontal coordinates of the fixed points P and Q) are still functions of μ and $\mathbf{f}$.

Our next objective is to adjust the tuning $\mathbf{f}$ so that the ordinates x/x_{st} of P and Q are equal. To solve Eq. (59) for $\mathbf{g}_1$ and $\mathbf{g}_2$, to substitute these values in (57), and then to equate the two expressions so obtained is very time consuming. Fortunately, it is not necessary. In the first place, we remember that at P and Q the value of x/x_{st} is *independent* of the damping, so we may as well select such a value of c/c_c that (57) reduces to its simplest possible form. This happens for $c = \infty$, when (57) becomes

$$\frac{x_1}{x_{st}} = \frac{1}{1 - \mathbf{g}^2(1 + \mu)} \tag{60}$$

Substituting $\mathbf{g}_1$ and $\mathbf{g}_2$ in this equation gives

$$\frac{1}{1 - \mathbf{g}_1^2(1 + \mu)} = \frac{1}{1 - \mathbf{g}_2^2(1 + \mu)} \tag{61}$$

However, this is not quite correct for the following reason. Equation (60) is really not represented by the curve $c = \infty$ of Fig. 79 but rather by a curve which is negative for values of $\mathbf{g}$ larger than $1/\sqrt{1 + \mu}$ (see also Fig. 38). Since P and Q lie on different sides of this value of $\mathbf{g}$, the ordinate of P is positive and that of Q negative, so that Eq. (61) should be corrected by a minus sign on one side or the other. By simple algebra the equation, thus corrected, becomes

$$\mathbf{g}_1^2 + \mathbf{g}_2^2 = \frac{2}{1 + \mu} \tag{62}$$

Now it is not even necessary to solve Eq. (59) for $\mathbf{g}_1$ and $\mathbf{g}_2$, if we remember that the negative coefficient of the middle term in a quadratic equation is equal to the sum of the roots. In Eq. (59) that sum is

$$\mathbf{g}_1^2 + \mathbf{g}_2^2 = \frac{2(1 + \mathbf{f}^2 + \mu\mathbf{f}^2)}{2 + \mu}$$

Substitute this in Eq. (62) with the result that

$$\mathbf{f} = \frac{1}{1 + \mu} \tag{63}$$

This very simple formula gives the correct "tuning" for each absorber size. For a very small absorber ($\mu \approx 0$) the tuning $\mathbf{f} \approx 1$, or the damper frequency should be the same as the main-system frequency. For a damper one-fifth as large as the main mass, $\mathbf{f} = \frac{5}{6}$ or the damper has to be made 17 per cent slower than the main system.

Now we know how to tune, but we do not know yet what amplitude x/x_{st} we shall finally get. Figure 80 is a case of such tuning for $\mu = \frac{1}{4}$. Two curves are drawn. One passes horizontally through P and then is *not* horizontal at Q; the other is horizontal at Q and not at P. It is seen that practically no error is made by taking the amplitude of either point as the maximum amplitude of the curve. This amplitude is easily

calculated. Merely substitute a root of (59) in the expression for x_1/x_{st}, and since at this point, (P or Q) x_1/x_{st} is independent of damping, take for it form (60). The result is

$$\frac{x_1}{x_{st}} = \sqrt{1 + \frac{2}{\mu}} \tag{64}$$

This represents the most favorable possibility, if the natural frequency of the damper differs from that of the main system in the manner prescribed by (63).

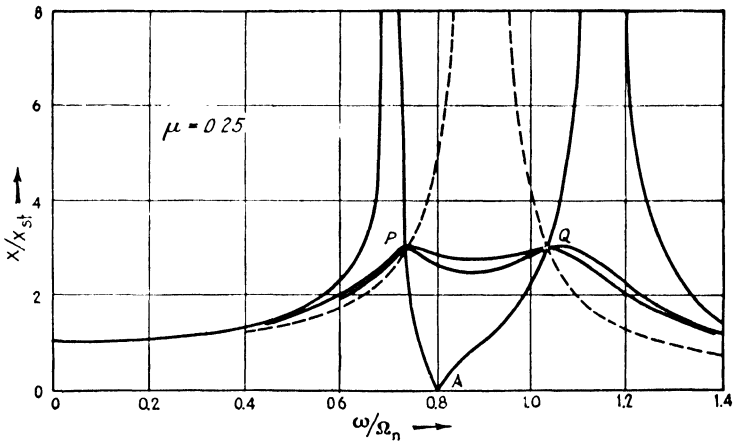


FIG. 80.—Resonance curves for the motion of the main mass fitted with the most favorably tuned vibration absorber system of one-fourth of the size of the main machine.

It is interesting to compare the result (64) with some other cases which are sometimes encountered in actual machines (Fig. 81).

First, consider the *vibration absorber with constant tuning*, $\mathbf{f} = 1$, where the small damper is tuned to the same frequency as the main system, independent of the size of the damper. The equation for the two fixed points (59) becomes

$$\mathbf{g}^4 - 2\mathbf{g}^2 + \frac{2}{2+\mu} = 0$$

or

$$\mathbf{g}^2 = 1 \pm \sqrt{\frac{\mu}{2+\mu}}$$

For the usual damper sizes, the peak for the *smaller* $\mathbf{g}$ is higher than for the larger $\mathbf{g}$ (see Fig. 79; also check the location of

the fixed points with the formula). Thus we substitute $\mathbf{g}^2 = 1 - \sqrt{\frac{\mu}{2+\mu}}$ in (60), with the result that

$$\frac{x_1}{x_{st}} = \frac{1}{-\mu + (1+\mu)\sqrt{\frac{\mu}{2+\mu}}} \tag{65}$$

Next, consider the apparatus known as the "Lanchester damper" (see page 255) with viscous friction, consisting of the system of Fig. 73, in which the damper spring has been replaced

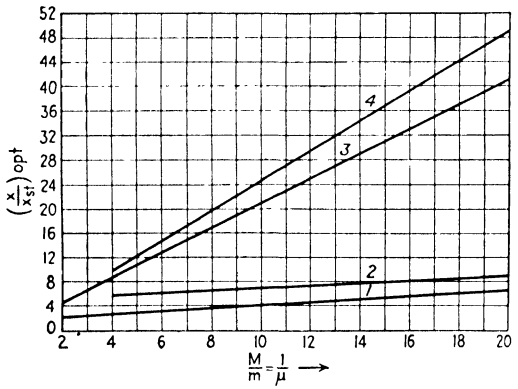


FIG. 81*a*.—Peak amplitudes of the main mass as a function of the ratio m/M for various absorbers attached to the main mass: curve 1 for the most favorably tuned and damped absorber; curve 2 for the most favorably damped absorber tuned to the frequency of the main system; curve 3 for the most favorably damped viscous Lanchester damper; curve 4 for the most favorably damped Coulomb Lanchester damper.

by a linear dashpot. Thus $k = 0$ and it is seen from Eq. (56) that ω_a and $\mathbf{f}$ also are zero. The fixed-point equation (59) becomes

$$\mathbf{g}^4 - 2\mathbf{g}^2\frac{1}{2+\mu} = 0$$

so that one of the fixed points is permanently at $\mathbf{g}_P = 0$, and the other is given by

$$\mathbf{g}_Q^2 = \frac{2}{2+\mu} \tag{66}$$

The undamped and the infinitely damped constructions are single-degree-of-freedom systems, because in the first case the damper mass is completely loose and in the second case it is rigidly

coupled to the main mass. This is shown clearly in Fig. 82, from which we also can conclude that the most favorable resonant amplitude is that of the fixed point Q. Substitute (66) in (60)

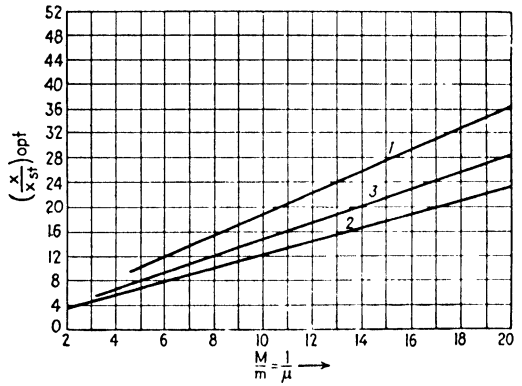


FIG. 81*b*.—Peak relative amplitudes between the masses M and m for various absorbers: curve 1 for the most favorably tuned and damped absorber; curve 2 for the most favorably damped absorber tuned to the frequency of the main system; curve 3 for the viscous Lanchester damper.

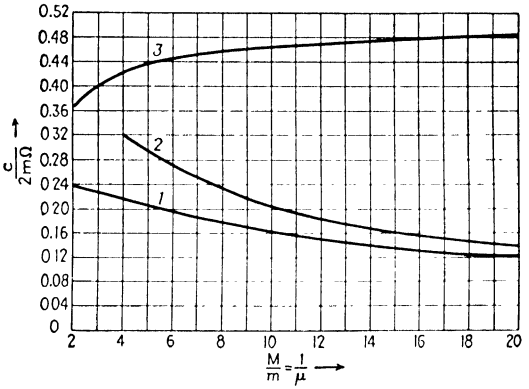


FIG. 81*c*.—Damping constants required for most favorable operation of the absorber, *i.e.*, for obtaining the results of Figs. 81*a* and 81*b*: curve 1 for the most favorably tuned absorber; curve 2 for the absorber tuned to the frequency of the main system; curve 3 for the viscous Lanchester damper (see Problem 53).

and find, for the optimum amplitude,

$$\frac{x_1}{x_{st}} = 1 + \frac{2}{\mu} \tag{67}$$

The usual construction of the Lanchester damper, however, does not have viscous friction but rather "Coulomb" or dry friction. The analysis of that case is more complicated and will

be discussed on page 257. The result for the most favorable resonant amplitude with such a damper is approximately

$$\frac{x_1}{x_{st}} = \frac{\pi^2}{4\mu} = \frac{2.46}{\mu} \tag{68}$$

The four cases already treated are shown in the curves of Fig. 81*a*. A damper of $\mu = 1/10$ or $1/12$ is a practical size. It is seen that the springless or Lanchester dampers are much less efficient than the spring dampers or "damped dynamic absorbers." However, the design of the correct spring in the dynamic absorber is often difficult, because the small amplitudes

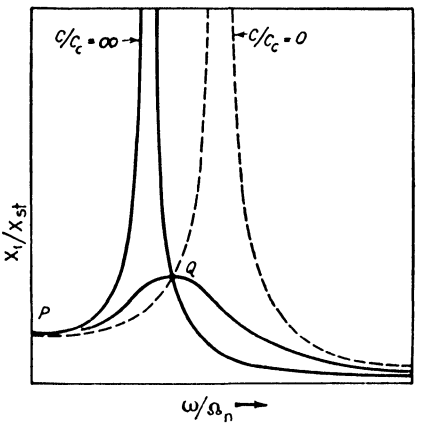


FIG. 82.—Resonance curves of a simple system equipped with a Lanchester damper with viscous friction for zero damping, infinite damping and optimum damping. All curves pass through the fixed points P and Q.

of the main mass are obtained at the expense of large deflections and stresses in the damper spring.

Before proceeding with the calculation of the stress in the damper spring, it is necessary to find the optimum damping; $(c/c_c)_{opt}$. The optimum amplitude was found merely by stating that there must be a value of c/c_c for which the curve passes horizontally through either P or Q in Fig. 80. The damping at which this occurs has not been determined as yet, and now for the first time complications arise.

Start from Eq. (57) and substitute Eq. (63) into it in order to make it apply to the case of "optimum tuning." Differentiate the so modified Eq. (57) with respect to **g**, thus finding the slope, and equate that slope to zero for the point P. From the equation thus obtained c/c_c can be calculated. This is a long and tedious job which leads to the result

$$\left(\frac{c}{c_c}\right)^2 = \frac{\mu(3 - \sqrt{\mu/\mu + 2}}{8(1 + \mu)^3},$$

as shown in the paper by Brock, quoted in the Bibliography. On the other hand, if $dx/d\mathbf{g}$ is set equal to zero, not at point P, but rather at point Q, and the resulting equation is solved for c/c_c, we get

$$\left(\frac{c}{c_c}\right)^2 = \frac{\mu(3 + \sqrt{\mu/\mu + 2}}{8(1 + \mu)^3},$$

A useful average value between the two gives *the optimum damping for the case, Eq.* (63), *of optimum tuning:*

$$\left(\frac{c}{c_c}\right)^2 = \frac{3\mu}{8(1 + \mu)^3}, \tag{69}$$

The same procedure applied to the case of the *constantly tuned absorber* $\mathbf{f} = 1$, for zero slope at P, gives

$$\left(\frac{c}{c_c}\right)^2 = \frac{\mu(\mu + 3)(1 + \sqrt{\mu/\mu + 2})}{8(1 + \mu)} \tag{69a}$$

Similarly, for the *Lanchester damper* $\mathbf{f} = 0$ (Fig. 82), zero damping at Q is attained for

$$\left(\frac{c}{c_c}\right)^2 = \frac{1}{2(2 + \mu)(1 + \mu)} \tag{69b}$$

These results are shown graphically in Fig. 81*c*.

Now we are ready to find the relative motion between the two masses M and m, determining the stress in the damper spring. An exact calculation of this quantity would be very laborious, because it would be necessary to go back to the original differential equations. Therefore we are satisfied with an approximation and make use of the relation found on page 63, stating that near a maximum or resonant amplitude the phase angle between force and motion is 90 deg.

Thus the work done per cycle by the force P_0 is [see Eq. (9), page 14]

$$W = \pi P_0 x_1 \sin 90° = \pi P_0 x_1$$

This is approximate, but the approximation is rather good because, even if φ differs considerably from 90 deg., $\sin \varphi$ does not differ much from unity.

On the other hand, the work dissipated per cycle by damping is, by the same formula, $\pi \times$ damping force $\times$ relative amplitude x_{rel}, since the damping force being in phase with the *velocity* has *exactly* 90-deg. phase angle with the displacement amplitude. Thus

$$W_{\text{dissipated}} = \pi(c\omega x_{\text{rel}}) \cdot x_{\text{rel}} = \pi c\omega x_{\text{rel}}^2$$

Equating the two,

$$\pi P_0 x_1 = \pi c\omega x_{\text{rel}}^2$$

or

$$x_{\text{rel}}^2 = \frac{P_0 x_1}{c\omega}$$

Written in a dimensionless form this becomes

$$\left(\frac{x_{rel}}{x_{st}}\right)^2 = \frac{x_1}{x_{st}} \cdot \frac{1}{2\mu g c/c_c} \tag{70}$$

This formula determines the relative motion and consequently the stress in the damper spring. Upon substitution of the proper values for μ, **g**, etc., this formula is applicable to the viscous Lanchester damper, as well as to the two kinds of dynamic absorbers.

The curves of Fig. 81*b* show the results of these calculations. It is seen that the relative motions or spring extensions are quite large, three or four times as large as the motion of the main system. If springs can be designed to withstand such stresses in fatigue, all is well, but this quite often will prove to be very difficult, if not impossible, within the space available for the springs. This is the reason why the Lanchester damper, though very much less effective than the spring absorber, enjoys a wide practical use.

Example: It is desired to design a damper for the system of Fig. 73, in which $Mg = 10$ lb.; $mg = 1$ lb.; $P_0 = 1$ lb., and $K = 102$ lb./in., which will operate for all frequencies of the disturbing force. If first the absorber spring is taken as $k = 10.2$ lb. in.,

a. What is the best damping coefficient across the absorber?

b. What is the maximum amplitude of the main mass?

c. What is the maximum stress in the absorber spring?

Further, if we drop the requirement $k/K = m/M$,

d. For what k is the best over-all effect obtained?

e. Same question as *a* but now for the new value of k.

f. Same question as *b* but now for the new value of k.

g. Same question as *c* but now for the new value of k.

Solution: The answers are all contained in Figs. 81*a*, *b*, and *c*.

a. From Fig. 81*c* we find: $c/2m\Omega_n = 0.205$ or

$$c = 0.41 m\Omega_n = 0.41 \tfrac{1}{386}\, 20\pi = 0.067 \text{ lb./in./sec.}$$

b. Figure 81*a* or Eq. (65) gives $x/x_{st} = 7.2$,

$$x_{st} = P_0/K = \tfrac{1}{102}, \text{ so that } x = 7.2/102 = 0.071 \text{ in.}$$

c. Figure 81*b* gives for the relative motion across the absorber spring $x_{rel}/x_{st} = 12.8$ so that $x_{rel} = 12.8/102 = 0.126$ in. The force is $kx_{rel} = 10.2 \times 0.126 = 1.28$ lb.

d. The most favorable tuning follows from Eq. (63): $\frac{\omega_a}{\Omega_n} = \frac{1}{1+\mu} = \frac{10}{11}$, so that $\left(\frac{\omega_a}{\Omega_n}\right)^2 = \frac{100}{121}$. Since m, M, and K are the same now as in all previous questions, $(\omega_a/\Omega_n)^2$ is proportional to k. Thus the new absorber spring should be

$$k = \tfrac{100}{121} \times 10.2 = 8.4 \text{ lb./in.}$$

e. Figure 81*c* gives $c/2m\Omega_n = 0.166$. Since $2m\Omega_n$ is the same as in question *a*, we have

$$c = \frac{0.166}{0.205} \times 0.067 = 0.054 \text{ lb. in.}^{-1} \text{ sec.}$$

f. From Fig. 81*a* or Eq. (64) we find $x/x_{st} = 4.6$. Since from *b* we have $x_{st} = 1/102$, the maximum amplitude is

$$x = \frac{4.6}{102} = 0.045 \text{ in.}$$

g. Figure 81*b* gives $x_{rel}/x_{st} = 19.5$, so that $x_{rel} = 19.5/102 = 0.191$ in. With $k = 8.4$ lb./in., this leads to a maximum force in the spring of $8.4 \times 0.191 = 1.60$ lb.

The principal applications of dampers and absorbers of this type are in internal-combustion engines (page 266) and in ship stabilization, which will be treated in the next section. However, an "absorber" may be present in a construction without being very conspicuous.

An example of this is found in the gears of electric street cars which, in operation, may be ringing like bells if no precautions are taken. In fact a great part of the objectionable noise in street cars is caused by their gears. It has been found by experience that this noise can be eliminated to a great extent (the wheels "deadened") by shrinking two steel or cast-iron rings *a*, *a* (Fig. 83) on the inside of the rim. If the shrink fit is too loose, no deadening occurs; if it is shrunk very tight the effect is again very small, but for some intermediate shrink pressure the deadening effect is astonishingly complete. Two identical gears, one with and the other without rings, may be placed upright on the ground and their rims struck with a hammer. The first gear will sound like a piece of lead while the second one will ring for ten or more seconds. The cast-iron inserts evidently act as Lanchester dampers.

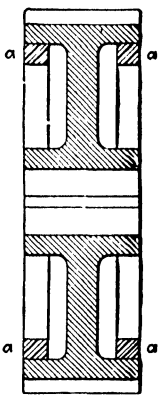


FIG. 83.—Gear with sound-deadening rings inserted. These should be either shrunk or tack-welded in a few spots so as to allow some relative rubbing during the vibration.

25. Ship Stabilization by Means of Frahm Tanks.—One of the most interesting applications of the rather lengthy theory of the preceding section is the prevention of the "rolling" of ships in a rough sea by means of certain devices installed on board.

First consider the rolling of the ship itself without any damping device. Imagine the ship to be floating in still water (Fig. 84*a*), the weight **W** and the buoyancy **B** being two equal and opposite forces both passing through the center of gravity *G*. Now hold the ship at a *slightly* inclined position by some external couple (Fig. 84*b*). The weight **W** still acts through the point *G*, but the buoyancy force **B** is displaced slightly to the left. The line of action of this force intersects the center line of the ship in some point *M*, which is technically known as the *metacenter*. It is clear that the location of this point is determined by the geometry of the hull of the ship. The distance *h* between *M* and *G* is called the *metacentric height*.

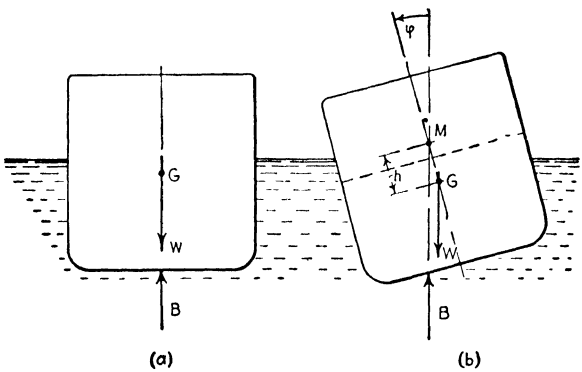


FIG. 84.—The buoyancy and weight forces acting on a ship. For stability the metacenter *M* has to be located above the center of gravity *G*. The distance *MG* is the metacentric height *h*.

The determination of this quantity from a drawing of the ship is an important task of the designer, since upon it the rolling *stability* depends. In Fig. 84*b* it is seen that the forces **W** and **B** form a couple tending to restore the ship to its vertical position. This is always the case when the metacenter is above the center of gravity or when the metacentric height *h* is positive. In case *h* were negative, the **W-B** couple of Fig. 84*b* would tend to increase the inclination of the ship and the equilibrium would be unstable.

Example: A ship has a rectangular cross section and the submerged part has a square section of which the sides have a length $2a$. The center of gravity lies in the vertical line of symmetry at a height x above the bottom of the ship. For small values of x the ship is stable, for large values of x it is statically unstable. Find the value of x where the equilibrium is just indifferent.

Solution: Consider a submerged piece of the ship of dimensions $2a \times 2a \times 1$ in. By taking such a slab of unit thickness we gain the advantage that the submerged volumes become numerically equal to the corresponding cross-sectional areas. By tilting through the angle φ the submerged figure changes from a square to a square from which a small triangle has been subtracted on the right side and to which a similar triangle has been added at the left side. The area of such a triangle is $a/2 \times a\varphi = a^2\varphi/2$. Since the center of gravity of these triangles is at one-third of the height from the base, the shift of the triangle from right to left shifts the center of gravity of an area $a^2\varphi/2$ through a distance of $\frac{2}{3} \cdot 2a$. The product of these quantities equals the total area of the square $4a^2$ multiplied by the horizontal shift y of the center of gravity of the whole figure. Thus

$$4a^2y = \tfrac{2}{3}a^3\varphi \qquad \text{or} \qquad y = \frac{a\varphi}{6}$$

The center of gravity of the submerged figure is shifted to the left over this distance from the original vertical axis of symmetry. A vertical line through this new center of gravity intersects the symmetry axis at a distance $a/6$ above the original location of the center of gravity. Since this intersection is the metacenter M, we find that M lies at a distance of $a + \frac{a}{6} = \frac{7}{6}a$ above the bottom of the ship. This is also the desired position of the center of gravity of the ship for indifferent equilibrium.

The ship is a vibratory system, since when it is displaced from its equilibrium position it shows a tendency to come back. For small angles φ the location of M is independent of φ. The restoring couple is $-\mathbf{W}h \sin \varphi$ or $-\mathbf{W}h\varphi$ for sufficiently small φ. By the action of this couple the ship will roll back about some longitudinal axis. Let the moment of inertia about that axis be I_s (the subscript s stands for ship). Newton's law can be written

$$I_s\ddot{\varphi} = -\mathbf{W}h\varphi$$

or

$$\ddot{\varphi} + \frac{\mathbf{W}h}{I_s}\varphi = 0 \tag{71}$$

which we recognize as Eq. (13) of page 42 for the undamped single-degree-of-freedom system. Consequently the ship rolls with a natural frequency

$$\omega_s = \sqrt{\frac{\mathbf{W}h}{I_s}} \tag{72}$$

Of the quantities appearing in this equation, $\mathbf{W}$ and h can be determined rather accurately from drawings before the ship is built. This is not so for I_s, which is somewhat open to conjec-

ture because we do not know exactly about what axis the ship rolls. It would be the axis through G, *if* during the rolling the water exerted no lateral forces on the hull. Since this is *not* the case, the center of rotation is somewhat below G. The exact location can best be determined by an experiment on a model in which $\mathbf{W}$ and ω_s are measured in the test, h is calculated or

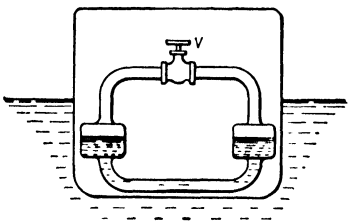


FIG. 85.—Frahm antirolling tanks, old type.

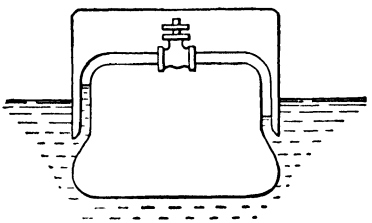


FIG. 86. Modern "blister" construction of Frahm's antirolling tanks.

possibly measured by a *static* test, and I_s is then calculated from (72).

Imagine the ship to be in a rough sea. Waves will strike it more or less periodically and exert a variable couple on it. Though this action is not very regular, it may be regarded approximately as a harmonic disturbing torque $T_0 \sin \omega t$ to be written on the right-hand side of Eq. (71). In case the wave frequency ω is near to the natural frequency ω_s of the ship's roll, the oscillations may become very large. In rough seas the angle φ has been observed to reach 20 deg. Equations (71) and (72) tell us that, as far as vibrational properties go, the system of Fig. 84 is equivalent to Fig. 24 or to the upper part of Fig. 73. Therefore the addition of a damper of the type shown in Fig. 73 should help. This has been done by Frahm, in 1902, who built into a ship a system of two tanks (Fig. 85) half filled with water, communicating through a water pipe below and through an air pipe with valve V above. The secondary or "absorber" system corresponds approximately to Fig. 31, page 48.

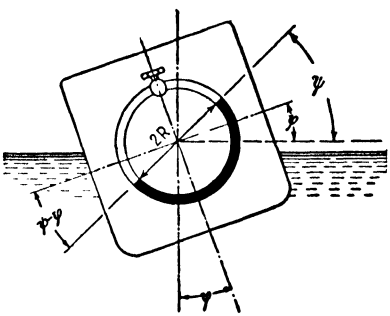


FIG. 87.—Idealized Frahm tank showing definition of R, φ, and ψ.

In more recent constructions the lower connecting pipe between the tanks is omitted and is replaced by the open ocean as indicated in Fig. 86. The "blisters" extend along two-thirds the length of the ship and are subdivided into three or more compartments by vertical partitions. Thus there are three or more air pipes with valves. Both these constructions are really more complicated than Fig. 77, though the older construction, Fig. 85, comes quite close to it.

In order to derive the differential equations, let us idealize Fig. 85 to such an extent that the tanks and the two connecting pipes are arranged in a circle of radius R with the center of rotation of the ship as center (Fig. 87). Moreover, there is so much water in this circular pipe of constant cross section A that just 180 deg. of it is filled. Further let

φ = angle of the ship
ψ = angle of tank-water level with respect to sea
$\psi - \varphi$ = angle of tank-water level with respect to ship
I_s = moment of inertia of ship + tank water clamped solid at $\psi - \varphi = 0$
I_w = moment of inertia of tank water about center of rotation
$K_s\varphi$ = static torque exerted on ship by ocean for a small angle φ with tank water clamped at $\psi - \varphi = 0$
$k_w\psi$ = static torque exerted on ship for $\varphi = 0$ and a small angle ψ (in radians)
c = friction torque on ship when φ, $\dot{\varphi}$, and ψ are zero while $\dot{\psi}$ is 1 rad. per second
$T_0 \sin \omega t$ = external torque on ship due to sea waves.

We shall now set up Newton's equation, first for the ship and then for the tank water. On the ship four external torques are acting: first, $-K_s\varphi$ due to the quiet ocean water trying to right the ship; second, $-k_w(\psi - \varphi)$ from the tank water which is displaced from one tank to the other; third, $-c(\dot{\varphi} - \dot{\psi})$ from the friction of the tank water moving through the pipes (and from the air through the throttle valve); and fourth, $T_0 \sin \omega t$, the disturbing torque from the waves. The sum of these, being the total torque on the ship, must be equal to $I_s\ddot{\varphi}$. The equation of motion of the tank water can be derived in a like manner:

$$\left.\begin{aligned} I_s\ddot{\varphi} + K_s\varphi - k_w(\varphi - \psi) + c(\dot{\varphi} - \dot{\psi}) &= T_0 \sin \omega t \\ I_w\ddot{\psi} + k_w\psi + c(\psi - \dot{\varphi}) &= 0 \end{aligned}\right\} \quad (73)$$

It is well to consider how the various constants K_s, k_w, etc., can be found from Fig. 87. The ship's "spring constant" K_s is Wh, the product of the weight and the metacentric height.

The spring constant of the water k_w should be calculated by the reader to be $2R^2A\gamma$, where γ is the weight of 1 cu. in. of water and A is the cross-sectional area of the tube. The unit friction torque c is caused not so much by the water flowing through the pipes directly as by the air passing through the throttle valve.

Comparing Eqs. (73) with (51) and (52), it is seen that they do not coincide completely, the difference being that the spring torque in the secondary equation is proportional to $x_2 - x_1$ in the first case and to ψ alone in the second case. Though this means that the numerical results of Fig. 81 are not directly applicable to the Frahm antirolling tank, the *general conclusions* are the same. These state that

1. When the throttle valve is completely closed ($c = \infty$), the roll of the ship is not diminished by the tank (Fig. 79).

2. When the throttle is completely open ($c = 0$), the roll is not diminished either; in fact, it becomes large for *two* different sea-wave frequencies.

3. There exists a setting of the throttle between the two extremes where the roll is effectively diminished at *all* sea-wave frequencies.

The foregoing analysis applies to Fig. 87, which is an idealization of Fig. 85. In the case of the construction shown in Fig. 86 it is still more difficult to precalculate exactly what happens. With the ship standing still, the water in the tanks is in itself a two-degree-of-freedom system. In Fig. 85 the water level in one tank determines that in the other, so that everything is described by giving the level in one of the tanks only. In Fig. 86, however, the two water heights are independent of each other and thus require two numbers to specify the configuration. Consequently the ship-tank assembly has three degrees of freedom and three resonant frequencies. This makes it practically impossible to make an exact calculation. But the three general conclusions just mentioned still hold.

In practice the tanks in either construction are designed so that the period of the water motion in them is approximately equal to the natural period of roll of the ship (corresponding to the absorber with "constant tuning" of Fig. 81). In a rough

sea the valve in the air pipe is adjusted to give the best possible operating condition.

Frahm antirolling tanks were installed on the large German liners "Bremen" and "Europa." For the more modern construction of "activated" tanks, where the water is pumped from one tank to the other, see page 142.

26. Gyroscopic Ship Stabilizers.—Another method of reducing ship roll, which apparently is entirely different from Frahm's tanks but really operates on much the same principle, is the *gyroscope of Schlick* (Fig. 88). This device consists of a heavy gyroscope rotating at high speed about a vertical axis. The gyroscope bearings AA are mounted in a frame which is suspended in two bearings BB so that the frame is capable of rotation about an axis across the ship. The axis BB lies *above* the center of gravity of the gyroscope and its frame. A brake drum C is attached to BB, so that the swinging motion of the gyroscope frame can be damped. The weight of the gyrorotor is of the order of 1 per cent of the ship's weight. It is driven electrically to the highest possible speed compatible with its bursting strength under centrifugal stress.

For an understanding of the operation of this device, it is necessary to know the main property of a gyroscope, namely that the torque exerted on it is represented vectorially by the rate of change of the angular momentum vector. For readers not entirely familiar with this theorem, a short exposition of it is given in Appendix I on page 453.

Let the direction of rotation of the rotor be counterclockwise when viewed from above, so that the momentum vector $\mathfrak{M}$ points upward. When the ship is rolling clockwise (viewed from the rear) with the angular velocity $\dot{\varphi}$, the rate of change of $\mathfrak{M}$ is a vector of length $\mathfrak{M}\dot{\varphi}$ directed across the ship to the right. This vector represents the torque exerted on the rotor by its frame. The torque exerted by the rotor on its frame is directed opposite to this, so that the frame is accelerated in the direction of increasing ψ (so that the lower part of the frame tends to go to the rear of the ship).

On the other hand, if the rotor frame is swinging with a positive angular velocity $\dot{\psi}$, the momentum vector $\mathfrak{M}$ increases by an amount $\mathfrak{M}\dot{\psi}$ each second in a direction pointing toward the front of the ship. This vector is a torque tending to rotate the rotor

clockwise, and consequently the ship counterclockwise, when viewed from the rear.

Thus the ship is "coupled" to the gyroscope in much the same sense as the ship is coupled to the Frahm water tanks, though the mechanism is entirely different. Consequently the differential equations will be different from (51), (52), but still it can be shown that the same three general conclusions hold.

Without damping in the swinging motion of the rotor frame, the presence of the gyroscope merely changes the *one* natural

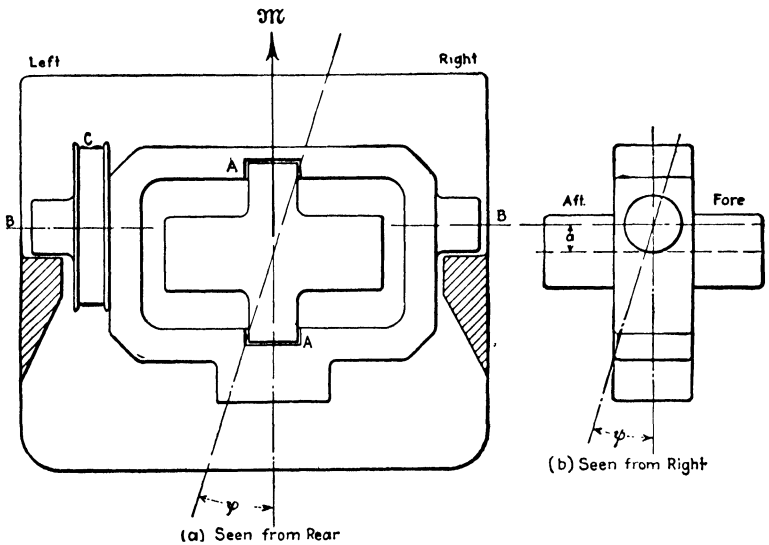


FIG. 88.—Scheme of Schlick's anti-ship-rolling gyroscope. It operates by virtue of energy dissipation at the brake drum *C*.

rolling frequency of the ship into *two* other natural rolling frequencies. A resonance with sea waves leads to infinite amplitudes φ of the ship. An infinite amount of damping clamps the rotor frame solidly in the ship. Then a roll of the ship merely creates a pitching torque on the ship's frame and conversely the clamped gyroscope will convert a pitching motion of the ship into a rolling torque on it. At resonance of the sea waves with the one natural rolling frequency again an infinite rolling amplitude results. But at some intermediate damping the two resonant peaks can be materially decreased.

In order to investigate more in detail the similarity and also the differences in behavior between the Schlick gyroscope and the Frahm tanks, we

shall derive the differential equations. The torques acting on the ship's hull in the φ-direction are the sea-wave torque $T_0 \sin \omega t$, the spring torque of the water $-K_s\varphi$, and the gyroscopic torque. It has been seen that this last torque has the magnitude $\mathfrak{M}\dot{\psi}$, its direction being such as to decrease φ when $\dot{\psi}$ is positive. Thus Newton's equation for the ship becomes

$$I_s\ddot{\varphi} = -K_s\varphi - \mathfrak{M}\dot{\psi} + T_0 \sin \omega t \tag{51a}$$

In the same manner the equation for the rotary motion of the gyroscope frame is

$$I_g\ddot{\psi} = -k_g\psi - c\dot{\psi} + \mathfrak{M}\dot{\varphi} \tag{52a}$$

In this the quantity k_g, the spring constant of the gyroscope frame as a pendulum, can be easily shown to be equal to $\mathbf{w}a$, where $\mathbf{w}$ is the weight of the frame and rotor combined and a is the distance between the center of gravity of $\mathbf{w}$ and the axis of support. The equations have been labeled here (51a) and (52a) in order to emphasize their similarity to (51) and (52) for the case of Fig. 73. Though the two sets of equations are not identical, the whole argument of Sec. 24 can be repeated word for word and similar results obtained. In particular, after going through the calculations corresponding to those performed on page 122, we arrive at the analogue of (57).

$$\frac{\varphi}{\varphi_{st}} = \sqrt{\frac{\left(2\frac{c}{c_c}\mathbf{g}\right)^2 + (\mathbf{g}^2 - \mathbf{f}^2)^2}{\left(2\frac{c}{c_c}\mathbf{g}\right)^2(g^2 - 1)^2 + [\mu\mathbf{f}^2\mathbf{g}^2 - (\mathbf{g}^2 - 1)(\mathbf{g}^2 - \mathbf{f}^2)]^2}} \tag{57a}$$

The various symbols used in this formula are not literally the same as those defined by (56), because they pertain to a different problem, but the difference is not great. For instance, $\mathbf{f}$ in this case is the ratio between the natural frequencies of the gyroscope and the ship:

$$\left.\begin{aligned} \mathbf{f} &= \frac{\omega_g}{\Omega_s} = \frac{\sqrt{\frac{\mathbf{w}a}{I_g}}}{\sqrt{\frac{\mathbf{W}h}{I_s}}} \\ \text{Also} \qquad \mathbf{g} &= \omega/\Omega_s \qquad \text{and} \qquad c_c = 2I_g\Omega_s \end{aligned}\right\} \tag{56a}$$

Equation 57a can be interpreted by diagrams like Figs. 79 and 80. But the fundamental difference lies in the definition of μ. In the dynamic absorber of Fig. 73, μ was defined as m/M, and with the Schlick gyroscope

$$\mu = \frac{\mathfrak{M}^2}{I_s I_g \omega_g^2} \tag{56a}$$

With the Frahm tank it is evident that $\mu = m/M$ cannot be much greater than $\frac{1}{20}$. On the other hand, it is easy to make the gyroscopic μ considerably greater than unity. (Schlick on his 8,500-ton experimental ship "Silvana" had $\mu = 20$ approximately.) One would be tempted to conclude from this relation in the values of μ that a gyroscope is of the order of 400 times as effective as a Frahm tank. This, however, is not so, because when

adjusting the damping c/c_c on the brake drum of Fig. 88 to the "optimum" value (such as to make the curve of Fig. 80 pass horizontally through P and Q), it is found that the "precessing" angle ψ of the rotor frame becomes many times 360 deg. This makes the analysis inapplicable, because in practice ψ is limited to about 30 deg. by stops on each side. It is necessary, therefore, to make the damping considerably greater than optimum to prevent the gyroscope from swinging too far, and this fact makes the Schlick gyroscope less effective than one would imagine from a comparison of the values of μ.

26a. Activated Ship Stabilizers.—The motion of the water in the Frahm tank, as well as the precession of the Schlick gyroscope, is brought about by the rolling of the ship itself, and in both cases is impeded by a brake. This is not a perfect solution, since the best brake adjustment is different for different frequencies and other conditions. These systems are designated as "passive" systems to distinguish them from the more modern "active" systems, where the Frahm water is *pumped* from one tank to the other, where the Schlick gyro precession is *forced*. There is no longer a brake, but there is a governor or device which feels the roll of the ship and gives the proper signals controlling the Frahm pump or the Schlick precession drive, so that the phase of the counter torque is always correct.

The first of these activated devices reaching practical perfection was the Sperry gyroscopic ship's stabilizer, illustrated schematically in Fig. 89. It consists of a main gyroscope, which differs from Schlick's only in the fact that the axis BB passes through the center of gravity, and that the brake drum C is replaced by a gear segment meshing with a pinion on the shaft of a direct-current motor D. Besides the main gyroscope there is the *pilot gyroscope* (Fig. 89*b*, *c*) which has an over-all dimension of some 5 in. and is nearly an exact replica of the main one. The only difference is that there is no gear C, but instead of that there are two electrical contacts d_1 and d_2, one in front and one behind the rotor frame.

The operation is as follows. When the ship has a clockwise rolling velocity φ (looking from the rear) the top of the pilot rotor frame is accelerated toward the front of the ship and closes the contact d_2. This action sets certain electrical relays working which start the precession motor D so as to turn the main frame about the axis BB in the same direction as the pilot frame. In other words, the top of the main frame moves to the front of the

ship. This necessitates a clockwise φ-torque on the main rotor, which has a counterclockwise reaction on the main-rotor frame and thus on the ship. Therefore the main gyroscope creates a torque on the ship which is in opposition to the *velocity* of roll and in that manner most effectively counteracts the roll. As soon as the velocity of roll of the ship becomes zero, the pilot torque

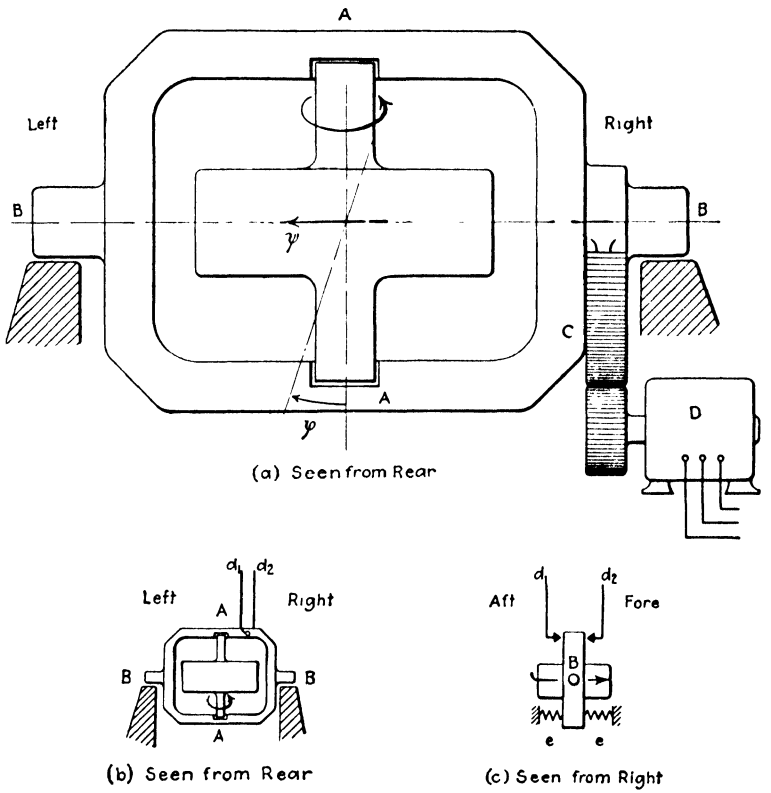


FIG. 89.—Sperry's gyroscope for diminishing ship roll. The precession is forced by a motor D, which is controlled by a small pilot gyroscope shown in (*b*) and (*c*).

disappears and the pilot rotor is pulled back to its neutral position by two springs e as shown in Fig. 89*c*. Only when the roll acquires a velocity in the opposite direction does the pilot go out of its equilibrium position again closing the contact d_1, which sets the precession motor going in the opposite direction. Thus there is always a torque acting on the ship in opposition to the instantaneous velocity of rolling. With the torque always

against the angular velocity, a maximum amount of energy of the rolling motion is destroyed. (See the three rules on pages 18 and 19.)

The direction of the desired ψ-precession of the main gyro was seen to be the same as that of the free pilot gyro, which means that the motor D turns the main gyro in the direction in which it would go by itself, if it were free to move in the bearings B. However, it can be easily verified that, if such freedom existed, the main gyro would precess extremely fast in an accelerated manner and would reach $\psi = 90$ deg. in a very short fraction of the roll period. At this position the roll would no longer affect the gyro. Therefore the motor D does not *push* the main gyro (except at the very beginning of the precession) but really acts like a brake, holding the speed of precession down to a proper value. Schemes have been proposed to do away altogether with the motor D, reverting to the old Schlick brake drum, with the difference, however, that the tightness of the brake would be controlled electrically by signals coming from the pilot gyro.

In actual constructions the pilot gyroscope has its axis AA horizontal and across the ship, while its frame axis BB is vertical. The line connecting the contacts d_1 and d_2 remains parallel to the ship's longitudinal axis as before. The reader should reason out for himself that with this arrangement the same action is obtained as with the one shown in Fig. 89.

Sperry gyro stabilizers have been installed with success on many yachts. An application to the Italian liner "Conte di Savoia" showed that a large roll was very effectively damped down by the device. However, in the roughest Atlantic storms *single* waves were found to tilt the ship 17 deg.; and since the power of the gyros was sufficient only to swing the ship 2 deg. at one time, the greatest roll angles with and without stabilizer did not differ materially. A gyroscope that would hold the ship down even in the roughest weather would become prohibitively large, of the order of 5 per cent of the weight of the ship.

Another antiroll device that has been proposed but never built utilizes the principle of lift on airplane wings. Imagine an airplane of a wing span of say 20 ft., and swell the fuselage of that plane to the size of an ocean liner, leaving the wing size unchanged. The wings are located below the water line. While the ship moves through the water, a lift will be developed on the wings. The wings can be rotated through a small angle about

their longitudinal (athwartship) axis. If the rotation of the wings (the leading edge downward, the sharp trailing edge upward) is some 15 deg., the "angle of attack" of the water on the wing is reversed and the "lift" is changed to a downpush. During the ship's roll one wing always has an uplift, the other one a downpush, giving a resulting torque opposite to the direction of roll. The angle of attack of the wings is continuously changed by a motor which is operated from the contacts of a pilot gyro. In order to obtain a sufficient torque, wings of comparatively small size and weight are adequate, but on the other hand the resistance of the ship is increased by them. Although the increase is of the order of only 1 per cent of the entire resistance, this means that 1 per cent of the weight and cost of the engines and fuel must be charged against the device.

Activated Frahm tanks with large centrifugal pumps transferring the water from one side to the other, governed by a pilot gyroscope, were installed experimentally in vessels of the U. S. Navy.

Example: A Sperry gyroscope of moment of inertia I_g and angular speed Ω is mounted on a ship with a moment of inertia I_s, which is rolling according to $\varphi = \varphi_0 \sin \omega_n t$. The gyroscope precesses in a damping sense all the time at a constant speed of either $+\omega$ or $-\omega$, depending on the direction of roll. During this process the angle of precession ψ remains small, say between $+20$ and -20 deg. Find the rate of decay of the rolling angle.

Solution: The momentum vector has the length $I_g\Omega$. Its increase per second in the direction of the roll axis (longitudinal axis of the ship) is $I_g\Omega \cdot \omega$, as is explained in Eq. (236) and Fig. 280 of Appendix I. Thus the roll-damping torque acting on the ship is $I_g\Omega \cdot \omega$. The angle through which this torque operates for a full roll from left to right is $2\varphi_0$, so that the work done per swing (half cycle) is $2\varphi_0 I_g \Omega\omega$.

The maximum angular velocity of roll in the middle of a swing is $\varphi_0\omega_n$ and thus the kinetic energy is $\frac{1}{2}I_s\varphi_0^2\omega_n^2$. The decrease of this must be equal to the damping work. Thus

$$\Delta(\tfrac{1}{2}I_s\varphi_0^2\omega_n^2) = \tfrac{1}{2}I_s\omega_n^2\Delta(\varphi_0^2) = I_s\omega_n^2\varphi_0\Delta\varphi_0 = 2\varphi_0 I_g\Omega w$$

from which

$$\Delta\varphi_0 = \frac{2I_g\Omega\omega}{I_s\omega_n^2}$$

This is the decrease in angle of roll per half cycle. The expression is independent of φ_0, so that the angle of roll diminishes as an arithmetic series and not geometrically as in Fig. 35.

27. Automobile Shock Absorbers.—An automobile of conventional design on its springs and tires is a very complicated vibrational system. There are three distinct "masses": the body, the front axle, and the rear axle; and eight distinct "springs":

the four springs proper and the four tires (Fig. 90). A solid body free in space has six degrees of freedom: it can bob up and down, sway back and forth, move forward and backward (*the three translations*); and, moreover, it can have three *rotations*, known under the technical names of:

1. *Rolling* about a longitudinal axis.
2. *Pitching* about a lateral axis.
3. *Yawing* or *nosing* about a vertical axis.

Since the automobile has three such bodies, it really has 18 degrees of freedom. However, a good many of those 18 are rather unimportant. For example, a sidewise motion of any axle, with the chassis fixed in space, is hardly possible on account of the great lateral stiffness both of the springs and of the tires. The most important motions are:

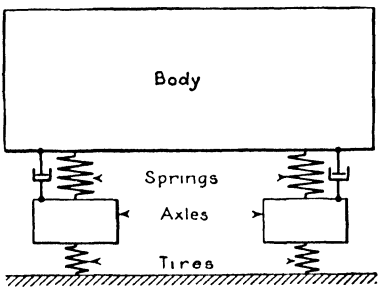


FIG. 90.—Idealized scheme of conventional automobile with front and rear axles and shock absorbers.

1. A bobbing up and down of the body with the axles practically steady.
2. A pitching of the body with the axles nearly steady.
3. A bobbing up and down of each axle on the tire elasticity with the chassis practically undisturbed.
4. A rolling of the axles with little motion of the body.

The first two motions were discussed on page 110. For an entirely symmetrical car (which naturally does not exist) the two natural modes are a pure vertical parallel motion and a pure pitching about the center of gravity, but in the actual unsymmetrical case each mode is a mixture of the two. In practice, the natural frequencies for the first two modes are close together, being somewhat slower than 1 cycle per second in modern cars. The motions 3 and 4 have frequencies roughly equal to each other but much faster than the body motions. With older cars the axle natural frequency may be as high as 6 or 8 cycles per second; with modern cars having balloon tires and heavier axles on account of front wheel brakes, the frequency is lower. On account of the fact that the body frequency and the axle frequency are so far apart, the one motion (1 or 2) can exist practically independent of the other (3 or 4). For when the body moves up and down at the rate of 1 cycle per second, the force

variation in the main spring is six times as slow as the natural frequency of the axle mass on the tire spring and thus the axle ignores the alternating force. And similarly, while the axle vibrates at the rate of 6 cycles per second, the main body springs experience an alternating force at that rate, which, however, is far too fast to make an appreciable impression on the car body (Fig. 38, page 59).

Resonances with either frequency occur quite often and can be observed easily on any old-model car or also on a modern car when the shock absorbers (dampers) are removed. The pitching motion of the body gets in resonance at medium speeds when running over a road with unevennesses of long wave length. For example, at some 30 m.p.h. on old concrete highways having joints spaced regularly at about 40 ft. apart, very violent pitching usually occurs in cars with insufficient shock absorbers. The other natural frequency often comes to resonance at rather low speeds when running over cobblestones. The axles then may vibrate so that the tires leave the ground at each cycle.

The worst of the evils just described have been eliminated by introducing shock absorbers across the body springs, which introduce damping in the same fashion as a dashpot would. Before starting a discussion of their action, it is well to consider first the influence of the springs and tires themselves on the "riding quality," or "riding comfort."

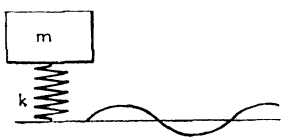


FIG. 91.—Automobile riding over a wavy road.

Assuming that the car is moving forward at a constant speed, what quantity should be considered to be a measure of comfort? It might be the vertical displacement of the chassis or any of its derivatives. It is not the displacement amplitude itself, for a ride over a mountain, being a "vibration" of amplitude 3,000 ft. at the rate of 1 cycle per hour, may be very comfortable. It is not the vertical velocity, for there are no objections to a fast ride up a steep slope. Nor is it the vertical acceleration, for a steady acceleration is felt as a steady force, which amounts only to an apparent change in g that cannot be felt. But *sudden* shocks produce uncomfortable sensations. Therefore a criterion for comfort is the rate of change of acceleration d^3y/dt^3, a quantity that has been called the "jerk."

Figure 91 represents a wheel or axle on its tire spring. The wheel runs over a road of which the surface is a sinusoid. If the

car moves at a constant speed, the bottom of the tire experiences a motion $a_0 \sin \omega t$. Consider various wheels of the same mass m running with the same speed over the same road $a_0 \sin \omega t$ but differing among each other in the elasticity k of their tire springs. The force F transmitted by the spring from the road to the wheel or axle is k times the relative displacement, which by Eq. (30), page 61, is

$$F = ky_0 = \frac{m\omega^2 a_0}{1 - \omega^2/\omega_n^2}$$

or in a dimensionless form,

$$-\frac{F}{m\omega^2 a_0} = \frac{(\sqrt{k/m\omega^2})^2}{1 - (\sqrt{k/m\omega^2})^2} \tag{74}$$

If the dimensionless force $F/m\omega^2 a_0$ is plotted vertically against the dimensionless square root of the tire spring constant $\sqrt{k}/\sqrt{m\omega^2}$, Eq. (74) shows that the diagram Fig. 40 (page 61) is obtained.

We see that stiff springs (large k or steel-rimmed wheels) are represented by points in the right-hand part of the diagram, which means considerable force transmission. Little force transmission occurs for weak springs (*i.e.*, balloon tires) represented by points close to the origin of Fig. 40.

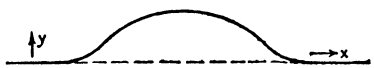


FIG. 92.—A bump in the road.

This can be appreciated also from a somewhat different standpoint. Consider a given "sinusoidal" road or a smooth road with a single bump on it, and let the steel-tired wheel be completely rigid. The vertical accelerations of the wheel now *increase with the square of the speed*, which can be seen as follows. Let the bump on the road be represented by $y = f(x)$ as in Fig. 92. For a car with speed v we have $x = vt$. Then the vertical velocity is

$$\frac{dy}{dt} = v\frac{dy}{d(vt)} = v\frac{dy}{dx}$$

and the vertical acceleration is

$$\frac{d}{dt}\left(\frac{dy}{dt}\right) = v\frac{d}{d(vt)} \cdot \left(\frac{dy}{dt}\right) = v\frac{d}{dx}\left(v\frac{dy}{dx}\right) = v^2\frac{d^2y}{dx^2}$$

Since d^2y/dx^2 is a property of the shape of the bump only, independent of the velocity, it is seen that the vertical acceleration increases with the square of the speed. If the wheel is rigid

(no tire), the forces acting on the wheel as well as on the road are the product of the wheel mass and this acceleration. Thus the force on the road also increases with the square of the speed, making the rubber tire an absolute necessity even for moderate speeds, which is a matter of common observation.

The tires are primarily there for a protection of the road and of the wheels, whereas the main springs take care of riding comfort. With a given axle movement a_0, how do we have to design the main springs for maximum riding comfort, *i.e.*, for minimum "jerk" d^3y/dt^3? From Eq. (30) we have

$$\ddot{y} = \frac{\omega^2 a_0}{1 - \omega^2/\omega_n^2} \sin \omega t$$

so that by differentiation

$$\frac{\dddot{y}}{\omega^3 a_0} = \frac{1}{1 - \omega^2/\omega_n^2} \cdot \cos \omega t \qquad (74a)$$

Again Fig. 40 represents this relation, and the springs have to be made as soft as possible in the vertical direction. Then most road shocks will be faster than the natural frequency of the car and will not give it any appreciable acceleration. The introduction of damping is undesirable at these high road frequencies. But the case of resonance is not excluded, and from that standpoint damping is very desirable.

There is still another viewpoint to the question. Figure 40 pertains to steady-state forced vibrations, *i.e.*, to road shocks following each other with great regularity. Practically this does not occur very often as the bumps on actual roads are irregularly spaced. Thus the motion will consist of a combination of forced and free vibrations, and damping is desirable to destroy the free vibrations quickly after the road is once again smooth.

The shock absorbers on most automobiles are hydraulic and operate on the dashpot principle. Any relative motion between the axle and the car body results in a piston moving in a cylinder filled with oil. This oil has to leak through small openings, or it has to pass through a valve which has been set up by a spring so that it opens only when a certain pressure difference exists on the two sides of the piston. In this manner a considerable force opposing the relative motion across the car body springs is created, and this force is roughly proportional to the *velocity* of the relative spring motion.

The most desirable amount of damping in these shock absorbers depends on the road condition. When running over a smooth road with rolling hills and valleys which are taken at the rate of approximately one hill per second, it is clear that critical damping is wanted. On the other hand, if the road has short quick bumps, a small damping is desirable. With this in mind, some cars had a "dash control" system, whereby the leakage openings in the shock absorbers could be adjusted from the dashboard of the car to suit the driver. However, it appeared that the variability in the types of road unevenness is too great for the driver to make an intelligent use of his opportunity for changing the damping constant.

Some shock absorbers have one-way valves in them, so that for a spreading apart of the axle and the body a different damping occurs than for their coming together. This is accomplished by forcing the oil through different sets of openings by means of check valves. Usually the arrangement is such that when the body and axle are spreading apart the damping is great, while when they are coming together a small force is applied by the shock absorbers. The theories and arguments given by the manufacturers as a justification of this practice do not seem to be quite rational.

Problems

40. Calculate the abscissas and ordinates of the points A, P, and Q in Fig. 80.

41. Calculate the natural frequency of the water in the tank system of Fig. 87 (see page 136).

42. Find the metacentric height of a body made of solid material of specific gravity $\frac{1}{2}$, floating in water, having the shape of a parallepiped with

a. Square cross section $h \times h$, floating with one of its sides parallel to the water.

b. Triangular cross section of base b and height h floating with the base down and the point emerging from the water.

c. The same triangular section with the point down.

43. *a.* Calculate the two natural frequencies of the system of Fig. 93*a*, consisting of a weightless bar of length $2l$, two masses m, and two springs k.

b. Find the location of the "node" or center of rotation of the bar in each of the two natural modes.

44. A weightless string is stretched with a large tension of T lb. between two solid immovable supports. The length of the string is $3l$ and it carries two masses m at distances l and $2l$ from one of the supports. Find the shapes of the natural modes of motion by reasoning alone (without mathematics), and then calculate the two natural frequencies (*cf.* Problem 20, page 100).

45. In the undamped vibration absorber of Fig. 73 let the mass ratio M/m be 5, and let the damper be tuned to the main system so that also $K/k = 5$. Further let the external force P_0 be absent. Find the two natural modes of motion, *i.e.*, the ratio between the amplitudes of M and m at the natural frequencies. Also calculate those frequencies.

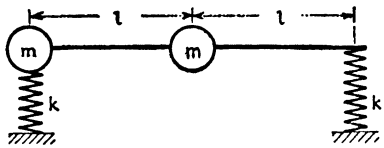


FIG. 93*a*.—Problem 43.

46. Let the system of Problem 45 be provided with a dashpot across the damper spring, having a damping constant of 5 per cent of "critical" ($c = \sqrt{4km}/20$). Assuming that the natural modes of motion calculated in Problem 45 are not appreciably altered by this small amount of damping, calculate the rate of decay in each of the two natural motions.

47. The period of roll of the "Conte di Savoia" (see page 144) is 25 sec., the metacentric height is 2.2 ft., and the weight of the ship is 45,000 tons. Calculate

a. Its moment of inertia about the roll axis.

b. Its maximum angular momentum when rolling 10 deg. to either side.

The characteristics of each one of the three gyroscopes installed on board the ship are:

Gyro moment of inertia, $4.7\ 10^6/32.2$ ft. lb. sec.^{2}
Gyro speed, 800 r.p.m.

Let these three gyroscopes precess from $\psi = -30$ deg. to $\psi = +30$ deg., and let this happen during a time (say 2 sec.) which is short in comparison with a half period of the ship's roll. Let this precession take place at the middle of a roll always in a sense to cause positive damping.

c. Find the rate of decay of a rolling motion of the ship, assuming that no damping action exists other than that of the gyroscopes.

48. An automobile has main springs which are compressed 4 in. under the weight of the body. Assume the tires to be infinitely stiff. The car stands on a platform which is first at rest and then is suddenly moved downward with an acceleration $2g$.

a. How far does the platform move before the tires leave it?

b. Assuming the car to have a speed of 30 m.p.h., draw the profile of the road which would correspond to the $2g$-accelerated platform. This question has meaning for *front* wheels only.

49. The car of Problem 48 runs over a road surface consisting of sine waves of 1 in. amplitude (*i.e.*, having 2 in. height difference between crests and valleys) and with distances of 42 ft. between consecutive crests. There are no shock absorbers.

a. Find the critical speed of the car.

b. Find the amplitude of vertical vibration of the chassis at a forward speed of 40 m.p.h.

50. A double pendulum consists of two equal masses m, hanging on weightless strings of length l each (Fig. 93*b*). In addition to gravity, there are two mechanical springs of stiffness k. The equilibrium position is a vertical line. Set up the differential equations of motion carefully and calculate the two natural frequencies. (Small angles.)

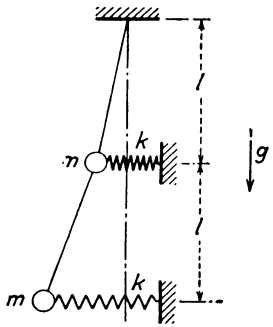


FIG. 93*b*.—Problem 50.

51. A weightless cantilever spring of length $2l$ and bending stiffness EI carries two concentrated weights, each of mass m, one at the free end $2l$ and the other at the center l. Calculate the two natural frequencies.

52. In the centrifugal pendulum of Fig. 77*b* let Ω be the speed of rotation of the disk, a the distance from the disk center to the center of swing of the pendulum, b the distance from the swing center to the center of gravity of the pendulum, and finally k the radius of gyration of the pendulum mass about its swing center. Find the natural frequency and try to design a pendulum that will swing back and forth three times per revolution.

53. Prove that the most favorable damping in the viscous Lanchester damper (curve 3 of Fig. 81*c*, page 129) is given by

$$\frac{c}{2m\Omega} = [2(1 + \mu)(2 + \mu)]^{-\frac{1}{2}}$$

54. A three-bladed airplane propeller is idealized as three flat massless cantilever springs, spaced 120 deg. apart and carrying concentrated masses m at their ends, at a distance R away from the shaft center. They are built in at a distance r from the shaft center into a hub having a moment of inertia I, with a definite angle α between the blade plane and the plane of the entire propeller (Fig. 93*c*). Let the spring constant of each blade in its limber direction be k_2 and let the blade be infinitely stiff against bending in its stiff direction (90 deg. from the limber direction). Let the hub be mounted on a shaft of torsional stiffness k_1. Find the two natural frequencies of the nonrotating system (the "blade frequency" and the "hub frequency"), as a function of the blade angle α, and find in particular whether the blade frequency is raised or lowered with increasing blade angle α.

55. The same as Problem 54; this time the shaft k_1 is stiff against torsion, but flexible against extension. The hub therefore can vibrate linearly in the shaft direction. Let k_1 mean the extensional spring constant of the shaft and let the inertia of the hub be expressed by its mass M rather than its moment of inertia.

56. The same as Problem 54, but this time the blade stiffness in its own plane is no longer considered infinite. Let the stiffness of one blade in its stiff plane be k_2 and in its limber plane k_3; let k_1 as before be the torsional stiffness of the shaft. For simplicity let $I = 0$.

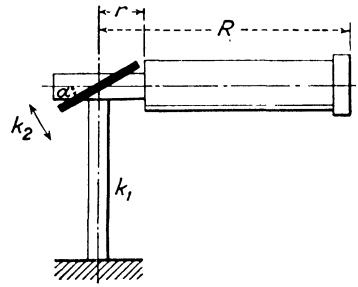


FIG. 93c.—Problems 54 to 57.

57. A combination of Problems 55 and 56, the blade having stiffnesses k_3 and k_2, the shaft being stiff in torsion and having k_1 in extension, and the hub mass M being zero for simplicity.

58. A mass m is suspended at distance l below the ceiling by two equal springs k arranged symmetrically at an angle α (Fig. 93*d*). This angle α is

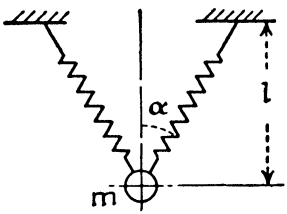


FIG. 93*d*.—Problem. 58.

the angle under the static influence of gravity with the springs carrying the weight. Find

a. The natural frequency of up-and-down motion.

b. The natural frequency of sidewise motion.

59. In Wilberforce's spring experiment (page 110) let m and $m\rho^2$ be the mass and moment of inertia of the suspended mass, let further k_{11} be the linear spring constant (pounds per inch deflection), k_{22} the torsional spring constant (inch-pounds per radian twist), and $k_{12} = k_{21}$ the coupling constant (inch pounds torque per inch deflection *or* pounds pull per radian twist). Note that $k_{12} >> k_{11}$.

a. Set up the differential equations of motion in terms of the longitudinal displacement x and the tangential displacement $y = \rho\varphi$, by the process of page 104.

b. Find the two natural frequencies and the two configurations x/y.

c. Determine the condition imposed on these values for x/y in order to insure good Wilberforce operation.

d. Find the two values for x/y numerically.

e. Find the ratio of the beat frequency to the natural frequency in terms of the spring constants, assuming the two natural frequencies to be so close together that their difference is negligible.

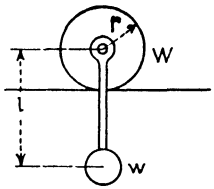


FIG. 93*e*. Problem 60.

60. A uniform disk of weight W and radius r rolls without sliding on a plane table. At its center it carries a hinge with a weightless pendulum of length l and a concentrated weight w at its end (Fig. 93*e*). Find the natural frequencies for motion in the plane of the paper.

CHAPTER IV

MANY DEGREES OF FREEDOM

28. Free Vibration without Damping.—When the number of degrees of freedom becomes greater than two, no essential new aspects enter into the problem. We obtain as many natural frequencies and as many modes of motion as there are degrees of freedom. The general process of analysis will be discussed in the next few sections for a three-degree system; for four or more degrees of freedom the calculations are analogous.

Consider for example Fig. 94, representing a weightless bar on two rigid supports, carrying three masses m_1, m_2, and m_3. If the upward deflections of these masses be denoted by x_1, x_2, and x_3, the first of the equations of motion can be obtained by equating $m_1\ddot{x}_1$ to the elastic force on the first mass. This force is the difference between the lateral shear forces in the bar to the left and to the right of m_1, a quantity depending on all three deflections x_1, x_2, and x_3, complicated and difficult to calculate.

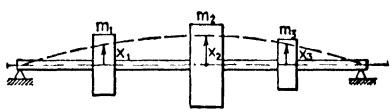


FIG. 94.—A round shaft with three disks on stiff bearings is a system having three degrees of freedom in bending.

It is more in the nature of this particular problem to describe its elasticity by the *influence numbers*. The definition of an influence number α_{12} is "the deflection of mass 1 caused by a force of 1 lb. at the location of mass 2." We have three *direct* influence numbers, α_{11}, α_{22}, and α_{33} where the unit force and the deflection are measured at the same location, and six *cross* influence numbers, α_{12}, α_{21}, α_{13}, α_{31}, α_{23}, and α_{32}, where the two locations are different. By Maxwell's theorem of reciprocity,

$$\alpha_{12} = \alpha_{21}$$

or, in words: the deflection at one location caused by a unit load at another location equals the deflection at this second location caused by a unit load at the first location. These influence numbers can be calculated for any system by the principles of

strength of materials. The equations of motion can be written with them as follows. In the position x_1, x_2, x_3 of maximum deflection of the bar (Fig. 94), the masses have accelerations $\ddot{x}_1$, $\ddot{x}_2$, $\ddot{x}_3$ and consequently experience forces $m_1\ddot{x}_1$, $m_2\ddot{x}_2$, $m_3\ddot{x}_3$. These forces are exerted *by* the bar *on* the masses. By the principle of action and reaction, the masses exert the inertia forces $-m_1\ddot{x}_1$, $-m_2\ddot{x}_2$, $-m_3\ddot{x}_3$ on the bar. The deflection at the first mass caused by these three forces is

$$\left.\begin{aligned} x_1 &= -\alpha_{11}m_1\ddot{x}_1 - \alpha_{12}m_2\ddot{x}_2 - \alpha_{13}m_3\ddot{x}_3 \\ \text{and analogously for the second and third masses,} & \\ x_2 &= -\alpha_{21}m_1\ddot{x}_1 - \alpha_{22}m_2\ddot{x}_2 - \alpha_{23}m_3\ddot{x}_3 \\ x_3 &= -\alpha_{31}m_1\ddot{x}_1 - \alpha_{32}m_2\ddot{x}_2 - \alpha_{33}m_3\ddot{x}_3 \end{aligned}\right\} \quad (75)$$

Although these equations cannot be interpreted directly as the Newton equation for each mass, nevertheless the three together determine the three unknown motions x_1, x_2, and x_3.

As before, on page 104, in order to reduce them from differential equations to algebraic equations, we put

$$\left.\begin{aligned} x_1 &= a_1 \sin \omega t \\ x_2 &= a_2 \sin \omega t \\ x_3 &= a_3 \sin \omega t \end{aligned}\right\} \quad (76)$$

and substitute, with the result

$$\left.\begin{aligned} a_1 &= \alpha_{11}m_1\omega^2 a_1 + \alpha_{12}m_2\omega^2 a_2 + \alpha_{13}m_3\omega^2 a_3 \\ a_2 &= \alpha_{21}m_1\omega^2 a_1 + \alpha_{22}m_2\omega^2 a_2 + \alpha_{23}m_3\omega^2 a_3 \\ a_3 &= \alpha_{31}m_1\omega^2 a_1 + \alpha_{32}m_2\omega^2 a_2 + \alpha_{33}m_3\omega^2 a_3 \end{aligned}\right\} \quad (76a)$$

These equations are homogeneous in a_1, a_2, and a_3, which can be seen better after rearranging and dividing by ω^2:

$$\left.\begin{aligned} \left(m_1\alpha_{11} - \frac{1}{\omega^2}\right)a_1 + m_2\alpha_{12}a_2 + m_3\alpha_{13}a_3 &= 0 \\ m_1\alpha_{21}a_1 + \left(m_2\alpha_{22} - \frac{1}{\omega^2}\right)a_2 + m_3\alpha_{23}a_3 &= 0 \\ m_1\alpha_{31}a_1 + m_2\alpha_{32}a_2 + \left(m_3\alpha_{33} - \frac{1}{\omega^2}\right)a_3 &= 0 \end{aligned}\right\} \quad (77)$$

If such homogeneous equations are divided by a_1, for example, we have *three* equations in *two* unknowns, a_2/a_1 and a_3/a_1. If we solve these unknowns from the first two equations of (77) and substitute the answers in the third one, we usually find that

the result is *not* zero. Only if a certain relation exists among the coefficients of a_1, a_2, and a_3, can there be a solution. In the theory of determinants it is shown that this relation is

$$\begin{vmatrix} m_1\alpha_{11} - \frac{1}{\omega^2} & m_2\alpha_{12} & m_3\alpha_{13} \\ m_1\alpha_{21} & m_2\alpha_{22} - \frac{1}{\omega^2} & m_3\alpha_{23} \\ m_1\alpha_{31} & m_2\alpha_{32} & m_3\alpha_{33} - \frac{1}{\omega^2} \end{vmatrix} = 0 \quad (78)$$

The argument is analogous to that given on page 105 for the two-degree-of-freedom system. The determinant expanded is a cubic equation in terms of $1/\omega^2$, known as the "frequency equation," which has three solutions and hence three natural frequencies. To each of these solutions belongs a set of values for a_2/a_1 and a_3/a_1, which determines a configuration of vibration. Thus there are three natural modes of motion.

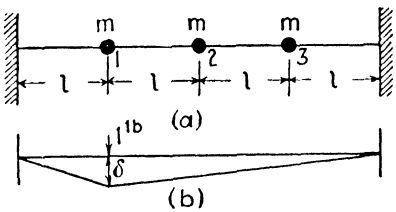


FIG. 95.—Showing calculation of influence numbers for a string with three masses.

We shall carry out these calculations in detail for the simplest possible example, obtained by making all masses equal $m_1 = m_2 = m_3 = m$ and replacing the bar by a string of tension **T** and length $4l$. If a load of 1 lb. is placed on location 1, the deformation will be as shown in Fig. 95*b*. The tension in the string is **T** and the vertical component of the tension in the part of the string to the left of m_1 is $\frac{\delta}{l}\mathbf{T}$ while to the right of m_1 it is $\frac{\delta}{3l}\mathbf{T}$. The sum of these vertical components must be equal to the load of 1 lb. so that $\delta = \frac{3}{4}\frac{l}{\mathbf{T}}$. This is the deflection at 1 caused by 1 lb. at 1, or $\alpha_{11} = \frac{3}{4}\frac{l}{\mathbf{T}}$.

The deflection at the masses 2 and 3 caused by the same load can also be found from Fig. 95*b*:

$$\alpha_{21} = \frac{2}{3} \cdot \frac{3}{4}\frac{l}{\mathbf{T}} = \frac{1}{2}\frac{l}{\mathbf{T}}$$

$$\alpha_{31} = \frac{1}{3} \cdot \frac{3}{4}\frac{l}{\mathbf{T}} = \frac{1}{4}\frac{l}{\mathbf{T}}$$

The other influence numbers can be found in a similar manner:

$$\left.\begin{aligned} \alpha_{22} &= \frac{l}{\mathbf{T}} \\ \alpha_{11} = \alpha_{33} &= \frac{3}{4}\frac{l}{\mathbf{T}} \\ \alpha_{12} = \alpha_{21} = \alpha_{32} = \alpha_{23} &= \frac{1}{2}\frac{l}{\mathbf{T}} \\ \alpha_{31} = \alpha_{13} &= \frac{1}{4}\frac{l}{\mathbf{T}} \end{aligned}\right\} \tag{79}$$

and Maxwell's reciprocity relations are seen to be true. The equations of motion are obtained by substituting these values for the influence numbers in Eq. (75). However, since nearly every term is proportional to $ml/\mathbf{T}$, we divide by this quantity and introduce the abbreviation

$$\frac{\mathbf{T}}{ml\omega^2} = \mathbf{F} \text{ (the frequency function)} \tag{80}$$

Then Eqs. (77) become

$$\left.\begin{aligned} (\tfrac{3}{4} - \mathbf{F})a_1 + \tfrac{1}{2}a_2 + \tfrac{1}{4}a_3 &= 0 \\ \tfrac{1}{2}a_1 + (1 - \mathbf{F})a_2 + \tfrac{1}{2}a_3 &= 0 \\ \tfrac{1}{4}a_1 + \tfrac{1}{2}a_2 + (\tfrac{3}{4} - \mathbf{F})a_3 &= 0 \end{aligned}\right\} \tag{81}$$

Dividing the first of these by a_1, the second by $2a_1$, and subtracting them from each other leads to

$$\frac{a_2}{a_1} = 2 - \frac{1}{\mathbf{F}} \tag{82}$$

Substituting this in the first equation of (81) and solving for a_3/a_1 gives

$$\frac{a_3}{a_1} = -7 + 4\mathbf{F} + \frac{2}{\mathbf{F}} \tag{83}$$

Substituting both these ratios in the third equation of (81) gives the following equation for $\mathbf{F}$ (the frequency equation):

$$\mathbf{F}^3 - \tfrac{5}{2}\mathbf{F}^2 + \tfrac{3}{2}\mathbf{F} - \tfrac{1}{4} = 0 \tag{84}$$

This result could have been found also by working out the determinant (78). Evidently (84) has three roots for $\mathbf{F}$. We note that none of these can be negative since for a negative $\mathbf{F}$ all four

terms on the left become negative and then their sum cannot be zero. Since by (80) a negative **F** corresponds to an imaginary ω, we see that our three-degree-of-freedom system must have three *real* natural frequencies. This is true not only for the particular system under consideration. In general it can be shown that *an n-degree-of-freedom vibrational system without damping has n real natural frequencies, i.e.,* the roots of a frequency equation such as (43), (78), or (84) are always real and positive.

The cubic (84) is solved by trial of some values for **F**. **F** = 0 makes the left-hand side $-\frac{1}{4}$, while **F** = 2 makes it $+\frac{3}{4}$; evidently at least one root must be between 0 and 2. A few trials will show that **F** = $\frac{1}{2}$ is a root, so that Eq. (84) can be written

$$(\mathbf{F} - \tfrac{1}{2})(\mathbf{F}^2 - 2\mathbf{F} + \tfrac{1}{2}) = 0$$

having the three roots

$$\mathbf{F}_2 = \tfrac{1}{2} \qquad \mathbf{F}_{1,3} = 1 \pm \sqrt{\tfrac{1}{2}}$$

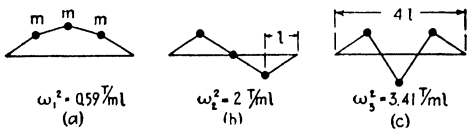


FIG. 96.—The three natural modes of a string with three equal and equidistant masses.

With the relations (80), (82), and (83) the complete result becomes

$$\mathbf{F}_1 = 1.707 \quad \omega_1^2 = 0.59\frac{\mathbf{T}}{ml} \quad \frac{a_2}{a_1} = 1.41 \quad \frac{a_3}{a_1} = 1$$

$$\mathbf{F}_2 = 0.500 \quad \omega_2^2 = 2\frac{\mathbf{T}}{ml} \quad \frac{a_2}{a_1} = 0 \quad \frac{a_3}{a_1} = -1$$

$$\mathbf{F}_3 = 0.293 \quad \omega_3^2 = 3.41\frac{\mathbf{T}}{ml} \quad \frac{a_2}{a_1} = -1.41 \quad \frac{a_3}{a_1} = 1$$

This gives the shapes of the vibration, or the "normal modes" as shown in Fig. 96. These are the *only* three configurations in which the system can be in equilibrium under the influence of forces which are proportional to the displacements x (as the inertia forces are). The second mode is of particular interest because the middle mass does not move at all. If that fact had been known in advance, the frequency could have been found very easily by considering the left half of the system as one of

a single degree of freedom with the spring constant $k = 2T/l$ (see Problem 20, page 100).

29. Forced Vibration without Damping.—Suppose an alternating force $P_0 \sin \omega t$ to be acting on the first mass of the previous example (Fig. 97*a*). The force $P_0 \sin \omega t$ *by itself* would cause "static" deflections at 1, 2, and 3 of $\alpha_{11}P_0 \sin \omega t$, $\alpha_{21}P_0 \sin \omega t$, and $\alpha_{31}P_0 \sin \omega t$. The equations of *forced* motion are obtained from (75) by adding these terms to the right-hand sides. With the assumption (76) the equations then are reduced to the algebraic form

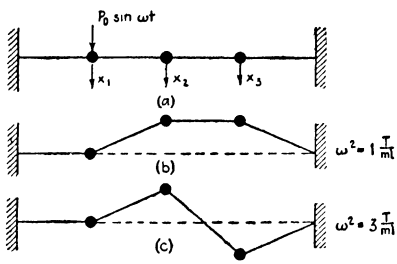


FIG. 97.—Forced vibrations of a string with three masses. There are two frequencies at which the disturbed mass does not move; these are the frequencies of the generalized-dynamic-vibration-absorber effect.

$$\begin{aligned}
\left(m_1\alpha_{11} - \frac{1}{\omega^2}\right)a_1 + \quad & m_2\alpha_{12}a_2 + \quad & m_3\alpha_{13}a_3 &= \alpha_{11}\frac{P_0}{\omega^2} \\
m_1\alpha_{21}a_1 + \left(m_2\alpha_{22} - \frac{1}{\omega^2}\right)a_2 + \quad & & m_3\alpha_{23}a_3 &= \alpha_{21}\frac{P_0}{\omega^2} \\
m_1\alpha_{31}a_1 + \quad & m_2\alpha_{32}a_2 + \left(m_3\alpha_{33} - \frac{1}{\omega^2}\right)a_3 &= \alpha_{31}\frac{P_0}{\omega^2}
\end{aligned}$$

With the influence numbers (79) and with the definition of $\mathbf{F}$ given in (80), they become

$$\left.\begin{aligned}
\left(\frac{3}{4} - \mathbf{F}\right)a_1 + \quad & \frac{1}{2}a_2 + \quad & \frac{1}{4}a_3 &= -\frac{3}{4}\frac{P_0}{m\omega^2} \\
\frac{1}{2}a_1 + (1 - \mathbf{F})a_2 + \quad & & \frac{1}{2}a_3 &= -\frac{1}{2}\frac{P_0}{m\omega^2} \\
\frac{1}{4}a_1 + \quad & \frac{1}{2}a_2 + \left(\frac{3}{4} - \mathbf{F}\right)a_3 &= -\frac{1}{4}\frac{P_0}{m\omega^2}
\end{aligned}\right\} \qquad (85)$$

These equations are no longer homogeneous in a_1, a_2, a_3, as were the corresponding ones (81) for free vibration. They are truly a set of three equations with three unknowns and can be solved by ordinary algebra. In the calculations, the cubic (84) appears in the denominators and is broken up into its three linear factors, with the result that

$$\left.\begin{aligned} a_1 &= \frac{P_0}{m\omega^2}\,\frac{\tfrac{3}{4}\mathbf{F}^2 - \mathbf{F} + \tfrac{1}{4}}{(\mathbf{F} - 1.707)(\mathbf{F} - 0.500)(\mathbf{F} - 0.293)} \\ a_2 &= \frac{P_0}{m\omega^2}\,\frac{\tfrac{1}{2}\mathbf{F}(\mathbf{F} - \tfrac{1}{2})}{(\mathbf{F} - 1.707)(\mathbf{F} - 0.500)(\mathbf{F} - 0.293)} \\ a_3 &= \frac{P_0}{m\omega^2}\,\frac{\tfrac{1}{4}\mathbf{F}^2}{(\mathbf{F} - 1.707)(\mathbf{F} - 0.500)(\mathbf{F} - 0.293)} \end{aligned}\right\} \qquad (86)$$

The physical meaning of these expressions is best disclosed by plotting them as resonance diagrams corresponding to Fig. 38 on page 59 or to Figs. 75*a* and *b* on page 116. For that purpose note that **F**, being proportional to $1/\omega^2$, is not a suitable variable. For the ordinate y of our diagrams we take the quantities

$$y_{1,2,3} = \frac{a_{1,2,3}}{\dfrac{P_0 l}{\mathbf{T}}}$$

The denominator $P_0 l/\mathbf{T}$ would be the "static deflection" of the middle of the string if the (constant) load P_0 were placed there ($\alpha_{22} = l/\mathbf{T}$), so that y is a "dimensionless amplitude." For the abscissa x we take

$$x = \frac{1}{\mathbf{F}} = \frac{\omega^2}{\mathbf{T}/ml}$$

The denominator $\mathbf{T}/ml$ can be interpreted as the ω^2 of a mass m on a spring constant $\mathbf{T}/l$, so that $\sqrt{x}$ is a "dimensionless frequency." With these two new variables, Eqs. (86) are transformed into

$$\left.\begin{aligned} y_1 &= \frac{-x^2 + 4x - 3}{(x - 0.59)(x - 2)(x - 3.41)} \\ y_2 &= \frac{(x - 2)}{(x - 0.59)(x - 2)(x - 3.41)} \\ y_3 &= \frac{-1}{(x - 0.59)(x - 2)(x - 3.41)} \end{aligned}\right\} \qquad (87)$$

plotted in Figs. 98, 99, and 100. The reader should satisfy himself that for the static case $x = 0$, all three expressions (87) give the proper static deflections. An interesting property of (87) is that the factor $(x - 2)$ can be divided out in the expression for y_2. This means physically that the middle mass does not get infinite amplitudes at the second resonance, while both the

first and third masses do go to infinity. A glance at the second normal mode of Fig. 96 shows that this should be so.

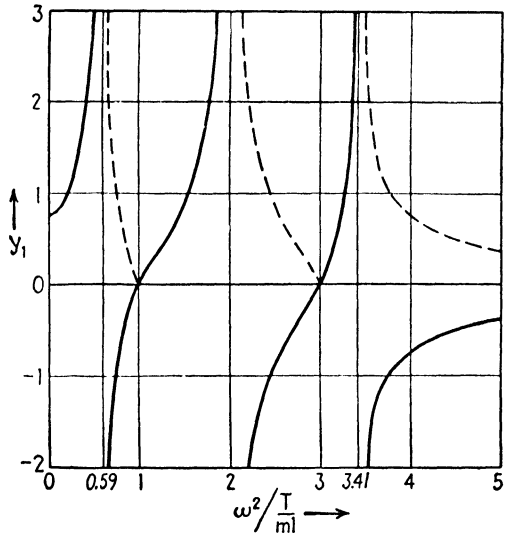


FIG. 98.—See legend under Fig. 100.

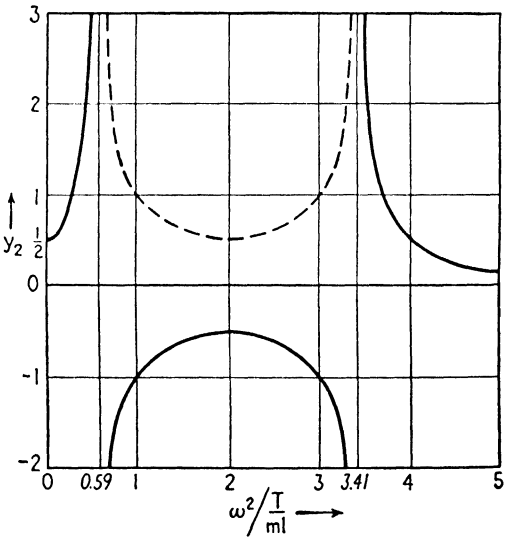


FIG. 99.—See legend under Fig. 100.

While the numerators of y_2 and y_3 show no peculiarities, it is seen that the numerator of y_1 is a quadratic which necessarily

becomes zero for two frequencies, *viz.*, for $x = 1$ and $x = 3$ (Fig. 98). At these frequencies the first mass, on which the force is acting, does not move, whereas the two other masses do vibrate. We have before us a *generalization of the dynamic vibration absorber* of page 112. If the first mass does not move,

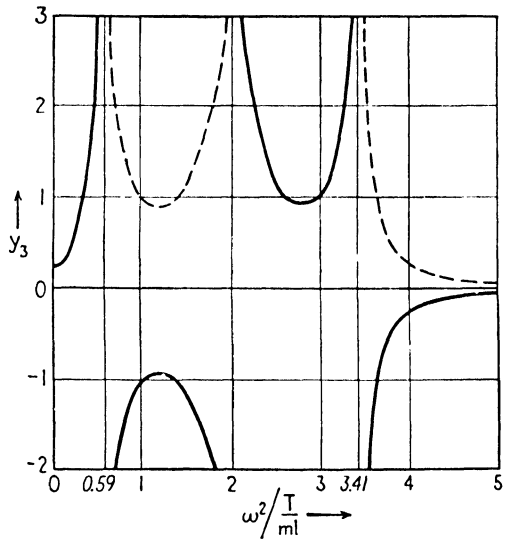


FIG. 100.

FIGS. 98–100.—Resonance diagrams for the motion of mass 1 (Fig. 98), mass 2 (Fig. 99) and mass 3 (Fig. 100) of the system of Fig. 97*a*, excited at the first mass. Only the first mass has two frequencies at which it does not move. The masses 2 or 3 move at all frequencies.

we can consider it clamped and the system reduces to one of two degrees of freedom (Fig. 97). Such a system has two natural frequencies which can easily be calculated to be $x = 1$ and $x = 3$. The action can then be imagined as follows. At two resonant frequencies the two-dimensional system can be excited to finite amplitudes by an infinitely small excitation, in this case by an infinitely small alternating motion of mass 1. On mass 1 in Fig. 97*b* or *c* two alternating forces are acting, one being the vertical component of the string tension from the right and the other one being the external force $P_0 \sin \omega t$. These two forces must be always equal and opposite, because m_1 does not move.

Generalizing, we thus might be tempted to make the following statement: If an alternating force acts on a mass of an n-degree-

of-freedom system, there will be $n - 1$ frequencies at which that mass will stand still while the rest of the system vibrates. Care has to be exercised, however, in making such sweeping generaliza-

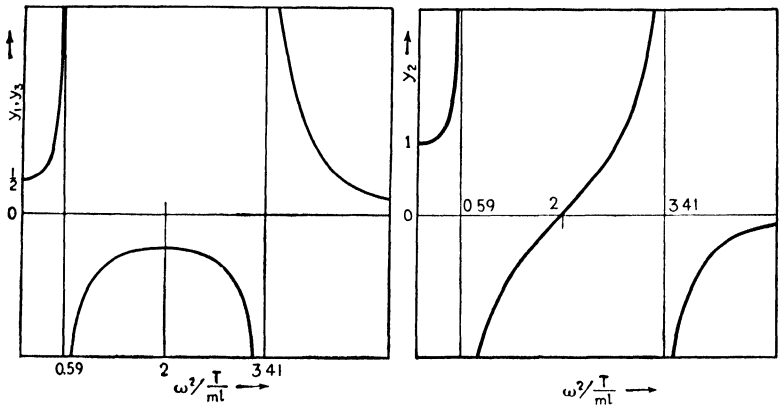


FIG. 101.—Resonance diagrams for the symmetrical string with three masses of which the middle mass is excited by an alternating force.

tions. For example, an exception to the rule can be pointed out immediately by exciting our system at the middle mass. On account of this mass being a *node* at the second resonance (Fig. 96), the force can perform no work on it at that frequency so that no infinite amplitudes can be built up. The "resonant frequency" and the "vibration absorber frequency" happen to coincide in this case. In reasoning out the shape of the three resonance curves for excitation at the middle mass, it should be borne in mind that the system is completely symmetrical so that the y_1 and the y_3 diagrams must be alike. Without carrying out the calculations in detail, we can conclude that the result must have the general shape shown in Fig. 101. Below $x = 2$ all three masses are in phase, somewhat like Fig. 96*a*; above that frequency they are in opposite phase, somewhat like Fig. 96*c*. At the second natural frequency, however, the configuration

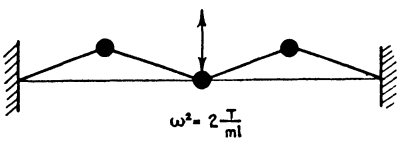


FIG. 102.—Vibration absorber effect in string with three masses of which the middle one is excited.

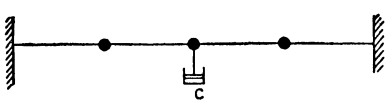


FIG. 103.—Damping at the central mass of the string.

must, for reasons of symmetry, be as shown in Fig. 102. The amplitude of motion of the masses 1 and 3 must be determined by the value of the exciting force, so that the sum of the vertical components of the tensions in the two pieces of string attached to m_2 must be equal and opposite to the exciting force.

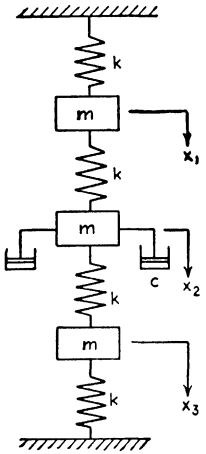


FIG. 104.—The longitudinal vibrations of this system are completely equivalent to the vibration of either Fig. 103 or Fig. 105.

30. Free and Forced Vibrations with Damping.—If there is damping in a system of many degrees of freedom, we are practically interested in two questions: (*a*) in the rate of decay of amplitude of the free vibration; (*b*) in the amplitude at resonance of the forced vibration. The method of calculation employed in the exact classical theory will be shown in the example of the string with three equal and equidistant masses.

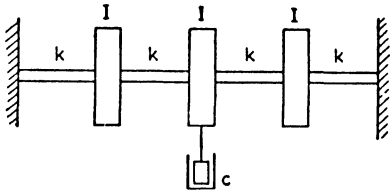


FIG. 105.—Torsional equivalent of the system of Fig. 103 or Fig. 104.

Let a damping force $-c\dot{x}_2$ be acting on the middle mass (Fig. 103). This force causes deflections of $-\alpha_{12}c\dot{x}_2$, $-\alpha_{22}c\dot{x}_2$, and $-\alpha_{32}c\dot{x}_2$ at the three masses. The differential equations (75) for the free vibration become

$$\left.\begin{aligned} x_1 &= -\alpha_{11}m\ddot{x}_1 - \alpha_{12}m\ddot{x}_2 - \alpha_{13}m\ddot{x}_3 - \alpha_{12}c\dot{x}_2 \\ x_2 &= -\alpha_{21}m\ddot{x}_1 - \alpha_{22}m\ddot{x}_2 - \alpha_{23}m\ddot{x}_3 - \alpha_{22}c\dot{x}_2 \\ x_3 &= -\alpha_{31}m\ddot{x}_1 - \alpha_{32}m\ddot{x}_2 - \alpha_{33}m\ddot{x}_3 - \alpha_{32}c\dot{x}_2 \end{aligned}\right\} \tag{88}$$

where the various influence numbers have the values expressed by (79). By algebraic manipulations these can be transformed into

$$\left.\begin{aligned} m\ddot{x}_1 + \frac{\mathbf{T}}{l}x_1 + \frac{\mathbf{T}}{l}(x_1 - x_2) &= 0 \\ m\ddot{x}_2 + \frac{\mathbf{T}}{l}(x_2 - x_1) + \frac{\mathbf{T}}{l}(x_2 - x_3) + c\dot{x}_2 &= 0 \\ m\ddot{x}_3 + \frac{\mathbf{T}}{l}(x_3 - x_2) + \frac{\mathbf{T}}{l}x_3 &= 0 \end{aligned}\right\} \tag{89}$$

The first equation of (89) is found by subtracting the second of (88) from twice the first of (88), *i.e.*, by forming $2x_1 - x_2$. The second equation of (89) is obtained by calculating $x_1 + x_3 - 2x_2$ and the third one by forming $x_2 - 2x_3$. The physical significance of Eqs. (89) is apparent. They are the Newtonian equations for the various masses, the first term being the inertia force, the second the vertical component of the string tension to the left of the mass, the third that same component to the right, and the fourth the damping force.

In this case it would have been possible and easier to write the equations in the last form directly without using the influence numbers. However, for the example of the beam with which this chapter started (Fig. 94), influence numbers afford the simplest manner of approach.

Before proceeding with the solution of (89), it may be well to point out that these equations may represent two other systems as well, shown in Figs. 104 and 105. In Fig. 104 the masses are restricted to vertical motion alone, and the spring constant k has to be made equal to $\mathbf{T}/l$ to give complete analogy with Fig. 103. The second example, Fig. 105, is a torsional one. The reader will do well to interpret the results shown in Figs. 95 to 102 for these two cases.

In solving Eqs. (89), we know from the last two chapters that an assumption of the form $x = a \sin \omega t$, which is perfectly justifiable for the undamped case, will not lead to a result if damping is present. The solution is rather expected to be of the form $x = a \cdot e^{-pt} \sin qt$. This is met by assuming

$$\left.\begin{aligned} x_1 &= a_1 e^{st} \\ x_2 &= a_2 e^{st} \\ x_3 &= a_3 e^{st} \end{aligned}\right\} \tag{90}$$

where s is a *complex* number, $s = p + iq$. The value $-p$ gives the exponent of decay of amplitude and q is the natural frequency (see page 51). Substituting (90) in (89),

$$\left.\begin{aligned} \left(ms^2 + 2\frac{\mathbf{T}}{l}\right)a_1 - \frac{\mathbf{T}}{l}a_2 + 0 &= 0 \\ -\frac{\mathbf{T}}{l}a_1 + \left(ms^2 + cs + 2\frac{\mathbf{T}}{l}\right)a_2 - \frac{\mathbf{T}}{l}a_3 &= 0 \\ 0 - \frac{\mathbf{T}}{l}a_2 + \left(ms^2 + 2\frac{\mathbf{T}}{l}\right)a_3 &= 0 \end{aligned}\right\}$$

This is a homogeneous set of equations in a_1, a_2, and a_3 and can have a solution only if the determinant vanishes:

$$\begin{vmatrix} ms^2 + 2\frac{\mathbf{T}}{l} & -\frac{\mathbf{T}}{l} & 0 \\ -\frac{\mathbf{T}}{l} & ms^2 + cs + 2\frac{\mathbf{T}}{l} & -\frac{\mathbf{T}}{l} \\ 0 & -\frac{\mathbf{T}}{l} & ms^2 + 2\frac{\mathbf{T}}{l} \end{vmatrix} = 0$$

or, written out,

$$\left(ms^2 + 2\frac{\mathbf{T}}{l}\right)\left[\left(ms^2 + 2\frac{\mathbf{T}}{l}\right)\left(ms^2 + cs + 2\frac{\mathbf{T}}{l}\right) - 2\left(\frac{\mathbf{T}}{l}\right)^2\right] = 0 \quad (91)$$

This equation of the sixth degree in s is known also as the "frequency equation," though s in this case is not the frequency but a complex number expressing frequency and rate of decay combined. The quantity s is called the "complex frequency."

In this particular case the equation falls into two factors of which the first one leads to

$$s^2 = -\frac{2\mathbf{T}}{ml} \qquad \text{or} \qquad s_{1,2} = \pm j\sqrt{\frac{2\mathbf{T}}{ml}}$$

with a solution of the form

$$Ae^{j\sqrt{\frac{2\mathbf{T}}{ml}}t} + Be^{-j\sqrt{\frac{2\mathbf{T}}{ml}}t}$$

which can be transformed to [see Eq. (8*a*), page 13]

$$C_1 \cos \sqrt{\frac{2\mathbf{T}}{ml}}t + C_2 \sin \sqrt{\frac{2\mathbf{T}}{ml}}t$$

This solution therefore gives a frequency $\omega^2 = 2\mathbf{T}/ml$, while the rate of decay of amplitude is zero, since s does *not* contain any real part. The frequency coincides with that of Fig. 96*b* for the undamped case, in which the middle mass is a node. Therefore the damping force can do no work, which is the reason for the absence of a rate of decay in this second mode and also the reason for the fact that the natural frequency is not affected at all by the damping.

The other factor of (91), after multiplying out, becomes

$$s^4 + \frac{c}{m}s^3 + 4\frac{\mathbf{T}}{ml}s^2 + 2\frac{\mathbf{T}}{ml}\frac{c}{m}s + 2\left(\frac{\mathbf{T}}{ml}\right)^2 = 0$$

having four roots for s, which we *do* expect to have *real* parts, since in the modes of Figs. 96*a* and *c* the damping does perform work. The roots of s will be of the form

$$\begin{aligned} s_3 &= -p_1 + jq_1 \\ s_4 &= -p_1 - jq_1 \\ s_5 &= -p_2 + jq_2 \\ s_6 &= -p_2 - jq_2 \end{aligned}$$

because the complex roots of algebraic equations always occur in conjugate pairs.

The numerical calculation of these roots from the numerical values of m, c, $\mathbf{T}$, and l is cumbersome even for the comparatively simple equation of the fourth degree.* Therefore this classical method is unsuited to a practical solution of the problem. It has been discussed here merely because in Chap. VII we shall consider cases in which the *real* parts of s become *positive*, which means a decay function of the form e^{+pt}, which is *not* decay but actually a building up of the vibration; the motion is then called "self-excited."

In practical cases the damping is usually so small that the natural frequency and the mode of motion are very little affected by it (Fig. 36, page 54). Hence the rate of decay of the free vibration may be calculated by assuming the configuration and frequency which would occur if no damping existed, as follows.

If the amplitude of the middle mass be a_2 and the frequency be ω, Eq. (34), page 68, gives for the work dissipated per cycle by the damping force $ca_2\omega$:

$$W = \pi c\omega a_2^2$$

The kinetic energy of the system when passing through its neutral position is

$$\tfrac{1}{2}m\omega^2(a_1^2 + a_2^2 + a_3^2) = \tfrac{1}{2}m\omega^2\mathbf{f}a_2^2 \qquad (92)$$

where the factor $\mathbf{f}$ depends on the configuration. This energy is diminished by $\pi c\omega a_2^2$ each cycle, or

$$d(\tfrac{1}{2}m\omega^2\mathbf{f}a_2^2) = m\omega^2\mathbf{f}a_2 da_2 = \pi c\omega a_2^2$$

Hence,

$$\frac{da_2}{a_2} = \frac{\pi c}{m\omega\mathbf{f}}$$

* The mathematical method by which this can be done is discussed in "Mathematical Methods in Engineering" by Th. von Kármán and M. A. Biot, p. 246.

If in a natural mode of motion one of the masses reduces its amplitude to one-half, all other masses do the same, so that

$$\frac{da_1}{a_1} = \frac{da_2}{a_2} = \frac{da_3}{a_3} = \frac{\pi c}{m\mathbf{f}\omega}$$

In the first mode of motion, Fig. 96*a*, the factor **f**, as defined by (92), is seen to be 2, whereas $\omega = \omega_1 = \sqrt{0.59\frac{\mathbf{T}}{ml}}$, so that the percentage decay per cycle is

$$\frac{da_1}{a_1} = 2.04c\sqrt{\frac{l}{\mathbf{T}m}}$$

In the third mode of motion **f** is also 2, but $\omega_3 = \sqrt{3.41\frac{\mathbf{T}}{ml}}$ so that

$$\frac{da_1}{a_1} = 0.85c\sqrt{\frac{l}{\mathbf{T}m}}$$

This method gives perfectly satisfactory results for the usual damping values. Of course, when the damping becomes an appreciable fraction of c_c, the procedure ceases to be reliable.

For *forced* vibrations with damping, the "classical" method is even more complicated than for free vibrations. It becomes so cumbersome as to be entirely useless for practical numerical purposes. However, for technically important values of the damping the above energy method gives us a good approximation for the amplitude at *resonance* in which we are most interested.

As before, we assume that at resonance the damping force and exciting force are so small with respect to the inertia and elastic forces (see Fig. 41, page 64, for the single-degree case) that the mode of motion is practically undistorted. Then the damping dissipation per cycle can be calculated in the same manner as has just been done for the free vibration. In the steady-state case this dissipation must be equal to the work per cycle done on the system by the exciting force or forces. In general, there is some phase angle between the force and the motion. At "resonance," however, this phase angle becomes 90 deg., as explained on page 68, at which value of the phase angle the work input for a given force and motion becomes a maximum.

As an example, take the combined Figs. 97*a* and 103. The work input of the force per cycle is $\pi P_0 a_1$, and the resonant amplitude is calculated from

$$\pi P_0 a_1 = \pi c \omega a_2^2 \qquad \text{or,} \qquad \pi P_0 = \pi c \omega \left(\frac{a_2}{a_1}\right)^2 a_1$$

Hence

$$(a_1)_{res} = \frac{P_0}{c\omega}\left(\frac{a_1}{a_2}\right)^2$$

In the first mode we have $a_2/a_1 = 1.41$ and $\omega = \sqrt{0.59\frac{T}{ml}}$ (page 162), so that

$$(a_1)_{res} = 0.65\frac{P_0}{c}\sqrt{\frac{ml}{T}}$$

For the two other natural frequencies we find

$$(a_1)_{res} = \infty \text{ (second mode)}$$
$$(a_1)_{res} = 0.27\frac{P_0}{c}\sqrt{\frac{ml}{T}} \text{ (third mode)}$$

The most important technical application of this method is in connection with torsional vibration in the crank shafts of Diesel engines, as discussed in Chap. V.

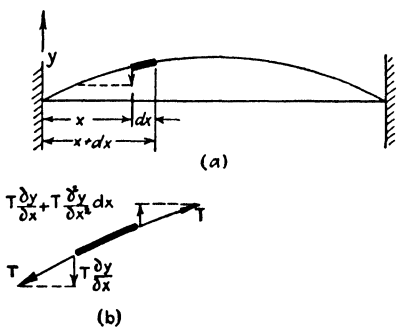


FIG. 106.—Vertical components of the tensions acting on an element *dx* of a stretched string.

31. Strings, Organ Pipes, Longitudinal and Torsional Vibration of Uniform Bars.—These four types of problem will be treated together because their mathematical and physical interpretations are identical.

In the last few sections a string with *three* masses has been investigated. The "string" itself was supposed to have no weight; the masses were supposed to be concentrated at a few distinct points. By imagining the number of masses to increase without limit we arrive at the concept of a uniform string with *distributed* mass.

The equation of motion is derived by writing Newton's law for a small element *dx* of the string, of which again the tension

T is assumed to be constant. Let the deflection curve during the vibration be $y(x, t)$, where the ordinate varies both with the location along the string and with the time. The vertical component of the tension **T** pulling to the left at a certain point x of the string is (Fig. 106)

$$-\mathbf{T}\frac{\partial y}{\partial x},$$

negative because it pulls downward, whereas y is positive upward. The differential coefficient is *partial*, because the string is considered at a certain instant, *i.e.*, t is a constant in the differentiation. At the right-hand end of the element dx, the vertical component of the tension is

$$+\mathbf{T}\frac{\partial y}{\partial x} + \partial\left(\mathbf{T}\frac{\partial y}{\partial x}\right) = \mathbf{T}\frac{\partial y}{\partial x} + \frac{\partial}{\partial x}\left(\mathbf{T}\frac{\partial y}{\partial x}\right)dx = \mathbf{T}\frac{\partial y}{\partial x} + \mathbf{T}\frac{\partial^2 y}{\partial x^2}dx$$

This quantity is positive because it pulls upward. The factor $\frac{\partial^2 y}{\partial x^2}dx$ expresses the increase in slope along dx. Since the two vertical forces on the element dx are not equal (Fig. 106*b*), there is an excess upward pull of

$$\mathbf{T}\frac{\partial^2 y}{\partial x^2}dx$$

which must accelerate the element in the upward direction. If we denote the mass per unit length of the string by μ_1, the mass of dx is $\mu_1 dx$ and Newton's law gives

$$\mu_1 dx\frac{\partial^2 y}{\partial t^2} = \mathbf{T}\frac{\partial^2 y}{\partial x^2}dx$$

Dividing by dx we obtain the partial *differential equation of the string:*

$$\mu_1\frac{\partial^2 y}{\partial t^2} = \mathbf{T}\frac{\partial^2 y}{\partial x^2} \tag{93}$$

The reader should compare the structure of this formula with the first of the equations (89) and determine the physical meaning of each term.

The problem of *longitudinal vibrations in a bar* is quite similar to that of the string and is a generalization of Fig. 104 (without damping) when we take more and smaller masses and more and

shorter springs. Now the masses are not numbered 1, 2, 3 as in Fig. 104 but designated by their position x along the bar (Fig. 107). Let the longitudinal displacement of each point x be indicated by the Greek equivalent of x, namely ξ. Thus the state of motion of the bar is known if we know $\xi(x, t)$, again a function of two variables.

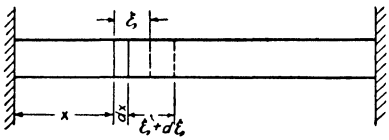


FIG. 107.—Longitudinal vibrations of a bar; x determines the position of any point, and ξ is the displacement during vibration of each point x.

The cross section x goes to $x + \xi$, and the section $x + dx$ goes to $(x + dx) + (\xi + d\xi)$. At some instant t the length dx becomes

$$dx + \frac{\partial \xi}{\partial x} dx$$

Thus $\partial\xi/\partial x$ is the unit elongation which causes at the section x of the bar a tensile stress of

$$E\frac{\partial \xi}{\partial x}$$

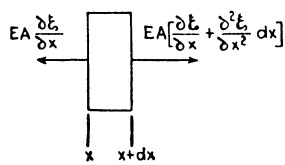


FIG. 108.—Longitudinal elastic forces on an element of the beam of Fig. 107.

where E is the modulus of elasticity. If the bar were stretched with a constant stress, $E\frac{\partial \xi}{\partial x}$ would be constant along the length of the bar, and the element dx would be pulled to the left with the same force as to the right. But if the stress $E\frac{\partial \xi}{\partial x}$ varies from point to point, there will be an excess force on the element to accelerate it longitudinally.

In Fig. 108 let the element dx be represented with its two forces which are the stresses multiplied by the cross-sectional area A. The force to the left is $AE\frac{\partial \xi}{\partial x}$, and that to the right is $AE\frac{\partial \xi}{\partial x}$ plus the increment due to the increase dx in the abscissa. This increment of force is $\frac{\partial}{\partial x}\left(AE\frac{\partial \xi}{\partial x}\right)dx$. Hence the excess force to the right is

$$AE\frac{\partial^2 \xi}{\partial x^2} dx$$

Let the mass per unit *length* of the bar be μ_1, and Newton's law becomes

$$(\mu_1 dx)\frac{\partial^2 \xi}{\partial t^2} = AE\frac{\partial^2 \xi}{\partial x^2}dx$$

or

$$\mu_1 \frac{\partial^2 \xi}{\partial t^2} = AE\frac{\partial^2 \xi}{\partial x^2} \tag{93a}$$

where AE is the tension stiffness of the bar. This is the same differential equation as (93).

A variant of this case is the *organ pipe*, where an air column instead of a steel column executes longitudinal vibrations. Equation (93*a*) evidently must be the same; μ_1 signifies the mass of air per unit length of pipe, and E is its modulus of elasticity. Instead of the *stress* in the above derivation, we have here the *pressure* and since the definition of E in elasticity is

$$\frac{\text{stress}}{E} = \frac{\text{elongation}}{\text{original length}},$$

we have correspondingly for the E in gases

$$\frac{\text{increase in pressure}}{E} = \frac{\text{decrease in volume}}{\text{original volume}},$$

or

$$E = -\mathrm{v}\frac{d\mathrm{p}}{d\mathrm{v}}$$

As in elasticity, the quantity E in gases is measured in pounds per square inch.

Finally, an inspection of Figs. 103, 104, and 105 will make it clear that the *torsional* vibration of a uniform shaft with distributed moment of inertia also leads to the same differential equation. The variable in this case is the angle of twist $\varphi(x, t)$, and the differential equation is

$$\mu_1 \frac{\partial^2 \varphi}{\partial t^2} = GI_p \frac{\partial^2 \varphi}{\partial x^2} \tag{93b}$$

where μ_1 is the moment of inertia per inch length of shaft and GI_p is the torsional stiffness of the shaft. It is left as an exercise to the reader to derive this result.

Proceeding to a solution of (93), (93*a*), or (93*b*), we assume that the string vibrates *harmonically* at some natural frequency

and in some natural or normal configuration. It remains to be seen whether such an assumption is correct. In mathematical language this means that we assume

$$y(x, t) = y(x) \sin \omega t \tag{94}$$

Substitute this in (93), which then becomes

$$\frac{d^2y}{dx^2} + \frac{\mu_1\omega^2}{\mathbf{T}} y = 0 \tag{95}$$

which is an ordinary differential equation. Whereas in all previous problems this sort of assumption simplified the ordinary differential equations to algebraic ones, we have here the simplification of a partial differential equation to an ordinary differential equation.

It is seen that (95) has the same mathematical form as Eq. (13), page 14, or in words: the amplitude of the string as a function of *space* acts in the same manner as the amplitude of a single-degree-of-freedom system as a function of *time*.

Therefore the general solution of (95) is by Eq. (14)

$$y(x) = C_1 \sin x\sqrt{\frac{\mu_1\omega^2}{\mathbf{T}}} + C_2 \cos x\sqrt{\frac{\mu_1\omega^2}{\mathbf{T}}} \tag{96}$$

which determines the shape of the string at the instant of maximum deflection. The integration constants C_1 and C_2 can be determined from the condition that at the ends of the string the amplitudes must be zero, or

$$y = 0 \quad \text{for} \quad x = 0 \quad \text{and for} \quad x = l$$

Substituting $x = 0$ gives

$$y(0) = 0 = C_1 \cdot 0 + C_2 \cdot 1$$

so that $C_2 = 0$. With $x = l$, we get

$$y(l) = 0 = C_1 \sin l\sqrt{\frac{\mu_1\omega^2}{\mathbf{T}}} \tag{97}$$

This can be satisfied by making $C_1 = 0$, which gives the correct but uninteresting solution of the string remaining at rest. However, (97) can also be satisfied by making the argument of the sine an integer multiple of π or 180 deg.

$$l\sqrt{\frac{\mu_1\omega^2}{T}} = 0, \pi, 2\pi, 3\pi, \cdots \tag{98}$$

This determines the natural frequencies, while the corresponding normal modes can be found at once by substitution of Eq. (98) in Eq. (96). The results are illustrated in Fig. 109.

There is an infinite number of normal elastic curves and correspondingly an infinite number of natural frequencies. The

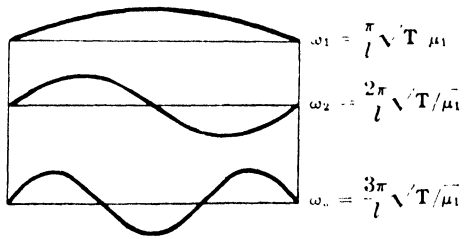


FIG. 109. The first three natural modes of motion of the lateral vibration of a uniform string or of the longitudinal or torsional vibration of a uniform bar built in at both ends.

motion in each one of these modes is such that the amplitude of every point of the string varies harmonically with the time, and consequently the normal curve remains similar to itself. Therefore, if a string is deflected in one of the shapes of Fig. 109 and then released, it will return to its original position in an interval of time determined by the natural period of the vibration. At that frequency and shape the inertia force and spring force of each element dx of the string are in equilibrium with each other at any instant.

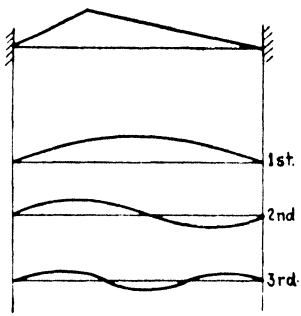


FIG. 110. Shape of a "plucked" string with the first three Fourier components of that shape.

If the string is given an initial displacement of a shape different from any of those of Fig. 109, *e.g.*, a displacement such as is shown in Fig. 110, the shape can be considered to be composed of a (Fourier) series of the normal shapes (see page 20). Each Fourier component then will execute a motion conformal to itself, but each one will do this *at its own particular frequency.* Thus after one-eighth period of the fundamental mode, the amplitude of that

fundamental component will have decreased to 0.707 of its original value, the second component will have zero amplitude, while the fourth mode will have reversed its amplitude. Thus the compound shape of Fig. 110 is *not* preserved during the motion. However, after a *full* period of the fundamental motion the original shape recurs.

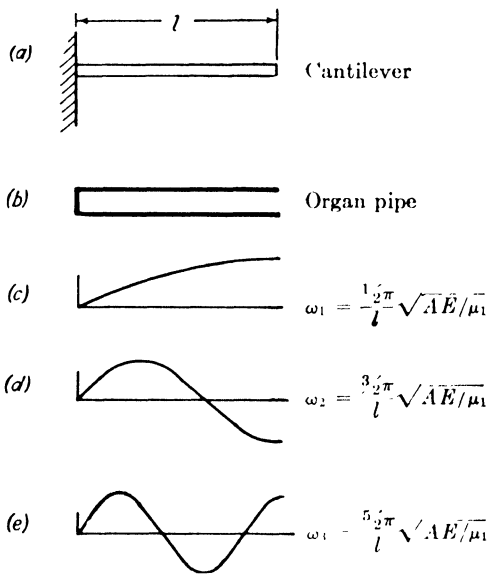


FIG. 111.—Longitudinal vibrations of a steel column or air column of which one end is fixed and one end free.

The shapes of Fig. 109 pertain also to the longitudinal (or torsional) vibrations of a bar with both ends built in or to the vibrations of an "organ pipe" with both ends closed. The ordinates then signify displacements along the bar. The frequencies are evidently the same, except for a substitution of the "tension stiffness" AE instead of the tension **T**.

For the longitudinal (or torsional) vibrations of a *cantilever* bar or of an organ pipe with one open end, the general expression (96) for the shape still holds, but the end conditions for determining C_1 and C_2 are different.

At the closed end $x = 0$, we still have $y = 0$, because the air cannot penetrate the solid wall at the closed end of the pipe. At the open end, however, there can be displacement but no stress (in the bar) or no pressure excess (in the organ pipe). In

the derivation of the differential equation this stress was seen to be proportional to $\partial\xi/\partial x$ (or dy/dx in the string notation). The end conditions are therefore

$$\begin{aligned} x &= 0 \qquad y = 0 \\ x &= l \qquad dy/dx = 0 \end{aligned}$$

The first of these makes $C_2 = 0$ in (96), while the second one can be satisfied by equating the length of the bar to $\frac{1}{4}$, $\frac{3}{4}$, $\frac{5}{4}$, etc., wave lengths, as shown in Fig. 111.

In conclusion, a number of results previously obtained are assembled in Fig. 112. The first of these is half of Fig. 96*b*;

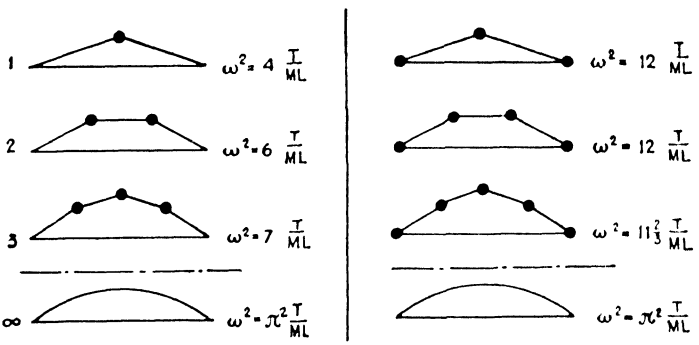


FIG. 112. By increasing the number of equidistant masses on the string the uniform mass distribution is approached gradually. The convergence is too slow to have practical significance.

the second one is Fig. 97*b*, and the third one is Fig. 96*a*. The inscribed frequencies also have been taken from the same sources, except that M now stands for all the masses combined and L for the total length of the string.

In the right half of Fig. 112 two masses have been added at the points of support. These masses do not affect the frequency since they do not move. However, they do affect the value of M, which is the total mass. By increasing the number of masses from 1 to 2, 3, etc., we must finally approach the fundamental frequency of the continuous string. In the left half of the figure the frequency of the continuous string is approached from below, because the masses are concentrated too close to the center where their inertia is very effective. Conversely, in the right half of the figure the mass is too close to the supports where it contributes a very small amount of kinetic energy; hence the frequencies are too large.

It is seen that the exact factor $\pi^2 = 9.87$ is approached very slowly, and therefore that a quick approximate method for finding the natural frequency based on such shifting of masses is rather unsatisfactory.

32. Rayleigh's Method.—The string problem is the simplest one among all those having an infinite number of degrees of freedom. Though for this problem an exact solution of the natural frequencies can be obtained, this is far from possible for the general problem of a system with distributed mass and distributed flexibility. Therefore it is of great importance to have an approximate method for finding the lowest or fundamental frequency, a method which will always work. Such a procedure has been developed by *Rayleigh;* it is a generalization of the energy method discussed on page 46.

Briefly, a shape is *assumed* for the first normal elastic curve; with this assumption the (maximum) potential and kinetic energies are calculated and are equated. Of course, if the *exact* shape had been taken as a basis for the calculation, the calculated frequency would be exactly correct also; for a shape differing somewhat from the exact curve a very useful and close approximation for the frequency is obtained. Since the exact solution for the string is known, we choose it as an example for the explanation of Rayleigh's method, which will enable us to judge the error of the approximate result.

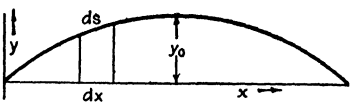


FIG. 113.—Calculation of the potential energy of a string.

For a calculation of the potential energy we observe that the deflected string has a greater length than the straight one. It is subjected to a tension **T** all the time, so that in going into the deflected shape an amount of work $\mathbf{T}\Delta l$ has to be performed on it. This is stored in the string in the form of potential energy. For a calculation of the increase in length Δl, we observe that the length of an element ds is (Fig. 113)

$$ds = \sqrt{(dx)^2 + (dy)^2} = dx\sqrt{1 + \left(\frac{dy}{dx}\right)^2} \approx dx\left[1 + \frac{1}{2}\left(\frac{dy}{dx}\right)^2\right]$$

The increase in length of that element is

$$ds - dx = \frac{1}{2}\left(\frac{dy}{dx}\right)^2 dx$$

so that

$$Pot = \frac{\mathbf{T}}{2}\int_0^l \left(\frac{dy}{dx}\right)^2 dx \tag{99}$$

This result can be derived somewhat differently as follows. In the derivation of Eq. (93), page 171, it was seen that the right-hand side $\mathbf{T}\frac{\partial^2 y}{\partial x^2}$ signifies the downward force per unit length of the string. Imagine the string to be brought into its deflected shape by a static loading $\mathbf{q}(x)$ which grows proportional to the deflection $y(x)$. The work done on an element dx by $\mathbf{q}(x)$ in bringing it to the fully deflected position $y(x)$ is $\frac{1}{2}\mathbf{q}(x)y(x)dx$, and the potential energy is

$$Pot = \tfrac{1}{2}\int_0^l \mathbf{q}(x)y(x)dx$$

Since $\mathbf{q}(x) = -\mathbf{T}\frac{d^2y}{dx^2}$,

$$Pot = -\frac{\mathbf{T}}{2}\int_0^l y \cdot \frac{d^2y}{dx^2}dx \tag{99a}$$

By a process of partial integration this can be shown to be equal to (99):

$$\int_0^l y\frac{d^2y}{dx^2}dx = \int_0^l yd\left(\frac{dy}{dx}\right) = y\frac{dy}{dx}\Big|_0^l - \int_0^l \frac{dy}{dx}dy$$

The first term is zero because y is zero at 0 and l. The integral in the second term can be written

$$-\int_0^l \frac{dy}{dx}\frac{dy}{dx}dx = -\int_0^l \left(\frac{dy}{dx}\right)^2 dx$$

The total kinetic energy is the sum of the kinetic energies $\frac{1}{2}mv^2 = \frac{1}{2}(\mu_1 dx)(y\omega)^2$ of the various elements:

$$Kin = \frac{1}{2}\mu_1\omega^2\int_0^l y^2dx \tag{100}$$

As in the case of a single degree of freedom (page 46), the expressions (99) and (100) are the *maximum* energies; the maximum potential energy occurs in the most deflected position, and the maximum kinetic energy occurs in the undeformed position where the velocity is greatest. Equating the two energies we find for the frequency:

$$\omega^2 = \frac{\mathbf{T}}{\mu_1}\frac{\int_0^l \left(\frac{dy}{dx}\right)^2 dx}{\int_0^l y^2dx} \tag{101}$$

The value ω^2 obtained with this formula depends on the form $y(x)$ which we assume. First consider the exact shape:

$$y = y_0 \sin \frac{\pi x}{l}$$

By Eq. (99) the potential energy is

$$Pot = \frac{\mathbf{T}}{2}\int_0^l \left(y_0 \frac{\pi}{l} \cos \frac{\pi x}{l}\right)^2 dx = \frac{\mathbf{T}}{2} y_0^2 \frac{\pi^2}{l^2} \frac{l}{2} \qquad \text{(see page 16)}$$

Similarly we find for the kinetic energy: $Kin = \frac{\mu_1 \omega^2}{2} y_0^2 \frac{l}{2}$, so that the frequency becomes

$$\omega_1 = \frac{\pi}{l}\sqrt{\frac{\mathbf{T}}{\mu_1}} = \frac{3.142}{l}\sqrt{\frac{\mathbf{T}}{\mu_1}} \qquad (102)$$

which is the exact value.

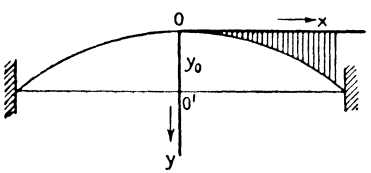


FIG. 114.—A parabolic arc as the approximate (Rayleigh) shape of a vibrating string.

Next assume a parabolic arc for the shape of the string. The equation of a parabola in the xy system of Fig. 114 is $y = px^2$. The parabola can be made to pass through the two points $y = y_0$ and $x = \pm l/2$ by giving p the value $4y_0/l^2$. The equation $y = 4y_0\frac{x^2}{l^2}$ describes the shaded ordinates of Fig. 114. The deflection of the string is y_0 minus the shaded ordinate:

$$y = y_0\left(1 - \frac{4x^2}{l^2}\right)$$

Using this value for y in (99) and (100), we have after a simple integration:

$$Pot = \frac{8}{3}\mathbf{T}\frac{y_0^2}{l}$$

$$Kin = \frac{4}{15}\mu_1 \omega^2 l y_0^2$$

and

$$\omega_1 = \frac{\sqrt{10}}{l}\sqrt{\frac{\mathbf{T}}{\mu_1}} = \frac{3.162}{l}\sqrt{\frac{\mathbf{T}}{\mu_1}}$$

which is only 0.7 per cent greater than the exact value. The error is surprisingly small, since it can be seen physically that the parabola cannot be the true shape. The spring effect driving a particle dx of the string back to equilibrium lies in the *curvature*, or d^2y/dx^2, of the string. At the ends the string particles do not

move, so that there they have obviously neither inertia force nor spring force. Therefore the exact shape must have no curvature at the ends, which condition is violated by the parabola.

To test the power of Rayleigh's method we shall now apply it to a most improbable shape of deflection curve (Fig. 115):

$$y = y_0 \frac{x}{l/2}, \text{ for } x = l/2$$

We find successively,

$$Pot = 2Ty_0^2/l$$
$$Kin = \mu_1\omega^2 l y_0^2/6$$

and

$$\omega_1 = \frac{\sqrt{12}}{l}\sqrt{\frac{T}{\mu_1}} = \frac{3.464}{l}\sqrt{\frac{T}{\mu_1}}$$

which is 10 per cent greater than the exact value (102).

Rayleigh's approximation always gives for the lowest natural frequency a value which is somewhat too high. Among a number of approximate results found in this manner the smallest is always the best one. A proof for this statement will be given on page 200.

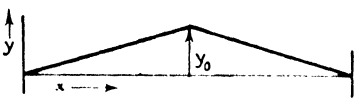


FIG. 115. Another Rayleigh approximation for half a sine wave.

Finally, we shall solve the combination problem of a heavy string of total mass M, in the middle of which is attached a single concentrated weight of the same mass M. This problem is again equivalent to that of the longitudinal (or torsional) vibrations of a bar clamped at both ends and having a concentrated disk in the middle with a mass (or moment of inertia) equal to that of the bar itself.

Regarding the elastic curve, it can be said that, if the central mass were absent, the curve would be sinusoidal, whereas if the string mass were absent, it would be as shown in Fig. 115. The actual shape will lie between these two. Assuming first a sinusoid, we note that the potential energy is not affected by the presence of the central mass. The kinetic energy, however, is increased by $\frac{1}{2}M\omega^2 y_0^2$, which is twice as great as the kinetic energy of the string itself, since $M = \mu_1 l$. Thus the total kinetic energy is three times as large as without the central mass and consequently the frequency is $\sqrt{3}$ times as small:

$$\omega_1 = \frac{\pi}{\sqrt{3}} \frac{1}{l} \sqrt{\frac{T}{\mu_1}} = 1.81 \sqrt{\frac{T}{Ml}}$$

With the string deformed as shown in Fig. 115, again the potential energy is not affected, and the kinetic energy becomes $M\omega^2 y_0^2/2$ larger, *i.e.*, $(\frac{1}{2} + \frac{1}{6})/\frac{1}{6} = 4$ times as great as before. Thus the frequency is

$$\omega_1 = \frac{\sqrt{12}}{2l} \sqrt{\frac{T}{\mu_1}} = 1.73 \sqrt{\frac{T}{Ml}}$$

Since this last value is smaller than the one found before, it is the better approximation. The exact solution for this problem is

$$\omega_1 = 1.721 \sqrt{\frac{T}{Ml}}$$

This exact solution, though somewhat complicated, can be found from the theory developed on page 174. Equation (96) gives the general shape of a vibrating string, which we apply now to the left half of our string. The condition that the left end is at rest gives $C_2 = 0$ as before, so that the shape of the left half of the string is determined by

$$y = C \sin x \sqrt{\frac{\mu_1 \omega^2}{T}} \tag{103}$$

where C and ω are unknown. The amplitude C is of no particular importance, but the frequency ω determines the "wave length" of the sine curve. In Fig. 116 the shape is shown, with the right half of the string as a mirrored image of the left half. The central mass M experiences an inertia force $M\omega^2 y_0$ and an elastic force $2T \tan \alpha$ and, as these two forces must be in equilibrium,

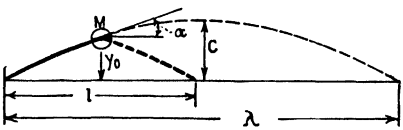


FIG. 116.—Exact calculation of heavy string with central mass.

$$2T \tan \alpha = M\omega^2 y_0 \tag{104}$$

The values y_0 and $\tan \alpha$ are the ordinate and the slope of (103) at the point where $x = l/2$, or

$$y_0 = C \sin \frac{l}{2} \sqrt{\frac{\mu_1 \omega^2}{T}}$$

$$\tan \alpha = C \sqrt{\frac{\mu_1 \omega^2}{T}} \cos \frac{l}{2} \sqrt{\frac{\mu_1 \omega^2}{T}}$$

Since $\mu_1 l = M$, a substitution of these expressions in (104) gives

$$\frac{\omega}{2} \sqrt{\frac{Ml}{T}} = \cot \frac{\omega}{2} \sqrt{\frac{Ml}{T}}$$

Thus we have to find an angle of which the magnitude in radians equals the value of the cotangent. For zero degrees the angle is zero and the cotangent infinite; for 90 deg. the angle is 1.6 radians and the cotangent is zero. Clearly the equality must occur somewhere between 0 and 90 deg. From a trigonometric table we find that it occurs at 49.3 deg. = 0.8603 radian. Thus

$$\frac{\omega}{2}\sqrt{\frac{Ml}{T}} = 0.8603$$

or

$$\omega_1 = 1.721\sqrt{\frac{T}{Ml}}$$

Since the smallest value obtained for the frequency is always the best one, Rayleigh sometimes writes down a formula for the shape which is not entirely determined but contains an arbitrary parameter. With this formula the frequency is calculated in the regular manner, giving a result which also contains the parameter. By giving the parameter various values, the frequency also assumes different values. The best value among these is the smallest one, *i.e.*, the minimum frequency as a function of the parameter. The approximation thus obtained is very much better than with the normal Rayleigh method.

Ritz has generalized this procedure to more than one parameter. The *Ritz method* of finding natural frequencies is very accurate but unfortunately requires rather elaborate calculations.

Example: A ship drive consists of an engine, a propeller shaft of 150 ft. length and 10 in. diameter, and a propeller of which the moment of inertia is the same as that of a solid steel disk of 4 in. thickness and 4 ft. diameter. The inertia of the engine may be considered infinitely great. Find the natural frequency of torsional vibration.

Solution: On account of the great engine inertia the engine end of the shaft can be considered as built in, so that the system might be described as a "torsional cantilever." The shape of the deflection curve (*i.e.*, angle φ *vs.* distance x from engine) would be a quarter sine wave if there were no propeller, and it would be a straight line through the origin if the shaft inertia were negligible with respect to that of the propeller. We choose the latter straight line as our Rayleigh shape, thus: $\varphi = Cx$.

From the strength of materials we take two results:

1. The relation between torque **M** and angle of twist φ:

$$d\varphi = \frac{\mathbf{M}dx}{GI_p}$$

2. The potential energy stored in a slice dx of the shaft:

$$d\,Pot = \frac{\mathbf{M}^2dx}{2GI_p}$$

where GI_p is the torsional stiffness of the shaft.

Since our assumed Rayleigh curve has a constant slope $d\varphi/dx = C$, it follows from the first of these equations that the torque $\mathbf{M} = CGI_p$ is constant along the length of the shaft. The second equation can thus be integrated immediately:

$$Pot = \frac{\mathbf{M}^2 l}{2GI_p}$$

The kinetic energy of a shaft element dx is $\frac{1}{2}(I_1 dx)\dot{\varphi}^2$, where I_1 is the mass moment of inertia per unit length of the shaft. But $\dot{\varphi} = \omega\varphi = \omega Cx = \omega \mathbf{M}x/GI_p$.

The kinetic energy of the shaft becomes

$$Kin. = \frac{I_1}{2}\left(\frac{\omega \mathbf{M}}{GI_p}\right)^2 \int_0^l x^2 dx = \frac{I_1}{6} \cdot \frac{\omega^2 \mathbf{M}^2 l^3}{G^2 I_p^2}$$

The angular amplitude of the propeller (of which the inertia is I) is $\varphi_p = Cl = \mathbf{M}l/GI_p$, and its kinetic energy:

$$Kin_p = \frac{I}{2}\omega^2 \frac{\mathbf{M}^2 l^2}{G^2 I_p^2}$$

Equating the sum of the two kinetic energies to the potential energy and solving for ω^2, we find:

$$\omega^2 = \frac{GI_p}{l\left(I + \frac{I_1 l}{3}\right)},$$

from which it is seen that one-third of the shaft inertia is to be thought of as concentrated at the propeller.

With the numerical data of the problem we find:

$$I = \frac{1}{2}mr^2 = \frac{1}{2}\left(\frac{0.28}{386}\pi r^2 4\right)r^2 = 1{,}510 \text{ in. lb. sec.}^2$$

$$I_1 l = \frac{1}{2}mr^2 l = \frac{1}{2}\left(\frac{0.28}{386}\pi r^2 1\right)r^2 l = 1{,}280 \text{ in. lb. sec.}^2$$

$$\frac{GI_p}{l} = \frac{G}{l}\frac{\pi}{2}r^4 = \frac{12.10^6}{150 \times 12} \cdot \frac{\pi}{2} \cdot 5^4 = 6.55\ 10^6 \text{ in. lb.},$$

so that

$$\omega^2 = \frac{6.55\ 10^6}{1{,}510 + 427} = 3{,}380 \text{ rad.}^2/\text{sec.}^2$$

and

$$f = \frac{\omega}{2\pi} = \frac{1}{2\pi}\sqrt{3{,}380} = 9.3 \text{ cycles/sec.}$$

An exact solution can be found by a process very similar to that discussed on page 182. In fact, Fig. 116 can be suitably interpreted for this propeller shaft. The frequency equation becomes

$$\alpha \tan \alpha = \frac{I_1 l}{I} = \frac{1{,}280}{1{,}510} = 0.846$$

where α is an abbreviation for

$$\alpha = l\sqrt{\frac{I_1\omega^2}{GI_p}}$$

By trial the solution of this transcendental equation is found to be

$$\alpha = 46.3 \text{ deg.} = 0.809 \text{ radian}$$

from which

$$\omega^2 = (0.809)^2 \frac{GI_p}{l^2 I_1} = 3{,}350 \text{ rad.}^2/\text{sec.}^2$$

which is 1 per cent smaller than the Rayleigh result.

33. Bending Vibrations of Uniform Beams.—In the various textbooks on strength of materials the differential equation of the static loading of a beam is usually given in the following form:

$$\left.\begin{aligned} \mathbf{M} &= EI\frac{d^2\eta}{dx^2} \\ \mathbf{q} &= \frac{d^2\mathbf{M}}{dx^2} \\ \text{or combined} \qquad \mathbf{q} &= \frac{d^2}{dx^2}\left(EI\frac{d^2y}{dx^2}\right) \end{aligned}\right\} \tag{105}$$

where $\mathbf{q}$ is the load per running inch and $\mathbf{M}$ is the bending moment.

If the cross section of the beam is constant along its length, the factor EI does not depend on x and the equation simplifies to

$$\mathbf{q} = EI\frac{d^4y}{dx^4} \tag{106}$$

The various diagrams for a beam on two supports under two stretches of uniform loading are shown in Fig. 117, but Eqs. (105) and (106) are generally true and hold just as well for other manners of support, *e.g.*, for cantilevers.

If a beam is in a state of sustained vibration at a certain natural frequency, the "loading" acting on it is an alternating inertia load. In order to get a physical conception of this statement, note that in the position of maximum *downward* deflection (Fig. 117*e*) each particle of the beam is subjected to a maximum *upward* acceleration. Multiplied by the mass of the particle, this gives an *upward* inertia force which the beam must exert on the particle. By the principle of action and reaction the particle in question must exert a *downward* force on the beam.

All these downward forces of the various particles constituting the beam form a loading q which is responsible for the deflection and is related to it by (105) or (106). Naturally, while the beam is passing through its equilibrium position, the accelerations and therefore the loadings are zero, but then the deflections are also zero.

Thus the differential equation of the vibrating *bar of uniform cross section* is

$$EI\frac{\partial^4 y}{\partial x^4} = -\mu_1\frac{\partial^2 y}{\partial t^2} \tag{107}$$

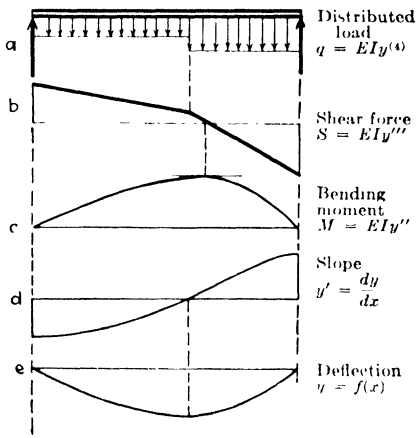


FIG. 117.—Illustrating the differential equations of a beam in bending.

where μ_1 is the mass of the beam per unit length. Assuming a sustained free vibration at a frequency ω, we have, as on page 174,

$$y(x, t) = y(x) \sin \omega t \tag{94}$$

which gives to (107) the form

$$EI\frac{d^4 y}{dx^4} = \mu_1\omega^2 y \tag{108}$$

The left side of this is the elastic expression for the loading [Eq. (106)], while the right side is the maximum value of the inertia load. From it we see that the physical characteristic of any "normal elastic curve" of the beam is that *the* q *loading diagram must have the same shape as the deflection diagram.* Any loading that can produce a deflection curve similar to the loading curve can be regarded as an inertia loading during a vibration;

the natural frequency appears merely in the numerical factor $\mu_1\omega^2$ connecting the two.

The functions which satisfy (108) must have the property that, when differentiated four times, they return to their original form multiplied by a positive constant $\mu_1\omega^2/EI$. We may remember four functions that will do this, *viz.*:

$$e^{ax}, \quad e^{-ax}, \quad \sin ax, \quad \text{and} \quad \cos ax$$

where the coefficient a has to be so chosen that

$$a = \sqrt[4]{\frac{\mu_1\omega^2}{EI}} \tag{109}$$

Thus the general solution of (108) containing four integration constants can be written

$$y(x) = C_1e^{ax} + C_2e^{-ax} + C_3 \sin ax + C_4 \cos ax \tag{110}$$

This expression determines the shape of the various "normal elastic curves." The four integration constants C have to be calculated from the end conditions. For each end of the beam there are two such conditions, making the required four for the two ends. They are for a

Simply supported end: $y = 0, y'' = 0$
(zero deflection and bending moment)

Free end: $y'' = 0, y''' = 0$
(zero bending moment and shear force)

Clamped end: $y = 0, y' = 0$
(zero deflection and slope)

which will be clear from a consideration of the physical meaning of the various derivatives as shown in Fig. 117. For any specific case the four end conditions substituted in (110) give four homogeneous algebraic equations in the four C's. The determinant of that system equated to zero is an equation in a, which by (109) is the frequency equation. This process has been carried out for the various kinds of beams (beam on two supports, cantilever or "clamped-free" beam, clamped-clamped beam, etc.), but we prefer here to find approximate solutions by using Rayleigh's method. Only for the beam on two simple supports can the exact solution be recognized from (110) in a simple manner. The end conditions are in this case

$$x = 0, y = y'' = 0 \quad \text{and} \quad x = l, y = y'' = 0$$

We see immediately that a sine-wave shape satisfies these conditions, and that the cosine or e-functions violate them. Thus for a beam on two supports (110) simplifies to

$$y(x) = C \sin ax$$

so that the normal elastic curves of a uniform beam on two supports are the same as those of the string shown in Fig. 109, but the frequencies are different. They are found by making the argument of the sine equal to an integer number times π or

$$al = l\sqrt[4]{\frac{\mu_1\omega^2}{EI}} = n\pi \qquad (n = 1, 2, 3, \cdots)$$

so that

$$\omega_1 = \frac{\pi^2}{l^2}\sqrt{\frac{EI}{\mu_1}},\ \omega_2 = \frac{4\pi^2}{l^2}\sqrt{\frac{EI}{\mu_1}},\ \cdots,\ \omega_n = \frac{n^2\pi^2}{l^2}\sqrt{\frac{EI}{\mu_1}} \qquad (111)$$

Whereas the consecutive natural frequencies of the string increase as 1, 2, 3, 4, etc. (page 175), for the beam on two supports they increase as 1, 4, 9, 16, etc.

We have seen that in a natural shape of the uniform beam the inertia loading diagram is similar to the deflection diagram, because the inertia load at each point is $\mu_1 dx\omega^2 y$, proportional to the deflection y. Thus to each natural shape there belongs a natural loading curve $\mu_1\omega^2 y$. This concept is useful for solving a group of problems, of which the following is a typical example:

A beam on two supports is in a state of rest. A load P is suddenly applied to the center and remains on it for t_0 seconds. Then it is removed. What is the ensuing state of motion?

The concentrated load, being not one of the natural loadings, will excite many of the natural motions. In order to see through the situation, the applied loading is resolved into a series of natural loadings, in this case into a Fourier series. A concentrated load P is hard to work with; we replace it by a distributed load of intensity q acting over a short length δ, such that $q\delta = P$. Then, by Eq. (11a), page 21, the various Fourier coefficients become

$$a_n = \frac{2}{\pi}\int_0^l F(x) \sin n\frac{\pi x}{l} \cdot d\frac{\pi x}{l} = \frac{2q}{\pi}\int_{-\frac{l}{2}-\frac{\delta}{2}}^{-\frac{l}{2}+\frac{\delta}{2}} \sin n\frac{\pi x}{l} d\frac{\pi x}{l}$$

$$= \pm\frac{2q}{\pi} \cdot \frac{\pi\delta}{l} = \pm\frac{2P}{l}$$

where the + sign holds for $n = 1, 5, 9$ and the − sign for $n = 3, 7, 11, \cdots$. Thus a concentrated force P at the center of a beam is equivalent to a series of sine loadings of the same intensity $2P/l$. The first few terms are illustrated in Fig. 118*a*.

We investigate the influence on the motion of each of these natural loadings individually. Any of them will influence only the natural motion to which they belong, and under one of these loadings the system acts as one of a single degree of freedom, to

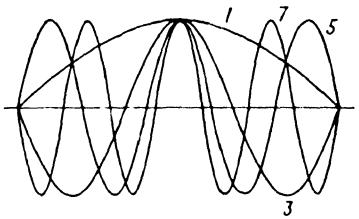


FIG. 118*a*.– Fourier components of a concentrated load.

which the solution of problem 32 (page 101) may be applied. Thus for the first loading

$$y = y_{st}[\cos \omega_1(t - t_0) - \cos \omega_1 t]$$

The static deflection curve under a loading $q = \frac{2P}{l} \sin \frac{n\pi x}{l}$ is found by integrating Eq. (106) four times:

$$(y_{st})_n = \frac{2Pl^3}{n^4\pi^4 EI} \cdot \sin \frac{n\pi x}{l}$$

The entire motion is the superposition of the individual motions for each mode and can be written as

$$y(x, t) = \frac{2Pl^3}{\pi^4 EI} \sum_{1,3,5}^{n=} (-1)^{\frac{n-1}{2}} \frac{\sin \frac{n\pi x}{l}}{n^4} [\cos \omega_n(t - t_0) - \cos \omega_n t]$$

where the values of ω_n are to be found from Eq. (111).

Suppose the load is applied during a time t_0 which is a multiple of a period of the first harmonic motion (and therefore a multiple of the period of any higher harmonic as well). Then $\cos \omega_n(t - t_0) = \cos \omega_n t$, and the whole solution $y(x, t)$ reduces to zero. No motion results after the load ceases to apply.

Next consider the case where the load stays on for ½ period of the first harmonic (and therefore for 9/2 period of the third harmonic, 25/2 period of the fifth, etc.). Then $\cos \omega_n(t - t_0) = -\cos \omega_n t$, and the square bracket becomes $-2 \cos \omega_n t$, so that

$$y(x, t) = \frac{4Pl^3}{\pi^4 EI} \sum_{1,3,5} \frac{1}{n^4} (-1)^{\frac{n-1}{2}} \sin \frac{n\pi x}{l} \cos \omega_n t$$

All harmonics are present in the motion, but their amplitudes are proportional to $1/n^4$. Thus, while the first harmonic has an

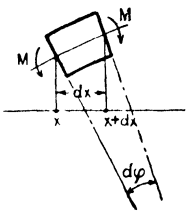


FIG. 118b.- Potential energy of flexure in a beam element.

amplitude of $2Pl^3/n^4EI$ at the center of the span, the third harmonic is only 1/81 times as large, the fifth 1/625, etc.

In applying Rayleigh's method, the expression (100) for the kinetic energy holds for the bar as well as for the string. But the expression (99) for the potential energy will be different since the spring effect in this case is due to the bending resistance EI rather than to the tension **T**. From strength of materials we have the following formulas for the potential or elastic energy stored in an element of length dx of the beam:

$$d\,Pot = \frac{\mathbf{M}^2}{2EI} dx$$

or

$$d\,Pot = \frac{EI}{2} \left(\frac{d^2y}{dx^2} \right)^2 dx$$

These can be derived simply as follows. Consider an element dx under the influence of the bending moment **M** (Fig. 118b). The element is originally straight and is bent through an angle $d\varphi$ by the moment **M**. If the left-hand end of the element be assumed to be clamped, the moment **M** at the right-hand end turns through the angle $d\varphi$. The work done by **M** on the beam is $\frac{1}{2}\mathbf{M}d\varphi$, where the factor ½ appears because both **M** and $d\varphi$ are increasing from zero together. This work is stored as potential energy in the beam element.

Now calculate the angle $d\varphi$. If the slope at the left-hand end x be dy/dx, then the slope at the right-hand end is $\frac{dy}{dx} + \left(\frac{d^2y}{dx^2}\right) \cdot dx$ and the difference in slope $d\varphi$ is

$$d\varphi = \frac{d^2y}{dx^2}dx$$

so that

$$d\ Pot = \tfrac{1}{2}\mathbf{M}y''dx$$

With the differential equation of bending $\mathbf{M} = EIy''$, the two forms given above follow immediately.

Thus the total potential energy in the beam is

$$Pot = \frac{EI}{2}\int_0^l \left(\frac{d^2y}{dx^2}\right)^2 dx \tag{112}$$

It is left as an exercise to the reader to derive the first natural frequency of a beam on two supports by substituting in the expressions (100) and (112) half a sine wave for the shape y.

Let us now calculate the fundamental frequency of a *cantilever* or "clamped-free" beam. We have to choose a curve (Fig. 119) which is horizontal at $x = 0$ and has no curvature or bending moment y'' at the end l. A quarter cosine wave has these properties:

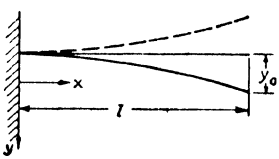


FIG. 119.—Quarter cosine wave as a Rayleigh shape for a cantilever.

$$y = y_0\left(1 - \cos\frac{\pi x}{2l}\right) \tag{113}$$

Since this expression cannot be forced into the form (110) by manipulating the four C's, (113) is not the *exact* form of the normal curve. Substituted in (112) and (100), we find with the aid of the integral of page 16:

$$Pot = \frac{\pi^4}{64}\frac{EI}{l^3}y_0^2$$

$$Kin = \mu_1\omega^2 y_0^2 l\left(\frac{3}{4} - \frac{2}{\pi}\right)$$

Equating these two expressions, the frequency becomes

$$\omega = \frac{\pi^2}{8\sqrt{\frac{3}{4} - \frac{2}{\pi}}}\sqrt{\frac{EI}{\mu_1 l^4}} = \frac{3.66}{l^2}\sqrt{\frac{EI}{\mu_1}} \tag{114}$$

The *exact* solution contains the factor 3.52 which is 4 per cent smaller than 3.66. Figure 120 gives the exact shape together with that of the second mode.

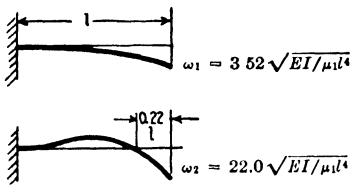


FIG. 120.—The first two natural modes of motion of a cantilever in bending.

The normal elastic curve of a beam which is built in at both ends (a "clamped-clamped" bar) must have a shape that is symmetrical and horizontal at both ends (Fig. 121). A full cosine wave displaced upward by y_0 is a simple curve fitting these conditions:

$$y = y_0\left[1 - \cos\frac{2\pi x}{l}\right]$$

We find successively:

$$Pot = \frac{EI}{2}y_0^2\frac{16\pi^4}{l^4}\frac{l}{2}$$

$$Kin = \frac{\mu_1}{2}y_0^2\omega^2 l[1 + \tfrac{1}{2}]$$

$$\omega = \frac{4\pi^2}{\sqrt{3}}\sqrt{\frac{EI}{\mu_1 l^4}} = \frac{22.7}{l^2}\sqrt{\frac{EI}{\mu_1}}, \tag{115}$$

whereas the exact solution is 22.4 or 1.3 per cent smaller than 22.7

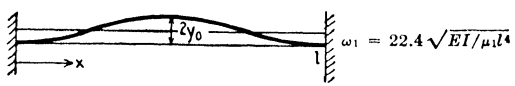


FIG. 121.—Normal elastic curve of a clamped-clamped bar.

Finally, we consider the "free-free" bar, *i.e.*, a bar which is suspended freely from one or more strings or which is floating on a liquid. The simplest mode of vibration (Fig. 122) must have two nodes and no curvature y'' at either end. Such a shape can be had conveniently in the form of half a sine wave displaced vertically through a short distance a:

$$y = y_0 \sin\frac{\pi x}{l} - a$$

The amount of vertical displacement a is important, since it determines the location of the two nodes. For $a = 0$ they are at the ends of the beam; for $a = y_0$ they are both at the center.

The actual value of a between 0 and y_0 can be found from the fact that since no external alternating force is acting on the beam, its total vertical momentum must be zero. While the beam is passing through its equilibrium position, the ends have downward velocities ωy and the middle has an upward velocity ωy. Since the beam is uniform, *i.e.*, since all particles dx have the same mass, these values ωy are proportional to the momentum as well. The total momentum is zero if the areas above and below the center line in Fig. 122 are equal or if

$$0 = \int_0^l y dx = y_0 \int_0^l \sin \frac{\pi x}{l} dx - \int_0^l a dx = \frac{2}{\pi} y_0 l - al$$

so that

$$a = \frac{2y_0}{\pi}$$

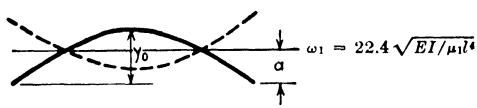


FIG. 122.—Normal elastic curve of a free-free bar.

With that expression for the shape of the vibration we find

$$Pot = \frac{\pi^4}{4} \frac{EIy_0^2}{l^3}$$

$$Kin = \mu_1 \omega^2 y_0^2 l \left[\frac{1}{4} - \frac{2}{\pi^2}\right]$$

$$\omega = \frac{\pi^2}{2\sqrt{\left(\frac{1}{4} - \frac{2}{\pi^2}\right)}} \sqrt{\frac{EI}{\mu_1 l^4}} = \frac{22.72}{l^2} \sqrt{\frac{EI}{\mu_1}} \qquad (116)$$

The exact result is the same as that of the clamped-clamped bar, namely 22.4 which is 1 per cent smaller than 22.72.

Example: A cantilever beam EI, of length l and of mass μ_1 per unit length (total mass $m = \mu_1 l$) carries a concentrated mass M at its end. Find the natural frequency by Rayleigh's method, and in particular find what fraction of m should be added to M in order to make the simple formula (16) applicable (page 43).

Solution: The shape of the deflection curve has to satisfy the same requirements that were used in deriving Eq. (113), so that we shall retain the expression employed there. The potential energy is not affected by the addition of a mass M at the end of the bar, but since the amplitude of that end is y_0, the kinetic energy is increased by $\frac{1}{2}M\omega^2 y_0^2$. With $m = \mu_1 l$, the total kinetic energy can be written as

$$Kin = \frac{1}{2}\omega^2 y_0^2\left[M + m\left(\frac{3}{2} - \frac{4}{\pi}\right)\right] = \frac{1}{2}\omega^2 y_0^2(M + 0.23m).$$

With the expression of page 184 for the potential energy the frequency becomes

$$\omega^2 = \frac{3.03EI}{l^3(M + 0.23m)}$$

Thus 23 per cent of the mass of the bar has to be added to the end mass. In case the bar is supposed weightless, $m = 0$ and the result for ω^2 found here is 1 per cent greater than the exact value, where the coefficient is 3.

34. Beams of Variable Cross Section.—In many practical cases the cross section of the beam is not constant over its length. The most common example of a beam on two supports is a shaft in its bearings, the shaft usually having a greater cross section in its middle portion than near its ends. A steel ship in the water sometimes executes vibrations as a free-free bar, somewhat in the form of Fig. 122. These vibrations become of importance if the unbalanced forces of the propelling machinery have the same frequency as the natural frequency of the ship. But the bending stiffness of a ship is by no means constant over its entire length.

The method of Rayleigh can be applied to such non-uniform beams also, since it is always possible to make some reasonable estimate regarding the shape of the deflection curve. The calculations are the same as those for the beam of constant section, with the evident exception that the expression (112) for the potential energy has to be modified by bringing the now variable stiffness EI under the integral sign. If the stiffness varies in a more or less complicated manner along the length x, the evaluation of the integral for the potential energy may become difficult, but, even if the exact calculation is impossible, the integral can always be evaluated graphically.

A somewhat different manner of finding the frequency has been developed by *Stodola*, primarily for application to turbine rotors. His process is capable of being repeated a number of times and of giving a better result after each repetition. Briefly it consists of drawing first some reasonable assumed deflection curve for the shaft in question. By multiplying this curve with the mass and the square of the (unknown) frequency $\mu_1(x)\omega^2$, it becomes an assumed inertia loading. Since ω^2 is not known, it is arbitrarily taken equal to unity to begin with. Then with the inertia loading $y(x)\mu_1(x)$ the deflection curve ${}_2y(x)$ is constructed by the regular methods of graphical statics. Of course

this second deflection curve ${}_2y(x)$ coincides with the originally assumed one $y(x)$ only if

1. $y(x)$ is exactly the normal elastic curve.
2. The natural frequency ω^2 is exactly unity.

The first of these conditions is fulfilled approximately, but the second is generally far from the facts. The deflection ${}_2y(x)$ has more or less the shape of the original assumption $y(x)$, but its ordinates may be 10,000 times smaller. If that is so, we could have obtained approximately equal ordinates for ${}_2y(x)$ and $y(x)$ by assuming a frequency $\omega^2 = 10{,}000$. In that case, the original inertia load would have been 10,000 times as large and the final deflection ${}_2y(x)$ also 10,000 times as large, *i.e.*, approximately equal to the original assumption. Therefore, the ratio of the ordinates of $y(x)$ and ${}_2y(x)$ gives a first approximation for the frequency ω^2.

With a fairly reasonable guess at a deflection curve, the accuracy obtained with this procedure is very good. If greater accuracy is desired, we can repeat the construction with ${}_2y(x)$ as our original estimate, finding a third curve ${}_3y(x)$. It will be proved on page 201 that the process for finding the fundamental mode of vibration is convergent, *i.e.*, each successive curve is nearer to the true shape than the previous one. In fact, the convergence is so rapid that usually no difference can be detected between the shape of ${}_3y(x)$ and ${}_2y(x)$.

For the second and higher modes of vibration the process is not convergent. Nevertheless Stodola's method, properly modified, can be used for the higher modes, as explained on page 202.

The details of the construction belong to the field of graphical statics rather than to vibration dynamics. As a practical example consider a shaft of 72 in. length, on two solid bearings, shown in Fig. 123, I. Dividing it into six sections of equal lengths, the masses and bending stiffness EI of the various sections are shown in the table below, where the modulus of elasticity E has been taken as 30.10^6 lb per square inch.

Section No	Mass per inch, lb. in.$^{-2}$ sec.^{2}	Section mass, lb. in.$^{-1}$ sec.^{2}	EI, lb. in.^{2}
1	0.0142	0.17	9.13×10^8
2	0.0320	0.38	46.2×10^8
3	0.0568	0.68	146×10^8
4	0.0568	0.68	146×10^8
5	0.0320	0.38	46.2×10^8
6	0.0142	0.17	9.13×10^8

The assumed deflection curve is designated by II. It has been made rather flat in the center portion because that part is much stiffer than the rest of the structure. In order to obtain the inertia load

$$y\mu_1\omega^2 = y\mu_1 \cdot 1,$$

the ordinates y have to be multiplied with the mass per running inch μ_1, *i.e.*, with the second column of the table. This gives curve III, which is drawn so that each ordinate "inch" represents 0.025 lb./in. All lengths are measured in actual shaft inches indicated by the scale above I. Thus one "inch" of the shaft is roughly $\frac{1}{25}$ in. in the printed figure. The ordinate of II in the center of the shaft is 15 in. and the middle ordinate of III is 0.852 lb./in. (15 × 0.0568).

In order to find the deflection curve under this loading, four integrations have to be performed, divided into two groups of two each. In the first group we integrate twice and arrive at the bending moment **M**:

$$\mathfrak{q} = \frac{d^2\mathbf{M}}{dx^2} \tag{105b}$$

The first integration is performed by evaluating the areas of the six sections of curve III. For instance, the area of the first section, being nearly triangular, is $\frac{1}{2}$ × 12 in. × 0.138 lb./in. = 0.83 lb. This is the combined inertia force (for ω = 1 rad./second) of the whole first section and thus is the change in the shear force between the left end and the right end of section 1. The six areas of curve III are set off vertically below each other in diagram IV, such that AB is 0.83 lb.; BC = 4.40 lb. = the area of section 2 of curve III. Thus the vertical line on the left of IV represents the shear forces S and is the result of the first integration. Now take an arbitrary horizontal distance H_1, here taken equal to 22.5 lb. and connect its end O with A, B, C, etc. Then, in curve V, draw lines parallel to the rays of diagram IV, so that the line parallel to OB in IV (which separates section 1 from section 2) runs between the vertical dotted lines through the centers of gravity of the areas 1 and 2 of curve III. The diagram V represents the bending moments; the scale being 1 in. = H_1 = 22.5 in. lb. Thus, for example, the bending moment in the middle of the shaft is 396 in. lb.

In order to pass from the bending moment curve V to the deflection curve VIII, we have to perform two more integrations:

$$\frac{\mathbf{M}}{EI} = \frac{d^2y}{dx^2}$$

This equation is built exactly like (105*b*); in fact, the deflection y can be considered to be the "bending moment curve of a beam with the loading $\mathbf{M}/EI$." The values of EI for the various sections are given in the last column of the table, and curve VI shows the $\mathbf{M}/EI$ diagram. We can repeat the process that has led from III *via* IV to V, and find VIII from VI *via* VII. The ordinates of III were measured in lb./in. and those of VI in in.$^{-1}$; so that the dimensions of VI, VII, VIII are found from their counterparts III, IV, V by dividing through by pounds. In particular, the horizontal distance H_2 of VII has no dimension; it is a pure number.

The deflection curve VIII has more or less the appearance of the first guess II; however, its middle ordinate is

$$12.2 \times 2.5 \times 10^{-6} \text{ in.} = 30.5 \times 10^{-6} \text{ in.},$$

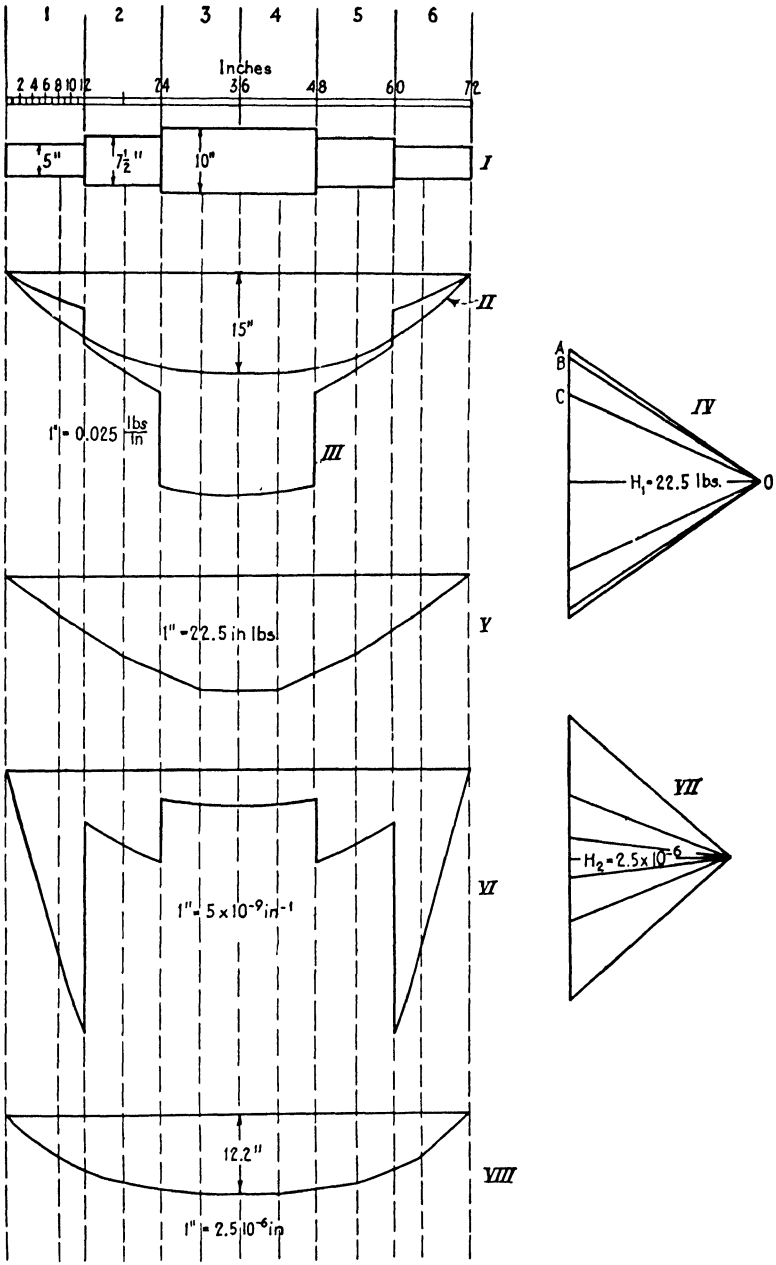


FIG. 123.—Stodola's construction for determining the fundamental frequency of a rotor.

whereas the same ordinate in diagram II was 15 in. Thus the first approximation for the natural frequency of the shaft is

$$\omega_1 = \sqrt{\frac{15}{30.5 \times 10^{-6}}} = 700 \text{ rad./sec.}$$

For other graphical and numerical methods to solve the problem of the natural frequencies of flexural vibration of a bar of variable stiffness and inertia, see page 290.

35. Normal Functions and Their Applications.—We now turn to the proofs of Rayleigh's minimum theorem and of the convergence of Stodola's process. Though these proofs are not essential for an understanding of the subsequent parts of the book, they may give the reader a clearer insight into the nature of "normal modes of motion."

With the *string* and the *beam on two supports*, it was seen that the various normal elastic curves are sine functions:

$$y_1 = \sin \frac{\pi x}{l}, \qquad y_2 = \sin \frac{2\pi x}{l}, \quad \cdots, \quad y_n = \sin \frac{n\pi x}{l}$$

In these expressions the amplitudes of the motions have been arbitrarily assumed to be such that their maximum deflections are 1 inch.

On the other hand, the normal elastic curves of a *cantilever beam* (page 192) or of a beam with non-uniform cross section are curves of much greater complication.

We know from page 20 that any arbitrary curve between 0 and l can be developed into a trigonometric or Fourier series and that one of the most important properties of such a series is

$$\int_0^l \sin \frac{m\pi x}{l} \sin \frac{n\pi x}{l} dx = 0, \qquad (m \neq n)$$

as explained on page 18.

Applied to the special case of string vibration, this means that any elastic curve $y(x)$ which may be given to the string by an external loading can be split up into a series of "normal" components. This is true not only for the string with its sine functions, but generally for any elastic system.

If the normal elastic curves of a system of length l are $y_1(x)$, $y_2(x)$, . . . , $y_n(x)$ . . . , then any arbitrary deflection curve $y(x)$ of that system can be developed into a series:

$$y(x) = a_1 y_1(x) + a_2 y_2(x) + \cdots a_n y_n(x) + \cdots \qquad (117)$$

Moreover, the relation

$$\int_0^l \mu_1(x) y_n(x) y_m(x) dx = 0 \qquad (n \neq m) \tag{118}$$

holds, so that any coefficient a_n in (117) can be found by exactly the same process as that employed on page 21:

$$a_n = \frac{\int_0^l \mu_1(x) y(x) y_n(x) dx}{\int_0^l \mu_1(x) y_n^2(x) dx} \tag{119}$$

This gives us a wide generalization of the concept of Fourier series.

To prove (118), consider an elastic system (beam) of length l of which the elastic properties are determined by the "influence functions" $I(x, x_1)$, with the following definition (Fig. 124): the deflection at a point x of the beam caused by a load of 1 lb. at a point x_1 is $I(x, x_1)$. In this expression both x and x_1 are variables running from 0 to l (see page 155).

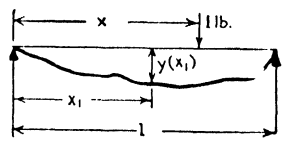


FIG. 124. Definition of influence function $I(x_1, x)$.

Maxwell's reciprocity theorem in the strength of materials states that the deflection at point 1 due to a unit load at point 2 equals the deflection at 2 due to a unit load at 1. Thus the influence function satisfies the relation

$$I(x, x_1) = I(x_1, x)$$

Let the beam be vibrating at one of its natural frequencies with the shape $y_n(x)$. The maximum inertia force acting on a section dx_1 of the beam with mass μ_1 per unit length is

$$\mu_1(x_1) dx_1 \omega_n^2 y_n(x_1)$$

and the deflection caused by that load at a point x is

$$\omega_n^2 y_n(x_1) I(x, x_1) \mu_1(x_1) dx_1$$

There are inertia loads of this kind on every section dx_1 between 0 and l, so that the actual deflection curve is the sum of all the partial deflection curves

$$y_n(x) = \omega_n^2 \int_0^l y_n(x_1) I(x, x_1) \mu_1(x_1) dx_1 \tag{120}$$

This relation holds only when $y_n(x)$ is a natural mode, because only then can the beam be in equilibrium with loads proportional to its own displacements.

In order to prove (118) we multiply (120) by $\mu_1(x) y_m(x) dx$ and integrate:

$$\int_0^l \mu_1(x) y_m(x) y_n(x) dx = \omega_n^2 \int_0^l \int_0^l y_n(x_1) y_m(x) I(x, x_1) \mu_1(x_1) \mu_1(x) dx_1 dx \tag{121}$$

Since (120) holds for any natural frequency, we may replace n by m. Then we can multiply by $\mu_1(x) y_n(x) dx$ and integrate, with the result:

$$\int_0^l \mu_1(x)y_m(x)y_n(x)dx = \omega_m^2 \int_0^l \int_0^l y_m(x_1)y_n(x)I(x, x_1)\mu_1(x_1)\mu_1(x)dx_1dx$$

In this last double integral we may reverse the order of integration, *i.e.*, reverse x and x_1:

$$\int_0^l \mu_1(x)y_m(x)y_n(x)dx = \omega_m^2 \int_0^l \int_0^l y_m(x)y_n(x_1)I(x_1, x)\mu_1(x)\mu_1(x_1)dxdx_1$$

This double integral is seen to be the same as that in (121) on account of Maxwell's theorem that $I(x, x_1) = I(x_1, x)$. Let the value of the double integral be A; then, on subtracting the last result from (121), we obtain:

$$0 = (\omega_n^2 - \omega_m^2)A$$

This means that for $\omega_m \neq \omega_n$, the double integral A is zero, which makes the left-hand side of (121) also zero, so that the proposition (118) is proved.

Proof of Rayleigh's Minimum Theorem.—The approximate curve $y(x)$ assumed in the Rayleigh procedure is not a normal elastic curve but can be expanded in a series of such curves:

$$y(x) = y_1(x) + a_2y_2(x) + a_3y_3(x) + \cdots + a_ny_n(x) + \cdots$$

In order to express the fact that $y(x)$ is an approximation of $y_1(x)$, its coefficient has been taken equal to unity, whereas the other coefficients a_2, a_3, etc., may be small numbers. A normal elastic curve $y_n(x)$ is a curve that can be caused by a static loading $\mu_1\omega_n^2y_n(x)$.

Thus the static loading $p(x)$ which causes the assumed curve $y(x)$ is

$$p(x) = \mu_1[\omega_1^2y_1(x) + a_2\omega_2^2y_2(x) + \cdots + a_n\omega_n^2y_n(x)]$$

The potential energy of an element dx is $\frac{1}{2}y(x)p(x)dx$, and the total potential energy is

$$Pot = \tfrac{1}{2}\int_0^l \mu_1[y_1(x) + a_2y_2(x) + a_3y_3(x) + \cdots + a_ny_n(x)][\cdots a_n\omega_n^2y_n(x)]dx$$

Since by (118) all integrals of products with $m \neq n$ are zero, this becomes

$$Pot = \tfrac{1}{2}\left(\omega_1^2\int_0^l \mu_1y_1^2dx + \cdots + a_n^2\omega_n^2\int_0^l \mu_1y_n^2dx + \cdots\right)$$

The kinetic energy of an element dx vibrating through the neutral position with a velocity $\omega y(x)$ is $\frac{1}{2}\omega^2y^2\mu_1dx$, and

$$Kin = \tfrac{1}{2}\omega^2\int_0^l \mu_1y^2dx = \tfrac{1}{2}\omega^2\left(\int_0^l \mu_1y_1^2dx + \cdots + a_n^2\int_0^l \mu_1y_n^2dx\right)$$

since again all terms with products y_my_n drop out.

It is seen that both the potential and kinetic energies consist of the sum of the various energies of the components y_1, y_2, etc. This is so only if y_1, y_2 are normal modes; if this is not the case, the integrals of the products y_ny_m have to be considered also.

By Rayleigh's procedure we equate the two energies and solve for ω^2:

$$\omega^2 = \frac{\omega_1^2\int_0^l \mu_1 y_1^2 dx + \cdots + a_n^2\omega_n^2\int_0^l \mu_1 y_n^2 dx + \cdots}{\int_0^l \mu_1 y_1^2 dx + \cdots + a_n^2\int_0^l \mu_1 y_n^2 dx + \cdots}$$

or

$$\omega^2 = \omega_1^2 \frac{1 + \frac{\omega_2^2}{\omega_1^2}a_2^2\binom{2}{1} + \frac{\omega_3^2}{\omega_1^2}a_3^2\binom{3}{1} + \cdots}{1 + a_2^2\binom{2}{1} + a_3^2\binom{3}{1} + \cdots} \tag{122}$$

where the symbols $\binom{n}{1}$ are abbreviations for

$$\binom{n}{1} = \frac{\int_0^l \mu_1 y_n^2 dx}{\int_0^l \mu_1 y_1^2 dx}$$

Since $\omega_2 > \omega_1$ and $\omega_3 > \omega_2$, etc., it is seen that in (122) the various entries in the numerator are larger than the ones just below them in the denominator. Thus the fraction in (122) is greater than 1, from which it follows that

$$\omega > \omega_1$$

or the frequency ω found by Rayleigh's procedure is greater than the first natural frequency ω_1, which was to be proved.

Moreover, an inspection of (122) will show that this property holds only for the first or lowest frequency but not for the second or higher ones.

Proof of the Convergence of Stodola's Process.—Let the first assumption for the deflection curve be $y(x)$, where

$$y(x) = y_1(x) + a_2y_2(x) + a_3y_3(x) + \cdots + a_ny_n(x) + \cdots$$

With a mass distribution $\mu_1(x)$ and an arbitrary frequency $\omega = 1$ the inertia loading becomes

$$\mu_1 y = \mu_1 y_1 + a_2\mu_1 y_2 + a_3\mu_1 y_3 + \cdots + a_n\mu_1 y_n + \cdots$$

The deflection curve for the loading $\mu_1\omega^2 y_n$ is y_n; consequently the loading $a_n\mu_1 y_n$ gives a deflection $a_n y_n/\omega_n^2$, so that the second deflection curve of the process becomes

$${}_2y(x) = \frac{y_1(x)}{\omega_1^2} + \cdots + \frac{a_n y_n(x)}{\omega_n^2} + \cdots,$$

which differs from the first curve in that each term is divided by the square of its natural frequency. Proceeding in this manner we find for the $(n+1)$st deflection curve

$${}_{n+1}y = \frac{1}{\omega_1^{2n}}\left[y_1 + \left(\frac{\omega_1}{\omega_2}\right)^{2n} a_2y_2 + \left(\frac{\omega_1}{\omega_3}\right)^{2n} a_3y_3 + \cdots\right]$$

Since $\omega_1 < \omega_2$ and $\omega_1 < \omega_3$, etc., it is seen that with increasing n the impurities $y_2, y_3 \ldots$ decrease, and the first mode y_1 appears more and more pure.

35a. Stodola's Method for Higher Modes.—The above proof shows that an attempt to construct the second normal elastic curve by Stodola's method will end in failure because any impurity of the fundamental elastic curve contained in the guess for the second curve will be magnified more than the second curve itself. After a large number of repetitions it will be found that the second mode disappears altogether and that only the fundamental mode is left. Still it is possible to find the second mode if before each operation the deflection curve is purified from its first-mode content. For this it is necessary first to know the shape of the first mode with sufficient accuracy.

Let $y(x)$ be the assumed shape for the second mode which unfortunately will contain some first harmonic impurity, say $Ay_1(x)$. Then we want to find

$$y(x) - Ay_1(x)$$

which will be free from first harmonic contamination. In order to find A, substitute the above expression in Eq. (118).

$$\int_0^l \mu_1(x)[y(x) - Ay_1(x)]y_1(x)\,dx = 0$$

or

$$\int_0^l \mu_1(x)y(x)y_1(x)\,dx = A\int_0^l \mu_1(x)y_1^2(x)\,dx$$

or

$$A = \frac{\int \mu_1(x)y(x)y_1(x)\,dx}{\int \mu_1(x)y_1^2(x)\,dx} \tag{118a}$$

The integrand in the numerator, apart from the factor $\mu_1(x)$, is the product of the known first harmonic deflection curve and the assumed approximation for the second harmonic deflection curve $y(x)$. In the denominator the integrand is the product of the mass $\mu_1(x)$ and the square of the first harmonic curve. Both integrals can be evaluated graphically; thus A is determined, and the assumed shape for the second mode can be purified from its first-mode contamination. Then the Stodola process is applied to this curve.

For the third or higher modes the procedure is similar, but the assumed curve for the third harmonic has to be purified from the first as well as from the second harmonic by Eq. (118*a*). Thus the Stodola process cannot be applied to a higher mode of vibration until after all lower modes have been determined with sufficient accuracy.

The method is not necessarily restricted to the graphical form of page 197. It is sometimes applied arithmetically, as will now be shown for the simple example of the string with three equal masses of Fig. 95. In the equations (76*a*) the terms on the right are the deflections caused by the individual inertia forces. With the influence numbers of Eq. (79), the elastic deflection equations (76*a*) are rewritten ($m_1 = m_2 = m_3 = m$).

$$\left.\begin{aligned} \frac{\mathbf{T}}{m\omega^2 l} a_1 &= \tfrac{3}{4} a_1 + \tfrac{1}{2} a_2 + \tfrac{1}{4} a_3 \\ \frac{\mathbf{T}}{m\omega^2 l} a_2 &= \tfrac{1}{2} a_1 + a_2 + \tfrac{1}{2} a_3 \\ \frac{\mathbf{T}}{m\omega^2 l} a_3 &= \tfrac{1}{4} a_1 + \tfrac{1}{2} a_2 + \tfrac{3}{4} a_3 \end{aligned}\right\} \qquad (76b)$$

With Stodola, we now assume a shape for the deformation in the first mode, and for the purpose of illustrating the convergence of the method we intentionally make a stupid choice: $a_1 = a_2 = a_3 = 1$. Substitute that into the right-hand sides of Eq. (76*b*), and calculate their sums.

$$Ca_1 = 1\tfrac{1}{2} \qquad Ca_2 = 2 \qquad Ca_3 = 1\tfrac{1}{2}$$

where $C = \mathbf{T}/m\omega^2 l$. By reducing the middle amplitude to unity (the same value as assumed first), we thus find for the second approximation of the deflection curve

$$a_1 = \tfrac{3}{4} \qquad a_2 = 1 \qquad a_3 = \tfrac{3}{4}$$

Put this into the right sides of Eq. (76*b*), and find

$$Ca_1 = 1\tfrac{1}{4}, \qquad Ca_2 = 1\tfrac{3}{4}, \qquad Ca_3 = 1\tfrac{1}{4}$$

or again reduced to unity at the center, the third approximation becomes

$$a_1 = \tfrac{5}{7}, \qquad a_2 = 1, \qquad a_3 = \tfrac{5}{7} = 0.714$$

Another substitution leads to the fourth approximation

$$a_1 = \tfrac{17}{24}; \qquad a_2 = 1; \qquad a_3 = \tfrac{17}{24} = 0.707$$

The fifth approximation is

$$a_1 = \tfrac{29}{41}; \qquad a_2 = 1; \qquad a_3 = \tfrac{29}{41} = 0.707$$

which is identical with the previous one within slide rule accuracy. Substituting this into the first of the equations (76*b*), we have

$$0.707\frac{\mathbf{T}}{m\omega^2 l} = 1.207 \qquad \text{or} \qquad \omega_1^2 = 0.586\frac{\mathbf{T}}{ml}$$

as found before on page 159.

Proceeding to the second mode, its shape is obvious (page 159) from the symmetry of the case. However, for the purpose of illustrating the method we start with a very bad assumption:

$$a_1 = 1.000, \qquad a_2 = 0.500, \qquad a_3 = -0.750 \qquad \text{(first)}$$

First this expression is to be purified from its fundamental harmonic content by means of Eq. (118*a*). All masses are equal and divide out from (118*a*). The expression thus is

$$A = \frac{1.000 \times 0.707 + 0.500 \times 1.000 - 0.750 \times 0.707}{0.707 \times 0.707 + 1.000 \times 1.000 + 0.707 \times 0.707} = 0.338$$

The first harmonic amount to be subtracted from the above assumption then is

$$a_1 = 0.338 \times 0.707 = 0.240, \qquad a_2 = 0.338, \qquad a_3 = 0.240$$

which leads to

$$a_1 = 0.760, \qquad a_2 = 0.162, \qquad a_3 = -0.990$$

or multiplying by a constant so as to make a_1 equal to unity, for purposes of comparison,

$$a_1 = 1.000, \qquad a_2 = 0.213, \qquad a_3 = -1.302 \qquad \text{(first, purified)}$$

Substituting this into Eq. (76*b*), and multiplying by a constant so as to make $a_1 = 1.000$ leads to

$$\begin{aligned} a_1 &= 1.000, \quad a_2 = 0.116, \quad a_3 = -1.181 \quad \text{(second)} \\ a_1 &= 1.000, \quad a_2 = 0.051, \quad a_3 = -1.125 \quad \text{(third)} \\ a_1 &= 1.000, \quad a_2 = -0.024, \quad a_3 = -1.148 \quad \text{(fourth)} \end{aligned}$$

By this time considerable first harmonic error has crept into the solution, so that it is necessary to purify again by means of Eq. (118*a*).

$$a_1 = 1.000, \qquad a_2 = +0.038, \qquad a_3 = -1.058 \qquad \text{(fourth, purified)}$$

Continuing

$$\begin{aligned} a_1 &= 1.000, \quad a_2 = +0.018, \quad a_3 = -1.035 \quad \text{(fifth)} \\ a_1 &= 1.000, \quad a_2 = 0.000, \quad a_3 = -1.034 \quad \text{(sixth)} \end{aligned}$$

Again it becomes necessary to throw out the first harmonic, which has crept in,

$a_1 = 1.000,$	$a_2 = +0.012,$	$a_3 = -1.018$	(sixth, purified)
$a_1 = 1.000,$	$a_2 = +0.006,$	$a_3 = -1.012$	(seventh)
$a_1 = 1.000,$	$a_2 = 0.000,$	$a_3 = -1.012$	(eighth)
$a_1 = 1.000,$	$a_2 = +0.004,$	$a_3 = -1.006$	(eighth, purified)
$a_1 = 1.000,$	$a_2 = +0.002,$	$a_3 = -1.004$	(ninth)
$a_1 = 1.000,$	$a_2 = 0.000,$	$a_3 = -1.004$	(tenth)

It is seen that the convergence is very slow, and that the first harmonic creeps in continually and has to be thrown out about every other step.

36. Rings, Membranes, and Plates.—The strings and beams thus far discussed suffice in many cases to give a tolerably accurate idealization of the actual constructions or machines with

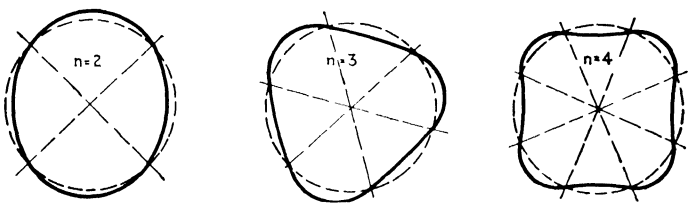


FIG. 125.—Normal modes of a ring bending in its own plane.

which we are dealing. Where this is no longer possible, an idealization in terms of rings (curved beams), membranes, or plates may be helpful. But the calculation of the natural frequencies of these elements is much more complicated than anything we have thus far considered. Therefore, in this section the results only will be given, while for the detailed derivations the reader is referred to the literature, especially to the book of Timoshenko, quoted on page 461.

Full Ring.—Of the many possible motions of a full ring, the bending vibrations are the most important. If the ring has uniform mass and stiffness, it can be shown that the *exact* shape of the mode of vibration consists of a curve which is a sinusoid on the developed circumference of the ring. In Fig. 125 these shapes are shown for the four, six, and eight noded modes or for two, three, and four full waves along the circumference of the ring.

The exact formula for the natural frequencies is

$$\omega_n = \frac{n(n^2 - 1)}{\sqrt{n^2 + 1}} \sqrt{\frac{EI}{\mu_1 R^4}} \tag{123}$$

where n is the number of full waves, μ_1 is the mass per unit length of the ring, EI the bending stiffness, and R the radius.

One of the most important applications of this result is to the frames of electric machines. As these machines often carry salient poles, which act as concentrated masses (Fig. 193, page 325), the exact shapes of vibration are no longer developed sinusoids, although in the spirit of Rayleigh's procedure the sinusoid may be considered as an approximate shape. The potential energy of deformation is not altered by the addition of the poles, but the kinetic energy changes from Kin_r to $Kin_r + Kin_p$, where the subscripts pertain to the ring and poles, respectively. Therefore, the result (123) for the frequency has to be corrected by the factor

$$\sqrt{\frac{Kin_r}{Kin_r + Kin_p}} \tag{124}$$

In case the number of poles is $2n$, *i.e.*, equal to the number of half waves along the ring, and in case these poles are located in the antinodes so that they move parallel to themselves (Fig. 194*b*), the correction (124) becomes specifically

$$\sqrt{\frac{M_r}{M_r + M_p \frac{2n^2}{n^2 + 1}}} = \sqrt{\frac{1}{1 + \frac{2n^2}{n^2 + 1} \frac{M_p}{M_r}}} \tag{124a}$$

where M_r is the mass of the complete ring and M_p is the mass of all poles combined, so that M_p/M_r is the ratio of one pole mass to the ring mass per pole.

Another important case occurs when the $2n$ poles are located at the nodes of the radial vibration and there execute rocking motions about the node axis. The correction factor for this case (Fig. 194*c*) is

$$\sqrt{\frac{1}{1 + \frac{n^5}{n^2 + 1} \cdot \frac{4I_p}{M_r R^2}}} \tag{124b}$$

in which I_p is the moment of inertia of a single pole for the axis about which it rotates during the vibration. The actual location of that axis is somewhat doubtful (on account of the fact that the

"node" of the ring is a node only in the radial motion but moves back and forth tangentially), but no great error is made by taking the axis on the center line of the ring at the node.

Partial Ring.—Quite often the stators of electric motors or generators are bolted on a foundation in the manner shown in Fig. 126*a*. If the foundation or bedplate is very stiff, the stator may be regarded as a partial ring of angle α built in (clamped) at both ends. The fundamental mode of vibration of such a ring in its own plane will be approximately as sketched in Fig. 126*b*. Its natural period, calculated by the procedure of Rayleigh, leads to a result which dimensionally is the same as (123), but the numerical factor depends on the central angle α and has to be written $f(\alpha)$:

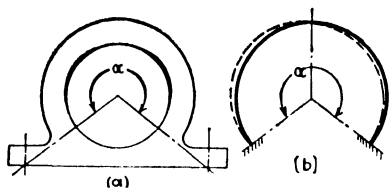


FIG. 126.—The fundamental flexural mode in its own plane of a partial ring.

$$\omega = f(\alpha)\sqrt{\frac{EI}{\mu_1 R^4}} \tag{125}$$

The values of the constant $f(\alpha)$ for the various angles between $\alpha = 180$ deg. (half circle) and $\alpha = 360$ deg. (full circle clamped at one point) are shown in Fig. 127.

In case the stator carries salient poles, the correction (124) has to be applied. No greater error is committed by distributing the pole masses uniformly along the ring, since the various pole-carrying points of Fig. 126*b* move through roughly the same amplitudes (which is totally different from some of the cases of Fig. 125). The natural frequency calculated from Eq. (125) and Fig. 127 is usually somewhat (of the order of 10 per cent) high on account of the fact that the feet of the stator do not constitute a complete "clamping" but admit some angular motion.

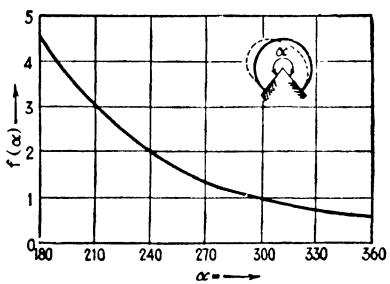


FIG. 127.—The coefficient $f(\alpha)$ in Eq. (125) for the frequency of Fig. 126.

If the ring of Fig. 126 has a small dimension in the direction perpendicular to the paper (*i.e.*, in the direction of the axis of the

cylinder), another motion has caused trouble in some cases. It is a vibration perpendicular to the plane of the paper. If Fig. 126 were viewed from the side, it would be seen as a cantilever beam of height h. The lateral vibration would then appear in a form similar to that shown in Fig. 120a. In this case the

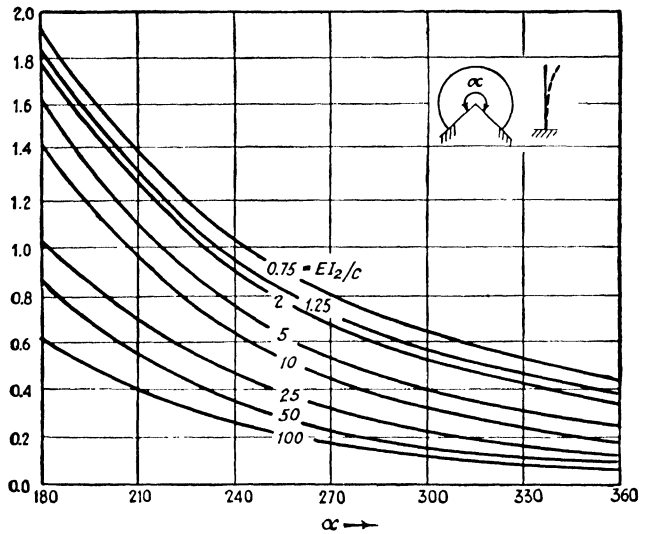


FIG. 128.—Coefficients $f(\alpha, EI_2/C)$ of Eq. (126) for the frequency of a partial ring vibrating perpendicularly to its own plane.

elastic resistance of the ring consists of a combination of bending and twist determined by the quantities

EI_2 = bending stiffness (now in a plane perpendicular to the paper, 90 deg. from the EI in Eqs. (123) and (125), and

C = torsional stiffness, which has the form GI_p for a bar of circular cross section.

The frequency can be written in the form

$$\omega = f\left(\alpha, \frac{EI_2}{C}\right)\sqrt{\frac{EI_2}{\mu_1 R^4}} \tag{126}$$

where the numerical constant is shown in Fig. 128. This figure was found by a modified Rayleigh method and subsequently verified by laboratory tests, showing the results to be substantially correct.

A *membrane* is a skin which is stretched with a great tension and which has no bending stiffness whatever. It is therefore to be considered as a two-dimensional generalization of a string. A circular membrane or drumhead has an infinite number of natural modes of motion whereby the nodes appear as diameters and also as smaller concentric circles. However, we shall discuss here the fundamental mode only, having no nodes except the boundary. The shape of the vibration is practically that of a hill formed by the revolution of a sine curve (Fig. 129). The frequency of this motion is

$$\omega = 2.40\sqrt{\frac{\mathbf{T}}{\mu_1 R^2}} = 4.26\sqrt{\frac{\mathbf{T}}{\mu_1 A}} \qquad (127)$$

where $\mathbf{T}$ is the tension per running inch across any section of the membrane, μ_1 is the mass per unit area, and A is the total area πR^2.

The formula in its second form is useful also when the membrane is no longer circular but has some other boundary which roughly resembles the circle (square, triangle, half or quarter circle, etc.). Even then (127) is approximately correct if the area A of the non-circular membrane is substituted. In such a case the numerical factor is somewhat greater than 4.26. An idea of the error involved can be had from the fact that for a square membrane the factor 4.26 in Eq. (127) becomes 4.44, for a 2×1 rectangular membrane 4.97, and for a 3×1 rectangle 5.74.

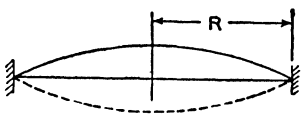


FIG. 129.—Fundamental mode of a drumhead with the frequency $\omega = 2.40\sqrt{\mathbf{T}/\mu_1 R^2}$.

Just as a membrane is a two-dimensional string, so a plate may be considered as a two-dimensional "beam." The theory of the vibrations of plates even in the approximate form of Rayleigh-Ritz is extremely complicated. The results are known for circular and rectangular plates with either free, clamped, or simply supported edges, and the reader who may have occasion to use these formulas should refer to the more elaborate books on the subject by Rayleigh, Prescott, or Timoshenko.

Problems

61. Derive Eq. (84) by working out the determinant (78).

62. A simple massless beam of bending stiffness EI and length $4l$, supported at its ends, carries a mass m at a distance l from each of the supports. Find:

a. The three influence numbers.

b. The two natural frequencies.

c. The two natural modes of motion.

63. A flexible weightless beam of section EI and length l is simply supported at its two ends and carries two equal masses m, each at $\frac{1}{4}l$ and at $\frac{1}{2}l$

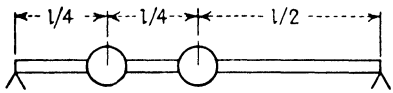


FIG. 129*a*. Problem 63.

from one of the ends (Fig. 129*a*). Calculate the two frequencies by the method of influence numbers (page 156).

64. In Fig. 68, let $m_1 = m$, $m_2 = 5m$, $k_1 = k$, $k_2 = 3k$, and $k_3 = 7k$. Let a force $P_0 \sin \omega t$ be acting on m_1. Find:

a. The frequency ω of P_0 at which m_1 does not move.

b. The amplitude of m_2 at this frequency.

Solve this problem without the use of large formulas by a physical consideration, as suggested in Fig. 97.

65. Derive Eq. (93*b*).

66. Check the various frequencies shown in Fig. 112.

67. By Rayleigh's method find the natural frequency of a string with tention **T** and length $3l$, carrying masses m at distances l and $2l$ from one end. The mass of the string itself is $3m$.

68. A beam EI on two supports, of length l and of mass μ_1 per unit length (total mass $m = \mu_1 l$) carries a concentrated mass M in the middle. Find the natural frequency by Rayleigh's method, and in particular find what fraction of m should be added to M in order to make the simple formula (16) applicable.

69. The same problem as 68, but for a beam of total mass m, clamped solidly at both ends, and carrying a mass M at its center.

70. A ship's propeller shaft has a length of 200 ft. between the engine and the propeller. The shaft diameter is 12 in. The propeller has the same moment of inertia as a solid steel disk of 4 ft. diameter and 6 in. thickness. The modulus of shear of the shaft is $G = 12 \times 10^6$ lb. per square inch. If the shaft is supposed to be clamped at the engine, find the natural frequency of torsional vibration, taking account of the inertia of the shaft by means of Rayleigh's method (steel weighs 0.28 lb. per cubic inch).

71. The coil springs of automobile-engine valves often vibrate so that the individual coils move up and down in the direction of the longitudinal axis of the spring. This is due to the fact that a coil spring considered as a "bar" with distributed mass as well as flexibility can execute longitudinal vibrations as determined by Eq. (93*a*). Find the equivalents for μ_1 and AE in (93*a*) in terms of the coil diameter D, wire diameter d, number of turns per inch n_1, modulus of shear G, mass per turn of spring m_1.

Calculate the first natural period of such a spring of total length $l (n = n_1 l)$ clamped on both sides.

72. A cantilever beam of total length $2l$ has a stiffness EI and a mass per unit length μ_1 along a part l adjacent to the clamped end, whereas the other

half of it has a stiffness $5EI$ and a unit mass $\mu_1/2$. Find the fundamental frequency by Rayleigh's method.

73. A small ⅛-hp. motor frame has the following characteristics (Fig. 126): $\alpha = 220$ deg., $R = 2.75$ in.; $I = 0.0037$ in.^{4}; $E = 27.10^6$ lb./in.^{2}; $\mu = 0.00052$ lb. sec.^{2}/in.^{2}

Find the fundamental frequency.

74. A mass hangs on a coil spring (Fig. 23 without damping or excitation). If the mass of the spring itself is not negligible with respect to the end mass, calculate what percentage of the spring mass has to be added to the end mass if the natural frequency is to be found from $\omega^2 = k/m$

a. By Rayleigh's method.

b. By the exact theory.

75. A uniform bar of length l, bending stiffness EI, and mass per unit length μ_1 is freely supported on two points at distance $l/6$ from each end. Find the first natural frequency by Rayleigh's method.

76. A ship drive, such as that discussed with reference to Fig. 147, consists of a propeller weighing 50,000 lb. and a line shaft of 19 in. diameter and 188 ft. length, on the other end of which there is a large gear weighing again 50,000 lb. The gear is driven by pinions and steam turbines which have no influence on the longitudinal vibrations of the system. On the inboard side of the main gear the thrust is taken by a Kingsbury thrust bearing, the supporting structure of which has a stiffness in the longitudinal direction of the shaft of 2.5×10^6 lb./in. The propeller has four blades and consequently gives four longitudinal impulses to the shaft per revolution.

Calculate the two critical speeds of the installation, considering it as a two-degree-of-freedom system, distributing the shaft mass equally to the propeller and to the gear mass.

77. Solve Problem 76 by the exact method, assuming the shaft mass to be uniformly distributed, and find the numerical answer for the lowest critical speed. The data of Problem 76 are taken from an actual case. The vibration was eliminated by stiffening the thrust bearing supports.

78. To calculate by Rayleigh's method the antisymmetrical, three-noded frequency of a free-free bar of length $2l$, assume for the curve a sine wave extending from -180 deg. to $+180$ deg., with a base line rotated through a proper angle about the mid-point, so that it intersects the sine curve in two points besides the center point.

a. Determine the slope of the base line so as to satisfy the condition that the angular momentum about the center remains zero during the vibration.

b. Calculate the frequency with the curve so found.

79. The potential energy of a membrane, such as is shown in Fig. 129, is calculated by multiplying the tension **T** by the increment in area of each element caused by the elastic deformation.

a. If the deformation has rotational symmetry about the central axis (as shown in Fig. 129), derive that this energy is

$$\text{Pot} = \int \frac{\mathbf{T}}{2}\left(\frac{dy}{dr}\right)^2 dA.$$

b. Assume for the deformation a sinusoid of revolution and calculate the frequency by Rayleigh's method.

80. In connection with the numerical Stodola or "iteration" method, discussed on page 203, carry out the following calculations:

a. Starting with the first assumption for the second mode, $a_1 = 1.000$; $a_2 = 0.500$; $a_3 = -0.750$; carry out the various steps without eliminating the first mode, and observe that gradually the solution converges to the first mode and not to the second.

b. In figuring the third mode start with an assumption such as $a_1 = a_3 = 1.000$, $a_2 = -1.000$, and eliminate from this solution the first and second harmonic contents by means of Eq. 76*b*. Note that the shape so obtained is the exact solution.

CHAPTER V

MULTICYLINDER ENGINES

37. Troubles Peculiar to Reciprocating Engines.—There are two groups of vibration phenomena of practical importance in reciprocating machines, namely:

1. Vibrations transmitted to the foundation by the engine as a whole.

2. Torsional oscillations in the crank shaft and in the shafting of the driven machinery.

Each one of these two effects is caused by a combination of the periodic accelerations of the moving parts (pistons, rods, and cranks) and the periodic variations in cylinder steam or gas pressure.

Consider a vertical single-cylinder engine. The piston executes an alternating motion, *i.e.*, it experiences alternating vertical accelerations. While the piston is accelerated downward there must be a downward force acting on it, and this force must have a reaction pushing upward against the stationary parts of the engine. Thus an alternating acceleration of the piston is coupled with an alternating force on the cylinder frame, which makes itself felt as a vibration in the engine and in its supports. In the lateral direction, *i.e.*, perpendicular to both the crank shaft and the piston rod, moving parts are also being accelerated, namely the crank pin and part of the connecting rod. The forces that cause these accelerations must have equal and opposite reactions on the frame of the engine. This last effect is known as "horizontal unbalance." In the longitudinal direction, *i.e.*, in the crank-shaft direction, no inertia forces appear, since all moving parts remain in planes perpendicular to the crank shaft.

The mathematical relation describing these effects is Newton's law, stating that in a mechanical system the rate of change of momentum equals the resultant $\bar{F}$ of all external forces:

$$\frac{d}{dt}(\Sigma m\bar{v}) = \bar{F} \tag{128}$$

This is a vector equation and is equivalent to three ordinary equations. Two of these equations are of importance, while the third (in the longitudinal direction) is automatically satisfied because $\bar{v}$ is always zero in that direction.

Equation (128) can be interpreted in a number of ways. First, consider the "mechanical system" as consisting of the *whole* engine, and assume it is mounted on extremely flexible springs so as to be floating freely in space. No external forces $\bar{F}$ are acting, and Eq. (128) states that, while the piston is accelerated downward (*i.e.*, acquires downward momentum), the cylinder must be accelerated upward. If the cylinder mass is 50 times the piston mass, the cylinder acceleration must be 50 times as small as the piston acceleration.

Next consider only the moving parts, *i.e.*, piston, rod, and crank shaft, as the mechanical system. During rotation these parts have a definite acceleration, or $\frac{d}{dt}(m\bar{v})$, in the vertical and lateral directions. Equation (128) determines the value of the force $\bar{F}$ acting on these parts, and consequently the value of the reaction $-\bar{F}$ on the stationary parts.

Equation (128) is sometimes written with the differentiation carried out:

$$\Sigma\left(m\frac{d\bar{v}}{dt}\right) = \bar{F} \qquad (128a)$$

The expression $m\ d\bar{v}/dt$ is called the "inertia force," and the theorem states that the external force acting on the system equals the sum of all the inertia forces of the moving parts.

These various inertia forces can form moments. Consider a two-cylinder vertical engine with the two cranks set 180 deg. apart. While one piston is accelerated downward the other one is accelerated upward, and the two inertia forces form a couple tending to rock the engine about a lateral axis. Similarly, the horizontal or lateral inertia forces of the two cranks are equal and opposite forming a couple tending to rock the engine about a vertical axis.

A rocking about the crank-shaft axis can occur even in a *single*-cylinder engine. If the piston be accelerated downward by a pull in the connecting rod, it is clear that this pull exercises a torque about the crank-shaft axis. Since the piston acceleration is alternating, this inertia torque is also alternating.

Newton's law for moments states that in a mechanical system on which an external torque or moment $\overline{\mathbf{M}}$ is acting

$$\frac{d}{dt}(\Sigma \overline{mva}) = \overline{\mathbf{M}} \tag{129}$$

where a is the moment arm of the momentum $m\bar{v}$. In words: the external torque equals the rate of change of moment of momentum. With the differentiation performed the relation reads

$$\Sigma a\left(m\frac{d\bar{v}}{dt}\right) = \overline{\mathbf{M}} \tag{129a}$$

or the sum of the moments of the inertia forces of the various moving parts equals the external moment.

As before, we can take for our mechanical system either the whole engine mounted on very weak springs, or we can take merely the moving parts. In the first case the external torque is zero, and therefore any increase in the clockwise angular momentum of the moving parts must be neutralized by an increase in counterclockwise angular momentum of the stationary parts of the engine. In the second case the increase in clockwise angular momentum of the moving parts must be caused by a clockwise torque or moment on these parts, which has a counterclockwise reaction torque on the frame. If this frame is mounted solidly on its foundation, this countertorque is communicated to the foundation and may cause trouble. On the other hand, if the engine is mounted on soft springs, no reaction to the foundation can penetrate through these springs and the countertorque is absorbed as an inertia torque of the frame and cylinder block. Hence that block must vibrate, but no appreciable torque gets into the foundation: we have "floating power" (page 97).

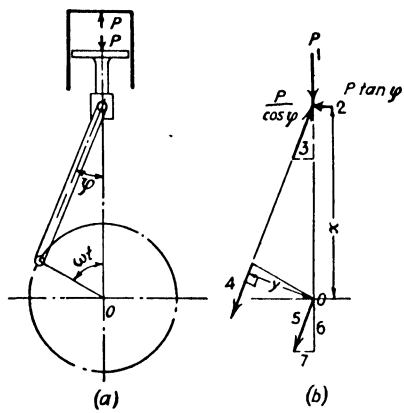


FIG. 130.—Gas pressure forces on a single-cylinder engine.

The formulas (128) and (129) suffice for a derivation of the *inertia* properties of the engine which will be carried out in the

next two sections. We shall turn our attention now to the effect of alternating steam or gas pressure in the cylinders.

In Fig. 130, let any inertia effect be excluded by assuming either that the moving parts have a negligible mass or that the engine is turning over very slowly at a constant speed ω. Let the pressure force on the piston be P, which is variable with the time (or with the crank angle ωt). The gas pressure not only pushes the piston downward, but it also presses upward against the cylinder head. The piston force P is transmitted through the piston rod (force 1) to the crosshead. Neglecting friction, it is there held in equilibrium by the forces 2 and 3. The forces 1, 2, and 3 of Fig. 130*b* are those acting on the crosshead; 3 is a compression in the connecting rod and 2 has a reaction pressure on the guide or frame to the *right* and of magnitude $P \tan \varphi$. The force 3 of magnitude $P/\cos \varphi$ is transmitted through the connecting rod to the crank pin (force 4). By shifting this force parallel to itself to O we add a torque $yP/\cos \varphi$, which is the driving torque of the gas pressure. The force 5 is taken up by the main bearings at O and can be resolved into a vertical component 6, and a horizontal component 7. From the similarity of the triangles 1, 2, 3 and 5, 6, 7 it can be seen immediately that the magnitude of 6 is P and that of 7 is $P \tan \varphi$.

The forces transmitted to the stationary parts of the engine are:

first, P upward on the cylinder head.
second, $P \tan \varphi$ to the right on the crosshead guide.
third, P downward on the main bearings at O.
fourth, $P \tan \varphi$ to the left on the main bearings at O.

The total *resultant* force on the frame is zero, but there is a resultant torque $Px \tan \varphi$. By Newton's law of action and reaction this torque must be equal and opposite to the driving torque on the crank shaft, $yP/\cos \varphi$. The truth of this statement can easily be verified because it can be seen in Fig. 130*b* that $y = x \sin \varphi$. Thus the gas pressures in the cylinder do not cause any resultant forces on the engine frame but produce only a torque about the longitudinal axis.

Summarizing, we note that no forces occur along the longitudinal axis of an engine, while in the lateral and vertical directions only inertia forces appear. About the vertical and lateral axes only inertia torques are found, whereas about a longitudinal

axis both an inertia torque and a cylinder-pressure torque occur.

If we assume the engine to be built up of solid bodies, *i.e.*, elastically non-deformable bodies, the problem is one of "balance" only. The frame or stationary parts usually fulfill this condition of rigidity, but as a rule the crank shaft can be twisted comparatively easily, which makes torsional vibrations possible. The subject is usually divided into three parts:

a. Inertia Balance: By this is meant the balance of the engine against vertical and lateral forces and against moments about vertical and lateral axes.

b. Torque Reaction: Under this heading we study the effect of the torque (due to inertia and cylinder-pressure effects) acting on the stationary parts about the longitudinal axis (floating power).

c. Torsional Vibrations of the Crank Shaft: Here we deal with the consequences of this same longitudinal torque on the moving parts of the engine.

The effect *c* is of particular importance since many crank shafts have been broken on account of it. Now that the theory is understood such failures are unnecessary.

The first step in the discussion of the subject is the derivation of the expressions for the vertical and lateral inertia forces of a single-crank mechanism as well as a formula for its inertia torque.

38. Dynamics of the Crank Mechanism.—Let Fig. 131 represent a simple piston and crank, and let

x_p = downward displacement of piston from top.
ωt = crank angle from top dead center.
r = crank radius.
l = length of connecting rod.

Assume the crank shaft to be rotating at uniform speed, *i.e.*, ω is constant. Our first object is the calculation of the position of the piston in terms of the angle ωt. The distance x_p would be equal to the length DB in the figure, were it not that the connecting rod has assumed a slanting position in the meantime. The distance DB, which is a first approximation of x_p can be written

$$r(1 - \cos \omega t)$$

In order to calculate x_p exactly, we must add to this as a correction term the difference between AC and BC or

$$l(1 - \cos \varphi)$$

The auxiliary angle φ can be expressed in terms of ωt by noting that

$$AB = l \sin \varphi = r \sin \omega t$$

or

$$\sin \varphi = \frac{r}{l} \sin \omega t \tag{130}$$

and consequently

$$\cos \varphi = \sqrt{1 - \frac{r^2}{l^2} \sin^2 \omega t}$$

Hence the exact expression for the piston displacement x_p in terms of the crank angle ωt is

$$x_p = r(1 - \cos \omega t) + l\left(1 - \sqrt{1 - \frac{r^2}{l^2} \sin^2 \omega t}\right) \tag{131}$$

On account of the square root this formula is not very convenient for further calculation. It can be simplified by noting that the second term under the square root is small in comparison to unity. In the usual engine, r/l differs little from $\frac{1}{4}$, so that the second term is less than $\frac{1}{16}$. Therefore, the square root is of the form $\sqrt{1 - \delta}$, where $\delta << 1$. Expanding this into a power series and retaining only the first term gives the approximation

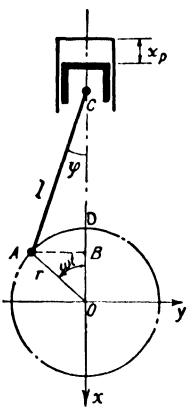


Fig. 131.—Crank mechanism.

$$\sqrt{1 - \delta} \approx 1 - \frac{\delta}{2}$$

With $\delta = \frac{1}{16}$, the error made is less than one part in 2,000. Equation (131) becomes

$$x_p \approx r(1 - \cos \omega t) + \frac{r^2}{2l} \sin^2 \omega t$$

A further simplification is obtained by converting the square of the sine into the cosine of the double angle by means of

$$\cos 2\omega t = 1 - 2 \sin^2 \omega t$$

or

$$\sin^2 \omega t = \frac{1 - \cos 2\omega t}{2}$$

Thus the piston displacement is

$$x_p = \left(r + \frac{r^2}{4l}\right) - r\left[\cos \omega t + \frac{r}{4l} \cos 2\omega t\right] \qquad (132a)$$

The velocity and acceleration follow from the displacement by differentiation:

$$\dot{x}_p = r\omega\left[\sin \omega t + \frac{r}{2l} \sin 2\omega t\right] \qquad (132b)$$

$$\ddot{x}_p = r\omega^2\left[\cos \omega t + \frac{r}{l} \cos 2\omega t\right] \qquad (132c)$$

After multiplication by the mass of the piston, these expressions become the vertical momentum and the vertical inertia force. They are seen to consist of two terms, one varying with the same frequency as the rotation and known as the "primary" term, and the other varying at double frequency and known as the "secondary" term. If the connecting rod is infinitely long, the secondary term disappears and the piston executes a harmonic motion. With a short connecting rod the motion, and especially the acceleration, deviates considerably from a sinusoid. As an example, Fig. 132 gives the piston acceleration (or inertia force) of an engine in which $l/r = 4$.

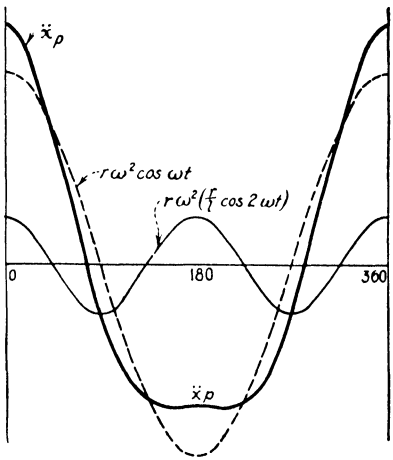


FIG. 132.—The piston acceleration as a function of the crank angle for $r/l = \frac{1}{4}$.

Having found the dynamic properties of the piston, we proceed to the rotating parts of the crank. The problem is first simplified by concentrating the entire rotating crank mass in its center of gravity. (The inertia force of this mass is the same as the resultant of all the small inertia forces on the various small parts of the crank.) Next the mass is shifted from the center of gravity to the crank pin A, but in this process it is diminished inversely proportional to the distance from the center of the shaft, so that the inertia force (which is here a centripetal force) remains unchanged.

In this manner the whole crank structure is replaced by a single mass m_c at the crank pin, and the vertical displacement can be found immediately from Fig. 131:

$$x_c = r(1 - \cos \omega t) \tag{133}$$

so that the vertical components of velocity and acceleration become

$$\left.\begin{aligned} \dot{x}_c &= r\omega \sin \omega t \\ \ddot{x}_c &= r\omega^2 \cos \omega t \end{aligned}\right\} \tag{134}$$

The horizontal components are

$$\left.\begin{aligned} y_c &= -r \sin \omega t \\ \dot{y}_c &= -r\omega \cos \omega t \\ \ddot{y}_c &= r\omega^2 \sin \omega t \end{aligned}\right\} \tag{135}$$

The momentum (or inertia force) is obtained from the velocity (or acceleration) by multiplying by the rotating crank mass m_c.

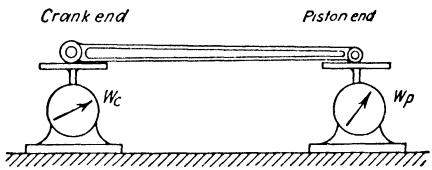


FIG. 133.—Division of the connecting rod weight into its reciprocating and rotating parts.

Returning to Fig. 131 we note that the inertia forces of the piston and the crank have been successfully put into formulas so that only the characteristics of the connecting rod remain to be determined. This seems to be the most difficult part of the problem, since the motion of the rod is rather complicated. The top point of the rod describes a straight line, while the bottom point moves on a circle. All other points describe ellipses, so that the determination and subsequent integration of the inertia forces of all these points require considerable algebra. Fortunately, however, this is not necessary. If the connecting rod is replaced by another structure, having the same mass and the same center of gravity, so that the path of the center of gravity is not changed, then the total inertia force of the rod is equal to that of the new structure. This follows directly from Newton's law which states that the component of the inertia force of a body in a certain direction equals the product of its mass and the acceleration of the center of gravity in that direction.

With the aid of this relationship the problem can be easily solved by replacing the rod by two concentrated masses, one at each end, so that the center of gravity stays where it is and so that the sum of the two concentrated masses equals the total mass of the original connecting rod. This division of mass is the same as the division of the weight into two parts by placing the rod horizontally on two scales as shown in Fig. 133.

Although the division of the connecting rod into two distinct masses leaves the center of gravity in its place and also leaves the total mass constant, the moment of inertia of the two distinct masses is different from the moment of inertia of the original connecting rod. Therefore the division of Fig. 133 is correct procedure for finding the inertia *forces*, but it is not exact for determining the moments of these forces, *i.e.*, the inertia *couple*.

Having thus divided the connecting-rod mass into a part moving with the piston (reciprocating) and another part moving with the crank pin (rotating), we can denote the total reciprocating and rotating masses by m_{rec} and m_{rot}. In other words, m_{rec} is the sum of the mass of the piston and of a part of the connecting rod and m_{rot} is the sum of the equivalent mass of the crank and the other part of the connecting rod.

With this notation the total vertical inertia force X (for *all* moving parts) of one cylinder is

$$\begin{aligned} X &= m_{\text{rec}}\ddot{x}_p + m_{\text{rot}}\ddot{x}_c \\ &= (m_{\text{rec}} + m_{\text{rot}})r\omega^2 \cos \omega t + m_{\text{rec}}\frac{r^2}{l}\omega^2 \cos 2\omega t \end{aligned} \tag{136}$$

and the horizontal inertia force Y is

$$Y = m_{\text{rot}}\ddot{y}_c = m_{\text{rot}}r\omega^2 \sin \omega t \tag{137}$$

In words: the vertical component of the inertia force consists of two parts, a "primary part" equal to the inertia action of the combined reciprocating and rotating masses as if they were moving up and down harmonically with crank-shaft frequency and amplitude r, and a "secondary part" equal to the inertia action of a mass $\frac{r}{4l}m_{\text{rec}}$ moving up and down with twice the crank-shaft frequency and with the same amplitude r.

The horizontal or lateral component has a primary part only, *viz.*, that due to the rotating mass.

Finally we have to determine the torque of the inertia forces about the longitudinal axis O. For the purpose of finding the

vertical and horizontal inertia *forces*, the connecting rod was replaced by two masses at the piston and crank pin in the manner of Fig. 133, and this procedure was shown to give exact results. For the inertia *torque* the result so obtained is no longer exact, but it will be correct to an acceptable degree of approximation. Thus again the complicated piston-rod-crank system is replaced by a mass m_{rec}, reciprocating according to (132), and a mass m_{rot} rotating uniformly round O so that it has no torque about O. The inertia torque is caused wholly by the reciprocating mass m_{rec}, and its magnitude can be deduced from Fig. 130*b*, where it was seen that the torque equals the downward piston force multiplied by $x \tan \varphi$. That the downward force in the present argument is an inertia force expressed by $-m_{\text{rec}} \ddot{x}_p$ instead of being a gas-pressure force as assumed in Fig. 130 does not make any difference. The distance x is

$$x = l \cos \varphi + r \cos \omega t \approx \left(l - \frac{r^2}{4l}\right) + r \cos \omega t + \frac{r^2}{4l} \cos 2\omega t$$

Further, $$\tan \varphi = \frac{\sin \varphi}{\sqrt{1 - \sin^2 \varphi}} \approx \sin \varphi \left(1 + \frac{1}{2} \sin^2 \varphi\right)$$

$$= \frac{r}{l} \sin \omega t \left(1 + \frac{r^2}{2l^2} \sin^2 \omega t\right),$$

so that the torque becomes

$$\mathbf{M} = -m_{\text{rec}} \ddot{x}_p \cdot x \tan \varphi$$

$$= -m_{\text{rec}} r \omega^2 \left(\cos \omega t + \frac{r}{l} \cos 2\omega t\right) \times \frac{r}{l} \sin \omega t \left(1 + \frac{r^2}{2l^2} \sin^2 \omega t\right)$$

$$\times \left\{\left(l - \frac{r^2}{4l}\right) + r \cos \omega t + \frac{r^2}{4l} \cos 2\omega t\right\}$$

Upon multiplying this out we disregard all terms proportional to the second or higher powers of r/l. This involves an error of the same order as that committed in passing from (131) to (132). Thus

$$\mathbf{M} = -m_{\text{rec}} \omega^2 r^2 \sin \omega t \left\{\frac{r}{2l} + \cos \omega t + \frac{3r}{2l} \cos 2\omega t\right\}$$

With the trigonometric relation

$$\sin \omega t \cos 2\omega t = \tfrac{1}{2} \sin 3\omega t - \tfrac{1}{2} \sin \omega t$$

the torque becomes finally

$$\mathbf{M} = \frac{1}{2} m_{\text{rec}} \omega^2 r^2 \left(\frac{r}{2l} \sin \omega t - \sin 2\omega t - \frac{3r}{2l} \sin 3\omega t\right) \quad (138)$$

This important formula for the inertia torque (acting on the shaft in the direction of its rotation, or also on the frame about O in the opposite direction) is quite accurate for the usual type of engine where the connecting rod consists of two substantial bearings at the ends, joined by a relatively light stem. On the other hand, in a radial aircraft engine, the "master connecting rod" has a crank end carrying not only the crank-pin bearing, but $n - 1$ other bearings to which the other $n - 1$ connecting rods are attached. It does not seem reasonable to replace this structure by two concentrated masses at the ends, and for this case the exact connecting rod analysis, given below, is of interest.

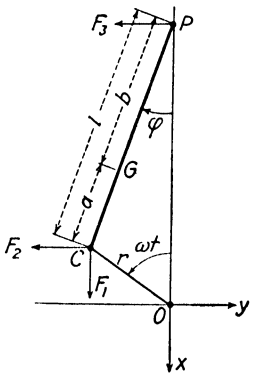


FIG. 134.

In Fig. 134 let the crank rotate in a counterclockwise direction at the uniform speed ω, and let it drag with it the connecting rod. The piston is supposed to be massless, since its inertia force is given by Eq. (132c). The piston moreover is supposed to have no friction, so that the reaction force of the cylinder wall on the rod must be F_3. Let further F_1 and F_2 be the forces exerted by the crank pin on the rod, which moves in its prescribed manner under the influence of the three forces F. This is a case of plane motion, governed by the three equations of Newton:

In the x-direction, $F_1 = m\ddot{x}_G$

In the y-direction $F_2 + F_3 = m\ddot{y}_G$

Moments about c.g., $-F_1 a \sin \varphi + F_2 a \cos \varphi - F_3 b \cos \varphi = I_G \ddot{\varphi}$

The geometry of the motion is prescribed; in particular the center of gravity moves thus:

$$x_G = x_p + (x_c - x_p)(b/l) = (x_p a/l) + (x_c b/l) \qquad \text{and} \qquad y_G = y_c b/l$$

where the subscripts c and p denote crank pin and piston, while a and b are the distances to the center of gravity G as shown in Fig. 134. The accelerations $\ddot{x}_p$, $\ddot{x}_c$, and $\ddot{y}_c$ are given by Eqs. (132), (134), and (135). The angle φ and its functions, including $\ddot{\varphi}$, are determined by Eq. (130). Thus the Newton equations can be solved for their three unknowns F_1, F_2, and F_3. It is noted that the first Newton equation becomes

$$F_1 = (m\ddot{x}_p a/l) + (m\ddot{x}_c b/l) = m_{\text{roc}}\ddot{x}_p + m_{\text{rot}}\ddot{x}_c$$

which leads to the result Eq. (136), known before. Similarly the combination $F_2 + F_3$ was designated before as Y in Eq. (137). Thus, for the inertia *forces* it is seen once more that the statement at the bottom of page 220 is correct. Now we wish to calculate the *torque* in the clockwise direction exerted on the shaft by the inertia of the rod. It is

$$\mathbf{M} = -F_1 r \sin \omega t - F_2 r \cos \omega t$$

so that it is necessary to find F_2 separately by eliminating F_3 from between

the last two Newton equations. This gives

$$F_2 = -m_{\text{rot}}\frac{b}{l}r\omega^2 \sin \omega t - \frac{I_G\dot{\varphi}}{\cos \varphi} + \frac{F_1 a \sin \varphi}{l \cos \varphi}$$

In working this out by means of Eq. (130) we neglect all terms containing powers of r/l higher than 2. This leads to

$$F_2 = -m_{\text{rot}}\frac{b}{l}r\omega^2 \sin \omega t - \frac{I_G}{l^2}r\omega^2 \sin \omega t + \frac{1}{2}m_{\text{rec}}\frac{r}{l}r\omega^2 \sin 2\omega t$$

With this expression the inertia torque, after some trigonometry becomes

$$\mathbf{M}_{\text{shaft}} = \frac{1}{2}m_{\text{rec}}\omega^2 r^2\left[\frac{r}{2l}\sin \omega t - \left(1 + \frac{ab - k^2}{al}\right)\sin 2\omega t - \frac{3r}{2l}\sin 3\omega t\right] \quad (139a)$$

in which k is the radius of gyration of the rod, defined by $mk^2 = I_G$. This result is approximate only in the sense that higher powers of r/l have been neglected; otherwise, it is exact. It differs from (138) only in the double-frequency term, which now depends on the moment of inertia mk^2.

Equation (138) is the expression for the inertia torque on the shaft of a connecting rod consisting of two concentrated masses ma/l and mb/l at distances b and a from the center of gravity. Such a rod has a radius of gyration $k^2 = ab$, and it is seen that Eq. (139a) reduces to Eq. (138) if this substitution is made.

It is interesting to consider two cases of rods that have no end concentrations in order to see how (139a) differs numerically from (138). First take the uniform rod, $a = b = l/2$ and $k^2 = l^2/12$. In this case the double-frequency term of (139a) is 33 per cent greater than the term in the approximate formula (138). Next consider a rod with $m_{\text{rec}} = 0$, ($b = l$), having its center of gravity at the crank pin and a certain dimension around it, which is a rough picture of the master rod of a radial aircraft engine. Assuming $k^2 = l^2/10$, we find a middle term in (139a) which is the same as that in (138) if only m_{rec} is replaced by $m/10$. But, moreover, *the sign is reversed.*

The aircraft master rod of actual practice is a combination of the two cases just discussed, and the increase in moment due to the "uniform rod effect" more or less balances the decrease in moment due to the large moment of inertia of the crank end. Thus, even for so unusual a rod as that of a radial aircraft engine, the approximate result (138) is fairly accurate.

The torque acting on the *frame* of the engine about the shaft center O (Fig. 134) is found by multiplying the force F_3 by its moment arm.

$$\mathbf{M}_{\text{frame}} = F_3(l \cos \varphi + r \cos \omega t)$$

Solving for F_3 from the Newton equation, substituting it into the above expression, and working it out, neglecting higher powers of r/l, involves more algebra than it is expedient to reproduce here. The answer becomes

$$\mathbf{M}_{\text{frame}} = \frac{1}{2}m_{\text{rec}}\omega^2 r^2\left\{\left[\frac{(r^2 + 8l^2)(k^2 - ab)}{4ral^2} + \frac{r}{2l}\right]\sin \omega t - \left[\frac{ab - k^2}{al} + 1\right]\sin 2\omega t - \left[\frac{3r(k^2 - ab)}{4al^2} + \frac{3r}{2l}\right]\sin 3\omega t\right\} \quad (139b)$$

Again, for the connecting rod with two concentrated ends ($k^2 = ab$) this

result reduces to Eq. (138). Thus for the general connecting rod the inertia torques on the shaft and the frame are not equal but differ by the moment of the inertia forces of the various rod points about O. Only when the rod degenerates into two concentrated masses is this moment zero, since the two inertia forces are along the center line and along a radius, both passing through O.

39. Inertia Balance of Multicylinder Engines.—The unbalance or inertia forces on a single-cylinder engine are given by Eqs. (136) and (137). In these formulas the reciprocating mass m_{rec} is always positive, but the rotating mass m_{rot} can be made zero or even negative by "counterbalancing" the crank (Fig. 135). It is therefore possible to reduce the horizontal inertia force Y to zero, but the vertical unbalance force X always exists.* Thus a single-cylinder engine is inherently unbalanced.

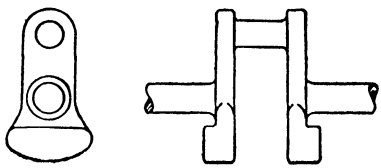


FIG. 135.—Counterbalanced crank.

Consider a two-cylinder engine with 180-deg. crank angle. Since the two cranks are opposed to each other, the two horizontal inertia forces are also in opposition and cancel each other (except for a moment about the vertical axis). Since the two pistons move against each other, the same is true for the primary vertical forces. However, the secondary vertical forces are in the same direction and add. To understand this, it is convenient to visualize the various forces as (the horizontal projections of) rotating vectors (page 3). We shall now explain this vector method for the general case of a multicylinder engine.

In such an engine let the distance between the nth crank and the first crank be l_n and the angle between the nth crank and the first crank be α_n (the nth crank angle). In Fig. 136 the first crank is shown in a vertical position, corresponding to a maximum value of the primary vertical inertia force. The second crank is α_2 radians ahead of the first one, and consequently its vertical primary inertia force has passed through its maximum value α_2/ω sec. earlier. If the rotating vector representing the primary vertical force of the first cylinder is in its vertical position, the vector representing the second cylinder is in the position α_2,

* A patent has been issued on a scheme whereby the connecting rod is extended beyond the crank pin so as to make $\mathbf{W}_p$ in Fig. 133 negative. In this manner M_{rec} may be made zero also. No such engine has ever been constructed on account of the large crank case required.

and generally the vector representing the nth cylinder is in the position α_n. The same statement is true for the primary *horizontal* inertia force.

Therefore, the crank diagram of Fig. 136*b*, regarded as a vector diagram (Fig. 136*c*), represents the primary force conditions in

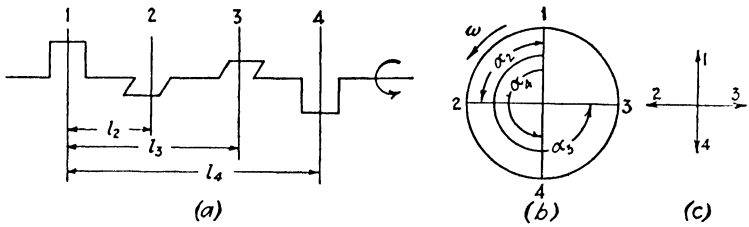


FIG. 136.—Primary inertia forces on a four-cylinder engine.

the engine. For example a four-cylinder engine of this type has balanced primary forces.

The secondary force vectors, however, rotate twice as fast as the crank shaft. Referring again to Fig. 136*a*, if the secondary force of crank 1 be a vertical vector, the vector of crank 2 *was* vertical at the time that crank 2 was vertical. Crank 2 has traveled α_2 radians from the vertical, and the vector of crank 2 consequently is $2\alpha_2$ radians from the vertical. The secondary-force diagram therefore is a star with the angles $2\alpha_2$, $2\alpha_3$, . . . , $2\alpha_n$ between the various vectors. Figure 137*a* shows this diagram for the engine of Fig. 136.

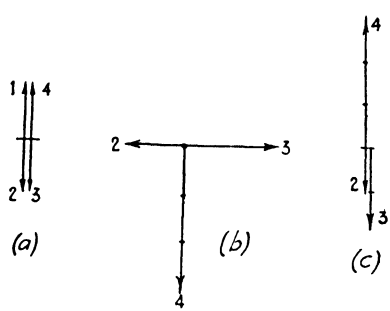


FIG. 137.—Secondary forces (*a*), primary moments (*b*) and secondary moments (*c*) for the four-cylinder engine of Fig. 136.

A similar reasoning holds for the *moments* of these forces about a lateral axis. The moment of the nth inertia force about the center of the first crank shaft is that force multiplied by the moment arm l_n (Fig. 136*a*). The plane in which such a moment operates is defined by the direction of the force and the longitudinal center line of the crank shaft. Therefore, the moment can be represented also by a vector in the same direction as the inertia force, its length being multiplied by the proper moment arm l_n.

The primary-moment diagram of the engine of Fig. 136*a* is given in Fig. 137*b*, where $l_1 = 0$, $l_2 = l$, $l_3 = 2l$ and $l_4 = 3l$. The secondary-moment diagram (Fig. 137*c*) follows in a similar manner.

With the aid of such vector diagrams the reader should prove the following propositions:

1. A four-cylinder engine of 0, 90, 270, 180 deg. crank shaft has balanced primary and secondary forces and also has balanced secondary moments, but the primary moments are unbalanced.

2. A four-cylinder engine of 0, 180, 180, 0 deg. crank shaft has balanced primary forces and moments, while the secondary forces and moments are unbalanced.

3. A six-cylinder engine (0. 120, 240, 240, 120, 0 deg.) has all forces balanced and all moments balanced

4. An eight-cylinder in-line engine (0, 180, 90, 270, 270, 90, 180, 0 deg.) is completely balanced.

In these examples it has been tacitly assumed that all pistons are alike and are spaced at equal distances, which is the case in modern internal-combustion engines. However, the method will work just as well for unequal piston masses and unequal spacings. In fact it was for the application to large triple and quadruple expansion steam engines for ship propulsion that the theory was originally developed (Schlick's theory of balancing, about 1900).

A particularly interesting case of balance occurs in the so-called V-8 engine, consisting of two ordinary four-cylinder blocks operating on a single common crank shaft. The crank shaft is of the 0, 90, 270, 180 deg. type, and on each throw two pistons act, one from each bank. It was seen above that each four-cylinder bank by itself is unbalanced only in terms of primary moments, the secondary forces and moments being completely balanced already in each bank. If the V-angle is made 90 deg., as usual, the vertical, or X-, force of a piston in one bank has the same space direction as the horizontal, or Y-, force of the other bank, and it is possible to make the primary components of these two forces annihilate each other. Thus the total primary force of each crank becomes zero and no primary moments can exist.

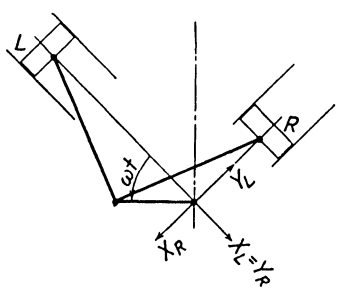


FIG. 138.

The manner in which this is done is illustrated in Fig. 138, in which the x- and y-axes are in the same direction as in Fig. 131, the subscripts L and R designating the left- and right-bank cylinders. Let further m_{rec} be the reciprocating mass of one piston and the corresponding part of one connecting rod, and let m_{rot} be the rotating mass of half of one crank and throw with the corresponding part of one single connecting rod. Then the primary force in the L-direction caused by the longitudinal component of the left cylinder, by Eq. (136), is

In L-direction: $(m_{rec} + m_{rot})r\omega^2 \cos \omega t$ due to L
Similarly by Eq. (137)
In R-direction: $-m_{rot}r\omega^2 \sin \omega t$ due to L

In computing the forces caused by the R-cylinder it is noted that the angle between its center line and the crank is $\omega t + \pi/2$, so that

In L-direction: $+m_{rot}r\omega^2 \sin [\omega t + (\pi/2)]$
$= +m_{rot}r\omega^2 \cos \omega t$ due to R
In R-direction: $(m_{rec} + m_{rot})r\omega^2 \cos [\omega t + (\pi/2)]$
$= -(m_{rec} + m_{rot})r\omega^2 \sin \omega t$ due to R

Summing these contributions we have

In L-direction: $(m_{rec} + 2m_{rot})r\omega^2 \cos \omega t$
In R-direction: $-(m_{rec} + 2m_{rot})r\omega^2 \sin \omega t$
$= +(m_{rec} + 2m_{rot})r\omega^2 \cos [\omega t + (\pi/2)]$

It is seen therefore that the unbalanced forces in the R- and L-directions are alike, and they can be reduced to zero by making $(m_{rec} + 2m_{rot})$ zero. Therefore complete balance of a V-8 engine can be attained by counterweighting each individual throw in such a way that it takes care of a full crank with the rotating parts of two rods and the reciprocating parts of one single piston and rod.

Example: A triple expansion steam engine has pistons of which the weights are to each other as $1 : \frac{1}{2} : 2$. If it is desired to balance this engine for primary forces, how should the crank angles be made?

Solution: The vectors in the diagram have lengths in the required ratios. Drawing the vector of two units length vertically, as in Fig. 139, the equilibrium requires that the two other vectors be arranged so that their horizontal components balance and that the sum of their vertical components be two units. With the angles α and β of Fig. 139, we have

$$1 \cdot \sin \alpha = 1\tfrac{1}{2} \sin \beta$$
$$1 \cdot \cos \alpha + 1\tfrac{1}{2} \cos \beta = 2$$

To solve these, calculate $\cos \alpha$ from the first equation:

$$\cos \alpha = \sqrt{1 - \sin^2 \alpha} = \sqrt{1 - 2\tfrac{1}{4} \sin^2 \beta}$$

and substitute in the second one:

$$\sqrt{1 - 2\tfrac{1}{4} \sin^2 \beta} = 2 - 1\tfrac{1}{2} \cos \beta$$

Square and simplify:

$$6 \cos \beta = 5\tfrac{1}{4}$$

from which $\cos \beta = 0.88$ and $\beta = 28$ deg

Further, $\cos \alpha = 2 - \tfrac{3}{2} \times 0.88 = 0.68$ and $\alpha = 47$ deg.

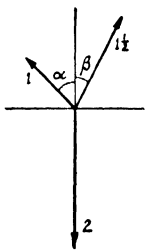


FIG. 139.

It is possible to express the results of these vector diagrams in simple mathematical language. The requirement for balanced primary forces is that the geometrical sum of all the vectors of Fig. 136c be zero. If this be so, the sum of their horizontal projections as well as the sum of their vertical projections must be zero or

$$\sum_n \sin \alpha_n = 0 \qquad \text{and} \qquad \sum_n \cos \alpha_n = 0 \tag{140}$$

Similarly, the conditions for balanced secondary forces are

$$\sum_n \sin 2\alpha_n = 0 \qquad \text{and} \qquad \sum_n \cos 2\alpha_n = 0 \tag{141}$$

For the primary moments

$$\sum_n l_n \sin \alpha_n = 0 \qquad \text{and} \qquad \sum l_n \cos \alpha_n = 0 \tag{142}$$

For the secondary moments

$$\sum l_n \sin 2\alpha_n = 0 \qquad \text{and} \qquad \sum l_n \cos 2\alpha_n = 0 \tag{143}$$

All these formulas are true only for *equal* piston masses.

For the four-cylinder engine of Fig. 136 we have $\alpha_1 = 0$, $\alpha_2 = 90$, $\alpha_3 = 270$, $\alpha_4 = 0$ deg., and consequently Eqs. (140) become

$$0 + 1 - 1 + 0 = 0 \qquad \text{and} \qquad 1 + 0 + 0 - 1 = 0$$

so that the primary forces are balanced.

But Eqs. (142) become

$$0 \cdot 0 + 1 \cdot 1 - 2 \cdot 1 + 3 \cdot 0 = 1 - 2 \neq 0$$
$$0 \cdot 1 + 1 \cdot 0 + 2 \cdot 0 + 3 \cdot 1 = 3 \neq 0$$

so that the primary moments are unbalanced.

Thus we are able to test the inertia balance of any engine design by using either the formulas (140) to (143) or the vector diagrams.

It may be well to recall that in this analysis the engine has been considered to be a "solid body." This is usually the case in automobile and aircraft engines where all cylinders are cast in a single block, but in marine engines the cylinders sometimes are mounted separately. Then the forces or moments of two cylinders may be in opposition to each other and not move the engine as a whole, but they may move the two cylinders against each other elastically. The problem becomes extremely complicated, and is not of sufficient practical importance to merit much time for its solution. In this connection the reader is referred to the analogous problem in rotating machinery discussed in Sec. 49.

An interesting case of balance occurs in radial engines for aircraft, having a single crank, rotating about O, on the crank pin of which operates the "master connecting rod" AB (Fig. 140). This master rod has a large lower head carrying $(n - 1)$ holes at a radius l_1 from the crank-pin center A. These holes are spaced at angles $2\pi/n$ apart and carry the $(n - 1)$ link rods of which one, CD, is shown. The length of the master rod $AB = L$ and that of a link rod $CD = L_1$. The first step in calculating the balance of this engine is the determination of the displacement of one of the $(n - 1)$ pistons. In the figure the distance OD is

$$x_p = r \cos (\omega t - \alpha) + l_1 \cos \varphi + L_1 \cos \varphi_1$$

The auxiliary angles φ and φ_1 are determined by the equations

$$\sin \varphi = \frac{r}{L} \sin \omega t \qquad \text{and} \qquad \sin \varphi_1 = \frac{r}{L_1} \sin (\omega t - \alpha) - \frac{l_1 r}{L L_1} \sin \omega t$$

Working out the cosines of φ and φ_1, neglecting powers of r/L higher than the second, in a manner quite similar to the process described on page 208, leads to

$$x_p = r \cos (\omega t - \alpha) + l_1 - \frac{r^2 l_1}{2L^2} \sin^2 \omega t + L_1 - \frac{r^2}{2L_1} \sin^2 (\omega t - \alpha) + \frac{r^2 l_1}{L L_1} \sin \omega t \sin (\omega t - \alpha) - \frac{l_1^2 r^2}{2 L_1 L^2} \sin^2 \omega t$$

or, after differentiation,

$$-\ddot{x}_p = r\omega^2 \left[\cos (\omega t - \alpha) + \frac{r l_1}{L^2} \left(1 + \frac{l_1}{L_1} \right) \cos 2\omega t + \frac{r}{L_1} \cos 2(\omega t - \alpha) - \frac{2 r l_1}{L L_1} \cos (2\omega t - \alpha) \right]$$

This expression, multiplied by the reciprocating mass m_{rec} of one piston and part of one link rod, gives the inertia force. There are $(n - 1)$ such forces

radially distributed round O, in addition to the force of the main cylinder B. The latter force is found from the above formula in which $\alpha = 0$, multiplied by the reciprocating mass of the master cylinder $m_{\text{rec mas}}$, which usually is different from the reciprocating mass of m_{rec} of one of the other cylinders. In order to form the resultant of the inertia forces of all the cylinders, it is necessary to divide each force into its components along and across the master-cylinder direction. The component along the master cylinder

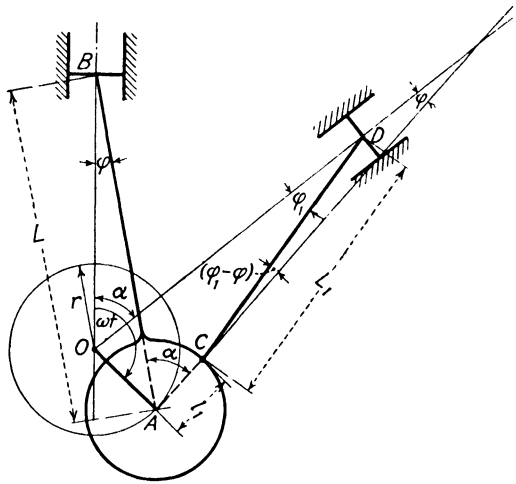


FIG. 140.

of the force of a cylinder at angle α away from the master is $m_{\text{rec}}\ddot{x}_p \cos \alpha$, and the component across the master cylinder is $m_{\text{rec}}\ddot{x}_p \sin \alpha$.

First we propose to add together the across-components of all cylinders, utilizing the trigonometric relation

$$\cos A \sin \alpha = \tfrac{1}{2} \sin (A + \alpha) - \tfrac{1}{2} \sin (A - \alpha)$$

Applying this to the first term in the bracket of x_p we find

$$\cos (\omega t - \alpha) \sin \alpha = \tfrac{1}{2} \sin \omega t - \tfrac{1}{2} \sin (\omega t - 2\alpha)$$

This expression is to be summed over all N cylinders, having angles α spaced at equal intervals $2\pi/N$ around the circle. The first term on the right side above is the same for all cylinders so that the sum is $\tfrac{1}{2}N \sin \omega t$. The second term, however, is the sum of a set of sines of angles that are $4\pi/N$ apart; sketching a vector diagram it is recognized that we have to form the vector sum of a uniformly spaced star diagram, so that the answer is zero. In the same manner we proceed with the three other terms in the bracket of $\ddot{x}_p$ with the result

$$\sum - x_p \sin \alpha = r\omega^2 \left(\frac{N}{2} \sin \omega t - \frac{N}{2} \cdot \frac{2rl_1}{LL_1} \sin 2\omega t \right)$$

In this summation it is noticed that for the master cylinder $\alpha = \sin \alpha = 0$, so that its contribution to the across-force is nil and the difference between m_{rec} and $m_{\text{rec mas}}$ does not come in. Thus the force across the center line of the master cylinder due to all reciprocating parts is

$$F_{\text{across}} = m_{\text{rec}} r\omega^2 \left(\frac{N}{2} \sin \omega t - \frac{N}{2} \frac{2rl_1}{LL_1} \sin 2\omega t \right)$$

In the same manner the force along the master cylinder is computed. Summing over all the cylinders, while considering the master cylinder as having the same mass as all the others, gives the same result as F_{across} except that cosines occur instead of sines. To this must be added the difference between the master reciprocating parts and those of an ordinary cylinder at its location, with the final result

$$F_{\text{along}} = m_{\text{rec}} r\omega^2 \left\{ \left[\frac{N}{2} + \left(\frac{m_{\text{rec mas}}}{m_{\text{rec}}} - 1 \right) \right] \cos \omega t + \right.$$
$$\left. + \left[-\frac{N}{2} \cdot \frac{2rl_1}{LL_1} + \frac{r}{L} \left(\frac{m_{\text{rec mas}}}{m_{\text{rec}}} - 1 \right) \right] \cos 2\omega t \right\}$$

Thus the total unbalance consists of a primary and a secondary force. The two components of primary force differ if $m_{\text{rec mas}}$ differs from m_{rec}. In that case it is not possible to balance the engine for primary force. The best counterbalance that can be provided interpolates between the two components. It must balance first the *rotating* parts of the crank, the master rod and the $(N - 1)$ link rods, and moreover it must balance a mass at the crank radius of $\frac{1}{2}(N - 1)m_{\text{rec}} + \frac{1}{2}m_{\text{rec mas}}$. If this counterweight is provided, there remain primary unbalanced forces in the two main directions of

$$\tfrac{1}{2} r\omega^2 (m_{\text{rec mas}} - m_{\text{rec}})$$

The secondary unbalanced forces cannot be balanced by ordinary means.

40. Natural Frequencies of Torsional Vibration.—The shafting of an internal-combustion engine with all its cranks, pistons, flywheel, and driven machinery is too complicated a structure to attempt an exact determination of its torsional natural frequency. It is necessary first to simplify or "idealize" the machine to some extent by replacing the pistons, etc., by equivalent disks of the same moment of inertia and by replacing the crank throws by equivalent pieces of straight shaft of the same torsional flexibility. In other words, the machine has to be reduced to the shape of Fig. 142*a*. This process is at best approximate.

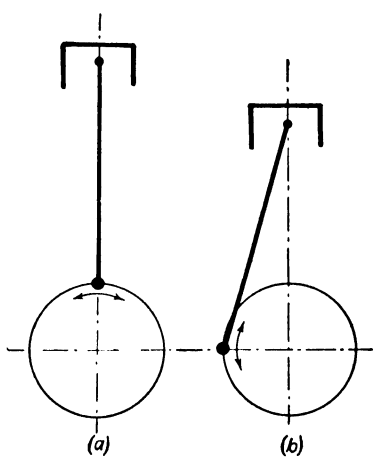


FIG. 141*a* and *b*.—The equivalent moment of inertia of a piston varies with its position.

First consider the equivalent moment of inertia of each crank mechanism. The moment of inertia I_{rot} of the purely rotating parts offers no difficulty, but it is not quite evident what should be done with the reciprocating weight. In Figs. 141*a* and *b* the piston is shown in two positions. Imagine the crank shaft to be non-rotating but to be executing small torsional oscillations. In Fig. 141*a* this takes place without any motion of the piston, but in Fig. 141*b* the motion (and acceleration) of the piston practically equals that of the crank pin. The equivalent inertia in position *a* is zero whereas in position *b* it is $m_{rec}r^2$. Thus while the crank shaft is rotating, the total equivalent moment of inertia of the crank mechanism varies between I_{rot} and $I_{rot} + m_{rec}r^2$, with an average value of $I_{rot} + \frac{1}{2}m_{rec}r^2$. The system with variable inertia (page 424) is now replaced by one of constant inertia I, where

$$I = I_{rot} + \tfrac{1}{2}m_{rec}r^2 \qquad (144)$$

Next consider the idealization of a crank throw into a piece of ordinary shafting of the same torsional flexibility. This is physically quite permissible, but the calculation of the flexibility is a very difficult matter. In Fig. 141*c* it is seen that, if the main shaft is subjected to twist, the crank webs *W* are subjected to bending moments and the crank pin *P* is in twist. It is possible to calculate the angle of twist produced by a certain torque by applying to the webs and pin the usual "beam" formulas for bending and twist. However, that will give very inaccurate results because these formulas are true only for long and slender beams and will lead to serious errors if applied to short stubs of a width and thickness nearly as great as the length. Moreover, it can be seen that the torque in Fig. 141*c* will cause not only a twisting rotation of the free end but also a sidewise displacement of it on account of the bending in the webs. In an actual machine the sidewise motion is impeded by the main bearings and the torsional stiffness of the crank shaft is increased by these bearings, especially if their clearance is small.

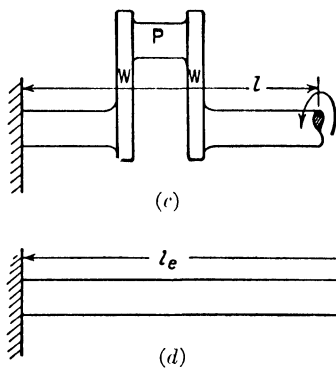


FIG. 141*c* and *d*.—A crank of length *l* is replaced by a piece of uniform shaft of length l_e having the same torsional flexibility.

Experiments have been carried out on a number of crank shafts of large, slow-speed engines showing that the "equivalent length" l_e of Fig. 141*d* (*i.e.*, the length of ordinary shaft having the same torsional stiffness) is nearly equal to the actual length l. The variation is between

$$0.95l < l_e < 1.10l$$

the lower value being for small throws and stiff webs and the higher value for large throws and thin flexible webs. In all tests the diameter of the main shaft was equal to that of the crank pin.

In cases where the crank pin has a different diameter (usually smaller) from that of the main bearing journal, the throw is replaced by a straight shaft of two different diameters; the point where the diameter jumps from one value to the other being located at the center of the crank web. For high-speed, light-weight engines, particularly aircraft engines, where the webs are no longer rectangular blocks but have shaved-off corners to save weight, the equivalent stiffness is very much smaller than would follow from the above simple calculation. In extreme cases the stiffness may be as low as 50 per cent of the value so calculated. The best guide is then a comparison of calculation and experiment of a number of previous crank shafts of similar characteristics.

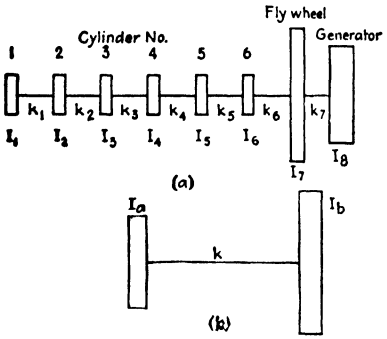


FIG. 142.—The engine is replaced by a two-mass system for the purpose of an approximate calculation of the lowest natural frequency.

In case one part of the system is connected to the other part through gears, it is convenient to reduce everything to one speed. As was explained on page 42, this is accomplished by eliminating the gears and multiplying the moments of inertia and the spring constants of the *fast* rotating parts by n^2 where $n > 1$ is the gear ratio.

Let Fig. 142*a* represent the idealized machine, in this case a six-cylinder Diesel engine driving a flywheel and an electric generator. There are eight degrees of freedom. It is theoretically possible to find the eight natural frequencies by the method of

Chap. IV, using a determinant with eight rows and eight columns and an eighth degree equation in ω_n^2. This is obviously undesirable from the standpoint of time consumption.

Instead, we use a method of successive approximations starting with a rough first guess at the frequency. Such a guess for the lowest natural frequency can be made by replacing Fig. 142*a* by Fig. 142*b*, where I_a is the inertia of all six cylinders combined and I_b that of the flywheel and generator rotor combined. The frequency of the latter system is [Eqs. (12*c*) and (16)]

$$\omega = \sqrt{k\frac{I_a + I_b}{I_a I_b}}$$

and is an approximation to the lowest frequency of Fig. 142*a*. In the reduction of Fig. 142*a* to 142*b* the judgment of the calculator enters. With some experience the frequency can be estimated to within 10 per cent.

The rough value ω_1, thus obtained, serves as the basis for the following method of calculation due to *Holzer*. Assume the whole system to be in a torsional oscillation with the frequency ω_1. If ω_1 were a natural frequency this could occur without any external torque on the system (a *free* vibration). If ω_1 is not a natural frequency, this can occur only if at some point of the system an external torque of frequency ω_1 is acting. We have then a *forced* vibration. Assume arbitrarily that the angular amplitude of the first disk in Fig. 142*a* is 1 radian. The torque necessary to make that disk vibrate is

$$I_1\omega_1^2 \sin \omega_1 t$$

This torque can come only from the shaft to the right of I_1. If that shaft has a torsional spring constant k_1, its angle of twist is $\frac{I_1\omega_1^2}{k_1} \sin \omega_1 t$ with a maximum value $\frac{I_1\omega_1^2}{k_1}$. Since the amplitude of disk I_1 is 1 radian and the shaft twists $\frac{I_1\omega_1^2}{k_1}$ radians, disk I_2 must vibrate with an amplitude of $1 - \frac{I_1\omega_1^2}{k_1}$ radians. This requires a torque of amplitude

$$I_2\omega_1^2\left(1 - \frac{I_1\omega_1^2}{k_1}\right)$$

This torque is furnished by the difference in the shaft torques left and right, and, since the torque in k_1 is known, the torque in k_2

can be calculated. From this we find the angle of twist of k_2, the angle of I_3, etc., finally arriving at the last disk I_8. But there is no shaft to the right of I_8 to furnish the necessary torque. In order to make the system vibrate as described, it is necessary to apply to I_8 an external torque T_{ext} of the value found by the calculation. Only when ω_1 happened to be a natural frequency would this T_{ext} be found equal to zero. The magnitude and sign of T_{ext} therefore are a measure of how far ω_1 is removed from the natural frequency. A number of such calculations with different values of ω_1 must be made, until finally the remainder torque T_{ext} is practically zero. The advantage of this method is that it gives not only the natural frequency but also the complete shape of the natural mode of vibration, and this will be needed for the calculation of the work input by the non-uniformities of the cylinder torques (page 255).

The actual course of the calculations can best be illustrated by a definite example, as follows.

41. Numerical Caclulation of Diesel Ship Drive.—Consider a six-cylinder Diesel engine with a flywheel directly coupled to a ship propeller through a long propeller shaft (Fig. 143). The characteristics of the installation are:

Crank radius r	15 in.
Crank-shaft diameter	12 in.
Weight of piston and crosshead	2,500 lb.
Connecting-rod weight	1,500 lb.
Moment of inertia of one crank equivalent to	1,180 lb. in. sec.^{2}
Flywheel inertia	75,000 lb. in. sec.^{2}
Cylinder spacing	36 in.
Distance, cylinder 6 to flywheel	36 in.
Distance, flywheel to propeller	150 ft.
Propeller-shaft diameter	12 in.
Propeller inertia	20,000 lb. in. sec.^{2}
Running speed	100 r.p.m.
Power at 100 r.p.m	$6 \times 250 = 1{,}500$ hp.

The moment of inertia of one crank is calculated as follows:

$$\text{Reciprocating weight: } 2{,}500 + \frac{1{,}500}{2} = 3{,}250 \text{ lb.}$$

$$\text{Rotating weight: } \frac{1{,}500}{2} = 750 \text{ lb.}$$

Half of the reciprocating weight is effective in rotatory inertia so

that the equivalent inertia of the piston and rod is

$$\frac{1{,}625 + 750}{386} \cdot 15^2 = 1{,}380 \text{ lb. in. sec.}^2$$

The total equivalent inertia of one crank thus is
1,180 (crank) + 1,380 (piston, etc.) = 2,560 lb. in. sec.^{2} = $I_{1\ldots6}$
The elasticity of the crank shaft between two cranks is calculated as if the equivalent length were equal to the actual length.

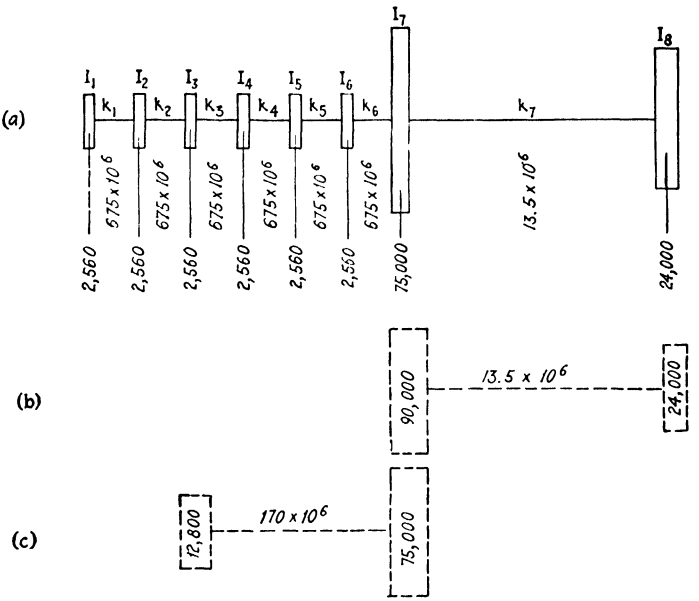


FIG. 143.— (*a*) Diesel ship drive with its approximations for calculating the first (*b*) and second (*c*) natural frequency.

Hence

$$k_{1\ldots6} = \frac{GI_p}{l} = \frac{G\pi d^4}{32l} = \frac{12 \cdot 10^6 \cdot \pi \cdot 12^4}{32 \cdot 36} = 675 \cdot 10^6 \text{ in. lb./rad.}$$

The elasticity of the long propeller shaft is

$$k_1 = \frac{GI_p}{l} = \frac{3}{150} \cdot 675 \cdot 10^6 = 13.5 \cdot 10^6 \text{ in. lb./rad.}$$

The inertia of the propeller is usually increased by 20 per cent to take care of the water which is moved with it, so that I_8 = 24,000 lb. in. sec.^{2}.

Thus the system is reduced to that shown in Fig. 143*a*. In the first mode of vibration with one node, the engine with its

flywheel will act practically as a solid body; then there are two masses, the engine-flywheel and the propeller, with the long shaft between. Consider a two-mass system with

$$I_1 = 75{,}000 + 6 \times 2{,}560 = 90{,}000$$

and $I_2 = 24{,}000$, with a shaft of $k = 13.5 \cdot 10^6$ between (Fig. 143*b*). Its natural frequency is

$$\omega = \sqrt{\frac{13.5 \cdot 10^6(24{,}000 + 90{,}000)}{24{,}000 \times 90{,}000}} = 26.2 \text{ rad./sec.}$$

The second (two-noded) mode will be in the engine itself, the flywheel swinging against the first few cylinders on the left with a node somewhere in the engine close to the flywheel. Since this motion is considerably faster than the previous one, the propeller on its shaft is far removed from resonance, and the propeller, being excited by the high-frequency flywheel motion, can have but little amplitude. Thus the propeller shaft cannot influence this mode very much. Assume (as is shown in Fig. 143*c*) two masses, the flywheel and the first five cylinders lumped at the location of cylinder 3. Then

$$\omega = \sqrt{\frac{170 \cdot 10^6(12{,}800 + 75{,}000)}{12{,}800 \times 75{,}000}} = 125 \text{ rad./sec.}$$

Higher modes of vibration usually are of no interest.

The Holzer calculation for the first mode becomes

First Mode $\omega = 26.2$ $\omega^2 = 680$ First Trial

No.	I (1)	$I\omega^2$ (2)	β (3)	$I\omega^2\beta$ (4)	$\Sigma I\omega^2\beta$ (5)	k (6)	$\frac{1}{k}\Sigma I\omega^2\beta$ (7)
1	2,560	1.74×10^6	1.000	1.74×10^6	1.74×10^6	675×10^6	0.003
2	2,560	1.74×10^6	0.997	1.73×10^6	3.47×10^6	675×10^6	0.005
3	2,560	1.74×10^6	0.992	1.72×10^6	5.19×10^6	675×10^6	0.008
4	2,560	1.74×10^6	0.984	1.71×10^6	6.90×10^6	675×10^6	0.010
5	2,560	1.74×10^6	0.974	1.70×10^6	8.60×10^6	675×10^6	0.013
6	2,560	1.74×10^6	0.961	1.67×10^6	10.27×10^6	675×10^6	0.015
7	75,000	51.0×10^6	0.946	48.2×10^6	58.5×10^6	13.5×10^6	4.33
8	24,000	16.3×10^6	−3.38	-55.0×10^6	$+3.5 \times 10^6 = T_{ext}$		

In this table columns 1, 2, and 6 were first filled in, and with an arbitrary amplitude $\beta_1 = 1$ radian in column 3 the calcu-

lation proceeds step by step to the right along the first row. The physical meaning of the second column is the inertia torque per unit angular amplitude of each disk. The fourth column is the inertia torque of each disk. Each entry in the fifth column is obtained by adding the value of column 4 to the previous value of column 5. Thus column 5 gives the sum of the inertia torques of all disks to the left of the one under consideration. This sum must equal the torque in the shaft immediately to the right of the disk under consideration. Thus, when this torque $\Sigma I\omega^2\beta$ is divided by the shaft elasticity k we obtain in column 7 the angular twist (in radians) in the shaft portion between two disks. This twist is subtracted from the amplitude in column 3 and thus gives the angular amplitude of the next disk. The reader should follow all calculations in this table and be clear about the physical meaning of each entry. In particular the last result 3.5×10^6 represents the sum of the inertia torques of all disks and thus is the torque T_{ext} that must be applied to the last disk in order to vibrate the system at $\omega = 26.2$ with 1 radian amplitude at the first disk. It is seen that T_{ext} is positive, *i.e.*, that it has the same phase as the motion of the first seven disks. From this we can conclude that the first natural frequency is *greater* than 26.2, which can be understood from Fig. 144 where T_{ext} is plotted as a function of ω.

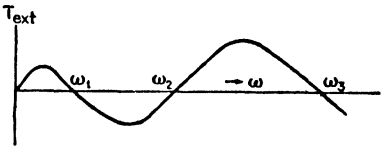


FIG. 144.—Behavior of the remainder torque of column 5 of the Holzer calculation.

When ω is taken zero, all entries in the columns 2, 4, 5, and 7 become zero, and thus T_{ext} is also zero. For a small ω the values in column 2 are small, and those of column 3 differ only slightly from unity. Thus column 5 shows a set of increasing values ending in a positive figure. At the first natural frequency (and at the higher ones as well) T_{ext} must be zero. Thus a diagram having the shape of Fig. 144 is obtained. Below the first natural frequency the last entry T_{ext} in the Holzer table is positive; between the first and second frequencies it is negative, and so on.

Since $\omega^2 = 680$ is apparently too small, and since the figures of column 3 show our original assumption of a stiff crank shaft and a flexible propeller shaft to be fairly correct, our next trial is $\omega^2 = 700$, very close to our first attempt.

First Mode $\omega = 26.5$ $\omega^2 = 700$ Second Trial

No.	I	$I\omega^2$	β	$I\omega^2\beta$	$\Sigma I\omega^2\beta$	k	$\frac{1}{k}\Sigma I\omega^2\beta$
1	2,560	$1\ 79 \times 10^6$	1.000	$1\ 79 \times 10^6$	$1\ 79 \times 10^6$	675×10^6	0 003
2	2,560	$1\ 79 \times 10^6$	0 997	$1\ 78 \times 10^6$	3.57×10^6	675×10^6	0 005
3	2,560	1.79×10^6	0.992	1.77×10^6	5.34×10^6	675×10^6	0 008
4	2,560	$1\ 79 \times 10^6$	0.984	1.76×10^6	7.10×10^6	675×10^6	0 011
5	2,560	1.79×10^6	0 973	1.74×10^6	$8\ 84 \times 10^6$	675×10^6	0 013
6	2,560	$1\ 79 \times 10^6$	0 960	$1\ 72 \times 10^6$	10.56×10^6	675×10^6	0.016
7	75,000	52.5×10^6	0 944	$49\ 55 \times 10^6$	$60\ 1 \times 10^6$	$13\ 5 \times 10^6$	4 45
8	24,000	$16\ 8 \times 10^6$	−3 50	$-58\ 9 \times 10^6$	$+1\ 2 \times 10^6 = T_{ext}$		

The torque T_{ext} is still positive, so that our estimate of the error was too optimistic. The next value to try is found by extrapolation from the two previous results based on the fact that a sufficiently small piece of the curve of Fig. 144 may be considered straight.

$$\omega^2 = 700 + \frac{1.2}{3.5 - 1.2}(700 - 680) = 710.5$$

First Mode $\omega = 26.7$ $\omega^2 = 711$ Third Trial

No.	I	$I\omega^2$	β	$I\omega^2\beta$	$\Sigma I\omega^2\beta$	k	$\frac{1}{k}\Sigma I\omega^2\beta$
1	2,560	$1\ 82 \times 10^6$	1 000	$1\ 82 \times 10^6$	1.82×10^6	675×10^6	0 003
2	2,560	$1\ 82 \times 10^6$	0 997	$1\ 81 \times 10^6$	$3\ 63 \times 10^6$	675×10^6	0 005
3	2,560	1.82×10^6	0 992	1.80×10^6	$5\ 43 \times 10^6$	675×10^6	0 008
4	2,560	1.82×10^6	0.984	1.79×10^6	7.22×10^6	675×10^6	0 011
5	2,560	1.82×10^6	0.973	1.77×10^6	8.99×10^6	675×10^6	0 013
6	2,560	1.82×10^6	0.960	1.75×10^6	10.74×10^6	675×10^6	0 016
7	75,000	53.3×10^6	0.944	50.32×10^6	61.1×10^6	13.5×10^6	4.52
8	24,000	17.1×10^6	−3.58	$-61\ 2 \times 10^6$	$-0\ 1 \times 10^6$		

In this table the external torque is negligibly small. Therefore the first natural frequency is 26.7 radians per second or $26.7/2\pi = 4.25$ cycles per second. The shape of the motion is illustrated in Fig. 145, where the angular amplitudes β of the various disks are plotted against their positions. The curve is known as the "normal elastic curve of the first mode of motion." It is seen that the crank shaft is practically solid and that nearly all the deformation is taking place in the propeller shaft.

Proceeding to the second mode of motion, the frequency was found to be, roughly, $\omega = 125$. The Holzer calculation is

Second Mode $\omega = 125$ $\omega^2 = 15625$ First Trial

No.	I	$I\omega^2$	β	$I\omega^2\beta$	$\Sigma I\omega^2\beta$	k	$\frac{1}{k}\Sigma I\omega^2\beta$
1	2,560	$40\ 0 \times 10^6$	1 000	$40\ 0 \times 10^6$	$40\ 0 \times 10^6$	675×10^6	0 059
2	2,560	$40\ 0 \times 10^6$	0 941	$37\ 6 \times 10^6$	$77\ 6 \times 10^6$	675×10^6	0 115
3	2,560	$40\ 0 \times 10^6$	0 826	$33\ 0 \times 10^6$	$110\ 6 \times 10^6$	675×10^6	0 164
4	2,560	$40\ 0 \times 10^6$	0 662	$26\ 4 \times 10^6$	$137\ 0 \times 10^6$	675×10^6	0 203
5	2,560	$40\ 0 \times 10^6$	0 459	$18\ 4 \times 10^6$	$155\ 4 \times 10^6$	675×10^6	0 230
6	2,560	$40\ 0 \times 10^6$	0 229	$9\ 2 \times 10^6$	$164\ 6 \times 10^6$	675×10^6	0 244
7	75,000	$1,172 \times 10^6$	− 0 015	$-17\ 6 \times 10^6$	$147. \times 10^6$	$13\ 5 \times 10^6$	10.89
8	24,000	375×10^6	−10 90	$-4,090 \times 10^6$	$-3,940 \times 10^6 = T_{ext}$		

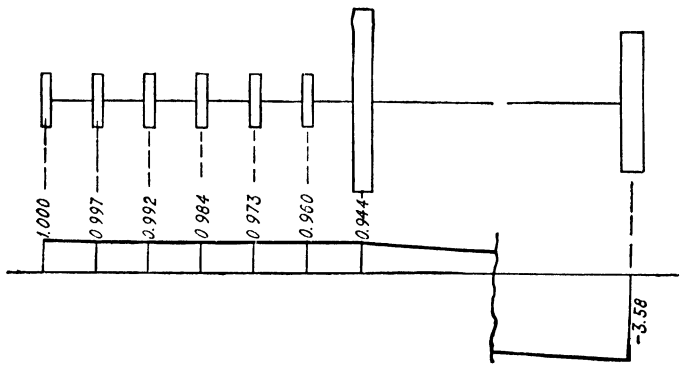


FIG. 145.—First natural mode of motion of Fig. 143.

The remaining torque is negative and rather large. Figure 144 tells us that our estimate is too low. Considering the large value of the external torque, the next trial is made very much higher.

Second Mode $\omega = 141$ $\omega^2 = 20,000$ Second Trial

No.	I	$I\omega^2$	β	$I\omega^2\beta$	$\Sigma I\omega^2\beta$	k	$\frac{1}{k}\Sigma I\omega^2\beta$
1	2,560	$51\ 2 \times 10^6$	1.000	$51\ 2 \times 10^6$	51.2×10^6	675×10^6	0 076
2	2,560	51.2×10^6	0 924	$47\ 3 \times 10^6$	$98\ 5 \times 10^6$	675×10^6	0 146
3	2,560	$51\ 2 \times 10^6$	0 778	$39\ 8 \times 10^6$	$138\ 3 \times 10^6$	675×10^6	0 205
4	2,560	51.2×10^6	0 573	$29\ 4 \times 10^6$	$167\ 7 \times 10^6$	675×10^6	0 248
5	2,560	51.2×10^6	0 325	16.6×10^6	$184\ 3 \times 10^6$	675×10^6	0 273
6	2,560	51.2×10^6	0 052	$2\ 7 \times 10^6$	187.0×10^6	675×10^6	0 278
7	75,000	$1,500 \times 10^6$	− 0.226	-339×10^6	-152×10^6	13.5×10^6	−11.24
8	24,000	480×10^6	+11.01	$+5,285 \times 10^6$	$+5,130 \times 10^6$		

Now the remainder is positive, so that the frequency is too high. The next value is found by interpolation:

$$\omega^2 = 15{,}625 + \frac{3{,}940}{3{,}940 + 5{,}130}(20{,}000 - 15{,}625) = 17{,}500$$

Second Mode $\omega = 132.4$ $\omega^2 = 17{,}500$ Third Trial

No.	I	$I\omega^2$	β	$I\omega^2\beta$	$\Sigma I\omega^2\beta$	k	$\frac{1}{k}\Sigma I\omega^2\beta$
1	2,560	44.8×10^6	1 000	$44\ 8 \times 10^6$	$44\ 8 \times 10^6$	675×10^6	0 066
2	2,560	44.8×10^6	0 934	$41\ 8 \times 10^6$	$86\ 6 \times 10^6$	675×10^6	0 128
3	2,560	44.8×10^6	0 806	36.1×10^6	$122\ 6 \times 10^6$	675×10^6	0 181
4	2,560	44.8×10^6	0 625	$27\ 9 \times 10^6$	$150\ 5 \times 10^6$	675×10^6	0 223
5	2,560	$44\ 8 \times 10^6$	0 402	$18\ 0 \times 10^6$	$168\ 5 \times 10^6$	675×10^6	0 250
6	2,560	44.8×10^6	0 152	$6\ 8 \times 10^6$	175.3×10^6	675×10^6	0 260
7	75,000	$1{,}312 \times 10^6$	−0 108	-141.8×10^6	$+\ 33\ 5 \times 10^6$	$13\ 5 \times 10^6$	+2 48
8	24,000	420×10^6	−2 59	$-1{,}088 \times 10^6$	$-1{,}054 \times 10^6$		

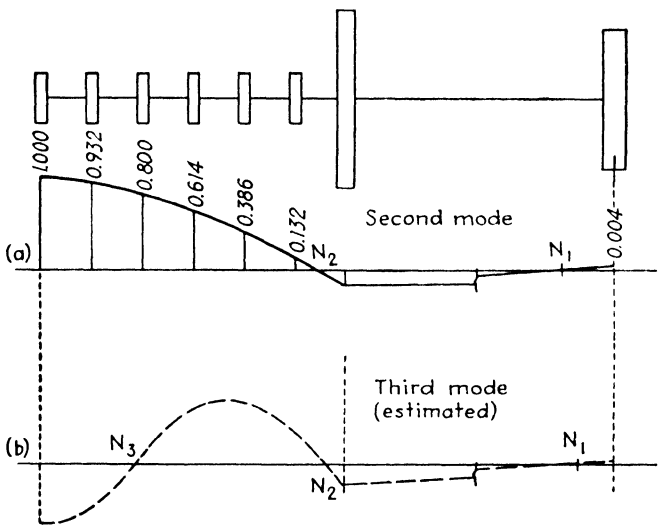


FIG. 146.—Second and third normal elastic curves.

Though this result is considerably better than the two previous ones it is still not sufficiently accurate. Linear interpolation gives

$$\omega^2 = 17{,}500 + \frac{1{,}054}{1{,}054 + 5{,}130}(20{,}000 - 17{,}500) = 17{,}930$$

A consideration of the result of the first trial makes us suspect that this is somewhat low. Thus the fourth calculation is

Second Mode $\omega = 134$ $\omega^2 = 18{,}000$ Fourth Trial

No.	I	$I\omega^2$	β	$I\omega^2\beta$	$\Sigma I\omega^2\beta$	k	$\frac{1}{k}\Sigma I\omega^2\beta$
1	2,560	46.05×10^6	1.000	46.0×10^6	46.0×10^6	675×10^6	0 068
2	2,560	46.05×10^6	0 932	42.8×10^6	$88\ 8 \times 10^6$	675×10^6	0 132
3	2,560	46.05×10^6	0 800	36.8×10^6	125.6×10^6	675×10^6	0 186
4	2,560	$46\ 05 \times 10^6$	0.614	28.2×10^6	153.8×10^6	675×10^6	0 228
5	2,560	46.05×10^6	0.386	17.7×10^6	171.5×10^6	675×10^6	0 254
6	2,560	$46\ 05 \times 10^6$	0.132	6.0×10^6	177.5×10^6	675×10^6	0 263
7	75,000	$1{,}350 \times 10^6$	−0 131	-176.8×10^6	$+ 0.7 \times 10^6$	13.5×10^6	0.052
8	24,000	432×10^6	−0.183	$-\ 79.0 \times 10^6$	-78.0×10^6		

The remainder is now sufficiently small. The only unsatisfactory thing about this solution is the value for the amplitude β of the propeller. A very slight change in ω^2 makes this amplitude vary tremendously. Consider the flywheel amplitude which has been underlined in the last two tables. A very small change in the frequency ω^2 will make the amplitude β_7 of the flywheel equal to -0.133 in the last table. Then the last two rows of that table become

7	75,000	$1{,}350 \times 10^6$	−0 133	$-179\ 3 \times 10^6$	$-1\ 84 \times 10^6$	$13\ 5 \times 10^6$	−0 1365
8	24,000	432×10^6	+0 004	$+\ 1\ 7 \times 10^6$	0		

Thus we have finally for the second natural frequency $\omega = 134$ radians per second or $f = 21.3$ cycles per second, and the normal elastic curve shown in Fig. 146*a*. The third mode of motion with three nodes will be somewhat as indicated in Fig. 146*c*, and its calculation probably would require six or more Holzer trials. Fortunately, however, such higher modes hardly ever attain practical importance.

The Holzer method, just outlined, does not take advantage of the fact that in the usual engine all cylinders and shaft sections between them are alike. A simplification of the computations can be obtained by using the methods of the calculus of finite differences, which is described in the book by von Kármán and Biot, quoted in the bibliography. This method leads to results identical with those of Holzer's method.

A very good approximation is obtained by the method of F. M. Lewis, in which the inertia of the engine disks is uniformly distributed along the engine shaft. Then the engine itself becomes a shaft in torsional vibration, subject to the differential

equation (93*b*) of page 173, with the general solution (96) of page 174. This simply means that the engine portions of the elastic curves of Fig. 145 and 146 are pieces of sine wave. If moreover the engine ends freely, without flywheel at its left-hand end, as shown in these figures, and if the end amplitude is 1.000 rad., as assumed, then Eq. (96) becomes

$$(x) = \cos x\sqrt{\frac{\mu_1\omega^2}{GI_p}}$$

where x is measured from the left to the right. With the notations $I = \mu_1 l$ = the total moment of inertia of the entire engine, $K = GI_p/l$ = the stiffness of the entire engine shafting of length l, and $\varphi = \beta$ = angle of twist along the shaft, as in the Holzer tables, the equation of the shaft deformation reads

$$\beta(x) = \cos \omega\sqrt{\frac{I}{K}} \cdot \frac{x}{l} \qquad (a)$$

The combination

$$\omega\sqrt{\frac{I}{K}} = \Theta \qquad (b)$$

is the number of radians of cosine wave along the engine shaft, and its numerical magnitude is easily visualized in Figs. 145 and 146. Then we have for the angle at the right-hand end of the engine, *i.e.*, for the angle of disk 7, the value

$$\beta_7 = \beta(l) = \cos \Theta \qquad (c)$$

The torque in the shaft just left of disk 7 is

$$\mathbf{M}_l = GI_p\left(\frac{d\beta}{dx}\right)_{x\ =\ l} = \omega\sqrt{IK} \cdot \sin \Theta \qquad (d)$$

With these four formulas the sixth line of the Holzer table can be calculated at once. We can assume either a value for ω, as before, or, also, we can assume a value for Θ, which in certain respects is even more physically obvious. Then β_7 can be calculated by Eq. (*c*), while $\mathbf{M}_l$, from (*d*), gives the value of the shaft torque, *i.e.*, of $\Sigma I\omega^2\beta$.

In assigning numerical values to the inertia I and the stiffness K of the uniform shaft, which is supposed to be the equivalent of the actual engine, some judgment is required. For instance, in Figs. 145 and 146 the mass at the left end should be smeared

out to the left as well as to the right. In this manner we arrive at an over-all length of 6½ shaft sections, and $K = 675 \times 10^6/6.5 = 104 \times 10^6$ inch lb./rad. Further, $I = 6 \times 2{,}560 = 15{,}360$ lb. in. sec.^{2} The two combinations of these quantities, occurring in the formulas (*a*) to (*d*), are

$$\sqrt{\frac{I}{K}} = 0.01215 \text{ sec.} \qquad \text{and} \qquad \sqrt{IK} = 1.265 \times 10^6 \text{ lb. in. sec.}$$

Entering with these values into the calculation of the first mode we assume $\omega \times 26.7$, as in the third Holzer trial. This gives

$\Theta = 26.7 \times 0.01215 = 0.324$ radian $= 18° 38'$

$\beta_7 = \cos 18° 38' = 0.948$

$\mathbf{M}_l = \Sigma I\omega^2\beta = 26.7 \times 1.265 \times 10^6 \times 0.319 = 10.75 \times 10^6$

These values are seen to differ from those in the Holzer table only in the last decimal place, so that the agreement is almost perfect.

Proceeding to the second mode with $\omega = 134$, as in the last Holzer trial for that mode, we find

$\Theta = 134 \times 0.01215 = 1.630$ radians $= 93.5$ deg.

$\beta_7 = \cos 93.5° = -0.061$

$\mathbf{M}_l = 134 \times 1.265 \times 10^6 \times \sin 93.5° = 169.5 \times 10^6$

The value of β_7 is far from the correct one. After some trial it is found that $\omega = 139$ gives a better fit.

$\Theta = 139 \times 0.01215 = 1.690$ radians $= 97.0$ deg.

$\beta_7 = \cos 97° = -0.122$

$I\omega^2\beta_7 = -176.5 \times 10^6$

$\mathbf{M}_l = 139 \times 1.265 \times \sin 97° = +176.0 \times 10^6$

Thus we see that Lewis's method gives us no error at all for the first mode and an error of only 3.7 per cent in the frequency of the second mode, with a large saving of labor. It is good practice to carry out the first rough trials with Lewis's method and to polish off with a Holzer table.

The method of F. P. Porter, which is used by several engine manufacturers, consists of replacing the entire engine by an "equivalent flywheel" I_{equiv}. The torque exerted by the entire engine on the rest of the system is expressed by formula (*d*), above. If the engine were to consist of a single flywheel I_{equiv}, oscillating at the amplitude of the end of the engine, Eq. (*c*), the torque would be

$$I_{\text{equiv}}\omega^2\beta(l) = I_{\text{equiv}}\omega^2 \cos \Theta$$

Equating this to the torque, Eq. (*d*), of the actual engine and considering Eq. (*b*) we get

$$I_{\text{equiv}} = I\frac{\tan\Theta}{\Theta} \qquad (e)$$

Thus the engine of actual inertia I with a flexible crank shaft acts as a solid flywheel (without flexibility) of inertia I_{equiv} at the assumed frequency determined by Θ. The rest of the calculation follows essentially Holzer's pattern.

The Holzer method can be applied conveniently to the calculation of the frequencies of *branched* systems, such as that in Fig. 147, which shows the main drive of a ship built in 1940 for the U.S. Maritime Commission. The disks 1 and 5 represent the inertia of a low-pressure and a high-pressure steam turbine, running at 7,980 r.p.m. The disks 2 and 4 are intermediate gears running at 730 r.p.m., while 3 is the main gear, running at 85 r.p.m. and coupled to the propeller 6. The inertias shown are in lb. in. sec.^{2} and are already multiplied with the squares of their speed ratios (page 42). The flexibilities shown must be multiplied by 10^9 to measure in in. lb./radian and likewise have been corrected for speed. To find the lowest natural frequency we notice that the engine shafting is stiff in comparison with the drive shaft. Thus for a first estimate all turbine masses are lumped at the main gear and

$$\omega^2 \approx \frac{k}{I} = \frac{0.071 \times 10^9}{416{,}000} = 170$$

A Holzer trial has shown this value to be low; and, with final value $\omega^2 = 176$, the last calculation proceeds as follows:

$$\omega^2 = 176, \qquad \beta_1 = 1.000, \qquad \mathbf{M}_1 = I_1\omega^2\beta_1 = 1.275 \times 10^9$$

$$\beta_{12} = \frac{\mathbf{M}_1}{k_1} = \frac{1.275}{643} = 0.002, \qquad \beta_2 = 0.998$$

$$\mathbf{M}_2 = I_2\omega^2\beta_2 = 0.181, \qquad \mathbf{M}_{23} = \mathbf{M}_1 + \mathbf{M}_2 = 1.456$$

$$\beta_{23} = \frac{\mathbf{M}_{23}}{k_{23}} = 0.279, \qquad \beta_3 = \beta_2 - 0.279 = 0.719$$

Now we do not know the amplitudes in the 3-4-5 branch, having once assumed $\beta_1 = 1.000$. Nevertheless we start fresh with the assumption $\beta_5 = 1.000$ and work back.

$$\beta_5 = 1.000, \qquad \mathbf{M}_5 = 0.083, \qquad \beta_{45} = 0.000, \qquad \beta_4 = 1.000$$
$$\mathbf{M}_4 = 0.191, \qquad \mathbf{M}_{34} = 0.274, \qquad \beta_{34} = 0.053, \qquad \beta_3 = 0.947$$

It is clear that β_3 cannot at the same time have an amplitude of 0.719 and of 0.947. It is possible to make the last value come out

equal to 0.719 simply by multiplying all figures in the last two lines by the ratio 0.719/0.947 = 0.760. Then these lines become

$$\beta_6 = 0.760, \quad \mathbf{M}_5 = 0.063, \quad \beta_{45} = 0.000, \quad \beta_4 = 0.760$$
$$\mathbf{M}_4 = 0.145, \quad \mathbf{M}_{34} = 0.205, \quad \beta_{34} = 0.04, \quad \beta_3 = 0.719$$

Proceeding with the main gear 3, it is seen that not only its own inertia torque $\mathbf{M}_3 = I_3\omega^2\beta_3 = 0.044$ is acting on it, but the torques $\mathbf{M}_{23}$ and $\mathbf{M}_{34}$ from the two branches as well. Thus the torque

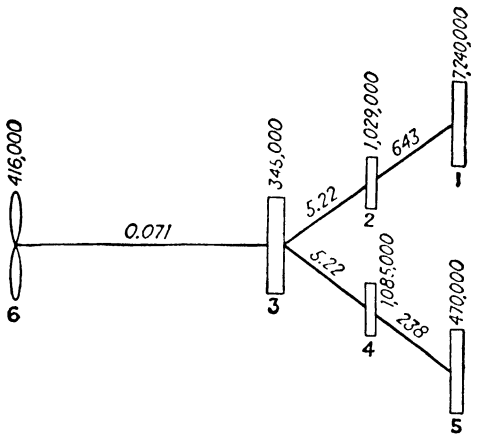


FIG. 147.—Ship drive consisting of high-speed turbines 1 and 5, double reduction-gear drive 2, 3, 4, and propeller 6.

entering the propeller shaft is

$$\mathbf{M}_{36} = 0.044 + 1.456 + 0.205 = 1.705$$

Further,

$$\beta_{36} = 24.01, \quad \beta_6 = -23.29, \quad \mathbf{M}_6 = -1.705$$

Remainder, 0

In a similar way the reader should find the second mode of motion of this system, which consists primarily of one turbine swinging against the other one. This leads to a frequency $\omega^2 = 1{,}929$, and an elastic curve

$$\beta_1 = 1.000, \quad \beta_2 = 0.978, \quad \beta_3 = -2.064, \quad \beta_4 = -4.87$$
$$\beta_5 = -4.89, \quad \beta_6 = +0.200$$

In carrying out this calculation it will be found that the last result comes out to be the small difference between two large numbers, which is very inaccurate. Therefore β_6 is calculated better by means of Eq. (30), page 61, considering the propeller and its shaft to be excited at $\omega^2 = 1.929$ by a motion $\beta_3 = -2.064$, which is known accurately.

42. Torque Analysis.—Since the torsional vibrations in the crank shaft are excited by the non-uniformities in the driving torque we proceed to an examination of the properties of this torque. We have seen in Sec. 38 that it is made up of two parts, one due to cylinder pressure and the other due to inertia.

In Fig. 148*a* the cylinder-pressure torque of a four-cycle Diesel engine is shown as a function of the crank angle. At the four

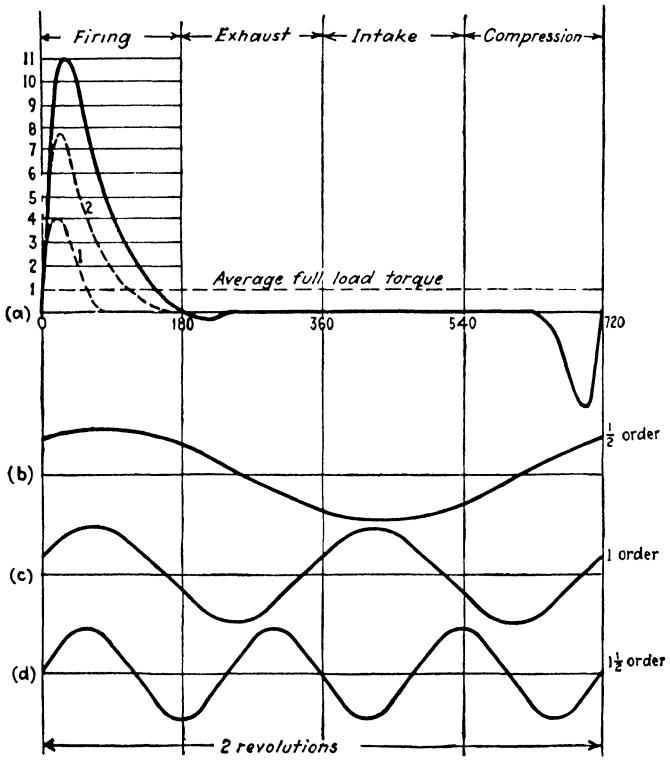


FIG. 148.—The gas torque of one cylinder of a Diesel engine and its first three harmonic components.

dead-center positions during the two revolutions of a firing cycle the torque is zero. When the engine is operated at partial load by a reduced injection of fuel, the curve is changed only in the firing quarter cycle. The dotted lines 1 and 2 indicate the shapes for zero and half load. At zero load the pressure during the firing period is equal to that during the compression period, so that even when there is no average torque at all there are alternating torques of considerable amplitude.

It is seen that the average torque delivered by the cylinder is only a small fraction of the maximum torque which occurs during the firing period. The fact that the torque is so irregular as shown constitutes one of the inherent disadvantages of the reciprocating engine as compared with the turbine where the torque curve is a straight horizontal line.

It is possible to break up Fig. 148*a* into its harmonic components as explained on page 20, and as an illustration the first three harmonics are shown. They are known as the harmonic components of the order ½, 1, and 1½ because they show as many full sine waves *per revolution* of the engine. In two-cycle engines and in steam engines, only harmonics of integer orders occur. It is only in the four-cycle internal-combustion engine that we have half-order harmonics due to the fact that the torque curve is periodic with a firing cycle, *i.e.*, with two revolutions.

It is seen that the 1- and 1½-order curves add up to a positive result near $\omega t = 45$ deg. and to a negative result near $720 - 45$ deg., while in a broad range near $\omega t = 360$ deg. they cancel each other approximately. Thus the three harmonic curves added together give a rough approximation of the actual torque curve, but many more harmonics are required to show the torque curve in all its detail.

The results of the harmonic analysis of the torque curve for this engine, a slow-speed, four-cycle Diesel, are given in Figs. 149*a* and *b*. Horizontally is plotted the loading condition of the engine, and vertically is plotted the amplitude of the various torque harmonics expressed in terms of the average full-load torque. It is seen, for example, that the harmonic of order 1½ has an amplitude of 1.97 times the average full-load torque when the engine is running at full load and has an amplitude of 0.69 times average full-load torque when the engine is idling and has no average torque whatever.

On page 222 it was seen that the inertia force of the reciprocating parts also causes a torque, and Eq. (138) indicates that only the harmonics of orders 1, 2, and 3 of this torque are of importance. With these three harmonics the torque due to cylinder pressure has to be properly compounded with the inertia torque. Since the Figs. 149*a* and *b* do not give the phase relation of the harmonics with respect to the compound torque curve (*e.g.*, order ½ in Fig. 148*b* is 50 deg. out of phase) and since the inertia-torque harmonics are all in phase with the sine (*i.e.*, at

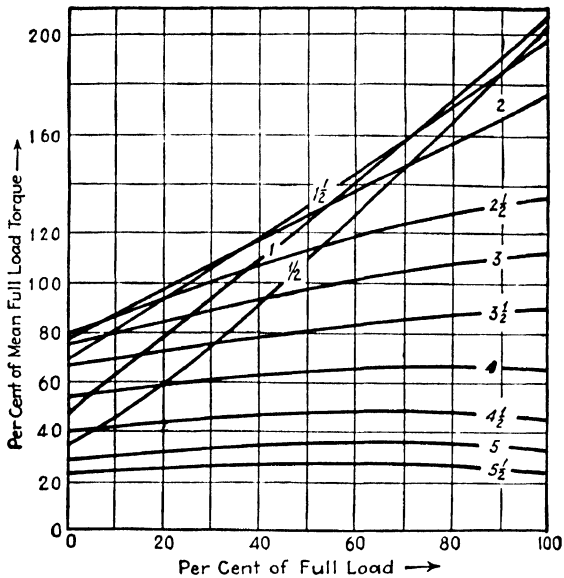


FIG. 149*a*.—Total harmonic components [*A* of Eq. (10), page 20] of Fig. 148*a* up to the order 5½ for slow-speed four-cycle Diesel engine. (Calculated by *F. M. Lewis.*)

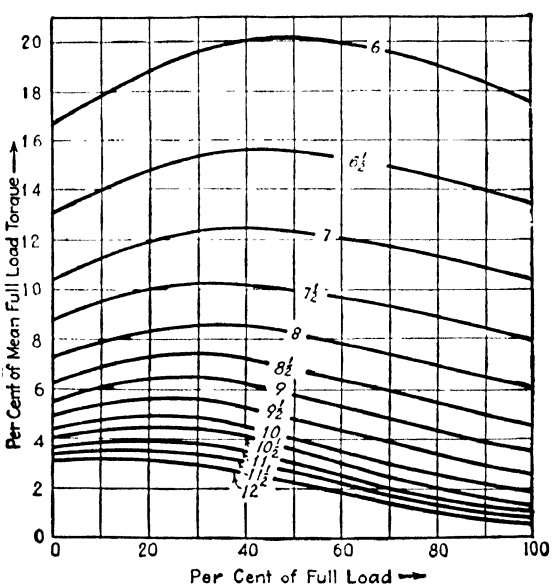


FIG. 149*b*.—Total harmonic components of Fig. 148*a*; orders 6 to 12 for slow-speed four-cycle Diesel engine. (Calculated by *F. M. Lewis.*)

$t = 0$ the ordinate of the torque harmonics is zero), it is necessary to specify the phase relation of the orders 1, 2, and 3 of the gas-pressure torque. This is done in Fig. 149*c*, where these harmonics are resolved into their sine and cosine components. As an

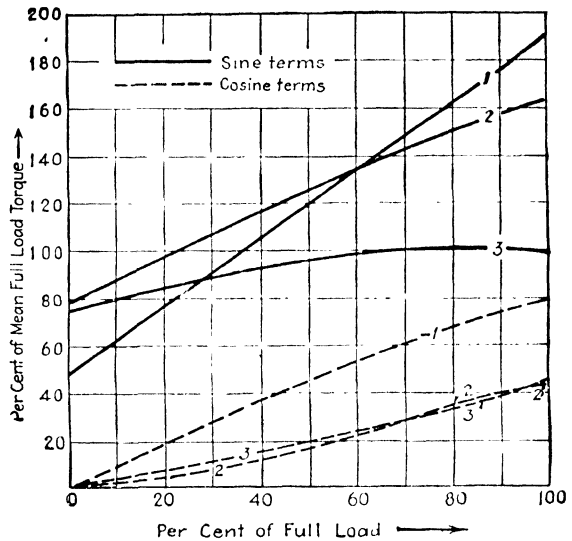


FIG. 149*c*.—Sine (a_n) and cosine (b_n) components of the harmonics of orders 1, 2, and 3. (*F. M. Lewis.*)

example consider the gas-pressure harmonic of order 1 at full load. The conditions are sufficiently clear from Fig. 150, in which the amplitude of the compound curve coincides with the result shown in Fig. 149*a*. The addition of the gas-pressure torque and the inertia torque is best explained by an example.

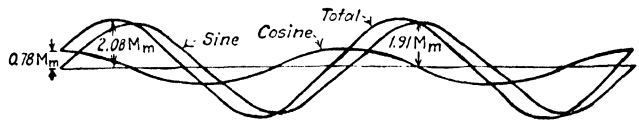


FIG. 150.—Compounding of the full-load sine and cosine components of the first order from Fig. 149*a*.

Take the harmonic of order 2 for the engine with the characteristics as given on page 236. The mean full-load torque per cylinder is

$$\mathbf{M}_m = \frac{33{,}000 \cdot \text{hp.}}{2\pi \cdot \text{r.p.m.}} \text{ft. lb.} = 13{,}150 \text{ ft. lb.}$$

By Fig. 149*c* the sine component of the harmonic of order 2 at full

load is $1.63 \times 13{,}150 = 21{,}400$ ft. lb., and the cosine component is $0.43 \times 13{,}150 = 5{,}650$ ft. lb.

The inertia torque is given by Eq. (138), page 222. Its amplitude of order 2 (*i.e.*, having 2 cycles per revolution) is $-\frac{1}{2}m_{rec}\omega^2 r^2$. Since the reciprocating weight is 3,250 lb. (page 236), the amplitude of the inertia torque at full speed is

$$-\frac{1}{2}\frac{3{,}250}{32.2}\left(2\pi\frac{100}{60}\right)^2\left(\frac{15}{12}\right)^2 = -8{,}600 \text{ ft. lb.}$$

This torque has the phase of a *sine* because the origin of time has always been taken at the position of top dead center (Figs. 130 and 131). Thus the total sine component has an amplitude of $-8{,}600 + 21{,}400 = 12{,}800$ ft. lb., which with a cosine amplitude of 5,650 ft. lb. gives a total harmonic of the order 2 of

$$\sqrt{(12{,}800)^2 + (5{,}650)^2} = 14{,}000 \text{ ft. lb.}$$

at 100 r.p.m. and full load. In this manner it is possible to calculate the amplitudes of the various harmonics of the torque.

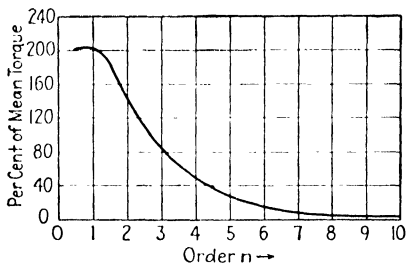


FIG. 151.—Harmonic torque components for four-cycle gas engine for aircraft. (*E. S. Taylor.*) An approximate expression for this graph is $7.7/n^2$.

The results of Fig. 149 are true for slow-speed four-cycle Diesel engines only. For other types of engine similar results have been obtained. Figure 151 gives the harmonic coefficients of four-cycle spark-plug engines used on aircraft. The values shown are independent of the operating conditions of the engine, but it is noted that the ordinates read in "per cent of mean torque," whereas in Fig. 149 they are in "per cent of mean *full-load* torque." Therefore, if an aircraft engine is run at half torque, all harmonic coefficients are half as small, a condition that is roughly true in the four-cycle Diesel only for the three lowest harmonics. The higher harmonic torques in the Diesel are roughly independent of the load, whereas in the aircraft engine

they are proportional to it. For full load it is seen that the coefficients of the two types of engine have about the same values.

The most complete and useful harmonic analyses were made by F. P. Porter in a paper entitled "Harmonic Coefficients of Engine Torque Curves."* In that paper, which is too large to reproduce here, curves similar to those of Fig. 149 are given for eight widely different types of engine (slow and fast, Diesel and spark plug, two- and four-cycle) so that one of the eight prototype engines of Porter is always sufficiently close for practical purposes to any engine that may come up.

In interpreting Porter's curves it is to be noted that the ordinate, which he calls m_1, is measured in pounds per square inch gas pressure, so that to find the corresponding nth harmonic torque T_n the ordinate has to be multiplied by the piston area A and by the crank radius $R(T_n = m_1 AR)$. Likewise his abscissas differ from those of Fig. 149, in that they are expressed in pounds per square inch M.I.P. (mean indicated pressure). The definition of M.I.P. is

$$\text{Work per cycle} = 2R \times \text{M.I.P.} \times A$$

where a "cycle" may be one revolution or two revolutions, depending on whether the engine is two- or four-cycle. Calling p the number of revolutions per cycle, the relation between the nth harmonic torque T_n and the mean engine torque T_{mean} is

$$\frac{T_n}{T_{\text{mean}}} = \frac{\pi p m_1}{\text{M.I.P.}} = \pi p \frac{\text{ordinate}}{\text{abscissa}}$$

In ship drives it is not only the Diesel engine that can excite torsional vibrations in the installation. The propeller itself, usually having three or four blades, does not experience a uniform reaction torque from the water. Each time a blade passes the rudder stem or some other near-by obstacle, the pressure field about the blade is influenced and the torque modified. Thus there will be torque fluctuations with propeller-blade frequency. Though little detailed information about the intensity of these variations is available at the present time, it has been found that an assumed torque variation of 7.5 per cent of the mean propeller torque leads to calculated torsional amplitudes that are in decent agreement with measured amplitudes on a considerable number of ships.

* *Trans. A.S.M.E.*, 1943, p. A33.

43. Work Done by Torque on Crank-shaft Oscillation.—Assume the crank shaft to be in a state of torsional oscillation, superposed on its main rotating motion. If one of the harmonics of the torque of a cylinder has the same frequency as the vibratory motion, that torque performs work upon the motion. The work so done may be either positive or negative (or zero), depending on the phase relation.

Generally speaking each torque harmonic will induce in the system a forced torsional vibration of its own frequency, so that the motion of the shaft is made up of as many harmonics as are present in the torque. However, nearly all of these harmonics have frequencies so far removed from the natural frequency that the corresponding vibrational amplitude is negligibly small. Only when one of the torque harmonics coincides with one of the natural frequencies is the response appreciable, and the ampli-

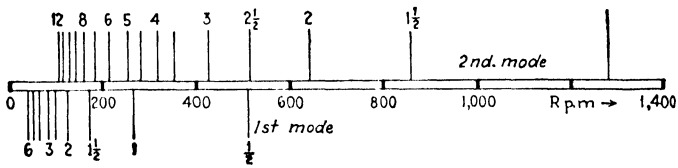


FIG. 152.—Critical-speed spectrum of the installation of Fig. 143.

tude of vibration then may become great. The "critical speeds" of the engine at which such resonance may occur are very numerous.

For example, the six-cylinder marine Diesel installation already discussed has natural frequencies of 4.25 and 21.3 cycles per second or 255 and 1,280 cycles per minute. Suppose this machine to be running at $2 \times 255 = 510$ r.p.m. There are 255 firing cycles per minute, and the torque harmonic of order $\frac{1}{2}$ produces resonance in the first mode. Similarly for a speed of 255 r.p.m., the first-order harmonic is in resonance and, in general, at $255/n$ r.p.m. the nth harmonic is in resonance. In the second mode of vibration the nth harmonic excites at $1{,}280/n$ r.p.m. This gives a spectrum of critical speeds as indicated in Fig. 152 and also in the table, page 259. This particular machine has near its running speed (100 r.p.m.) the harmonics of orders $2\frac{1}{2}$ and 3 of the first mode.

Most of the critical speeds thus found are not dangerous as very little work is put into them by the torque. The amplitude builds up until the work done by the torque equals the work

dissipated in damping in the manner indicated in Fig. 43, page 68. It is now our object to calculate the work input at the various critical speeds in order to find their comparative danger, while a discussion of the dissipation by damping will be postponed to the next section.

The work done per cycle by one cylinder (the nth one) is $\pi \mathbf{M}_n \beta_n \sin \varphi_n$, where $\mathbf{M}_n$ is the torque harmonic, β_n the torsional amplitude, and φ_n the phase angle between the two (see page 17). Let us investigate how these three quantities vary from cylinder to cylinder. The torque harmonic $\mathbf{M}_n$ has the same magnitude but a different phase at the various cylinders, because we assume

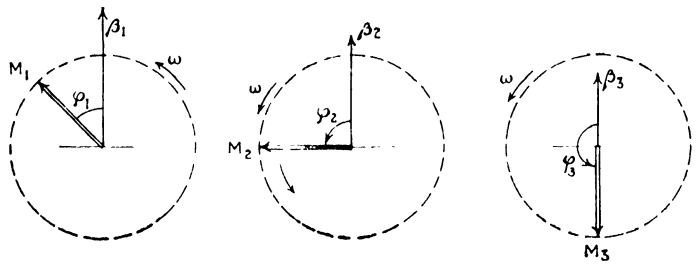


FIG. 153 Torque harmonic **M** and vibration amplitude β for the cylinders 1, 2, and 3. The subscripts 1, 2, 3 under **M** denote the cylinder and not the order of the harmonic. The diagram holds for *any* order of harmonic.

that they all fire with the same intensity but naturally not all at the same time. On the other hand the angular displacement β_n varies in magnitude from cylinder to cylinder according to Fig. 145 or 146, but it has the sample phase everywhere because all disks reach their maximum amplitude (or go through zero) simultaneously. The phase angle φ_n therefore varies from cylinder to cylinder. This is shown in Fig. 153, where the (horizontal projection of the rotating) doubly lined vector represents the torque harmonic and the (h.p.o.t.r.) single vector represents the angular vibration amplitude for the various cylinders. The velocity of rotation of all the diagrams is ω, the natural circular frequency of the vibration. This is *not* the angular velocity of the crank shaft which is m times as slow as ω for the mth-order critical speed.

Since the work done by the nth cylinder is $\pi \mathbf{M}_n \beta_n \sin \varphi_n$, it is not changed if, as in Fig. 154, the *directions* of the torque and displacement vectors in each individual diagram are interchanged, so that we now consider the fictitious case of torques in phase at the various cylinders and torsional amplitudes out of phase.

This is convenient for adding the work done by the individual cylinders. Since $\beta_n \sin \varphi_n$ is the horizontal projection of the single-lined vector β_n in Fig. 154*a*, the work by one cylinder is $\pi \mathbf{M}_n$ times the vector obtained by projecting β_n horizontally. Hence the work done by all cylinders combined is $\pi \mathbf{M}_n$ times the vector obtained by projecting the *resultant* of all β-vectors horizontally as indicated in Fig. 154*b*. There will be some phase

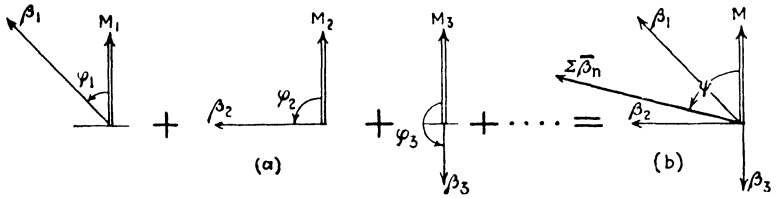


FIG. 154.—The work input by all cylinders is found by adding the work of the various cylinders individually.

angle ψ in this result which will depend on the original φ_1 at the first crank.

The φ_1 or ψ is unknown, and its exact determination for each frequency ω is out of the question. However we can state that *at resonance* ψ must be 90 deg., which can be understood as follows. At "resonance" the amplitude (considered as a function of the frequency) is a maximum, and consequently the work dissipated by damping is a maximum. But this work is equal to the input of Fig. 154*b*. Thus the phase angle ψ is such as to

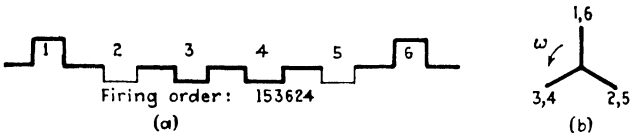


FIG. 155.—Direction of the torque vectors of order 1 for a six-cylinder engine.

make that work a maximum, *i.e.*, ψ must be 90 deg. Hence we do not need the doubly lined arrows of Fig. 154 for the determination of the work input. It is necessary merely to draw a star of vectors with the phases of the torques $\mathbf{M}_n$ and the magnitudes of the angular displacements β_n. The vector sum of this star, numerically multiplied by π times the torque amplitude $\mathbf{M}_n$, is the work done by all the cylinders per cycle of oscillation.

Consider the specific example of the Diesel ship drive discussed earlier. Let the crank shaft be as shown in Fig. 155, which is the usual construction, having complete "inertia bal-

ance" (see page 229). The sequence with which the various cylinders fire, *i.e.*, the "firing order," is limited somewhat by this choice of crank shaft, but it is not completely determined. For each one-third revolution two pistons come to the top, of which one is fired and the other begins its charging stroke. Thus there are only four possible firing orders for counterclockwise rotation, namely: 1 5 3 6 2 4, 1 5 4 6 2 3, 1 2 3 6 5 4, and 1 2 4 6 5 3. The first of these will be assumed to exist in this case.

We proceed to construct the star diagram of Fig. 154*b* for the various orders of vibration first considering the phase angles only and paying no attention to the *length* of the vectors.

At the critical speed of order $\frac{1}{2}$, *i.e.*, when half a vibration occurs during one revolution, the crank shaft makes a full turn

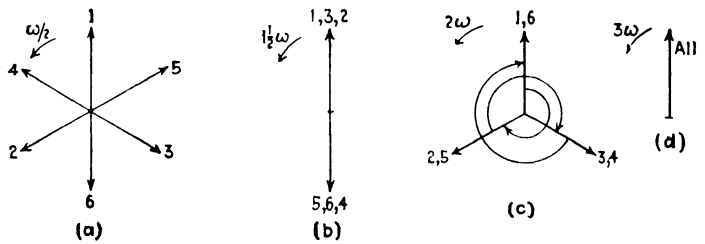


FIG. 156.—Direction of torque vectors for various orders. As in Fig. 155*b* the lengths of all vectors have been made equal, for simplicity.

while the vibration vector turns through only 180 deg. Or, while the crank shaft turns 120 deg. (Fig. 155*b*) between two firings, the vibration vector turns only 60 deg. This gives Fig. 156*a*, rotating with *half* the crank-shaft speed. After a 60-deg. turn, arrow 5 is on top and fires, which occurs at the same time that arrow 5 in Fig. 155*b* is on top.

Next consider the vibration of order 1, *i.e.*, one vibration per revolution. The motion vector turns just as fast as the crank shaft, and the star diagram coincides with Fig. 155*b*. The $1\frac{1}{2}$-order vibration gives a vector diagram turning $1\frac{1}{2}$ times as fast as the crank shaft, *i.e.*, the angle between consecutive vectors is $1\frac{1}{2} \times 120 = 180$ deg. (Fig. 156*b*). The order 2 gives an angle of $2 \times 120 = 240$ deg. between consecutive vectors as shown in Fig. 156*c*. The diagram 156*c* is seen to be the mirrored image of 155*b*, so that the length of the resultant arrow will be the same. Similarly with the order $2\frac{1}{2}$ the angles between the vectors are 300 deg., which is 360 − 60 deg. making the diagram a mirrored image of that of order $\frac{1}{2}$ (Fig. 156*a*). The order 3 gives angles

of $3 \times 120 = 360$ deg. between the various vectors (Fig. 156*d*), and order $3\frac{1}{2}$ is again the same as order $\frac{1}{2}$, because the angle between vectors is 360 + 60 deg.

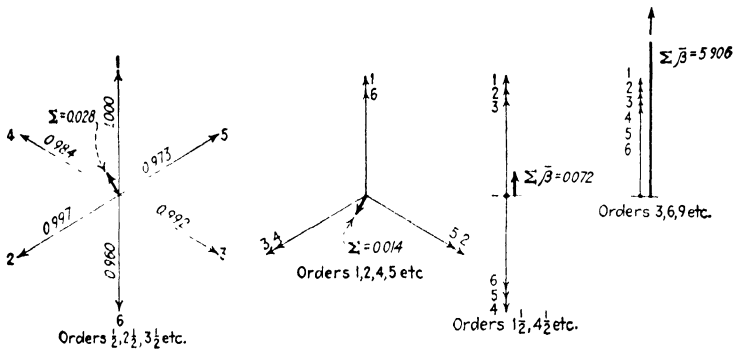


Fig. 157. Complete star diagrams (direction *and magnitude*) for the first normal mode of motion of the engine of Fig. 155.

Thus we find that only four different diagrams exist, namely:

Figure 156*a* for the orders $\frac{1}{2}$, $2\frac{1}{2}$, $3\frac{1}{2}$, $5\frac{1}{2}$, $6\frac{1}{2}$, $8\frac{1}{2}$, etc.

Figure 156*c* for the orders 1, 2, 4, 5, 7, 8, etc.

Figure 156*b* for the orders $1\frac{1}{2}$, $4\frac{1}{2}$, $7\frac{1}{2}$, etc.

Figure 156*d* for the orders 3, 6, 9, etc.

Now we are ready to construct the diagrams completely including the proper *lengths* of the vectors. Figure 157 gives

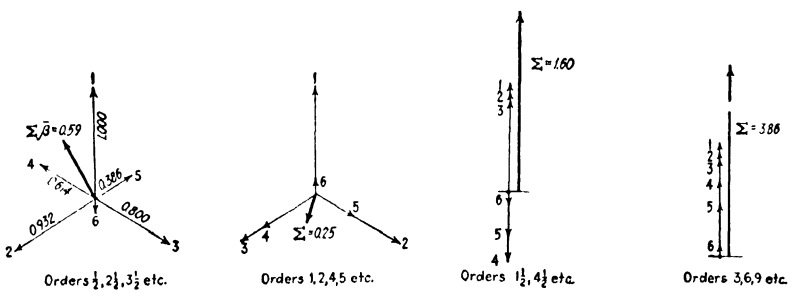


Fig. 158.—Complete star diagrams for the second normal mode of motion.

them for the first mode of motion (Fig. 145) and Fig. 158 for the second or two-noded mode.

The critical speeds of order 3, 6, etc., are known as *major* critical speeds, all others being *minor* critical speeds. The characteristic property of a major critical speed is that all the vectors in the diagram have the same phase. The physical significance is that with a *rigid* engine (in which the crank shaft

cannot twist) the major critical speeds are the only speeds at which work can be done on the vibration, because, as all magnitudes of β_n are then equal, the resultants of the star diagrams of all minor critical speeds are zero.

The distinction between major and minor critical speed does not imply that a major speed is always more dangerous than a minor. In fact, for engines with a more or less symmetrical normal elastic curve, as shown in Fig. 159, the resultant of the

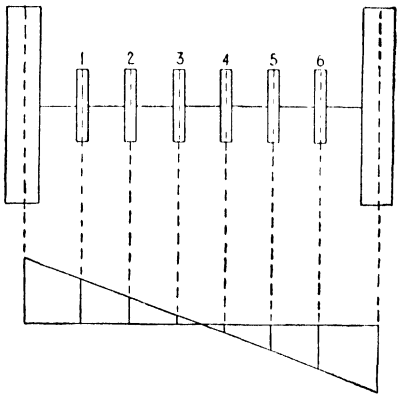


FIG. 159.—First normal elastic curve for symmetrical engine with two very heavy flywheels.

major critical speeds is zero, whereas for the minor speeds of order $1\frac{1}{2}$, $4\frac{1}{2}$, etc., the resultant becomes very large (Fig. 156*b*, *d*).

The work input per vibration cycle at the various first-mode critical speeds that may be encountered is calculated in the table below.

All critical speeds below order 12 of the *second* mode lie above the running speed and need not be considered. The figures in

Order	R.p.m.	$\Sigma\bar{\beta}_n$	Per cent of full torque	$\mathbf{M}_n$ ft. lb.	Work/cycle, $\pi\mathbf{M}\Sigma\bar{\beta}_n$
(1)	(2)	(3)	(4)	(5)	(6)
$2\frac{1}{2}$	102	0.028	104	17,800	1,560
3	85	5.906	72	10,200	189,000
$3\frac{1}{2}$	73	0.028	53	10,600	930
4	64	0.014	41	8,230	362
$4\frac{1}{2}$	57	0.072	33	6,050	1,370
5	51	0.014	26	4,340	191
$5\frac{1}{2}$	46	0.028	21	3,430	302
6	42	5.906	18	2,150	45,300

column 4 have been calculated from those in column 2 by assuming that the torque varies as the square of the speed as is approximately true for a ship drive. Column 5 has been calculated from column 4 in connection with Figs. 148, 149, and 150 and from formula (138). The formula (138) comes in only for the critical speed of order 3, and in the calculation it has to be remembered that the inertia torque also varies as the square of the speed. The entries in column 6 are the work input per cycle and are a measure of the relative severity of the critical speeds. The amplitude of vibration can be calculated by equating column 6 to the energy dissipated per cycle by damping. It is to the calculation of this latter quantity that we now turn.

44. Damping of Torsional Vibration.—In marine engines the damping provided by the action of the water on the *propeller* is usually particularly effective. A damping torque is one which is opposite in phase to the angular velocity. In the free vibration of the first mode, shown in Fig. 145, the propeller speed will alternately be faster and slower than normal. Since the resisting torque of the surrounding water increases with the speed there is positive damping action, which can be explained as follows. During the half cycle that the propeller speed is greater than average $(\Omega_p + d\Omega_p)$, the retarding torque is also greater than average $(\mathbf{M}_p + d\mathbf{M}_p)$, so that the excess torque $d\mathbf{M}_p$ tends to retard the motion, *i.e.*, $d\mathbf{M}_p$ is directed opposite to the excess velocity $d\Omega_p$. Conversely, during the half cycle that the propeller speed is smaller than average $(\Omega_p - d\Omega_p)$, the retarding torque is $\mathbf{M}_p - d\mathbf{M}_p$, so that the excess $-d\mathbf{M}_p$ is accelerating. The excess velocity $d\Omega_p$ is directed against the rotation Ω_p, which also is against the direction of the excess torque.

If for these small variations in torque and speed the torque-speed characteristic is straight, the damping constant c, being the retarding torque per unit angular velocity, is $c = d\mathbf{M}_p/d\Omega_p$.

By (Eq. 34), page 68, the work dissipation per cycle is

$$W = \pi c\omega\beta_p = \pi\omega\beta_p^2\frac{d\mathbf{M}_p}{d\Omega_p}, \tag{145}$$

where β_p is the amplitude of vibration at the propeller. The work input per cycle by the cylinder torques doubles if all amplitudes of vibration are doubled, since the torques are not affected by a change in amplitude. However, by (145) the propeller dissipation quadruples if the amplitudes are doubled. Thus there will

be a definite amplitude at which input and output of energy balance each other (Fig. 43, page 68). It is necessary merely to find the value of $d\mathbf{M}_p/d\Omega_p$.

In Fig. 160 the *steady-state* relation between the torque and the propeller speed of a typical ship is shown. The curve is a parabola or a somewhat steeper curve expressed by $\mathbf{M}_p = \Omega_p^n$ with an exponent n between 2 and 3. This curve can be easily obtained for a given ship by the actual measurement of the torque (indicator diagrams), and the shaft revolutions per minute for a number of speeds. But the slope of *this* curve is not the damping constant we are seeking, because in it the ship's forward speed grows with the revolutions per minute, whereas during the rapid Ω_p-variations of the torsional vibration, the ship's speed is constant. It is shown below in small print that at a definite torque and speed (point P in Fig. 160) the slope $d\mathbf{M}_p/d\Omega_p$ for a constant ship speed is considerably greater than the slope of the steady-state curve. The dotted line through P indicates the curve for constant ship speed, and it is usually assumed that its slope at P is twice as large as the slope of the fully drawn steady-state characteristic.

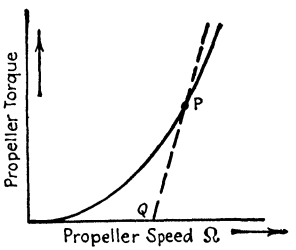


FIG. 160.—Marine propeller characteristic.

Consider a propeller-blade element cut out by two cylinders concentric with the shaft and with radii r and $r + dr$. The section of the propeller blade so obtained has the appearance of an airplane-wing section. Let this blade be moving forward (Fig. 161*a*) with the ship's velocity V and tangentially with the velocity $\Omega_p r$. The water will flow against it from the upper left corner of the drawing with the relative velocity V_{rel}. The propeller is so designed that this direction includes a small angle α (the angle of attack) with the main direction of the blade. This causes a hydrodynamic lift force **L** on the blade perpendicular to the direction of flow (Fig. 161*b*). There will be also a small drag or resistance force in the direction of flow which we may disregard in this argument. The lift **L** can be resolved into two components **T** and **R**: **T** being the thrust, and **R** the reaction, thus causing a torque **R***r* about the shaft axis. The sum of all **T**'s for the various blade elements of the propeller add up to the thrust on the ship, and the sum of the various **R***r*'s is equal and opposite to the engine torque in the steady-state case.

Imagine a periodic variation in the propeller speed Ω_p while the ship's speed V is constant. In Fig. 161*a* the length $\Omega_p r$ varies, and consequently the angle of attack α varies. This varies the lift **L** and the torque **R***r*. Let Ω_p diminish to such an extent that the angle α and with it the lift and **R***r* become zero. Then the propeller torque is zero, because the propeller

freely screws through the water, which in this case acts as a stationary nut. The forward speed and the rotation are adjusted so that this screwing takes place without any effort. In the usual designs the blade angle $\tan^{-1}\frac{\Omega_p r}{V}$ varies between 20 and 80 deg. along the blade, whereas the angle of attack α is of the order of 5 deg. Thus we see that a diminishing of Ω_p by 10 or 20 per cent is sufficient to make the torque zero. This condition is indicated by the point Q in Fig. 160.

In this argument it has been tacitly assumed that the rate of change $d\Omega_p/dt$ is of no influence on the phenomenon, *i.e.*, we have assumed that the flow in Fig. 161*a* is a steady-state flow for each ratio $\Omega_p r/V$. In case the variation in Ω_p is *slow*, such a succession of steady-state flows is practically the same as the actual flow, but for *rapid* variations ($d\Omega_p/dt$ = large), this analysis is inapplicable. A completely satisfactory theory of propeller damping does not exist as yet, and for important cases where the frequency is high, only an experiment on a model can give reliable information.

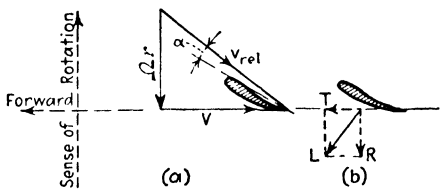


FIG. 161.—Direction of water flow (*a*) and the forces (*b*) acting on a propeller-blade element.

The torque $\mathbf{M}_p$ of our 1,500-hp. engine at 85 r.p.m. is

$$\mathbf{M}_p = \frac{1{,}500 \cdot 33{,}000}{2\pi \cdot 100}\left(\frac{85}{100}\right)^2 = 57{,}000 \text{ ft. lb.}$$

and the angular speed Ω_p of the propeller is

$$\Omega_p = 2\pi\tfrac{85}{60} = 8.90 \text{ radians per second}$$

The equation of a parabolic relation (Fig. 160) between the two would be

$$\mathbf{M}_p = \frac{57{,}000}{(8.9)^2}\Omega_p^2 = 720\Omega_p^2$$

and its slope at 85 r.p.m.

$$\frac{d\mathbf{M}_p}{d\Omega_p} = 2 \cdot 720\Omega_p = 12{,}800 \text{ ft. lb. sec./rad.}$$

The actual propeller-damping constant at this speed is assumed to be twice as great, or

$$c_p = 25{,}600 \text{ ft. lb. sec./rad.}$$

The energy dissipation per cycle in the first mode of vibration is

$$\pi\omega_1\beta_p^2 c_p = \pi \cdot 26.7 \cdot 25{,}600\beta_p^2 = 2{,}150{,}000\beta_p^2 \text{ ft. lb.}$$

The work input of the table on page 259 is calculated on the basis of the amplitude of 1 radian at cylinder 1 and 3.58 radians at the propeller. Thus the energy input is

$$\frac{189{,}000}{3.58}\beta_p = 53{,}000\beta_p$$

Equating the two energies, we find for the amplitude at the propeller

$$\beta_p = 0.025 \text{ radian} = 1.4 \text{ deg.}$$

From Fig. 145 we see that the twist in the propeller shaft is $(3.58 + 0.94)/3.58$ times as large as β_p. With a spring constant in this shaft of $k = 13.5 \times 10^6$ in. lb./rad., the torque amplitude is

$$\frac{4.52}{3.58} \cdot 0.025 \cdot 13.5 \cdot 10^6 = 426{,}000 \text{ in. lb.} = 35{,}500 \text{ ft. lb.}$$

The mean engine torque is 57,000 ft. lb., so that the variation in the engine torque is about 62 per cent of the mean torque. Though this is not particularly smooth, it may be without danger for the shaft. We see that even the worst major critical speed may not be dangerous on account of the propeller damping. This is generally true for direct propeller drives where the propeller inertia is small compared with the engine-flywheel inertia. On account of the relatively great propeller amplitude and the small engine amplitude it is easier for the damping to destroy work than it is for the torque harmonics to create it. However, under the circumstances it would be wise to stiffen the propeller shaft so as to bring the major critical above the running speed.

In high-speed ship engines it may happen that some critical speeds of the two-noded mode come into the running range. Then usually (Fig. 146) the propeller amplitude is very small and consequently the propeller damping is nearly zero. In such cases and also in those where the Diesel engine and its flywheel are directly coupled to an electric generator, there is hardly any damping which we can calculate except that due to mechanical hysteresis in the crank-shaft fibers, which are alternately in tension and in compression.

The stress-strain relation of any steel under alternating load is represented by a thin loop as in Fig. 162*a*, the area of which equals the energy dissipated per cycle in 1 cu. in. of the material. Plotting the area of the loop against the maximum stress gives a curve of the character shown in Fig. 162*b*. If the hysteresis loss in the crank shaft is calculated on the basis of an experimental curve (Fig. 162*b*), we find that only about 10 to 15 per cent of the actual energy loss in the engine can be accounted for. The major portion of the energy is dissipated in the bearings and through them into the foundation. The argument given with Figs. 111*c* and *d*, page 233, showed that during a torsional oscillation alternating forces are imparted to the main bearings which

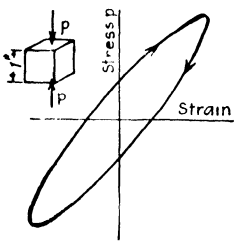


FIG. 162*a*. Mechanical hysteresis loop.

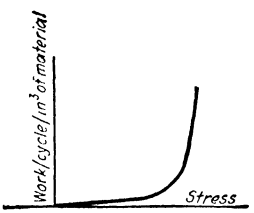


FIG. 162*b*.—Hysteresis-dissipation curve for typical shaft steel.

set the whole machine vibrating. (Incidentally this is responsible for the fact that a torsional oscillation can be observed on the machine by a rumbling noise or by a vibration in the frame which can be felt by the hand. The purely ideal system shown in Fig. 143 will not give any external evidence of a state of torsional vibration.) The motions thus caused in the several parts of the foundation may result in rubbing and a consequent dissipation by friction. Obviously this effect is beyond calculation.

In spite of the fact that only some 10 per cent of the dissipation is caused by hysteresis, it has become customary to calculate this loss and multiply it by an empirical factor, which was determined so as to make the calculated torsional amplitudes coincide statistically with the measured ones on a number of installations.

For this calculation two formulas are used in practice, the first one being the Lewis-Porter formula:

$$\text{Loss per cycle} = \frac{635{,}000 D^{4.3} \Sigma \beta^{2.3}}{l^{1.3}} \text{ in. lb./cycle}$$

where D is the diameter of the crank shaft or crank pin in inches, l is the distance in inches between two crank throws and $\Sigma\beta^{2.3}$ is the sum of the 2.3 powers of the angles of twist of the various shaft sections between cylinders. These angles are *not* found in the fourth or β-column of the Holzer table, but rather in the last column (page 238). The energy dissipation of the engine, thus found, will be proportional to the 2.3 power of the end amplitude. The energy input of the engine is proportional to the first power of the end amplitude, so that when the energy-equilibrium equation is written it can be solved for that amplitude.

The second, more recent, formula is due to Dorey:

$$\text{Loss per cycle} = 90{,}000 D^4 l^{-1} \Sigma\beta^2 \text{ in. lb./cycle}$$

where the letters D and β have the same meaning as in the Lewis formula above, but the length l is the distance in inches between two crank throws less the thickness of two crank webs, thus including only the length of one crank pin and of one main shaft section.

It is apparent that for large stresses and angles in the shaft Lewis's formula gives higher values, while for small angles Dorey gives higher values for the work dissipated. The two formulas give the same result for an average value of the angles occurring in practice. Both are empirical, based on a number of actual calculations, and under the circumstances the simpler one by Dorey is preferable. The Lewis formula is retained in this book because of its widespread occurrence in the literature.

In engine installations without active propeller damping, without badly constructed couplings or without other visible sources of energy dissipation, a critical speed with a comparatively large entry in the last column of the table on page 259 will inevitably cause such large amplitudes that the crank shaft or driving shaft breaks in fatigue. To prevent this we can apply one of the following procedures:

1. If the engine is to operate always at the same speed, *e.g.*, a synchronous-generator drive, changes in the elasticity of the shaft or in the inertia of the masses can be made such as will remove the running speed sufficiently far from any important critical speed.

2. If the engine has to operate over a narrow speed range, course 1 usually suffices. If it does not suffice, the relative severity of the minor critical speeds may be influenced by changing the firing order. This is explained on page 280.

3. If operation over a very wide speed range is required, as for instance in Diesel locomotives or in ship drives, it may become very difficult, if not impossible, to avoid all danger of torsional vibration by the means 1 and 2. An artificial damper should then be applied. Three such devices will now be discussed, *i.e.*, the friction damper of Lanchester, the tuned centrifugal pendulum described on page 119, and the hydraulic coupling or "fluid flywheel."

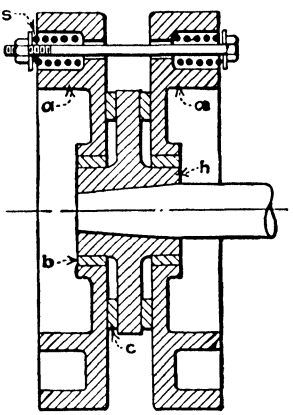


FIG. 163*a*.—Lanchester damper.

45. Dampers and Other Means of Mitigating Torsional Vibration.—The Lanchester damper (Fig. 163*a*) consists of two disks *a*, which can rotate freely on the shaft bearings *b*. Between them is a hub disk *h* solidly keyed to the shaft. This hub *h* carries brake lining *c* on its faces against which the disks *a* can be pressed by screwing down the springs *s*.

If the engine, *i.e.*, the hub *h*, is in uniform rotation, the friction carries the disks *a* with the shaft, so that the disks then merely increase the inertia of the engine by a small percentage. If, however, the hub executes a torsional vibration, the motion of the disks depends on the amount of friction between them and the hub. If the friction torque is extremely small, the disks rotate uniformly and there is a relative slip between the hub and the disks with the amplitude of the hub motion. Since the friction torque is nearly zero, very little work is converted into heat. On the other hand, if the friction torque is very large, the disks lock on the hub and follow its motion. There is then no relative slip and hence no energy dissipation. Between these two extremes there is both slip and a friction torque, so that energy is destroyed. There must be some optimum value of the friction torque at which the energy dissipated is a maximum, as indicated in Fig. 163*b*. At the optimum damping torque $\mathbf{M}_{opt}$, let

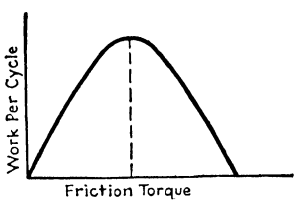


FIG. 163*b*.—Energy dissipation in the Lanchester damper as a function of the friction torque.

$\mathbf{f}\beta_h$ be the amplitude of relative motion $\beta_{rel} = \beta_a - \beta_h$
$\mathbf{g}\beta_h$ be the amplitude of disk motion β_a.

The factors **f** and **g** are yet unknown. The friction torque is usually of the dry friction or Coulomb type, *i.e.*, not proportional to the slip velocity but constant in magnitude and opposed in sign to the slip. The work destroyed per cycle is

$$W = 4\mathbf{M}_f\beta_{\text{rel}} = 4\mathbf{f}\mathbf{M}_f\beta_h$$

The friction torque $\mathbf{M}_f$ is the cause of the oscillatory motion of the disks a, which have a combined moment of inertia I_a. Thus by Newton's law

$$\mathbf{M}_f = I_a\ddot{\beta}_a$$

and, if the disk motion is approximately sinusoidal, we have roughly

$$\mathbf{M}_f = I_a\omega^2\beta_a = I_a\mathbf{g}\omega^2\beta_h$$

Substituting this in the energy dissipation per cycle,

$$W = 4\mathbf{f}\mathbf{g}I_a\omega^2\beta_h^2$$

For a damper with a *viscous* damping torque the analysis is similar and gives the same result except for a factor π instead of 4. The numerical value of the factor $4\mathbf{fg}$ (or $\pi\mathbf{fg}$) for the optimum friction torque has been found by a somewhat elaborate calculation, with the results

$$W = \frac{4}{\pi}I_a\omega^2\beta_h^2 \qquad \text{(for dry friction)} \qquad (146a)$$

$$W = \frac{\pi}{2}I_a\omega^2\beta_h^2 \qquad \text{(for viscous friction)} \qquad (146b)$$

The optimum friction torque at which this maximum dissipation occurs is determined by

$$\mathbf{M}_{\text{opt}} = \pm\frac{\sqrt{2}}{\pi}I_a\omega^2\beta_h \qquad \text{(for dry friction)} \qquad (146c)$$

$$\mathbf{M}_{\text{opt}} = \frac{I_a\omega^2\beta_h}{\sqrt{2}}\sin\omega t \qquad \text{(for viscous friction)} \qquad (146d)$$

The derivation of the results (146*b*) and (146*d*) for the case of viscous damping, though somewhat lengthy, offers no particular difficulties and is left as an exercise to the reader. For a *dry*-friction damper, however, the problem is more complicated. If

ω_a = angular velocity of friction disks a.
ω_h = angular velocity of the hub,
$\pm\mathbf{M}_f$ = the friction torque,

the angular velocity of slip (relative motion) is $\omega_h - \omega_a = \omega_{rel}$, and the work done per cycle is

$$fM_f d\beta_{rel} = fM_f \omega_{rel} dt = M_f \int (\omega_h - \omega_a) dt$$

with the proper limits of integration. Figure 164 serves to illustrate this integral. The angular velocities of the hub and friction disks are plotted against the time. The velocity of the hub, *i.e.*, of the engine as a whole, is supposed to be harmonic with the amplitude $\omega\beta_h$, where ω is the frequency of the vibration and β_h its angular amplitude at the hub. The friction disks are acted upon by an alternating *constant* torque $\pm M_f$, *i.e.*, they have alternating constant accelerations $\pm M_f/I_a$ and thus the velocity diagram ω_a must consist of pieces of straight line of slope $\pm M_f/I_a$. The difference between the ordinates of the two curves of Fig. 164 is $\omega_{rel} = \omega_h - \omega_a$, and

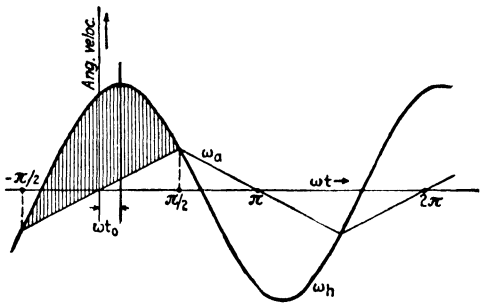


FIG. 164.—Angular velocity diagrams of the hub and the inertia disks of the Lanchester damper.

thus the shaded area multiplied by M_f is the work dissipated per half cycle.

Taking the origin of time at the instant that $\omega_a = 0$ (*i.e.*, at the instant that the angular velocity of the disks equals the average angular velocity of the hub), the phase relation between the disk and hub motions is determined by the quantity ωt_0, which is as yet unknown.

The motions during the shaded interval are

$$\omega_h - \beta_h \omega \cos(\omega t - \omega t_0)$$

$$\omega_a = +\frac{M_f}{I_a} t$$

The phase ωt_0 can be found from the fact that at $\omega t = \pm\pi/2$ the two angular velocities are equal.

$$\pm\frac{M_f}{I_a} \cdot \frac{\pi}{2\omega} = \beta_h \omega \cos\left(\pm\frac{\pi}{2} - \omega t_0\right) = \pm\beta_h \omega \sin \omega t_0$$

or

$$\sin \omega t_0 = \frac{\pi}{2} \frac{M_f}{I_a \omega^2 \beta_h}$$

The work dissipated per cycle is $2M_f$ times the shaded area, or

$$W = 2M_f \int_{-\frac{\pi}{2\omega}}^{+\frac{\pi}{2\omega}} \left[\beta_h \omega(\cos \omega t \cos \omega t_0 + \sin \omega t \sin \omega t_0) - \frac{M_f}{I_a} t\right] dt$$

The integral contains three terms. The first term is

$$2\mathbf{M}_f\beta_h \cos \omega t_0 \int_{-\frac{\pi}{2}}^{+\frac{\pi}{2}} \cos \omega t \, d\omega t = 4\mathbf{M}_f\beta_h \cos \omega t_0$$

The second term is a sine integrated between equal positive and negative angles and thus is zero. The third term is the area under the straight line of Fig. 164 between $-\pi/2 < \omega t < \omega/2$ and is also zero.

Thus

$$W = 4\mathbf{M}_f\beta_h \cos \omega t_0 = 4\mathbf{M}_f\beta_h \sqrt{1 - \left(\frac{\pi}{2} \frac{\mathbf{M}_f}{I_a\omega^2\beta_h}\right)^2}$$

For which value of the friction torque $\mathbf{M}_f$ does this dissipation become a maximum? By differentiation,

$$0 = \frac{dW}{d\mathbf{M}_f} = 4\beta_h \cos \omega t_0 - \frac{2\mathbf{M}_f\beta_h}{\cos \omega t_0} \cdot 2\mathbf{M}_f\left(\frac{\pi}{2I_a\omega^2\beta_h}\right)^2$$

A short calculation shows that

$$\mathbf{M}_f = \frac{\sqrt{2}}{\pi}\beta_h I_a\omega^2 \qquad \text{and} \qquad \cos \omega t_0 = \frac{1}{\sqrt{2}} \tag{146c}$$

This is the optimum value of the friction torque. The dissipated energy is found by substituting into the above equations

$$W = 2\sqrt{2}\mathbf{M}_f\beta_h = \frac{4}{\pi} I_a\omega^2\beta_h^2 \qquad \text{q.e.d.} \tag{146a}$$

It is clear from (146*a*) that the damper should be placed at a point of the shaft where the torsional amplitude is great, and that the device becomes entirely useless if placed at a node of the vibration. This is a property which the damper has in common with the ship's propeller.

In order to make the Lanchester damper dissipate more energy for a given inertia of the flywheel *a* of Fig. 163*a*, the relative motion between the flywheel *a* and the hub *h* may be increased by mounting the flywheel on tuned springs. This produces the "damped tuned vibration absorber" of which the theory for viscous damping is discussed on pages 119 to 133. That theory gives the complete behavior of such a damper when applied to a simple *K*-*M* system. In order to apply it to a multimass system the theory would become hopelessly complicated. However the results of pages 119 to 133 can be applied with decent accuracy to a multimass system as well, by replacing the multimass system by an equivalent *K*-*M* system as follows:

1. The mass M of the one-mass system is so chosen that for equal amplitudes at M and at the point of the multimass system where the damper is attached, the kinetic energy of M equals the kinetic energy of the multimass system in the mode of motion considered.

2. The spring K of the one-mass system is then so chosen that K/M is equal to the ω^2 of the multimass system in the mode of motion under consideration.

3. The exciting force P on the single mass M is so chosen that its work $\pi P x_1$ at resonance is equal to the total work input by all the exciting forces of the multimass system adjusted to the same amplitude x_1 at the point of attachment of the damper.

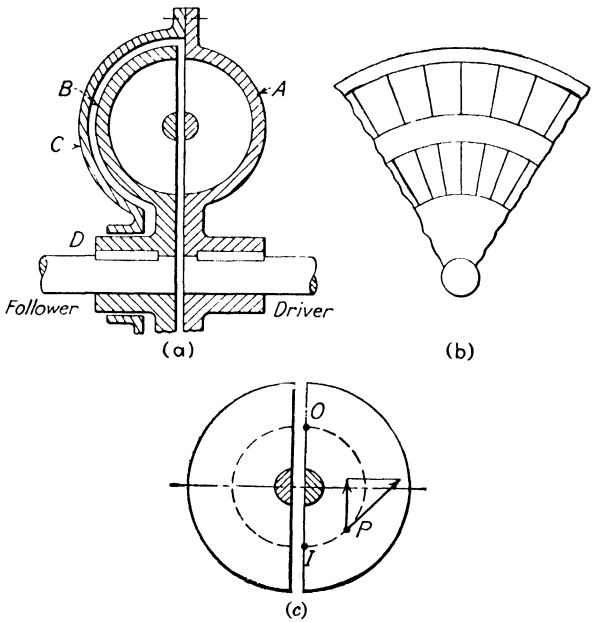
Another device useful for avoiding or damping torsional vibration is *Foettinger's* hydraulic coupling, also known as "fluid flywheel" (Fig. 165*a*). It consists of a piece A in the shape of half a doughnut keyed to the driver shaft. A similar piece B is keyed to the follower shaft. A cover C is attached solidly to A on the driver shaft and can turn with respect to the follower shaft. At D there is a hydraulic seal with little friction. The entire interior of the doughnut is filled with a fluid, thin oil or water, and the sole purpose of the cover C is to hold that fluid in place. The doughnut-shaped space is subdivided into a large number of open compartments by many thin vanes, each having the form of a semicircle, and arranged in purely radial planes (Fig. 165*b*). By Newton's law of action and reaction the torques on driver and follower must be equal and opposite. Since the device does not operate at ideal efficiency, the speed of the follower must be somewhat less than that of the driver, the speed ratio being the same as the efficiency, which is between 97 and 99 per cent. The fluid in the coupling is under the influence of centrifugal force, which is greater in the driver than in the follower on account of the speed difference. Thus a circulation is set up, moving the fluid outward in the driver and inward in the follower. This circulation, for the existence of which a speed difference is essential, is the cause of torque transmission between the two shafts.

Consider a particle of fluid dm at point P in Fig. 165*c*. Its velocity will have a radial component v_r, and the Coriolis acceleration is $2\Omega v_r$, directed tangentially. The Coriolis force is $2\Omega v_r\, dm$ and its moment is $2\Omega v_r r\, dm$, in a direction such as to retard the rotation Ω of the driver. For all the particles in the stream tube of P the torque integrates to

$$\int 2\Omega_r v\, dm = 2\Omega \int \frac{dr}{dt} \cdot r\, dm = 2\Omega \int r\, dr \cdot \frac{dm}{dt}$$
$$= 2\Omega \frac{dm}{dt} \int_I^O r\, dr = \Omega \frac{\Delta m}{T}(r_O^2 - r_I^2)$$

The factor dm/dt appearing in this integration is the mass flowing by P per second, which is constant and equal to $\Delta m/T$, *i.e.*, the total mass Δm of the entire steam tube from I to O in the driver and from O to I in the follower divided by the period of circulation T in seconds.

The Coriolis torque on the follower is in the direction of rotation and is calculated similarly with the same form of answer. Only the angular speed



FIGS. 165*a*, *b*, and *c*.—The hydraulic coupling or "fluid flywheel" transmits torque primarily by the action of Coriolis forces

of the follower is less, say $\Omega - \Delta\Omega$, so that the Coriolis torque is

$$(\Omega - \Delta\Omega)\frac{\Delta m}{T}(r_O^2 - r_I^2)$$

which is different from the Coriolis torque of the driver. This apparent discrepancy is removed by considering that there are some other contributions to the torques. At O, fluid of tangential velocity Ωr_0 from the driver is received by the follower of which the tangential speed is less by an amount $\Delta\Omega \cdot r_0$. The loss in tangential momentum per second thus is $\Delta\Omega \cdot r_0 \cdot \Delta m/T$ which is equal to the force exerted by the stream tube of P on the follower, in the direction of rotation. The moment arm of this force is r_0 giving a moment $\Delta\Omega r_O^2 \Delta m/T$. Consequently the total amount on the follower

is the sum of the Coriolis torque and the torque caused by the change in momentum:

$$\mathbf{M} = \frac{\Delta m}{T}[\Omega(r_O^2 - r_I^2) + \Delta\Omega \cdot r_I^2] \tag{147}$$

Similarly at the inlet point I slow water from the follower enters the driver which rotates faster, thus causing a retarding torque on the driver of $\Delta\Omega r_I^2 \Delta m/T$, which in conjunction with the driver's Coriolis torque gives the same expression (147) for the total retarding torque on the driver.

The torque (147) is that due to a single stream tube only. The torque of the complete device is found by still another integration, in which r_O, r_I, and T are variables, since the period of circulation will be different for different stream lines. However, Eq. (147) can be interpreted as the total torque if we consider Δm to be the mass of water in the entire doughnut, r_O and r_I the radii belonging to the center stream line, and T some average period of circulation.

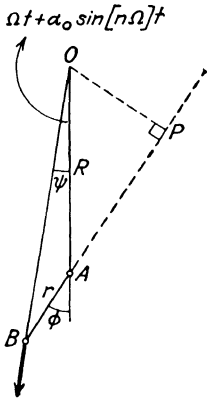


Fig. 166a.

So far we have considered only uniform or steady-state operation of the coupling. To investigate its damping characteristics both halves of it are now given non-uniform motions. Let the driver speed be $\Omega + \varphi_d$, and let the follower speed be $\Omega - \Delta\Omega + \varphi_f$, where the φ are variable with time. If these variations are sufficiently rapid, the consequent changes in centrifugal force are so fast that the velocity of the fluid circulation is not affected. Then we can apply the above steady-state analysis, merely substituting the variable angular speeds for the constant ones. Thus the torque on the follower (in the direction of rotation) is

$$(\Omega - \Delta\Omega + \varphi_f)\frac{\Delta m}{T}(r_O^2 - r_I^2) + (\Delta\Omega - \varphi_f + \varphi_d)r_O^2\frac{\Delta m}{T}$$

which is seen to be the sum of the steady-state torque (147) plus the variable part:

$$\mathbf{M}_{\text{var}} = \frac{\Delta m}{T}[\varphi_d r_O^2 - \varphi_f r_I^2] \tag{147a}$$

In the same manner the torque on the driver, in a direction opposite to that of the rotation, is written as the sum of the Coriolis and momentum transfer components. The answer again is (147) plus the variable part (147*a*). It is noted that the torque (147*a*) is proportional to the angular *speeds* and thus acts as a damping torque. It may be a positive or a negative damping torque, on account of the second term in the bracket of (147*a*), but in all actual installations it is found to be a positive damping torque. See further problems 122 and 123 on page 405.

Another means of correcting a troublesome condition of torsional vibration is the tuned centrifugal pendulum mentioned on page 119. Since there is no energy loss in the device, it cannot be considered a "damper," but, just as the Frahm absorber of

page 112, it acts like an infinite mass for the frequency to which it is tuned, thus enforcing a node at the point of its application. For other frequencies it acts like a mass which is *not* infinitely large and thus does not affect the situation particularly. The proof of this statement is as follows:

Let the shaft in Fig. 166*a* rotate about its center O with an average angular speed Ω on which is superposed a rotational oscillation $\alpha = \alpha_0 \sin \omega t = \alpha_0 \sin n\Omega t$, the number n being the "order" of the vibration. The (mathematical) pendulum of length r and mass m swings about A, with the *small* angle $\varphi = \varphi_0 \sin n\Omega t$ relative to the shaft. The angle AOB denoted by ψ satisfies $\psi = \varphi r/(R + r)$.

Considering the relative motion of the system with respect to a uniformly rotating coordinate system Ω, the Coriolis forces can be neglected for small oscillations. The tangential component of the centrifugal force (*i.e.*, normal to AB) is

$$-m\Omega^2(R + r) \sin (\varphi - \psi) = -m\Omega^2 R \sin \varphi \approx -m\Omega^2 R\varphi$$

and the tangential displacement of B with respect to the coordinate system is $\alpha(R + r) + \varphi r$. Thus the equation of motion is

$$(R + r)\ddot{\alpha} + r\ddot{\varphi} = -\Omega^2 R\varphi$$

which, after substitution of the harmonic values for α and φ, yields

$$\frac{\varphi_0}{\alpha_0} = \frac{n^2(R + r)}{R - n^2 r} \tag{148a}$$

The tension in the pendulum string $m\Omega^2(R + r)$ furnishes the only reaction from the pendulum on the shaft and with the moment arm $\overline{OP} = R\varphi$ gives the reaction torque

$$\mathbf{M} = m\Omega^2(R + r)R\varphi = m\Omega^2(R + r)R\left(\frac{\varphi_0}{\alpha_0}\right) \cdot \alpha_0 \sin n\Omega t$$

After substitution of (148*a*), this becomes

$$\mathbf{M} = \frac{m(R + r)^2}{1 - \dfrac{r}{R}n^2} \cdot \omega^2 \alpha_0 \sin \omega t = -\frac{m(R + r)^2}{1 - \dfrac{r}{R}n^2} \cdot \ddot{\alpha}$$

If instead of the pendulum a moment of inertia I_{equiv} had been attached to the shaft, its reaction torque to an acceleration $\ddot{\alpha}$ would have been $-\ddot{\alpha} I_{\text{equiv}}$, from which follows that the undamped

pendulum for small oscillations is completely equivalent to a flywheel of inertia:

$$I_{\text{equiv}} = \frac{m(R + r)^2}{1 - \frac{r}{R}n^2} \tag{148b}$$

The numerator of this expression is the moment of inertia of the pendulum when clamped to the shaft; the denominator is

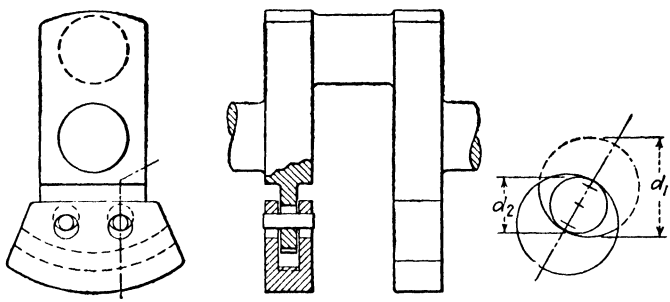


FIG. 166b.—The "bifilar" or Sarazin-Chilton type of tuned centrifugal pendulum

a multiplication factor. Thus a "tuned" pendulum

$$n^2 = \frac{R}{r} \tag{148c}$$

is equivalent to an infinite moment of inertia; an "overtuned" pendulum ($R/r > n^2$) represents a (large) positive inertia, while an "undertuned" pendulum behaves like a large negative moment of inertia (see Fig. 38, page 59).

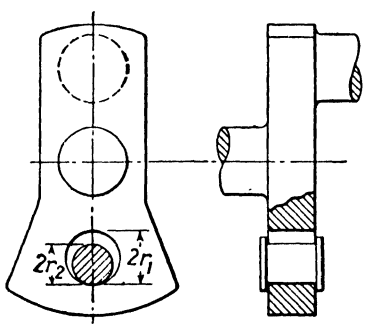


FIG. 166c.—The roller or Salomon type of centrifugal pendulum.

The tuning formula (148c) carries within itself a difficult problem of design. The order of an objectionable harmonic vibration in a multicylinder engine is at least $n = 3$, usually higher. The radial distance R is limited by space considerations; in a radial aircraft engine, for instance, where the pendulum is conveniently located in the crank counterweight, the maximum distance R is of the order of 5 in. Thus, by (148c), the pendulum length r is about ½ in. for $n = 3$, and considerably shorter for higher orders of vibration.

Since the pendulum must have appreciable mass, the construction indicated in Fig. 77*b* is impossible. Two solutions of the problem have been found; they are shown in Figs. 166*b* and *c*, both located in the counterweight of a crank shaft.

The first one, known as the "bifilar" type, was invented by *Sarazin* in France and, independently, by *Chilton* in the United States. The pendulum is a large U-shaped weight, fitting loosely around the crank-shaft overhang. That overhang carries two circular holes of diameter d_1. The U-shaped loose counterweight has holes of the same diameter. The two pieces are joined by two pins of a diameter d_2, smaller than that of the holes. It is now possible for the pendulum to roll without slipping on the pins, and in doing this the center of the hole in the pendulum describes a small circle about the center of the crank-shaft hole as a center. Thus the radius of this circular path is $(d_1 - d_2)$, and it is seen that all points of the U-pendulum describe similar paths. The pendulum swings parallel to itself in a circular path of radius $d_1 - d_2$. Thus in Eq. (148*c*), $R + r$ is the distance from the shaft center to the center of gravity of the pendulum, while $r = d_1 - d_2$. Thus it is possible to make r very small and still retain a large mass.

The other construction is due to *Salomon* in France and consists of a cylinder of radius r_2, rolling or sliding in a cylindrical cavity of radius r_1 (Fig. 166*c*).

In case the cylinder slides without rotation, all its points describe similar paths of radius $r_1 - r_2$; this quantity thus is the equivalent pendulum length r. For a rolling cylinder the swing is slower, so that r is greater than $r_1 - r_2$. Since the mass involved in this construction is much smaller than that of Fig. 166*b*, the amplitude through which it must swing for correct operation is much greater, which creates some additional difficulties.

A single pendulum arranged as a loose counterweight exerts a torque on the crank shaft by virtue of the fact that the force exerted on its guide does not pass through the center O (Fig. 166*a*) but is directed along BA. Thus the tangential component of the force along BA by its moment arm R furnishes the desired reaction torque, but in addition to that torque the pendulum exerts a *force* on the crank shaft. This alternating force is entirely unbalanced and can cause a linear vibration of the center O. If two pendulums were installed, one in the counter-

weight and another one diametrically opposite, *i.e.*, at the crank pin, these two pendulums would enforce nodes at the two points of their application. In case the shaft excitation were purely torsional, the two pendulums would acquire equal and opposite amplitudes, their reactions forming a pure torque. If, however, the shaft excitation were a purely lateral force, the two pendulums would swing in phase, furnishing a pure force as a reaction. In the case of mixed excitation, the two pendulums would assume different amplitudes such that the sum of their reactions would be a force and a torque, equal and opposite to the excitation. The argument in connection with Fig. 166*a* makes it clear that the pendulum can furnish a reaction force only in a direction perpendicular to the radius OA, while along that radial direction it simply acts like a dead body. Thus the two pendulums just discussed cannot prevent motion along the line OA. In order to prevent all motion in the plane of the crank throw when the excitation consists of a torque, a lateral force, and a radial force, three pendulums are necessary, located 120 deg. apart for convenience. They will respond with three different amplitudes causing three reactions of which the sum is equal and opposite to the sum of the excitations.

The application of a centrifugal pendulum to a multicylinder engine requires some calculations, which will be discussed with reference to the example of Fig. 143. It was seen on page 259 that the only dangerous critical is that of order 3, occurring at 85 r.p.m. We wish to investigate the possibility of applying a centrifugal pendulum of order 3 to the end cylinder I_1 of the installation. If this pendulum works properly, it enforces a node there, and therefore we must now calculate what torque is necessary at I_1 to ensure that. The torque so found must be supplied by the pendulum and determines its necessary size.

The introduction of the pendulum removes the resonance from the 85-r.p.m. speed, so that we have to deal with a *forced* vibration rather than a free one. The gas torques at the individual cylinders play an important part, and, in this case of the major order 3, they all have the same phase with respect to the motion. The magnitude of this torque, taken from the table on page 259, is 10,200 ft. lb., or 0.122×10^6 in. lb. We proceed through the Holzer table in the usual manner, except that now this gas torque at each cylinder must be added to the inertia torque of that cylinder.

Another change in the Holzer table from the previous practice is that it is no longer necessary to guess at the frequency ω because that frequency is known, being the third harmonic of the r.p.m. In our particular case

This form of the Holzer table is used for calculating the necessary size of a centrifugal pendulum attached at cylinder 1, which is the last line of the table. The amplitude at mass 8 (see Fig. 143) is assumed to be x, and the influence of gas torque is taken into consideration. The frequency $\omega^2 = 711$ is *not* assumed, but is the frequency of vibration at the definite speed for which the pendulum is to be designed. The final criterion is that the last entry in the β-column must be zero (for a correct damper), so that x can be calculated. Then the size of the damper follows from the fact that it must produce a reaction torque given by the last entry of the $\Sigma/10^6$ column.

$\omega^2 = 711$

Number	I	$I\omega^2/10^6$	β	$I\omega^2\beta/10^6$	Gas torque/10^6	Inertia and gas torque/10^6	$\Sigma/10^6$	$k/10^6$	Σ/k
8	24,000	17.1	$+1.00x$	$17.1x$	0	$17.1x$	$17.1x$	13.5	$1.27x$
7	75,000	53.3	$-0.27x$	$-14.4x$	0	$-14.4x$	$+ 2.7x$	675	$0.004x$
6	2,560	1.82	$-0.274x$	$- 0.500x$	-0.122	$-0.122 - 0.500x$	$-0.122 + 2.2x$	675	$-0.00018+0.0033x$
5	2,560	1.82	$+0.00018-0.2773x$	$+0.00033- 0.504x$	-0.122	$-0.1217- 0.504x$	$-0.2437+ 1.7x$	675	$-0.00035+0.0025x$
4	2,560	1.82	$+0.00053-0.2798x$	$+0.00097- 0.51x$	-0.122	$-0.121 - 0.51x$	$-0.3647+ 1.19x$	675	$-0.00054+0.0018x$
3	2,560	1.82	$+0.00107-0.2816x$	$+0.00195- 0.51x$	-0.122	$-0.120 - 0.51x$	$-0.4847+ 0.68x$	675	$-0.00072+0.0010x$
2	2,560	1.82	$+0.00179-0.2826x$	$+0.00326- 0.515x$	-0.122	$-0.119 - 0.515x$	$-0.6037+ 0.165x$	675	$-0.00089+0.00024x$
1	2,560	1.82	$+0.00268-0.2828x$	$+0.00488- 0.515x$	-0.122	$-0.117 - 0.515x$	$-0.7207- 0.35x$		

for 85 r.p.m., we have $\omega^2 = 711$, as in the third trial on page 240. It is no longer permissible to assume an end amplitude of unity, as was done in the usual form of the Holzer table; for, the motion being a forced vibration, the amplitudes are definite quantities that are determined by the gas torques. We therefore assume an end amplitude x and proceed through the table with this unknown x, which is determined at the end of the calculation by the necessary condition of zero motion at the damper end of the engine. In order to arrive at the damper last, we start the Holzer table from the end opposite that from which we started in the process described on page 240 and proceed in the opposite direction so that we finish at cylinder 1 at which the damper is located. The table is shown on page 277. It is seen that a few additional columns appear, *viz.*, that of the gas torque and that of the sum of the inertia and gas torque at each cylinder. Beyond this, the table does not differ essentially from the familiar form. It is noticed that at the end of the table the amplitude at cylinder 1 comes out to be $+0.00268 - 0.2828x$. This quantity must be equal to zero if the damper works correctly, and from it we find $x = 0.0095$ radian. The last entry in the table shows the remainder torque, being equal to $(-0\,721 - 0.35x)10^6 = 724{,}000$ in. lb. This is the torque that is necessary to enforce a node at cylinder 1 and consequently is the torque to be supplied by the pendulum.

If $R = 15$ in., the pendulum length by Eq. (148*c*) must be $r = 1.667$ in. At 85 r.p.m. the centrifugal field at 15 in. radius is $\Omega^2 R = 3.08$ g. If we design the pendulum to swing 30 deg. each way, the lateral component of force is half the centrifugal force, or 1.54 times the weight of the pendulum. The moment is this force times 15 in., or $23.1W$ in.-lb. Setting this equal to the required torque of 724,000 in.-lb. gives the prohibitive pendulum weight of 31,000 lb. The principal reason for the fact that the device is not practical for this application is the low speed. Since the centrifugal force grows with the square of the speed, the required pendulum weight is inversely proportional to that quantity, everything else being equal. For engines of high and medium speed the pendulum size becomes reasonable.

A few remarks remain to be made in connection with the above Holzer table. First it is noticed that the final torque of the pendulum, 719,000 in.-lb., is practically equal to the sum of the six gas torques on the six cylinders. The reason for this becomes clear by comparing the relative values of columns 5 and 6, *i.e.*, by comparing the inertia torque to the gas torque of each cylinder. On account of the very low speed the gas torques are overwhelming, so that the pendulum must furnish the countertorque to their sum. For higher speed machines the inertia torques become of the same order as the gas torques and then the above simple rule no longer obtains.

Another observation is that only for a *major* order of disturbance are the gas torques of the various cylinders in phase with each other (Fig. 157*d*), while for all minor orders (Figs. 157*a*, *b*, *c*) there are phase angles. In these cases it is necessary to perform the Holzer calculation twice, once for gas torques found by the vertical projections of the vectors of Fig. 157 and once again for their horizontal projections. At the conclusion of these computations *two* remainder torques are found, one for the components of

gas torque in phase with those of the first cylinder and the other one for the components at quadrature. The total torque to be furnished by the pendulum is the Pythagorean sum of these two (Fig. 6, page 6).

In the special case of the third diagram of Fig. 157, for order 1½, etc., the phase angles can be accounted for by changes in sign of the gas torques, and a single calculation suffices.

Formula (148*b*) shows that by proper tuning of the pendulum it can be made to behave like a moment of inertia of almost any magnitude, large or small, positive or negative. This property has been used in a number of practical applications; pendulums have been built of orders different from that of the excitation, so that they acted as flywheels of an inertia different from infinity. Each different pendulum tuning gives the system a different set of natural frequencies for each order of excitation. If the system contains several pendulums of different tunings, the number of possibilities becomes overwhelmingly large. In order to obtain a bird's-eye view over all these relations, preliminary to designing the pendulums, we can proceed as follows:

1. Make a plot of "equivalent moment of inertia of pendulum-damper flywheel" plotted vertically against "natural frequency" horizontally. This can be done by a number of Holzer tables without gas torque. Take a frequency and make a Holzer table, starting at the end away from the damper. Proceed to the damper end. Then, arbitrarily, give the damper moment of inertia such a value as to make the Holzer table come out with a zero remainder. Plot that moment of inertia against the frequency. Each Holzer table gives a point on the graph; no trials or other fumbling. The frequency range calculated for is the one where trouble might be expected from the engine excitation. This graph looks like a resonance diagram with many branches and asymptotes. The curve intersects the horizontal line at the natural frequencies of the system without pendulum dampers; the curve goes to infinity at the natural frequencies of the system with perfectly tuned pendulum dampers.

2. Two other useful curves can be drawn into the same diagram without further calculations:

a. The angular motion at damper hub (based on unit motion at the other end of the engine) *vs.* natural frequency.

b. The torque reaction of the pendulum damper (the shaft torque in the last shaft section) *vs.* the natural frequency. These points can be taken directly from the Holzer tables.

Curve (2*a*) goes through zero where the moment of inertia curve becomes infinite. Curve (2*b*) goes to zero where the moment of inertia curve becomes zero.

3. The diagram thus constructed gives a bird's-eye view of the system for any damper tuning that is desired. At this stage a preliminary decision has to be made as to number of pendulums and their sizes. With these values fixed, different pin diameters (different tunings) for the same weight can be investigated as follows:

a. Assume certain tunings, and find the I_{equiv} of all dampers combined for a particular order of vibration n by means of Eq. (148*b*).

b. Find the natural frequencies of the system for this particular order n

by inserting this equivalent inertia in the diagram. Also, from the diagram find the damper torque reaction and the damper hub motion, both per degree at the free end for this particular order. Find the critical speeds for this order and for any other orders that may be troublesome.

c. Repeat (*a*) and (*b*) for a number of tunings and choose from among them one set, for which all important criticals are outside the running range.

d. With this tuning perform a full set of forced vibration calculations, including the influence of gas torque, by means of Holzer tables, such as are shown on page 277.

The statement was made that the relative danger of minor critical speeds could be affected by a change in the firing order. The reader can easily verify this fact by drawing the star diagrams of Fig. 157 or 158 for two different firing orders and observing that the resultant vector is the same *only* for integer order critical speed and not for half-integer orders. This can be seen particularly well with the "symmetrical" engine of Fig. 159.

Consider the major critical of order 3. There are three oscillations per revolution, or one oscillation per 120-deg. rotation, *i.e.*, one oscillation per firing. Figure 159 shows that during a clockwise (+) vibrational velocity of 1, 2, 3, the disks 4, 5, 6 move in a counterclockwise (−) direction. Just after the firing of a cylinder, that cylinder exerts a particularly heavy torque on the crank shaft. Assume cylinder 1 to fire first while disk 1 has a clockwise (+) velocity. Cylinder 1 then does work on the motion. When the next firing occurs, 1, 2, 3 again have a + velocity and 4, 5, 6 a counterclockwise or − velocity. Suppose that the next cylinder to fire is 5. It does negative work, because 5 has a negative angular speed. After six firings, the total work done is positive for 1, 2, 3 and negative for 4, 5, 6. It is seen that a change in the firing order does *not* affect this result.

Now consider the 1½-order minor critical speed, *i.e.*, one-half vibration per firing. When cylinder 1 fires, let 1, 2, 3 have a (+) velocity and 4, 5, 6 a (−) velocity. At the next firing this condition is reversed, 1, 2, 3 are moving counterclockwise, because one-half vibration period has passed. If the next cylinder to fire is 5, it does positive work; but if it is 2, it does negative work. If cylinder 5 is chosen, 2 gets its turn to fire after one revolution, *i.e.*, after one and one-half vibrations and then does positive work. We see that the sign of the work done by cylinder 2 depends on whether it is made to fire immediately after 1 or one revolution later.

Of the four possible firing orders of Fig. 159 with the crank shaft of Fig. 155, the order

1	5	3	6	2	4
+	+	+	+	+	+

puts a maximum amount of work into the 1½-order vibration, because the firing always occurs when the corresponding disk is moving in a positive (clockwise) sense. For the three other possibilities we have

1	5	4	6	2	3		1	2	3	6	5	4		1	2	4	6	5	3
+	+	−	+	+	−		+	−	+	+	−	+		+	−	−	+	−	−

where the signs indicate positive or negative work done. The reader should verify these statements carefully. As an example verify that in the 8-cylinder engine of Problem 91, page 283, when vibrating in a mode such as shown in Fig. 159 in the order ½ or 4½, etc., the best possible firing order is 1 2 4 6 8 7 5 3, and that the worst possible firing order is 1 7 4 3 8 2 5 6. What are the best and the worst firing orders for order 1½?

This changing of the firing order acts as a shift of severity rather than as a cure. If one particular minor critical speed is made less dangerous by such a change, the result is obtained at the expense of another critical speed becoming more serious. If this other speed is outside the running range, our object is attained; but if the machine is required to operate over a very wide speed range, it may not be possible to avoid danger by changing the firing order. Then a damper is practically the only resource left to us.

Problems

81. A single-cylinder engine weighs complete 300 lb.; its reciprocating weight is 10 lb., and the rotating weight is 5 lb. The stroke $2r = 5$ in., and the speed is 500 r.p.m.

a. If the engine is mounted floating on *very* weak springs, what is the amplitude of vertical vibration of the engine?

b. If the engine is mounted solidly on a solid foundation, what is the alternating force amplitude transmitted?

Assume the connecting rod to be infinitely long.

82. Construct the piston-acceleration curve (Fig. 132) for an engine with a very short connecting rod, $l/r = 3$.

83. Sketch one full cycle of the inertia-torque variation [Eq. (138)] for an engine with $l/r = 3$.

84. Prove the four propositions on inertia balance stated on page 227. Find also the balance properties of a three-cylinder (0-120-240) engine.

85. A 4-cylinder engine has all 4 cylinders in one plane, on a crank shaft of 2 cranks in line, 90 deg apart (Fig. 166*d*). Find:

a. The amount of necessary counterweight at A or A^1 in order to reduce the primary inertia force of one crank and pair of pistons to a force of constant magnitude rotating in a direction opposite to that of the crank shaft.

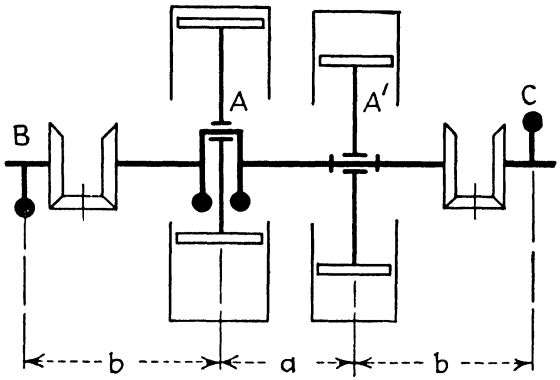


FIG. 166*d*.

b. The secondary inertia force of one crank.

c. The necessary counterweight and its angular location at B and C (gears rotating at 1:1 speed opposite to the crank shaft) in order to balance for primary forces and moments.

86. Figure 166*e* shows a "wobble-plate" engine. A number of stationary cylinders are equally spaced angularly around the central shaft. By prop-

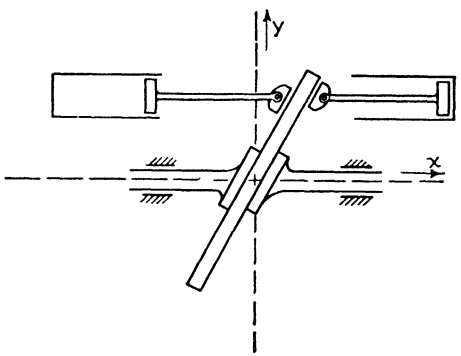


FIG. 166*e*.

erly proportioning the inertia of the piston and piston rods in relation to the inertia of the wobble plate, the engine can be balanced perfectly. For purposes of this analysis the pistons and rods may be assumed to have a uniformly distributed mass around the axis of rotation. The wobble plate is assumed to be a disk of total weight W_{disk}, uniformly distributed over its circular area of radius R_{disk}. The total weight of all pistons and connecting

rods is W_{pi}, supposedly concentrated on a circle of radius R_{pi} from the x-axis. Find the relation between these variables for which perfect balance is accomplished.

87. The torsional amplitudes of any engine at slow speeds are very large but the crank shaft stresses associated with it are small. In order to visualize this condition, consider a two-disk system I_1, I_2, connected by a shaft k, with a torque $T_0 \sin \omega t$ acting on disk I_1 only. Calculate and plot:

a. The amplitude of the engine I_1 as a function of frequency.

b. The shaft torque as a function of frequency.

88. Find the first natural frequency of a four-cylinder oil engine driving an electric generator of the following characteristics:

$I_{1,2,3,4}$ of the cranks, pistons, etc. = 50 lb. in sec.^{2} each
I_5 of flywheel-generator assembly = 1,000 lb. in sec.^{2}
$k_1 = k_2 = k_3 = k_4 = 10^7$ in. lb./rad.

89. *a.* Sketch the steam-torque curve of a double-acting steam cylinder of which the inlet valve is open for one-fourth revolution after the dead-center position. During the next quarter revolution the steam expands according to **pv** = constant. The engine works without compression.

b. Sketch the combined torque curve of an engine made up of three such cylinders on a 120, 240, 360 deg. crank shaft and also the combined torque curve of a six-cylinder Diesel engine based on Fig. 148*a*. Compare the two.

90. Draw the four fundamental star diagrams (Figs. 157 and 158) for the engine Fig. 159, for each of the four possible firing orders listed on page 281.

91. Discuss the star diagrams for the eight-cylinder engine (0, 180, 90, 270, 270, 90, 180, 0) without considering the elastic curve (Figs. 155 and 156). How many fundamental diagrams are there, and to which orders of vibration do they belong?

92. The turbine ship drive of Fig. 147, page 247, is excited by the four-bladed propeller only, the intensity of the exciting torque being 0.075 times the mean torque. Assume a propeller damping corresponding to twice the slope of the diagram, Fig. 160, and assume that diagram to be a parabola. Neglect damping in other parts of the installation.

a. Calculate the amplitude at resonance at the propeller.

b. From the Holzer calculations of pages 246 and 247 find the resonant torque amplitudes in the shafts 2-3 and 3-4.

c. At what propeller r.p.m. does this critical condition occur?

93. Problem 92 determines the resonant amplitude of the ship drive, Fig. 147. The resonance curve about that critical condition is found by calculating the undamped resonance curve and sketching in the damped one. Points on the undamped curve are determined by calculating a Holzer table for neighboring frequencies and by interpreting the "remainder torque" of these tables as a forced propeller-exciting torque. The mean propeller torque is 6,300,000 in. lb. at the rated speed of 90 r.p.m. and is proportional to the square of the speed. Find the amplitudes of forced vibration at the propeller for $\omega^2 = 145$ and $\omega^2 = 215$, and from the results sketch the resonance curve.

94. A recent aircraft engine consists of two six-cylinder-in-line blocks arranged parallel to each other and coupled to each other at each end by

three identical spur gears, so that the two blocks run at equal speeds in the same direction. One set of natural modes has nodes at both ends of each block.

a. What modification has to be made in the first line of the ordinary Holzer table to accommodate the node at one end?

b. What is the Holzer criterion at the other end?

c. What is the Θ in Lewis's method (page 244)?

d. Calculate the lowest natural frequency of a system of six equal inertias I, coupled to each other and to two solid walls at either end by seven identical shafts of stiffness k.

95. A variation (due to Chilton) of the damper of Fig. 166*a* consists of a steel block of weight W with a hardened cylindrical bottom that can roll on a hard cylindrical guide (Fig. 166*f*). The two radii of curvature R_1 and R_2 are large and their difference $\Delta R = R_2 - R_1$ is small. The distance between the center of gravity G and the contact point is a, and the radius of gyration about G is ρ.

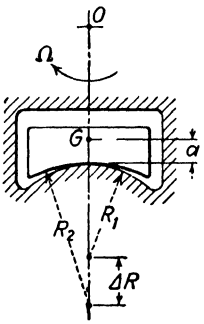


Fig. 166*f*.

a. Calculate the natural frequency of small rolling oscillations in a gravity field g.

b. The assembly rotates with speed Ω about a center O; the distance $OG = r_G$, and gravity is neglected. Calculate the frequency of small rolling oscillations.

96. Prove the results (146*b*) and (146*d*) of page 267 on the operation of the viscous Lanchester damper.

97. An eight-cylinder, four-cycle engine has a firing order 1 7 4 6 8 2 5 3 and crank angles 0, 90, 270, 180, 180, 270, 90, 0 deg.

a. Sketch the vector diagrams for the various orders of vibration without considering the magnitude of the vectors.

b. If at a certain mode the Holzer amplitudes are as follows:

No. 1, 1.000; No. 2, 0.900; No. 3, 0.800; etc.

down to No. 8, 0.300, and, if the 3½ order harmonic torque is 100,000 in. lb., find the work input per cycle at the resonance of this order if cylinder No. 1 vibrates ± 1 deg.

c. If the above mode occurs with a value $\omega^2 = 2{,}000$ in the Holzer table, what is the critical r.p.m. of order 3½?

d. What is the most dangerous r.p.m. of this engine?

e. What is the state of balance of this engine?

98. An idealized single-acting steam engine with constant pressure during the entire stroke (no cutoff) and an infinitely long connecting rod has a torque-angle diagram consisting of 180 deg. of sine wave, then 180 deg. of zero torque, etc; the torque never becomes negative. Find the harmonic torque components by a Fourier analysis, in terms of the mean torque T_{max}/π.

CHAPTER VI

ROTATING MACHINERY

46. Critical Speeds.—Consider a disk of mass m on a shaft running at constant angular speed ω in two bearings, as shown in Fig. 167. Let the center of gravity of the disk be at a radial distance e (= eccentricity) from the center of the shaft. If the disk were revolving about the shaft center line, there would be a rotating centrifugal force $m\omega^2 e$ acting on the disk. Such a rotating force can be resolved into its horizontal and vertical components and thus is seen to be equivalent to the sum of a vertical and a horizontal vibratory force of the same amplitude $m\omega^2 e$. Hence we expect the disk to execute simultaneous vertical and horizontal vibrations, and in particular we expect the disk to vibrate violently when these impulses are in resonance with the natural frequency, *i.e.*, when the angular speed ω of the shaft coincides with the natural frequency ω_n of the non-rotating disk on its shaft elasticity.

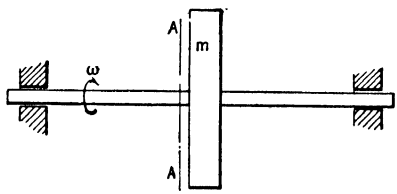


FIG. 167.—Unbalanced rotating disk.

This conclusion is not restricted to a single disk symmetrically mounted on rigid bearings but holds for more complicated systems as well. The speeds at which such violent vibrations occur are known as "critical speeds." In general the critical speeds ω of any circular shaft with several disks running in two or more rigid bearings coincide with the natural frequencies of vibration of the non-rotating shaft on its bearings. The critical speeds can be calculated from the influence numbers in the manner discussed in Chap. IV, and the determination of the influence numbers is a problem in the strength of materials.

The same result can be obtained also in a slightly different manner as follows. Figure 168 is drawn in the plane AA of Fig. 167 perpendicular to the shaft. The origin of the x-y coordinate system is taken in the point B which is the intersec-

tion with the plane AA of the center line connecting the two bearings. In the whirling unbalanced shaft there are three points of importance:

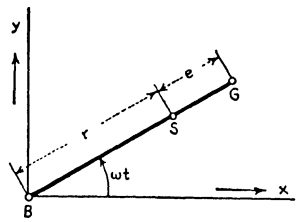


FIG. 168.—Cross section AA of Fig. 167 where B = bearing center, S = shaft center, and G = gravity center.

B = the center of the Bearings

S = the center of the Shaft (at the disk)

G = the center of Gravity (of the disk)

In Fig. 168 these three points have been drawn in a straight line BSG, which is supposed to rotate about B with the angular velocity ω of the disk. It will be seen that this apparently arbitrary assumption is the only one for which all forces are in equilibrium.

Further let

e = constant distance between S and G (eccentricity).

$r = BS$ = the deflection of the shaft at the disk.

If the effect of gravity be omitted, there are two forces acting on the disk: first, the elastic pull of the shaft which tends to straighten the shaft or to pull S toward B, and, second, the centrifugal force on the center of gravity G, which point is traveling in a circle of radius $(r + e)$. The first force depends on the bending stiffness of the shaft and is proportional to its deflection; thus we write for it kr (toward the center). The centrifugal force is $m\omega^2(r + e)$ directed from the center outward. For a steady whirling motion these two forces must be in equilibrium:

$$kr = m\omega^2 r + m\omega^2 e \tag{149a}$$

and solving for the shaft deflection r,

$$r = e\frac{\omega^2}{\frac{k}{m} - \omega^2} = e\frac{\omega^2}{\omega_n^2 - \omega^2} = e\frac{\left(\frac{\omega}{\omega_n}\right)^2}{1 - \left(\frac{\omega}{\omega_n}\right)^2} \tag{149b}$$

This formula coincides with Eq. (30) on page 61 for the case of a simple k-m-system excited by a force proportional to the square of the frequency. Hence Eq. (149b) may be represented also by the diagram of Fig. 40, which is shown again in Fig. 169. Taking the points S and G at the fixed distance e apart, the location of B

with respect to these two points at each frequency is the projection of the ordinate of the curve on the vertical axis. It is seen immediately that for very slow rotations ($\omega \approx 0$) the radius of whirl BS is practically zero; at the critical speed, $r = BS$ becomes infinite, while for very large frequencies B coincides with G. Thus at very high speeds the center of gravity remains at rest, which can be easily understood physically, since, if it were not so, the inertia force would become very (infinitely) great.

Equation (149a) shows that for a perfectly balanced shaft ($e = 0$), the spring force kr and the centrifugal force $m\omega^2 r$ are in equilibrium. Since both are proportional to the deflection, the shaft is in a state of indifferent equilibrium at resonance. It can rotate permanently with any arbitrary amount of bend in it. Whereas below the critical speed the shaft offered some elastic resistance to a sidewise force, this is no longer true at the critical speed. The smallest possible sidewise force causes the deflection to increase indefinitely.

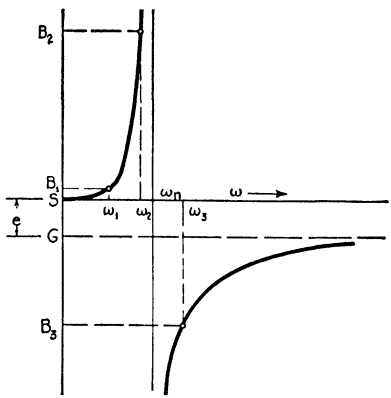


FIG. 169.—The relative location of S, G, and B for various speeds.

Another interesting conclusion that can be drawn from Fig. 169 is that, for speeds below the critical, G lies farther away from the center B than S does, whereas, for speeds above the critical, S lies farther outside. The points S and G are on the same side of B at all speeds. Thus below the critical speed the "heavy side flies out," whereas above the critical speed the "light side flies out."

The inertia force or centrifugal force is proportional to the eccentricity of G, which is $r + e$; and the elastic force is proportional to the eccentricity of S, which is r. The proportionality constants are $m\omega^2$ and k, respectively. For speeds below the critical, $m\omega^2$ is smaller than k, so that $r + e$ must be larger than r since the two forces are in equilibrium. At the critical speed, $r + e$ is equal to r, which necessitates that r be infinitely large. Above the critical speed, $r + e$ is smaller than r, which makes r negative.

It is difficult to understand why the shaft, when it is accelerated gradually, should suddenly reverse the relative positions of the three points B, S, and G at the critical speed. In fact the above analysis states merely that at a *given constant* speed the configuration of the three points, as determined by Fig. 169, is the only one at which equilibrium exists between the two forces. Whether that equilibrium is stable or unstable, we do not know as yet. It can be shown that for certain types of friction the equilibrium is stable below as well as above the critical speed.

The stability above the critical speed is due to the *Coriolis* acceleration which is set up as soon as the center of gravity of the disk moves radially away from the center B. Then G is accelerated sidewise and ultimately driven to the other side of B, destroying the collinearity of B, S, and G during the process. If this sidewise escape is prevented, *i.e.*, if the collinearity of the three points is enforced, the equilibrium above the critical speed is indeed *unstable*.

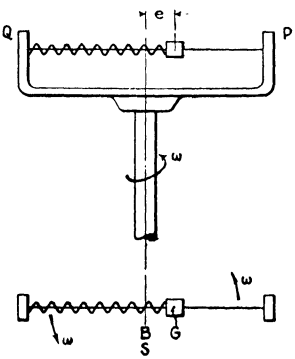


FIG. 170.—Rotating wire PQ along which the mass m can slide. This system is *unstable* above the critical speed.

The theory leading to Fig. 169 applies also to the system of Fig. 170 where the mass m is constrained to move without friction along a straight wire which in turn rotates with speed ω. When $\omega = 0$, the spring is not stretched and the equilibrium position of the mass is at a distance e from the vertical-shaft center. With increasing ω the mass will move more and more toward P, and just below the critical speed it will rest against P. Above the critical speed the equilibrium position of the mass is on the other side (the Q-side) of the vertical shaft, so that the centrifugal force toward Q is in equilibrium with the spring force toward P caused by the compression in the spring. This equilibrium, however, is unstable, as can be easily verified by displacing the mass by a small amount from the equilibrium position. Then the centrifugal force either increases or decreases at a faster rate than the spring force, with the result that the mass flies either to Q or to P, depending on the direction of the small initial displacement. In this experiment the collinearity of the three points B, S, and G is enforced by the wire, and sidewise escape is impossible. While the mass is moving along the wire, the Coriolis effect is felt only as a sidewise pressure on the wire and this does not influence the motion. In case the wire were absent, as in our original set-up of Fig. 167, a radial velocity of the mass would be associated with a sidewise acceleration (Coriolis) so that the above argument would be no longer valid.

In order to prove the stability of the system of Fig. 167 we have to write Newton's equations for the disk in the general case, *i.e.*, dropping the assumption of collinearity. The only assumption we retain is that the disk

rotates at a uniform speed ω about its center S, which is permissible of its moment of inertia is sufficiently large. In Fig. 171 the distance SG is constant and equal to e, whereas BS is variable and is denoted by r.

Let the coordinates of S be x and y, then the coordinates x_G and y_G of the center of gravity are $x + e\cos\omega t$ and $y + e\sin\omega t$. The only tangible force acting on the disk is the elastic force kr toward B and this force has the components $-kx$ and $-ky$ along the axes. Newton's equations for the center of gravity G are therefore

$$m\ddot{x}_G = -kx \qquad \text{and} \qquad m\ddot{y}_G = -ky$$

or written out

$$\left.\begin{aligned} m\ddot{x} + kx &= m\omega^2 e\,.\cos\omega t \\ m\ddot{y} + ky &= m\omega^2 e\,.\sin\omega t \end{aligned}\right\} \qquad (150)$$

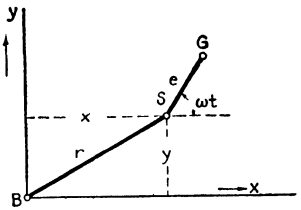


FIG. 171.—Proof of the stability of the system of Fig. 167 above the critical speed.

From Chap. II we know that the solution of these equations states that the motion of S in the x-direction as well as in the y-direction is made up of two parts, a free vibration of frequency $\omega_n^2 = k/m$ and a forced vibration of frequency ω. The two forced vibrations in the x- and y-directions being 90 deg. out of phase in time as well as in space make up the steady rotation of Fig. 168 (see Problem 27, page 101). If the usual type of friction exists, the free vibrations will be damped out after a time, so that indeed the circular motion with amplitude (149*b*) is reached ultimately. The "free vibration" which gradually dies down expresses the sidewise escape from collinearity as before discussed. However, there are types of friction for which the whirl above the critical speed is unstable, as discussed on page 362.

Until now the bearings of the machine have been assumed rigid. By making them flexible the argument already given needs no change whatever, provided the flexibility of the bearings is the same in all directions. The meaning of k, as before, is the number of pounds to be applied at the disk in order to deflect it 1 in. With flexible bearings, k is numerically smaller than with rigid bearings, but that makes no difference in the behavior of the shaft other than somewhat lowering its critical speed.

This situation is slightly altered if the bearings have different flexibility in the horizontal and vertical directions. Usually with pedestal bearings the horizontal flexibility is greater (k is smaller) than the vertical flexibility. We merely split the centrifugal force $m\omega^2 e$ into its horizontal and vertical components $m\omega^2 e\cos\omega t$ and $m\omega^2 e\sin\omega t$ and then investigate the vertical and horizontal motions separately. In Eqs. (150) this procedure introduces the difference that k in the x-equation is not the same as the k in the y-equation. At the frequency ω_1, the horizontal motion gets into resonance whereas the amplitude of the

vertical motion is still small (Fig. 172). The path of the disk center S is an elongated horizontal ellipse. At a greater speed ω_2, there is vertical resonance and the path is an elongated vertical ellipse. Thus there are two critical speeds and the shaft can hardly be said to "whirl" at either of them. Rather the shaft center vibrates almost in a straight line at either critical speed.

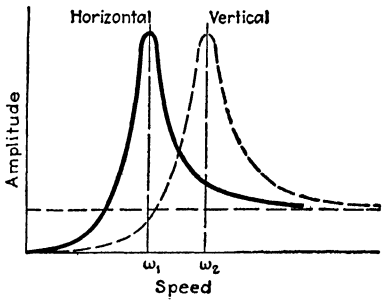


FIG. 172.—Resonance diagram for a shaft on bearings which are stiffer vertically than they are horizontally.

The generalization of this theory to shafts with many disks on more than two bearings with different flexibilities in the two principal directions is obvious. In general, there will be twice as many critical speeds as there are disks.

46a. Holzer's Method for Flexural Critical Speeds.—The usual method for determining the natural frequencies or critical speeds of shafts or beams in bending is the "iteration" method of Stodola, either in its graphical form (page 197) or its numerical form (page 203). Recently another manner of arriving at the result was suggested by several authors; this method can be properly called an extension of the Holzer method, familiar in torsional calculations, to flexural vibration. The beam in question is first divided into a convenient number of sections 1, 2, 3, etc., just as in Fig. 123 (page 197). The mass of each section is calculated, divided into halves, and these halves concentrated at the two ends of each section. Thus the beam is weightless between cuts and at each cut there is a concentrated mass equal to half the sum of the masses of the two adjacent sections. As in the Holzer method, we assume a frequency and proceed from section to section along the beam. In the torsional problem (governed by a second-order differential equation) there are *two* quantities of importance at each cut: the angle φ and the twisting moment, proportional to $d\varphi/dx$ (page 173). In the flexural problem (governed by a fourth-order equation) there are *four*

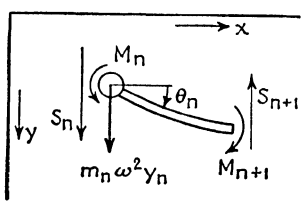


FIG. 172a.

quantities of importance at each cut: the deflection y, the slope $\theta = y' = dy/dx$, the bending moment $\mathbf{M} = EIy''$, and the shear force $\mathbf{S} = d\mathbf{M}/dx = EIy'''$; and it is necessary to find the relations between these quantities from one cut to the next. Figure 172*a* shows the section between the nth cut and the $n + 1$st cut, together with the various quantities. The sign of these quantities is defined as positive as shown in Fig. 172*a*. It is noted that the cut is made at and immediately to the left of the concentrated mass. The mass m_n shown in the figure thus equals half the mass of the section between cut $n - 1$ and n plus half the mass of the section between n and $n + 1$. Then we can write the following four equations for the section of length l:

$$\mathbf{S}_{n+1} = \mathbf{S}_n + m_n\omega^2 y_n \qquad (a)$$

$$\mathbf{M}_{n+1} = \mathbf{M}_n + \mathbf{S}_{n+1}l \qquad (b)$$

$$\theta_{n+1} = \theta_n + \frac{\mathbf{M}_{n+1}l}{EI} - \frac{\mathbf{S}_{n+1}l^2}{2EI} \qquad (c)$$

$$y_{n+1} = y_n + \theta_n l + \frac{\mathbf{M}_{n+1}l^2}{2EI} - \frac{\mathbf{S}_{n+1}l^3}{3EI} \qquad (d)$$

of which (*a*) and (*b*) are the equilibrium equations of the section, subject to the inertia force or centrifugal force $m_n\omega^2 y_n$ at the chosen frequency ω^2. The equations (*c*) and (*d*) are the deformation equations of the section, considered to be a cantilever built in at the left at the proper angle θ_n, and deformed by the force $\mathbf{S}_{n+1}$ and the moment $\mathbf{M}_{n+1}$ at its right-hand end.

The equations (*a*) to (*d*) allow us to calculate y, θ, $\mathbf{M}$, and $\mathbf{S}$ at the right-hand end of a section where they are known at the left-hand end. This can be done with a Holzer table, similar to the familiar one in torsional vibration, but much more elaborate, containing 17 columns instead of 7.

If we start from a simply supported end, where $y = 0$ and $\mathbf{M} = EIy'' = 0$, the slope θ and the shear force $\mathbf{S}$ are unknown. In the torsional case *only* the amplitude was unknown, which was arbitrarily assumed to be 1.000. Here we assume $\theta = 1.000$ and $\mathbf{S} = \mathbf{S}_0$. If we have a single span, by the Holzer table we find values for y, θ, $\mathbf{M}$, and $\mathbf{S}$ at the other end bearing, all in terms of the symbol $\mathbf{S}_0$ and the assumed numerical value of ω^2 and the assumed slope 1.000. At the end bearing we must have $y = 0$, and from this condition $\mathbf{S}_0$ is calculated numerically and substituted in. Then we find a definite numerical value for the bending moment $\mathbf{M}$ at the end bearing, which is the counterpart

of Holzer's "remainder torque" in the torsional case. Repeating the calculation a number of times for different values of ω^2 and plotting the end moment against ω^2 leads to a curve like Fig. 144 on page 239, and the natural frequencies are the zero points of that curve.

The case of a multispan beam is essentially the same. The start is as usual and upon arriving at the first intermediate bearing we set $y = 0$ and solve for $\mathbf{S}_0$. But there is a new unknown reaction and consequently a new shear force $\mathbf{S}_1$ at the intermediate bearing. Thus, between the first and second intermediate bearings the calculation proceeds as before; only with the unknown symbol $\mathbf{S}_1$ instead of $\mathbf{S}_0$ in the previous span.

Suppose the beam starts with an overhang instead of a bearing-supported end. Then $\mathbf{M} = \mathbf{S} = 0$ at that end, while y and θ are unknown. We start with $y = 1.000$ and $\theta = \theta_0$ and the calculation is the same as before. For a built-in end $y = \theta = 0$, and we start with $\mathbf{M} = 1.000$ and $\mathbf{S} = \mathbf{S}_0$.

Whereas the calculation for the torsional problem can be carried out with three decimal places on the slide rule, this is no longer feasible for the more complicated case of flexure. Eight or more decimal places are necessary to arrive at a final result accurate to three places, so that calculating machines become essential. This method is being used by the General Electric Company for the calculation of their turbogenerator critical speeds by means of the punched-card type of calculating machine, originally developed for bookkeeping purposes by the International Business Machines Corporation.

47. Balancing of Solid Rotors.—The disk of Fig. 167, of which the center of gravity lies at a distance of e in. from the shaft center, will vibrate and also will cause rotating forces to be transmitted to the bearings. The vibration and the bearing forces can be made to disappear by attaching a small weight to the "light side" of the disk so as to bring its center of gravity G in coincidence with the shaft center S. If the original eccentricity is e, the disk mass M, and the correction mass m, applied at a radial distance r from S, then

$$mr = eM \qquad \text{or} \qquad m = \frac{e}{r}M$$

The "unbalance" mr of the disk is usually measured in "inch ounces." It is, of course, correct to double the balance weight

for a given disk if the double weight is applied at half the original radius, since the centrifugal force is proportional to the product mr.

The determination of the location of the correction is a problem of statics. The shaft can be placed on two parallel horizontal rails, for example, then the heavy spot will roll down, and a correction weight can be attached tentatively to the top side of the disk. The amount of this weight is then varied until the disk is in indifferent equilibrium, *i.e.*, shows no tendency to roll when placed in any position. In order to minimize the errors of such a procedure (or as is sometimes said, in order to increase the sensitivity of the balancing machine), the rails must be made of hard steel and must be firmly embedded in heavy concrete, so that their elastic deformation under the load is as small as possible.

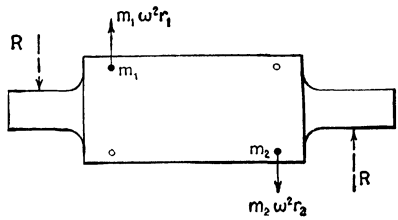


FIG. 173.—A dynamically unbalanced rotor causes equal and opposite rotating reactions on its bearings.

The set of horizontal rails is the simplest *static balancing machine* in existence. For machines in which the rotating mass is of disk form, *i.e.*, has no great dimensions along the axis, static balance is the only balance required to insure quiet operation at all speeds.

In case the rotor is an elongated body, static balance alone is not sufficient. Figure 173 shows a rotor which is supposed to be "ideal," *i.e.*, of perfect rotational symmetry, except that two equal masses, m_1 and m_2, are attached to two symmetrically opposite points. The rotor is evidently still in static balance, since the two masses do not remove the center of gravity from the shaft center line. When in rotation, the centrifugal forces on m_1 and m_2 form a moment which causes rotating reactions R on the bearings as indicated. This rotor is said to be statically balanced but *dynamically unbalanced*, because this type of unbalance can be detected by a dynamic test only, while on a static balancing machine the rotor appears to be perfect.

We shall now prove that any unbalance whatever in a rigid rotor (static, dynamic, or combined) can be corrected by placing appropriate correction weights in two planes, the end planes I and II of the rotor usually being chosen on account of their easy accessibility (Fig. 174). Let the existing unbalance mr consist

of 4 in. oz. at one-quarter of the length of the rotor and of 3 in. oz. in the middle between the planes I and II but turned 90 deg. with respect to the first unbalance. In determining the corrective masses to be placed in the planes I and II, we shall first find the corrections for the 4-unit unbalance, then find them for the 3-unit unbalance, and finally add the individual corrections together. The 4-unit unbalance will cause a 4-unit rotating centrifugal force, which can be held in static equilibrium by a 3-unit force at I and by a one-unit force at II. Thus we have to place a 3-unit correction mass in plane I, 180 deg. away from the original unbalance, and similarly a single-unit correction mass in plane II, also 180 deg. away from the original unbalance.

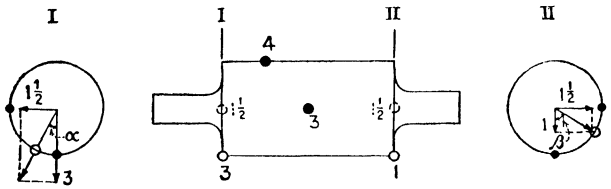


FIG. 174.—The most general unbalance in a rigid rotor can be corrected by placing one weight in each of two planes I and II.

The 3-unit unbalance is corrected by 1½-unit masses in each of the two planes. Thus in total we have to place in plane I a 3-unit mass and a 1½-unit mass, 90 deg. apart. The two centrifugal forces due to these can be added together by the parallelogram of forces so that instead of placing two correction masses in plane I we insert a single mass of $\sqrt{(3)^2 + (1\frac{1}{2})^2} = 3.36$ units at an angle $\alpha = \tan^{-1} 0.5$ from the diameter of the 4-unit unbalance. Similarly, the total correction in plane II consists of a correction mass of $\sqrt{1 + (1\frac{1}{2})^2} = 1.80$ units at an angle $\beta = \tan^{-1} 1.5$ from the same diameter.

The process can be extended to a larger number of unbalanced masses, so that any unbalance in a rigid rotor can be corrected by a single mass in each of the two balancing planes.

In any given rotor the size and location of the existing unbalance are unknown. They can be determined in a dynamic balancing machine. A type of construction of such a machine, used for small and medium-sized rotors, is shown in Fig. 175. The rotor is put in two bearings which are rigidly attached to a light table T. This table in turn is supported on springs and can be made rotatable about either one of two fulcrum axes F_1 or F_2,

located in the two balancing planes I and II. The rotor is driven either by a belt or by a flexible shaft, in which cases the driving motor is separate from the table T, or sometimes is driven by direct coupling to a small motor rigidly mounted on T. The latter scheme increases the weight of the table, which is undesirable. The drive is not shown in the figure.

The balancing process is as follows. Make F_1 a fulcrum by releasing F_2 and run the rotor until it, together with the table, comes to resonance on the springs. The maximum oscillating motion takes place at the right-hand end of T, and its amplitude is read on a dial indicator. By a series of operations to be described presently, the location and magnitude of the correction weight in the plane II are determined. With this weight inserted, the rotor and table do not vibrate at all. Any unbalance which still may exist in the rotor cannot have a moment about the fulcrum F_1, so that such unbalance must have a resultant located in plane I.

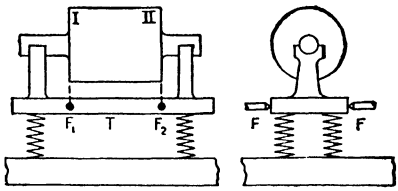


FIG. 175.—Balancing machine for small and medium size rotors with two interchangeable fulcrums F_1 and F_2.

Next, fulfrum F_1 is released and fulcrum F_2 is tightened, and the correction weight in plane I is determined by the same process, to be described. After this correction has been applied, the moments of all centrifugal forces are zero about the axes through F_1 *and* F_2. But, then, by the rules of statics, there can be no moment about any other axis, and the rotor is balanced completely.

Now we proceed to discuss how the correction weights can be determined. Apparently the simplest method is by means of the phase-angle relation shown in Fig. 42*b*, page 66. If a pencil or a piece of chalk is held very close to the rotating and whirling shaft, it will "scribe the heavy spot" when the shaft runs below its critical speed; it will "scribe the light spot" when above resonance, while exactly *at* the critical speed it will scribe at a point which is 90 deg behind the heavy spot. Thus the *location* of the unbalance can be found by scribing, and the *magnitude* of the correction is then determined by a few trials.

In practice this phase-angle method is very inaccurate, since near resonance the phase angle varies rapidly with small variations in speed, whereas at speeds markedly different from the

critical the amplitudes of the vibration are so small that no satisfactory scribing can be obtained.

A more reliable method is based on observations of the amplitude only. It consists of conducting three test runs with the rotor in three different conditions: (1) without any additions to the rotor, (2) with a unit unbalance weight placed in an arbitrary hole of the rotor, and (3) with the same unbalance weight placed in the diametrically opposite hole. In Fig. 176 let OA represent to a certain scale the original unbalance in the rotor and also, to another scale, the vibrational amplitude observed as a result of this unbalance at a certain speed. Similarly let OB represent vectorially the total unbalance of the rotor after the unit addition has been placed in the first hole. It is seen that the vector OB may be considered as the sum of the vectors OA and AB, where AB now represents the extra unbalance introduced. If now this unbalance is removed and replaced in the diametrically opposite hole, necessarily the new additional unbalance is represented by the vector AC equal and opposite to AB, and consequently the vector OC, being the sum of the original unbalance AC, represents the complete unbalance in the third run.

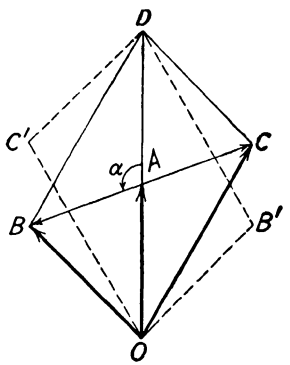


FIG. 176.—Vector diagram for determining the unbalance in a plane by three or four observations of amplitude.

As a result of the amplitude observations in these three runs, we know the relative lengths of the vectors OB, OA, and OC, but we do not as yet know their absolute lengths or their angular relationships. However, we do know that OA must be the median of the triangle OBC and the problem therefore consists in constructing a triangle OBC, of which are known the ratios of two sides and a median. Its construction by Euclid's geometry is carried out by doubling the length OA to OD and then observing that in the triangle ODC the side DC is equal to OB, so that in triangle OCD all three sides are known. Thus the triangle can be constructed, and as soon as this has been done we know the relative lengths of AB and OA. Since AB represents a known unbalance weight artificially introduced, we can deduce from it the magnitude of the original unknown unbalance

OA. Also the angular location α of the original unbalance OA with respect to the known angular location AB is known.

There is one ambiguity in this construction. In finding the original triangle OCD, we might have obtained the triangle $OC'D$ instead. Consequently we would have obtained the direction $C'B'$ instead of the direction CB for our artificially introduced unbalances. This ambiguity can be removed by a fourth run which also will act as a check on the accuracy of the previous observations. It is noted that in the construction of Fig. 176 no other assumptions have been made than that the system is linear, *i.e.*, that all vibration amplitudes are proportional to the unbalance masses. This relation is not entirely true for actual rotors but it is a good approximation to the truth. If after going through the motions shown in Fig. 176 and if after inserting the correction weight so found there still is vibration present in the machinery, that vibration will be very much less than the original one and the process of Fig. 176 may be repeated once more.

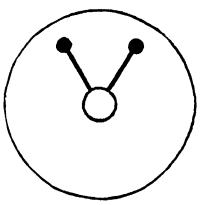


FIG. 177.—A balancing head with two unbalanced arms.

In factories where great numbers of small- or moderate-sized motors have to be balanced as a routine operation, the process of Fig. 176 takes too much time. For such applications the movable fulcrum machine of Fig. 175 was developed into an intricate precision apparatus in which the balancing is done by means of a so-called "balancing head."

A *balancing head* is an apparatus which is solidly coupled to the rotor to be tested and which contains two arms with weights (Fig. 177). These arms rotate with the rotor and keep the same relative position with respect to it, at least as long as the operator does not interfere. The possibility of rotating these arms *relative* to the rotor exists in the form of an intricate system of gears, clutches, and magnets or motors. The power for its operation is introduced necessarily through slip rings, since the whole head is rotating. The operator has before him two buttons. If he presses the first one, the two arms rotate in the same direction; if he presses the second one, the arms rotate in opposite directions at the rate of about one revolution per 5 sec. relative to the rotor in each case.

Since the two arms form the only unbalance in the head, this makes it possible for the operator to change the magnitude as

well as the direction of the added unbalance. By letting the two masses rotate in the same direction (button 1) and watching the vibration indicator, a maximum and a minimum amplitude appear every 5 sec. After taking his finger off button 1 at the minimum amplitude, the operator makes the two arms rotate against each other by pressing button 2. Since during this operation the bisecting line of arms remains at rest with respect to the rotor, the direction of the additional unbalance does not change, but the magnitude varies from two masses (when the arms coincide) to zero (when they are 180 deg apart). After the vibration has been reduced to zero, the rotor is stopped and from the position of the arms in the head the desired correction is determined immediately. As before, the process has to be performed twice for different locations of the fulcrum.

Another entirely different balancing head is the one invented by *Thearle* (1930). The machine is of the type of Fig. 175 with two fulcrums and with a head like Fig. 177 but with the important difference that the two arms are entirely free to rotate with respect to the rotor, except for the possibility of clamping them. There are no gears or magnets, merely a clutch which either clamps or releases the arms. In operation the arms are first clamped and the machine brought to above its critical speed. Upon releasing the arms, *they will automatically seek the position of complete balance* where all vibration ceases. They are clamped again in that position and the rotor is brought to rest.

The theory of operation of this device is very interesting. Suppose that the two arms are clamped in a 180-deg. position so that the head with the arms included is in perfect balance. The only unbalance in the system is in the rotor.

In Fig. 178, let B (center line of bearings), S (center of shaft, *i.e.*, balancing head), and G (center of gravity) have the usual meanings. We know from Fig. 169 that these three points appear in different sequences for speeds below and above the critical speed. The whirl of the whole assembly is about the bearing center line B, so that the centrifugal forces acting on the clamped arms must be directed away from B.

If at some speed below the critical (Fig. 178*a*) the arms are released, then the centrifugal forces will turn them toward each other to the top of the figure. Having arrived there they find themselves on the side of G, *i.e.*, on the *heavy* side. On the

other hand, if they are released above the critical speed, Fig. 178*b* shows that the centrifugal forces tend to drive the arms again to the top of the figure, which is now the *light* side. In coming closer together, the arms bring the location of G up and, after they have gone a certain distance, G coincides with S (and also with B) and all vibration ceases.

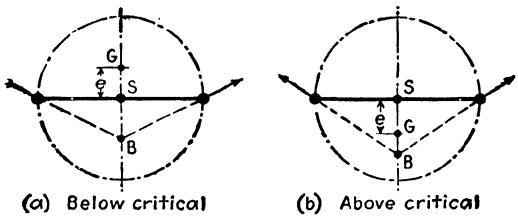


FIG. 178.—Explains the Thearle balancing machine.

Another balancing machine is shown in Fig. 179. The rotor R is supported in bearings on a table, which may rock about a fulcrum F. The rotor carries an arm A, which sweeps over the face of a stationary disk B. The disk is made of an electrically insulating material but carries a copper insert to which a wire is attached. By this means the magnet M receives an electric

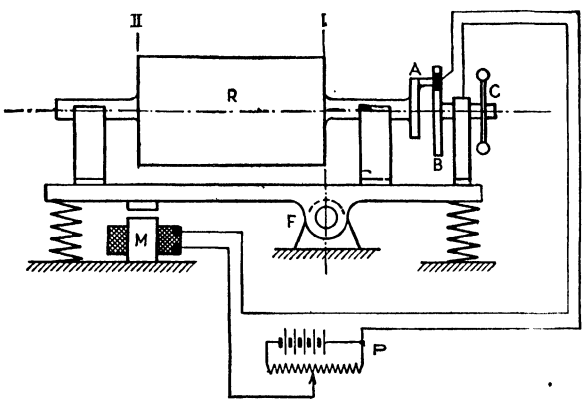


FIG. 179.—Automatic balancing machine of Spaeth-Losenhausen in which the counterforce is furnished by synchronous pulses of current in an electromagnet M.

impulse once per revolution of the rotor, so that the table experiences a downward force once per revolution. If this impulse occurs at the instant that the unbalance is on top of the rotor and if, moreover, the intensity of the impulse has a certain magnitude, the table does not vibrate. By slowly turning the handwheel C the phase of the impulse can be changed and by

adjusting the potentiometer P the magnitude can be varied, until all vibration disappears. From the positions of C and P the location and magnitude of the unbalance can be deduced immediately.

In Fig. 179 the fulcrum coincides with plane I, but by reversing the rotor in its bearings plane II can be made to pass through F. As with all other machines having balancing heads, the device is run at its critical speed, which insures a great sensitivity.

With the modern developments in radio technique, it is now no longer necessary to run balancing machines at resonance. They can be operated at speeds well removed from the resonant one, the very small vibrations at the bearing being picked up by electrical devices, of which the output can be magnified to any desired degree by a vacuum-tube amplifier. Machines utilizing such amplifiers are discussed in the next section.

48. Simultaneous Balancing in Two Planes.—It is possible to simplify the methods of balancing described in the previous section if means are available to measure the phase angle between the location of the unbalance in the rotor and the "high spot" of the vibration. Let the rotor be supported in two bearings a and b which are flexible in, say, the horizontal direction and stiffly supported vertically. The balancing planes I and II do not coincide with the locations of the bearings a and b. Now imagine the rotor to be ideally balanced so that while it is rotating in the bearings no bearing vibration occurs. Then unbalance the ideal rotor by placing a unit weight in the angular location 0° of balancing plane I. This will cause a vibration in both bearings and these vibrations are denoted as α_{aI} and α_{bI}, where the first subscript denotes the bearing at which the vibration occurs and the second subscript denotes the balancing plane in which the unit unbalance at zero angular location has been placed. When there is no damping in the system, these numbers α are real numbers, by which we mean that the maximum displacement in the horizontal direction of the bearings occurs at the same instant that the unbalance weight finds itself at the end of a horizontal radius. If there is damping in the system, there will be some phase angle between the unbalance radius and the horizontal at the moment that the bearing has its maximum displacement, and this condition can be taken care of by assigning complex values to the α numbers.

In a similar manner the ideal rotor may be unbalanced with a unit weight in the zero angular location of plane II, which then

causes the bearing vibrations $\alpha_{a\text{II}}$ and $\alpha_{b\text{II}}$. The four numbers α so found are known as the complex *dynamic influence numbers* of the set-up. If the rotor is run well above its critical speed, the phase angles are close to 180 deg. and the influence numbers are nearly real. These four influence numbers completely determine the elastic and inertia properties of the system for the r.p.m. at which they are determined, but they are entirely independent of the amount of unbalance present.

Next suppose that the unbalance in plane I is not a unit unbalance at zero angular location but an unbalance which numerically as well as angularly differs from the unit unbalance, and is represented by the complex number $\bar{U}_{\text{I}}$. Then this unbalance $\bar{U}_{\text{I}}$ will cause a vibration at the bearing a, expressed by the product $\alpha_{a\text{I}}\bar{U}_{\text{I}}$ of two complex numbers. This can be easily seen for the case where the unbalance is, say, two units in angular location 0°, but it also holds true for any other angular location of the vector $\bar{U}_{\text{I}}$.

With these notations, it is now possible to write the vibration vectors $\bar{V}$ at the two bearings in terms of a general unbalance $\bar{U}_{\text{I}}$ and $\bar{U}_{\text{II}}$ as follows:

$$\left.\begin{aligned} \bar{V}_a &= \alpha_{a\text{I}}\bar{U}_{\text{I}} + \alpha_{a\text{II}}\bar{U}_{\text{II}} \\ V_b &= \alpha_{b\text{I}}\bar{U}_{\text{I}} + \alpha_{b\text{II}}\bar{U}_{\text{II}} \end{aligned}\right\} \qquad (150a)$$

The eight symbols used in these equations are all vectors or complex numbers. It is possible to measure the vibration vectors $\bar{V}_a$ and $\bar{V}_b$ and calculate from them by means of the set (150a) the unknown unbalance vectors $\bar{U}_{\text{I}}$ and $\bar{U}_{\text{II}}$, with the following result:

$$\left.\begin{aligned} \bar{U}_1 &= \frac{\alpha_{b\text{II}}}{\Delta}\bar{V}_a - \frac{\alpha_{a\text{II}}}{\Delta}\bar{V}_b \\ \bar{U}_2 &= \frac{\alpha_{a\text{I}}}{\Delta}\bar{V}_b - \frac{\alpha_{b\text{I}}}{\Delta}V_a \end{aligned}\right\} \qquad (150b)$$

In these equations $\Delta = \alpha_{a\text{I}} \cdot \alpha_{b\text{II}} - \alpha_{b\text{I}}\alpha_{a\text{II}}$ is the determinant of the coefficients of Eq. (150a). The set of equations (150b) enables us to calculate the unknown unbalance vectors if we can measure the vibration vectors at the two bearings and if we know the four dynamic influence numbers.

These $\bar{V}$ vectors can be measured in various ways. A very convenient method consists of inverted loud-speaker elements such as are described on page 81. These elements are attached

to the two bearing shells a and b of the balancing machine, and their output is an electric alternating voltage which in magnitude and phase determines the vibration vector. The *Gisholt-Westinghouse* balancing machine uses such elements and also has an electric circuit by which Eqs. (150*b*) are automatically solved. In order to understand the operation of this circuit, shown in Fig. 180, we rewrite the first of Eqs. (150*b*) as follows:

$$\bar{U}_{\mathrm{I}} \cdot \frac{\Delta}{\alpha_{b\mathrm{II}}} = \bar{V}_a - \frac{\alpha_{a\mathrm{II}}}{\alpha_{b\mathrm{II}}} \cdot \bar{V}_b \tag{150c}$$

In this equation we notice that the ratio $\alpha_{a\mathrm{II}}/\alpha_{b\mathrm{II}}$ is smaller than 1 because the numerator is the response of a bearing to a unit unbalance far away from it, while the denominator is the response to an unbalance close to it. In all ordinary systems this ratio is smaller than unity. Thus we see from Eq. (150*c*) that the unbalance in plane I is found by taking the vibration vector of bearing a, subtracting from it a *fraction* of the vibration vector of bearing b, and multiplying the result by $\alpha_{b\mathrm{II}}/\Delta$. The fraction of V_b in general is a complex fraction but it is made real by running the machine at a speed far above its resonance. The subtraction of these two quantities is accomplished in Fig. 180 by connecting in series the full output of the loud-speaker coil on bearing a with a fraction of the voltage output of loud-speaker coil $\bar{V}_b$. This fraction is picked off by a potentiometer knob 1. In this way it is possible to adjust that fraction to any real number smaller than one. The fact that there is a minus sign on the right-hand side of Eq. (150*c*) instead of a plus sign has no further importance than that the terminals of one of the coils have to be reversed. The voltage representing the right-hand side of Eq. (150*c*) is then fed into an amplifier, and the amplified voltage is multiplied by the number $\alpha_{b\mathrm{II}}/\Delta$, by picking off a fraction of it through the potentiometer knob 2. The output of the circuit is then read on a milliammeter and is simultaneously used to actuate a stroboscopic lamp which flashes once per revolution of the rotor. If it is only possible to set knob 1 so as to represent the ratio $\alpha_{a\mathrm{II}}/\alpha_{b\mathrm{II}}$ and to set knob 2 so as to represent the ratio $\alpha_{b\mathrm{II}}/\Delta$, then the milliammeter to a certain scale will read directly the amount of the unbalance, while the stroboscopic lamp will apparently freeze the rotor at such an angular position that a fixed needle points at the angular location of the unbalance.

The circuit thus described solves the first of Eqs. (150*c*). For

the solution of the second equation (150c) it is necessary to combine the full output of $\bar{V}_b$ with a fraction of $\bar{V}_a$ and multiply the amplified output by a different number. This is done by a new circuit with knobs 3 and 4 instead of 1 and 2 in a similar manner.

The interesting feature of this circuit is that the proper setting of these knobs is not calculated but found by a series of very simple experiments. Suppose that a large number of identical rotors have to be balanced in a mass-production process. We start with balancing one rotor in any convenient

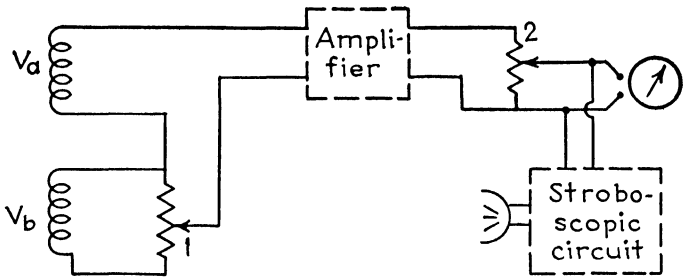


FIG. 180.—Circuit diagram of the Gisholt-Westinghouse balancing machine. (*J. G. Baker.*)

manner until it is perfect and this may take us a considerable time. This *perfect* rotor placed in the two bearings a and b will cause no vibration in them, therefore no voltage $\bar{V}_a$ or $\bar{V}_b$, and hence no reading in the milliammeter. Then a unit unbalance at zero angular location is deliberately placed in plane I. This ought to cause a unit reading on the milliammeter and a zero angular reading on the stroboscope in the case where the circuit of Fig. 180 with knobs 1, 2 is switched in, *i.e.*, in the case where a left-right switch is set on the position I. If this switch is set to the position II, the other circuit with knobs 3 and 4 is in force and the milliammeter ought to give a zero reading. Naturally, these readings will not be as they should, because the four adjustments have not been made as yet. It follows from Eq. (150c) that with the switch in the position II the zero reading on the milliammeter (due to unit unbalance in plane I) is not affected by the knob 4 but can be accomplished entirely by 3. We therefore turn knob 3 until the milliammeter reading becomes zero.

Now the unit unbalance in plane I is removed and brought to plane II, while the selector switch is thrown to position I.

Again the milliammeter should read zero, which is accomplished quickly by adjusting knob 1. Now, leaving the unit unbalance in plane II, the selector switch is thrown to the position II and the knob 4 is adjusted until the milliammeter reads a unit unbalance and the stroboscope a zero angular position. Finally, the unit unbalance is brought back to plane I, the selector switch is set on plane I, and knob 2 adjusted to get unit reading on the milliammeter and zero angular reading on the stroboscope. This process of making the four adjustments takes only a few minutes for an experienced operator, and thereafter these adjustments are correct for every other rotor in the series to be balanced. The balancing process then consists of placing an unbalanced rotor in the bearings, starting the rotor by a foot-operated switch (belt drive), reading the milliammeter and the angular position, throwing the selector switch to the other side, and again reading the unbalance numerically as well as angularly. This process takes only a few seconds and is extremely accurate.

In cases where a *single* rotor has to be balanced instead of a whole series in mass production, such as, for example, a turbine or a generator rotor in its own bearings in a powerhouse, the problem is to produce one "ideal rotor." The procedure outlined above does not solve the difficulty, but it is still possible to use the apparatus of Fig. 180 by a clever expedient, due to J. G. Baker, which consists of fooling the circuit of Fig. 180 into believing that it deals with an ideal rotor, whereas in reality it deals with an ordinary unbalanced rotor. For this purpose two small alternating-current generators are made to be driven by the turbine to be balanced. These generators produce currents of a frequency equal to that of the r.p.m., and their voltage output can be regulated in magnitude as well as in phase. Now the circuit of Fig. 180 is opened in two spots at the two coils V_a and V_b. The output of the generators, suitably modified, is now fed into these openings and regulated so that the voltage induced by the vibration in each pickup coil is bucked by an equal and opposite voltage artificially introduced by the generators. With this set-up the circuit of Fig. 180 gets no impulses and therefore reacts as if an ideal rotor were run. Now with the bucking voltages in force, the three runs of the existing rotor are made: (1) "as is," (2) with a unit unbalance in plane I, and (3) with a unit unbalance in plane II. In this manner the adjustment on all four knobs is carried through as outlined above. After this,

the artificially introduced bucking voltages are removed and now the circuit responds to the actual rotor with the existing unbalance in it.

A still simpler method of balancing without fulcrums is suggested by Eqs. (150*a*). It is clear that the vibration readings can be made at such a position along the rotor that the influence numbers α_{aII} and α_{bI} become zero. This means that the measurement $\bar{V}_a$ (or $\bar{V}_b$) has to be made at a position along the rotor which will not experience any vibration if an unbalanced weight is placed in plane II (or I). This position is known as the "center of percussion," belonging to the "center of shock" II (or I). In that case each loud-speaker element or other type of electrical indicator reads only the vibration caused by one of the balancing planes alone and, instead of solving a set of four algebraic simultaneous equations (150*a*) with four unknowns, the problem is reduced to finding a solution to two sets of two unknowns each. This method has been used for some time in a machine developed by the General Motors Research Laboratory.

49. Balancing of Flexible Rotors: Field Balancing.—In discussing the effects of unbalanced masses in the last two sections, we have assumed that the rotor was not deformed by them. When running at speeds far below the first critical, this assumption is perfectly justified, but for speeds higher than about half of the first critical the rotor assumes deformations which can no longer be neglected since they set up new centrifugal forces in addition to the ones caused by the original unbalance. If, for example, a unit unbalance is located in the center of a symmetrical rigid rotor, the unit centrifugal force due to this unbalance will have reactions of half a unit at each of the bearings. On the other hand, if the rotor is flexible, the unit centrifugal force will put a bend in the structure and bring its center line off the original position. Consequently, the bent center line whirls around and additional centrifugal forces are set up which will alter the bearing reactions.

The machine can evidently be balanced by adding a corrective mass in the middle directly opposite the original unbalance. But we prefer to balance it in two definite planes near the ends. Assume that the rotor consists of a straight uniform shaft and that the balancing planes are at one-sixth of the total length from each end. Evidently the rigid rotor will be balanced by putting in corrections of magnitude $\frac{1}{2}$ in each plane (Fig. 181*a*).

When the unbalanced rotor is running at its first critical speed, its deflection curve is a sinusoid (page 188) of which the amplitude is so large that the newly "induced" unbalance is far greater than the original unit balance. Thus the original unbalance does not influence the shape of the deflection curve, which at the balancing planes has half the amplitude of the middle. The proper corrections have to be of the same amount as the original unbalance. This can be understood by bending the shaft a little more. The centrifugal forces of the shape itself (exclusive of the original unbalance) are in equilibrium with the elastic forces at any position of the shaft, since there is resonance. When increasing the deflection at the center by δ, the work done by the unbalance is $\delta \times 1$ and the work done by each of the two correction weights $\frac{1}{2}\delta \times 1$. It is seen that the equilibrium remains indifferent (characteristic of a balanced rotor at a critical speed) when the correction weights are made a full unit (Fig. 181*b*).

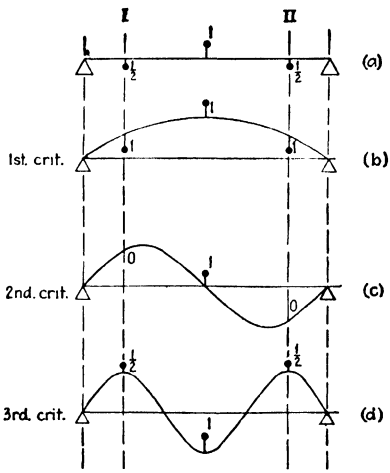


FIG. 181.—The proper correction weights to be inserted in the planes I and II vary with the speed in a flexible rotor.

At the second critical speed the central unbalance is not displaced in position so that no correction weights are necessary. At the third critical speed the correction weights have to be made half a unit on the side opposite to where they were at slow speeds (Fig. 181*c*, *d*).

We thus draw the conclusion that *a flexible rotor can be balanced in two planes for a single speed only;* as a rule the machine will become unbalanced again at any other speed. Large turbine spindles or turbogenerator-rotors in modern applications usually run between their first and second critical speeds. When such units are balanced at a rather low speed in the machine sketched in Fig. 175, they quite often become rough when run at full speed in their permanent bearings. This is one of the reasons why shop balancing is not sufficient, and why such machines have to be balanced again in the field under service conditions.

In the field no movable fulcrums are available and the process of balancing takes a considerable time. As a rule, the amplitude method discussed on page 296 is applied, but in order to secure good balance it is necessary to repeat the operation a number of times, shuttling back and forth from one balancing plane to the other.

There are cases on record where even several weeks of systematic field balancing did not produce a smooth machine. In such cases the trouble is evidently caused by something other than unbalance. In one particular machine it was found that a careless workman had dropped a balancing weight in the hollow interior of a turbine spindle and had failed to report the fact. Consequently a loose weight of 1 lb. was flying around freely in that space, and it was impossible to balance the machine.

A remarkable series of cases of steam-turbine vibration, observed off and on during the last fifteen years, was explained recently. The turbine would vibrate with the frequency of its rotation, obviously caused by unbalance, but the intensity of the vibration would vary periodically and extremely slowly. On some turbines the period of time between two consecutive maxima of vibration intensity was as low as 15 min.; on others this period was as much as 5 hr. The seriousness of the trouble consisted in the fact that each maximum was worse than its predecessor, so that after half a dozen of these cycles the machine had to be shut down.

Observations were made of the phase angle of the vibration, *i.e.*, the angle between the vertical and the radial direction of a definite point of the rotor at the instant that, say, the horizontal vibrational displacement of a bearing was maximum to the right. This angle was observed by watching the needle of a vibrometer placed on the bearing by a stroboscopic light, flashing once per revolution and operated by a contactor driven off the rotor. The phase angle was found to increase indefinitely, growing by 360 deg. each time the vibration reached a maximum. This was explained as a "rotating unbalance" which would creep through the rotor and which would be additive to the original steady unbalance when the vibration was a maximum and in phase opposition to the steady unbalance at times of minimum vibration. A detailed explanation of how an unbalance can creep so slowly through a rotor was given recently by R. P. Kroon, as follows.

Let Fig. 182 represent a cross section of the rotor and let the vector $\overline{OS}$ be the static unbalance of the rotor; *i.e.*, O is the geometric center of the rotor and S is its center of gravity when not rotating. For very slow rotation the rotor will bow out under the influence of the centrifugal force in the direction OS, but at higher speeds the "high spot" will no longer coincide with the "heavy spot" S. The high spot will be given by the dynamic unbalance vector $\overline{OD}$, where D is the location of the geometric center of the rotor while running. Since $\overline{OS}$ is the "force" and $\overline{OD}$ the "displacement," the result of Figs. 41 and 42*b* can be applied from which it is seen that the high spot always trails behind the heavy spot by an angle φ which is less than 90 deg. below resonance and between 90 and 180 deg. above resonance.

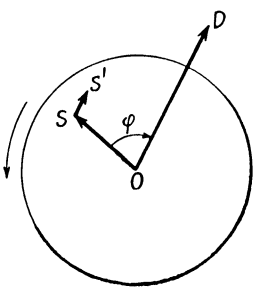


FIG. 182.—This illustrates a spiral wandering of the unbalance within the rotor caused by unsymmetrical heating or cooling.

The unsymmetry in the direction $\overline{OD}$ caused by the bowing out of the rotor may be the cause of local heating at D. This may be in the form of actual rubbing on the periphery at D or, in the case of a hollow rotor, may be the result of condensation. The water droplets from the condensing steam will be moved by centrifugal force to D, thus causing further condensation and heating at that point. The heating at D in turn causes the rotor fibers to expand, thus producing an elastic bowing out of the rotor with a consequent shift in the location of the center of gravity. The point S therefore shifts to S', the vector $\overline{SS'}$ having the direction $\overline{OD}$. The new static unbalance $\overline{OS'}$ is angularly displaced with respect to $\overline{OS}$; the angle φ remains the same, so that $\overline{OD}$ also shifts clockwise. In this manner we see a slow rotation of the unbalance in a direction opposite to that of rotation. Also $\overline{OS'}$ is slightly greater than $\overline{OS}$, so that the result will be that the point S describes a spiral within the rotor. We have thus seen that for local heating at the high spot below resonant speed we get a retrograde and increasing spiral. In a similar manner it is shown that above resonant speed ($\varphi > 90$ deg.) the spiral is still retrograde but now decreasing. If there happens to be cooling at the high spot, instead of heating, the spiral is

forward and decreasing below resonance, forward and increasing above that speed.

For very flexible rotors, running well above their first critical speed and close to the second critical, the phase angle φ becomes greater than 180 deg. and the analysis in terms of a single degree of freedom can no longer be applied. However, the general reasoning is the same; only the value of φ is different.

In this connection it may be of interest to mention another temperature effect observed in steam turbines. After a turbine has stood still for some time, the temperature of the top fibers of the rotor is usually somewhat higher than that of the bottom fibers, so that the rotor is "humped up." When rotating the unit, this evidently corresponds to a huge unbalance, since a bend of 0.001 in. in the center line of a 20-ton rotor means an unbalance of 40 in.-lb. Thus an attempt to bring the machine to full speed at once would end in disaster. It is necessary to rotate the spindle at a low speed for about an hour before the temperature differences are sufficiently neutralized and the machine can be put in operation.

50. Secondary Critical Speeds.—Besides the main or ordinary critical speed caused by the centrifugal forces of the unbalanced masses, some disturbance has been observed at half this critical speed, *i.e.*, for the single disk of Fig. 167 at $\omega = \frac{1}{2}\sqrt{k/m}$.

This effect has been observed on horizontal shafts only. On vertical shafts it is absent, indicating that gravity must be one of the causes of it. There exist two types of this disturbance, caused by gravity in combination with unbalance and by gravity in combination with a non-uniform bending stiffness of the shaft.

These phenomena are known as "secondary critical speeds," and, as the name indicates, their importance and severity are usually less than for the ordinary or "primary" critical speeds. The theory of the actual motion is very complicated, and its detailed discussion must be postponed to the last chapter, pages 406 to 424. Here, we propose to give merely a physical explanation of the phenomena and a calculation of the amplitude of the disturbing forces involved.

To this end we imagine the simple shaft of Fig. 167 to be rotating without any vibration or whirl, and then we calculate which alternating forces are acting on the disk. For the ordinary critical speed of page 287 we have a rotating centrifugal force

$m\omega^2 e$ (m = mass of the entire disk, e = eccentricity of its center of gravity), and this force can be resolved into its horizontal and vertical components. Each of these is an alternating force of frequency ω and amplitude $m\omega^2 e$.

Consider next the case of a perfectly balanced disk ($e = 0$) running on a shaft which is not equally stiff in all directions. Since a shaft cross section has two principal axes about which the moment of inertia is maximum and minimum, it is seen that for each quarter revolution the stiffness of the shaft in the vertical direction passes from a maximum to a minimum (Fig. 183). For a full revolution of the shaft the stiffness is twice a maximum and twice a minimum, or for each revolution the stiffness variation passes through two full cycles.

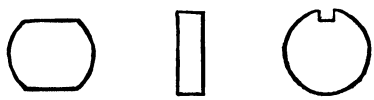


FIG. 183. – Shaft cross sections of non-uniform flexibility.

If the spring constant of the shaft varies between the minimum value $k - \Delta k$, and the maximum value $k + \Delta k$, with an average value of k, then for uniform rotation ω the stiffness can be expressed by

$$k + \Delta k \cdot \sin 2\omega t$$

If the disk is not vibrating and its downward deflection during rotation is δ, there are two vertical forces acting on it, *viz.:*

The weight mg downward.

The spring force $(k + \Delta k \cdot \sin 2\omega t)\delta$ upward.

Naturally the weight and the constant part of the spring force are in equilibrium, so that we have a vertical disturbing force of frequency 2ω and of amplitude

$$\Delta k \cdot \delta = \Delta k \cdot \frac{mg}{k} = \mathbf{W} \cdot \frac{\Delta k}{k}$$

If the shaft is running at half its critical speed, the impulses of this force occur at the natural frequency so that we expect vibration.

The next case, that of an unbalanced disk on a uniform shaft, is somewhat more difficult to understand. Assuming no vibration, *i.e.*, the center S of the shaft being at rest and coinciding with B, and assuming an eccentricity e, the center of gravity G describes a circular path of radius e (Fig. 184). The weight $\mathbf{W}$ of the disk exerts a torque on the shaft which retards the rotation

when G is in the left half of Fig. 184 and accelerates it when G is in the right half. The magnitude of this torque is $\mathbf{W}e \sin \omega t$. If the moment of inertia of the disk about the shaft axis is $m\rho^2$ (ρ = radius of gyration), the angular acceleration of the shaft caused by this torque is $(\mathbf{W}e/m\rho^2) \sin \omega t$. The point G in its circular path has an acceleration of which the radial or centripetal component is of no interest to us in this case, since it will lead to the ordinary (primary) critical speed. However, on account of the angular acceleration, G has a tangential component of acceleration of magnitude

$$\frac{\mathbf{W}e^2}{m\rho^2} \sin \omega t$$

This means that there must be a tangential force acting on G of value $(\mathbf{W}e^2/\rho^2) \sin \omega t$. The vertical component of this force is $\sin \omega t$ times as large, or

$$\left(\frac{\mathbf{W}e^2}{\rho^2}\right) \sin^2 \omega t = \text{const.} - \frac{\mathbf{W}e^2}{2\rho^2} \cos 2\omega t$$

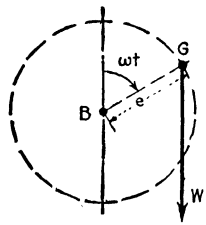


FIG. 184. Explains the secondary critical speed caused by unbalance and gravity.

The constant part of this force is taken up as a small additional constant deflection of the shaft and is of no interest. However, the variable part has the frequency 2ω and the amplitude $\mathbf{W}e^2/2\rho^2$.

Summarizing, we have for amplitudes of the disturbing forces the following expressions:

$$\left.\begin{array}{ll} \text{At the ordinary critical speed,} & m\omega^2 e \\ \text{At the "unbalance" secondary speed,} & \dfrac{\mathbf{W}}{2} \cdot \left(\dfrac{e}{\rho}\right)^2 \\ \text{At the "flat-shaft" secondary speed,} & \mathbf{W} \cdot \dfrac{\Delta k}{k} \end{array}\right\} \quad (151)$$

In practice, the order of magnitude of e/ρ to be expected in a machine is about the same as that of $\Delta k/k$, both being very small, say 0.001. It is seen that the disturbing force of the "unbalance" secondary critical speed is of a much smaller order than that of the "flat-shaft" critical speed, since e/ρ appears as a square. Therefore, in most cases where the secondary critical is observed, it is due to non-uniformity of the shaft rather than to unbalance. The nature of the trouble can be established by balancing the machine at its primary critical speed. If the amplitude of the secondary critical speed is not

affected by this procedure, that speed is clearly due to shaft flatness.

A more detailed analysis of this problem is given on pages 406 to 424.

50a. Critical Speeds of Helicopter Rotors.—About the year 1940, helicopter rotors with the usual hinged-blade construction were observed to come to a violent critical condition at a speed very much lower than that calculated from the $\omega^2 = k/M$ formula. This happens while the aircraft is standing still on the ground prior to take-off and consequently is called the "ground critical." The phenomenon was explained by R. P. Coleman of Langley Field in N.A.C.A. reports of 1942 and 1943, and the simpler portion of his results are here reproduced for the great interest attached to them.

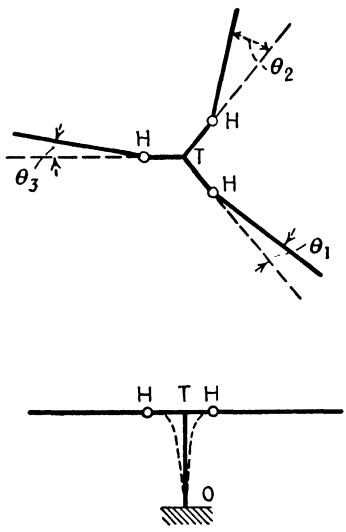


FIG. 184a.

The system is as shown in Fig. 184*a*. The blades of a helicopter rotor are hinged at H, so that they can swing freely about H in the plane of rotation. The hub of the rotor coincides with the top T of a "pylon" OT, which at O is supposed to be built-in into the helicopter structure. If k be the stiffness of this pylon against a force at T in the plane of the rotor and if M be the total mass of the hub and all attached blades, then the observed critical speed ω^2 was very much smaller than k/M.

Consider the three-bladed rotor of Fig. 184*b*, where O is the bottom of the pylon seen from above and T is the top of the pylon, displaced to the right through the distance $OT = e$, the eccentricity. The pylon is supposed to be bent elastically through distance e, and the entire figure as a solid body rotates or whirls at speed ω about the vertical axis O. The blades will turn about their hinge axes H through small angles ϵ, so that the blade lines up with the centrifugal field through the center of rotation O. During the whirling motion these angles ϵ are constant and no relative motion takes place across any of the hinges H. We now

calculate the centrifugal forces of all three blades and of the hub and set their sum equal to ke, the elastic homing force of the pylon. This will give the critical speed.

In the triangle OTH the angle OTH is 120 deg., the angle $THO = \epsilon$ is considered "small," the hinge radius $TH = a$, and the eccentricity $OT = e$ is again "small" with respect to a. From the geometry of this triangle the reader should derive as follows:

$$\sin \epsilon = \epsilon = \frac{\sqrt{3}}{2} \cdot \frac{e}{a}. \qquad OH = a + \frac{e}{2}.$$

Thus the centrifugal force of blade 2, Fig. 184*b* is

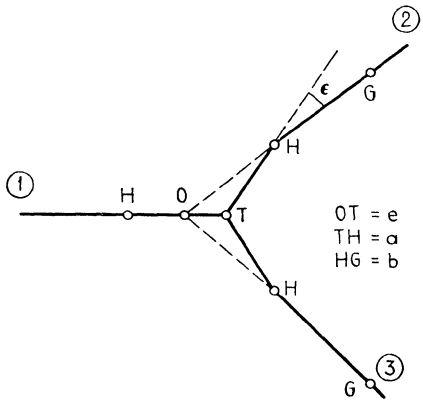


FIG. 184*b*.

$m_b\omega^2(a + b + e/2)$, directed along GH. This force is now resolved into components parallel and perpendicular to OT. The component parallel to OT (to the right) is

$$m_b\omega^2\left(a + b + \frac{e}{2}\right)\cos\left(60° - \epsilon\right)$$

$$= m_b\omega^2\left(a + b + \frac{e}{2}\right)(\cos 60° + \epsilon \sin 60°)$$

$$= m_b\omega^2\left(a + b + \frac{e}{2}\right)\left(\frac{1}{2} + \frac{3}{4}\frac{e}{a}\right)$$

$$= m_b\omega^2\left[\frac{1}{2}(a + b) + e\left(1 + \frac{3}{4}\frac{b}{a}\right)\right] \quad (a)$$

For blade 3 the result is the same for reasons of symmetry, while the components of centrifugal force perpendicular to OT for

blades 2 and 3 cancel each other. The centrifugal force of blade 1 in the direction OT (to the left) is

$$m_b\omega^2(a + b - e) \tag{b}$$

The centrifugal force of the hub itself (to the right) is

$$m_{\text{hub}}\omega^2 e \tag{c}$$

Thus the total centrifugal force to the right is twice Eq. (*a*) less Eq. (*b*) plus Eq. (*c*):

$$\omega^2 e\left[m_{\text{hub}} + m_b\left(3 + \frac{3}{2}\cdot\frac{b}{a}\right)\right]$$

Let

$$m_{\text{hub}} + 3m_b = M, \text{ the total mass,}$$

and

$$\mu = \frac{3m_b}{M}, \text{ ratio of hinged mass to total mass.}$$

Then the total centrifugal force can be written:

$$M\omega^2 e\left(1 + \frac{\mu b}{2a}\right)$$

Equate this to the elastic force ke, and the critical frequency comes out:

$$\omega^2 = \frac{k}{M}\cdot\frac{1}{1 + \mu b/2a} \tag{d}$$

It is seen that for the case of no hinged mass, $\mu = 0$, the natural frequency is k/M: the presence of the hinged mass diminishes this frequency. The relation is shown graphically by the fully drawn curve of Fig. 184*c*. Although the above analysis was carried out for a three-blade rotor, the result is good also for a rotor with more than three blades, which is shown in small type on page 316.

In the case of a *two*-bladed rotor, however, the result comes out differently. Figure 184*d* shows the equivalent of Fig. 184*b*, this time for two blades. Before repeating the analysis for this case, we notice that in Fig. 184*d* the eccentricity OT has been drawn perpendicular to the line HH connecting the two hinges. If we had assumed the other extreme case: that of an eccentricity OT in the direction of the hinge line HH, the angle ϵ would have been zero, the hinges would not have deflected at all, and consequently

the frequency would have come out just $\omega^2 = k/M$, without any hinge effect. With the position shown in Fig. 184*d* the hinge effect is as great as it can be. The principal steps in the calcula-

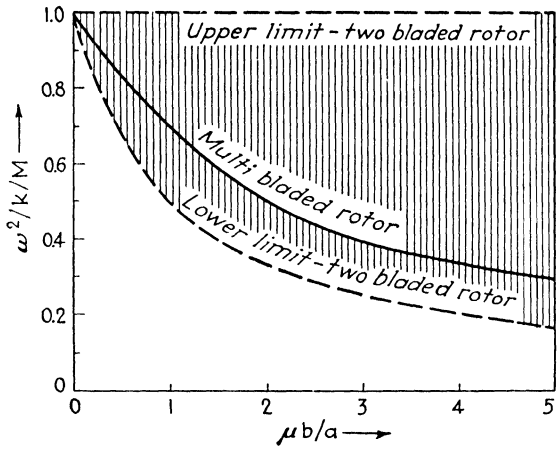


FIG. 184*c*.

tion of Fig. 184*d* are

$$\sin \epsilon = \epsilon = \frac{e}{a} \qquad OH = a$$

$$\text{Centrifugal force of one blade} = m_b\omega^2(a + b)$$

$$\text{Component parallel } OT = m_b\omega^2(a + b)\frac{e}{a}$$

$$\text{Total centrifugal force to right} = 2m_b\omega^2(a + b)\frac{e}{a} - m_{\text{hub}}\omega^2 e$$

$$= M\omega^2 e\left[1 + \frac{\mu b}{a}\right],$$

in which μ is again the ratio of the hinged mass to the total mass:

$$\mu = \frac{2m_b}{(2m_b + m_{\text{hub}})} = \frac{2m_b}{M}$$

Setting the total centrifugal force again equal to the spring force ke leads to the critical speed:

$$\omega^2 = \frac{k}{M}\frac{1}{1 + \mu b/a} \qquad (e)$$

represented by the dotted line in Fig. 184*c*.

For the case that the whirl eccentricity is at angle α_0 with respect to the hinge line *II*, *II*, it

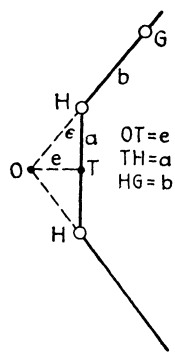


FIG. 184*d*.

will be shown in small type below that Eq. (*e*) modifies to the more general

$$\omega^2 = \frac{k}{M}\frac{1}{1 + \mu b \sin^2 \alpha_0/a} \qquad (f)$$

which reduces to Eq. (*e*) for $\alpha_0 = 90$ deg., and which gives plainly $\omega^2 = k/M$ for $\alpha_0 = 0$ deg. and a value for the frequency in between these two extremes for α_0 between zero and 90 deg. It must be concluded then that for a two-bladed rotor a large amplitude whirl at some value of α_0 is possible for any speed of rotation in the shaded region of Fig. 184*c*. Thus the two-bladed rotor has a *region* of instability, shown shaded in Fig. 184*c*, whereas a multibladed rotor just has a simple critical speed above which it becomes stable again. All of this is in good agreement with experiment.

In order to write the general theory for a multibladed rotor we start with a single blade located at an arbitrary angle α with respect to the direction of eccentricity OT as shown in Fig. 184*e*. With the same assumption as before, that the eccentricity e is small with respect to a, we have in the triangle OTH:

$$OS = e \sin \alpha; \qquad \epsilon = \frac{e}{a} \sin \alpha; \qquad OH = HS = HT - ST = a - e \cos \alpha$$

The centrifugal force of this blade thus is

$$m_b\omega^2(a + b - e \cos \alpha)$$

The component of this force in the direction OT of the eccentricity is

$$\begin{aligned}
&-m_b\omega^2(a + b - e \cos \alpha) \cos (\alpha + \epsilon) = \\
&-m_b\omega^2\left[(a + b) \cos \alpha - e\left(1 + \frac{b}{a} \sin^2 \alpha\right) + \cdots\right] = \\
&-m_b\omega^2\left[(a + b) \cos \alpha - e\left(1 + \frac{b}{2a}\right) + e\frac{b}{2a} \cdot \cos 2\alpha\right]
\end{aligned}$$

Now let the rotor have N equally spaced blades. The angle between blades is $2\pi/N = \Delta$, and if the angle α of the first blade be α_0, then the angle α of the $(p + 1)st$ blade is $\alpha_0 + p\Delta$. Substituting this value for the angle α and adding for all blades we find for the component along OT of the centrifugal forces of all blades:

$$-m_b\omega^2\left[(a + b) \sum_{p=r}^{p=N-1} \cos (p\Delta + \alpha_0) - Ne\left(1 + \frac{b}{2a}\right) + \frac{be}{2a} \sum_{p=0}^{p=N-1} \cos (2p\Delta + 2\alpha_0)\right], \qquad (g)$$

The first of the sums appearing in this expression can be interpreted as the sum of the horizontal projections of the individual vectors of the star of the blades. Since the total resultant of the vectors themselves is zero, so is the horizontal projection. The second sum is a star of vectors with double angles 2Δ between them, which for a multibladed rotor again has a zero resultant. Thus both sums disappear and the OT component of centrifugal force is simply

$$m_b\omega^2 Ne\left(1 + \frac{b}{2a}\right)$$

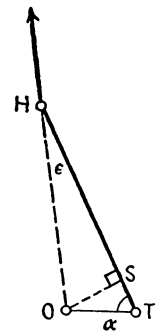


FIG. 184e.

Adding to this the hub force $m_{hub}\omega^2 e$ and setting the sum equal to the elastic force ke leads to the result equation (d), independent of the number of blades N or of the direction of the whirl α_0.

For a two-bladed rotor the summations in Eq. (g) come out differently. The first sum is $\cos\alpha_0 + \cos(180 + \alpha_0)$, which is zero as before. The second sum however becomes $\cos 2\alpha_0 + \cos(360 + 2\alpha_0) = 2\cos 2\alpha_0$. This makes the centrifugal force component for a two-bladed rotor equal to

$$m_b\omega^2\left[2e\left(1 + \frac{b}{2a}\right) - \frac{be}{a}\cdot\cos 2\alpha_0\right] = 2m_b\omega^2 e\left[1 + \frac{b}{a}\sin^2\alpha_0\right]$$

Adding to this the centrifugal force of the hub and equating the sum to ke leads to the result equation (f).

51. Gyroscopic Effects.—The disk of Fig. 167, being in the middle of the span, will vibrate or whirl in its own plane. When the disk is placed near one of the bearings, and especially when it is located on an overhung shaft, it will *not* whirl in its own plane. Then the system of Fig. 185b will have a (primary) critical speed different from the one of Fig. 185a, the mass and shaft stiffness being the same in both cases. This is due to the fact that the centrifugal forces of the various particles of the disk do not lie in one plane (Fig. 186) and thus form a couple tending to straighten the shaft. Before calculating this moment, it is necessary to have a clear picture of the mode of motion.

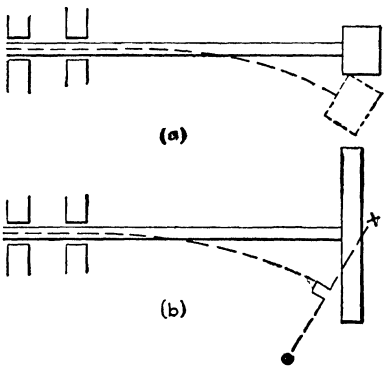


FIG. 185.—The critical speeds of (a) and (b) are *not* equal if the shafts are identical and the masses at the end are equal.

We assume the machine to be completely balanced and whirling at its critical speed in some slightly deflected position. The angular velocity of the whirl of the center of the shaft is assumed to be the same as the angular velocity of rotation of the shaft. This implies that a particular point of the disk which is outside (point · in Fig. 185*b*) will always be outside; the inside point × always remains inside; the shaft fibers in tension always remain in tension while whirling, and similarly the compression fibers always remain in compression. Thus any individual point of the disk moves in a circle in a plane perpendicular to the undistorted center line of the shaft.

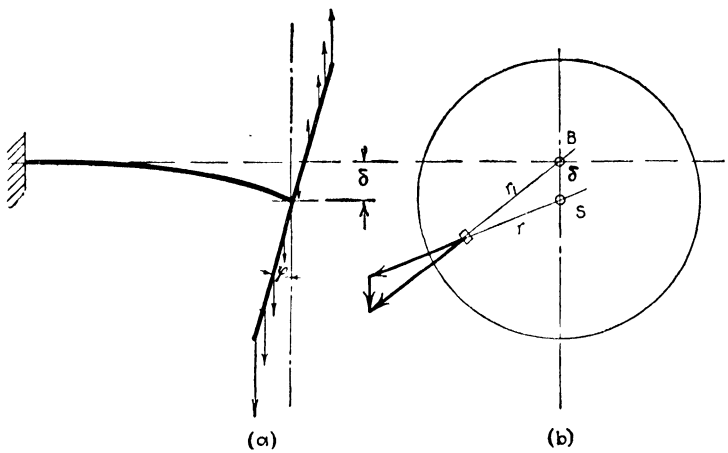


FIG. 186.—The centrifugal forces on the disk tend to bend the disk to a plane perpendicular to the equilibrium position of the shaft. Thus these forces act as an additional spring.

Figure 186 shows the centrifugal forces set up by this motion. In Fig. 186*b* we see that the centrifugal force of a mass element dm is $\omega^2 r_1 dm$ directed away from the point B. This force can be resolved into two components: $\omega^2\delta \cdot dm$ vertically down and $\omega^2 r\, dm$ directed away from the disk or shaft center S. The forces $\omega^2\delta \cdot dm$ for the various mass elements add together to a single force $m\omega^2\delta$ (where m is the total mass of the disk) acting vertically downward in the point S of Fig. 186*b*. The forces $\omega^2 r\, dm$ all radiate from the center of the disk S, and their influence becomes clear from Fig. 187, as follows. The y-component of the force $\omega^2 r dm$ is $\omega^2 y\, dm$. The moment arm of this elemental force is $y\varphi$, where φ is the (small) angle of the disk with respect to the vertical. Thus the moment of a small particle dm being $\omega^2 y^2 \varphi$

dm, the total moment $\mathbf{M}$ of the centrifugal forces is

$$\mathbf{M} = \omega^2\varphi\int y^2 dm = \omega^2\varphi I_d$$

where I_d is the moment of inertia of the disk about one of its diameters.

Thus the end of the shaft is subjected to a force $m\omega^2\delta$ and to a moment $\omega^2 I_d\varphi$, under the influence of which it assumes a deflection δ and an angle φ. This can happen only at a certain speed ω, and the calculation of the critical speed is thus reduced to a static problem, namely that of finding at which value of ω a shaft will deflect δ and φ under the influence of $P = m\omega^2\delta$ and $\mathbf{M} = I_d\omega^2\varphi$.

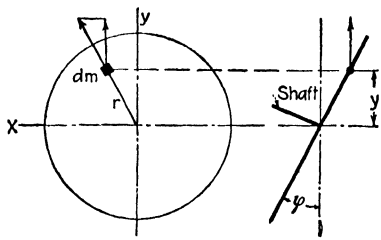


FIG. 187.—Calculation of the moment of the centrifugal forces.

For a rotating overhung cantilever shaft of stiffness EI and length l, this calculation will now be carried out in detail.

From the strength of materials the formulas for the deflection and angle of the end of a cantilever due to a force P or a moment $\mathbf{M}$ are

$$\delta_P = \frac{Pl^3}{3EI}; \qquad \varphi_P = \frac{Pl^2}{2EI}; \qquad \delta_{\mathbf{M}} = \frac{\mathbf{M}l^2}{2EI}; \qquad \varphi_{\mathbf{M}} = \frac{\mathbf{M}l}{EI}$$

With these formulas we write

$$\delta = (m\omega^2\delta)\frac{l^2}{3EI} - (I_d\omega^2\varphi)\frac{l^2}{2EI}$$
$$\varphi = (m\omega^2\delta)\frac{l^2}{2EI} - (I_d\omega^2\varphi)\frac{l}{EI}$$

which after rearranging become

$$\left(m\omega^2\frac{l^3}{3EI} - 1\right)\delta + \left(-I_d\omega^2\frac{l^2}{2EI}\right)\varphi = 0$$
$$\left(-m\omega^2\frac{l^2}{2EI}\right)\delta + \left(\omega_d I_d\frac{l}{EI} + 1\right)\varphi = 0$$

This homogeneous set of equations can have a solution for δ and φ only when the determinant vanishes (see page 157 or 167), which gives the following equation for ω^2:

$$\omega^4 + \omega^2\frac{12EI}{mId^3}\left(\frac{ml^2}{3} - I_d\right) - \frac{12E^2I^2}{mId^4} = 0$$

This can be solved for ω^2. Before doing so we prefer to bring the equation to a dimensionless form with the variables:

$$K = \omega\sqrt{\frac{ml^3}{EI}} \qquad \text{(the critical speed function)}$$

and

$$D = \frac{I_d}{ml^2} \qquad \text{(the disk effect)}$$

The equation then becomes

$$K^4 + K^2\left(\frac{4}{D} - 12\right) - \frac{12}{D} = 0$$

with the solution

$$K^2 = \left(6 - \frac{2}{D}\right) \pm \sqrt{\left(6 - \frac{2}{D}\right)^2 + \frac{12}{D}} \tag{152}$$

of which only the plus sign will give a positive result for K^2 or a real result for K.

The formula (152) is plotted in Fig. 188 of which the ordinate K^2 is the square of the "dimensionless natural frequency," *i.e.*,

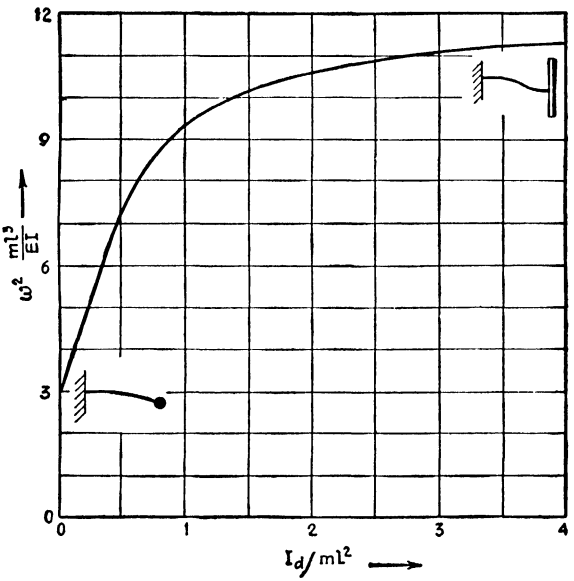


FIG. 188.—Change in the natural frequency caused by the stiffening effect of the centrifugal forces in the system Fig. 185.

the square of the factor by which $\sqrt{EI/ml^3}$ must be multiplied to obtain that frequency. The abscissa is the "disk effect" D, which is zero for a concentrated mass. In that case the frequency of Fig. 185*a* is $\omega^2 = 3EI/ml^3$. On the other hand for $I_d = \infty$ (a disk for which all mass is concentrated at a large radius), no finite angle φ is possible, since it would require an infinite torque, which the shaft cannot furnish. The disk remains parallel to itself and the shaft is much stiffer than without the disk effect. The frequency is $\omega^2 = 12EI/ml^3$.

The phenomenon just described is generally referred to in the literature as a *gyroscopic effect.* The name is unfortunate since in the usual sense of the word a gyroscope is a body which rotates very fast and of which the axis of rotation moves slowly. In the disk just considered the whirl of the axis of rotation is just as fast as the rotation itself, so that it could hardly be called a gyroscope.

A true gyroscope effect occurs in the experimental set-up of Fig. 212, page 361, where a small motor is suspended practically

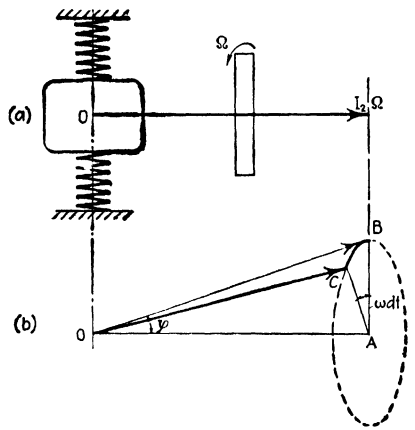


FIG. 189.—Explains the gyroscopic effect of the apparatus shown in Fig. 212 (page 361).

at its center of gravity by three very flexible springs. We want to calculate the natural frequencies of the modes of motion for which the center of gravity O remains at rest and the shaft whirls about O in a cone of angle 2φ (Fig. 189*b*). The disk on the motor shaft rotates very fast, and, as the springs on which the motor is mounted are flexible, the whirl takes place at a very much slower rate than the shaft rotation.

Let

Ω = (fast) angular velocity of disk rotation,

ω = (slow) angular velocity of whirl of the shaft center line,

I_1 = moment of inertia of the stationary and rotating parts about an axis through O perpendicular to the paper,

I_2 = moment of inertia of rotating parts about shaft axis,

k = torsional stiffness of the spring system, *i.e.*, the torque about O for $\varphi = 1$ radian.

Further let the direction of rotation of the disk be counterclockwise when viewed from the right so that the angular momentum vector $I_2\Omega$ is as shown in Fig. 189*a*. In case the whirl is in the same direction as the rotation, the time rate of change of the angular momentum of the disk is directed from B toward C in Fig. 189*b*, *i.e.*, out of the paper toward the reader. This is equal to the moment exerted *by* the motor frame on the disk. The reaction, *i.e.*, the moment acting *on* the motor, is pointing into the paper and therefore tends to make φ smaller. This acts as an addition to the existing spring stiffness k, so that it is seen that a whirl in the direction of rotation makes the natural frequency higher. In the same manner it can be reasoned that for a whirl opposite to the direction of rotation the frequency is made lower by gyroscopic effect.

To calculate the magnitude of the effect we see in Fig. 189*b* that

$$\frac{d(I_2\Omega)}{I_2\Omega} = \frac{BC}{OB} = \frac{BC}{AB} \cdot \frac{AB}{OB} = \omega\, dt \cdot \varphi$$

Consequently

$$\frac{d}{dt}(I_2\Omega) = \omega\varphi I_2\Omega$$

is the gyroscopic moment. The elastic moment due to the springs k is $k\varphi$, and the total moment is

$$(k \pm \omega\Omega I_2)\varphi$$

where the plus sign holds for a whirl in the same sense as the rotation and the minus sign for a whirl in the opposite sense. Since the parenthesis in this last expression is the equivalent spring constant, we find for the natural frequencies

$$\omega_n^2 = \frac{k \pm \omega\Omega I_2}{I_1}$$

or

$$\omega_n^2 \mp \frac{I_2}{I_1}\Omega\omega_n - \frac{k}{I_1} = 0$$

or

$$\omega_n = \pm\frac{I_2}{2I_1}\Omega \pm \sqrt{\left(\frac{I_2\Omega}{2I_1}\right)^2 + \frac{k}{I_1}} \tag{153}$$

Of the $\pm$ ambiguity before the square root, only the plus sign need be retained since the minus sign gives two negative values

for ω_n which are equal and opposite to the two positive values obtained with the plus sign before the square root.

The result (153) is shown in Fig. 190, where the ordinate is the ratio between the actual natural frequency and the one without gyroscopic effect, *i.e.*, with a non-rotating shaft. The abscissa is the rotor speed multiplied by some constants so as to make the quantity dimensionless. It is seen that the natural frequency is split into two frequencies on account of the gyroscopic effect: a slow one whereby the whirl is opposed to the rotation, and a fast one where the directions are the same.

In the quasi-gyroscopic phenomenon of Fig. 186 the frequency is raised by the disk effect for a whirl having the *same* direction as the rotation. The case of a whirl *opposed* to the rotation with a lowered frequency is said to have been observed also in the system of Fig. 186, but it is difficult to understand how such a mode could be excited.

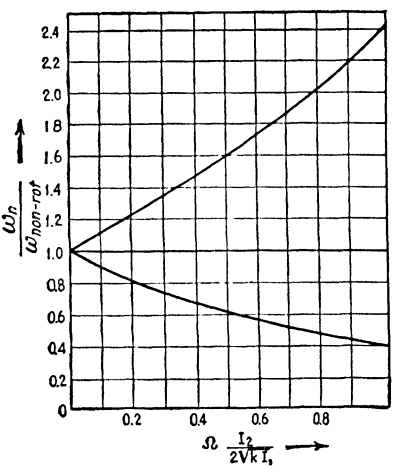


FIG. 190.—The two natural frequencies of Fig. 189; with the faster one of the two, the precession ω has the same direction as the rotation Ω; with the slower frequency these directions are opposite.

52. Frame Vibration in Electrical Machines.—Between the stator and rotor of any electric motor or generator magnetic forces exist which have a small rapid variation in intensity with a frequency equal to the number of rotor teeth passing by the stator per second. These alternating forces may cause vibrations in the stator frame if they are in resonance with one of its natural frequencies. For constant-speed machinery such trouble, if it ever appears, can easily be corrected by changing the stiffness of the frame and thus destroying the resonance. If, however, the machine is to run satisfactorily over a wide range of speeds, it is necessary to look for other means of avoiding the trouble. The situation in this respect is quite analogous to that for Diesel engines as discussed in Secs. 43 to 45.

The number of teeth in the rotor multiplied by its r.p.m.

usually leads to a very high frequency, and the amplitudes of vibration observed in practice are invariably so small that no danger for the structural safety of the machine need be feared. The frequency, however, is in the range of greatest sensitivity of the human ear so that noise considerations become of importance. In submarine motors, which have very light frames and thus are apt to be noisy, the problem is of special interest since such noise may be picked up by the enemy sound detectors.

The details of the phenomenon will first be explained with the help of Fig. 191, which represents one stator pole and a part of the rotor. The magnetic force $\mathbf{R}_1$ acting between the stator and the rotor can be conveniently resolved into its normal and tangential components $\mathbf{N}_1$ and $\mathbf{T}_1$. These forces are nearly

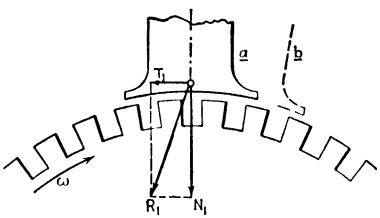


FIG. 191.—The normal and tangential components of the force R_1 exerted by the rotor on a pole of the stator.

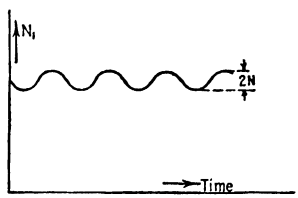


FIG. 192.—Variation of the magnetic force with the time.

constant with respect to time; however, they are subjected to small variations of amplitude $\mathbf{N}$ and $\mathbf{T}$ with the frequency of the rotor teeth passing by the stator (Fig. 192). A calculation of the exact phase relation of this variation (*i.e.*, a calculation of the position of the rotor teeth with respect to the pole at the instant that $\mathbf{N}$ or $\mathbf{T}$ becomes zero) requires electrical theory which is not necessary for our present purpose. It is sufficient to know that both $\mathbf{N}$ and $\mathbf{T}$ go through a full cycle of variation each time a tooth goes by, *i.e.*, each time that the relative position between rotor and pole passes from *b* to *a* in Fig. 191.

Before investigating how the variation of $\mathbf{N}$ and $\mathbf{T}$ can excite vibration, we shall discuss the possible motions of the frame.

Consider an eight-pole machine for submarine application (Fig. 193). In such a construction the poles are comparatively heavy and the "frame" consists of a rolled-up steel plate to which the poles are bolted. Thus the poles practically form the "masses" and the frame shell the "elasticity" of the system.

Since each pole as a solid body has six degrees of freedom (page 34), the whole frame must have 48 different natural modes of motion. Some of these are trivial (*e.g.*, the six possible motions of the whole frame as a solid body), and many of the others pos-

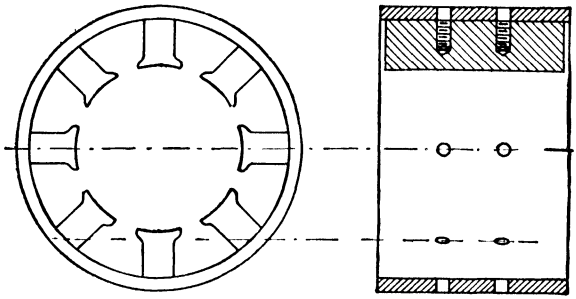


FIG. 193.—Stator of submarine motor generator.

sess natural frequencies which are far removed from the frequency of the variation of the magnetic forces **N** and **T.** Four of the natural modes that have been causing trouble in an actual installation are shown in Figs. 194*a* to *d*.

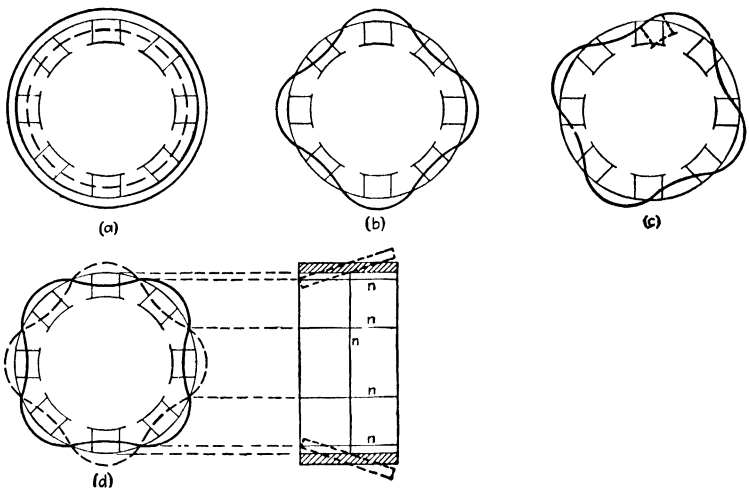


FIG. 194.—Four natural modes of motion of the frame shown in Fig. 193.

In the first of these figures the poles move parallel to themselves in a radial direction, while the frame ring alternates between the purely extended and compressed states. In Fig. 194*b* the motion of the individual poles is the same as before, but the consecutive poles are 180 deg. out of phase and the frame is in bending.

Figure 194*c* shows a rotation of the poles about their longitudinal axes with bending in the frame. These three cases have the common property that all cross sections of a pole lying in planes perpendicular to the axis of rotation have the same motion. This is not the case in Fig. 194*d*. Here the poles rotate about their transverse axes, and the frame ring is in combined twist and bending. There are eight nodal generators and one central nodal circle on the cylinder, all denoted by n in the figure.

Assume first that the rotor teeth and slots are parallel to the axis of rotation, the forces **T** or **N** reaching their maximum value at the same instant all along a pole. It is clear that the motions of Fig. 194*a* and *b* may be affected by the normal force **N**; the tangential force **T** will act only on Fig. 194*c*, while the motion of Fig. 194*d* will not be excited at all, because, if the normal force helps the motion at one end of a pole, it opposes the motion at the other end of the same pole.

Even if there is a large variation in **N** of the same frequency as the natural frequency of modes 194*a* or *b*, these modes are not necessarily excited. If the number of rotor teeth per pole (total number of teeth divided by 8) is an integer, the force $\mathbf{N}_1$ becomes a maximum at all poles at the same time. Then, of course, Fig. 194*a* is excited, but the work input for Fig. 194*b* is zero over a full cycle of the vibration. (While the force **N** pulls the four downgoing poles downward and does positive work, the same force pulls down on the upgoing poles and there does equal negative work.) On the other hand, if there are $n + \frac{1}{2}$ teeth per pole, Fig. 194*b* is excited and Fig. 194*a* is not. A similar consideration holds for Fig. 194*c* which is excited by the tangential variation **T** if there are $n + \frac{1}{2}$ teeth per pole.

It is clear that a changing of the number of teeth per pole is not alone sufficient to avoid an excitation of all four modes of motion at once.

Another possibility of affecting the phenomenon consists in "skewing" the slots or teeth of the armature with respect to the axis of rotation. Figure 195 shows how the teeth are skewed by one full tooth pitch over the length of the rotor. In this case the forces **N** or **T** at any one instant vary from point to point along the length of the pole, and it can be seen that the diagram of the force as a function of position along the pole must be identical with the diagram of the force at one point

of the pole as a function of the time. At the side of Fig. 195 the diagram of force as function of position is drawn, the force variation not being necessarily sinusoidal.

Since **N** and **T** are the variable parts of N_1 and T_1, their integrated values over a full cycle are zero (Fig. 192). In particular, in Fig. 195 it is seen that the pull between pole and rotor along one half of the pole length is compensated by a push on the other half of the pole length.

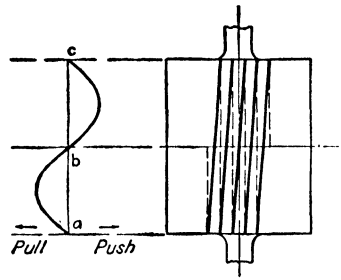


FIG. 195.—Variation of the time-variable part of the magnetic force along a generating line of a rotor with whole-pitch skewing.

With a machine built as in Fig. 195, it is clear that no excitation at all is given to the modes of Figs. 194*a*, *b*, and *c*, irrespective of the number of teeth per pole. Now, however, trouble is to be expected from the motion of Fig. 194*d*. It is true that the total integrated value of the forces **N** and **T** over the whole pole length is zero, but that is of no consequence in connection with Fig. 194*d*. The total force is zero only because it is pulling down on one side and pushing up on the other side. The motion 194*d*, however, is also up on one side and down on the other side, which creates the possibility of a great input of energy.

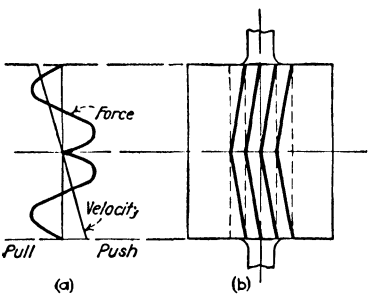


FIG. 196.—Force diagram for herringbone skewing.

In order to circumvent this difficulty, "herringbone" skewing has been proposed in the fashion of Fig. 196*b*, where the slope of the teeth is at the rate of one full tooth pitch over *half* the rotor length. In this arrangement the force diagram (which again may or may not be sinusoidal) is shown in Fig. 196*a*. The radial velocity diagram of the various points along the pole is a straight line (Fig. 194*d*). It can be easily verified that the work input per cycle, which is proportional to the integrated product of the two curves of Fig. 196*a*, is zero. It is also seen that the force by itself, integrated over the pole length, is zero. A herringbone skewed rotor of full tooth pitch over half the rotor length will make the frame free from vibration in any

of the four modes of Fig. 194, independent of the number of teeth per pole.

53. Vibration of Propellers.—Since the introduction of aluminum-alloy propellers in airplanes, a number of fatigue failures have occurred. Some of these were noted in time to avoid failure, being seen in the form of cracks, but in other cases either an entire blade or the tip of a blade has blown away in mid-air. The fact that these failures were unmistakably due to fatigue makes it certain that they were caused by vibration. Before entering into the possible excitations to which a propeller blade may be subjected, it is of interest to consider the determination of its natural frequencies. These are different for various running speeds, because the centrifugal force tends to force the vibrating beam back to its middle position, thus acting like a spring force.

A propeller blade is a complicated system. It can be idealized as a cantilever beam, but the mass per unit length and the bending stiffness EI vary along the length. An exact calculation of the natural frequency, even without the centrifugal effect, is out of the question. For each particular case we can calculate the frequency by Rayleigh's method by choosing some probable shape of the deformation and determining the potential and kinetic energies. In this case the potential energy will consist of two parts, one due to bending and one due to the centrifugal effect. As is always true with Rayleigh's method, the answer thus found for the natural frequency is somewhat *too large* (pages 181 and 200).

The actual evaluation of the frequency in this manner requires involved calculations, which can be avoided by applying the following theorem:

Theorem of Southwell: If in an elastic system the spring forces can be divided into two parts so that the total potential energy is the sum of the two partial potential energies, then the natural frequency ω of that system can be calculated approximately from

$$\omega^2 = \omega_1^2 + \omega_2^2 \tag{154}$$

where ω_1 and ω_2 are the *exact* natural frequencies of the (modified) system in which one of the spring effects is absent. The value ω thus found is somewhat *too small*.

A very simple case illustrating this statement is that of a single mass m connected to a wall with two coil springs k_1 and k_2 in parallel (Figs. 32*a*, *b*, page 49). The natural frequency of this system is $\omega^2 = (k_1 + k_2)/m$ which is exactly equal to $\omega_1^2 + \omega_2^2 = \frac{k_1}{m} + \frac{k_2}{m}$. The answer is exact in this case because the configuration of the vibration is not changed by omitting one of the springs.

Applied to the propeller blade, the theorem states that a good approximation for the natural frequency when rotating (ω) can be derived by the relation (154) from the exact natural frequency at standstill (ω_1) and the exact natural frequency of a chain without bending stiffness of the same mass distribution as the blade and rotating at full speed (ω_2).

For the proof of Southwell's theorem we apply Rayleigh's procedure to the exact shape of the vibrating blade while rotating. In that shape let

P_{ben} = potential energy due to bending,

P_{cen} = potential energy due to centrifugal forces,

$\omega^2 K$ = kinetic energy, where ω^2 is the (exact) natural frequency of vibration.

Then,

$$\omega^2_{\text{exact}} = \frac{P_{\text{ben}} + P_{\text{cen}}}{K} = \frac{P_{\text{ben}}}{K} + \frac{P_{\text{cen}}}{K}$$

We find the *exact* answer for the natural frequency because the exact configuration was assumed (see page 172). But the exact shape of vibration while rotating is different from the exact shape at standstill and also differs from the shape of the rotating chain. Yet the first shape may be considered as an approximation to the latter two. Thus the two terms on the right side of the above equation are Rayleigh approximations of ω_1 and ω_2 (*i.e.*, of the exact standstill frequency and the exact chain natural frequency). Since Rayleigh's approximations are always *too large*,

$$\frac{P_{\text{ben}}}{K} + \frac{P_{\text{cen}}}{K} \geqslant \omega_1^2 + \omega_2^2$$

or

$$\omega^2 \geqslant \omega_1^2 + \omega_2^2$$

the error being of the same order as usually obtained with Rayleigh's method.

The usefulness of the theorem lies in the fact that the standstill frequency ω_1 can be easily determined by experiment on the actual propeller. The chain frequency ω_2, which expresses the effect of rotation, can be calculated without much difficulty.

In the case of a central hub of negligible dimension compared with the blade length we find for the chain frequency the remarkably simple result

$$\omega_2 = \Omega \tag{155}$$

i.e., the natural frequency of vibration of a chain rotating about one of its ends O as a center is equal to the angular velocity of its rotation. This is true independent of the mass distribution along the chain, which can be understood as follows.

Since the flat side of a propeller blade lies practically in the plane of its rotation, in the slowest type of vibration the various particles will move nearly perpendicular to the plane of rotation, *i.e.*, parallel to the axis of rotation. Assume that the deflection curve of the chain is a straight line at a small angle φ with respect to the plane of rotation OA (Fig. 197*a*). Consider an element dm at a distance r from O. On this element are acting the tensions above and below (which are in line with the chain) and the centrifugal force $\Omega^2 r\ dm$. If φ is small, equilibrium in the vertical direction requires that the tension below exceeds the tension above by this amount. In the horizontal direction there is a resultant force of $\varphi \cdot \Omega^2 r\ dm$ toward the equilibrium position. The deflection of the element dm from equilibrium is φr, since the "curve" was assumed straight. Thus this excess force can be considered as a spring force with a spring constant $k = \Omega^2 dm$. The frequency of vibration of *this particle* is $\omega_n = \sqrt{k/m} = \sqrt{\Omega^2 dm/dm} = \Omega$. The same answer is found for any particle along the line. Hence we may conclude that the assumed straight line is the exact deformation curve, for, if this were not so, we should have found different frequencies for the individual particles. (In Rayleigh's procedure a nonexact curve is presupposed; in this case the individual particles have different calculated frequencies. In integrating the energies over all the particles, Rayleigh finds some sort of average of all these frequencies.)

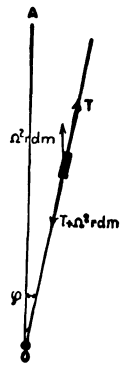


FIG. 197*a*.—Calculating the natural frequency of a rotating heavy chain.

We have proved that the first natural frequency of the small vibrations of a chain, as shown in Fig. 197*a*, equals its angular speed, and, since in the proof no mention was made of the mass distribution, the result is true for any distribution of the mass.

Another manner of showing this is by means of Rayleigh's method. Again assume a straight line for the deformation curve. On a particle dm the centrifugal force is $\Omega^2 r\, dm$. When moving from the equilibrium position A to the position C of Fig. 197*b*, the particle travels against the centrifugal force over a distance $AB = r\varphi^2/2$. Thus the potential energy in the element is $\Omega^2 r\, dm \cdot r\varphi^2/2$ and the total potential energy of the chain is

$$Pot = \frac{\Omega^2\varphi^2}{2}\int_0^l r^2 dm = \frac{1}{2}\Omega^2\varphi^2 I_0$$

If the chain is vibrating harmonically with a frequency ω_2, the kinetic energy of the particle dm is $\frac{1}{2}\, dm \cdot v^2 = \frac{1}{2}\, dm \cdot \overline{BC}^2 \cdot \omega_2^2 = \frac{1}{2}\, dm\varphi^2 r^2 \omega_2^2$, and for the whole chain

$$Kin = \frac{\omega_2^2\varphi^2}{2}\int_0^l r^2\, dm = \frac{1}{2}\omega_2^2\varphi^2 I_0$$

Equating the two energies gives the desired result, $\omega_2 = \Omega$, which is independent of mass distribution.

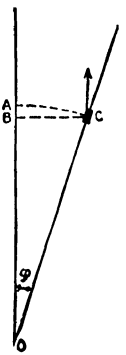


FIG. 197*b*.—Potential energy of an element of a rotating chain.

We obtain finally as an approximation for the first natural frequency of the rotating propeller blade

$$\omega^2 = \omega_1^2 + \Omega^2$$

For higher modes the result is quite similar; it can be expressed generally by

$$\omega_{\text{rot}}^2 = \omega_{\text{non-rot}}^2 + a\Omega^2 \qquad (156)$$

where Ω is the speed of rotation and a a numerical factor which differs for the different modes and which has been found to be approximately as follows:

Mode 1, $a \approx 1.5$
Mode 2, $a \approx 6$
Mode 3, $a \approx 12$

The principal source of excitation of blade vibration is found in torsional impulses on the crank shaft of the engine. A common manner in which the relation (156) is plotted is shown in Fig. 198, in which two families of curve are given. The first set are parabolas showing the relation between the natural frequencies of a blade in its various modes and the speed of rotation as expressed by Eq. (156). The other set is a star of straight lines passing through the origin, expressing the relation between the exciting frequency and the speed. These

straight lines have slopes equal to the order of vibration, *i.e.*, to the number of oscillations per revolution. For four-cycle, internal-combustion engines, such as are commonly used on aircraft, the orders occurring are either integer or half-integer numbers, as shown in the figure. Any intersection of one of the straight lines of exciting frequency with one of the curves of natural frequency indicates a possible condition of resonance in torsional vibration.

The determination of the natural frequencies of the non-rotating blade, *i.e.*, the intersections of the parabolas with the ordinate axis of Fig. 198, is not so simple as appears on first sight. This is because the bending frequency of a blade cannot be considered

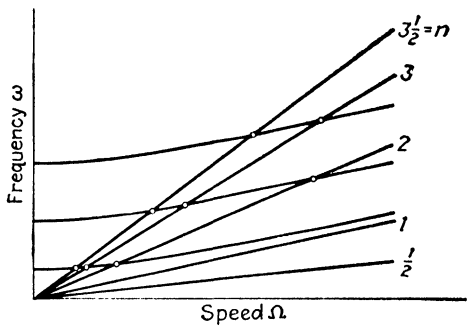


FIG. 198.—Diagram showing straight lines of exciting frequency and parabolas of natural frequency. Intersections are points of resonant speed.

separately from the torsional oscillation of an engine crank shaft; the two effects are coupled together. Thus the frequency of vibration of a blade is different for different engines attached. Still it is desirable to have a criterion by which to determine the characteristics of an arbitrary propeller, independently of the engine to which it is attached. This is possible by means of the reasoning shown in connection with Figs. 199*a*, *b*, and *c*.

Imagine the shaft cut at the hub of the propeller, as in Fig. 199*a*. The amplitude of torque transmitted through the cut is $\mathbf{M}_0 \sin \omega t$ and the amplitude of torsional oscillation at the cut is $\varphi_0 \sin \omega t$. Looking at the propeller alone, *i.e.*, at the left-hand side of Fig. 199*a*, there is a definite ratio between $\mathbf{M}_0$ and φ_0 which is independent of the magnitude of φ_0 but which will be a function of the frequency of oscillation. This ratio $\mathbf{M}_0/\varphi_0$, sometimes known as the *mechanical impedance* of the propeller, is plotted in the full line of Fig. 199*b*. The various shapes

of natural vibration belonging to various frequencies are shown in their proper positions in Fig. 199*c*. The curve of Fig. 199*b* shows a number of points of zero ordinate and another series of points of infinite ordinate. In the first set of points the torque at the propeller hub is zero, so that these points are the natural frequencies of the propeller with a free hub. The other series of points of infinite ordinate show a zero angle for a finite torque and therefore are the natural frequencies with clamped hub. The actual condition of the hub lies between that of completely

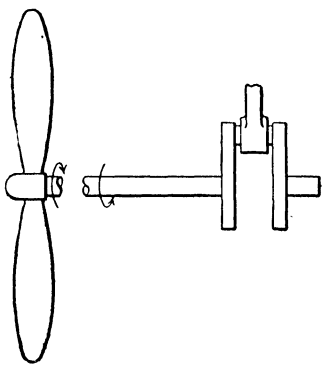


FIG. 199*a*.—The system divided into two parts for purpose of analysis.

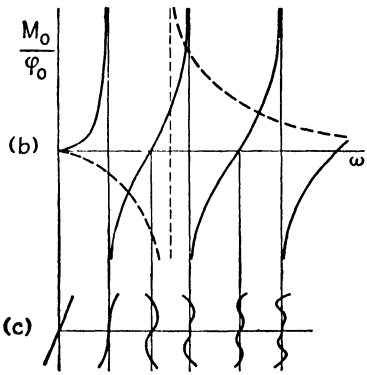


FIG. 199*b*.—Impedance diagram for the left half of Fig. 199*a* (full line) and for the right half of Fig. 199*a* (dashed line). FIG. 199*c*.—Shapes of blade vibration at various frequencies.

free and that of completely clamped and depends on the properties of the engine to which it is attached.

Now turning our attention to the right-hand half of Fig. 199*a* and again plotting the ratio of torque to angle (with a negative sign), we obtain the dotted line of Fig. 199*b*. This is the curve for the (negative) "mechanical impedance" of the engine and is the usual resonance curve for the single-degree-of-freedom system of Fig. 40. For a natural frequency of the combined system, Fig. 199*a*, it is necessary that the moment-angle ratios to the left and to the right are the same. In other words, the natural frequencies of the combined system are the intersections between the dotted curve and the full curve of Fig. 199*b*. These are the frequencies that must be inserted on the ordinate axis of Fig. 198, and then Fig. 198 determines the critical speeds of the system caused by a purely torsional excitation.

Vibrations due to other causes have been observed in propeller blades. When the engine is out of balance, the center of the propeller hub may move back and forth laterally, which is a motion entirely independent of torsion, and associated with a displacement of the center of gravity of the engine. The primary cause of such a condition is of course unbalance, but it has also been found as a direct result of torque variation. If, for instance, there is a certain clearance in the main bearings of the engine, or if the crank-shaft structure is flexible, the periodic thrust variations on the crank pin due to the firing cylinders may cause the crank shaft to deform and move within its bearing clearance so that the center of gravity is displaced. Since all of this is due to internal forces in the system, a displacement of the center of gravity of the rotating parts must be associated with a displacement of the center of gravity of the stationary parts, which include the bearing near the hub of the propeller. In this manner, lateral motions of the center of the propeller hub with the firing frequency are possible.

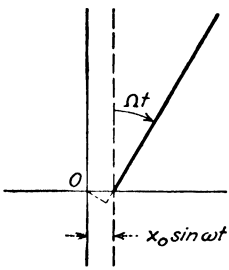


FIG. 200.

A lateral motion of the center of the propeller hub with a frequency ω does not, however, cause stress variations in the propeller of that same frequency, but rather of the frequency $\omega + \Omega_{\text{prop}}$ or $\omega - \Omega_{\text{prop}}$, as will be explained presently. If, as usual, the propeller is geared to the engine so that the propeller speed is related to the engine speed by a fairly complicated fraction such as $9/16$, then an observation of the frequency of stress variation in the propeller makes it possible to distinguish between a vibration caused by pure torsional excitation and one caused by lateral excitation. In order to understand the frequency relation just mentioned, consider Fig. 200. A propeller blade is shown to rotate with angular speed Ω_{prop}, while its hub is moving back and forth laterally through the distance $x_0 \sin \omega t$. The displacement $x_0 \sin \omega t$ is now resolved into its components along the blade and perpendicular to the blade. The displacement along the blade does not excite any bending in it, but the displacement across the blade is entirely responsible for just that. Thus the displacement of the blade root in a direction perpendicular to that of the blade is

$$x_0 \sin \omega t \cdot \sin \Omega_{\text{prop}} t$$

which, by means of the trigonometric relations of page 17, is equal to

$$\frac{x_0}{2}\cos(\omega - \Omega_{\text{prop}})t - \frac{x_0}{2}\cos(\omega + \Omega_{\text{prop}})t$$

This lateral motion of the blade root will cause bending vibrations in the blade of the same frequencies as the root displacement, which proves the contention made above. If the lateral displacement of the blade root had been assumed vertically or in a different phase with respect to the rotation, exactly the same result would have been obtained, as can be easily verified.

Still another possible excitation of bending vibrations in propeller blades is that due to aerodynamic forces. In the usual construction of large airplanes a propeller is mounted in front of a wing and consequently each blade comes close to the wing twice in the course of one revolution. The velocity field of the air close to the wing is different from that at some distance from it so that the aerodynamic forces acting on the propeller blade will pass through a periodic change twice per revolution. This has been found to cause bending vibrations in the blade.

Summarizing, it may be stated that bending vibrations in a propeller blade caused by torsional excitation have a frequency equal to an integer or a half-integer multiple of the engine speed; those caused by lateral vibration of the propeller hub have a frequency equal to an integer or a half-integer multiple of the engine speed $\pm$ the propeller speed; and finally, the bending vibrations caused by aerodynamic excitation have a frequency which is a multiple of the propeller speed.

The internal friction in propeller blades of steel or aluminum is very small and the only damping that the vibrations experience is aerodynamic and is of the same nature as that discussed with reference to ship propellers on page 262. In Fig. 161, a vibratory motion of the blade in its limber direction causes periodic variations in the angle of attack α and consequently periodic variations in the aerodynamic lift force. The reader is urged to follow this phenomenon in detail and to verify the statement that the lift-force variation caused by this motion will be directed against the velocity of the motion and thus constitutes a true damping. This is true only for relatively slow frequencies, for the reasoning leading to this conclusion concerning damping presupposes a "succession of steady states." It will be seen in Chap. VII, page 392, that for very fast frequencies and high air

speeds this reasoning is no longer valid and that under such circumstances the blade may experience "negative damping" and get into a state of "flutter." When such a condition obtains, the aerodynamic forces become very large, of the same order almost as the spring forces and the inertia forces, so that even the frequency of the fluttering blade is considerably different from the natural bending frequency as calculated without air forces.

Not only aircraft propellers but also ship propellers have been responsible for serious cases of vibration during the last decade. The excitation of a ship propeller falls into two classes: torsional and linear. When an individual blade passes close by the hull of the ship or by the "bossing" that holds the propeller tube in place, it finds itself in a region of flow which is different from that in the more or less open water. Consequently the hydrodynamic forces are different so that these forces experience variations with the blade frequency, *i.e.*, the frequency of revolution of the propeller multiplied by its number of blades. The torque variation caused by this effect is more serious when the bossings are close to the propeller than when they are cut away. At present there is not a great deal of detailed knowledge available on the subject but a figure which represents a good average condition is a torque variation equal to 7.5 per cent of the total propeller torque. This effect is responsible for the fact that even in steam-turbine drives the main propulsion shafting of a ship has been found to experience definite resonant speeds. It has become standard practice to precalculate these speeds, as discussed on page 247 and in Problem 92.

The other effect caused by the variation in the hydrodynamic forces of the propeller is found in their reactions on the ship's hull and on the bossings. These force variations were determined by F. M. Lewis on an experimental model in a tank and were found to be as large as 12.5 per cent of the total propeller thrust. Naturally, this figure is very much dependent on the bossing clearance and the tip clearance of the propeller but it represents a good average figure for ships of conventional design up to date. These hull forces are responsible for the vibrations usually observed on the afterdecks of steamships. They were not considered to be of any great importance until the great French liner "Normandie" brought the matter into the lime-

light. In that case it happened that the propeller forces were of the same frequency as one of the natural frequencies of the entire ship as a "free-free" beam (page 193) so that oscillations of considerable magnitude were set up. The trouble was cured primarily by replacing the three-bladed propellers by four-bladed ones which eliminated this resonant condition. The reader is further referred to the interesting literature on the subject.

54. Vibration of Steam-turbine Wheels and Blades.—In the mechanical construction of large-reaction steam turbines we can distinguish two principal types, which may be designated as the disk type and the drum type. In the disk type the rotor or spindle consists of a shaft on which a number of disks are shrunk. The diameter of these disks is about four times as large as the shaft diameter, and the turbine blades are attached to the rim of the disks. With the drum type the spindle consists of a hollow forging of a diameter equal to the outside diameter of the disks in the disk type, and the blades are fastened directly to the outside of this spindle.

In both types fatigue failures of the blades have occurred. Whereas in the drum type the failures have been restricted to the blades themselves, in the disk type the breaks have been found to extend into the solid parts of the disks as well.

As in the case of the airplane propeller we have a resonance phenomenon between the natural frequency of vibration of the disk and some multiple of the running speed. Before proceeding to an explanation of the origin of the disturbing forces, it is necessary to have a clear understanding of the natural modes of vibration. First consider a disk at standstill (*i.e.*, without rotation). The center is clamped on the shaft, and the periphery with the blades is free to vibrate. In such a system there are infinitely many modes of natural motion, of which only a few are of importance for this problem. The four modes which have caused failures in the past are those in which the periphery bends into a sine wave with 4, 6, 8, or 10 nodes designated as the flexural modes of $n = 2, 3, 4, 5$, respectively.

The first two of these, being the most important ones, are illustrated in Fig. 201. In producing these figures the disk is held in a horizontal plane and evenly covered with light sand. Vibration is excited (usually by an alternating-current magnet of variable frequency), and at resonance the sand is thrown away from the vibrating parts of the disk and accumulates on the nodal

lines. The circumference of the disk thereby divides up into an even number of equal parts which alternate in moving up and down. The signs + and − written in at the locations of the antinodes pertain to a certain instant of time. At that instant, the plus sign indicates that the disk is deflected upward and the minus sign that it is deflected downward. After half a vibration period these signs are reversed. At the nodes, of course, no motion takes place at all. The 8- and 10-noded motions are not illustrated but can be easily visualized. The deflections along the circumference are such that, if the perimeter is developed into

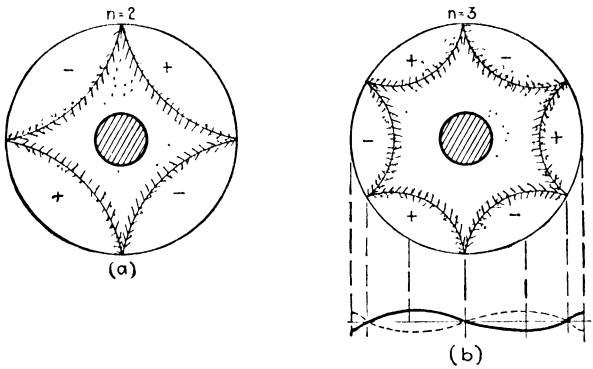


FIG. 201.—The four- and six-noded modes of vibration of a turbine disk.

a straight line, the deflections appear approximately as sine curves with n full cycles for the $2n$-noded vibration.

In the *rotating* disk the conditions are only slightly different. The whole Fig. 201 now revolves with the angular velocity Ω of the wheel. Moreover, the centrifugal forces which are set up by the rotation will raise the frequency of the vibration and also alter the shape of the natural mode. The latter effect is of little importance and will not be considered. The rise in the natural frequency ω follows the same trend as in the propeller blade of the previous section, *i.e.*, it is expressed approximately by the parabolic relation

$$\omega^2 = \omega^2_{\text{non-rot}} + B\Omega^2 \tag{157}$$

where Ω is the angular velocity of rotation and B is a numerical factor which is greater than unity and has different values for different modes of vibration, as discussed on page 331. The derivation of this formula is very similar to the derivation of Eq. (156); only it is much more complicated on account of the substitution of a plate for the beam of the previous problem.

A vibration in the modes of Fig. 201 may be excited in the rotating disk by a constant force standing still in space, *e.g.*, by the steam jet of a stationary nozzle playing on the disk. This can be understood from Fig. 202, which represents one nth part of the developed perimeter of the disk vibrating in its $2n$-noded mode. The amplitude varies periodically with the

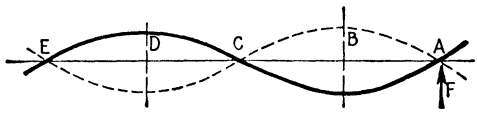


FIG. 202.—A steady, stationary force F can put work into a rotating and vibrating disk.

time between the full-drawn and the dotted curves. Simultaneously the curve (with its nodal points A, C, and E) moves to the right with the circumferential speed of the wheel. The force F remains fixed in space. Let the period of vibration and the circumferential speed be related in such a manner that when the point C has arrived at A one-half period of oscillation has passed so that the periphery will then have the dotted shape. To be more precise, let the relation be such that, when the force F is

opposite A, the full curve exists;
opposite B, no deflections exist anywhere;
opposite C, the dotted line is the shape;
opposite D, no deflections, etc.

Thus while the piece AC of the curve passes by the force F, that curve goes from its full-drawn to its dotted shape. During this time all points of the curve AC have an upward velocity so that F does positive work. But while CE passes by F, the shape goes from the dotted to the full line, which again is associated with upward velocities in the stretch CE, so that F again does positive work. The stretch AC in that interval of time goes downward to its full line position, but then it is not situated opposite F.

The speed at which this relation holds is called the "critical speed" of the disk; it exists when $1/n$th revolution occurs during one vibration period:

$$\left.\begin{aligned} \text{r.p.s.} = \frac{f}{n}; \qquad \Omega = \frac{\omega}{n} \\ \omega^2 = \omega^2_{\text{non-rot}} + B\Omega^2 = n^2\Omega^2 \end{aligned}\right\} \tag{158}$$

As was stated before, B is larger than unity, so that this equation coincides with (156). Therefore, it can be represented by Fig. 198, with the understanding that resonance in the $2n$-noded mode occurs at the intersection point of the parabola with the line of slope n. In particular we see that the two-noded mode ($n = 1$, one nodal diameter) can never be excited by a constant force F. Also, excitations of half-integer order do not occur in the turbine.

It is clear from Fig. 198 that a great number of critical speeds are possible. The disks in a turbine vary considerably in size from the high-pressure to the low-pressure ends, and in most cases there will be one or more disks among them in which the cluster of critical speeds ranges around the operating speed. This accounts for the great number of failures which occurred before the cause was understood.

To overcome the trouble, the disks are so designed that their criticals do not coincide with the running speed. Since in the first place the analysis is too crudely developed to permit great accuracy in this calculation, and since the frequency depends quite sensibly on the amount of shrink pressure at the center, the design is carried out in an empirical manner by comparison with previous constructions. After the turbine is built and assembled, the frequencies of those disks in which trouble may be expected are determined by experiment (excitation at variable frequency either by a mechanical vibrator or by means of an alternating-current magnet). In case such a frequency lies too close to the service speed, it is changed by a "tuning" process consisting of machining a thin layer of metal from the disk, usually near its periphery. The minimum difference between the critical and the running speed which is tolerated in practice is given as 15 per cent for the 4-noded mode and as 10 per cent for the 6- and 8-noded vibrations.

With turbines of the *drum* type fatigue failures of the individual blades or of groups of blades have occurred repeatedly. The explanation is exactly the same as for the disks; a drum with a row of blades can be regarded as a disk of which the central portion is infinitely stiff. There exist, however, other possibilities of resonance than the one just described. Imagine a turbine (disk or drum type) in which the blades are attached only at their base and are not connected either by a shrouding ring or

by lashing wires, so that each blade can vibrate individually. If there is a single nozzle, the first mode of vibration of the blade (without nodes except at the base) can be excited if the rotational speed is such that an integer number of vibration cycles occurs during one revolution. This is because if the blade passes by the jet, while the blade is receding in its vibratory motion, the jet does positive work on it. If the number of vibrations per revolution is an integer, the phase of the vibratory motion is the same each time the blade comes in contact with the jet. This opens up a large number of possibilities for trouble. In practically all turbines, however, the blades are connected either completely or else in groups of approximately eight blades. Such a group of blades has natural frequencies that may be excited in the manner just described.

This particular phenomenon has been responsible for a series of serious failures during the last few years. The blades in question were in the first impulse stage of turbines of very high pressure and temperature: 1,200 lb./sq. in. pressure at 900°F. The blades themselves were about 1 in. high and 1 in. deep, and under the influence of the very thick steam at high velocity developed 100 hp. each. They are found to fail in fatigue after an operation of some 5 hr. The natural frequency of the blades was such that approximately 60 full cycles occurred during one revolution. This put the various consecutive critical speeds only 1.5 per cent apart so that it was impossible to avoid resonance by tuning. Ordinarily it would be expected that a blade, after having passed the steam nozzle and having acquired a certain amplitude of vibration by the steam impact of that nozzle, would execute a damped vibration from there on and in the ensuing 60 cycles practically lose all of its amplitude. Then, coming back to the nozzle, it would get a new impact. The blades in question were calculated to be sufficiently strong to stand this variable loading. It was found, however, that the internal damping in the blades were so small that at the end of 60 cycles, *i.e.*, at the end of a full revolution, the amplitude of vibration had hardly diminished so that the blade would enter the jet with a substantial amplitude. Thus with proper phase conditions the amplitude could be pushed up to a value many times greater than that caused by a single exposure to the jet. The surprising fact was brought to light that the internal

hysteresis at temperatures approaching that of the red-hot state is considerably smaller than the hysteresis at room temperature. A partial cure for the trouble consists in rounding off the edges of the steam jet by providing suitable leakage passages in the nozzle. For further details, the reader is referred to the publications by Kroon quoted in the Bibliography.

In reaction turbines no actual nozzles exist in the blading such as would account for the definite force F of Fig. 202. However, any deviation from radial symmetry of the pressure distribution acts in the same manner as a nozzle. While rotating, the blade passes through a periodic pressure field of which the fundamental component has the frequency of revolution, and in which most of the higher harmonics are present as well. Consider as an example the nth harmonic of this field. It is capable of exciting vibration, if the blade rotates at the rate of n natural periods per revolution. The phase of the motion will be such that while passing through the regions of great nth harmonic pressure, the blade recedes in its vibratory motion, whereas in regions of low pressure it is coming forward. We see that, in principle, resonance can occur if any natural frequency of a blade or blade group is an integer multiple of the speed of rotation, provided the pressure is unevenly distributed around the circumference.

Problems

99. On a horizontal platform are two small motors A and B, their shafts parallel and horizontal, at distance $2a$ apart. The motors are unbalanced, each producing a rotating centrifugal force. The motors rotate at equal speeds in the same direction and their two centrifugal forces are equal in magnitude, but one of them runs by the constant angle α ahead of the other.

a. If C denotes the instantaneous intersection of the two centrifugal forces through A and B, prove that the locus of C is a circle passing through A and B with its center somewhere on the perpendicular bisecting AB.

b. Using this result, prove that the resultant of the two centrifugal forces is a single rotating force rotating about a fixed point located on the perpendicular bisector of AB at a distance $a \tan \alpha/2$ from AB.

100. Find the critical speed in revolutions per minute of the system shown in Fig. 167 in which the disk is made of solid steel with a diameter of 5 in. and a thickness of 1 in. The total length of the steel shaft between bearings is 20 in., and its diameter is $\frac{1}{2}$ in. The bearings have equal flexibility in all directions, the constant for either one of them being $k = 100$ lb./in.

101. The same as Problem 100 except that the bearings have different vertical and horizontal flexibilities: $k_{\text{hor}} = 100$ lb./in. and $k_{\text{vert}} = 200$ lb./in. for *each* of the bearings.

102. Figure 203 shows a machine with a rigid overhung rotor. The initial unbalance consists of 1 in. oz. in the center of the main rotor and of 2 in. oz.

on the overhung disk, 90 deg. away from the first unbalance. Find the corrections in the planes I and II.

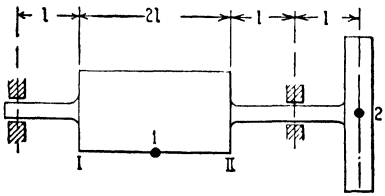


FIG. 203.

103. A rotor is being balanced in the machine of Fig. 175, pivoted about the fulcrum F_1. The following amplitudes of vibration are observed at the critical speed:

1. 14 mils for the rotor without additional weights.
2. 10 mils with 3 oz. placed in location 0 deg.
3. 22 mils with 3 oz. placed in location 90 deg.
4. 22 mils with 3 oz. placed in location 180 deg.

Find the weight and location of the correction (Fig. 176).

104. In the balancing process we make the following observations:

a_0 = amplitude of vibration of the unbalanced rotor "as is."

a_1 = amplitude with an additional one-unit correction at the location 0 deg.

a_2 = same as a_1 but now at 180 deg.

The ideal rotor, unbalanced only with a unit unbalance (and thus *not* containing the original unbalance), will have a certain amplitude which we cannot measure. Call that amplitude x. Let the unknown location of the original unbalance be φ.

Solve x and φ in terms of a_0, a_1, and a_2, and show that in this answer there is an ambiguity in sign. Thus *four* runs are necessary to determine completely the diagram of Fig. 176.

105. In a Thearle balancing machine (page 298), the total mass of the rotating parts is M, the eccentricity e, the mass of each of the balls at the ends of the arms is m, and the arm radius r. Find the angle α which the arms will include in their equilibrium position when released about the resonant speed.

106. A steel disk of 5 in. diameter and 1 in. thickness is mounted in the middle of a shaft of a total length of 24 in. simply supported on two rigid bearings (Fig. 167). The shaft diameter is ½ in.; it is made of steel also. The shaft has filed over its entire length two flat spots (Fig. 183*a*), so that the material taken away on either side amounts to $\frac{1}{500}$ part of the cross section (total loss in cross section $\frac{1}{250}$). Find the primary and secondary critical speeds.

Find the amplitude of the secondary alternating force, and calculate the unbalance which would cause an equal force at the primary critical speed.

107. A shaft of length $2l$ and bending stiffness EI is supported on two bearings as shown in Fig. 204. The bearings allow the shaft to change its

angle freely but prevent any deflection at those two points. The disk at the end has a moment of inertia I_p about its axis of rotation. (Thus I is measured in in.^{4}, and I_p in lb. in sec.^{2}). The mass of the disk is m. Find the critical speed.

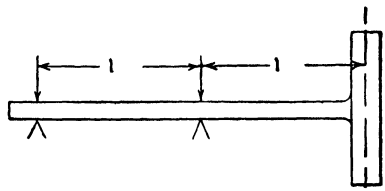


FIG. 204.

108. Calculate the abscissas and ordinates of several points on the curves of Fig. 198 by means of Eq. (156).

109. A solid disk of mass M and radius R is keyed to a stiff and weightless shaft, supported by springs k_1 and k_2 at distances a_1 and a_2. The nearer

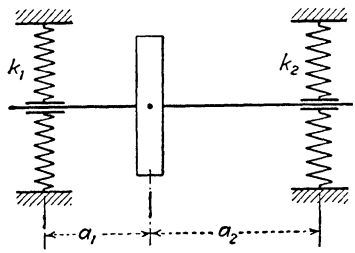


FIG. 205*a*.

spring is the stiffer one, so that $k_1a_1 = k_2a_2$ (Fig. 205*a*). The shaft rotates at speed Ω. Calculate the natural frequencies of the system and plot them in the form ω/ω_a against Ω/ω_a, where $\omega_a^2 = (k_1 + k_2)/M$ and $\omega_b^2 = (k_1a_1^2 + k_2a_2^2)/\frac{1}{4}MR^2 = 4\omega_a^2$.

110. Generalize the problem of page 318 by dropping the assumption that the disk whirls at the same speed as its rotation. Let the rotational speed be ω as before and the whirl speed be ω_w, positive forward and negative backward. Show that there are four natural frequencies; plot them against the speed ω for the special case where the shaft length equals the disk diameter.

111. A cantilever shaft has a stiffness EI over a length l and is completely stiff over an additional distance l_1 (Fig. 205*b*). The stiff part has a total

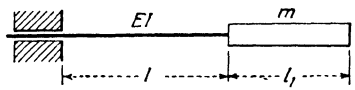


FIG. 205*b*.

mass m while the flexible part is supposedly massless. Calculate the natural frequencies as a function of l_1/l between the values $0 < l_1/l < 1$, and plot the result in a curve.

112. In a laboratory experiment one small electric motor drives another through a long coil spring (n turns, wire diameter d, coil diameter D). The two motor rotors have inertias I_1 and I_2 and are distance l apart.

a. Calculate the lowest torsional natural frequency of the set-up.

b. Assuming the ends of the spring to be "built in" to the shafts, calculate the r.p.m. of the assembly at which the coil spring bows out at its center, due to whirling.

113. The drive of an aerodynamic wind tunnel consists of a driving motor I_1 coupled to a large fan I_2 which drives the air through the wind tunnel. The torsional elasticity between the motor and the fan is k, and the tunnel is idealized as an organ pipe of length l and cross section A (Fig. 205*c*).

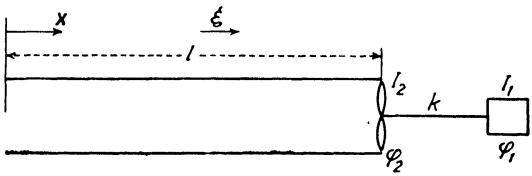


FIG. 205*c*.

The coupling between the fan and the air column is expressed by two constants C_1 and C_2 with the following meaning: C_1 is a pitch constant relating the air displacement in the tunnel to the angular displacement of the fan: $\xi = -C_1\varphi_2$. The second constant C_2 relates the forward torque on the fan to the pressure variation in the air column at the fan, so that the fan torque variation is $C_2 d\xi/dx$. In both these expressions x is the distance along the tunnel measured from left to right and ξ is the alternating component of the air displacement, positive to the right.

Set up the differential equations of the system and from it deduce the frequency equation.

CHAPTER VII

SELF-EXCITED VIBRATIONS

55. General.—The phenomena thus far discussed were either free vibrations or forced vibrations, accounting for the majority of troublesome cases which occur in practice. However, disturbances have been observed which belong to a fundamentally different class, known as *self-excited vibrations*. The essence of the difference can best be seen from a few examples.

First consider an ordinary single-cylinder steam engine, the piston of which executes a reciprocating motion, which may be considered a "vibration." Evidently the force maintaining this vibration comes from the steam, pushing alternately on the two sides of the piston.

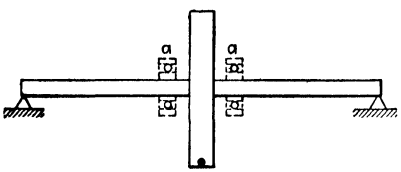


FIG. 206.—Unbalanced shaft as an example of forced vibration.

Next consider an unbalanced disk mounted on a flexible shaft running in two bearings (Fig. 206). The center of the disk vibrates, the motion being maintained by the centrifugal force of the unbalance pushing the disk alternately up and down.

The steam engine is a case of *self-excited* vibration, while the disk executes an ordinary *forced* vibration. Imagine that the piston is prevented from moving by clamping the crosshead or the flywheel. Then the valves do not move either, and hence *no alternating* steam *force* acts on the piston.

On the other hand, let us prevent the disk from vibrating. This can be done, for example, by mounting two ball bearings *a*, *a* on the shaft adjacent to the disk and attaching their outer races to a solid foundation, thus preventing vibration of the disk but leaving the rotation undisturbed. Since the unbalance is still rotating, *the alternating force remains.*

Thus we have the following distinction:

In a self-excited vibration the alternating force that sustains the motion is created or controlled by the motion itself; when the motion stops the alternating force disappears.

In a forced vibration the sustaining alternating force exists independently of the motion and persists even when the vibratory motion is stopped.

Another way of looking at the matter is by defining a self-excited vibration as a free vibration with *negative damping.* It must be made clear that this new point of view does not contradict the one just given. An ordinary positive viscous damping force is a force proportional to the velocity of vibration and directed opposite to it. A negative damping force is also proportional to the velocity but has the same direction as the velocity. Instead of diminishing the amplitudes of the free vibration, the negative damping will increase them. Since the damping force, whether positive or negative, vanishes when the motion stops, this second definition is in harmony with the first one.

Examine the differential equation of a system having a single degree of freedom with negative damping:

$$m\ddot{x} - c\dot{x} + kx = 0 \qquad (18A)$$

Since this equation differs from (18) on page 49 only in the sign of c, its solution can be written as

$$x = e^{+\frac{c}{2m}t}(A \cos qt + B \sin qt) \qquad (24A)$$

which is clearly a vibration with exponentially increasing amplitude (Fig. 207).

A system with positive damping is sometimes said to be *dynamically stable,* whereas one with negative damping is known as *dynamically unstable.* There is a difference between *static* and *dynamic* stability. A mechanical system is statically stable if a displacement from the equilibrium position sets up a force (or couple) tending to drive the system back to the equilibrium position. It is statically unstable if the force thus set up tends to increase the displacement. Therefore static instability means a *negative spring constant* k or, more generally, a negative value of one of the natural frequencies ω^2.

Figure 207 shows the behavior of a system in three different stages of stability. It is to be noted that dynamic stability always presupposes static stability (Fig. 207*c*), but that the converse is not true: a statically stable system may yet be dynamically unstable (Fig. 207*b*).

Regarding the *frequency* of the self-excited vibration, it may be said that in most practical cases the negative damping force is very small in comparison to the elastic and inertia forces of the motion. If the damping force were zero, the frequency would be the *natural* frequency. A damping force, whether positive or negative, lowers the natural frequency somewhat, as expressed by Fig. 36, page 54. However, for most practical cases in mechanical engineering this difference is negligible, so that then *the frequency of the self-excited vibration is the natural frequency of the system.* Only when the negative damping force is large in comparison with the spring or inertia forces does the frequency differ appreciably from the natural frequency. Such

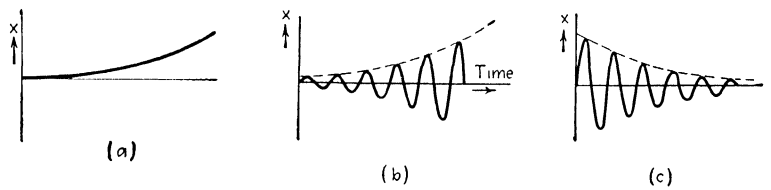


FIG. 207.—The free motion of a system in various states of stability. (*a*) Statically unstable; (*b*) statically stable but dynamically unstable; (*c*) statically and dynamically stable.

cases, which are known as "relaxation oscillations," are discussed on page 439. The steam engine is an example, as the negative damping force of the steam is very much greater than the spring force (which is wholly absent). Hence, for the engine, the frequency of vibration differs appreciably from the natural frequency (which is zero).

A consideration of the energy relations involved will also serve to give a better understanding. With positive damping, the damping force does negative work, being always opposed to the velocity; mechanical energy is converted into heat, usually in the dashpot oil. This energy is taken from the vibrating system. Each successive vibration has less amplitude and less kinetic energy, and the loss in kinetic energy is absorbed by the damping force. In the case of negative damping the damping force (which is now a driving force) does positive work on the system. The work done by that force during a cycle is converted into the additional kinetic energy of the increased vibration. It is clear that self-excited vibration cannot exist without an extraneous source of energy, such as the steam boiler in our first example. The source of energy itself should not have the alter-

nating frequency of the motion. In most cases the energy comes from a source without any alternating properties whatever, for example, a reservoir of steam or water under pressure, a steady wind, the steady torque of an engine, etc. However, there are a few cases (discussed on page 449) where the source is alternating with a high frequency, much higher than that of the vibration it excites.

With a truly *linear* self-excited system the amplitude will become infinitely large in time, because during each cycle more energy is put into the system (Fig. 207*b*). This infinitely large amplitude is contrary to observation. In most systems the mechanisms of self-excitation and of damping exist simultaneously and separately. In Fig. 43 the energy per cycle is plotted against the amplitude of vibration. For a linear system this energy follows a parabolic curve since the dissipation per cycle is $\pi c\omega x_0^2$ (see page 68). If the negative damping force is also linear, another parabola will designate the energy input per cycle. The system is self-excited or is damped according to which parabola lies higher. In all practical cases, however, either the input or the damping, or both, are non-linear and the input and dissipation curves intersect. If in Fig. 43 the amplitude happens to be OA, more energy is put in than is dissipated, so that the amplitude grows. On the other hand, if the amplitude happens to be OC, there is more damping than self-excitation and the vibration will decrease. In both cases the amplitude tends toward OB where energy equilibrium exists. The motion thus executed is an undamped steady-state free vibration.

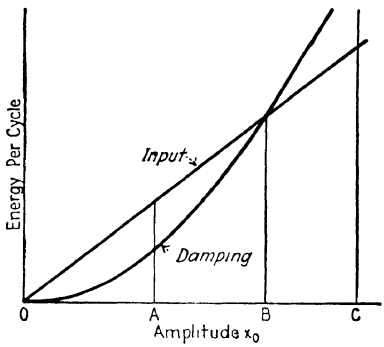


FIG. 43.—Work per cycle performed by a harmonic force and by a viscous damping force for various amplitudes.

Since the non-linearity of the damping or input forces leads to great mathematical complication (see Chap. VIII), we usually assume linear systems of very small amplitude and determine whether the damping or the energy input is the stronger. If the system is found to be unstable, it means merely that the amplitude will *begin* to build up; how far this building up will develop depends on the nature of the non-linearity.

In electrical engineering, self-excited vibrations are of even greater importance than in the mechanical field. The electrical analogue of a forced vibration was seen to be an LC circuit with an alternator all in series (Fig. 25, page 38). An electrical self-excited system is exemplified by an oscillating vacuum-tube circuit. The B-battery is the non-alternating source of energy; the frequency is determined by the L and C values of the plate circuit, and the negative damping or feed-back is supplied by the grid.

56. Mathematical Criterion of Stability.—For single-degree-of-freedom systems, such as are discussed in Secs. 57 to 60, a simple physical reasoning usually suffices to show the negativity of the damping constant c. Thus the criterion of dynamic stability can be derived by physical rather than by mathematical means. With systems of two or three degrees of freedom, a physical conception is always very helpful but usually does not give a complete interpretation of what happens. A mathematical approach is necessary, and this involves at first the setting up of the differential equations of the problem. As long as we deal with small vibrations (and thus disregard any non-linearities that may exist), the equations are all linear and of the second order, of the type (52) or (89). Their solution, as usual, is found by assuming

$$\left.\begin{aligned} x_1 &= x_{1\max} e^{st} \\ x_2 &= x_{2\max} e^{st} \\ &\cdots\cdots \\ x_n &= x_{n\max} e^{st} \end{aligned}\right\} \tag{159}$$

where s is a complex number the real part of which determines the damping and the imaginary part of which is the natural frequency. Substituting (159) into the differential equations of the free vibration transforms these equations into a set of n homogeneous, linear algebraic equations in the (complex) unknowns $x_{1\max} \ldots x_{n\max}$. A process of algebraic elimination is then performed with the result that one equation is obtained which does not contain any of these variables. This equation, known as the "frequency equation," is generally of the degree $2n$ in s. Thus, for a two-degree-of-freedom system we obtain a quartic; for a three-degree-of-freedom system we obtain a sixth-degree equation, etc.

An algebraic equation of degree $2n$ in the variable s has $2n$ roots or $2n$ values of s. Real roots of s would lead to terms e^{st} in the solution, which rarely occur in ordinary vibrating systems

(Fig. 34, page 52). The roots of s are usually complex and then they always occur in conjugate pairs:

$$\begin{aligned} s_1 &= p_1 + jq_1 \\ s_2 &= p_1 - jq_1 \\ s_3 &= p_2 + jq_2 \\ s_4 &= p_2 - jq_2 \\ &\cdots \end{aligned}$$

The solution of the first differential equation is

$$x_1 = C_1 e^{s_1 t} + C_2 e^{s_2 t} + C_3 e^{s_3 t} + \cdots$$

From Eqs. (21), (23), and (24), page 53, we know that these terms can be combined by pairs as follows:

$$C_1 e^{s_1 t} + C_2 e^{s_2 t} = e^{p_1 t}(A \sin q_1 t + B \cos q_1 t)$$

so that the imaginary part of s is the frequency, and the real part of s determines the rate of damping. *If the real parts of all the values of s are negative, the system is dynamically stable; but if the real part of any one of the values of s is positive, the system is dynamically unstable.*

Therefore the stability can be determined by an examination of the signs of the real parts of the solutions of the frequency equation. It is not necessary to solve the equation, because certain rules exist by which from an inspection of the coefficients of the equation a conclusion regarding the stability or instability can be drawn. These rules, which were given by *Routh* in 1877, are rather complicated for frequency equations of higher degree, but for the most practical cases (third and fourth degree) they are sufficiently simple.

Let us consider first the cubic equation

$$s^3 + A_2 s^2 + A_1 s + A_0 = 0 \tag{160}$$

which occurs in the case of two degrees of freedom where one mass or spring is zero (in a sense one and one-half degrees of freedom). If its roots are s_1, s_2, and s_3, (160) can be written

$$(s - s_1) \cdot (s - s_2) \cdot (s - s_3) = 0$$

or

$$s^3 - (s_1 + s_2 + s_3)s^2 + (s_1 s_2 + s_1 s_3 + s_2 s_3)s - s_1 s_2 s_3 = 0 \tag{161}$$

A comparison with (160) shows that

$$\left.\begin{aligned} A_2 &= -(s_1 + s_2 + s_3) \\ A_1 &= s_1s_2 + s_1s_3 + s_2s_3 \\ A_0 &= -s_1s_2s_3 \end{aligned}\right\} \tag{162}$$

One of the three roots of a cubic equation must always be real, and the other two are either real or conjugate complex. Separating the roots s_1, s_2, s_3 into their real and imaginary parts, we may write

$$\begin{aligned} s_1 &= p_1 \\ s_2 &= p_2 + jq_2 \\ s_3 &= p_2 - jq_2 \end{aligned}$$

Substituted into (162) this leads to

$$\left.\begin{aligned} A_2 &= -(p_1 + 2p_2) \\ A_1 &= 2p_1p_2 + p_2^2 + q_2^2 \\ A_0 &= -p_1(p_2^2 + q_2^2) \end{aligned}\right\} \tag{163}$$

The criterion of stability is that both p_1 and p_2 be negative. It is seen in the first place that *all coefficients* A_2, A_1, *and* A_0 *must be positive,* because, if any one of them were negative, (163) requires that either p_1 or p_2, or both p_1 and p_2, must be positive. This requirement can be proved to hold for higher degree equations as well. Hence a frequency equation of any degree with one or more negative coefficients determines an unstable motion.

Granted that the coefficients A_0, A_1, and A_2 are all positive, the third equation (163) requires that p_1 be negative. No information about p_2 is available as yet. However, on the boundary between stability and instability, p_2 must pass from a positive to a negative value through zero. Make $p_2 = 0$ in (163) and

$$\left.\begin{aligned} A_2 &= -p_1 \\ A_1 &= q_2^2 \\ A_0 &= -p_1q_2^2 \end{aligned}\right\} \tag{164}$$

These relations must be satisfied on the boundary of stability. By eliminating p_1 and q_2, we find

$$A_0 = A_1A_2$$

We do not know yet on which side of this relation stability exists. That can be found in the simplest manner by trying out one particular case. For example let $s_1 = -1$ and $s_{2,3} = -1 \pm j$,

which obviously is a stable solution. Substitution in (163) gives

$$A_2 = 3 \qquad A_1 = 4 \qquad A_0 = 2$$

so that

$$A_0 < A_1 A_2$$

The complete criterion for stability of the cubic (160) *is that all coefficients A are positive and that*

$$A_1 A_2 > A_0 \tag{165}$$

Practical examples of the application of this result are given in Sec. 61 and 62.

Next consider the quartic

$$s^4 + A_3 s^3 + A_2 s^2 + A_1 s + A_0 = 0 \tag{166}$$

for which the procedure is similar. Since a quartic can be resolved into two quadratic factors, we may write for the roots

$$\left.\begin{aligned} s_1 &= p_1 + jq_1 \\ s_2 &= p_1 - jq_1 \\ s_3 &= p_2 + jq_2 \\ s_4 &= p_2 - jq_2 \end{aligned}\right\} \tag{166a}$$

and substitute in (166), which leads to

$$\left.\begin{aligned} A_3 &= -2(p_1 + p_2) \\ A_2 &= p_1^2 + p_2^2 + q_1^2 + q_2^2 + 4p_1 p_2 \\ A_1 &= -2p_1 \cdot (p_2^2 + q_2^2) - 2p_2(p_1^2 + q_1^2) \\ A_0 &= (p_1^2 + q_1^2) \cdot (p_2^2 + q_2^2) \end{aligned}\right\} \tag{167}$$

The requirement for stability is that both p_1 and p_2 be negative. Substitution of negative values of p_1 and p_2 in (167) makes all four A's positive, so that the first requirement for stability is that all coefficients A be positive. Granted that this is so, the first equation of (167) requires that at least one of the quantities p_1 or p_2 be negative. Let p_1 be negative. We still need another requirement to make p_2 also negative. On the boundary between stability and instability, $p_2 = 0$, which substituted in (167) gives

$$\left.\begin{aligned} A_3 &= -2p_1 \\ A_2 &= p_1^2 + q_1^2 + q_2^2 \\ A_1 &= -2p_1 q_2^2 \\ A_0 &= (p_1^2 + q_1^2) q_2^2 \end{aligned}\right\} \tag{168}$$

being four equations in the three variables p_1, q_1, and q_2.

Elimination of these variables leads to a relation between the A's:

$$A_1 A_2 A_3 = A_1^2 + A_3^2 A_0$$

To find out on which side of this equality stability exists, we try out a simple stable case, for example,

$$s_{1,2} = -1 \pm j \qquad s_{3,4} = -2 \pm 2j$$

which, on substitution in (167), gives

$$A_3 = 6 \qquad A_2 = 18 \qquad A_1 = 24 \qquad A_0 = 16$$

so that

$$A_1A_2A_3 > A_1^2 + A_3^2A_0$$

The complete criterion for stability of the quartic (166) *is that all coefficients A are positive and that*

$$A_1A_2A_3 > A_1^2 + A_3^2A_0 \tag{169}$$

Applications of this relation are made in Sec. 61, 63, and 64.

Systems with three degrees of freedom generally have a sextic for their frequency equation and in degenerated cases a quintic. In such cases there are three real parts of the roots s, and besides the requirement of positive signs for all coefficients A there are *two* other requirements, each of which is rather lengthy. For further information in this field the reader is referred to the original work of Routh, mentioned in the Bibliography.

57. Instability Caused by Friction.—There are a number of cases where friction, instead of being responsible for positive damping, gives rise to negative damping. One of the well-known examples is that of the violin string being excited by a bow. The string is a vibrating system and the steady pull of the bow is the required source of non-alternating energy. The friction between the string and the bow has the characteristic of being greater for small slipping velocities than for large ones. This property of dry friction is completely opposite to that of viscous friction (Fig. 208). Consider the bow moving at a constant speed over the vibrating string. Since the string moves back and forth, the relative or slipping velocity between the bow and the string varies constantly. The absolute velocity of the bow is always greater than the absolute vibrating velocity of the string, so that the direction of slipping is always the same. However, while the string is moving in the direction of the bow, the slipping velocity is small and consequently the friction force great; but during the receding motion of the string, the slipping velocity is large and the friction small.

We note that the *large* friction force acts in the direction of the motion of the string, whereas the *small* friction force acts

against the motion of the string. Since the string executes a harmonic motion, the work done by the friction force during one-half stroke in $2Fx_0$, where F is an average value of the friction force and x_0 the amplitude of vibration. Since F if greater during the forward stroke (when the friction does positive work on the string) than during the receding stroke (when negative work is done), the total work done by the friction over a full cycle is positive and hence the vibration will build up.

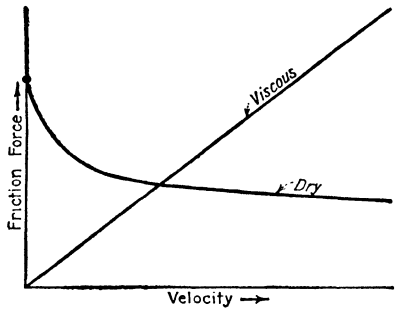


FIG. 208.—Damping forces with positively and negatively sloping characteristics.

In mechanical engineering certain vibrations, usually referred to as "chatter," can be explained in the same manner. The cutting tool of a lathe may chatter and also the driving wheels of a locomotive. When starting a heavy train these drivers are sometimes seen to slip on the rails. While, as a rule, the slipping takes place in a uniform manner, "chattering slip" has been sometimes observed. Besides the major slipping rotation, the wheels then execute torsional oscillations which may cause very large alternating stresses in the crank pins and side rods. A negative slope (Fig. 208) of the friction-velocity characteristic between the wheels and the rails is essential for this phenomenon.

The phenomenon may be observed in many homely examples such as the door that binds and screeches when opened, and the piece of chalk that is held perpendicular to the blackboard while writing. Another case is the familiar experiment in the physics laboratory of rubbing the rims of water glasses with a wet finger to cause them to sing.

A torsional vibration of this type has been observed in ships' propeller shafts when rotating at very slow speeds (creeping speeds). The shaft is usually supported by one or two outboard bearings of the lignum-vitae or hard-rubber type, which are water-lubricated. At slow speeds no water film can form and the bearings are "dry," causing a torsional vibration of the shaft at one of its natural frequencies, usually well up in the audible range. The propeller blades have natural frequencies not too far removed and act as loud-speakers, making this "starting squeal" detectable at great distances under water.

A striking technical example of the self-excited vibrations caused by dry friction is shown in Fig. 208*a* which represents a drawbridge of rather large dimensions. The bridge deck *a* is counterbalanced by a large concrete counterweight *b* which, together with its guiding links and the supporting tower, forms a parallelogram as shown.

After about a year's operation one of the towers of this bridge broke and on inspection the failure proved to be unmistakably caused by fatigue. Experiments with the other half of the bridge, still standing, showed that, when the deck was raised and lowered, violent vibrations of the whole structure took place at a very slow frequency, of about six cycles during the entire time of raising the bridge deck. The explanation was found in the bearing *c* which carries the tremendous load of the counterweight *b*. Whatever grease happened to be in this bearing at the beginning of the life of the bridge was soon squeezed out and the bearing was found to be entirely dry. The dry-friction chatter thus caused was sufficiently violent to cause the failure.

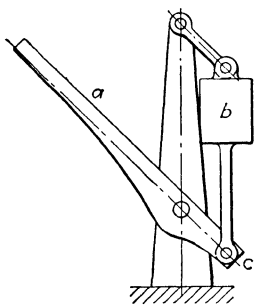


FIG. 208*a*.—Drawbridge which failed structurally because of a negative friction characteristic in the pin bearing c.

Obviously the remedy for this case consists in proper grease cups, which have to be kept in proper order and must be inspected daily.

Another interesting phenomenon caused by a "negative characteristic" is shown in Figs. 208*b* and *c*. A fan is blowing air into a closed chamber *A* of fairly large dimensions and the air is leaking out of that chamber through definite orifices *B*. The practical case of which Fig. 208*b* is a schematic representation was a boiler room in a ship which was kept under a slight pressure by the fan, and the orifices *B* were the boilers and stacks through which the air was forced out. It was observed that for a certain state of the opening *B*, *i.e.*, for a certain steam production, violent pressure variations of a frequency of about one cycle per second took place in the boiler room.

The explanation is partly given by Fig. 208*c*, which is the characteristic curve of a blower. The volume delivered by the blower is plotted againt the pressure developed by it. The point *P* of the characteristic obviously refers to the condition where the orifice *B* is entirely closed so that no volume is delivered, but a

maximum of pressure is developed. The point Q of the characteristic refers to operation of the fan in free air where no pressure is developed but a large volume is delivered. By changing the opening at B in Fig. 208*b*, operation of the fan can be secured over a range in Fig. 208*c* from the point P almost down to Q. It is seen that most of this curve has a slope descending from P to Q but that there is a short section between C and D in which the

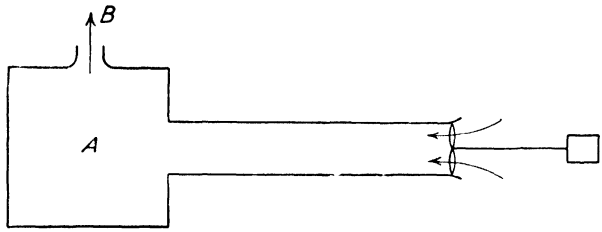


FIG. 208*b*.—Fan blowing air through a long tube into a chamber A.

slope is reversed. This is a characteristic of the construction of the fan and it is very difficult to build a fan in which the characteristic curve drops from P to Q with the slope in one direction only, and at the same time have good efficiency in the region between Q and D, for which the fan is built primarily.

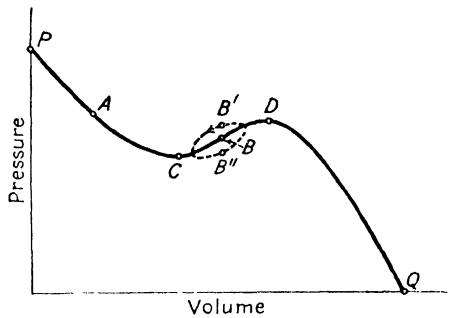


FIG. 208*c*.—Pressure-volume characteristic of a fan. At point P the discharge opening is closed, while at Q the fan discharges freely into the open atmosphere. Between C and D the slope of the characteristic is reversed, causing unstable operation.

It can be shown that operation near the point A in Fig. 208*c* is stable, whereas operation near the point B is unstable and will lead to the surging condition just described. Imagine operation near the point A and let the pressure in the chamber of Fig. 208*b* be slightly higher than normal. This means a decreased volume delivered by the fan, as can be seen from Fig. 208*c*. Thus an

output of the fan less than normal will cause the pressure in the chamber to drop again, and since the pressure was higher than normal, the equilibrium condition tends to be restored. Similarly, if by an accident the pressure were temporarily lower than normal at A, the volume delivered would be increased, which tends to boost the pressure and restore the equilibrium.

On the other hand, consider operation near the point B of Fig. 208*a*. If now the pressure in the chamber is higher than normal instantaneously, the fan delivers more volume than in the normal condition and thus increases the pressure in the chamber still more. Therefore, if the pressure in the chamber is increased by accident, the fan operation will immediately increase it still more, which means an unstable condition.

Imagine an operation which consists of a sliding up and down of the point B in Fig. 208*c* along the characteristic curve. Starting from the normal position of B and rising along the curve to the maximum height, then coming back down again to the normal position of B, constitutes a period in which more than the usual volume is delivered to the chamber. Consequently at the end of this period the pressure in the chamber will be higher than normal, and we find ourselves at the point B'. Now going from B' down along the curve to the bottom position, and back up again to the normal position, is a period in which less than the normal volume is delivered, so that at the end of this period the pressure in the chamber will be less than normal; *i.e.*, we are at the point B''. Consequently, instead of sliding up and down the characteristic curve, we describe a closed curve of some elliptical form in a counterclockwise direction. The work done *by the air on the fan* is the area of this closed curve and, since it is run through in a counterclockwise direction, this work is negative. Consequently, the work done *by the fan on the air* is positive and the phenomenon is seen to be unstable.

An important case of dry-friction excitation, which repeatedly has led to serious trouble in practice, is the so-called "shaft whipping" caused by a loose guide or by a poorly lubricated bearing with excessive clearance. In Fig. 209 let the circle A designate the inside of a bearing or guide and B the cross section of the vertical shaft rotating in it. Let the shaft be rotating clockwise and be temporarily deflected from its equilibrium position in the center of A so that it strikes A at the left. On account of its rotation the shaft sets up friction forces F and F', of which

F is the force acting on the shaft and $F' = -F$ acts on the guide or bearing. The force F can be replaced by a parallel force of equal magnitude through the center of the shaft B and a couple Fr. The couple acts merely as a brake on the shaft, which is supposed to be driven at uniform speed, so that the only effect of the couple is to require some increase in the driving torque and is inconsequential. The force F through the center of the shaft, however, drives it downward or rather in a direction tangent to the circle A. The direction of F changes with the position of the shaft B in A, so that the shaft will be driven around as indicated by the dotted circle. It will be noticed that the shaft is driven around the clearance in a direction opposite to that of its own rotation. If the shaft rotates in the center of the guide without touching it, the shaft is stable; but as soon as it strikes the guide for any reason, the shaft is set into a violent whirling vibration.

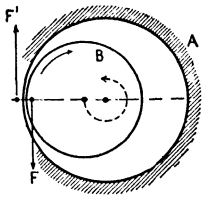
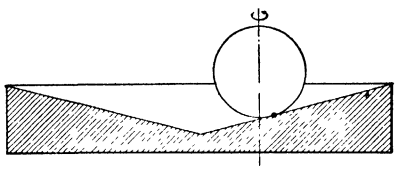


FIG. 209.—Shaft whirl caused by dry friction.

This effect is present in many modifications. A very simple model for demonstrating it is as follows. Take a shallow conical cup (Fig. 210) and a steel ball of about 1 in. diameter. Spin the ball between the fingers at the bottom of the cup. This position is an unstable one for the rotating ball because, if it is accidentally displaced a very small distance from the center of the cup, the point of contact with the cup no longer coincides with the (vertical) axis of rotation. There will be slip and a friction force perpendicular to the paper tending to drive the ball around in a circle. The direction of rolling of the ball will be opposite to the direction of spin.


FIG. 210.—The ball whirls around on account of the friction at the point of contact.

The phenomenon is not restricted to cylindrical guides or bearings but has also been observed on thrust bearings. Figure 211 represents schematically a thrust bearing and shaft, of which the equilibrium position is central and vertical. Suppose that the elastic system of which the shaft forms a part is capable of a natural mode of motion whereby the shaft center line whirls

around the vertical with an eccentricity δ and an inclination α. The center A of the collar disk describes a circle of radius δ and the shaft a cone of apex angle 2α. This mode of motion will be self-excited by friction, because during the vibration the collar rests on the bearing on one side only. This causes a tangential friction force on that side urging the point A around the center line in a direction opposite to that of the rotation of the collar disk. The obvious way to prevent this sort of disturbance is to make the bearing support so flexible that, in spite of the angular deviation, the pressure on the various parts of the bearing remains uniform.

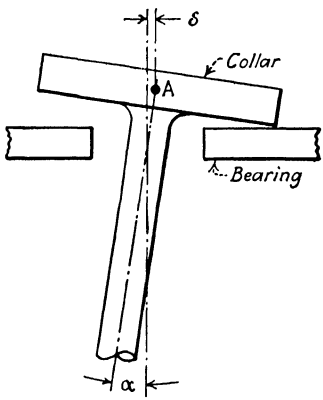


FIG. 211.—Whirl on account of dry friction in a thrust bearing.

A very instructive model demonstrating this effect may be built as follows (Fig. 212). A small motor A carries a disk B on the end of its horizontal shaft and is supported very flexibly on three springs lying in a plane through the center of gravity and perpendicular to the shaft. When running, this motor is capable of a large number of natural modes of vibration, two of which are particularly interesting. They are illustrated by Fig. 212*c* and also by Fig. 189 (page 321.) The shaft describes a cone characterized by δ and α and whirls either in the direction of rotation or opposite to it. The natural frequencies of these two modes of motion are shown in Fig. 190.

Imagine a piece of felt or paper C held against the front side of the disk near its circumference. It will strike (or press hard) when α (and consequently δ) is just in the position shown in Fig. 212*c*. Assume B to be rotating clockwise in Fig. 212*a*. The obstacle C will cause a friction force tending to push the disk *down*. As in the argument given with Fig. 209, this friction force is replaced by a retarding couple and a force through the shaft center. The retarding couple merely retards the motion slightly, but the force through the center of the disk pushes that center down, *i.e.*, in a direction of clockwise whirl. Thus friction on the *front* side C of the disk will encourage a precessional motion in the *same* direction as the rotation.

On the other hand, if D is pressed against the back of the rotating disk B, it will strike and cause friction when α and δ have reached the position just opposite to that of Fig. 212*c*. The friction again kicks the disk down, because the direction of rotation is still clockwise. This downward force now excites a counterclockwise whirl, because the deflection δ is opposite to that shown in Fig. 212*c*.

The experiment consists of rubbing the front of the disk and noticing the self-excitation of the mode of vibration of rather high frequency with the precession in the same direction as the rotation. Then, taking the rub from the front and applying it to the back side, this motion is seen to damp out very fast, and the second mode (precession against the rotation) with a much slower frequency is seen to build up. This latter motion can be damped very effectively by again rubbing the front of the disk. The difference in the two frequencies is caused by the gyroscopic action of the disk as explained on page 321.

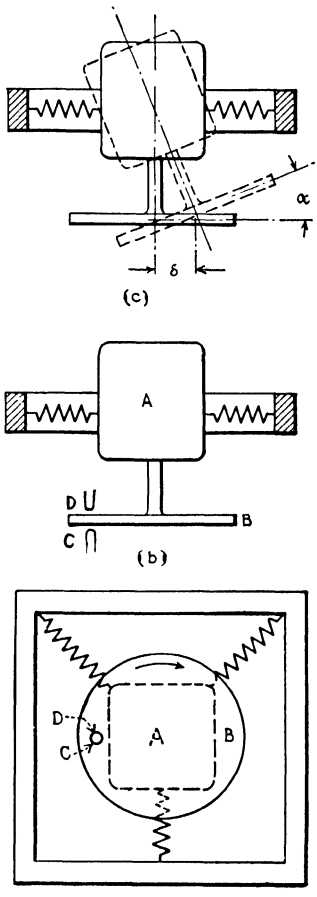


FIG 212.—Self-excited whirl caused by friction on the disk B.

58. Internal Hysteresis of Shafts and Oil-film Lubrication in Bearings as Causes of Instability.—Another highly interesting case of self-excited vibration is that caused by internal hysteresis of the shaft metal. *Hysteresis* is a deviation from Hooke's stress-strain law and appears in most materials with alternating stresses. In the diagram 213*a* Hooke's law would be represented by a straight line, and a fiber of a vibrating shaft, which experiences alternately tension and compression, should move up and down that line between P_1 and P_3. Actually the stress-strain relation is represented by a long narrow elliptic figure which is always run through

in a clockwise direction. The ellipse as shown in Fig. 213 has its width greatly exaggerated; in reality it is so narrow that it can hardly be distinguished from the straight line P_1P_3.

Consider a vertical rotating shaft in two bearings with a central disk as shown in Fig. 213*b*. During the whirling motion the center of the shaft S describes a circle about the point B on the bearing center line. The point B is the normal or equilibrium position of S when no whirl exists. Figure 213*c* shows a cross section of the middle of the shaft, $P_1Q_1P_2P_3P_4$ being the outline of the shaft and the dotted circle being the path of S during the

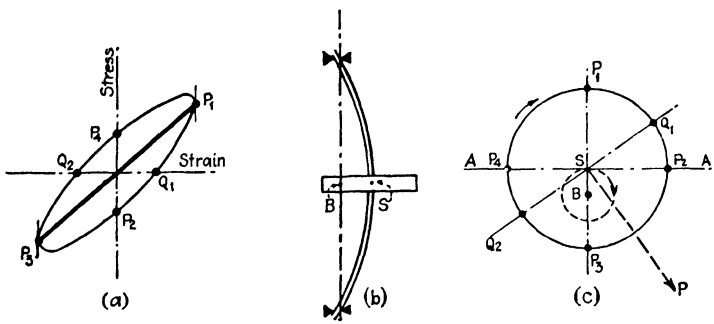


FIG. 213.—Shaft whirl caused by internal hysteresis.

whirl. The deflection BS of Fig. 213*c* is a practical possibility; that of Fig. 213*b* is enormously exaggerated.

It is assumed that the rotation of the shaft and the whirl are both clockwise as shown. The shaft is bent, and the line AA divides it in two parts so that the fibers of the shaft above AA are elongated and those below AA are shortened. The line AA may be described as the *neutral line of strain*, which on account of the deviation from Hooke's law does not coincide with the *neutral line of stress*.

In order to understand the statement just made consider the point P_1 in Fig. 213*c* which may be thought of as a red mark on the shaft. In the course of the shaft rotation that red mark travels to Q_1, P_2, P_3, etc. Meanwhile the shaft whirls, whereby S and the line AA run around the dotted circle. The speed of rotation and the speed of whirl are wholly independent of each other. In case the speed of rotation is equal to the speed of whirl, the red mark P_1 will always be in the elongation of the line BS, or in other words, P_1 will always be the fiber of maximum

elongation. In case the rotation is faster than the whirl, P_1 will gain on S and consecutively reach the position P_2 (of no elongation), P_3 (of maximum shortening), etc. On the other hand, if the rotation is slower than the whirl, P_1 will go the other way (losing on S) and go through the sequence P_1, P_4, P_3, P_2, etc.

First, investigate a rotation faster than the whirl. The state of elongation of the shaft fibers of the various points P_1, P_2, P_3, P_4 of Fig. 213*c* is indicated by the same letters in Fig. 213*a*. In Fig. 213*a* the point Q_1 of *no stress* lies between P_1 and P_2. The point Q_1 is now drawn in Fig. 213*c* and the same is done with Q_2 between P_3 and P_4. Thus the line Q_1Q_2 is the line of no stress (neutral line of stress) and all fibers above Q_1Q_2 have tensile stress while those below Q_1Q_2 have compressive stress. The stress system described sets up an elastic force $\overline{P}$, as shown. This elastic force $\overline{P}$ has not only a component toward B (the usual elastic force) but also a small component to the right, tending to drive the shaft around in its path of whirl. Thus there is a self-excited whirl.

The reader will determine for himself the truth of the statement that, if the rotation is slower than the whirl, the inclination of Q_1Q_2 reverses and the elastic force has a damping instead of a driving component.

The whirling motion is determined primarily by the elastic force of the shaft toward the center B combined with the inertia forces of the disk (see page 321) and therefore takes place with the natural frequency. The very small *driving* component of the elastic force merely overcomes damping. Internal hysteresis of the shaft acts as damping on the whirl below the critical speed, whereas above that speed a self-excited whirl at the critical frequency may build up.

Internal hysteresis in the shaft material is usually very small, but a more pronounced hysteresis loop is found in cases where actual slipping occurs, as in loose shrink fits or other joints. Thus a shaft with a loosely shrunk disk will probably develop a whirl at the natural frequency above the critical speed.

A self-excited vibration known as *oil whip* is caused by certain properties of the oil film in generously lubricated sleeve bearings. In order to understand this phenomenon, it is necessary to know that a horizontal shaft rotating in a counterclockwise direction in an oil-film lubricated bearing does not seek a central position

but is deflected somewhat to the right (Fig. 214). The direction of this deviation can easily be remembered by noting that it is opposite to the direction in which one would expect the journal to climb. Since on such a journal the load or weight **W** is acting downward, as indicated in the figure, the resultant P of the oil pressures on the journal is equal and opposite to **W** and makes a certain angle α with the line OA connecting the center of the bearing and the center of the journal.

Consider a *vertical* guide bearing with a shaft in it. If there are no lateral loads acting, the shaft will seek the center of the bearing. If, for some reason, the shaft starts whirling around in the bearing, it will occupy an eccentric position at any instant. Moreover, if during that whirling the oil pressures are the same as in Fig. 214 (where **W** now must be replaced by a centrifugal force in the direction OA), there is no equilibrium between P and the centrifugal loading, but there is a small resultant force tending to drive the journal around in the bearing in a counterclockwise direction. Thus the oil-pressure distribution will encourage or self-excite a whirl in the direction of rotation but will damp a counterrotating whirl, if one ever sets in.

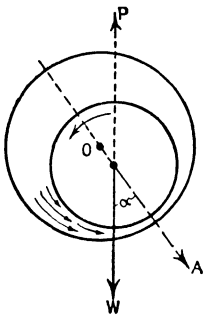


FIG. 214.—Oil-film lubrication in a bearing causes whirling because the weight **W** and the axis of symmetry OA are not in line.

There remains to be considered the condition under which the oil-film pressures during the whirling will be the same as in the steady-state case for a horizontal bearing with gravity loading. Consider two extreme cases, namely those in which the ratio of the angular velocity of whirl to the angular velocity of rotation is either very small or very great.

In the first case the shaft makes say 100 revolutions while the whirl moves forward 5 deg. It is clear that such a slow drift can have no effect on the pressure distribution, so that for a *slow* whirl the succession of steady states actually occurs and the oil whip will develop. In the second case the journal center whirls around while the journal itself hardly rotates. Then, of course, no oil film develops at all and the shaft merely vibrates in a bath of oil, which effectively damps the motion.

Therefore we recognize that for whirl frequencies which are slow with respect to the angular velocity of rotation the oil

whip develops, while for comparatively fast whirls all vibratory motions are damped. The ratio of $\omega_{\text{rotation}}/\omega_{\text{whirl}}$, at which the damping passes from a positive value to a negative one, can be determined only by experiment.

It has been found in this manner that if the ω of the whirl is equal to or smaller than half the ω of the shaft (*i.e.*, if the shaft runs faster than twice its critical speed), the oil whip develops. This constitutes a serious trouble for high-speed machines with vertical shafts in oil-lubricated guide bearings, which is very difficult to overcome.

An interesting justification for this result is due to Hagg (see Bibliography). In Fig. 214*a* let the radial clearance be ϵ and the radius of whirl be δ, the diameter of the journal D. For a slow whirl, the velocity distribution across the oil film is linear, and, with the journal peripheral velocity being V, the volume of oil (per unit shaft length) transported up at A is $\frac{V}{2} \cdot (\epsilon - \delta)$, while the volume passing downward through B is $\frac{V}{2} \cdot (\epsilon + \delta)$.

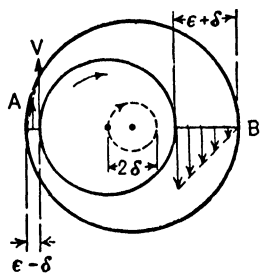


FIG. 214*a*.

Thus assuming no end leakage, the net transport of oil into the lower half of the film is $V\delta$. Now the journal whirls with a frequency f and the whirl velocity v of the journal center is $v = f \cdot 2\pi\delta$. The area of the lower half of the oil film increases at the rate $vD = f2\pi\delta D$. If the whirl frequency is slow enough, the rotation of the shaft will wipe enough oil into the lower half of the film to fill the cavity caused there by the upward whirling motion. For faster whirl the rotation will not transport enough oil and the film breaks. This occurs therefore at $V\delta = f2\pi\delta D$. The peripheral velocity V is related to the shaft speed by $V = \pi D \cdot \text{r.p.s.}$ Substituting this we obtain

$$f = \frac{\text{r.p.s.}}{2}$$

This shows that if the whirl is faster than half the shaft speed, the oil film breaks down and no self-excitation can take place. In the presence of end leakage this breakdown will occur at a whirl frequency below half the shaft rotation.

Comparing Fig. 214 with Fig. 209 we note that while for dry

friction the direction of whirl is opposite to that of shaft rotation, the two directions are the same for oil-film excitation.

For horizontal bearings with a certain loading, the oil whip appears also for speeds above twice the critical. The explanation is along the same lines as for the vertical shaft. During the whirl the oil pressures will not have a purely radial direction but will have a tangential component as well. That tangential component may be driving during a part of the whirling cycle and retarding during another part. For excitation it is necessary merely that the total work done by the tangential force component on the motion during a *whole* whirling cycle be positive, *i.e.*, that the average value of the tangential force component be positive or driving.

59. Galloping of Electric Transmission Lines.—High-tension electric transmission lines have been observed under certain weather conditions to vibrate with great amplitudes and at a very slow frequency. The line consists of a wire, of more or less circular cross section, stretched between towers about 300 ft. apart. A span of the line will vibrate as a half wave (Fig. 109*a*) with an amplitude as great as 10 ft. in the center and at a rate of 1 cycle per second or slower. On account of its character this phenomenon is hardly ever described as a vibration but is commonly known as "galloping." It has never been observed in countries with a warm climate, but it occurs about once every winter in the Northern states and in Canada, when the temperature hovers around 32°F. and when a rather strong transverse wind is blowing. In most cases sleet is found on the wire. A rough calculation shows that the natural frequency of the span is of the same order as the observed frequency. The fact that, once started, the disturbance is very persistent and continues sometimes for 24 hr. with great violence makes an explanation on the basis of "forced" vibration quite improbable. Such an explanation would imply gusts in the wind having a frequency equal to the natural frequency of the line to a miraculous degree of precision. For example, letting $T = 1$ sec., if in 10 min. there were not exactly 600 equally spaced gusts in the wind but 601 instead, the vibration would build up during 5 min. and then be destroyed during the next 5 min. To keep the line vibrating for 2 hr. would require an error in the gustiness of the wind of less than 1 part in 7,200, so that this explanation may be safely dismissed.

We have a case of self-excited vibration caused by the wind acting on the wire which, on account of the accumulated sleet, has taken a non-circular cross section. The explanation involves some elementary aerodynamic reasoning as follows.

When the wind blows against a circular cylinder (Fig. 215*a*), it exerts a force on the cylinder having the same direction as the wind. This is evident from the symmetry. For a rod of non-circular cross section (Fig. 215*b*) this in general does not hold true, but an angle will be included between the direction of the wind and that of the force. A well-known example of this is given by an airplane wing where the force is nearly perpendicular to the direction of the wind (Fig. 215*c*).

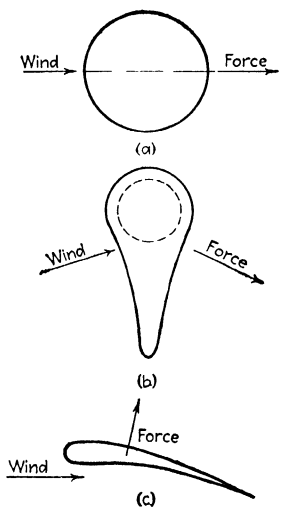


FIG. 215.—The directions of the wind and the force it causes include an angle for nonsymmetrical cross sections.

Let us visualize the transmission line in the process of galloping and fix our attention on it during a downward stroke. If there is no wind, the wire will feel air blowing from below because of its own downward motion. If there is a horizontal side wind of velocity V, the wire, moving downward with velocity v, will experience a wind blowing at an angle $\tan^{-1} v/V$ slightly from below. If the wire has a circular cross section, the force exerted by that wind will have a small *upward* component (Fig. 216). Since the wire was moving *downward* this upward component of the wind exerts a force in opposition to the direction of motion of the wire and thus damps it. However, for a *non*-circular cross section, it may well be that the force exerted by the wind has a downward component and thus furnishes negative damping (Fig. 215*b*).

Considering the conditions during the upward stroke of the vibration, it can be seen in a similar manner that the relative wind felt by the wire comes obliquely from above, and the force caused by it on a circular wire has a downward component which causes damping. For a non-circular section, it may be that the force has some upward component, and this component being in the direction of the motion acts as a negative damping.

If the sleet on the wire gives a cross section exhibiting the relation between the wind and force directions shown in Fig. 215*b*, we have a case of dynamic instability. If by some chance the wire acquires a small upward velocity, the wind action pushes it even more upward, till the elastic or spring action of the wire stops the motion. Then this elastic force moves the wire downward, in which process the wind again helps, so that small vibrations soon build up into very large ones.

There remains to be determined which cross sections are dynamically stable (like the circular one) and which are unstable. This brings us into the domain of aerodynamics, a science which unfortunately is still very little developed. Usually all we can do is to make a direct test, but in some very pronounced cases

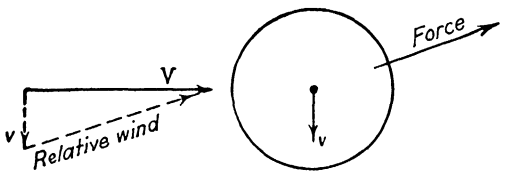


FIG. 216.—A horizontal side wind appears to come from below if the line moves in a downward direction.

a qualitative reasoning may give information. The most "unstable" section so far known is the semicircle turned with its flat side toward the wind. Figure 217 shows such a section in a wind coming slightly from above, corresponding to the upward stroke of a galloping transmission line. The air stream leaves the wire at the sharp edge at the bottom but can follow around the upper sharp edge for some distance on account of the wind coming from above in a slightly inclined direction.

The region indicated by dots is filled with very irregular turbulent eddies, the only known property of which is that in such a region the average pressure is approximately equal to atmospheric. On the lower half of the circular surface of the cylinder we have atmospheric pressure, *i.e.*, the pressure of the air at some distance away from the disturbance created by the line. Above the section the streamlines curve downward. This means that the pressure decreases when moving from *a* to *b*, which may be seen as follows. Consider an air particle in a streamline. If no force were acting on it, the particle would move in a straight line. Since its path is curved downward, a force must be pushing it from above. This force can be caused only by a

greater pressure above the particle than below it, so that the pressure at *a* must be larger than at *b*. Since at *a* there is atmospheric pressure (being far away from the disturbance), the pressure at *b* must be below atmospheric. Thus the semicircular section experiences an upward force on account of the pressure difference below and above, and, since the upward force is caused by a wind coming from above, we recognize the case of Fig. 217 as definitely unstable.

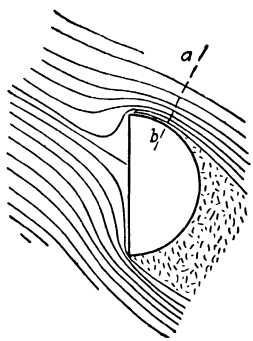


FIG. 217.—The flow of air round a semicircular cylinder.

This may be shown by a simple experiment. A semicircular bar of very light wood (2 in. diameter and 15 in. long) is suspended by four springs so as to have a vertical natural frequency of about 6 cycles per second (Fig. 218). If sufficient care is taken to reduce damping to a minimum in the connections between the springs and the frame or bar, the apparatus will build up vibrations with more than one radius amplitude when placed in front of an ordinary desk fan. The bar in this device is made as light as possible which, for a given frequency and amplitude, makes both the spring force and inertia force small. The input force of the wind is determined only by the shape and size of the bar and is independent of the weight. Thus, by making the bar light, the ratio

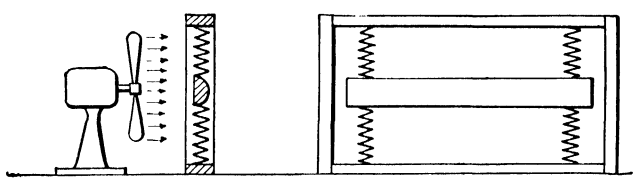


FIG. 218.—Apparatus for demonstrating transmission line galloping.

between the wind force and the spring force is made as great as possible.

Another cross section which is known to be unstable is an elongated rectangle exposed with its broad side to the wind. The explanation is the same as for the semicircular bar (Fig. 219), only the effect is less pronounced. It can be observed easily by means of any flat stick held in the hand at one end and dipped vertically into a tub of water. When the stick is pulled through the water with the broad side of the rectangle perpendicular to the motion,

it moves in zigzag fashion. On the other hand, when pulled with the narrow side perpendicular to the motion, it moves forward quite steadily.

If, instead of mounting the unstable section in springs as shown in Fig. 218, it is pivoted in the middle and placed before a fan (Fig. 220), we have a case of self-excited *rotation*. While the apparatus stands still, the wind evidently exerts no torque on it, but, as soon as it starts rotating, the torque of the wind urges it on in the same direction. The direction of rotation naturally is determined only by the direction at the start, *i.e.*, by accident. This very interesting toy is known as Lanchester's "aerial tourbillion."

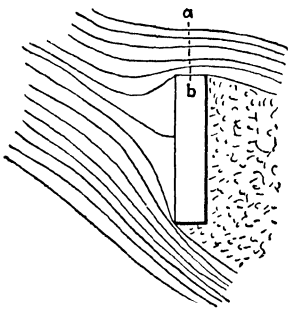


FIG. 219.—The effect for a rectangle is less pronounced than that for a semicircle.

In aerodynamic work it is customary to resolve the total air force on an object into two components:

a. In the direction of the wind (the *drag* or resistance **D**).

b. Perpendicular to the wind (the *lift* **L**).

These two forces can be measured easily with the standard wind-tunnel apparatus.

Let Fig. 221 represent a section moving downward in its vibrational motion so that the wind appears to come from below at an angle $\alpha = \tan^{-1} v/V$. The lift and drag forces **L** and **D** have vertical upward components (*i.e.*, components opposite to the direction of the motion) of $\mathbf{L} \cos \alpha$ and $\mathbf{D} \sin \alpha$. The total upward damping force F of the wind is

$$F = \mathbf{L} \cos \alpha + \mathbf{D} \sin \alpha$$

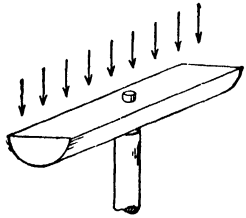


FIG. 220.—The Lanchester tourbillion.

We are not interested in the force F itself but rather in $dF/d\alpha$, *i.e.*, in the variation of the upward force with a variation in α or in v/V. Assume that F has a large value and that $dF/d\alpha$ is zero. The result would be that part of the weight of the line would not be carried by the towers but by the wind directly. Any vibration or galloping of the line would not change the wind-carried weight ($dF/d\alpha = 0$) so that the vibration would not be affected. On the other hand, assume that $dF/d\alpha$ is negative,

which means that the upward wind force increases for negative α and decreases for positive α. Then clearly we have the case of an encouraging alternating force as already explained. The criterion for dynamic stability is

$$\frac{dF}{d\alpha} < 0 \quad \text{(unstable)}$$

and

$$\frac{dF}{d\alpha} > 0 \quad \text{(stable)}$$

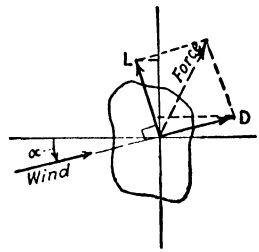


FIG. 221.—The total wind force resolved into a lift **L** and a drag **D**.

In performing the differentiation on (170), it is to be noted that, for small vibrations, v is small with respect to V, so that α is a small angle of which the cosine equals unity and the sine is negligible with respect to unity:

$$\begin{aligned}\frac{dF}{d\alpha} &= \frac{d\mathbf{L}}{d\alpha} \cdot \cos\alpha - \mathbf{L}\sin\alpha + \frac{d\mathbf{D}}{d\alpha}\sin\alpha + \mathbf{D}\cos\alpha \\ &= \sin\alpha\left(-\mathbf{L} + \frac{d\mathbf{D}}{d\alpha}\right) + \cos\alpha\left(\frac{d\mathbf{L}}{d\alpha} + \mathbf{D}\right) \\ &\approx \frac{d\mathbf{L}}{d\alpha} + \mathbf{D}\end{aligned}$$

Thus the system is *unstable* when

$$\frac{d\mathbf{L}}{d\alpha} + \mathbf{D} < 0 \tag{171}$$

The values of the lift and drag of an arbitrary cross section cannot be calculated from theory but can be found from a wind-tunnel test. The results of such tests are usually plotted in the form of a diagram such as Fig. 222. In words, (171) states that

A section is dynamically unstable if the negative slope of the lift curve is greater than the ordinate of the drag curve.

In Fig. 222 it is seen that an elongated section is always stable when held "along" the wind ($\alpha = 0$), whereas it is usually unstable when held "across" the wind ($\alpha = 90$ deg.). A transmission line which is being coated with sleet at approximately freezing temperature has the tendency to form icicles that are more or less elongated in a vertical direction, corresponding to $\alpha = 90$ deg. in the diagram.

At this angle, for small amplitudes of vibration (say varying between 89 and 91 deg.), there is energy input during a cycle. This will increase the amplitude, and the increase will continue so long as there is an excess of energy furnished by the wind. At some large amplitude this excess of energy will become zero so that we have energy balance and reach the final amplitude. In Fig. 222 this will take place presumably at α varying between 30 and 150 deg., say. Near the ends of each stroke, energy is put in; but in the middle of the stroke, energy is destroyed by

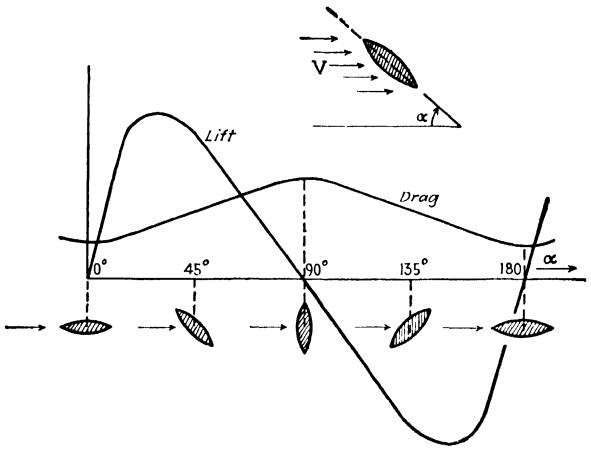


FIG. 222.—Lift and drag as a function of the angle of attack for an elongated, symmetrical cross section.

damping, since $\frac{dL}{d\alpha} + D$ is larger than zero at these places (see also Fig. 268, page 440). The final amplitude can be found by a process of graphical or numerical integration over the known curve of the diagram, in the manner already indicated.

Thus far in the discussion the system has been assumed to be one of a single degree of freedom, which certainly is not the case with a span of transmission line, of which each point vibrates with a different amplitude (large in the center of the span and small near the towers). Since the wind force is small in comparison to the elastic and inertia forces of the vibration, the form of the motion is the same as if the wind force were absent; in other words, the line vibrates in its first natural mode. The final amplitude can be determined by finding the energy input for the whole span. If for a certain assumed amplitude this energy comes out positive, the amplitude assumed was too small;

whereas, if the energy comes out negative (damping), the assumed amplitude was too great. The determination of the energy involves a *double* graphical integration, first with respect to α for each point of the line and then with respect to the position x along the line. This process is straightforward and involves no difficulties, though it may require much time.

The phenomenon discussed so far is one of very *slow* frequency and *large* amplitude in the transmission line. It has been observed but rarely, where the weather conditions brought together sleet deposits as well as a lateral wind of considerable strength. There is another case of vibration of transmission lines characterized by *high* frequency and *small* amplitude which is much more common and for the occurrence of which only a lateral

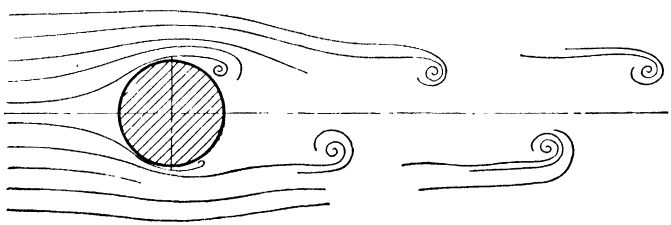


FIG. 222*a*.—Kármán vortices in a wake.

wind is necessary. The explanation of this phenomenon is found in the so-called "Kármán vortex trail," illustrated in Fig. 222*a*.

When a fluid flows by a cylindrical obstacle, the wake behind the obstacle is no longer regular but in it will be found distinct vortices of the pattern shown in Fig. 222*a*. The vortices are alternately clockwise and counterclockwise, are shed from the cylinder in a perfectly regular manner, and are associated with an alternating sidewise force. This phenomenon has been studied experimentally and it has been found that there is a definite relation among the frequency f, the diameter of the cylinder D, and the velocity v of the stream, expressed by the formula $fD/v = 0.22$, or the cylinder moves forward by about five diameters during one period of the vibration. It is seen that this fraction is dimensionless and that therefore the value 0.22 is independent of the choice of units. The figure 0.22 is not a very rigid quantity. It depends somewhat on the velocity of flow but the value always lies between say 0.18 and 0.27.

As an example, consider a transmission line of 1 in. diameter exposed to a sidewise wind of 30 m.p.h. The frequency of eddy

shedding thus is $0.22 \times 528 = 116$ cycles per second. If a transmission line vibrates at this frequency, the span will be subdivided into many waves; *i.e.*, the span will be excited at one of its high harmonics. Vibrations caused by this phenomenon have been responsible for fatigue failures in many a transmission line. On account of the high frequency and comparatively small amplitude, it is possible to use friction dampers of the Lanchester type with advantage. Telephone wires have considerably smaller diameter and consequently higher frequency, which is the explanation of the musical tones given off by them.

An example of technical importance has been discussed in the literature recently. A steel smokestack of 11 ft. diameter had a natural frequency of cantilever vibration of about 1 cycle per second. It was found that with a wind of about 40 m.p.h. the stack would sway violently in a direction perpendicular to that of the wind, which necessitated the construction of guy wires. Checking on the Kármán frequency with the above formula gives a constant of 0.19, which differs but slightly from the constant given above.

Submarine periscopes, being cylindrical cantilever beams of some 20 ft. exposed length and some 8 in. diameter, have shown vibrations of considerable amplitude in a direction perpendicular to that of the motion through the water when the submarine was proceeding submerged, with only the tip of the periscope protruding from the water. Resonance of the Kármán frequency with the natural cantilever frequency of the periscope in many instances has occurred at service speeds with the result of blurring the picture seen by the observer.

Another phenomenon of considerable practical importance is that of the "singing propeller." Ships' propeller blades have been observed to go into a violent vibration at one of the natural frequencies and in one of the natural modes. Usually the frequency is in the audible range, say 200 cycles per second, and the resulting noise is so great that it makes the aft spaces in the ship unlivable. The noise also carries through the water so that the ship can be detected at great distances by underwater listening devices, which in wartime is not comfortable. In extreme cases the propeller blades have broken in fatigue as a result of the singing. It is obviously a case of self-excited motion caused by the water stream as the source of energy, but the exact details are not well understood at present. In the olden days the cross

section of a propeller blade usually was "ogival," *i.e.*, flat on one side, and with a circular arc on the other, with presumably sharp leading and trailing edges, and singing was practically unknown. The influence of airplane wing theory brought about a change in the cross section towards an airfoil shape with a definitely blunt, rounded leading edge. It is with sections of this sort that singing has often been found to occur and a practical remedy for the trouble is known to be a sharpening of the *leading* edge. This suggests a rough theory of what takes place. Obviously during the self-excited vibration the water stream changes its flow pattern periodically with the frequency of the vibration and presumably the dividing point of the flow on the leading edge (the "stagnation point") jumps back and forth across that edge. When the edge is sharpened, this is prevented and the dividing point is forced to remain at the sharp edge, thus effectively impeding the self-excited singing vibration.

The singing has been observed not only in ships' propellers but also in large Francis turbines. Here again it has been found by experience that sharpening of the leading edges of the buckets of the Francis runner eliminates the trouble.

60. Autorotation; Instability Caused by Finite Speed of Formation of Turbulence.—Perform the following three experiments. First, take a strip of paper about 1 by 4 in. and drop it in a room with tolerably still air. The strip is seen to rotate and to descend along an inclined path. Second, make a rectangular vane of thin metal plate and pivot it about its longitudinal axis with the smallest possible friction. Blow air against this vane perpendicular to the axis of rotation by means of a fan. It will be observed that, once started, the vane is capable of sustained rotation in either direction. Third, take a piece of wood 2 by 10 by $\frac{1}{8}$ in., and fasten a 3-ft. length of string to one end. Take the end of the string in one hand and swing the board in a circle above the head in a horizontal plane. When the string has been given some initial twist, the board will spin about its axis very rapidly and emit a roaring sound. Moreover, the string is seen to describe not a plane but a cone with the hand as apex. This cone opens alternately toward the floor and toward the ceiling; at each transition the spin of the board is observed to stop and to start again in the reverse direction. This is a toy, which has been called a "bullroarer."

The aerodynamic explanation of these experiments is based on

the fact that a turbulent flow takes a certain time for its formation. If the semicircle of Fig. 217 were held in still air and then suddenly started moving at a uniform speed to the left and slightly upward, the flow pattern during the first instant would not look at all like Fig. 217. The turbulent region behind the cylinder would be absent, and only after a few seconds would complete turbulence have developed. The picture that is formed at the very first instant after starting is known as the *potential flow* pattern, because it can be calculated by means of the potential theory of hydrodynamics.

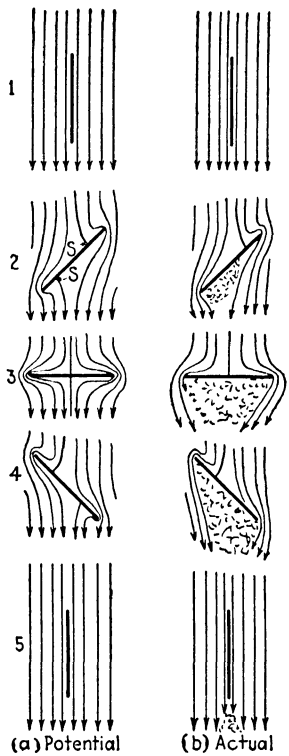


Fig. 223.—The flow around a rotating strip shown in five positions during one-half revolution.

On the left side of Fig. 223 the steady-state potential flow around the vane is shown in five consecutive positions. It is seen that in position 1*a* no torque is exerted by the wind on the vane. In position 2*a* the theoretical flow has two stagnation points *S* of no velocity and of maximum pressure. The position of these is such that the stream exerts a clockwise torque on the vane, which in this instance is a driving torque. The flow in position 3*a* is symmetrical so that no torque is exerted. Position 4*a* looks the same as position 2*a*, except that the torque is now acting counterclockwise and, since the vane is still rotating clockwise, this amounts to a retarding torque. We see that in the quarter revolution between 1*a* and 3*a* the stream does positive work on the vane, but between 3*a* and 5*a* it does exactly the same amount of negative work on it.

For a potential flow, or for any other flow where the pictures 2 and 4 look alike, the stream performs zero work during a full revolution, so that neither damping nor self-excitation takes place. However, the actual flow differs from the potential one and is shown in the right half of Fig. 223. Between 1*b* and 3*b* turbulence behind the vane builds up gradually and between 3*b*

and 5*b* this turbulent air is washed away with the stream. On account of this, the pictures 2*b* and 4*b* differ; 2*b* resembles the potential-flow picture much more than 4*b* does. The effect of turbulence on the pictures in the position 2 is primarily to diminish the torque exerted by the stream on the plate. Similarly in picture 4*b* the retarding torque is less than that of 4*a*. But the "less" is more pronounced in 4 than in 2. Thus there is more positive work done between 1*b* and 3*b* than negative work between 3*b* and 5*b*, and a net positive work results for a full revolution. This explains the self-excited rotation or "autorotation" of the strip.

Besides a torque, the stream also exerts a sidewise force on the strip. Figure 2*b* resembles the flow around an airplane wing, and as such the vane experiences a lift force to the right. Similarly in 4*b* there is a lift force to the left, but this force is smaller than in 2*b* because the turbulence is so much further developed ("stalled" airplane wing). Thus there is a net lift force to the right during a full revolution. This furnishes the explanation for the *inclined* fall of the paper strip in the first experiment and for the *conical* paths of the string in the third one. There the string is twisted on account of the rapid rotation of the vane and exerts an elastic countertorque, which after some time stops the vane and then reverses the rotation. With this reversal of rotation the direction of the lift is also reversed, so that the vane is pushed alternately up and down.

This last experiment may be described as a self-excited *vibration* having the period of the reversals in the rotation of the vane. Briefly, any object capable of self-excited rotation in either direction can be transformed into a self-excited vibrating system by mounting it in springs.

61. Hunting of Steam-engine Governors.—Quite interesting self-excited vibration phenomena have been observed in steam engines or turbines operating in conjunction with an inertia governor of the direct-acting type. By this is meant that the speed-sensitive part of the governor, *i.e.*, the flyballs, is in direct mechanical connection with the steam-supply throttle valve. In very large engines or turbines too much power is required to open and close the throttle directly, so that the governor merely operates electric contacts or oil valves (a relay) which in turn set the throttle valve in motion. Such *indirect* governor systems will not be discussed here.

In Fig. 224 the system is shown schematically. When the speed of the engine a increases for any reason, the flyballs lift the sleeve b of the governor somewhat higher, thereby reducing the opening of the main steam valve c. In this fashion less steam is admitted to the engine, and its speed falls. Since there is inertia in the system, the speed will decrease below normal, which will result in the governor opening the valve more than normal. In this manner, oscillations in the speed of the engine occur, which may be damped or self-excited, depending on the circumstances. The unstable case has occurred repeatedly. Technically it is known as *hunting*, and if such a hunting engine drives an electric generator, its voltage will fluctuate so that a marked flicker in the lights is observed.

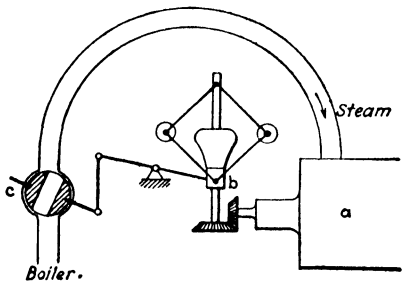


FIG. 224.—Watt governor directly coupled to a throttle valve regulating the steam supply to a turbine. Without damping this system is unstable and will hunt.

In order to understand this phenomenon in greater detail, it is convenient to start from the differential equations. In the first place, the governor is an ordinary vibrating system consisting of a mass, a spring, and a dashpot. This will give three terms in the differential equation. Moreover, the governor is coupled to the engine in such a manner that, when the engine speed $\dot{\varphi}$ increases, an additional upward force on the governor mass ensues, caused by the centrifugal action of the flyballs. This gives the equation

$$m\ddot{x} + c\dot{x} + kx = C_1\dot{\varphi} \tag{172}$$

where x = upward displacement of the governor sleeve, measured from the normal position at a certain load.

m = equivalent mass of the governor sleeve.

c = damping coefficient at the governor sleeve.

k = stiffness of governor spring.

$\dot{\varphi}$ = difference between the instantaneous engine speed and the normal or average speed at a certain load.

C_1 = increase in the upward force on the governor sleeve (from centrifugal action) caused by an increase in engine speed of 1 radian per second.

It is seen that the two coordinates x and φ are based on a certain "normal" condition which exists when the engine is running at a constant speed with a constant load and constant throttle opening, while the governor sleeve stands vertically still. In this condition $x = 0$, so that x is positive when the governor sleeve is higher than normal and negative when lower than normal; similarly, $\dot{\varphi}$ is negative while the engine is temporarily running at a speed slower than normal.

Properly speaking, the engine in itself is not a vibrating system since it has no spring pulling it back into an equilibrium position. There is, however, a mass or rather a moment of inertia I. The damping torque of the engine will be neglected in this investigation. The engine is coupled to the governor in the sense that, when the governor sleeve is lower than normal (negative x), the throttle is opened wider than usual so that an extra positive or driving torque is exerted on the engine. Its equation of motion becomes

$$I\ddot{\varphi} = -C_2 x \tag{173}$$

where I = equivalent moment of inertia of the engine.

C_2 = increase in steam torque of engine caused by a lowering of the governor sleeve by 1 in.

Equations (172) and (173) represent the *free* vibrations of the engine-governor system, since no periodic force is present. The solution therefore must be a function of the shape

$$e^{pt} \cos qt \tag{174}$$

where q is the (damped) natural frequency and p is a measure for the damping, which may be positive or negative. Instead of writing the solution in the form (174), we may write

$$e^{(p+jq)t}$$

the real part of which is the same as (174); or, still shorter, we may assume that

$$\left.\begin{aligned} x &= x_{\max} e^{st} \\ \varphi &= \varphi_{\max} e^{st} \end{aligned}\right\} \tag{159}$$

where s is a complex number (the "complex frequency").

Substitute (159) in the differential Eqs. (172) and (173), which then can be divided by e^{st}, giving

$$\begin{aligned} (ms^2 + cs + k)x_{\max} - C_1 s\varphi_{\max} &= 0 \\ C_2 x_{\max} + Is^2\varphi_{\max} &= 0 \end{aligned}$$

These are a set of homogeneous algebraic equations which have a solution for x_{max} and φ_{max} only if

$$\frac{ms^2 + cs + k}{C_2} = \frac{-C_1 s}{Is^2}$$

or if

$$s^3 + \frac{c}{m}s^2 + \frac{k}{m}s + \frac{C_1 C_2}{mI} = 0, \tag{175}$$

Equation (175) is the frequency equation of the set (172) and (173). On account of the absence of a "spring" in the engine system, the equation is a cubic and not a quartic as would be expected for an ordinary two-degree-of-freedom system.

Of the two criteria for stability on page 353, the first one, requiring all coefficients to be positive, is satisfied. The other criterion, expressed by (165), becomes

$$\frac{c}{m} \cdot \frac{k}{m} > \frac{C_1 C_2}{mI}$$

or

$$c > \frac{mC_1C_2}{kI} \tag{176}$$

If the damping in the governor dashpot is greater than the value indicated by this formula, the system will come to rest after a sudden change in load, but for any damping less than this the system is inoperative (Fig. 207*b*).

In case the engine is rigidly coupled to an electric generator feeding a large network, the problem becomes more complicated. Then, there is an "engine spring," since the network tends to keep the generator rotor in a definite angular position. Any deviation from that synchronous position is opposed by a torque caused by the magnetic spring in the air gap of the generator. In such cases Eq. (173) contains one more term $k_e\varphi$, and, if there is generator damping in an electric damper winding, Eq. (173) contains two more terms. The two simultaneous differential equations of the problem are

$$\left.\begin{aligned} m\ddot{x} + c_g\dot{x} + k_g x &= C_1\dot{\varphi} \\ I\ddot{\varphi} + c_e\dot{\varphi} + k_e\varphi &= -C_2 x \end{aligned}\right\} \tag{177}$$

where the subscript g stands for governor and e for engine. Clearly I means the inertia of all the rotating parts, *i.e.*, of the engine and generator combined.

The damper winding in the generator just mentioned is a device invented by Leblanc in 1901 with the object of alleviating the hunting trouble. It consists of a short-circuited copper winding in the pole faces of the rotating part of the generator. As long as the generator runs at constant (synchronous) speed, no current flows in this winding and consequently it does not impede the motion. With changes in speed, however, currents are induced in the winding, which together with the magnetic field in the air gap produce a torque proportional to the deviation of the angular velocity from synchronous ($\dot{\varphi}$) and directed opposite to $\dot{\varphi}$, *i.e.*, braking while the engine temporarily runs too fast and driving while it runs too slow.

Assuming the solution of (177) in the form (159) and substituting in (177), the frequency equation becomes

$$s^4 + s^3\left(\frac{c_e}{I} + \frac{c_g}{m}\right) + s^2\left(\frac{k_e}{I} + \frac{k_g}{m} + \frac{c_e \cdot c_g}{Im}\right) + s\left(\frac{c_g}{m} \cdot \frac{k_e}{I} + \frac{c_e}{I}\frac{k_g}{m} + \frac{C_1C_2}{Im}\right) + \frac{k_e k_g}{Im} = 0 \quad (178)$$

in which all coefficients are seen to be positive. The criterion of stability (169) becomes

$$\left(\frac{c_e}{I} + \frac{c_g}{m}\right) \cdot \left(\frac{k_e}{I} + \frac{k_g}{m} + \frac{c_e c_g}{Im}\right)\left(\frac{c_g}{m} \cdot \frac{k_e}{I} + \frac{c_e}{I} \cdot \frac{k_g}{m} + \frac{C_1C_2}{Im}\right) > \left(\frac{c_g}{m} \cdot \frac{k_e}{I} + \frac{c_e}{I} \cdot \frac{k_g}{m} + \frac{C_1C_2}{Im}\right)^2 + \frac{k_e k_g}{Im}\left(\frac{c_e}{I} + \frac{c_g}{m}\right)^2 \quad (179)$$

which depends on the governor damping c_g/m, on the engine damping c_e/I, on the natural frequencies $\omega_e^2 = k_e/I$ and $\omega_g^2 = k_0/m$, and on the "coupling" C_1C_2/Im. The only simple conclusion that can be drawn from (179) is that, when no damping exists at all ($c_g = c_e = 0$), the left-hand side is zero, while the right-hand side is $(C_1C_2/Im)^2$, so that the inequality is violated. *Without any damping the system hunts.*

In order to see the physical meaning of (179), consider first the special case where engine damping is absent, $c_e = 0$. Equation (179) reduces to

$$c_g \frac{I}{C_1C_2}(\omega_g^2 - \omega_e^2) > 1 \quad (180)$$

In case the governor frequency ω_g is less than the engine frequency ω_e, the left-hand side is negative and the inequality is

violated, which means unstable operation even if c_g is very large. Conversely, when ω_g is greater than ω_e, the left-hand side is positive and stable operation prevails if the governor damping is larger than

$$c_g > \frac{C_1 C_2}{I(\omega_g^2 - \omega_e^2)}.$$

It is seen that (176) is a special case of this more general result.

The second simple case to be considered is when the only damping is in the engine and none is in the governor, $c_0 = 0$. The large form (179) can then be reduced to

$$c_e \frac{m}{C_1 C_2}(\omega_e^2 - \omega_g^2) > 1 \tag{181}$$

which shows that instability exists if the governor frequency is greater than the engine frequency. When the opposite is the case, the system may be stable if the engine damping is sufficiently large.

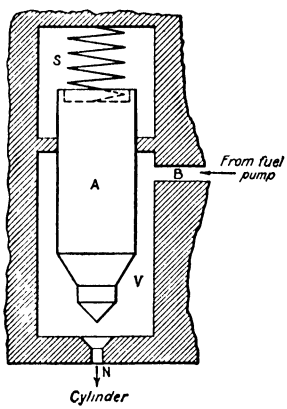


FIG. 225.—Diesel-engine fuel-injection valve. Without damping, the valve is dynamically unstable.

Summarizing, if a system determined by Eqs. (177) is found to be unstable, it should be cured by increasing the damping in the governor dashpot in case the governor frequency is greater than the engine frequency; on the other hand, if the governor frequency is the smaller of the two, damping should be introduced in the engine or generator.

62. Diesel-engine Fuel-injection Valves.—A common construction of a liquid fuel-injection valve and nozzle for Diesel engines is sketched in Fig. 225. The chamber V is permanently filled with liquid fuel oil and is connected to the fuel pump through a short passage B. The normal position of the valve A is on its seat N. At the instant that the engine piston is ready to start on its firing stroke the fuel pump pushes a certain amount of fuel into V, where the pressure rises greatly. Since the valve stem has a greater diameter above than below, this pressure tends to push the valve up. As soon as the pressure is sufficiently large to overcome the force of the set-up in the spring

S, the stem will go up and the liquid is forced through the nozzle *N* into the cylinder head. At the end of the pump stroke the pressure in *V* falls and the spring *S* closes the valve again.

With this mechanism self-excited vibrations of the valve have been observed of the type shown in Fig. 226, I. In these figures the upward displacement x of the valve has been plotted against time. The shading refers to the interval during which the fuel pump is delivering, *i.e.*, during which fuel is actually flowing through the passage *B*. Case III is that of positive damping, case II is neutral, and case I shows negative damping.

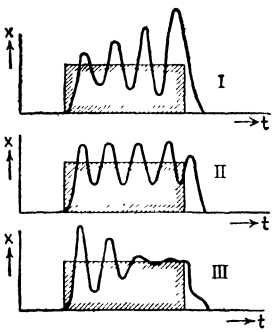


FIG. 226.—Oscillations of an unstable (I), neutral (II), and stable (III) valve system.

The physical action may be understood as follows. During the vibration, part of the valve stem retreats from the chamber *V*, oil flows in at *B* and out at *N*, all of which affects the pressure in *V*. In case the average pressure is greater during the upward stroke than during the downward stroke of the valve stem, there is a feeding of energy into the vibration. If this energy is greater than the friction loss in the gland, the vibration is self-excited.

Indeed, in the absence of gland damping, the system is unstable, which can be seen physically as follows. Consider only the period during which the fuel pump is operating, and assume that the fuel oil is flowing in at a constant rate through the passage *B*. The outflow of oil through the nozzle is varying, depending on the position of the valve stem. Let the valve stem vibrate about some average position. In this average position the outflow through the nozzle equals the inflow through *B*; while the stem is $\left\{\begin{matrix}\text{higher}\\ \text{lower}\end{matrix}\right\}$ than the average position, the outflow is $\left\{\begin{matrix}\text{smaller}\\ \text{greater}\end{matrix}\right\}$ than the inflow. The pressure in the chamber *V* depends on the amount of oil in it; the more oil, the greater the pressure. Consider the valve stem in the neutral or average position in the act of going up. During the next two quarter cycles of vibration, the outflow exceeds the inflow and the pressure diminishes. Thus, when the valve stem finds itself in the

neutral position going down, the pressure is at a minimum. In the same manner it can be shown that, when the stem is in the middle of its upward stroke, the pressure is a maximum. Thus the pressure does work on the vibration.

In the above argument one fact has not been mentioned, namely, that, on account of its motion, the valve stem changes the volume of oil in the chamber V, thus causing pressure variations. The total pressure caused by the fuel pump is so great that these variations are supposed not to affect the outflow, which is determined by the nozzle opening only. Moreover, these pressure variations are in phase with the valve displacement and thus act as an oil *spring* and not as a damping.

Mathematically we come to the same conclusions. Our two dependent variables are the upward displacement x of the valve stem and the pressure $\mathbf{p}$ in the chamber, both measured as deviations from their average values during a vibration cycle; the independent variable is the time. There are three upward forces acting on the valve stem:

1. The spring force $-F_0 - kx$.
2. The damping force $-c\dot{x}$.
3. The pressure force $+\mathbf{p}A + \mathbf{p}_0 A$.

In the first expression, F_0 is the set-up force of the spring S and k is its stiffness; in the third expression, A is the cross section of the stem at the gland and $\mathbf{p}_0$ is the average value of the pressure. The constant forces $-F_0$ and $+\mathbf{p}_0 A$ are equal and opposite; they keep each other permanently in equilibrium. Thus the equation of motion of the valve stem is

$$m\ddot{x} + kx + c\dot{x} - \mathbf{p}A = 0 \tag{182}$$

in which both variables x and $\mathbf{p}$ occur.

The second equation is found by considering the change in volume of the oil in the chamber V and correlating it with a change in the pressure. It is assumed that the flow of oil in the passage B occurs at constant speed during the stroke of the pump. It has also been found with a good degree of approximation that the velocity of oil flow through the nozzle is proportional to the distance of the valve from the nozzle. This distance consists of the average distance x_0 with the variation x superposed on it. The amount of fuel flowing out of the nozzle for a valve set at x_0 equals the amount coming in through B. Thus the *excess*

volume of fuel oil flowing in per second is $-Cx$, where C is the total volume flowing through the nozzle per second when x_0 equals one unit of length. However, the volume of the chamber $\mathbf{V}$ does not remain constant, since the stem moves in and out of it. The change in volume per second on account of this motion of the stem is $A\dot{x}$. The difference

$$-Cx - A\dot{x}$$

is the excess rate of fluid flow inward for a constant volume $\mathbf{V}$. It can be written as $d\mathbf{V}/dt = \dot{\mathbf{V}}$. The definition of the modulus of elasticity E of a fluid in compression is

$$\frac{d\mathbf{V}}{\mathbf{V}} = \frac{d\mathbf{p}}{E}$$

from which follows that

$$\frac{\dot{\mathbf{V}}}{\mathbf{V}} = \frac{\dot{\mathbf{p}}}{E}$$

so that the second differential equation is

$$\dot{\mathbf{p}} = -\frac{E}{\mathbf{V}}(Cx + A\dot{x}) \tag{183}$$

The variable $\mathbf{p}$ can be eliminated between (182) and (183) by differentiating (182) and then substituting (183), giving

$$m\dddot{x} + c\ddot{x} + \left(k + \frac{A^2E}{\mathbf{V}}\right)\dot{x} + \frac{AEC}{\mathbf{V}}x = 0 \tag{184}$$

A substitution of (159) leads to the frequency equation:

$$s^3 + \frac{c}{m}s^2 + \left(\frac{k}{m} + \frac{A^2E}{m\mathbf{V}}\right)s + \frac{AEC}{\mathbf{V}} = 0 \tag{185}$$

in which all the coefficients are positive, so that the stability criterion (165) becomes

$$\frac{c}{m}\left(\frac{k}{m} + \frac{A^2E}{m\mathbf{V}}\right) > \frac{AEC}{m\mathbf{V}}$$

or

$$c > \frac{CE}{\mathbf{V}} \cdot \frac{mA}{\left(k + \frac{A^2E}{\mathbf{V}}\right)} \tag{186}$$

Only when the damping in the gland or elsewhere is as large as is shown in this expression is the motion stable.

It is of interest to note that the bracket in the denominator is the combined spring constant due to S and to the oil chamber, and also that the combination CE/V means the rate of increase in the oil pressure caused by a deflection of 1 in. from the average position of the valve stem. In this light it can be seen that the frequency equations (175) and (185) for the apparently widely different problems of Watt's governor and the Diesel nozzle have exactly the same structure. The coefficient A_2 is a measure of the damping, A_1 is the square of the natural frequency, and A_0 determines the intensity of back-feeding of energy.

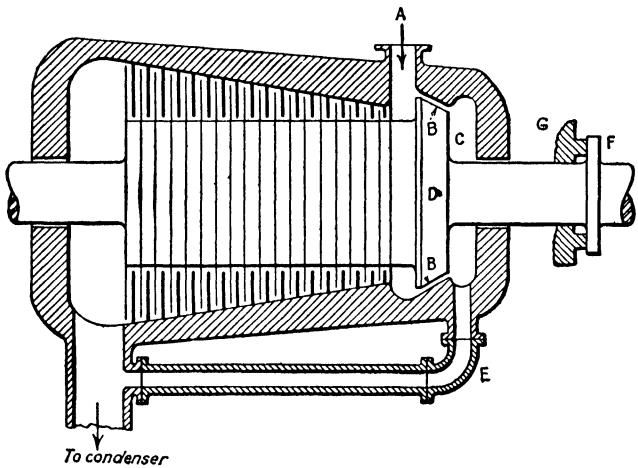


FIG. 227.—Steam turbine showing dummy piston D, labyrinth B, thrust bearing F, G, and equilibrium pipe E.

63. Axial Oscillation of Turbine Caused by Steam Leakage.—A case quite similar to the one just discussed has been observed on some large reaction steam turbines in an electric generating station. The turbine spindle and the rigidly coupled generator rotor were found to be oscillating in an axial direction in the bearings at a frequency of the order of 20 cycles per second. The explanation of this trouble was found in a pressure variation in the space behind the "dummy piston" and was caused by leakage of steam into this space. As with the Diesel valve, the rate at which this leakage takes place depends on the longitudinal position of the turbine spindle.

The construction is roughly indicated in Fig. 227. The high-pressure steam enters through A and passes to the left through the blading to the condenser. On account of the pressure differ-

ence between the boiler and the condenser, an appreciable force to the left is exerted on the spindle and this force has to be balanced. This is done partly by the dummy piston D and partly by the thrust bearing F.

A very small quantity of high-pressure steam leaks by the labyrinth B into the chamber C, which is connected by the "equilibrium pipe" E (of some 16 ft. length) to the condenser. Thus the pressure in C is about equal to (slightly above) the condenser vacuum, and this results in a force tending to pull the dummy piston D to the right and thus partly balances the steam thrust. The details of the labyrinth B vary widely in construction, but usually they are such that an axial displacement of the rotor changes the rate of leak. Since the pipe E is rather long, longitudinal oscillations of its steam column are associated with pressure variations in C, which react on the spindle motion. To have damping of the axial oscillation, it is necessary that the average pressure in C during the spindle motion to the left be smaller than during the stroke to the right. The frequency at which the motion takes place is practically the natural one of the spindle on the springs G of the thrust-bearing structure, since the steam forces are usually small compared with the spring forces.

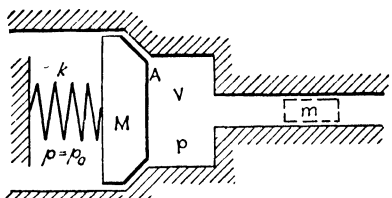


FIG. 228.—Idealized system of the axially vibrating turbine.

The vibration of the steam column in the equilibrium pipe E becomes rather complicated if the length of this pipe approaches one-quarter wave length of the standing sound wave having the frequency of the axial turbine oscillation (Figs. 111*b*, *c*). In most cases, however, the length is appreciably less than this, which means that the steam in the pipe surges back and forth as an incompressible body. The spring on which this steam mass oscillates is found in the volume C, where the pressure changes as a result of an alternating motion of the steam column in E. Thus the system is as shown schematically in Fig. 228, where the mass m may be regarded as a piston (made of steam) sliding back and forth in the equilibrium pipe. There is a general drift of steam in the pipe m to the right. For our analysis we subtract from the total steam velocity its average value so that only the variable part of the velocity of m is considered.

In the actual construction, the volume **V** is very small, and thus some physical reasoning on the behavior of Fig. 228 for zero volume **V** is of interest. Assume the mass M (being the turbine spindle and the generator rotor) to be vibrating back and forth according to Fig. 229. Since the volume **V** is assumed to be zero, the motion of m is directly determined by the amount of steam leaking past M. Thus the velocity of m to the right is maximum when the leakage is maximum or when M is in its extreme left position (point A of Fig. 229). While M is in its extreme right position, the leakage is minimum, less than average, so that m has its maximum velocity to the left (point B of Fig. 229). In this manner the curve determining the position of m is found.

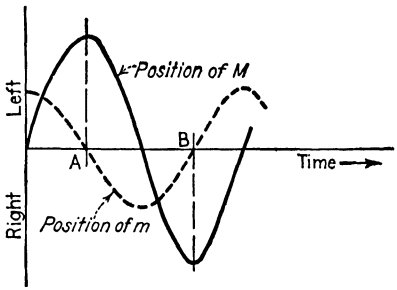


FIG. 229.—Motion diagrams of Fig. 228 for the case of zero volume **V**.

There is no spring acting on m, so that its motion is wholly caused by the steam pressure in (the small volume) **V**. Between A and B the steam column is being accelerated to the left, which means that the pressure in **V** is less than the average. This in turn means that between A and B the steam force in **V** pulls M to the right. But in this interval AB, M is moving toward the right also, so that we conclude that the motion is self-excited.

On the other hand, suppose the volume **V** is very large. Then any variation in leakage can hardly affect the pressure in **V**, so that the variation in the steam force on M, be it positive or negative, is very small. A little friction in the system is then certain to neutralize any small negative damping that may exist.

The trouble in the actual machines was cured by the insertion of a chamber of about 2 cu. ft. volume between the space C and the equilibrium pipe E (Fig. 227).

The more precise theory in mathematical form leads to the same results. If the variable part of the pressure in **V** be denoted by **p** (a function of the time), the dummy-piston area by A, and the displacement of M to the left by x, the equation of motion of M is

$$M\ddot{x} + c_M\dot{x} + kx = A\mathbf{p} \tag{187}$$

If the displacement of the steam column to the right be y, its equation of motion is (Fig. 228)

$$m\ddot{y} + c_m\dot{y} = a\mathbf{p} \tag{188}$$

where a is the cross-sectional area of the pipe.

We have only two equations with the three variables x, y, and $\mathbf{p}$. The third equation is found by considering that $\mathbf{p}$ is affected by the steam flow.

The amount of steam flowing through the labyrinth leak can be considered as consisting of two parts, one, the average flow, remaining constant with the time, and the other a more or less harmonic function of the time. The latter flow is negative during half the time, *i.e.*, it is backward from $\mathbf{V}$ into the high-pressure chamber. This takes place while the total leakage is less than average. Let x be considered the displacement of M from the average position. Then the volume of steam (more than average) flowing per second through the leak is roughly proportional to x, say it is bx, where b is a constant of the dimension in.^{2}/sec. The volume flowing out (more than average) per second is the velocity (more than average) $\dot{y}$ of the steam column times its area a. Thus the volume per second more in than out is $bx - a\dot{y} = d\mathbf{V}/dt$. If the modulus of elasticity of the steam in compression be denoted by E,

$$\frac{d\mathbf{p}}{E} = \frac{d\mathbf{V}}{\mathbf{V}} \qquad \text{or} \qquad \frac{d\mathbf{p}/dt}{E} = \frac{d\mathbf{V}/dt}{\mathbf{V}}$$

Thus the third differential equation is

$$\frac{bx - a\dot{y}}{\mathbf{V}} = \frac{\dot{\mathbf{p}}}{E}$$

or

$$\dot{\mathbf{p}} = \frac{E}{\mathbf{V}}(bx - a\dot{y}) \tag{189}$$

For a solution of the set (187), (188), and (189), assume

$$x = x_0e^{st}$$
$$y = y_0e^{st}$$
$$\mathbf{p} = \mathbf{p}_0e^{st}$$

Substitute this in Eqs. (187), (188), and (189), and eliminate $\mathbf{p}$, x, and y. The frequency equation thus obtained is

$$s^4 + s^3\left[\frac{c_M}{M} + \frac{c_m}{m}\right] + s^2\left[\frac{k}{M} + \frac{a^2E}{m\mathbf{V}} + \frac{c_m c_M}{mM}\right] + s\left[\frac{k}{M}\cdot\frac{c_m}{m} + \frac{a^2E}{m\mathbf{V}}\cdot\frac{c_M}{M} - \frac{AEb}{M\mathbf{V}}\right] + \left[\frac{a^2E}{m\mathbf{V}}\cdot\frac{k}{M} - \frac{AEb}{M\mathbf{V}}\cdot\frac{c_m}{m}\right] = 0 \quad (190)$$

The similarity between this result and (178) is striking. The quantity $a^2E/m\mathbf{V}$ is the natural frequency of the steam column m on the spring $a^2E/\mathbf{V}$ of the steam chamber (Problem 121). The quantity $AEb/M\mathbf{V}$, being proportional to the leakage constant b, represents the coupling or backfeed. The only differences between (178) and (190) consist in the negative sign in the coupling term and in the added appearance of this term in the constant of (190).

For stability it is necessary in the first place that all coefficients in (190) be positive, which means that

$$\frac{k}{M}\cdot\frac{c_m}{m} + \frac{a^2E}{m\mathbf{V}}\cdot\frac{c_M}{M} > \frac{AEb}{M\mathbf{V}} \quad (191)$$

and

$$\frac{c_m}{m} < \frac{\dfrac{a^2E}{M\mathbf{V}}\cdot\dfrac{k}{M}}{\dfrac{AEb}{m\mathbf{V}}} \quad (192)$$

Equation (191) shows that, if no damping exists anywhere, the system is always unstable. Even with a small amount of damping in m and M, instability may exist if $\mathbf{V}$ is sufficiently small. By increasing the volume $\mathbf{V}$, the right side of the inequality (191) can be made small enough to satisfy that stability requirement.

The second equation, Eq. (192), states that the damping in the steam pipe has to be smaller than a certain amount if stability is to be had. This apparently strange result becomes clear when it is noted that the right side is the product of the two natural frequencies divided by the backfeed term. This ratio will be very large, so that the inequality (192) is always satisfied. In this

connection it may be noted that the entire analysis is based on the assumption (166*a*), which implies a *true* vibration. In case a damping constant becomes greater than critical, no true vibration occurs and the analysis is no longer applicable.

The other requirement for stability, expressed by (169), is a very complicated form like (179). To understand its physical meaning it is more useful to investigate the special cases where one of the two dampings is absent. In the case of no damping in pipe ($c_m = 0$), the criterion is

$$\mathbf{V} < \frac{EM}{k}\left(\frac{a^2}{m} - \frac{Ab}{c_M}\right) \tag{193}$$

where the bracket must be a positive quantity by virtue of (191).

When the engine damping is absent ($c_M = 0$), the stability requirement becomes

$$\mathbf{V} > \frac{\dfrac{AEb}{M} + \dfrac{a^2E}{m} \cdot \dfrac{c_m}{m}}{\dfrac{c_m}{m}\left(\dfrac{k}{M} + \dfrac{c_m^2}{m^2}\right)} \tag{194}$$

It is understood that stability exists only when all three inequalities (191), (192), and (193) or (194) are satisfied simultaneously. In case the steam damping is absent, the volume **V** has to be below a certain limit (193), whereas for non-existing engine damping that volume has to be made greater than a certain amount (194). This complicated relation is due to the fact that by changing the volume **V** we really change two quantities:

1. The frequency of the steam column $a^2E/m\mathbf{V}$.
2. The coupling constant $AEb/M\mathbf{V}$.

The inherent significance of the expressions (193) and (194) is disclosed better by writing them in a slightly different form as follows:

$$\frac{A^2E}{m\mathbf{V}} - \frac{k}{M} > \frac{AEb}{M\mathbf{V}} \cdot \frac{M}{c_M} \tag{193a}$$

$$\frac{k}{M} - \frac{a^2E}{m\mathbf{V}} > \frac{AEb}{M\mathbf{V}} \cdot \frac{m}{c_m} - \left(\frac{c_m}{m}\right)^2 \tag{194a}$$

Thus, if we depend only on the engine damping to prevent instability, the frequency of the steam column has to be made greater than the engine frequency (by decreasing **V**). If only

steam-column damping is available, the engine frequency has to be the greater of the two (which can be attained by increasing the volume **V**).

64. Airplane-wing Flutter.—In certain airplanes flying at very high speed, particularly when diving, the wings have been repeatedly observed to develop a very violent vibration. On a number of occasions this "flutter" has been so excessive that it has caused the wing to break off in mid-air.

An explanation on the basis of the phenomenon of Sec. 59 might be attempted. For wings in a "stalled" position the slope of the lift curve is negative (Fig. 222), and the up-and-down motion of a cantilever wing is unstable. This has been observed; however, it is not a condition of actual flight and in the typical "flutter" cases on record the angle of attack of the wing is small and the slope of the left curve decidedly positive. This, by the argument of Sec. 59, leads to a definite positive damping.

Any attempt at an explanation along the lines of Sec. 60 or 61 is not adequate, because in regular flight the air about the wing is practically in a state of potential flow and very little turbulence exists. In fact any attempt at an explanation in terms of a single degree of freedom (for example, where the wing vibrates up and down only, like a cantilever beam) does not succeed. We have another case of a coupled two-degree-of-freedom system, since the wing not only vibrates up and down, but simultaneously executes a twisting motion. The interplay of the vertical and twisting vibrations with the air stream as the source of energy may lead to instability. The possibility of such an occurrence can be explained physically in a rather simple manner.

For a certain value of the *angle of attack* α (defined in Fig. 230*c*) the wing experiences an aerodynamic lift and also a clockwise twisting moment. While the wing executes a twisting vibration, the angle α varies; and therefore we are interested in knowing how the lift and the moment vary with this angle.

Figures 230*a* and *b* show these relations are obtained by a wind-tunnel test. For the angles α at which flight takes place (0 to 10 deg.), these characteristics are practically straight lines.

Assume that the vertical and the twisting motions of the wing are coupled in such a manner that during the upward stroke the angle α is larger than during the downward stroke. According to Fig. 230*a* the lift during the upward motion is larger than

during the downward stroke, which means that the wind feeds energy into the vibration. An energy input is also possible by virtue of Fig. 230*b*. This follows from the fact that even without any twisting motion the angle of attack varies on account of the vertical vibration as explained in Fig. 216. Due to this effect the angle of attack and consequently the twisting moment are made larger during the downward stroke and smaller during the upward stroke. Thus, if during the downward motion the wing twists clockwise, energy will be put into the system and the vibration will grow.

A form of flutter which occurred commonly a few years ago was that of bending of the wing associated with flapping of the aileron. Suppose the aileron is hinged about an axis *not* passing

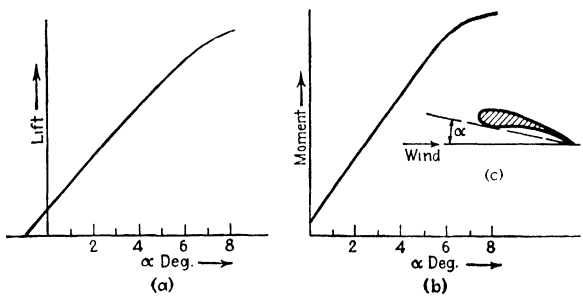


FIG. 230.—The lift and moment diagrams of an airfoil are practically straight lines for small angles of attack.

through its center of gravity and suppose the wing to be vibrating up and down. Independent of any aerodynamic forces the alternating vertical motion of the hinge axis will force the aileron to execute an angular motion, since the hinge axis does not pass through the center of gravity. The aileron is restrained from doing this by the control wires attached to it, which act as springs, since they are necessarily flexible. Thus the aileron-pendulum has a natural frequency of its own which may be above or below the natural frequency of the flutter motion of the wing, so that the aileron motion may be in phase with or in opposition to the wing motion (when the difference between the two frequencies is great) or the aileron motion may have a phase angle near 90 deg. with respect to the wing motion (when the two frequencies are close together, page 66). In the latter case the aileron motion lags behind the force, so that in the middle of the downward stroke of the wing the aileron is up, causing a downward air force

on the wing: hence instability. Trouble of this sort was recognized early and the obvious remedy is to locate the aileron hinge axis through the center of gravity of the aileron by the addition of counterbalance weights if necessary. Even this in itself is not always sufficient to prevent "inertia coupling." To understand this, assume a uniform rectangular aileron hinged about its center line of symmetry. Add to this aileron two equal weights in two opposite corners of the rectangle, leaving the center of gravity where it was. For a purely up-and-down disturbance of the hinge axis the aileron is still balanced and has no tendency to rotate; but if this aileron is placed in an actual wing performing a cantilever vibration with a large amplitude at the tip and a smaller one in the middle, the inertia forces on the two added weights will differ from each other and the aileron will have a

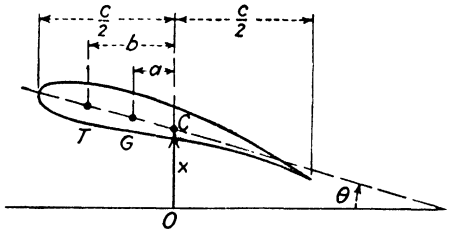


FIG. 231.—The airplane wing with its two characteristic points: the center of gravity G and the center of twist T.

turning moment about its hinge axis. Complete balance against all possible motions can be obtained by insisting not only that the center of gravity lies in the hinge axis, but also that the hinge axis is a principal axis of inertia (so that there is zero product of inertia about the hinge axis). This is an ideal that the designer will satisfy as well as design conditions make feasible and as well as flutter difficulties demand. It applies not only to ailerons, but to other movable surfaces (rudder and elevators) as well, which incidentally also have given rise to flutter phenomena in conjunction with the entire fuselage of the airplane.

We now proceed to a more quantitative analysis of the torsion-bending flutter of a solid wing without aileron, and start by setting up the differential equations of motion. In reality the wing acts more or less as a cantilever beam built in at the fuselage, but for simplicity we assume the wing to be a solid body supported on springs so that it can move up and down as well as rotate about its longitudinal axis. In Fig. 231 the origin of coordinates O is

taken to be at the center point of the span in the position of equilibrium of the wing. The wing departs from this position by the amounts x and θ as shown. Besides the center of the span C, two other points in the wing section are of importance, *viz.*, G and T. The point G is the center of gravity, by which the inertia properties are determined. The location of the point T determines the elastic properties of the spring suspension. The point T is known as the "center of twist" and is defined in one of the following manners: T is that point on the wing where a vertical force causes only a vertical displacement and *no rotation*. T is also that point of the wing which does not displace itself if the wing is subjected to a pure torque causing a rotation of the section. These two properties of T always go together as can be shown by Maxwell's theorem of reciprocity.

Let k_x be the up-and-down spring constant and k_θ the torsional spring constant per unit length of wing, let $\mathbf{L}$ be the aerodynamic lift force (a function of x, θ, and the time), and let $\mathbf{M}$ (also a function of x, θ, and t) be the moment of all aerodynamic forces about O, positive when clockwise, again per unit span. Then the equations of motion are

$$\left.\begin{aligned} m(\ddot{x} + a\ddot{\theta}) + k_x(x + b\theta) &= \mathbf{L} \\ I_G\ddot{\theta} + k_\theta\theta + k_x(x + b\theta)(b - a) &= \mathbf{M} - \mathbf{L}a \end{aligned}\right\} \tag{195}$$

The combinations $(x + a\theta)$ and $(x + b\theta)$ occurring in these equations are the vertical displacements of G and T, respectively. The symbols m and I_G not only refer to the inertia of the wing itself but include that of the surrounding air as well. Usually we take for this a cylinder of air of radius $c/2$. Although this effect is rather insignificant for propeller blades, it is important for airplane wings, which may weigh not more than three times as much as the cylinder of air around them.

The alternating air force $\mathbf{L}$ in actual wings is quite considerable, of the same order of magnitude as the spring and inertia forces. In practically all previous cases treated in this book, the exciting forces (and damping forces) were small in comparison to the inertia and spring forces, so that the resonant frequency was determined by k/m only and was independent of the exciting force. Here the exciting force $\mathbf{L}$, being of the same order of magnitude as the spring force, *does* affect the frequency and the system will flutter at a frequency distinctly different from any of the natural frequencies of the structure in still air.

The expressions for the air force and moment per unit length of the flapping wing have been derived by a complicated analysis with the result

$$\left.\begin{aligned} \mathbf{L} &= \pi\rho V^2 c\left[Y\left(\theta - \frac{\dot{x}}{V}\right) + (1 + Y)\frac{\theta c}{4V}\right] \\ \mathbf{M} &= \pi\rho V^2 \frac{c^2}{4}\left[Y\left(\theta - \frac{\dot{x}}{V}\right) - (1 - Y)\frac{\theta c}{4V}\right] \end{aligned}\right\} \tag{196}$$

in which the worst complication is that the quantity Y not only is complex but depends on the frequency of flutter as well:

$$Y = F + iG \tag{197}$$

where both F and G are functions of $\omega c/2V$, in which ω is the circular frequency of flutter. The values of F and G are given in Fig. 231a, taken from Theodorsen's paper. In these expressions for F and G it has already been assumed that the wing is fluttering, *i.e.*, that it is on the borderline between positive and negative damping and hence executing a purely harmonic

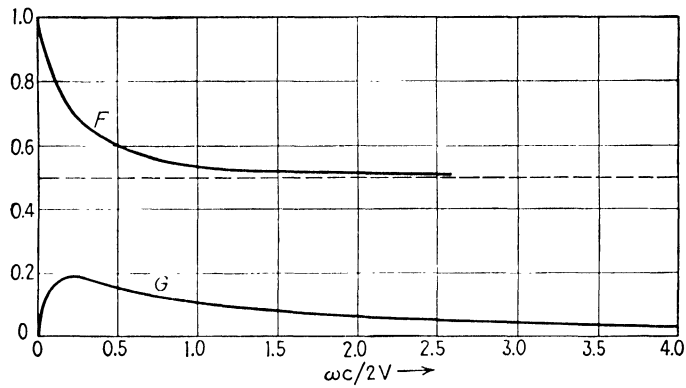


FIG. 231a.—The functions F and G of Eq. (197).

motion. The s of page 351 therefore is already assumed to be without real part p and the imaginary part q is identified with the flutter frequency ω. This, of course, makes stability conditions such as Eqs. (165) or (169) inapplicable.

If still we would proceed to set up the frequency equation, in the manner outlined on page 350, that equation would contain F and G and hence, also, s or ω in a much more complicated manner than a fourth degree algebraic. Theodorsen in the paper quoted in the Bibliography proceeds to set $x = x_0 e^{i\omega t}$ and $\theta = \theta_0 e^{i\omega t}$ into Eqs. (195) and then eliminates x_0 and θ_0 by setting the determinant zero as before. The frequency equation now contains real and imaginary parts, each of which must be zero individually. In this manner *two* equations are found, which must be true on the border between positive and negative damping. These two equations are in terms of two unknowns: the flutter speed V and the flutter frequency ω, but they are not linear in either V or ω, since they contain the curve Fig. 231a. The details of Theo-

dorsen's solution of V and ω from this pair of equations are too complicated to be reproduced here and the reader is referred to the original publication. In a subsequent paper by Kassner and Fingado a nomogram is given, based on an analysis similar to Theodorsen's, by which the flutter speed of any individual wing can be determined in a few minutes after the constants have been found.

Another method, originally suggested by Bleakney and Hamm, and now in extensive use, consists of assuming numerical values for the flutter speed V, and for the flutter frequency ω. Then the forces (196) can be calculated and substituted into Eqs. (195), which of course are not satisfied by the substitution because V and ω are not correct. But they can be made to satisfy Eq. (195) by assigning proper values to the stiffnesses k_x and k_θ, which appear linearly in (195) and thus can be calculated very easily. This means physically that the arbitrarily chosen V and ω are the true flutter speed and frequency for a wing with stiffnesses different from those of the wing we are considering. The result of this calculation is plotted in Fig. 231*b* in the form of two points marked 1, one each in the V-, ω-diagram and in the k_x-, k_θ-diagram. The entire calculation is then repeated for a different value

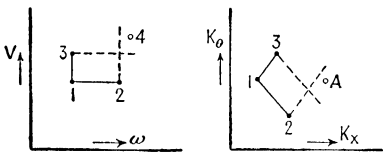


FIG. 231*b*.

of the flutter frequency ω with the same flutter speed V (point 2 in the V-, ω-diagram) and the result plotted as point 2 in the k_x-, k_θ-diagram. A third calculation for the points 3 follows. The actual wing has stiffness values designated by point A in the diagram. Looking at the relative positions of the points, we then pick point 4 in the ω-, V-diagram as a likely next approximation. These trials are continued until we have found a point in the V-, ω-plane whose image in the k_x-, k_θ-plane is sufficiently close to the desired point A.

So far the problem has been one of two degrees of freedom only, *i.e.*, of a wing in which the amplitudes are constant along the span. An approximate value for the flutter speed is obtained by replacing the actual wing by one of the same stiffness but with all its inertia concentrated at a point 70 per cent of the span length distant from the root of the wing, and thus reducing the structure to that of Fig. 231. A better result can be found by numerical integration over the length of the wing. Assume, as with the Rayleigh method, a likely shape of deformation. In practice we take for this the shapes of the bending and torsion modes of the wing without air forces, Eq. (196), and assume that the bending and torsion motions occur in phase with each other at the same frequency of flutter ω. Assume, next, with Bleakney and Hamm, numerical values for V and ω. Then the air force, Eq. (196), the inertia force $\omega^2 y\, dm$, and the elastic force $EIy^{(4)}$ [Eq. (106), page 185] are all known numerically. Also the corresponding moments are known numerically. *If* the assumed shape were the correct one, the sum

of all these three forces would be zero for each individual element of the beam, as expressed by the first equation of Eq. (195), and likewise the sum of the inertia, elastic , and air moments at each element would be zero as expressed by the second equation (195). Since the assumed shape is *not* the correct one, the equilibrium is violated for each individual element dx, but, with Rayleigh, we can integrate along the entire length of the beam and satisfy the over-all equilibrium. Thus the individual terms of Eq. (195) become integrals extending over the length of the wing:

$$\left.\begin{aligned} \omega^2 \int_0^l y(x)\mu(x)\,dx + EI_0 \int_0^l \frac{EI(x)}{EI_0} \cdot \frac{d^4y}{dx^4} \cdot dx &= \int_0^l \mathbf{L}(x)\,dx \\ \omega^2 \int_0^l \theta(x) I_G(x)\,dx + C_0 \int_0^l \frac{C(x)}{C_0} \cdot \frac{d^2\theta}{dx^2}\,dx &= \int_0^l [\mathbf{M}(x) - a\mathbf{L}(x)]\,dx \end{aligned}\right\} \quad (195a)$$

These equations are written for a wing of non-uniform cross section in which the mass μ, the bending stiffness EI, the torsional stiffness C, the deflection of the center of gravity $y = x + a\theta$, the angle θ, and the distance a are all functions of x, variable along the length from 0 to l. The bending stiffness at the root EI_0 and the torsional stiffness at the root C_0 have been brought outside the integrals, Eq. (195*a*). Instead of the constants k_x and k_θ we plot in Fig. 231*b* against the stiffness factors EI_0 and C_0 at the root of the wing. Calculations carried out with this procedure come out with errors in the flutter speed of the order of 10 per cent.

Obviously this is a prodigious job, no longer within the power of an engineer with his slide rule. It is rather in the class of a large, well-lighted, chromium-fixtured office, filled with 20 young ladies and 20 electric calculating machines working full time for a week to find the flutter speed for a single wing.

Another approach is by model testing. Consider a model of the wing to a reduced scale, made of the same material as the original, but scaled down equally in all dimensions and details. Put this model in a wind tunnel with the *same* air-speed as the original wing. In order to leave the values in the square brackets of Eq. (196) unchanged, it is necessary to assume that the time unit is reduced by the same scale as the length unit. But then, as the reader should reason out carefully for himself, the spring force, air force, and inertia force on the model wing all are reduced by a factor l^2, *i.e.*, by the square of the scale ratio for length and time. Thus the flutter speed V (having the dimension l/t) will remain unchanged, and the flutter frequency ω will go up by the scale ratio. Such a test has the additional advantage of still being valid for air speeds near to or exceeding the velocity of sound, where the expressions (196) break down completely. However, a model test as described involves very careful building of the model and elaborate testing apparatus in a wind tunnel. For subsonic air speeds the chromium-appointed room with its charming occupants may be preferable, but for sonic and supersonic air speeds the model test is the only possibility at the present time.

A spectacular case of flutter failure under unusual circumstances occurred when the great suspension bridge across the Narrows near Tacoma, Wash., broke down under the influence

of lateral winds of moderate speed, about 30 m.p.hr. This was a case of flutter with a very low frequency, as the bridge was seen, and photographed, to exhibit large amplitudes both in the bending and in the torsional modes. As with airplane wings the remedy lies in increasing the torsional stiffness, and in post-mortem publications it was recognized that this particular bridge was much more flexible torsionally than any other suspension bridge built. Since future suspension bridges undoubtedly will have greater torsional stiffness, the Tacoma bridge very probably will be the only case of its kind.

65. Automobile "Shimmy."—The familiar phenomenon of shimmy in automobiles, which consists of a rotary oscillation of the front wheels about vertical axes, is usually a self-excited vibration. For a proper explanation it is necessary to consider *three* degrees of freedom, so that the problem is more complicated than any of those previously discussed.

Let Fig. 232*a* represent an elevation looking from the front of the car, A being the axle and B the "king-pins." The axle is capable of tilting in a vertical plane (through the angle φ with respect to the road) by virtue of the vertical elasticity in the tires. It is also capable of shifting sidewise with respect to the body or the road (deviation x) on account of the lateral flexibility of the main springs or of the tires. Looking in Fig. 232*b* from the top, the wheels can flutter through an angle ψ, which constitutes the motion usually referred to as shimmy. Since the two wheels are connected to each other by the rigid steering connecting rod C, the angle of flutter ψ has to be the same for both wheels. Several other motions are possible, but these may be neglected for the purpose in hand.

There are thus three degrees of freedom, φ, ψ, and x. In order to show the possibility of self-excited vibration, it has to be demonstrated that these three are coupled to one another and also that some source of energy is available.

The mass of the front wheel and axle is considerably smaller than that of the spring-supported body of the car. Since the shimmy vibration takes place at a rather rapid rate, the body is practically unable to take part in the motion. In the following discussion it will be assumed that the car body moves forward in a straight line along the road while the front wheels and axle vibrate.

Consider the sidewise vibrating motion $x = x_0 \sin \omega t$ of the

wheels with respect to the body or to the road. This takes place by distorting the *main springs* laterally and sets up an alternating external force on the axle. A part of this main-spring force is used to accelerate the axle in the x-direction and the rest of it finds a reaction which can occur only in the form of lateral road friction at the tires. This reaction force causes a couple in the plane of Fig. 232*a*, tending to set up an alternating angular motion φ. The motion φ, on the other hand,

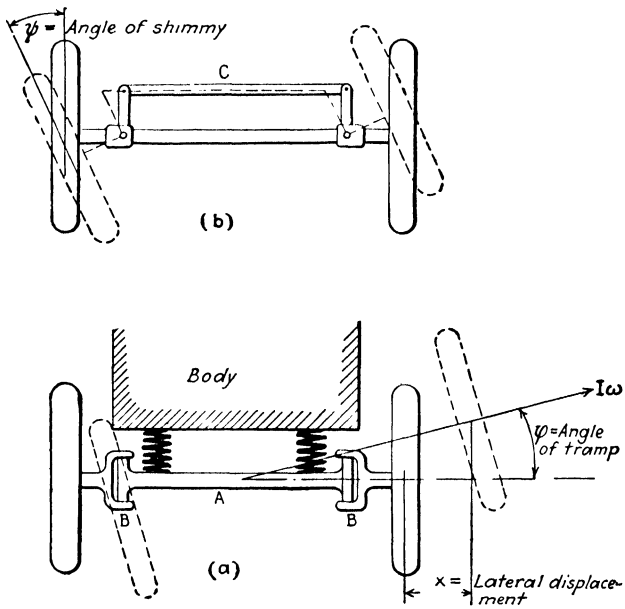


FIG. 232.—Illustrating the coupling between the shimmy motion ψ, the tramping motion φ, and the lateral vibration x.

is coupled to the shimmy ψ by the gyroscopic action of the rapidly rotating wheels. If, for example, the wheel has a "tramping" velocity φ, a gyroscopic couple will be created tending to make ψ smaller. (Incidentally the gyroscopic coupling is responsible for the fact that when *one* wheel rides over a bump in the road the steering wheel gets a rotational jolt.) Finally, the alternating shimmy angle ψ causes the front wheels to follow a wavy path and thus sets up a lateral displacement x. Thus each one of the three degrees of freedom is definitely coupled to the two others.

A source of energy can also be readily found. It was seen

that the sidewise motion x is associated with lateral friction forces at the tread of the tires. These forces in turn cause slipping, if not over the *whole* area of the tire in contact with the road, at least over a part of it. Therefore the sidewise displacement x and the lateral force F on the tire do not bear to each other the simple spring relation $F = kx$ but this relation is much more complicated. Without entering into technical details, it is clear that with certain phase relations between the motion x and the road force F this force may do work on the vibration. The ultimate source of energy naturally is the forward kinetic energy of the car.

In case the proper phase relations for instability do exist, the vibration will be all the more violent the smaller the flexibilities and the stronger the coupling. The most important change in the front-wheel construction of the last few years has consisted in the introduction of balloon tires, the great flexibility of which make large φ-motions possible. The general application of superballoon tires, which are very desirable for the riding quality, has been retarded for a number of years on account of this shimmy trouble.

A mathematical analysis of the problem is possible, but even in the most elementary case (where many important simplifications have been made) it leads to a sixth-degree frequency equation, whereas a more complete investigation gives an equation of the eighth degree. The complications of such calculations make them hardly worth while. A cure of the trouble is better effected by the experimental approach. It is possible to make modifications in the construction of the steering gear so as to alter the various flexibilities, and this may change the phase angles between the various motions with the result of rendering them stable. Also damping may be introduced.

Though most cases of shimmy are self-excited vibrations, this is not invariably so. The disturbance may be excited by unbalance of the wheels, which always exists to a certain extent, especially with unevenly worn tires. Suppose the unbalance weight at the left wheel to be on top, while at the right wheel it is at the bottom. Then the centrifugal forces of these unbalances will cause a tramping φ-vibration and this in turn causes a shimmy. At a speed such that the frequency of rotation of the wheels coincides with the natural shimmy frequency, the disturbance will be great, as we have an ordinary resonance phe-

nomenon. Since the diameters of the two wheels are different, say by 1 part in 500, the unbalances in the two wheels will be in the same direction after 250 revolutions and then excite only an up-and-down motion, which is not coupled with shimmy. In this manner typical and very slow beats are observed, as indicated in Fig. 233.

The most effective method of eliminating shimmy, whether forced or self-excited, is to do away with the gyroscopic coupling. This has been accomplished in some cars by an independent wheel suspension. There is no front axle and the wheel is supported in such a manner that it can move only up and down in its own

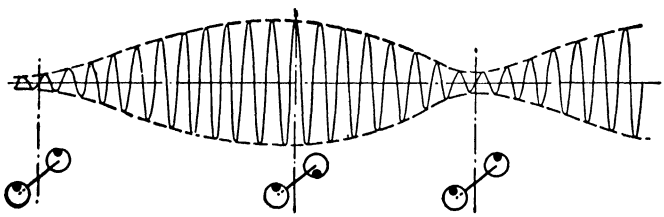


FIG. 233.—A forced shimmy motion caused by unbalanced wheels.

plane parallel to itself and can execute no φ-deviation. With such a construction extremely flexible tires and front springs can be used without any undesirable results.

Finally, it is of interest to mention another self-excited phenomenon very similar to that of shimmy, *viz.*, the "nosing" of electric street cars or locomotives. This disturbance occurs frequently with cabs mounted on trucks with some lateral flexibility and consists of a violent lateral sway of the cab with a period of several seconds per cycle. It is obviously a self-excited vibration with the energy furnished by the rail friction. However, there is no gyroscopic coupling as in the automobile. The details of the mechanism of this phenomenon are not fully understood at the present time.

Problems

114. Test the stability of the following frequency equations:

(*a*) $s^3 + 5s^2 + 3s + 2 = 0$.

(*b*) $s^4 + 8s^3 + 10s^2 + 5s + 7 = 0$.

(*c*) $s^4 - 2s^3 + 5s^2 - 3s + 2 = 0$.

115. The landing gear of an airplane consists of two wheels whose axes are rigidly attached to the fuselage and a third trailing wheel which is castored, *i.e.*, can swivel about a vertical axis (Fig. 234*a*). Necessarily the center of gravity of the airplane is located so that its projection falls

within the triangle formed by the three wheels. Prove that, if this gear is rolling over the ground with the two wheels forward as usual, the operation is unstable, *i.e.*, a small angular deviation of the rear wheel will increase and the plane will execute a "ground loop."

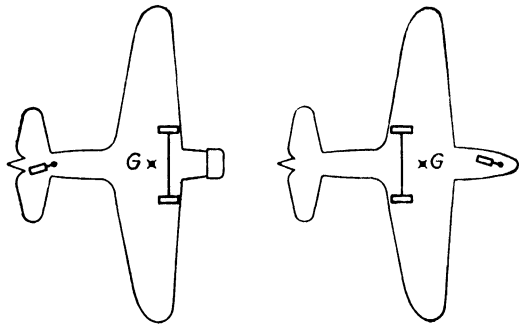


FIG. 234.

Prove that if the castored wheel is located in front of the two steady wheels, as with a so-called "tricycle," landing gear (Fig. 234*b*), the operation is stable.

116. A pendulum with a light rod a and a heavy weight of mass M at a distance l from the point of support is hanging on a round shaft S (Fig. 235).

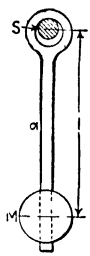


FIG. 235.

If the shaft S is rotating at a large angular velocity ω and the friction torque on the shaft is T_0, find:

a. The equilibrium position of the pendulum in terms of the angle α_0 with the vertical.

Discuss the small vibrations which the pendulum may execute about this equilibrium position for the following three cases:

b. The friction torque T_0 is absolutely constant.

c. T_0 increases slightly with increasing velocity of slip.

d. T_0 decreases slightly with increasing velocity of slip.

117. A weight **W** rests on a table with the coefficient of friction f (Fig. 236). A spring k is attached to it with one end while the motion of the other end is prescribed by

$$t < 0 \qquad v = 0$$
$$t > 0 \qquad v = v_0$$

or, in words, at the time $t = 0$ the spring end suddenly starts moving with a constant velocity v_0. Discuss the motion and construct displacement-time diagrams of the mass for the three cases *b*, *c*, and *d* of Problem 116.

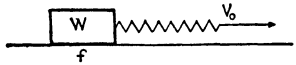


FIG. 236.

118. A certain cross section has a diagram Fig. 222 with the following curves:

$$\text{Lift} = L_0 \sin 2\alpha$$

$$\text{Drag} = D_0 - \frac{D_0}{2} \cos 2\alpha$$

If a piece of such a section is mounted in the apparatus of Fig. 218 in the position $\alpha = 90$ deg., for what ratio L_0/D_0 does instability start?

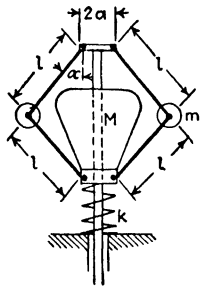


FIG. 237.

119. Figure 237 shows a Watt's governor with the dimensions l, a, m, M, and k. At standstill the spring k is such that the angle α of the flyball arms is 30 deg. At the full rotational speed Ω the angle α is 45 deg.

a. Express k in terms of the other variables.

b. Calculate the natural frequency at standstill.

c. Calculate the natural frequency while the governor is rotating with speed Ω.

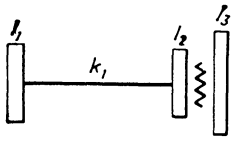


FIG. 237*a*.

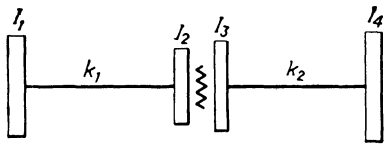


FIG. 237*b*.

120. Transform Eq. (179) into a relation between four dimensionless variables: one frequency ratio $\mathbf{f} = \omega_g/\omega_e$, two damping ratios $C_e = (c/c_e)_{\text{eng}}$ and $C_2 = (c/c_c)_{\text{gov}}$, and a dimensionless feedback or coupling quantity Γ. Plot the results so found on a diagram for one certain value of $\mathbf{f}$; C_e = ordinate, C_g = abscissa, and Γ = parameter for the various curves. Interpret these graphs.

121. Referring to Fig. 228, find the natural frequency of the steam column m on the "steam spring" of the chamber **V.** The mass M is supposed to be held clamped.

122. A system consists of an engine I_1, driving a shaft k_1 (Fig. 237*a*). At the other end of k_1 is attached a fluid-flywheel coupling (page 271), the "driver" of which has an inertia I_2. The "follower" is attached to a piece of driven machinery of inertia I_3. Set up the differential equations of motion, using Eq. (147*a*), write the frequency equation, and find whether the system is or is not capable of self-excited oscillations.

123. The same as Problem 122, only the "follower" of inertia I_3 drives a shaft k_2, at the other end of which is a flywheel I_4 (Fig. 237*b*).

CHAPTER VIII

SYSTEMS WITH VARIABLE OR NON-LINEAR CHARACTERISTICS

66. The Principle of Superposition.—All the problems thus far considered could be described by linear differential equations with constant coefficients, or, physically speaking, all masses were constant, all spring forces were proportional to the respective deflections, and all damping forces were proportional to a velocity. In this chapter it is proposed to consider cases where these conditions are no longer true, and, on account of the greater difficulties involved, the discussion will be limited to systems of a single degree of freedom. The deviations from the classical problem (12), page 35, are twofold.

First, in Sec. 67, 68, and 69, we shall consider differential equations which are linear but in which the coefficients are functions of the time. In the remainder of the chapter non-linear equations will be discussed. The distinction between these two types is an important one. Consider the typical linear equation with a variable coefficient:

$$m\ddot{x} + c\dot{x} + f(t)x = 0 \tag{198}$$

which describes the motion of a system where the spring constant varies with the time. Assume that we know two different solutions of this equation:

$$x = \varphi_1(t) \qquad \text{and} \qquad x = \varphi_2(t)$$

Then $C_1\varphi_1(t)$ is also a solution and

$$x = C_1\varphi_1(t) + C_2\varphi_2(t) \tag{199}$$

is the *general* solution of Eq. (198). Any two known solutions may be added to give a third solution, or

The principle of superposition holds for the solutions of linear differential equations with variable coefficients.

The proof of this statement is simple.

$$m\ddot{\varphi}_1(t) + c\dot{\varphi}_1(t) + f(t)\varphi_1(t) = 0$$
$$m\ddot{\varphi}_2(t) + c\dot{\varphi}_2(t) + f(t)\varphi_2(t) = 0$$

Multiply the first equation by C_1 and the second by C_2 and add:

$$m[C_1\ddot{\varphi}_1(t) + C_2\ddot{\varphi}_2(t)] + c[C_1\dot{\varphi}_1(t) + C_2\dot{\varphi}_2(t)] + f(t)[C_1\varphi_1(t) + C_2\varphi_2(t)] = 0$$

This shows that $[C_1\varphi_1(t) + C_2\varphi_2(t)]$ fits the differential Eq. (198) and therefore is a solution.

In mechanical engineering it is usually the *elasticity* that is variable (Eq. 198). There is, however, one important case where the *mass* is variable with time (Fig. 141, page 232). This case can be discussed on the same mathematical basis as that of variable elasticity, provided damping is absent. We have

$$m(t) \cdot \ddot{x} + kx = 0 \tag{200}$$

where $m(t)$ is the variable mass. Dividing by $m(t)$,

$$\ddot{x} + \frac{k}{m(t)}x = 0 \tag{200a}$$

This equation describes a system of unit mass (constant mass) and of variable elasticity.

A *non-linear* equation is one in which the displacement x or its derivatives do not appear any more in the first power, such, for example, as

$$m\ddot{x} + kx^2 = 0 \tag{201}$$

or more generally

$$m\ddot{x} + f(x) = 0 \tag{202}$$

The principle of superposition is not true for the solutions of non-linear equations.

This can be easily verified. Let $x_1 = \varphi_1(t)$ and $x_2 = \varphi_2(t)$ be solutions of (201):

$$m\ddot{\varphi}_1(t) + k[\varphi_1(t)]^2 = 0$$
$$m\ddot{\varphi}_2(t) + k[\varphi_2(t)]^2 = 0$$

Hence, by addition,

$$m[\ddot{\varphi}_1(t) + \ddot{\varphi}_2(t)] + k[\{\varphi_1(t)\}^2 + \{\varphi_2(t)\}^2] = 0$$

If $(\varphi_1 + \varphi_2)$ were a solution, the last square bracket should be $(\varphi_1 + \varphi_2)^2$. But the term $2\varphi_1\varphi_2$ is missing, so that $(\varphi_1 + \varphi_2)$ is *not* a solution of (201).

The general solution of (201) or (202) can still be written in a form containing two arbitrary constants C_1 and C_2, since the

process of solution is, in principle, a double integration. But although for linear equations a knowledge of two particular solutions immediately leads to the general solution in the form (199), this is no longer true for a non-linear equation. Very few non-linear equations exist for which the general solution is known. As a rule all we can do is to find particular solutions and even these in an approximate manner only.

67. Examples of Systems with Variable Elasticity.—In this section seven cases are discussed physically and a partial explanation of their behavior is given. The more fundamental treatment is necessarily mathematical and will be taken up in the next two sections.

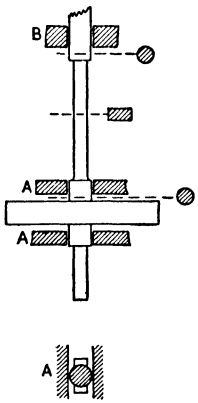


FIG. 238.—A disk mounted on a shaft with non-uniform elasticity. The disk is confined to motion in one plane only.

First consider a disk mounted on the middle of a vertical shaft running in two bearings B of which only the upper one is shown in Fig. 238. The cross section of the shaft is not completely circular but is of such a nature that two principal directions in it can be distinguished, one of maximum and one of minimum stiffness as, for example, in a rectangular section. Assume the shaft to have two circular spots A, A close to the disk. These round spots A can slide without friction in two straight guides restricting the motion of the shaft to one plane, *e.g.*, to the plane perpendicular to the paper. The disk on the shaft flexibility is a vibrating system of a single degree of freedom. While the shaft is rotating, the spring constant varies with the time, from a maximum $k + \Delta k$ to a minimum $k - \Delta k$, twice during each revolution, so that the equation of motion is

$$m\ddot{x} + (k + \Delta k \sin \omega_k t)x = 0 \tag{203}$$

where ω_k is *twice* the angular speed of rotation of the shaft and the subscript k is used to suggest variation in the elasticity k.

Next, place the same shaft horizontal with the guides A vertical so that the vibration of the disk is restricted to the vertical direction. The weight $\mathbf{W}$ of the disk acts as an additional force so that Eq. (203) changes to

$$m\ddot{x} + (k + \Delta k \sin \omega_k t)x = \mathbf{W} \tag{204}$$

If the elasticity were constant, there would be no significant difference between (203) and (204), because (204) could be transformed into (203) by merely taking another origin for the coordinate x (the distance between these two origins would be the static deflection of the disk). With variable elasticity, however, this is not so. Let us take a new variable

$$y = x + C$$

where C is a constant to be determined so as to make the result as simple as possible. Substitute in (204) which becomes

$$m\ddot{y} + (k + \Delta k \sin \omega_k t)y = \mathbf{W} + kC + C\Delta k \sin \omega_k t \quad (205)$$

If the variation in elasticity Δk were zero, we could choose C equal to $-\mathbf{W}/k$ and thus transform (205) into (203). With $\Delta k \neq 0$, this cannot be done. By imagining $\mathbf{W} = 0$ in the last result, it is interesting to see that (203) by a mere shift of the origin of x can be given a right-hand member which can be classed as an extraneous exciting force of frequency ω_k [see Eq. (151c), page 311].

We see that (203) and (204) cannot be transformed into one another; they are definitely different and have to be so treated.

Assume that the *variations* in k are small with respect to k (Δk is 10 per cent of k or less). Then the elastic force is principally that of k and the motion of the disk is nearly harmonic with the frequency $\omega_n = \sqrt{k/m}$. When this natural frequency of motion ω_n has a proper relation to the frequency of spring variation ω_k and when also a proper phase relation exists, it is possible to build up large vibrations. Consider the curves Fig. 239*a* and *b*, illustrating the motion x of the disk with a frequency ω_n and a variation in shaft stiffness taking place at twice that frequency. These diagrams pertain to the vertical shaft (no gravity) so that OA is the equilibrium line where there are no bending stresses in the shaft. The elastic force is therefore the product of the ordinates of Figs. 239*b* and 239*a*, measured from OA. With the phase relation shown in the figure it is seen that, while the disk is moving away from the center position (1-2 and 3-4), the spring force is smaller than its average value, whereas, while the disk is moving toward the center, the spring force is greater than its average value (2-3 and 4-5). Thus the spring

force is small while opposing the motion and large while helping the motion. Hence, over a full cycle the spring force does work on the system and the vibration, once started, builds up: we have instability.

With gravity, the spring force is still the product of k and the amplitude of Fig. 239*a*, but this time the ordinate is not measured from base OA, but rather from the base BB, distant from OA by the static deflection δ_{st}. The presence of the extra δ_{st} does not change the previous argument with respect to the k-variation shown in Fig. 239*b*, but it is now possible to obtain work input

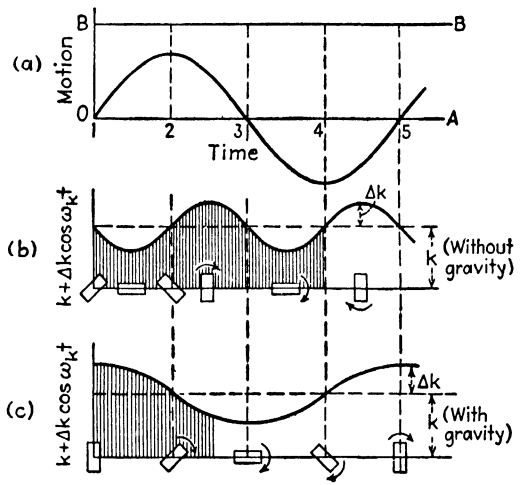


FIG. 239.—Explains instability in the flat shaft at half and full critical speed.

with another k-variation, shown in Fig. 239*c*, with $2\omega = \omega_n$ (shaft running at *half* critical speed). This is so because the spring force is small (2 to 4) while the disk is going away from its equilibrium position BB and large (1 to 2 and 4 to 5) while it is coming toward BB.

The work input per cycle in general is $\int F\,dx = -\int kx\,dx$, where $x = \delta_{st} - x_0 \sin \omega t$. In the case of Fig. 239*b* we write for $k = k - \Delta k \sin 2\omega t$, and the reader is asked to substitute this into the integral and verify that the work input per cycle is $+\frac{\pi}{2}\Delta k x_0^2$, which is independent of δ_{st}. For the case of Fig. 239*c* we write for $k = k + \Delta k \cos \omega t$, and the work input becomes

$+\pi\ \Delta k x_0 \delta_{st}$, which is seen to exist only in the presence of gravity.

Thus the physical analysis leads to the following conclusions:

1. In the system described by Eq. (203), *i.e.*, in the vertical shaft with flats, any small vibrations at the natural frequency $\omega_n = \sqrt{k/m}$ that may exist will be increased to large amplitudes if the shaft runs at its full critical speed ($\omega_k = 2\omega_n$).

2. For the system of Eq. (204), *i.e.*, for the horizontal shaft with flats, the same type of instability exists at the full critical speed as well as at half the critical speed ($\omega_k = \omega_n$).

These conclusions are tentative; an analysis of the equation in the following sections will show to what extent they have to be supplemented.

Practical cases in which shafts of non-circular section have given rise to critical speeds of one-half the normal are illustrated in Fig. 240. The first of these is a shaft with a keyway cut in it. There the trouble can be corrected by cutting two additional dummy keyways, symmetrically placed, which makes the stiffness uniform in all directions.

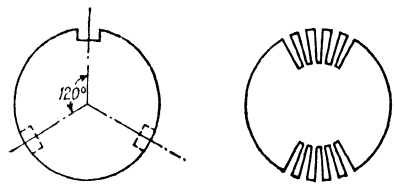


FIG. 240.—Cases of non-uniform flexibility in shafts and rotors.

The other example is found in the cross section of a two-pole turbogenerator rotor, in which slots are cut for the electric windings, the solid parts forming the pole faces. In this case the non-uniform elasticity cannot be avoided, so that a two-pole rotor will always be rough at half its critical speed.

A *second* case quite similar to the example of the shaft is that of a string with a mass m in the center. The tension in the string is varied with a frequency ω_k between a maximum $\mathbf{T} + \mathbf{t}$ and a minimum $\mathbf{T} - \mathbf{t}$ by pulling at the end (Fig. 241). If we pull hard while m is moving toward the center and slack off while m is moving away from the center, a large vibration will be built up. While m is describing a full cycle, the end of the string describes two cycles. We have the case of Fig. 239*b*. If the string is horizontal a gravity effect comes in, making the system subject to Eq. (204) and Fig. 239*c*.

The periodic change in tension may also be brought about by a change in temperature. A wire in which an alternating current is flowing has temperature variations and consequently variations in tension having double the frequency of the current. Lateral oscillations will build up if the natural frequency is either equal to or twice as large as the electric frequency.

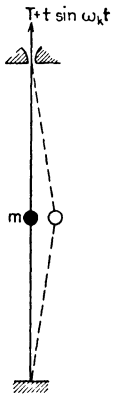


FIG. 241.—String with variable tension as the second example of Eq. (203).

A *third* case is illustrated in Fig. 242. A pendulum bob is attached to a string of which the other end is moved up and down harmonically. The spring constant k of a "mathematical pendulum" is mg/l, so that a periodic change in the length l means a corresponding change in the spring constant. Thus the sidewise displacements of the bob are governed by Eq. (203). In order to build up large oscillations by a length variation of $\omega_k = 2\omega_n = 2\sqrt{g/l}$, the string has to be pulled up in the middle of the swing and let down at the extreme positions, the bob describing a figure eight as indicated in Fig. 242. The tension in the string is larger for small angles φ than for great angles on account of two factors. In the extreme position the tension in the string is the weight of the bob multiplied by cos φ, which is less than unity. In the center, the tension is the weight plus the centrifugal force of the bob moving in its curved course. Thus the string is pulled up in the center against a large tension and let down at the extreme positions against a small tension. In this way work is put into the system, and this work is converted into the additional kinetic and potential energy of the larger vibrations.

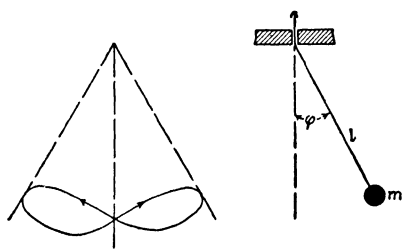


FIG. 242.—Pendulum of variable length.

The *fourth* example is more difficult to understand physically. It is nearly the same as the previous one, except that the pendulum is a stiff rod of constant length and the point of support (about which it can turn freely) is given a rapid up-and-down harmonic motion by means of a small electric motor. It will be

seen later (on page 422) that such a pendulum has the astounding property of being able to stand up vertically on its support. The spring constant of a pendulum *rod* is again mg/λ, but λ in this case is the "equivalent length." In this experiment the length λ is constant, but the gravity constant g varies periodically. This can be understood by considering the pressure of a man on the floor of an elevator car. While the elevator is standing still or moving at constant speed, this pressure is equal to the weight of the man; in an upward accelerated elevator it is more and in a downward accelerated car it is less. An impartial experimenter in the accelerated elevator may conclude that the value of g differs from its value on the earth. The same is the case with the pendulum. While it is being accelerated upward, g is apparently larger. Thus a periodically varying spring constant and the validity of Eq. (203) are shown. A more satisfactory derivation is given on page 423.

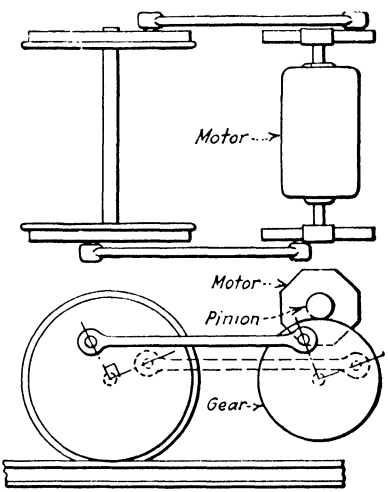


FIG. 243.—Torsional vibration in electric side-rod locomotive.

The *fifth* case to be discussed is technically the most important one. In electric locomotives of the side-rod type violent torsional vibrations in the drive system have been observed in several speed ranges. They are caused by a periodic pulsation in the spring constant, which can be understood from Fig. 243 representing one of the simplest constructions of this type. An electric motor is mounted on the frame and coupled to a driving axle by one connecting rod on each side of the locomotive. The two rods are 90 deg. offset so that the system as a whole does not have any dead center. With the usual operating conditions the wheels are locked to the rails by friction, but the motor can rotate slightly against the flexibility of the two side rods. When a side rod is at one of its dead centers, it does not prevent the motor from turning through a small angle, *i.e.*, its share in k is zero. When it is 90 deg. from its dead center, it constitutes a very stiff spring since it has to be elongated or the crank pins have to be

bent to allow a small rotation of the motor. The spring constant of *one* side rod, therefore, varies between a maximum and practically zero and performs two full variation cycles for each revolution of the wheel. The variation in the flexibility of the combination of two side rods is less pronounced and shows four cycles per revolution. The curves 1 and 2, Fig. 244, show the torque at the motor necessary for one unit of twisting angle, if only side rod 1 or 2 is attached. Curve 3, being the sum of curves 1 and 2, gives the resultant k for the whole system.

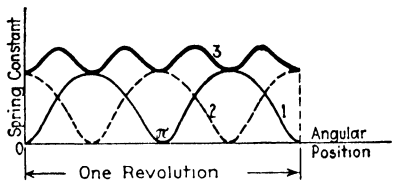


FIG. 244.—The torsional spring constant of Fig. 243 as a function of the angular position.

The torsional oscillations of the motor on its side-rod springs will take place superposed on the general rotation of the motor. The phenomenon is represented by Eq. (203) where ω_k is four times as large as the angular velocity of the wheels. It is to be expected, therefore, that serious vibrations will occur when $\omega_n = \frac{1}{2} \cdot [4(2\pi \text{ r.p.s.})]$.

A *sixth* example has been found in the small synchronous motors of electric clocks (Fig. 245). The rotating part of these motors usually consists of a very light piece of sheet metal A running around the poles B which carry the alternating current. The rotor can slide axially in its bearing but is held in a certain position by the magnetic field of the poles B. These poles act as magnetic springs of which the intensity becomes zero 120 times per second in a 60-cycle circuit, so that the variation in the spring constant is large (100 per cent). The trouble experienced consists in a noisy axial vibration of the rotor.

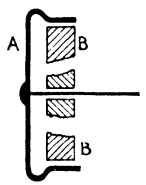


FIG. 245.—An electric clock motor is an axially vibratory system on the magnetic springs B.

The *seventh* and last illustration of (203) is the electrical analogue. A glance at the table on page 38 shows that we are dealing with a simple inductance-condenser circuit of which the condenser capacity is periodically varying, for instance by means of the crank mechanism of Fig. 246. The x of Eq. (203) stands for the charge Q on the condenser plates. A constant right-hand member in Eq. (204) can be provided by a direct-current battery in the circuit. First consider the system without battery.

Two charged condenser plates attract each other mechanically. The current in the L, C circuit will surge back and forth with the frequency $\omega_n = \sqrt{1/LC}$. Let the crank mechanism be so timed that the plates are pulled apart while the charge Q is large and pushed together again while Q and hence the attractive force are close to zero. Thus the crank mechanism (moving at double the current frequency: $\omega_k = 2\omega_n$) does mechanical work on the system and this work is converted into electrical energy. With a strong battery and small oscillations the charge on the condenser never changes its sign and the crank mechanism has to operate at the frequency $\omega_k = \omega_n$ in the fashion indicated in Fig. 239c.

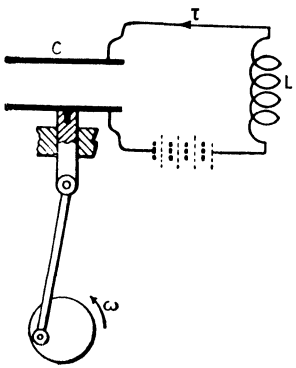


Fig. 246.—Electric circuit with variable condenser (spring).

68. Solution of the Equation.—Most of the problems discussed in the previous section depend for their solution on the differential equation

$$m\ddot{x} + [k + \Delta k \cdot f(t)]x = 0 \qquad (203a)$$

where $f(t)$ is a periodic function of the time, usually of the form $f(t) = \sin \omega_k t$. It is known as *Mathieu's* equation, and its general solution, containing two arbitrary integration constants, has not yet been found. In fact, there are very few equations with variable coefficients of which solutions are known. However, we are not so much interested in the solution itself, *i.e.*, in the exact shape of the motion, as in the question whether the solution is "stable" or "unstable." The simplest solution of (203*a*) is $x = 0$; in other words, the system remains at rest indefinitely. If it is given some initial disturbance ($x = x_0$ or $\dot{x} = v_0$), it cannot remain at rest and the distinction between stable and unstable motion refers to this case. By a stable solution we mean one in which the disturbance dies down with time as in a damped vibration, whereas an unstable motion is one where the amplitudes become larger and larger with time (Fig. 207).

If the "ripple" $f(t)$ on the spring constant has the frequency ω_k, the motion, though it may not be periodic, will show certain regularities after each interval $T = 2\pi/\omega_k$.

Suppose that the system starts off at the time $t = 0$ with the amplitude $x = x_0$ and with the velocity $\dot{x} = v_0$. Let the (unknown) solution be $x = F(t)$ and assume that after the end of one period $T = 2\pi/\omega_k$ the amplitude and velocity of the system are given by their values at the beginning, multiplied by a factor **s** (positive or negative):

$$(x)_{t=\frac{2\pi}{\omega_k}} = \mathbf{s}x_0 \qquad (\dot{x})_{t=\frac{2\pi}{\omega_k}} = \mathbf{s}v_0 \tag{206}$$

Whether this assumption is justified remains to be seen. If it is justified, we find ourselves at the beginning of the second cycle with an amplitude and velocity **s** times as great as at the beginning of the first cycle. Then it can easily be proved that the motion throughout the *whole* of the second cycle is **s** times as large as the motion during the corresponding instants of the first cycle and in particular that the third cycle starts with an amplitude $\mathbf{s}^2x_0$.

The proof is as follows: Let $x = F(t)$ be the solution of (203*a*) with the conditions

$$(x)_{t=0} = x_0 \qquad \text{and} \qquad (\dot{x})_{t=0} = v_0 \tag{207}$$

Take as a new variable during the second cycle $y = \mathbf{s}x$. The differential equation becomes (after multiplication by **s**)

$$my + [k + \Delta k f(t)]y = 0 \tag{208}$$

If the time is now reckoned from the beginning of the second cycle, the initial conditions are

$$(y)_{t=0} = \mathbf{s}x_0 = y_0 \qquad \text{and} \qquad (\dot{y})_{t=0} = \mathbf{s}v_0 = \dot{y}_0 \tag{209}$$

It is seen that (208) and (209) are exactly the same as (203*a*) and (207) so that the solution is $y = F(t)$. Therefore, $y = \mathbf{s}x$ behaves during the second cycle in exactly the same manner as x behaves during the first cycle.

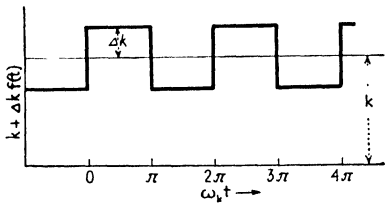


FIG. 247.—Variation in elasticity for which Eq. (203*a*) can be solved.

Thus, if the supposition (206) is correct, we have solutions that repeat in ω_k-cycles but multiplied by a constant factor in much the same manner as Eq. (24) or Fig. 207. If **s** is smaller than unity, the motion is damped or stable; if **s** is larger than unity, the motion is unstable. For any general periodic $f(t)$, Eq. (203*a*) cannot be solved. The particular case of a "rectangular ripple"

Δk on the spring constant k, however, is comparatively simple of solution (Fig. 247). In most practical cases the ripple is more sinusoidal than rectangular, but the general behavior of a system such as is shown in Fig. 247 is much the same as that of a system with a harmonic ripple on the spring force.

With the notation $k/m = \omega_n^2$ and $f(t) = \pm 1$, the differential equation (203a) becomes for $0 < \omega_k t < \pi$,

$$\ddot{x} + \left(\omega_n^2 + \frac{\Delta k}{m}\right)x = 0 \tag{210}$$

and for $\pi < \omega_k t < 2\pi$,

$$\ddot{x} + \left(\omega_n^2 - \frac{\Delta k}{m}\right)x = 0 \tag{211}$$

Both of these equations are easily solved, since the coefficient of x is now constant. The solution for the first half cycle is [see Eqs. (13) and (14), page 42]

$$x_1 = C_1 \sin p_1 t + C_2 \cos p_1 t \qquad \left(p_1 = \sqrt{\omega_n^2 + \frac{\Delta k}{m}}\right) \tag{212}$$

and for the second half cycle

$$x_2 = C_3 \sin p_2 t + C_4 \cos p_2 t \qquad \left(p_2 = \sqrt{\omega_n^2 - \frac{\Delta k}{m}}\right) \tag{213}$$

These two solutions should be fitted together at $\omega_k t = \pi$ with the same amplitude and velocity; moreover, they should describe a motion which at the end of a full cycle is s times as large as at the beginning. Thus

$$\left.\begin{aligned} (x_1)_{\omega_k t = \pi} &= (x_2)_{\omega_k t = \pi} \\ (\dot{x}_1)_{\omega_k t = \pi} &= (\dot{x}_2)_{\omega_k t = \pi} \\ (x_2)_{\omega_k t = 2\pi} &= \mathbf{s}(x_1)_{\omega_k t = 0} \\ (\dot{x}_2)_{\omega_k t = 2\pi} &= \mathbf{s}(\dot{x}_1)_{\omega_k t = 0} \end{aligned}\right\} \tag{214}$$

are four equations from which the four arbitrary constants in (212) and (213) can be determined.

Written out fully the first equation of (214) is

$$C_1 \sin \frac{\pi p_1}{\omega_k} + C_2 \cos \frac{\pi p_1}{\omega_k} - C_3 \sin \frac{\pi p_2}{\omega_k} - C_4 \cos \frac{\pi p_2}{\omega_k} = 0$$

and the remaining three are of the same type, homogeneous in C_1, C_2, C_3, and C_4. This set of four algebraic equations can have

solutions for the C's only if their determinant is zero as explained on pages 105 and 157. Therefore,

$$\begin{vmatrix} \sin\frac{\pi p_1}{\omega_k} & \cos\frac{\pi p_1}{\omega_k} & -\sin\frac{\pi p_2}{\omega_k} & -\cos\frac{\pi p_2}{\omega_k} \\ p_1\cos\frac{\pi p_1}{\omega_k} & -p_1\sin\frac{\pi p_1}{\omega_k} & -p_2\cos\frac{\pi p_2}{\omega_k} & p_2\sin\frac{\pi p_2}{\omega_k} \\ 0 & \mathbf{s} & -\sin\frac{2\pi p_2}{\omega_k} & -\cos\frac{2\pi p_2}{\omega_k} \\ \mathbf{s}p_1 & 0 & -p_2\cos\frac{2\pi p_2}{\omega_k} & p_2\sin\frac{2\pi p_2}{\omega_k} \end{vmatrix} = 0$$

is a condition that has to be satisfied if our original assumption (206) is correct. Of all the quantities appearing in this determinant only $\mathbf{s}$ has no definite value and is at our disposal. It is seen that the determinant is a quadratic equation in $\mathbf{s}$. After a somewhat laborious working out, it becomes

$$\mathbf{s}^2 - 2\mathbf{s}\left\{\cos\frac{\pi p_1}{\omega_k}\cos\frac{\pi p_2}{\omega_k} - \frac{p_1^2+p_2^2}{2p_1p_2}\sin\frac{\pi p_1}{\omega_k}\sin\frac{\pi p_2}{\omega_k}\right\} + 1 = 0 \quad (215)$$

If, for brevity, the expression within the braces be denoted by A, the solution of (215) is

$$\mathbf{s} = A \pm \sqrt{A^2 - 1} \quad (216)$$

In case $A > 1$, one of the two possible values of $\mathbf{s}$ is greater than unity and the solution is unstable. After each ω_k-cycle the magnified deflection is in the same direction, so that in each ω_k-cycle there have taken place 1 or 2 or 3 . . . cycles of the free vibration ω_n.

If A lies between -1 and $+1$, the two values for $\mathbf{s}$ become complex, which means that the original assumption (206) is untenable. However the real part of $\mathbf{s}$ is less than unity, so that we expect a motion which does not increase regularly with the time: the system is stable.

Finally, when A is smaller than -1, one of the values of $\mathbf{s}$ will also be smaller than -1. This means physically that after one ω_k-cycle, the amplitude and velocity of the system are reversed and are somewhat larger. After two ω_k-cycles they have the same sign and are also larger (multiplied by $\mathbf{s}^2$ which is positive and larger than one). Again we have instability, but during each ω_k-cycle we see $\frac{1}{2}$, $1\frac{1}{2}$, $2\frac{1}{2}$ cycles of the free vibration ω_n.

Thus briefly the system is *unstable* if $|A| > 1$, or if

$$\left|\cos\frac{\pi p_1}{\omega_k}\cos\frac{\pi p_2}{\omega_k} - \frac{p_1^2 + p_2^2}{2p_1p_2}\sin\frac{\pi p_1}{\omega_k}\sin\frac{\pi p_2}{\omega_k}\right| > 1 \qquad (217)$$

where the symbol | | means "numerical value of" and the significance of p_1 and p_2 is given by (212) and (213). In this relation there are two variables, p_1/ω_k and p_2/ω_k, or more significantly, ω_n/ω_k (the ratio of the "free" and "elasticity" frequencies) and $\Delta k/k$ (the "percentage of variation," Fig. 247).

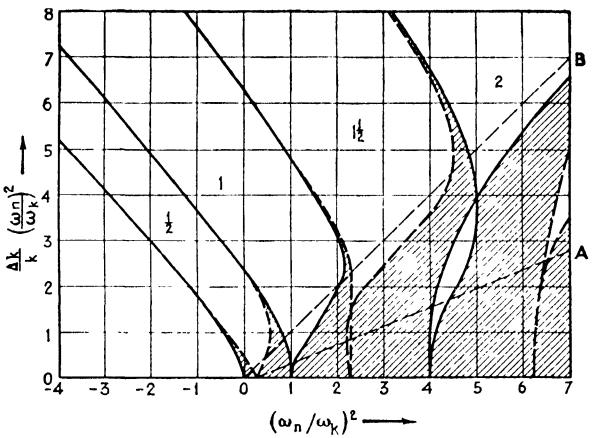


FIG. 248.—Fundamental diagram determining the stability of a system with variable elasticity. The shaded regions are stable and the blank regions are unstable. (Van der Pol and Strutt).

The result (217) is shown graphically in Fig. 248, where for convenience the abscissas are taken as $(\omega_n/\omega_k)^2$ and the ordinates as $(\Delta k/k)\cdot(\omega_n/\omega_k)^2$. The reason for this choice of abscissa is that with the second power, a negative spring constant (such as appears in the vertical pendulum) can be plotted as a negative $(\omega_n/\omega_k)^2 = -k/m\omega_k^2$, whereas with the first power of ω_n/ω_k the abscissa for a negative spring would become imaginary. For the ordinate the case of no steady spring constant, $k = 0$, would lead to an infinite ratio $\Delta k/k$; this defect is avoided by taking $\frac{\Delta k}{k}\left(\frac{\omega_n}{\omega_k}\right)^2 = \frac{\Delta k}{m\omega_k^2}$. In the figure the lines where (217) equals $+1$ are drawn in full, while those along which (217) is -1 are dashed. In the shaded regions the expression (217) is less than unity, which indicates stability, while in the non-shaded regions its

value is greater than unity, denoting instability. The numbers ½, 1, 1½, etc., inscribed in the regions of instability indicate the number of vibrations of the system during one ω_k-period of the variation in stiffness.

69. Interpretation of the Result.—From Fig. 248 the behavior of the various systems of Sec. 67 can be deduced more accurately than was possible from the simple physical considerations given in Sec. 67. The examples come in three groups:

a. The shaft, the string, the locomotive, and the variable condenser all have a frequency of variation ω_k which can vary over a considerable range and have also a *small* variation percentage $\Delta k/k \ll 1$ with a *positive* k.

b. The electric-clock motor has a constant ω_k-frequency, large variations ($\Delta k/k = 1$), and a positive k.

c. The pendulum standing on end has a variable ω_k-frequency and a *negative* k, *i.e.*, it is statically unstable.

Before discussing any one case in detail, it should be remembered that the diagram, Fig. 248, has been derived for a "rectangular ripple," so that only approximate results are to be expected from its use for most actual cases where the variation is nearly harmonic. However, the approximation is a very good one. Moreover, no *damping* has been considered.

First we shall discuss the examples of group *a*. In each case the percentage of variation $\Delta k/k$ and the average natural frequency $\omega_n = \sqrt{k/m}$ are constant. The only variable in the system is the frequency of variation in elasticity ω_k. In the diagram the ordinate is always $\Delta k/k$ times as large as the corresponding abscissa. Each system, therefore, can move only along a straight line through the origin of Fig. 248 at an inclination $\tan^{-1} \Delta k/k$ with the horizontal. The line for $\Delta k/k = 0.4$ (40 per cent variation) is drawn and marked OA. A slow variation ω_k corresponds to a point on that line *far* from the origin O, while the points close to the origin have a small value of $(\omega_n/\omega_k)^2$ and therefore a large ω_k. It is seen that most of the points on OA are in stable regions where no vibration is to be feared, but we also note that there are a great (theoretically an infinitely great) number of rather narrow regions of instability. These occur approximately at $\omega_n/\omega_k = ½, 1, 1½, 2, 2½$, etc.

Now imagine the electric locomotive to start very slowly and to increase its speed gradually, until finally the variation in side-rod elasticity (being four times as fast as the rotation of the

wheels) equals twice the natural frequency of torsional vibration. Along *OA* in Fig. 248 this means a motion from infinity to the point where $(\omega_n/\omega_k)^2 = \frac{1}{4}$, *and it is seen that an infinite number of critical speeds has been passed.*

From Sec. 67 it seems that the two speeds, for $\omega_n/\omega_k = 1$ and $\omega_n/\omega_k = \frac{1}{2}$ are the most significant and that the other critical speeds are much less important. Nevertheless it is impossible to avoid these low-speed instabilities by changes in the design, unless of course the variation Δk can be made zero. Vibrations of this sort have caused great trouble in the past. They were overcome chiefly through introducing torsionally flexible couplings with springs between the motor gear and its crank or between the driving wheel and its crank. These couplings act in two ways. First, they shift the natural frequency ω_n to a low value so that all critical regions lie below a rather low speed, say 20 m.p.h. At these low speeds the intensity of the input cannot be expected to be very great. Furthermore, the springs, especially if they are of the leaf type, have some internal friction in them so that they introduce damping.

Similar results hold for any of the other examples in group *a*. In particular a shaft with two flat sides will pass through a great number of critical-speed regions. In the actual experiment, however, only the highest two of these critical speeds prove to be of importance, one occurring at half the usual "primary" critical speed and the other at that speed itself.

In group *b* we have the axial vibrations of the electric-clock motor caused by a periodically vanishing elasticity. Here $\Delta k/k = 1$, which for variable speed ω_k is represented by a straight line at 45 deg. (shown as *OB* in the diagram). In this case, it is seen that the regions of instability are wider than the regions of stability, so that the chance for trouble is far greater than before.

The last case, that of the inverted pendulum, is technically the least important but philosophically the most interesting.

In the first place, the spring constant k for such a pendulum is negative. This will be clear if we remember the definition of k, which is the force tending to bring the system *back* to its equilibrium position from a unit deflection. The gravity component attempts to *remove* the pendulum from the vertical so that k is negative. Hence $\omega_n^2 = k/m$ is also negative. For the *hanging* pendulum $\omega_n^2 = g/\lambda$ where λ is the equivalent length ($\lambda = \frac{2}{3}$ of

the over-all length in the case of a uniform bar). For the inverted pendulum,

$$\omega_n^2 = -\frac{g}{\lambda}$$

Let the motion of the supporting point be $e \sin \omega_k t$ which gives an acceleration $-e\omega_k^2 \sin \omega_k t$. The variation in elasticity amounts to

$$\frac{\Delta k}{k} = \frac{\Delta g}{g} = \frac{-e\omega_k^2}{g}$$

and the ordinate in Fig. 248 becomes

$$\frac{\Delta k}{k}\left(\frac{\omega_n}{\omega_k}\right)^2 = \frac{e}{\lambda}$$

being the ratio of the amplitude of the base motion to the equivalent length of the pendulum. The abscissa is

$$\left(\frac{\omega_n}{\omega_k}\right)^2 = -\frac{g}{\lambda\omega_k^2}$$

a negative quantity and small for rapid motions of the base.

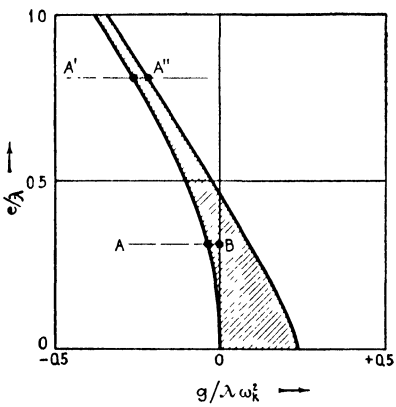


FIG. 249.—Detail of Fig. 248 giving an explanation for the stability of the inverted pendulum.

Figure 249 shows a detail of the main diagram of Fig. 248 which is important for the inverted pendulum. To be precise, Fig. 249 has been taken from the exact solution for a *sinusoidal* ripple (not given in this book), while Fig. 248 refers to a rectangular ripple. Incidentally it is seen that very little difference exists between the two.

If the pendulum is started with a given base amplitude e and with an increasing frequency ω_k, we move along the horizontal line from A toward B. For slow ω_k the system is clearly unstable, but at a certain speed it enters the stable region and remains there until at B the base speed ω_k becomes infinitely large. However, when the ratio e/λ is taken greater than about 0.5,

there is a large speed at which the pendulum becomes unstable for the second time, as indicated by the point A'' of the line $A'A''$.

The proof for the statement that the variation in elasticity may be considered as a variation in the gravity constant can be given by writing down Newton's laws of motion.

In Fig. 250 let

a = distance between point of support and center of gravity G,
$s = e \sin \omega_k t$ = displacement of support,
I = moment of inertia about G,
θ = angle with the vertical,
x, y = vertical (up and horizontal (to right) displacements of G,
X, Y = vertical (up) and horizontal (to right) reaction forces from support on pendulum.

Then the displacements of G are

$$x = s + a \cos \theta \approx s + a \qquad \text{(for small } \theta\text{)}$$
$$y = a \sin \theta \approx a\theta \qquad \text{(for small } \theta\text{)}$$

The three equations of Newton for the vertical and horizontal motion of G and for the rotation about G are

$$X - mg = m\ddot{x} = m\ddot{s}$$
$$Y = m\ddot{y} = ma\ddot{\theta}$$
$$Xa \sin \theta - Ya \cos \theta \approx Xa\theta - Ya = I\ddot{\theta}$$

The reactions X and Y can be eliminated by substituting the first two equations in the third one:

$$I\ddot{\theta} = m\ddot{s}a\theta + mga\theta - ma^2\ddot{\theta}$$

or

$$(I + ma^2)\ddot{\theta} - ma(g + \ddot{s})\theta = 0$$

The expression $I + ma^2$ is the moment of inertia about the point of support and the spring constant is

$$ma(g + \ddot{s})$$

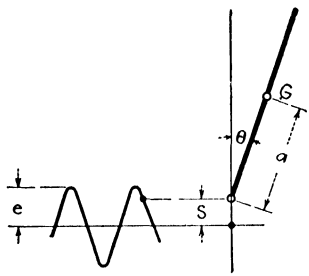


FIG. 250.—A pendulum with a harmonically moving point of support is equivalent to a pendulum with a stationary support in a space with a periodically varying constant of gravity g.

It is negative and its variation can be interpreted as a variation in g by the amount $\ddot{s}$, the acceleration of the support.

Finally we shall discuss the case of variable *mass*, illustrated in Fig. 141, page 232. Consider a simple piston and crank mechanism coupled through a flexible shaft k to a flywheel of infinite inertia (Fig. 251). Let the flywheel be rotating at uniform speed. This system is a torsional one of a single degree of freedom with the constant elasticity k and a variable moment of inertia (mass).

It was seen on page 407 that such a system is mathematically equivalent to one with variable elasticity and constant mass so that Fig. 248 applies. According to Fig. 248 we ought to experience critical speeds when the average natural frequency $\omega_n = \sqrt{k/I}$ is $\frac{1}{2}$, 1, $1\frac{1}{2}$, 2 · · · times the frequency ω_k of mass variation. It can be easily seen that the main frequency of mass variation is twice the r.p.m., so that the critical speeds should appear for $\omega_n = 1, 2, 3 \cdots$ times ω_{rpm}. The simple approximate theory culminating in Eq. (138), page 222, gives only one critical speed occurring at $\omega_n = 2\omega_{\text{rpm}}$ for a connecting rod of infinite length.

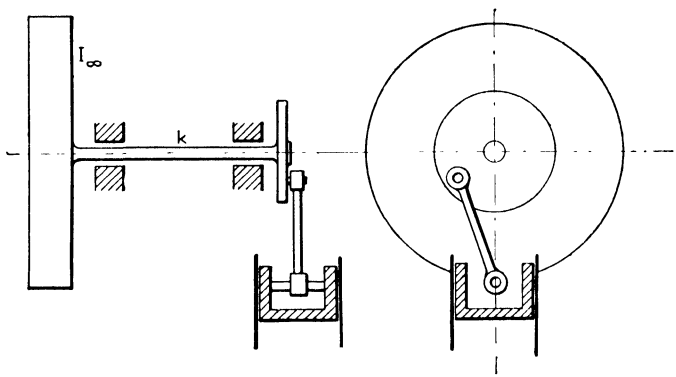


FIG. 251.—A system with periodically varying inertia.

70. Examples of Non-linear Systems.—Non-linearity consists of the fact that one or more of the coefficients m, c, or k depend on the displacement x. In mechanical cases the most important non-linearities occur in the damping or in the springs, whereas in electrical engineering the most common case is that of a non-linear inductance (mass).

Let us first consider some examples of non-linear springs. Figure 252 shows three cases where the spring force is not proportional to the displacement, but where the individual springs employed are yet ordinary linear coil springs. The first case is the very common one of clearances in the system. The mass can travel freely through the clearance without experiencing any spring force at all, but from there on the force increases linearly. The second case is that in which the springs have an initial compression and are prevented from expanding by the thin washers a resting against the lugs b. The mass m, being loose

from the washers, cannot move until a force is applied to it equal to the initial compressive force F of the springs. The third example is that of a spring with so-called "stops." For a small displacement the system is affected only by one set of springs,

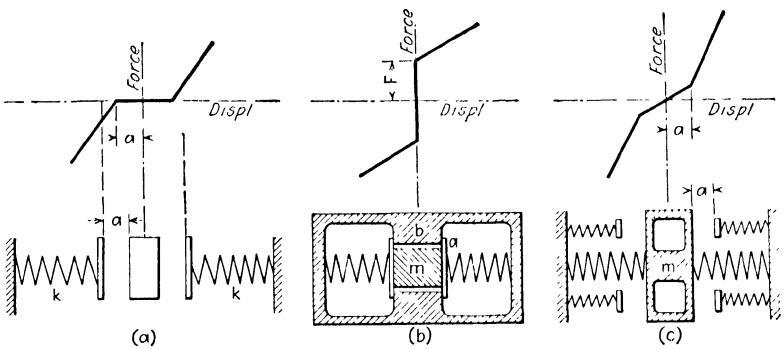


FIG. 252.—Combination of linear coil springs which form a non-linear elasticity. (*a*) Clearances; (*b*) set-up springs; (*c*) stops.

but after that another set comes into action and makes the combined spring much stiffer. The second set of springs sometimes consists of a practically solid stop, in which case the characteristic becomes nearly vertical after the stop is hit.

All three cases shown in Fig. 252 naturally have their torsional equivalents. In particular, set-up springs (Fig. 252*b*) are used often in the construction of torsionally flexible couplings.

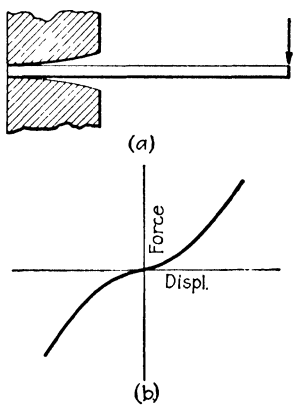


FIG. 253.—Spring with gradually increasing stiffness.

Figure 253 represents a cantilever spring which, when deflected, lies against a solid guide, thus shortening its free length and becoming stiffer. Hence its force-deflection characteristic becomes steeper for increasing deflections. More or less curved spring characteristics occur quite often in practice. In fact, most actual springs have a straight characteristic for small deflections only and then become stiffer for larger deflections.

Next consider some forms of non-linear *damping*. The linear damping force is $c\dot{x}$, proportional to the velocity. It is known

also as a *viscous* damping force, because it occurs in a dashpot with a viscous fluid.

Other types of damping which occur frequently are dry-friction or Coulomb damping and air or turbulent-water damping. The

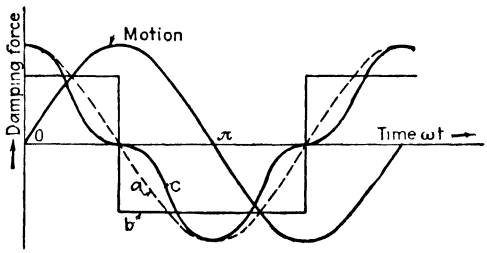


FIG. 254.—Various damping forces for the case of harmonic motion. *a*, viscous friction $c\dot{x}$; *b*, Coulomb friction $\pm F$; *c*, turbulent air damping $\pm cx^2$.

first of these is independent of the magnitude of the velocity, but is always opposite in direction to the velocity. The air or turbulent-water damping is approximately proportional to the square of the velocity and also is directed against it. The various forces plotted against the time for a sinusoidal motion are shown in Fig. 254.

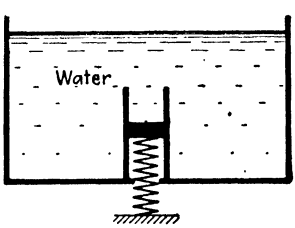


FIG. 255.—A system with a non-linear mass.

In practical mechanical problems the *mass* is usually a constant quantity. It is possible, however, to imagine a system where even this coefficient varies with the displacement. In Fig. 255, let the piston be very light and the amount of water in the cylinder small in comparison with that in the tank. Evidently the piston with the water column above it in the cylinder is a vibratory system since the rest of the water in the tank moves very little during the oscillation. But the length of the water column and therefore its mass depend on the displacement x. While for small oscillations of the piston the mass is practically constant, this ceases to be the case for larger motions, so that we have a system with a non-linear inertia coefficient (mass).

This example is of little practical value, and we turn to the electrical field to find important cases where the mass varies with x. Consider the simple *L-C*-circuit of Fig. 256 with or without alternating-current generator. The coil contains a soft iron core, which becomes magnetically saturated for a certain

value of the current. This is illustrated in Fig. 257 where, for a given frequency, the voltage across the coil is plotted against the current, giving a distinctly non-linear relation for larger values of the current. Since the voltage across the inductance coil is the electrical equivalent of the mechanical inertia force, it is seen that indeed we have before us a case of a mass depending on the displacement.

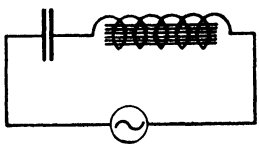


FIG. 256.—Non-linear electric circuit with a saturated core in the inductance.

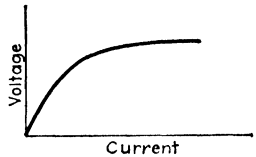


FIG. 257.—Saturation curve of the inductance of Fig. 256.

71. Free Vibrations with Non-linear Elasticity or Damping.—The most important new fact arising in a discussion of the *free* vibrations of these systems is that with the non-linearity in the *springs* the natural frequency is no longer independent of the amplitude of vibration. With non-linear *damping*, however (if it is not too great), the frequency depends very little on the amplitude. The reason for this can be readily understood. In a sense the natural frequency is the ratio of the intensity of the spring force to the inertia force for unit frequency. In the linear case these are both proportional to the deflection, and their ratio therefore must be independent of the deflection. If, however, the spring force is not proportional to the amplitude, as with a non-linear system, the natural frequency cannot remain constant.

On account of its 90-deg. phase angle a damping force disturbs the frequency as a second-order effect only (Fig. 36, page 54). This is true whether the damping is linear or not. Therefore no appreciable influence of the amplitude on the frequency should be found in the case of non-linear damping.

Consider the specific case of a motion with clearances a and springs with a constant k as shown in Fig. 252*a*. If the amplitude is smaller than a, there is no spring force whatever and the natural frequency is zero. On the other hand, for very large amplitudes x_{max}, the little irregularity between $+a$ and $-a$ is completely buried by the large motion, and we should expect a frequency $\omega_n = \sqrt{k/m}$. To find the complete relation $\omega_n = f(x_{max})$, we

fix our attention on the mass at the instant that it is in an extreme position, $x = x_{max}$ and $\dot{x} = 0$. In the absence of damping, the only force acting on the mass is the spring force, under the influence of which the mass will return to its central position in a certain time which is one quarter period $T/4$. We now proceed to calculate $T/4$, from which ω_n can be found immediately. With $x_{max} = a + x_0$ we introduce the distance x_0, along which the spring is acting. From $x = x_{max}$ to $x = a$, the system acts as a linear one with a frequency $\sqrt{k/m}$. The time it takes for this distance is one quarter period of the harmonic motion or $\frac{1}{4} \cdot \frac{2\pi}{\omega_n} = \frac{\pi}{2}\sqrt{\frac{m}{k}}$. At the end of this interval of time the mass is at $x = a$ and has acquired the maximum velocity $\omega_n x_0 = x_0\sqrt{k/m}$. From there to the center O no forces act on the mass so that it goes through the distance a with a constant velocity. This distance a takes $\frac{a}{x_0}\sqrt{\frac{m}{k}}$ sec.

The total time, being one quarter period of the non-linear motion, is

$$\left(\frac{a}{x_0} + \frac{\pi}{2}\right)\sqrt{\frac{m}{k}}$$

from which the natural frequency is found as

$$\left.\begin{aligned} \omega_n &= \sqrt{\frac{k}{m}} \cdot \frac{1}{1 + \frac{2a}{\pi x_0}} \\ x_0 &= x_{max} - a \end{aligned}\right\} \tag{218}$$

This relation is shown in the full line of Fig. 258. The dotted line represents an approximate solution obtained by the construction in Fig. 260. When the clearance $a = 0$, or the motion $x_{max} = x_0 = \infty$, the natural frequency reduces to $\sqrt{k/m}$, whereas for $x_0 = 0$ the frequency becomes zero.

For the *general* case of a curved characteristic this same procedure, involving the calculation of one quarter period, can be followed. With a spring characteristic $f(x)$ the equation of motion becomes

$$m\ddot{x} = -f(x)$$

But

$$m\ddot{x} = m\frac{dv}{dt} = m\frac{dv}{dx} \cdot \frac{dx}{dt} = mv\frac{dv}{dx} = -f(x)$$

Integrating,

$$m\frac{v^2}{2} = \int_{x_{max}}^{x} -f(x)dx$$

The limits of integration are from x_{max} where the velocity is zero, to the general position x where the velocity is v.

Further,

$$v = \sqrt{\frac{2}{m}} \cdot \sqrt{\int_{x_{max}}^{x} -f(x)dx} = \frac{dx}{dt}$$

Thus

$$t = \sqrt{\frac{m}{2}} \int_{x_{max}}^{x} \frac{dx}{\sqrt{\int -f(x)dx}}$$

which is the time it takes to go from x_{max} to x.

Clearly $t = T/4$ when the second integral extends from x_{max} to zero and

$$\frac{1}{f} = \frac{2\pi}{\omega_n} = T = \sqrt{8m} \int_{x_{max}}^{0} \frac{dx}{\sqrt{\int_{x_{max}}^{x} -f(x)dx}} \qquad (219)$$

This general formula enables us to calculate the natural frequency of a non-linear system having any kind of characteristic. Sometimes the two integrations can be performed directly, but, if this is not possible, they can always be evaluated graphically or numerically by subdividing the distance between x_{max} and 0 into a sufficient number of steps and assuming that in each step the spring force is constant. A rather well-known example of (219) is the mathematical pendulum with *large* oscillations. The equation is

$$ml^2\ddot{\varphi} + mgl \sin \varphi = 0$$

which for small oscillations is made linear by setting sin φ equal to φ. The frequency for large vibrations is found from (219) by substituting ml^2 for m, mgl sin φ for $f(x)$, and φ for x. In mathematical texts the integration is given as a classical example of elliptic functions.

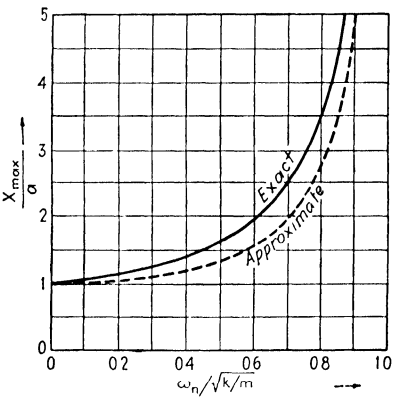


FIG. 258.—Natural frequency as a function of the maximum amplitude of vibration for the system with clearances (Fig. 252*a*).

If the non-linearity is located in the *damping* of the system, the natural frequency is not affected by the amplitude and remains approximately $\sqrt{k/m}$. The only question of interest here is the rate of dying down of the amplitude. An exact

solution to this problem can be found by a step-by-step (graphical or numerical) integration of the equation of motion, but this is too laborious. (Only for the simple case of Coulomb dry friction does a simple exact solution exist.)

A sufficiently accurate approximation for practical purposes is obtained by calculating the energy spent by the friction force during a cycle and equating this energy to the loss in kinetic energy of the motion. In order to be able to calculate these energy losses, we have to know the shape of the motion, which obviously is not sinusoidal but yet resembles a sinusoid for small values of the damping. The smaller the damping the better is this resemblance, because with a harmonic motion the *large* spring and inertia forces are harmonic and only the *small* damping force causes a deviation from this harmonic motion. Thus we assume harmonic motion $x = x_0 \sin \omega t$. If the damping force is represented by $f(\dot{x})$, its work per cycle is

$$W = \int f(\dot{x})dx = \int_0^T f(\dot{x})\dot{x}dt = x_0 \int_0^{2\pi} f(\dot{x}) \cos \omega t \, d(\omega t)$$

The loss in kinetic energy per cycle is

$$\tfrac{1}{2}m\omega^2 x_0^2 - \tfrac{1}{2}m\omega^2(x_0 - \Delta x)^2 = m\omega^2 x_0 \Delta x - \tfrac{1}{2}m\omega^2(\Delta x)^2 \approx m\omega^2 x_0 \Delta x$$

Equating the two expressions we find for the decrease in amplitude per cycle

$$\Delta x = \frac{1}{m\omega^2} \int_0^{2\pi} f(\dot{x}) \cos \omega t \, d(\omega t) \tag{220}$$

This integral can always be evaluated, even though it may sometimes be necessary to do it graphically.

As an example, consider Coulomb damping, where $f(\dot{x}) = \pm F$. The velocity and the damping force are shown in Fig. 259. The integral in (220) is seen to consist of four equal parts,

$$4 \int_0^{\frac{\pi}{2}} F \cos \omega t d(\omega t) = 4F$$

and the decrement in amplitude per cycle is

$$\Delta x = \frac{4F}{m\omega^2} = 4\frac{F}{k} \cdot \frac{k}{m} \cdot \frac{1}{\omega^2} = 4\frac{F}{k} \tag{221}$$

or four times the static deflection of the friction force on the spring. The result is significant in that the amplitude decreases in equal decrements as an arithmetic series, whereas in the case of viscous damping the amplitude decreases in equal percentage ratios as a geometric series (page 54). Incidentally it is of interest to know that (221) happens to coincide with the exact solution before mentioned.

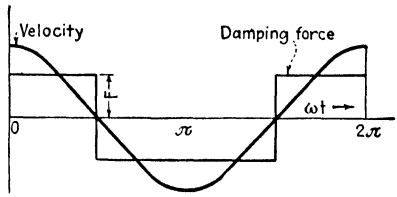


FIG. 259.—Coulomb damping force.

72. Forced Vibrations with Non-linear Springs.—The problem is that of an undamped system with a curved spring characteristic under the influence of a harmonic disturbing force or

$$m\ddot{x} + f(x) = P_0 \cos \omega t \tag{222}$$

Thus far an exact solution to this problem exists only for the simple characteristic of Fig. 252*b* and is so complicated as to be without much practical value. In the following pages an approximate solution will be given, based on the assumption that the motion $x = f(t)$ is sinusoidal and has the "forced" frequency. This is obviously not true, and the degree of approximation can be estimated only by the seriousness of the deviation from this assumption. Assume

$$x = x_0 \cos \omega t \tag{222a}$$

The inertia force $m\ddot{x}$ is $-mx_0\omega^2 \cos \omega t$, and this force attains its maximum value $-m\omega^2 x_0$ at the same instant that the external force reaches its maximum value P_0 and the spring force its maximum $f(x_0)$. Equation (222) is a condition of equilibrium among three forces at *any* time during the (non-harmonic) motion. Let us satisfy that condition for the harmonic motion (by a proper choice of x_0) at the instant that $x = x_0$. Thus

$$-m\omega^2 x_0 + f(x_0) = P_0$$

or

$$f(x_0) = P_0 + m\omega^2 x_0 \tag{223}$$

At the time when $x = 0$ (in the middle of the stroke), all three forces are zero so that the equilibrium condition is again satisfied. In case $f(x)$ were equal to kx, all three terms of (222) would be

proportional to sin ωt, so that (222) divided by sin ωt would give (223) with $f(x_0) = kx_0$ and the equilibrium condition would be satisfied at *all* values of x between 0 and x_0. However, when $f(x) \neq kx$, this is no longer true, and the equilibrium is violated at most points between 0 and x_0. To satisfy the equilibrium at the two points $x = 0$ and $x = x_0$ is the best we can do under the circumstances. Thus the amplitude of the forced vibration will be found approximately from the algebraic equation (223).

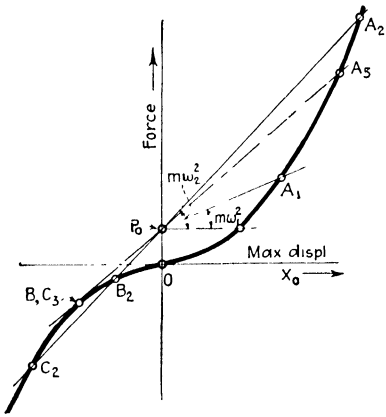


FIG. 260.—Approximate construction of the amplitudes of forced non-linear vibrations.

The most convenient and instructive manner in which this can be done is graphical. Plot the forces vertically and the amplitude x_0 horizontally as in Fig. 260. The left side of (223) is the (curved) spring characteristic, while the right side of the equation expresses a straight line with the ordinate intercept P_0 and the slope $\tan^{-1}$ $(m\omega^2)$. Where the two curves intersect, the left-hand force of (223) equals the right-hand force, so that equilibrium exists (at the end of a stroke). This determines x_0 as the abscissa of the point of intersection. For slow frequencies (small slopes $m\omega^2$), there is only one such point of intersection A_1, but for greater frequencies and the same force P_0 there are three intersections A_2, B_2, and C_2. In other words, there are then three possible solutions. To see this more clearly, we plot in Fig. 261 the amplitude x_0 against the frequency ω for a given constant value of the force P_0, which gives a resonance diagram corresponding to Fig. 38, page 59, for the linear case. (Incidentally, Fig. 38 can be constructed point by point in an exact manner from Fig. 260 with a straight-line characteristic.) It is left for the reader to develop Fig. 261 from Fig. 260 and in particular to see that for frequencies below BC_3 only one solution exists, and for frequencies above BC_3 three solutions exist; also that the A-branch of the diagram represents motions *in phase* with the force P_0 sin ωt, while the BC-branch is 180 deg. out of phase with this force. This peculiarity is the same as in Fig. 38.

Of the three possible motions A, B, or C, it has been found that C is *unstable*, whereas A and B represent *stable* motions which can be realized by experiment. In order to make this statement seem reasonable, it is necessary to complete the diagram of Fig. 261 with curves for other values of P_0, and this is done in Fig. 262. The central thick curve is the one for $P_0 = 0$, or, in other words, for the free vibration. It is found by drawing lines with slopes $m\omega^2$ from the origin O (Fig. 260) and determining their intersections with the characteristic. For frequencies ω below a certain value ω_0 the slope in Fig. 260 is too small to give any intersection at all. For increasing slope the x_0 becomes greater and greater. For a very small exciting force P_0 we obtain curve 1 of Fig. 262, while for greater values of P_0 the curves 2 and 3 result.

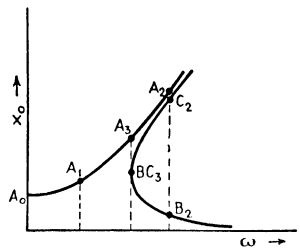


FIG. 261.—Resonance diagram for a system with a gradually stiffening spring.

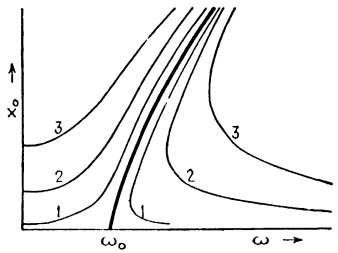


FIG. 262.—Explains the instability of the C-branch of Fig. 261.

Consider a point on the A-branch of one of the curves of Fig. 262. If for a given frequency the force P_0 is increased, the amplitude x_0 also increases (we move along a vertical line in Fig. 262). The same is true for any point on the B-branch of the curves. But on the C-branch an increase in the force P_0 means a downward motion in Fig. 262 (from curve 1 toward curve 2) and this means that an *increase* in the force results in a *decrease* in the amplitude. This cannot happen, however, and what actually takes place is shown in Fig. 263, representing the same curve as Fig. 261 with the influence of damping taken into account. This damping rounds off the resonance peak in the same manner as with a linear system. If the force amplitude P_0 is kept constant and the frequency ω is gradually increased, the amplitude x_0 suddenly drops from B to C and continues to D. With diminishing ω we pass D, C, and E, where the amplitude suddenly jumps up to F, then continues on to A. The unstable branch BE represents motions that cannot occur.

The characteristic of Fig. 260 represents a spring which becomes gradually stiffer with increasing amplitudes. This leads to a natural frequency which increases with the amplitude, as shown by the thick curve bending off to the right in Fig. 262. For a spring of *diminishing* stiffness (as, for example, Fig. 252*b*) the natural-frequency curve bends to the left and the unstable *C*-branch of the curves lies to the left of the central curve. In Fig. 264 the upward jump in amplitude happens with *increasing* frequency.

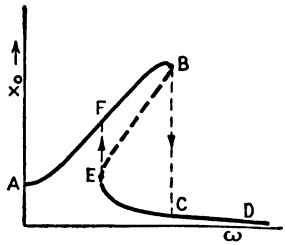


FIG. 263.—Discontinuous jumps in the amplitudes of a non-linear system with a gradually stiffening spring.

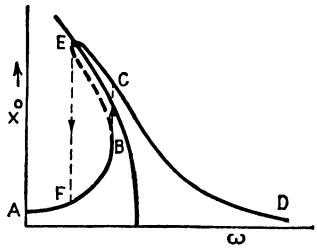


FIG. 264.—Resonance diagram for a spring in which the stiffness *decreases* with the amplitude.

An interesting method of solving this problem accurately by successive approximations for any spring characteristic is due to *Rauscher*. Instead of starting with a given frequency and then solving for the amplitude x_0, as was done in Fig. 260, Rauscher starts with an amplitude ratio x_0/P_0 and then solves for the frequency. In Eq. (222) the frequency ω is regarded as not fixed, and a first guess at the motion is Eq. (222*a*), in which x_0 is given a definite value, while ω is the frequency of the force, as yet floating. Then we may write $P_0 \cos \omega t = P_0 x/x_0$, which transforms the exciting force from a time function to a displacement function. The exciting force is now brought to the left-hand side of Eq. (222) and combined with the spring force $f(x)$. The problem reduces to one of free vibration, which can be solved by means of Eq. (219). The displacement-time curve so obtained will not be the same as the first guess (222*a*) for it, but it *will* have the same maximum amplitude x_0. With this new displacement function we enter once more into the differential equation (222), transform the exciting force from a t-function to an x-function, and throw it to the left so as to combine it with the spring force. In this manner the third solution for $x = f(t)$

is obtained. These successive solutions for the motion converge very rapidly to the exact one. Being a method of "iteration" it is very closely related to *Stodola's* procedure, discussed on pages 194 to 205. Again, as in that process, if the first guess for the motion happens to be the correct one, the second result will be identical with the first. This can best be shown by applying Rauscher's procedure to the linear case,

$$m\ddot{x} + kx = P_0 \cos \omega t.$$

The first guess is $x = x_0 \cos \omega t$, which, if x_0 has a definite value, is the exact motion for some frequency ω. Then

$$P_0 \cos \omega t = \frac{P_0 x}{x_0} \qquad \text{and} \qquad m\ddot{x} + \left(\frac{k - P_0}{x_0}\right)x = 0.$$

This is a free vibration of a linear system like Eq. (13) with the solution (222*a*) in which the frequency ω is determined by $\omega^2 = \dfrac{k - P_0/x_0}{m}$. This is seen to be the *exact* result (28) of page 57. The unusual feature of Rauscher's procedure is that, instead of finding the intersection of the curves of Fig. 262 with a vertical line (*i.e.*, solving for x_0 with ω given), the intersection with a horizontal line is determined (*i.e.*, ω is solved for a given x_0) which, of course, is just as good.

The analysis of the electric circuit of Fig. 256 follows exactly the same lines except that the inertia force (inductance voltage) has a curved characteristic, whereas the spring force (condenser voltage) follows a straight line.

In the analysis it was assumed that the motion has the same frequency as the force, which would be the case in a linear system. Though this is the only possible motion for *slightly* non-linear systems, it will be seen later (page 448) that for very pronounced non-linearity motions of a frequency 1, 2, 3, 4 . . . times as *slow* as the disturbing frequency ω may be excited.

73. Forced Vibration with Non-linear Damping.—The differential equation of this case is

$$m\ddot{x} + f(\dot{x}) + kx = P_0 \sin \omega t \qquad (224)$$

where $f(\dot{x})$ is not equal to $c\dot{x}$. On account of the presence of the non-linear damping term $f(\dot{x})$, the motion is not harmonic. An exact solution of (224) is known only for the case of Coulomb damping, $f(\dot{x}) = \pm F + c\dot{x}$ and even then in a limited region of frequencies only.

In practical cases the damping is reasonably small, and the curve of motion is sufficiently close to a sinusoid to base an approximate analysis on it. The most general method replaces the term $f(\dot{x})$ by an "equivalent" $c\dot{x}$ and then proceeds to determine the "equivalent damping constant" c in such a manner that with sinusoidal motion the actual damping force $f(\dot{x})$ does the same work per cycle as is done by the equivalent damping force $c\dot{x}$. The value for c thus obtained will not be a true constant but a function of ω and of the amplitude x_0. Therefore, approximately, the system (224) can be replaced by a linear one, but the damping constant c has a different numerical value for each value of ω or of x_0.

In carrying out this analysis we first assume for the motion,

$$x = x_0 \sin \omega t$$

The work done per cycle by the equivalent damping force $c\dot{x}$ is $\pi c\omega x_0^2$ as calculated on page 68. For the work per cycle of the general damping force $f(\dot{x})$ we have already found on page 430:

$$x_0 \int_0^{2\pi} f(\dot{x}) \cos\omega t \, d\omega t$$

Equating the two values we obtain for the equivalent damping constant c:

$$c = \frac{1}{\pi\omega x_0} \int_0^{2\pi} f(\dot{x}) \cos\omega t \, d\omega t \tag{225}$$

The amplitude of the "linearized" Eq. (224), as given on page 64, is

$$x_0 = \frac{P_0}{k} \frac{1}{\sqrt{\left(1 - \frac{\omega^2}{\omega_n^2}\right)^2 + \left(\frac{c\omega}{k}\right)^2}} \tag{32a}$$

in order to calculate the amplitude, the value (225) for c has to be substituted in (32a).

This general procedure may be applied to any type of damping, even if its law is given merely in curve form, where the integral (225) must be evaluated graphically. As an example we shall take the case of dry friction $f(\dot{x}) = \pm F$. On page 430, the value of the integral in (225) was found to be $4F$. Hence

$$c = \frac{4F}{\pi\omega x_0}$$

indeed an equivalent damping constant depending on both frequency and amplitude. Substituting in (32*a*):

$$x_0\sqrt{\left(1-\frac{\omega^2}{\omega_n^2}\right)^2+\left(\frac{4F}{\pi k x_0}\right)^2}=\frac{P_0}{k}$$

or

$$\left(1-\frac{\omega^2}{\omega_n^2}\right)^2 x_0^2=\left(\frac{P_0}{k}\right)^2-\left(\frac{4F}{\pi k}\right)^2$$

Hence

$$x_0=\frac{P_0}{k}\cdot\frac{\sqrt{1-\left(\frac{4}{\pi}\frac{F}{P_0}\right)^2}}{1-\frac{\omega^2}{\omega_n^2}} \tag{226}$$

An *exact* solution of this case also exists. The analysis is too elaborate to be given here in detail, but the results, which do not differ much from those of (226), are shown in Figs. 265 and 266. The reader should compare these with Fig. 42, page 66.

With Coulomb friction (below the value of $F/P_0 = \pi/4$), the amplitudes at resonance are infinitely large, independent of the damping. At first sight it seems strange that a *damped* vibration can have infinite amplitude. The paradox is explained, however, by considering that the exciting force $P_0 \sin \omega t$ performs work on the system, and, since work is the product of force and displacement, this energy input is proportional to the amplitude. The energy dissipated by damping is also proportional to the amplitude since the friction force F is constant. Thus, if the friction force is small with respect to the exciting force $\left(F < \frac{\pi}{4}P_0\right)$, the work input by the latter is greater than the dissipation by the former, no matter how great the amplitude becomes. Thus the amplitude increases without limit, which is another way of saying that it is infinitely large in the steady state. With viscous damping, however, the friction *force* itself is proportional to the amplitude, so that its work dissipation is proportional to the square of the amplitude. Hence, even for a very small friction constant c there will always be a finite amplitude at which the dissipation by damping is equal to the energy input by the exciting force.

In connection with the fact that infinite amplitudes occur at resonance with Coulomb damping, the phase angle shows a discontinuous jump at resonance, as can be seen in Fig. 266.

For Coulomb friction the (non-linear) friction force is constant, whereas the (linear) inertia and spring forces increase with the

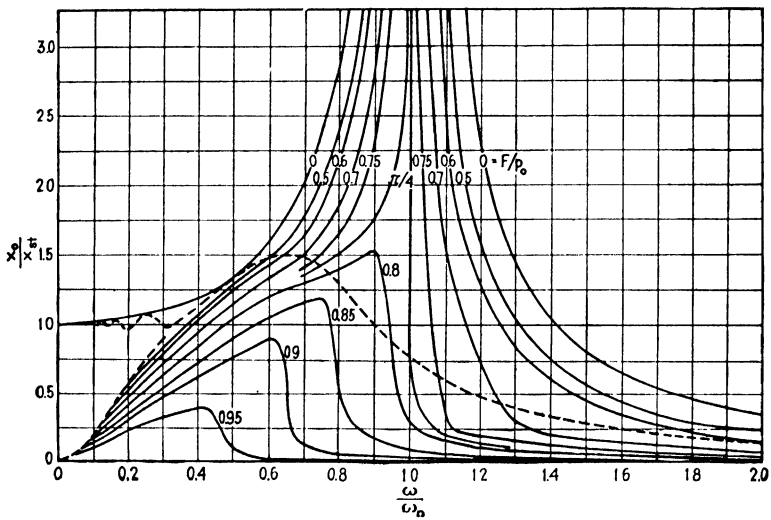


FIG. 265.—Resonance diagram for a system with dry friction damping. Compare with Fig. 42*a* on page 66.

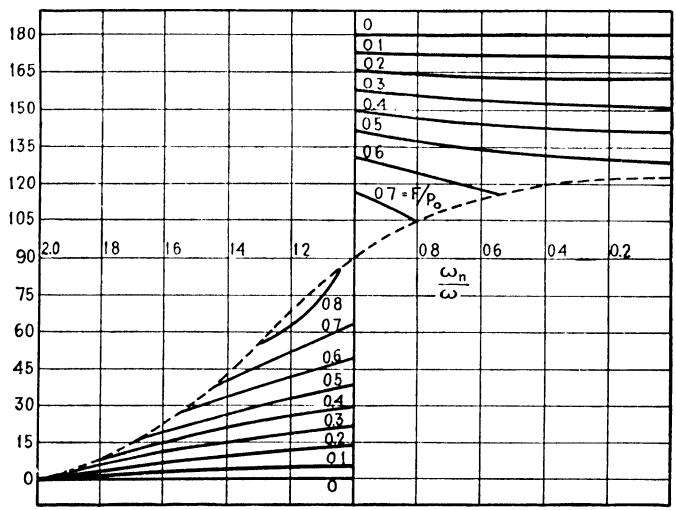


FIG. 266.—Phase-angle diagram with dry friction damping. Compare with Fig. 42*b*.

amplitude. Thus for large amplitudes the motion will be practically sinusoidal and the approximation (226) should be very

satisfactory. For smaller amplitudes the curve of motion becomes very much distorted and consequently the approximation for the amplitude is poor. Below the dotted line running through Fig. 265 we have motions with one "stop" per half cycle, as shown in Fig. 267*a*. In the blank part in the left-hand lower corner of Fig. 265 the motion has more than one stop per half cycle as shown in Fig. 267*b*. No solution could be obtained in that region. For all motions of the types of Fig. 267 the approximate formula (226) is unreliable. In practice, however, we are interested only in the conditions near resonance, and here the errors of (226) are of the order of a few per cent. Thus the general method of (225) and (32*a*) is of great practical value. Its consequences for the case of turbulent-air damping, *i.e.*, $f(\dot{x}) = c\dot{x}^2$, have been worked out in the form of diagrams like Figs. 265 and 266. For further details the reader is referred to the literature.

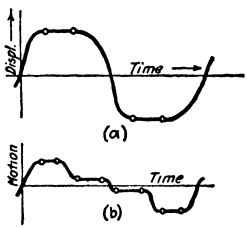


FIG. 267.—Forced motion with one (*a*) or two (*b*) stops per half cycle occurring with great Coulomb damping at slow frequencies.

74. Relaxation Oscillations.—A linear vibratory system with negative damping builds up oscillations of infinite amplitude (Fig. 207*b*). Of course, this is physically impossible and in all actual systems the damping becomes positive again for sufficiently large amplitudes, thus limiting the motion. An example of this is the electric transmission line discussed on page 372.

The actual relation between the damping coefficient and the amplitude varies from case to case, but for a general understanding it is useful to write down the simplest possible mathematical expression that will make the damping force negative for small amplitudes x and positive again for larger ones. Such an expression is

$$\text{Damping force} = -(C_1 - C_2x^2)\dot{x} \tag{227}$$

The damping coefficient as a function of x is shown in Fig. 268. It is seen that zero damping occurs at an amplitude $x = \sqrt{C_1/C_2}$.

The differential equation of a single-degree-of-freedom system with this type of non-linear damping is

$$m\ddot{x} - (C_1 - C_2x^2)\dot{x} + kx = 0 \tag{228}$$

Since we shall now give a general discussion of this equation, it is of importance to simplify it as much as possible first, by reducing the number of system characteristics of which there are now four, *viz.*, m, C_1, C_2, and k. To this end we divide by m, and with the notation $k/m = \omega_n^2$ we obtain

$$\ddot{x} - \left(\frac{C_1}{m} - \frac{C_2}{m}x^2\right)\dot{x} + \omega_n^2 x = 0 \quad (228a)$$

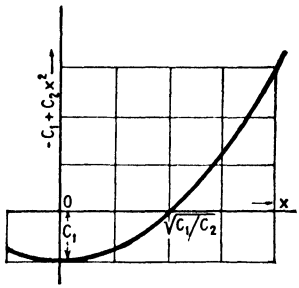


FIG. 268.—Simplest mathematical expression for a non-linear damping coefficient which is negative for small amplitudes and becomes positive for greater amplitudes.

Of the three system characteristics now remaining, two can be absorbed by making the variables x and t dimensionless. First consider the time t, which is measured in seconds. Instead of using this standard unit, we shall now measure time in terms of a unit inherent in the system, for example, $T/2\pi$. This means that for a slowly vibrating system the new time unit is large, while for a rapidly vibrating system it is small. The time is measured in "periods/2π" rather than in "seconds." Let the new time (measured in units of $T/2\pi$) be denoted by t' and the old time (measured in seconds) by t.

Then

$$t' = \frac{t}{T/2\pi} = \omega_n t$$

The new differential coefficients become

$$\frac{d^2x}{dt^2} = \frac{d^2x}{dt'^2} \cdot \frac{t'^2}{t^2} = \omega_n^2 \cdot \frac{d^2x}{dt'^2}$$

and

$$\frac{dx}{dt} = \omega_n \frac{dx}{dt'}$$

Substituting in (228a) and dividing the equation by ω_n^2,

$$\ddot{x} - \frac{C_1}{m\omega_n}\left(1 - \frac{C_2}{C_1}x^2\right)\dot{x} + x = 0$$

where the dots now signify differentiation with respect to the dimensionless time t'.

There are now only two parameters, $C_1/m\omega_n$ and C_1/C_2. The amplitude x still has the dimension of a length, and in order to

make it dimensionless we measure it also in a unit inherent in the equation. A convenient unit is indicated in Fig. 268, *viz.*, the amplitude $\sqrt{C_1/C_2}$, for which the positive and negative damping forces balance. Thus we take for our new "dimensionless displacement"

$$y = \frac{x}{\sqrt{C_1/C_2}}$$

which gives the differential equation in the form

$$\ddot{y} - \epsilon(1 - y^2)\dot{y} + y = 0 \tag{229}$$

The equation is finally reduced to a single parameter $\epsilon = C_1/m\omega_n$, which has an important physical significance. For harmonic motion this quantity equals the ratio between the maximum negative damping force and the maximum spring force:

$$\frac{C_1}{m\omega_n} = \epsilon = \frac{\text{input force}}{\text{spring force}} \tag{230}$$

This can be shown as follows. Let $x = x_0 \sin \omega_n t$, and $\dot{x} = x_0\omega_n \cos \omega_n t$. From (227) the maximum negative damping force in the middle of a stroke ($x = 0$) is $C_1\dot{x}_{\max} = C_1x_0\omega_n$. The maximum spring force $kx_{\max} = kx_0 = \omega_n^2 m x_0$, so that (230) is verified.

In all cases thus far discussed, the input force was much smaller than the spring force, so that ϵ was a small quantity, $\epsilon << 1$. This implies a motion practically harmonic and of the natural frequency ω_n. The final amplitude to which the motion will build up can be found from an energy consideration. For amplitudes smaller than this final one, the damping force $F = \epsilon(1 - y^2)\dot{y}$ puts energy into the system; while for amplitudes greater than the final one, the damping dissipates energy. At the final amplitude we have for a full cycle:

$$0 = \int F dy = \int_0^{2\pi} F\dot{y}dt' = \int_0^{2\pi} \epsilon(1 - y^2)\dot{y}^2 dt'$$

The motion is harmonic:

$$y = y_0 \sin \omega_n t = y_0 \sin t'$$

Hence

$$0 = \epsilon \int_0^{2\pi} (1 - y_0^2 \sin^2 t')y_0^2 \cos^2 t' dt'$$

or

$$y_0^2 = \frac{\int_0^{2\pi} \cos^2 t' dt'}{\int_0^{2\pi} \sin^2 t' \cos^2 t' dt'} = \frac{\pi}{\pi/4} = 4$$

(The evaluation of these integrals is discussed on page 16.) Thus for small values of the parameter ϵ the amplitude of vibration x is

$$x_0 = 2\sqrt{\frac{C_1}{C_2}} \tag{231}$$

or, in words, the amplitude is twice as large as the amplitude at which the damping force just becomes zero. Figure 268 shows that this is a reasonable result: the energy put in by the negative damping force in the center part of the motion is neutralized by the energy dissipated by the positive force near the end of the stroke.

So far the introduction of the differential equation (228) or (229) has not brought us anything new. The importance of these equations is centered rather in the case where the input force or negative damping force is *great* in comparison with the elastic force:

$$\epsilon \gg 1$$

Then the non-linear middle term in (229) becomes more important than the other two, so that the assumption of a harmonic motion (which was justified for a small middle term) is untenable. Thus we should expect the motion to be very much distorted, containing a great number of higher harmonics, and we also expect the frequency to differ from ω_n.

The shape of the motion can be obtained by means of a graphical integration as follows. In (229) we may write for the first term:

$$\ddot{y} = \frac{d\dot{y}}{dt'} = \frac{d\dot{y}}{dy}\frac{dy}{dt'} = \frac{d\dot{y}}{dy} \cdot \dot{y}$$

so that after a division by $\dot{y}$, Eq. (229) becomes

$$\frac{d\dot{y}}{dy} = \epsilon(1 - y^2) - \frac{y}{\dot{y}} \tag{232}$$

in which only the (dimensionless) amplitude y and the (dimensionless) velocity $\dot{y}$ appear, the time having been eliminated.

Take a coordinate system in which y is plotted horizontally and $\dot{y}$ vertically, as in Fig. 269. Then (232) states that the slope $d\dot{y}/dy$ at each point in the diagram can be calculated directly from its coordinates $\dot{y}$ and y and the parameter ϵ. This enables us to draw in a set of tangent directions. For example, for $\dot{y} = 0$ (the horizontal axis) the slope $d\dot{y}/dy$ becomes infinite, *i.e.*, vertical, whereas for $y = 0$ (the vertical axis) the slope is given by $d\dot{y}/dy = \epsilon$. Having the whole field of tangents, a solution can be found by starting from any arbitrary point (*i.e.*, with any arbitrary initial displacement y and velocity $\dot{y}$) and constructing a curve following the tangents. Figure 269 ($\epsilon = 10$) shows, for example, that starting at $\dot{y} = 15$ and $y = -2$ the curve goes down, bends up, then goes down again, and thereafter describes a closed figure continuously. Also when starting from rest (*i.e.*, from the origin), it reaches the same closed curve after a short run. An ordinary steady-state harmonic vibration would be pictured as a circle in this diagram, so it is seen that for $\epsilon = 10$ the motion is far from harmonic.

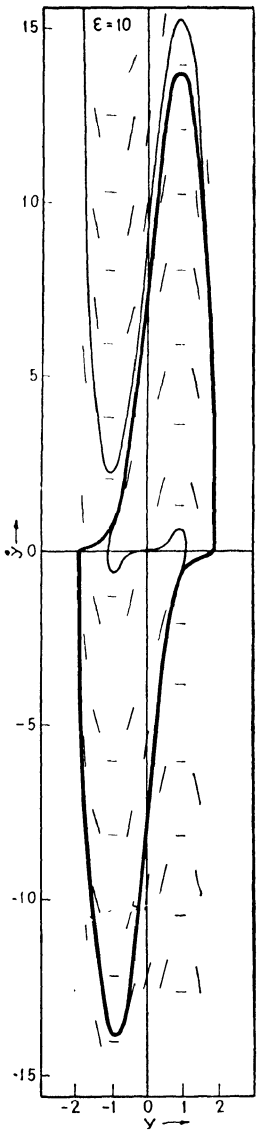


FIG. 269.—First integration of Eq. (229) for relaxation oscillations in the case that $\epsilon = 10$.

Next transform Fig. 269 into the corresponding diagram in terms of $y = f(t')$, as shown in Fig. 270. The abscissa of a point in Fig. 269 corresponds to the ordinate of Fig. 270, whereas the ordinate of that point in Fig. 269 is the slope of Fig. 270. Thus the construction of Fig. 270 from Fig. 269 amounts to a second graphical integration.

Our expectations regarding the nature of the motion are fully corroborated by the final result, Fig. 270. The motion is seen to be distinctly non-harmonic. The period is not 2π units of time (the unit being $T/2\pi$) but rather 2ϵ

units or $2\epsilon \cdot T/2\pi$ sec. This, by virtue of (230), is

$$\text{Period} = \frac{2\epsilon}{\omega_n} = \frac{2C_1}{m\omega_n^2} = 2\frac{C_1}{k} \text{ sec.} \tag{233}$$

i.e., the period no longer depends on the ratio of mass to spring constant but rather on the ratio of negative damping coefficient to spring constant. The expression (233) is twice the *relaxation time* (see page 54) of a system with a positive coefficient C_1. For this reason oscillations of the nature of Fig. 270 have been called *relaxation oscillations*.

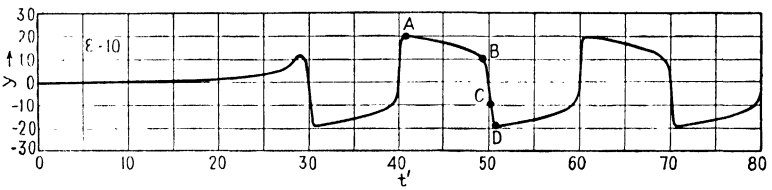


FIG. 270.—A typical relaxation oscillation, being an integration of Fig. 269.

The result (233), as well as the general shape of the vibration, Fig. 270, can be made to seem reasonable by a physical analysis as follows.

For $\epsilon = 10$ the damping action is large in comparison to the spring action. Follow the motion in Fig. 270 starting from the point A where the amplitude is $x = 2\sqrt{C_1/C_2}$. On account of Fig. 268 the damping coefficient at A is positive and remains positive until the amplitude has diminished to one-half its value (point B). Between A and B the velocity will be very small because the weak spring force is opposed by a damping force of which the coefficient is large. Hardly any inertia effect will come in during that time. At the point B the damping reverses, and becomes negative and large, which hurls the mass at a high speed through the point C, where the damping force again reverses. Between B and C the negative damping force has done work on the mass and thus has given it considerable momentum. This momentum is destroyed by the positive damping force from C on, until the mass comes to rest again at D. That the point D should be approximately at $x = 2\sqrt{C_1/C_2}$ seems reasonable from the result (231) for the case of harmonic motion.

Since it takes hardly any time to move from B to D we might calculate the period by taking twice the time between A and B. The answer thus found would be slightly too small.

In simplifying the calculation we see in Fig. 268 that the damping coefficient between $x = \sqrt{C_1/C_2}$ and $x = 2\sqrt{C_1/C_2}$ can be expressed very well by a straight-line relation.

$$\text{Damping coefficient} = -3C_1 + \frac{3C_1}{\sqrt{C_1/C_2}} \cdot x$$

The damping force is

$$\left(-3C_1 + \frac{3C_1 x}{\sqrt{C_1/C_2}}\right)\dot{x}$$

and this force is opposed only by the spring force $-kx$. Thus the differential equation of the creeping or relaxation motion between A and B is

$$\left(-3C_1 + \frac{3C_1}{\sqrt{C_1/C_2}}x\right)\frac{dx}{dt} = -kx$$

or

$$\frac{3C_1}{k}\left(-\frac{1}{x} + \frac{1}{\sqrt{C_1/C_2}}\right)dx = -dt$$

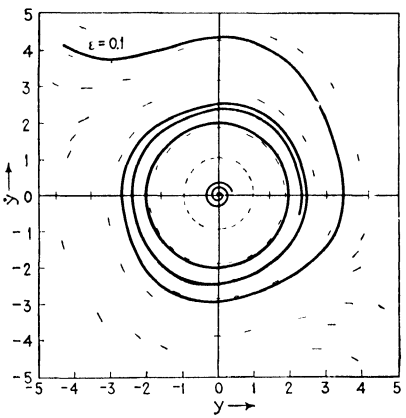


FIG. 271.—First integration of Eq. (229) for a small damping force, $\epsilon = 0.1$.

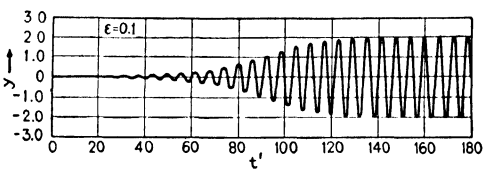


FIG. 272.—Second integration of Eq. (229) for $\epsilon = 0.1$, showing the building up of a non-linear, self-excited vibration to its final amplitude.

In integrating this expression we notice that the time progresses from 0 to $T/2$ (half period), while x goes from $2\sqrt{C_1/C_2}$ to $\sqrt{C_1/C_2}$, so that

$$\frac{3C_1}{k}\left(-\log_e x + \frac{x}{\sqrt{C_1/C_2}}\right)\Bigg|_{2\sqrt{C_1/C_2}}^{\sqrt{C_1/C_2}} = -t\Big|_0^{T/2}$$

After substitution of the limits we find

$$\frac{3C_1}{k}(-\log_e 2 + 1) = \frac{T}{2}$$

or

$$T = 6(1 - \log_e 2)\frac{C_1}{k} = 1.84\frac{C_1}{k}$$

With the slight additional time taken in going from B to D it is seen that (233) is verified.

The corresponding results of the graphical integration for the more usual case $\epsilon = 0.1$ are shown in Figs. 271 and 272.

Relaxation oscillations have been found to occur very often in radio engineering, and the reader is referred to the original papers of Van der Pol for quite a number of applications in that field. In mechanical engineering thus far they have been of little importance.

A case on the border between the electrical and mechanical fields is that of the periodic speed reversals of a separately excited direct-current motor fed by a direct-current series generator driven at a constant speed (Fig. 273). The voltage generated in a constant-speed generator is proportional to its magnetic field strength. If there were no magnetic saturation, this field strength would be proportional to the field current i, which in a series machine is the same as the main current. The influence of saturation amounts to a less rapid increase of the field strength, and the characteristic of the generator (Fig. 274) may be expressed approximately by the relation

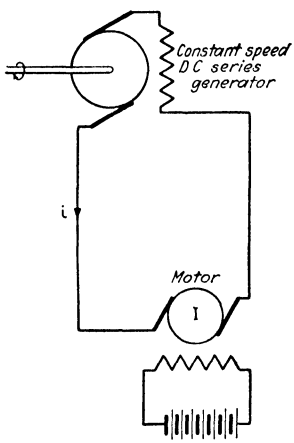


FIG. 273.—A separately excited motor driven by a series generator has periodic speed reversals of the character shown in Fig. 270.

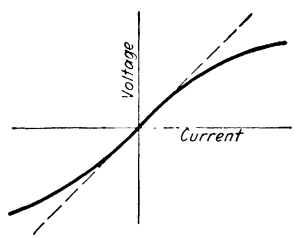


FIG. 274.—Voltage-current characteristic of a constant-speed series generator.

$$E_{gen} = C_1 i - C_2 i^3$$

This generated voltage overcomes first the inductance of its own field coils $\left(L\frac{di}{dt}\right)$, second the resistance of the circuit (Ri), and third the countervoltage of the motor. The motor has a *constant* magnetic field and a variable angular speed ω. Its voltage is proportional to the speed, $C_3\omega$. No effect of saturation enters since the field is maintained constant. The voltage equilibrium equation is

$$C_1 i - C_2 i^3 = C_3\omega + L\frac{di}{dt} + Ri \tag{234}$$

Another relation between i and ω is obtained from the fact that the energy input per second in the motor is given by its voltage $C_3\omega$ multiplied by its current i. Since the motor drives no load, this energy is used in accelerating its rotating parts of which the moment of inertia is I. The kinetic energy of the motor is $\frac{1}{2}I\omega^2$ and

$$C_3\omega i = \frac{d}{dt}(\tfrac{1}{2}I\omega^2) = I\omega\frac{d\omega}{dt}$$

or

$$\frac{d\omega}{dt} = \frac{C_3 i}{I} \tag{235}$$

The angular speed ω can be eliminated from (234) by differentiating and substituting (235), giving

$$C_1\frac{di}{dt} - 3C_2 i^2\frac{di}{dt} = C_3\frac{d\omega}{dt} + L\frac{d^2i}{dt^2} + R\frac{di}{dt}$$

$$L\frac{d^2i}{dt^2} - (C_1 - R - 3C_2 i^2)\frac{di}{dt} + \frac{C_3^2}{I}i = 0$$

This equation is equivalent to (228). Moreover, the values of $C_1 - R$, C_3, and I in the usual motor are such that $\epsilon = \frac{C_1 - R}{C_3}\sqrt{\frac{I}{L}}$ is much larger than unity. Thus the current i will reverse periodically according to Fig. 270, and the velocity of rotation ω will also show periodic reversals on account of Eq. (235). By Eq. (233) the period of these reversals is

$$T = 2\frac{C_1 - R}{C_3^2}I$$

that is, proportional to the inertia of the motor. If the oscillation were *harmonic* its period would be proportional to the *square root* of the inertia.

75. Subharmonic Resonance.—In this section some cases will be discussed for which the motion differs greatly from a harmonic motion on account of some non-linearity in the system. It does not matter where this non-linearity appears, whether it be in the spring or in the damping.

In *linear* systems subjected to an "impure" disturbance, large amplitudes may be excited at a frequency which is a multiple of the fundamental frequency of the disturbance. The most important technical example of this was discussed in Chap. V, namely the torsional vibration in internal-combustion engines. The converse of this, *i.e.*, the excitation of large oscillations of a *lower* frequency than ($\frac{1}{2}$, $\frac{1}{3}$ $\frac{1}{4}$ . . . of) the fundamental frequency of the disturbance, never happens in a linear system.

In *non-linear* cases, however, this may occur. Consider, for example, a self-excited relaxation oscillation as in Fig. 270. Subject this system to a small harmonic force of a frequency 2, 3, 4 . . . times as fast as the free or natural frequency $\frac{1}{2\epsilon}$. Since the free motion contains all higher harmonics generously, the disturbance (if phased properly) will do work on one of these harmonics and excite it. But this harmonic is an integral part of the whole motion of Fig. 270 and will pull all other harmonics with it. The result is that a large motion is excited at a frequency lower than (a submultiple of) the disturbing frequency. This phenomenon is known as "subharmonic resonance" or "frequency demultiplication."

No practical cases of this sort have thus far occurred in mechanical engineering, but in electrical engineering they are of some importance and are beginning to find applications.

Let an electric circuit containing a neon tube, a condenser, a resistance, and a battery be arranged so as to produce a relaxation oscillation of the type of Fig. 270, and excite this circuit by a small alternating voltage of constant frequency ω. The natural period T_n of the system (which in this case is not proportional to $\sqrt{LC}$ but to RC) is slowly varied by changing the capacity C. If there were no ω-disturbance, the self-excited period would gradually vary along the dotted line of Fig. 275. With the ω-disturbance, however, this does not happen. The system always vibrates at a multiple of the exciting period T_{exc} (*i.e.*, at a submultiple of the exciting *frequency* ω) and picks *that* multiple which is closest to the natural period, as shown in

Fig. 275. With circuits of this sort, frequency demultiplication up to 200 times has been obtained.

Although the phenomenon was first observed with relaxation oscillations, the explanation given shows that it is not limited to that type of vibration but may occur in any pronounced non-linear system with small "effective" damping. By "effective damping" is meant the total energy dissipation per cycle by the positive and negative damping forces combined. Thus the argument applies to non-linear self-excited vibrations and also to non-linear forced vibrations without any or with very little damping. In the latter case the non-linearity is usually caused by the springs. Two examples will now be considered.

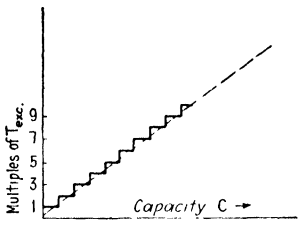


Fig. 275.—Subharmonic resonance in self-excited relaxation circuit.

Let a cantilever with an iron bob be placed between two permanent magnets (Fig. 276*a*). The "spring" is then made up of two parts, an elastic one (the beam) which is linear, and a magnetic one which is negative and distinctly non-linear. The closer the iron bob approaches to one of the magnets, the greater the

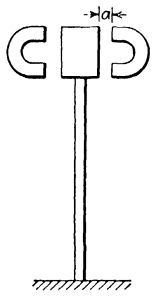


Fig. 276*a*.

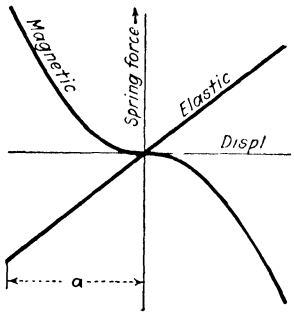


Fig. 276*b*.

Fig. 276*a*.—Mechanical subharmonic resonant system. The mass can be made to vibrate at its natural frequency by an exciting force of much higher frequency.

Fig. 276*b*.—The magnetic and elastic spring forces acting on the mass of Fig. 276*a*.

attractive (or negative restoring) force, as shown in Fig. 276*b*. With a combined spring of this sort, the free vibration contains many higher harmonics. Imagine the bob of the cantilever to be subjected to a small alternating force of a frequency which is approximately a multiple of the natural frequency. This force

can be realized in many ways, among others by attaching a small unbalanced motor to the bob. The alternating force can then do work on the nth harmonic of the motion and thus keep the system in vibration. In this example no source of energy exists other than the alternating one, and it is seen that the frequency of the alternating source of energy must be a multiple of the natural frequency.

It is not necessary to have an extraneous exciting force acting on the system: subharmonic resonance can be brought about also by a variable spring. The cases discussed in Sec. 67 to 69 had *linear* springs for which the constant or intensity varied with the time. It was shown there that resonance could occur at higher frequencies than that of the spring variation and also at *half* this frequency but not at any of the *lower* subharmonics ($\frac{1}{3}$, $\frac{1}{4}$, etc.). However, if we have a non-linear spring varying with the time (*i.e.*, a spring for which the stiffness varies with *both* the displacement and the time), these lower subharmonics may be excited. An example of such a system is Fig. 276*a*, in which the magnets now consist of soft iron and carry alternating-current windings. The attractive force of such magnets varies not only with the displacement according to Fig. 276*b* but also with the time at twice the current frequency. That it is possible for the magnetic forces to do work on the vibration if the phase is proper, is clear from Fig. 277. Curve I of that figure represents the motion of the bob, curve II is the spring force of the magnets if there were direct current in them, and curve III shows the intensity variation of the magnets with the time in case the mass were standing still (taken here to be six times as fast as the motion). The actual force exerted by the magnets on the bob is the product of the ordinates of II and III. Just to the left of line AA the magnetic force is against the direction of motion, and just to the right of it the force helps the motion. But III has been placed so that to the left of AA the intensity is small and to the right of AA it is great. The same relations obtain near BB. Thus energy is put into the system. The non-linearity of the system is essential because without it

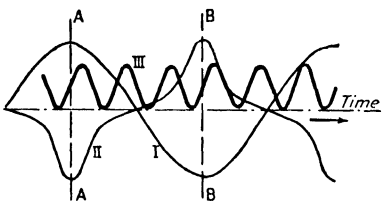


FIG. 277.—Operation of the system of Fig. 276 with alternating current in the magnet windings.

curve II would be sinusoidal and the argument of Fig. 16, page 18, would show no energy input. Only the fact that at some distance from either AA or BB the curve II has a negligible ordinate accounts for the energy input.

Under which conditions the "proper phase" between the curves I and III occurs is a question that can be answered only by mathematical analysis. Since this implies a non-linear equation with variable coefficients, it is evident that such an analysis will be extremely difficult.

Problems

124. In the center of the cylinder AA of cross section A (Fig. 278) a piston of mass m can slide without friction. The pistons BB are moving back and forth in opposite phase and change the pressure of the air in the cylinder A between 95 and 105 per cent of atmospheric pressure. Assume that this change in pressure takes place isothermally or that $\mathbf{pv} = \text{const}$. The volume of one half of A together with its pipe and the cylinder B is **V**. Find the frequency or frequencies of motion of BB at which the mass m is in unstable equilibrium. Give a general discussion with the aid of Fig. 248.

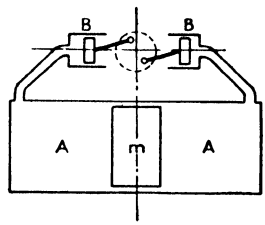


Fig. 278.

125. A pendulum consists of a uniform bar of 5 in. length and ½ lb. weight. The base is given an alternating harmonic motion in a vertical direction with an amplitude $e = 0.5$ in. At what speed of the driving motor will the pendulum become stable in an upright position? Assume the curve of Fig. 249 to be a parabola passing through the origin and through the point $y = 0.5$ and $x = -0.1$.

126. Calculate and plot the natural frequency of the system Fig. 252*b* as a function of the amplitude. Do this by the exact method of Eq. (219) as well as by the approximate method of Fig. 260.

127. Give a discussion and derive a result corresponding to Eq. (226) for the forced vibrations of a system with a damping proportional to the square of the velocity ($F = \pm c\dot{x}^2$).

128. Find a few of the slopes drawn in Fig. 269, and from that figure construct one cycle of Fig. 270.

129. Prove that in a velocity-displacement diagram, such as is shown in Fig. 269 or 271, the energy of the system is represented by the square of the radius from the origin to any point in the diagram. Verify that for harmonic motion the diagram has to be a circle and from Fig. 269 deduce in which part of the cycle the system energy is maximum. Where does the work come from?

Prove also that in this diagram the acceleration at any point P is represented by the length of the "subnormal," *i.e.*, the distance along the y-axis between the intersection of it with the normal at P and the projection of P on the y-axis.

APPENDIX I

THE GYROSCOPE

Thus far, all phenomena discussed have been explained by Newton's fundamental law stating that force equals mass times acceleration. The gyroscope will be no exception to this rule.

As was stated on page 213, another way of writing Newton's law for a particle is

$$\bar{F} = \frac{d}{dt}(m\bar{v}) \tag{128}$$

or, in words, the force $\bar{F}$ acting on a particle is equal to the rate of change of the momentum $m\bar{v}$. This is a *vector* equation and can be resolved into three algebraic equations in the x-, y-, and z-directions. The expression (128) is true not only for a single particle but holds also for the motion of the center of gravity of any larger body, provided $\bar{F}$ means the vector sum of all external forces acting on that body and m means the mass of the body, which is thought of as concentrated at its center of gravity.

If we take the moments of the two forces of Eq. (128) about any axis we obtain

$$\text{Moment of } \bar{F} = \text{moment of } \frac{d}{dt}(m\bar{v}) = \frac{d}{dt}(\text{moment of } m\bar{v})$$

again a vector equation, since a moment can be represented by a vector, usually taken along the moment axis. The length of the moment vector is made equal to the numerical value of the moment and its sense is chosen so that the vector together with the direction of rotation forms a right-handed screw.

The various particles of a body (Fig. 279) which is rotating with the angular speed ω about an axis through O and perpendicular to the paper have differently directed velocities $\bar{v}$. But the *moment* vectors of all these velocities have the same direction, *viz.*, through O and perpendicularly into the paper. Thus the (moment of $m\bar{v}$)-vectors for all particles can be added algebraically, and, since $v = \omega r$, we have for this sum

$$\int dm \cdot \omega r \cdot r = \omega \int r^2 dm = \omega I_O$$

where I_O is the moment of inertia about the moment axis. Thus Newton's theorem becomes

$$\text{Moment of forces} = \frac{d}{dt}(\overline{I\omega}) = \frac{d}{dt}(\overline{\mathfrak{M}}) \qquad (129)$$

or, in words, the vector of the moment of all forces acting on a body about some axis equals the rate of change of the $\overline{I\omega}$- or $\overline{\mathfrak{M}}$-vector. This $\overline{\mathfrak{M}}$-vector is known as the "moment of momentum" vector and also as the vector of "angular momentum."

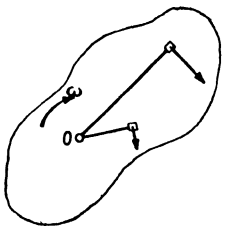


FIG. 279.—The angular momentum of a body rotating about an axis O is ωI_O.

Equation (129) is sufficient to explain the main property of the gyroscope. By a gyroscope we usually mean a body which rotates very rapidly and for which the direction of the axis of rotation varies comparatively slowly.

Figure 280 respresents a disk which is spinning in its own plane with a large speed Ω and of which the axis of rotation rotates slowly (at the rate ω) about the axis BB. The $\overline{\mathfrak{M}}$-vector is pointing upward and its length is $I\Omega$. On account of the ω-motion this vector tilts slowly toward the right through an angle ωdt. The increment in $\overline{\mathfrak{M}}$ is $d\overline{\mathfrak{M}} = \overline{I\Omega \cdot \omega dt}$ and consequently

$$\frac{d}{dt}(\overline{\mathfrak{M}}) = \overline{I\Omega\omega} \qquad (236)$$

which is a vector directed to the right, *i.e.*, parallel to AA. By Eq. (129) the length $I\Omega\omega$ of this vector must be equal to the value of the force moment applied to the disk. Since this moment acts about the axis AA, we have to push down on P and pull up on Q in order to make the disk move so that R goes up and S goes down. Hence there are three axes involved:

1. The axis of rotation of the disk ($\overline{\mathfrak{M}}$-vector).
2. The axis about which the external moment acts (AA).
3. The axis about which the disk drifts or "precesses" (BB).

These three axes are mutually perpendicular.

The result (236) can be derived from Newton's law in a somewhat different manner as follows.

Let the disk be exactly horizontal at the instant of time $t = 0$. At a later instant dt it is dipped to the right through an angle ωdt. If the precessing angular velocity ω were zero, all particles of the disk would move in circles in horizontal planes and would have no vertical velocity component whatever. On account of ω the various particles do have small vertical velocities. At the instant $t = 0$ these velocities are upward for particles to the left of BB and downward for particles to the right of BB, and their magnitude is expressed by ωx. Consider the particle dm at r, φ in Fig. 280 at the instant $t = 0$. Its vertical velocity is ωx directed downward. Somewhat later, at time dt, this velocity has changed for two reasons. First the particle is then farther away from the axis BB, and second the disk is slightly tilted so that the large circumferential velocity of that point has acquired a small vertical component.

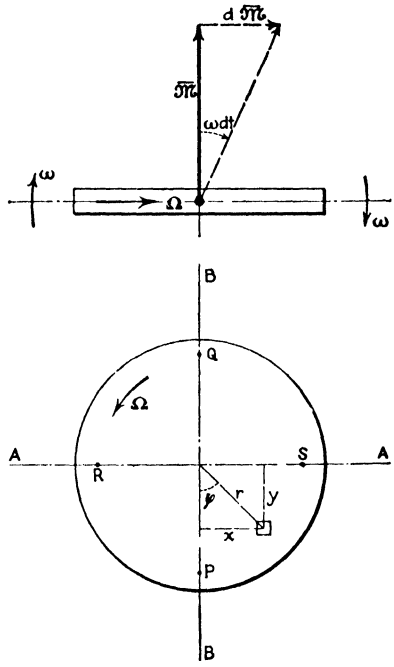


FIG. 280.—Illustrating the fundamental formula (236) of the gyroscope.

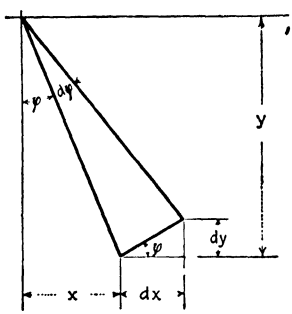


FIG. 281.

The increase in vertical velocity due to the first reason is $\omega dx = \omega \cdot r d\varphi \cdot \frac{y}{r} = \omega y d\varphi$ (Fig. 281). But since $d\varphi = \Omega dt$ this is equal to $\Omega\omega y dt$. The inclination of the disk about the BB-axis at the instant dt is ωdt, and the circumferential velocity of a point is Ωr. The component of that velocity perpendicular to the BB-axis is $\Omega r \cdot \frac{y}{r} = \Omega y$. The vertical component of Ωy, due to the inclination is $\Omega y \cdot \omega dt$. (The vertical component of the component which is parallel to

BB is zero.) Thus the change in vertical velocity on account of the second reason is the same as that owing to the first reason. Since both changes are downward, the total effect is $2\Omega\omega y dt$, and the vertical acceleration of the particle is $2\Omega\omega y$. Its inertia force is $2\Omega\omega y dm$, which is directed downward for positive y (*i.e.*, below AA in Fig. 280) and upward for negative y.

The *moment* of this inertia force about AA is y times the force, or $2\Omega\omega y^2 dm$. For all particles combined,

$$\int 2\Omega\omega y^2 dm = 2\Omega\omega \int y^2 dm = 2\Omega\omega I_d = \Omega\omega I_o$$

where I_d is the moment of inertia about a diameter and I_o the moment of inertia about the axis of rotation, being twice as great as I_d. The moment $\Omega\omega I_o$ by Eq. (129) must be supplied from outside the disk to make the disk perform the prescribed ω-motion. Since the particles below AA are accelerated downward and those above AA upward, it is necessary to push down on P and to pull up on Q in Fig. 280. Thus the result (236) is proved.

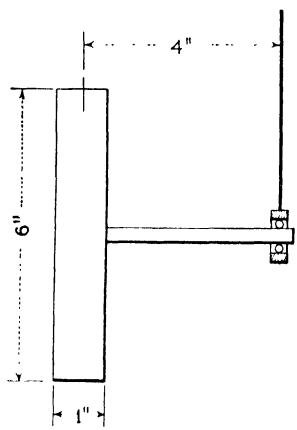


FIG. 282.

Of the two viewpoints which we have set forth on the gyroscopic theorem, the first one employing the rate of change of the $\overline{\mathfrak{M}}$-vector is by far the more useful. It is this concept which has been used in the various applications in the book.

Problems

130. A solid steel disk of 1 in. thickness and 6 in. diameter rotates at 1,800 r.p.m. It is keyed to a shaft 4 in. long which is supported at the end by a string attached to the outer race of a ball bearing, as shown in Fig. 282. Under the influence of gravity, the disk will precess in such a manner that the 4-in. shaft rotates slowly in a horizontal plane.

a. If the disk rotates in a clockwise sense when viewed from the string, find the sense of the precession.

b. Calculate the angular velocity of precession.

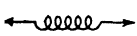
131. A ship carries turbines rotating at 1,800 r.p.m. with a moment of inertia of 50,000 in. lb. sec.^{2}. The axis of rotation is parallel to the propeller shaft. The ship is *pitching* in a rough sea through an angle of ± 5 deg. with a period of 10 sec. The distance between the two main bearings of the turbine is 15 ft. Find the maximum value of the gyroscopic bearing reaction.

APPENDIX II

A COLLECTION OF FORMULAS

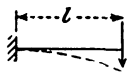
I. Linear Spring Constants

(Pounds per inch deflection)



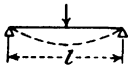
Coil dia. D; wire dia. d; n turns

$$k = \frac{Gd^4}{8nD^3} \tag{1}$$



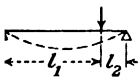
Cantilever

$$k = \frac{3EI}{l^3} \tag{2}$$



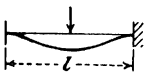
Beam on two supports; centrally loaded

$$k = \frac{48EI}{l^3} \tag{3}$$



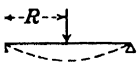
Beam on two supports; load off center

$$k = \frac{3EIl}{l_1^2 l_2^2} \tag{4}$$



Clamped-clamped beam; centrally loaded

$$k = \frac{192EI}{l^3} \tag{5}$$



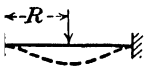
Circular plate, thickness t; centrally loaded; circumferential edge simply supported

$$k = \frac{16\pi D}{R^2}\,\frac{1+\mu}{3+\mu} \tag{6}$$

in which the plate constant is

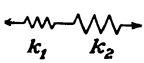
$$D = \frac{Et^3}{12(1-\mu^2)} \tag{6a}$$

μ = Poisson's ratio ≈ 0.3



Circular plate; circumferential edge clamped

$$k = \frac{16\pi D}{R^2} \tag{7}$$

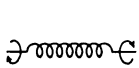


Two springs in series

$$k = \frac{1}{1/k_1 + 1/k_2} \tag{8}$$

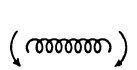
II. Rotational Spring Constants

(Inch-pounds torque per radian rotation)



Twist of coil spring; wire dia. d; coil dia. D; n turns

$$k = \frac{Ed^4}{64nD} \tag{9}$$



Bending of coil spring

$$k = \frac{Ed^4}{32nD} \cdot \frac{1}{1 + E/2G} \tag{10}$$



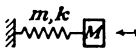
Twist of hollow circular shaft, outer dia. D, inner dia. d, length l

$$k = \frac{GI_p}{l} = \frac{\pi}{32}\,\frac{G(D^4 - d^4)}{l} \tag{11}$$

For steel

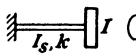
$$k = 1.18 \times 10^6 \times \frac{D^4 - d^4}{l}$$

III. Natural Frequencies of Simple Systems



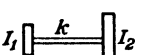
End mass M; spring mass m, spring stiffness k

$$\omega_n = \sqrt{k/(M + m/3)} \qquad (12)$$



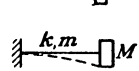
End inertia I; shaft inertia I_s, shaft stiffness k

$$\omega_n = \sqrt{k/(I + I_s/3)} \qquad (13)$$



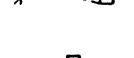
Two disks on a shaft

$$\omega_n = \sqrt{\frac{k(I_1 + I_2)}{I_1 I_2}} \qquad (14)$$



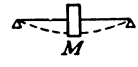
Cantilever; end mass M; beam mass m, stiffness by formula (2)

$$\omega_n = \sqrt{\frac{k}{M + 0.23m}} \qquad (15)$$



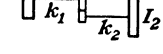
Simply supported beam; central mass M; beam mass m; stiffness by formula (3)

$$\omega_n = \sqrt{\frac{k}{M + 0.5m}} \qquad (16)$$



Massless gears, speed of I_2 n times as large as speed of I_1

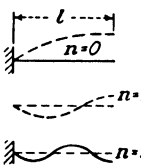
$$\omega_n = \sqrt{\frac{1}{\frac{1}{k_1} + \frac{1}{n^2 k_2}} \times \frac{I_1 + n^2 I_2}{I_1 \cdot n^2 I_2}} \qquad (17)$$



$$\omega_n^2 = \frac{1}{2}\left(\frac{k_1}{I_1} + \frac{k_3}{I_3} + \frac{k_1 + k_3}{I_2}\right) \pm \frac{1}{2}\sqrt{\left(\frac{k_1}{I_1} + \frac{k_3}{I_3} + \frac{k_1 + k_3}{I_2}\right)^2 - 4\frac{k_1 k_3}{I_1 I_2 I_3}(I_1 + I_2 + I_3)} \qquad (18)$$

IV. Uniform Beams

(Longitudinal and torsional vibration)



Longitudinal vibration of cantilever: A = cross section, E = modulus of elasticity. μ_1 = mass per unit length, n = 0,1,2,3 = number of nodes

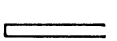
$$\omega_n = \left(n + \frac{1}{2}\right)\pi\sqrt{\frac{AE}{\mu_1 l^2}} \qquad (19)$$

For steel and l in inches this becomes

$$f = \frac{\omega_n}{2\pi} = (1 + 2n)\frac{51{,}000}{l}$$

cycles per second (19a)

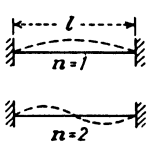
For air at atm. pressure, l in inches:



Organ pipe open at one end, closed at the other

$$f = \frac{\omega_n}{2\pi} = (1 + 2n)\frac{3{,}300}{l}$$

cycles per second (19b)



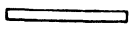
Longitudinal vibration of beam clamped at both ends; n = number of half waves along length

$$\omega_n = n\pi\sqrt{\frac{AE}{\mu_1 l^2}} \qquad (20)$$

For steel, l in inches:

$$f = \frac{\omega_n}{2\pi} = \frac{102{,}000}{l}$$

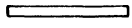
cycles per second (20a)



Organ pipe closed at both ends (air)

$$f = \frac{\omega_n}{2\pi} = \frac{6{,}600}{l}$$

cycles per second (20b)



Torsional vibration of beams

Same as (19) and (20); replace tensional stiffness AE by torsional stiffness GI_p; replace μ_1 by the moment of inertia per unit length $i_1 = I_{bar}/l$.

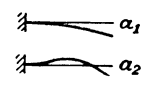
V. Uniform Beams

(Transverse or bending vibrations)

The same general formula holds for all the following cases,

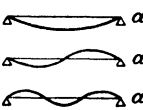
$$\omega_n = a_n \sqrt{\frac{EI}{\mu_1 l^4}} \tag{21}$$

where EI is the bending stiffness of the section, l is the length of the beam, μ_1 is the mass per unit length $= W/gl$, and a_n is a numerical constant, different for each case and listed below



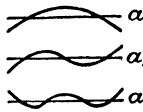
Cantilever or "clamped-free" beam

$a_1 = 3.52$
$a_2 = 22.4$
$a_3 = 61.7$
$a_4 = 121.0$
$a_5 = 200.0$



Simply supported or "hinged-hinged" beam

$a_1 = \pi^2 = 9.87$
$a_2 = 4\pi^2 = 39.5$
$a_3 = 9\pi^2 = 88.9$
$a_4 = 16\pi^2 = 158.$
$a_5 = 25\pi^2 = 247.$



"Free-free" beam or floating ship

$a_1 = 22.4$
$a_2 = 61.7$
$a_3 = 121.0$
$a_4 = 200.0$
$a_5 = 298.2$



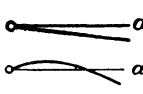
"Clamped-clamped" beam has same frequencies as "free-free"

$a_1 = 22.4$
$a_2 = 61.7$
$a_3 = 121.0$
$a_4 = 200.0$
$a_5 = 298.2$



"Clamped-hinged" beam may be considered as half a "clamped-clamped" beam for even a-numbers

$a_1 = 15.4$
$a_2 = 50.0$
$a_3 = 104.$
$a_4 = 178.$
$a_5 = 272.$



"Hinged-free" beam or wing of autogyro may be considered as half a "free-free" beam for even a-numbers

$a_1 = 0$
$a_2 = 15.4$
$a_3 = 50.0$
$a_4 = 104.$
$a_5 = 178.$

VI. Rings, Membranes, and Plates

Bending vibrations of ring, radius r, mass per unit length μ_1, in its own plane with n full "sine waves" of disturbance along circumference

$$\omega_n = \frac{n(n^2 - 1)}{\sqrt{1 + n^2}} \sqrt{\frac{EI}{\mu_1 r^4}} \tag{22}$$

Circular membrane of tension **T**, mass per unit area μ_1, radius r

$$\omega_n = a_{cd} \sqrt{\frac{\mathbf{T}}{\mu_1 r^2}} \tag{23}$$

The constant a_{cd}, is shown below, the subscript c denotes the number of nodal circles, and the subscript d the number of nodal diameters:

d \ c	1	2	3
0	2.40	5 52	8.65
1	3.83	7 02	10.17
2	5.11	8.42	11.62
3	6.38	9.76	13.02

Membrane of any shape of area A roughly of equal dimensions in all directions, fundamental mode:

$$\omega_n = \text{const.} \sqrt{\frac{T}{\mu_1 A}} \tag{24}$$

circle..... const. $= 2.40\pi = 4.26$
square..... const. $= 4.44$
quarter circle..... const. $= 4.55$
2×1 rectangle ..... const. $= 4.97$

Circular plate of radius r, mass per unit area μ_1; the "plate constant D" defined by Eq. (6a), p. 429

$$\omega_n = a \sqrt{\frac{D}{\mu_1 r^4}} \tag{25}$$

For free edges, 2 perp. nodal diameters..... $a = 5.25$
For free edges, one nodal circle, no diameters.... $a = 9.07$
Clamped edges, fundamental mode..... $a = 10.21$
Free edges, clamped at center, umbrella mode.... $a = 3.75$

BIBLIOGRAPHY

A. General Books

RAYLEIGH, LORD: "Theory of Sound."

TIMOSHENKO, S.: "Vibration Problems in Engineering."

KIMBALL, A. L.: "Vibration Prevention in Engineering."

LAMB, HORACE: "The Dynamical Theory of Sound."

STODOLA, A.: "Steam and Gas Turbines."

MORSE, PHILIP M.: "Vibration and Sound."

WILSON, W. KER: "Practical Solution of Torsional Vibration Problems."

KÁRMÁN, TH. VON, and M. A. BIOT: "Mathematical Methods in Engineering."

B. Specific References

(The numbers prefixed refer to sections in the book)

3. STEINMETZ, C. P.: "Alternating Current Phenomena," Chaps. 3 and 4.

4. Mechanical Vibrations in Penstocks of Hydraulic Turbine Installations, *Trans. A.S.M.E.*, 1929, Paper HYD-51-13.

7. EAGLE, A.: "A Practical Treatise on Fourier's Theorem and Harmonic Analysis for Physicists and Engineers," London, 1925.

KLOCK, NANCY: Forty-eight Ordinate Harmonic Spectrum of the Two-cycle Diesel Torque, *Trans. A.S.M.E.*, 1940.

RUNGE, KARL: *Zeit. Math.*, 1903, p. 443, and 1905, p. 117.

SCARBOROUGH, J. B.: "Numerical Mathematical Analysis," Oxford, 1930.

MANLEY, R. G.: "Wave-form Analysis," 1945.

WENTE, E. C.: U. S. Patent 2,098,326.

MONTGOMERY, H. C.: An Optical Harmonic Analyzer, *Bell System Tech. Jour.*, vol. 17, p. 406, 1938.

16. ORMONDROYD, J.: The Use of Vibration Instruments on Electrical Machinery, *Trans. A.I.E.E.*, vol. 45, p. 443, 1926.

18. EDGERTON, H. E.: Stroboscopic Moving Pictures, *Elec. Eng.*, 1931, p. 327.

DRAPER, C. S., and G. P. BENTLEY: Measurement of Aircraft Vibration during Flight, *Jour. Aero Sciences*, 1936, pp. 116–121.

DRAPER, C. S., and W. WRIGLEY: An Instrument for Measuring Low Frequency Accelerations in Flight, *Jour. Aero. Sciences*, vol. 7, p. 388, 1940.

KEARNS, C. M., and R. M. GUERKE: Vibration Stress Measurements in Strong Centrifugal Fields, *Jour. Applied Mechanics*, December, 1937.

"Evaluation of Effects of Torsional Vibration," a publication of the Society of Automotive Engineers, 1945.

Various catalogues of the firms mentioned in the text.

19. SODERBERG, C. R.: Vibration Absorbers for Large Single-phase Machines, *Elec. Jour.*, vol. 20, p. 383, 1924.

TAYLOR, E. S. and K. A. BROWNE: Vibration Isolation of Aircraft Power Plants, *Jour. Aero. Sciences*, vol. 6, pp. 43–49, 1938.

MINDLIN, R. D.: Dynamics of Package Cushioning, *Bell System Tech. Jour.*, vol. 24, pp. 353–461, 1945.

22. POESCHL, T.: Der Frequenzenkreis, *Zeit. techn. Phys.*, vol. 14, p. 565, 1933.

23. FRAHM, H.: U. S. Patent 989,958, April, 1911, Device for Damping Vibrations of Bodies.

ORMONDROYD, J., *et al.*: The Theory of the Dynamic Vibration Absorber, *Trans. A.S.M.E.*, 1928, Paper APM-50-7.

MINER, I. O.: U. S. Patent 1,895,292, Jan. 24, 1933, on Hair Clipper with Dynamic Vibration Absorber (Brown & Sharpe Manufacturing Company).

24. HAHNKAMM, E.: Dissertation, Göttingen, 1931, also: *Ing. Arch.*, vol. 4, p. 192, 1932.

BROCK, JOHN E.: A Note on the Damped Vibration Absorber, *Trans. A.S.M.E.*, 1946, A284.

WAHL, A. M., and E. FISHER: Self-excited Torsional Oscillation and Vibration Damper for Induction Motor Drives, *Trans. A.S.M.E.*, 1942, pp. A175–A183, and 1943, p. A176.

24, 25. KLEIN, F., and A. SOMMERFELD: "Die Theorie des Kreisels," vol. IV.

26. "The Sperry Gyro-stabiliser," booklet issued by Sperry Gyroscope Co., New York.

DE SANTIS, R., and M. RUSSO: Rolling of the S.S. Conte di Savoia in Tank Experiments at Sea, *Trans. Soc. Nav. Arch. Marine Eng.*, vol. 44, pp. 169–194, 1936.

26*a*. MINORSKY, N.: Note on the Angular Motion of Ships, *Trans. A.S.M.E.*, 1941, pp. A111–A120, containing a good bibliography on the entire subject.

27. KINDL, C. H.: New Features in Shock Absorbers with Inertia Control, *Jour. S. A. E.*, 1933, p. 172.

SCHILLING, R., and H. O. FUCHS: Modern Passenger Car Ride Characteristics, *Trans. A.S.M.E.*, 1941, pp. A59–A66.

30–35. Books of Rayleigh and Timoshenko mentioned in the general bibliography.

MCBRIDE, E. J.: The Free Lateral Vibration of a Cantilever Beam with a Terminal Dashpot, *Trans. A.S.M.E.*, 1943, pp. A33–A48.

36. Vibrations of Frames of Electrical Machines, *Trans. A.S.M.E.*, 1928, Papers APM-50-6 and APM-50-11.

BROWN, T. H.: Lateral Vibrations of Ring-shaped Frames, *Jour. Franklin Inst.*, 1934.

PRESCOTT, JOHN: "Applied Elasticity," London, 1924.

39. BENTLEY, G. P.: Vibration of Aircraft Engines, *Jour. Aero. Sciences*, vol. 6, pp. 278–283, 333–341, 1939.

40. TIMOSHENKO, S.: "Vibration Problems in Engineering," 2d ed., pp. 270–272 (crank-shaft stiffness formula).

CONSTANT, H.: On the Stiffness of Crankshafts, Reports and Memoranda No. 1201 (1928) of the British Aeronautical Research Committee.

HOLZER, H.: "Die Berechnung der Drehschwingungen," Berlin, 1921.

BIOT, M.: Vibration of Crankshaft-Propeller Systems. New Method of Calculation, *Jour. Aero. Sciences*, vol. 7, pp. 107–112, 1940.

LI, J. P., *et al:* Forced Torsinal Vibrations with Damping: An Extension of Holzer's Method, *Trans. A.S.M.E.*, 1946, p. A276.

40–45. LEWIS, F. M.: Torsional Vibration in the Diesel Engine, *Trans. Soc. Nav. Arch. Marine Eng.*, 33, 1925 (contains excellent bibliography up to the year 1925).

PORTER, F. P.: The Range and Severity of Torsional Vibrations in Diesel Engines, *Trans. A.S.M.E.*, 1928, Paper APM-50-14.

TAYLOR, E. S.: Eliminating Crankshaft Torsional Vibration in the Radial Aircraft Engine, *Trans. Soc. Automotive Eng.*, 1936, p. 82.

Tuned Pendulums as Torsional Vibration Eliminators, an article in "Contributions to the Mechanics of Solids," dedicated to Stephen Timoshenko, Macmillan, 1938.

42. PORTER, F. P.: Harmonic Coefficients of Engine Torque Curves, *Trans. A.S.M.E.*, 1943, pp. A33–A48.

TAYLOR, E. S., and E. W. MORRIS: Harmonic Analysis of Engine Torque Due to Gas Pressure, *Jour. Aero. Sciences*, vol. 3, pp. 129–131, 1936.

BENTLEY, G. P., and E. S. TAYLOR: Gas Pressure Torque of Radial Engines, *Jour. Aero. Sciences*, vol. 6, pp. 1–6, 1938.

ORMONDROYD, J., *et al.*: Torsional Vibration Dampers, *Trans. A.S.M.E.* 1930, Paper APM-52-13.

46. ALEXANDER, WILLIAM: Hydraulic Analysis of Vulcan Couplings, *The Marine Engineer and Motorship Builder*, November, 1930, pp. 417–421.

SINCLAIR, H.: Recent Developments in Hydraulic Couplings, *Proc. Inst. Mech. Eng., London*, October, 1935, pp. 75–190.

46*a*. PROHL, M. A.: A General Method for Calculating Critical Speeds of Flexible Rotors, *Trans. A.S.M.E.*, 1945, pp. A142–A148.

RANKIN, A. W.: Calculation of Multiple-Span Critical Speeds by Means of Punched Card Machines, *Trans. A.S.M.E.*, 1946, p. A117.

47–49. SODERBERG, C. R.: The Vibration Problem in Engineering, *Elec. Jour.*, vol. 21, p. 89, 1924.

RATHBONE, T. C.: Turbine Vibration and Balancing, *Trans. A.S.M.E.*, 1929, Paper APM-51-23.

48. THEARLE, E. L.: A New Type of Dynamic Balancing Machine, *Trans. A.S.M.E.*, 1932, Paper APM-54-12.

BAKER, J. G.: Methods of Rotor-unbalance Determination, *Trans. A.S.M.E.*, March, 1939, page A1.

BAKER, J. G., and F. C. RUSHING: Balancing Rotors by Means of Electrical Networks, *Jour. Franklin Inst.*, August, 1936.

49. KROON, R. P., and W. A. WILLIAMS: Spiral Vibration of Rotating Machinery, *Proc. Fifth International Congress for Applied Mechanics*, 1938, p. 712.

50. SODERBERG, C. R.: On the Subcritical Speeds of the Rotating Shaft, *Trans. A.S.M.E.*, 1932, Paper APM-54-4.

FOOTE, W. R., H. PORITSKY, and J. J. SLADE, Jr.: Critical Speeds of a Rotor with Unequal Shaft Flexibilities, etc., *Trans. A.S.M.E.*, 1943, pp. A77-A81.

50*a*. COLEMAN, R. P.: Theory of Self-excited Mechanical Oscillations of Hinged Rotor Blades, *N.A.C.A. Repts.*, July, 1942, and July, 1943.

51. STODOLA, A.: "Steam and Gas Turbines," vol. I, pp. 430–437, New York.

52. MIKINA, S. J.: The Effect of Pole Skewing and Pole Spacing on Magnetic Noise in Electrical Machinery, *Elec. Jour.*, 1934.

LAMB, H., and R. V. SOUTHWELL: *Proc. Roy. Soc. London*, vol. 99, 1921.

53. CARTER, B. C.: Airscrew Blade Vibration, *Proc. Roy. Aeronautical Soc.*, 1937, pp. 749–790.

CALDWELL, F. W.: The Vibration Problem in Aircraft Propeller Designing, *Jour. Soc. Automative Eng.*, 1937, pp. 372–380.

LEWIS, F. M.: Propeller Vibration, *Trans. Soc. Nav. Arch. Marine Eng.*, vol. 43, pp. 252–285, 1935, and vol. 44, pp. 501–519, 1936.

COQUERET, F., and P. ROMANO: Some Particulars Concerning the Design of the "Normandie" and the Elimination of Vibration, *Trans. Soc. Nav. Arch. Marine Eng.*, vol. 44, pp. 127–145, 1936.

CONN, J. F. C.: Marine Propeller Blade Vibration, *Trans. Inst. Eng. and Shipbuilders in Scotland*, 1939, p. 225.

SHANNON, J. F., and R. N. ARNOLD: Statistical and Experimental Investigations on the Singing Propeller Problem, *Trans. Inst. Eng. and Shipbuilders in Scotland*, 1939, p. 256.

54. CAMPBELL, W.: The Protection of Steam Turbine Disk Wheels from Axial Vibration, *Trans. A.S.M.E.* vol. 46, pp. 31–140, 1924.

KROON, R. P.: Turbine Blade Vibration due to Partial Admission, *Trans. A.S.M.E.*, 1940, p. A161.

KROON, R. P., and C. A. MEYER: U. S. Patent 2,341,148.

MEYER, C. A. and H. B. SALDIN: Model Tests of Two Types of Vibration Dampers, *Trans. A.S.M.E.*, 1942, pp. A59–A64.

56. ROUTH, E. J.: On the Stability of a Given State of Motion, Adams Prize Essay, 1877.

HURWITZ: *Math. Ann.*, vol. 46, pp. 273–284, 1895.

57. BAKER, J. G.: Self-induced Vibrations, *Trans. A.S.M.E.*, 1933, Paper APM-55-2.

WAHL, A. M., and E. G. FISHER: See Section 24.

For the Hackensack Bascule Bridge Failure see *Eng. News-Record*, Nov. 14, 1929, top of p. 784.

58. KIMBALL, A. L.: Internal Friction Theory of Shaft Whipping, *Gen. Elec. Rev.*, April, 1924.

KIMBALL, A. L.: Friction and Damping in Vibration (with 52 references), *Trans. A.S.M.E.*, 1941, pp. A37–A41.

NEWKIRK, B. L., and H. D. TAYLOR: Shaft Whipping Due to Oil Action in Journal Bearings *Gen. Elec. Rev.*, 1925, p. 559.,

NEWKIRK, B. L., and L. P. GROBEL: Oil Film Whirl—A Non-whirling Bearing, *Trans. A.S.M.E.*, 1934, Paper APM-56-10.

HAGG, A. C.: The Influence of Oil Film Journal Bearings on the Stability of Rotating Machines, *Trans. A.S.M.E.*, 1946, p. A211.

59. Transmission Line Vibration Due to Sleet, *Trans. A.I.E.E.*, 1932, p. 1074.

PAGON, W. W.: Vibration Problems in Tall Stacks Solved by Aerodynamics, *Eng. News-Record*, July 12, 1934.

REISSNER, H.: "Oscillations of Suspension Bridges" (with references to Tacoma Bridge failure), *Trans. A.S.M.E.*, 1943, pp. A23-A32.

60. BAKER, J. G.: On the Falling of a Strip of Paper, *Phil. Mag.*, vol. 16, p. 175, 1933.
61. STONE, M.: Parallel Operation of A. C. Generators, *Trans. A.I.E.E.*, June, 1933, p. 332.
62. LUTZ, O.: "Die Vorgänge in federbelasteten Einspritzdüsen von kompressorlosen Oelmaschinen," *Ing. Arch.*, 1933, p. 155.
64. THEODORSEN, TH.: General Theory of Aerodynamic Instability and the Mechanism of Flutter, *N.A.C.A. Rept.* 496, 1935.

KASSNER, R., and H. FINGADO: Das ebene Problem der Flügelschwingung, *Luftfahrtforschung*, vol. 13, pp. 374–387, 1936.

BLEAKNEY, W. M., and J. D. HAMM: Vector Methods of Flutter Analysis, *Jour. Aero Sciences*, vol. 9, pp. 439–451, 1942.

GOLAND, M.: The Flutter of a Uniform Cantilever Wing, *Trans. A.S.M.E.*, 1945, pp. A197–A208.

MYKLESTAD, N. O.: "Vibration Analysis," New York, 1944. The entire latter half of this book is devoted to flutter.

65. BECKER, FROMM, and MARUHN: "Schwingungen in Automobillenkungen," Berlin, 1931.

LANGER, B. F., and H. P. SHAMBERGER: Lateral Oscillations of Rail Vehicles, *Trans. A.S.M.E.*, vol. 57, pp. 481–493, 1935.

67. TIMOSHENKO: "Vibration Problems in Engineering," 2d ed., pp. 151–160.
68. VAN DER POL, B., and M. J. O. STRUTT: On the Stability of the Solutions of Mathieu's Equation, *Phil. Mag.*, vol. 5, p. 18, 1928.
72. MIKINA, S. J., *et al.*: Forced Vibrations with Non-linear Spring Constants, *Trans. A.S.M.E.*, 1932, Paper APM-54-15.

RAUSCHER, M.: Steady Oscillations of Systems with Non-linear and Unsymmetrical Elasticity, *Trans. A.S.M.E.*, 1938, p. A169.

73. JACOBSEN, L. S.: Steady Forced Vibration as Influenced by Damping, *Trans. A.S.M.E.*, 1930, Paper APM-52-15.

Forced Vibrations with Combined Coulomb and Viscous Friction, *Trans. A.S.M.E.*, 1931, Paper APM-53-9.

74. VAN DER POL, B.: On Relaxation Oscillations, *Phil. Mag.*, vol. 2, p. 978, 1926.

SHOHAT, J.: A New Analytical Method for Solving Van der Pol's Equations, *Jour. Applied Phys.*, vol. 14, pp. 40–48, 1943.

75. VAN DER POL, B.: Frequency Demultiplication, *Nature*, Sept. 10, 1927

ANSWERS TO PROBLEMS

1. (*a*) -157.0 in.-lb. (*b*) $+0.40$ in.-lb.

7. When $n = 1, 3, 9, \cdots, \quad b_n = +\dfrac{a\sqrt{2}}{\pi n}.$

$n = 5, 7, 13, \cdots, \quad b_n = -\dfrac{a\sqrt{2}}{\pi n}.$

$n = 2, 10, 18, \cdots, \quad b_n = -\dfrac{2a}{\pi n}.$

$n = 4, 8, 12, \cdots, \quad b_n = 0.$

$n = 1, 7, 9, \cdots, \quad a_n = +\dfrac{2a}{\pi n}\left(\dfrac{2 + \sqrt{2}}{2}\right).$

$n = 3, 5, 11, \cdots, \quad a_n = +\dfrac{2a}{\pi n}\left(\dfrac{2 - \sqrt{2}}{2}\right).$

$n = 2, 6, 10, \cdots, \quad a_n = +\dfrac{2a}{\pi n}.$

$n = 4, 12, 20, \cdots, \quad a_n = +\dfrac{4a}{\pi n}.$

$n = 8, 16, 24, \cdots, \quad a_n = 0.$

8. $y = \dfrac{a}{3} + \dfrac{4a}{\pi^2}\sum_{n=1}^{n=\infty}\dfrac{(-1)^n}{n^2}\cos\dfrac{2n\pi x}{l}.$

9. $a_1 = 0.267 \qquad b_1 = 0.134$

$a_2 = 0.313 \qquad b_2 = -0.0109$

$a_3 = 0.214 \qquad b_3 = -0.037$

$b_0 = 0.120$

12. $\omega^2 = \dfrac{r^2}{R - r}\cdot\dfrac{W}{\dfrac{Wr^2}{g} + I}.$ **13.** $\omega^2 = r_1\dfrac{w}{\dfrac{Wr^2}{g} + I}.$

14. (*a*) $\omega^2 = \dfrac{fg}{a}.$ (*b*) Unstable.

15. $\omega^2 = \dfrac{g}{l} + \dfrac{2ka^2}{ml^2}$ (see theorem on page 307).

16. (*a*) $a^2 > \dfrac{mgl}{2k}.$ (*b*) $\omega^2 = -\dfrac{g}{l} + \dfrac{2ka^2}{ml^2}.$

17. $\omega^2 = \dfrac{4ka^2}{I}.$ **18.** $\omega^2 = \dfrac{2Ea^2wt^3}{Il_1^2(2l_1 + 3l_2)}.$

19. $\omega^2 = \dfrac{a}{l}\cdot\dfrac{g}{h}.$ **20.** $\omega^2 = \dfrac{4T}{ml}.$

21. $\omega^2 = \frac{4}{3}\frac{k}{m}\left(1 + \frac{2a}{D}\right)^2$.

22. (*a*) $k = \frac{Gd^4}{8nD^3}$. (*b*) $k = 4.45$ lb. per inch.

23. (*a*) $k = EI/l$, where EI is the bending stiffness and l is the total length πDn of the spring.

(*b*) $k = 3.13$ in.-lb. per radian.

24. (*a*) $k = \frac{\pi d^4}{32l} \cdot \frac{E}{\left(1 + \frac{E}{2G}\right)}$.

(*b*) $k = 2.78$ in.-lb. per radian.

25. (*a*) $\frac{3EI}{l^3}$. (*b*) $\frac{48EI}{l^3}$. (*c*) $\frac{192EI}{l^3}$.

26. $\omega^2 = \frac{4}{m\left[\frac{1}{4k_1} + \frac{1}{4k_2} + \frac{1}{k_3} + \frac{1}{k_4}\right]}$.

27. (*a*) $\sin\varphi = \frac{AB}{h}$. (*b*) Straight line through origin.

(*c*) Ellipse with vertical and horizontal major axes.

28. (*a*) $\omega = 27.8$ radians per second or $f = 4.42$ cycles per second

(*b*) $c = 0.0023$ lb. in.$^{-1}$ sec. (*c*) $P_0 = 0.064$ lb.

(*d*) One per cent per cycle at the beginning; slower later on.

(*e*) 2 in. (*f*) $x = 2 - e^{-(ct/2m)}$

29. (*a*) Torque $= T_0 \cdot \frac{I_2}{I_1 + I_2} \cdot \frac{1}{1 - \frac{\omega^2}{\omega_n^2}}$,

where $\omega_n^2 = \frac{k(I_1 + I_2)}{I_1 I_2}$.

(*b*) Same as (*a*), except that I_2 becomes $n^2 I_2$ and $\frac{1}{k}$ becomes $\frac{1}{k_1} + \frac{1}{n^2 k_2}$.

30. (*a*) $I\ddot{\varphi} + mgr \sin\alpha \sin\varphi = 0$. (*b*) $\omega^2 = \frac{mgr \sin\alpha}{I}$.

31. $\omega^2 = \frac{8g}{r(9\pi - 16)}$.

32. $x = \frac{P}{k}[\cos\omega_n(t - t_0) - \cos\omega_n t]$ where t starts upon application of the load.

33. $\frac{I_1 I_2 n^2}{I_1 + I_2 n^2}\ddot{\psi} + \frac{k_1 k_2 n^2}{k_1 + k_2 n^2}\psi = T_0 \cdot \frac{I_2 n^2}{I_1 + I_2 n^2} \sin\omega t$.

34. $\omega^2 = \frac{9k}{m} - \frac{4c^2}{m^2}$. (*b*) $x = \frac{3P_0}{4c}\sqrt{\frac{m}{k}}$. (*c*) $x_0 = \frac{4}{3}\frac{P_0}{k}\left[1 = \frac{32}{81}\frac{c^2}{km}\right]$

35. (*a*) $\omega^2 = \frac{2g}{l}$. (*b*) $\omega^2 = \frac{g}{l}$.

37. $\dfrac{\text{Work/cycle}}{ka_0^2} = 2\pi\dfrac{c}{c_c}\cdot\dfrac{\omega}{\omega_n}\cdot\left(\dfrac{y}{a_0}\right)^2$ where y is the relative motion (across the dashpot), described by Eq. (32*a*) in which the force $P_0 = m\omega^2 a_0$.

39. (*a*) $\omega_{\max}/\omega_{\min} = I_{\min}/I_{\max}$

(*b*) Torque $= \omega\Omega(I_{\max} - I_{\min})\sin 2\Omega t$, very large, so that (*a*) is the practical alternative.

41. $\omega^2 = \dfrac{2g}{\pi R}$.

42. (*a*) $-\dfrac{h}{12}$ (unstable). (*b*) $\dfrac{b^2}{h\cdot 6\sqrt{2}} - h\dfrac{2-\sqrt{2}}{3}$. (*c*) Same as (*b*).

43. $\omega_1^2 = 0.76k/m$ with the node at $2.62l$ to right of left mass.
$\omega_2^2 = 5.24k/m$ with the node at $0.38l$ to right of left mass.

44. $\omega_1^2 = \dfrac{\mathbf{T}}{ml}$. $\omega_2^2 = \dfrac{3\mathbf{T}}{ml}$.

45. $\omega_1^2 = 0.64k/m$ with $x_1/x_2 = +0.36$.
$\omega_2^2 = 1.56k/m$ with $x_1/x_2 = -0.56$.

46. First mode: 10 per cent per cycle decay in amplitude.
Second mode: 24 per cent per cycle decay in amplitude.

47. (*a*) 3.1×10^9 ft.-lb. sec.^{2} (*b*) 1.38×10^8 ft.-lb. sec.

(*c*) Arithmetic decay; roll angle diminishes by 2.7 deg. each half cycle of roll.

48. 4.37 in.

49. (*a*) 45 m.p.h. (*b*) 4.75 in.

50. $\omega^2 = \dfrac{k}{m} + \dfrac{g}{l}(2 \pm \sqrt{2})$.

51. $\omega_1 = 0.59\sqrt{\dfrac{EI}{ml^3}}$. $\omega_2 = 3.89\sqrt{\dfrac{EI}{ml^3}}$.

52. $\omega = \Omega\sqrt{\dfrac{ab}{k^2}}$.

54. $\omega^4[1 + 3mR^2\cos^2\alpha/I] - \omega^2[\omega_1^2 + \omega_2^2 + 3k_2R^2/I] + \omega_1^2\omega_2^2 = 0$.
where $\omega_1^2 = k_1/I$ and $\omega_2^2 = 3k/3m$.

55. $\omega^4[1 + 3m\sin^2\alpha/M] - \omega^2[\omega_1^2 + \omega_2^2 + 3k_2/M] + \omega_1^2\omega_2^2 = 0$.
where $\omega_1^2 = k_1/M$ and $\omega_2^2 = 3k_2/3m$.

56. $\omega^4[1 + 3k_2R^2\cos^2\alpha/k_1 + 3k_3R^2\sin^2\alpha/k_1] -$
$\omega^2[\omega_1^2 + \omega_2^2 + 3k_2k_3R^2/mk_1] + \omega_1^2\omega_2^2 = 0$
where $\omega_1^2 = 3k_2/3m$ and $\omega_2^2 = 3k_3/3m$.

57. $\omega^4[1 + 3k_2\sin^2\alpha/k_1 + 3k_3\cos^2\alpha/k_1]$
$$-\omega^2\left(\omega_1^2 + \omega_2^2 + \frac{3k_2k_3}{mk_1}\right) + \omega_1^2\omega_2^2 = 0.$$

In all four problems the solutions are simple and physically lucid for $\alpha = 0$ and $\alpha = 90$ deg. Check up what these frequencies are. Increasing blade angle α means increased "coupling" between the two modes, and this always causes the two uncoupled frequencies to spread apart (see Figs. 69 and 74). Therefore the blade frequency is either raised or lowered by an increase in α depending on whether it is higher or lower than the engine frequency to start with.

58. (*a*) $\omega^2 = 2\dfrac{k}{m} \cdot \sin^2 \alpha$

(*b*) $\omega^2 = 2\dfrac{k}{m} \cdot \cos^2 \alpha$

59. (*a*) $-x + \dfrac{m\omega^2 x}{k_{11}} + \dfrac{m\omega^2 y}{k_{12}/\rho} = 0$

$-y + \dfrac{m\omega^2 y}{k_{22}/\rho^2} + \dfrac{m\omega^2 x}{k_{12}/\rho} = 0$

(*b*) $\omega_{1,2}^2 = \dfrac{1}{2}\left(\dfrac{m}{k_{11}} + \dfrac{m}{k_{12}/\rho}\right) \pm \dfrac{1}{2}\sqrt{\left(\dfrac{m}{k_{11}} - \dfrac{m}{k_{22}/\rho^2}\right)^2 + \left(\dfrac{2m}{k_{12}/\rho}\right)^2}$.

$$\frac{x}{y} = \frac{\dfrac{1}{\omega^2} - \dfrac{m}{k_{22}/\rho^2}}{\dfrac{m}{k_{12}/\rho}}.$$

(*c*) $\left(\dfrac{x}{y}\right)_1 = -\left(\dfrac{x}{y}\right)_2$

(*d*) $\dfrac{x}{y} = \pm 1$

(*e*) $\dfrac{\Delta\omega}{\omega} = \dfrac{k_{11}}{k_{12}/\rho}$

60. $\omega_1^2 = 0$

$\omega_2^2 = \dfrac{g}{l}\left[1 + \dfrac{2}{3}\dfrac{w}{W}\right]$.

62. (*a*) $\alpha_{11} = \alpha_{22} = \dfrac{3l^3}{4EI}$; $\alpha_{12} = \dfrac{7l^3}{12EI}$.

(*b*) $\omega^2 = \dfrac{1}{m(\alpha_{11} \pm \alpha_{12})}$ with $\dfrac{x_1}{x_2} = \pm 1$.

63. $\alpha_{11} = \dfrac{16}{768}\dfrac{l^3}{EI}$ $\alpha_{12} = \dfrac{11}{768}\dfrac{l^3}{EI}$ $\alpha_{22} = \dfrac{9}{768}\dfrac{l^3}{EI}$

$\omega_1 = 1.14\sqrt{\dfrac{EI}{ml^3}}$ $\omega_2 = 28.5\sqrt{\dfrac{EI}{ml^3}}$.

64. (*a*) $\omega = \sqrt{\dfrac{2k}{m}}$. (*b*) $x_2 = \dfrac{P_0}{7k}$.

67. $\omega^2 = \dfrac{6}{11}\dfrac{\mathbf{T}}{ml}$ assuming a shape consisting of three straight stretches of string.

68. Half the mass of the beam has to be added to the central mass. Curve assumed is half a sine wave.

69. Three-eighths of the beam mass is effective. Assumed curve is a full (360-deg.) sine wave, vertically displaced.

70. $\omega^2 = 2{,}960$ rad.^{2}/sec.^{2} $f = 8.66$ cycles per second.

71. Equivalent of μ_1 is $m_1 n_1$; equivalent of AE is $\dfrac{Gd^4}{8n_1D^3}$; $\omega^2 = \dfrac{\pi^2 Gd^4}{8n_1^2 D^3 m_1 l^2}$.

72. $\omega^2 = 2.80\dfrac{EI}{\mu_1 l^4}$ for a quarter cosine wave; the coefficient 2.80 becomes 1.35 if the stiff half of the beam does not bend so that the deflection curve is one-eighth cosine wave and a piece of straight line.

73. 745 cycles per second.

74. (*a*) Assuming straight line deformation one-third of spring mass is to be added to end mass.

(*b*) Frequency determined by the transcendental equation

$$\frac{\omega^2}{k/m} = \frac{\omega/\sqrt{k/m_s}}{\tan \omega/\sqrt{k/m_s}}.$$

For $m_s \ll m$, and retaining the first two terms of the Taylor series development we find again that one-third of the spring mass is to be added to the end mass.

75. $\omega^2 = \dfrac{\pi^4}{\frac{3}{2} - \frac{4}{\pi}} \cdot \dfrac{EI}{\mu_1 l^4}$ assuming curve a sine wave passing through $\dfrac{l}{6}$ and $\dfrac{5l}{6}$.

76. 132 r.p.m. and 376 r.p.m.

77. $\tan pl = \dfrac{p(q + r)}{qr - p^2}$ where $p^2 = \dfrac{\mu_1 \omega^2}{AE}$; $q = \dfrac{M_1 \omega^2}{AE}$; $r = \dfrac{M_2 \omega^2 - k}{AE}$.

Solve by trial and error assuming values for ω^2. Plot left and right side of equation against ω^2 and get intersection of the two curves. The first critical speed is at 127.5 r.p.m.

78. (*a*) $y = \sin \dfrac{\pi x}{l} - \dfrac{3}{\pi} \dfrac{x}{l}$.

(*b*) $\omega^2 = \dfrac{\pi^4}{1 - 6/\pi^2} \cdot \dfrac{EI}{\mu l^4} = 15.75 \dfrac{EI}{\mu l^4}$.

The exact solution, listed on p. 459 as a_2 of the hinged-free beam, has a factor 15.4.

79. $\omega^2 = \dfrac{\pi^2}{4} \cdot \dfrac{\pi^2 + 4}{\pi^2 - 4} \cdot \dfrac{\mathbf{T}}{\mu l^2} = 5.80 \dfrac{\mathbf{T}}{\mu l^2}$

The exact answer, involving Bessel's functions, has a factor 5.74.

81. (*a*) $\frac{1}{8}$ in. vertically.

(*b*) 267 lb. vertically.

84. Primary and secondary forces balanced; both moments unbalanced.

85. (*a*) $\frac{1}{2} W_{\text{rec}}$, or half the rec. wt. of a crank, *i.e.*, one piston and fraction of one rod.

(*b*) Zero.

(*c*) $W_{\text{rec}} \sqrt{\dfrac{(a + b)^2 + b^2}{(a + 2b)^2}}$; $\alpha_A = 0$; $\alpha_{A1} = 90°$;

$$\alpha_B = 180° + \tan^{-1} \frac{b}{a + b}$$

$$\alpha_C = 180° + \tan^{-1} \frac{a + b}{b}.$$

86. $\dfrac{W_{\text{pis}} R_{\text{pis}}^2}{W_{\text{disk}} R_{\text{disk}}^2} = \dfrac{\cos \alpha}{2}$.

87. (*a*) $\dfrac{\varphi_1}{T_0/k} = \dfrac{(\omega/\omega_n)^2 - I_1/I_1 + I_2}{1 - (\omega/\omega_n)^2} \cdot \left(\dfrac{\omega_n}{\omega}\right)^2 \cdot \dfrac{I_2}{I_1 + I_2}$,

showing $\varphi_1 \to \infty$ for $\omega = 0$.

(*b*) $\dfrac{k(\varphi_1 - \varphi_2)}{T_0} = \dfrac{I_2/I_1 + I_2}{1 - (\omega/\omega_n)^2}$

88. $\omega_1 = 168$ radians per second.

91. Five fundamental diagrams:
(1) For orders ½, 3½, 4½, 7½, etc.
(2) For orders 1, 3, 5, 7, etc.
(3) For orders 1½, 2½, 5½, 6½, etc.
(4) For orders 2, 6, 10, etc.
(5) Majors 4, 8, 12, etc.

92. (*a*) 0.0047 radian.
(*b*) 293,000 in.-lb.; 41,300 in.-lb.
(*c*) 31.6 r.p.m.

93. −0.00359 radian.
+0.00423 radian.

94. (*a*) $\beta = 0$; first shaft torque arbitrarily assumed.
(*b*) End $\beta = 0$.
(*c*) $\Theta = \pi = 180$ deg.
(*d*) $\omega^2 = \frac{\pi^2}{42} \cdot \frac{k}{I}$.

95. (*a*) $\frac{g}{\rho^2 + a^2}\left(\frac{R_1R_2 - a\,\Delta R}{\Delta R}\right)$.
(*b*) $\frac{\Omega^2 r_G}{\rho^2 + a^2}\left[\frac{R_1R_2 - a\,\Delta R - a^2\,\Delta R/r_G}{\Delta R}\right]$.

97. (*b*) 4,000 in.-lb.
(*c*) 122.0 r.p.m.
(*d*) 107 r.p.m.
(*e*) Balanced.

98. $a_1 = \frac{\pi}{2}$; all other a's are zero.

$b_n = \frac{2}{n^2 - 1}$ for even n; $b_n = 0$ for odd n.

Order:	1	2	3	4	5	6
Per cent of mean torque:	157	66.7	0	13.3	0	5.7

100. 990 r.p.m.

101. 990 r.p.m. horizontally and 1,260 r.p.m. vertically.

102. Counting angles from the +1 unbalance toward the +2 unbalance (at which $\varphi = 90$ deg.), the corrections are:
In Plane I: 2.06 in. oz. at 104 deg.
In Plane II: 4.03 in. oz. at 263 deg.

103. 4.2 oz. at 315 deg.

104. $x^2 = \frac{a_1^2 + a_2^2}{2} - a_0^2$; $\cos\varphi = \frac{a_1^2 - a_2^2}{4a_0x}$.
Ambiguity between $+\varphi$ and $-\varphi$.

105. $\alpha = 2\cos^{-1}\frac{Me}{2mr}$.

106. Primary speed, 1440 r.p.m.; secondary speed, 720 r.p.m. Secondary force amplitude is 0.044 lb., corresponding to an unbalance of 7.1 $\times 10^{-4}$ in.-lb.

107. $K^2 = \frac{12}{7}\left[\left(2 - \frac{1}{D}\right) + \sqrt{\frac{1}{D^2} - \frac{9}{4D} + 4}\right]$
where K and D are the abbreviations used in Eq. (152).

109. With x of the disk center and φ of the shaft there are two differential equations, the latter having the gyroscopic term $\frac{1}{2}MR^2\Omega\omega\varphi$, where ω is the angular speed of the forward whirl of shaft center line. The frequency equation falls apart into two quadratics:

$$\left[\left(\frac{\omega}{\omega_a}\right)^2 - 1\right]\left[\left(\frac{\omega}{\omega_a}\right)^2 - \left(\frac{\omega}{\omega_a}\right)\cdot 2\frac{\Omega}{\omega_a} - \left(\frac{\omega_h}{\omega_a}\right)^2\right] = 0$$

so that two roots are $\omega/\omega_a = \pm 1$ independent of Ω (a forward and backward whirl with the shaft parallel to itself) and two other roots, one a forward whirl the frequency of which increases with Ω and a backward whirl of a frequency decreasing with Ω.

110. $x^4 - 2Ax^3 - 25\frac{1}{3}x^2 + 8Ax + 21\frac{1}{3} = 0$

where $x = \omega_w/\sqrt{3EI/ml^3}$ and $A = \omega/\sqrt{3EI/ml^3}$.

For $A = 0$, $x = \pm 4.95$ and ± 0.93.

For $A = 2$, $x = +7.17$, -3.66 and $+1.20$, -0.70.

For $A = 5$, $x = +11.58$, -3.47 and $+2.13$; -0.25.

111. If plotted as: $\omega^2/EI/m\left(l + \frac{l_1}{2}\right)^2 = f(l_1/l)$ the curve is nearly straight at an ordinate falling from 3 to 2.90 between the points $l_1/l = 0$ and 1. A second critical with a node somewhere in the stiff part has a very high frequency running from ∞ at $l_1/l = 0$ to 567 at $l_1/l = 1$ in the same diagram.

112. (*a*) $\omega^2 = \dfrac{Ed^4(I_1 + I_2)}{64DnI_1I_2}$.

(*b*) $22.4\sqrt{\dfrac{Ed^2}{8\pi^2D^2n^2l^2\rho_{\text{steel}}(1 + E/2G)}}$.

113. $I_1\ddot{\varphi}_1 + k(\varphi_1 - \varphi_2) = 0$.

$I_2\ddot{\varphi}_2 + k(\varphi_2 - \varphi_1) - C_1C_2\frac{\omega}{c}\tan\frac{\omega l}{c}\cdot\varphi_2 = 0$.

$-k^2 + (-I_1\omega^2 + k)\cdot\left(-I_2\omega^2 + k - C_1C_2\frac{\omega}{c}\tan\frac{\omega l}{c}\right) = 0$.

in which $c = \sqrt{AE/\mu}$, the velocity of sound; see p. 173.

114. (*a*) Stable. (*b*) Unstable. (*c*) Unstable.

116. (*a*) $\sin\alpha_0 = \dfrac{T_0}{Mgl}$.

(*b*) Undamped vibrations of frequency $\omega^2 = g\cos\alpha_0/l$.

(*c*) Damped vibrations; same frequency.

(*d*) Increasing vibration.

117. (*b*) $x = v_0t - v_0\sqrt{\frac{m}{k}}\cdot\sin\left(t + \sqrt{\frac{k}{m}}\right)$ (undamped oscillations).

(*c*) Damped oscillations about $x = v_0t$.

(*d*) Oscillations with increasing amplitude which lead to a motion with periodic stops of the mass.

118. $\dfrac{L_0}{D_0} > \dfrac{3}{4}$.

119. (*a*) $k = \dfrac{m\Omega^2}{\sqrt{6} - 2}\left(1 + \dfrac{a\sqrt{2}}{l}\right)$. (*b*) $\omega^2 = \dfrac{k}{M + 2m}$.

(*c*) $\omega^2 = \dfrac{k - \frac{1}{2}m\Omega^2}{m + M}$ (the second term in the numerator expresses the influence of the "negative spring" of the centrifugal forces on m).

120. For complete solution with curves see *Trans. A.I.E.E.*, 1933, p. 340.

121. $\omega^2 = \dfrac{a^2E}{mV}$.

122. $I_1\ddot{\varphi}_1 + k_1(\varphi_1 - \varphi_2) = 0.$

$I_2\ddot{\varphi}_2 + k_1(\varphi_2 - \varphi_1) + \dfrac{\Delta m}{T}(r_B^2\dot{\varphi}_2 - r_A^2\dot{\varphi}_3) = 0.$

$I_3\ddot{\varphi}_3 + \dfrac{\Delta m}{T}(r_A^2\dot{\varphi}_3 - r_B^2\dot{\varphi}_2) = 0.$

$$s^3 + s^2\left(\frac{r_A^2}{I_3} + \frac{r_B^2}{I_2}\right)\frac{\Delta m}{T} + s\left(\frac{k_1}{I_2} + \frac{k_1}{I_1}\right) + \frac{\Delta m}{T}\left[\frac{k_1r_A^2}{I_2I_3} + \frac{k_1r_A^2}{I_1I_3} + \frac{k_1r_B^2}{I_1I_2}\right] = 0.$$

The system is stable.

123. $I_1\ddot{\varphi}_1 + k_1(\varphi_1 - \varphi_2) = 0$

$I_2\ddot{\varphi}_2 + k_1(\varphi_2 - \varphi_1) + \dfrac{\Delta m}{T}r_B^2\dot{\varphi}_2 - \dfrac{\Delta m}{T}r_A^2\dot{\varphi}_3 = 0$

$I_3\ddot{\varphi}_3 + k_2(\varphi_3 - \varphi_4) + \dfrac{\Delta m}{T}r_A^2\varphi_3 - \dfrac{\Delta m}{T}r_B^2\dot{\varphi}_2 = 0$

$I_4\ddot{\varphi}_4 + k_2(\varphi_4 - \varphi_3) = 0$

$s^5 + A_4s^4 + A_3s^3 + A_2s^2 + A_1s + A_0 = 0$

where $A_4 = \dfrac{\Delta m}{T}\left[\dfrac{r_A^2}{I_3} + \dfrac{r_B^2}{I_2}\right]$; $A_3 = \dfrac{k_1}{I_1} + \dfrac{k_1}{I_2} + \dfrac{k_2}{I_3} + \dfrac{k_2}{I_4}$

$$A_2 = \frac{\Delta m}{T}\left(\frac{r_A^2k_1}{I_2I_3} + \frac{r_A^2k_1}{I_1I_3} + \frac{r_B^2k_1}{I_1I_2} + \frac{r_A^2k_2}{I_3I_4} + \frac{r_B^2k_2}{I_2I_4} + \frac{r_B^2k_2}{I_2I_3}\right)$$

$$A_1 = \frac{k_1k_2}{I_2I_3} + \frac{k_1k_2}{I_1I_4} + \frac{k_1k_2}{I_2I_4} + \frac{k_1k_2}{I_1I_3}$$

$$A_0 = \frac{\Delta m}{T}\left(\frac{k_1k_2r_A^2}{I_2I_3I_4} + \frac{k_1k_2r_A^2}{I_1I_3I_4} + \frac{k_1k_2r_B^2}{I_1I_2I_4} + \frac{k_1k_2r_B^2}{I_1I_2I_3}\right).$$

The system is stable.

124. Unstable frequencies are $\omega = \alpha\sqrt{\dfrac{2A^2\mathbf{p}}{MV}}$ where $\alpha = 2, 1, \frac{2}{3}, \frac{2}{4}, \frac{2}{5}$, etc., and $\mathbf{p}$ is atmospheric pressure = 14.6 lb. per square inch. The slope of the line in the diagram of Fig. 248 is 0.10.

125. 1,085 r.p.m.

126. Exact: $\omega = \sqrt{\dfrac{k}{m}} \cdot \dfrac{\pi/2}{\cos^{-1}\left(\dfrac{1}{1 + \dfrac{kx_0}{F}}\right)}$; approximate; $\omega = \sqrt{\dfrac{k}{m} + \dfrac{F}{mx_0}}$.

127. $x_0^2 = \left(\dfrac{P_0}{k}\right)^2 \cdot \dfrac{3\pi}{8D}\left[-\dfrac{3\pi}{16D}\left(1 - \dfrac{\omega^2}{\omega_n^2}\right)^2 + \sqrt{\dfrac{9\pi^2}{256D^2}\left(1 - \dfrac{\omega^2}{\omega_n^2}\right)^4 + 1}\right]$

where $D = c\omega^2P_0/k^2$ is a dimensionless variable involving the damping constant c, the damping force being $c\dot{x}^2$.

130. (*a*) Counterclockwise viewed from above.

(*b*) T = 3.45 sec. per revolution.

131. 2,880 lb.

INDEX

A

Absorbers, automobile shock, 134
  dynamic vibration, 112
Accelerometer, 77
Airplane vibration, propeller, 327
  wing flutter, 392
Analogues, table, 40
Automatic balancing, 301
Automobile vibration, chassis, 110
  floating power, 97
  shimmy, 399
  shock absorber, 145
Autorotation, 376
Axial vibration, clock motor, 413
  steam turbine, 387

B

Balancing, diagram, 296
  flexible rotors, 305
  reciprocating engines, 225
  solid rotors, 292
Balancing machines, 294
  automatic, 301
Bars (*see* Natural frequency formulas)
Beams (*see* Natural frequency formulas)
Bearings, oil whip, 364
  thrust, 360
Beats, 7, 402
Blades, turbine, 341
Bullroarer, 376

C

Centrifugal pendulum, 119, 272, 284
Chattering slip, 355
Clearances, 424
Clock motor, electric, 414
Complex numbers, 11
Compounding of springs, 49
Connecting rod, 220
Conversion table, 40
Coriolis force, 259, 270, 288
Coulomb damping, 438
Coupled pendulums, 109
Couplings, slipping, 363
Crank mechanism, 217
Critical damping, 52
Critical speeds, Diesel engines, 255
  major, minor, 259
  rotating machines, 286
  secondary, 309
Cubic equation, stability criterion, 353

D

Dampers, general properties, 128
  Lanchester, 129, 267
Damping, air (Prob. 127), 451
  dry, 355, 438
  hysteresis, 265, 362
  negative, 347
  non-linear, 440
  propeller, 262
  viscous, 51
Decay, rate of, 53, 169, 348
Decrement, logarithmic, 54
Degree of freedom, definition, 34
Demultiplication, 448
Diesel engines, firing order, 279
  fuel valves, 383
  torque analysis, 249
  torsional vibration, 236
Differential equation (*see* Natural frequency formulas)
Disks, steam turbine, 336

Dynamic absorber, damped, 119, 133
undamped, 112, 160
Dynamic balancing, 293

E

Electric circuits, 38, 120, 414, 448
Electric clock motor, 414
Electric conversion table, 40
Electric locomotive, 413
Electric machines, frames, 324
single phase, 93
Electric transmission line, 367
Energy method, 46, 172, 178
Equivalents, table, 40

F

Firing order, 279
Fixed points, 123
Flat shafts, 310
Floating power, 97
Fluid flywheel, 270
Flutter, airplane wing, 392
Forced vibration, definition, 58
Fourier series, 20, 175
Frahm, ship tanks, 136
tachometer, 75
Frame vibration, 207, 303, 324
Free vibration, definition, 45
Freedom, degree of, 34
Frequency (*see* Natural frequency formulas)
Frequency demultiplication, 448
Frequency equation, real-root theorem, 159
Frequency meters, 73
Friction, instability caused by, 354
(*See also* Damping)
Fuel-injection valves, 383

G

Galloping transmission line, 367
Gear noise, 133
Geared systems, 41
Governor vibration, 378
Gravity effects, 37, 311, 409
Gyroscope, automobile shimmy, 400
effect on frequency, 320
ship stabilization, 139
theory, 453

H

Hair clipper, 118
Harmonic analyzer, 23
Head, balancing, 300
Helicopter, 312
Herringbone skewing, 327
Holzer's method, 239, 290
Hunting governors, 378
Hydraulic turbines, 8
Hysteresis, 264, 362

I

Imaginary numbers, 11
Inertia balance, 226
radial aircraft engine, 230
Influence number, 155, 199
Injection valve, Diesel, 383
Instability criteria, 350
Internal friction, 265, 340, 362
Inverted pendulum, 422
Isolation, 89
Iteration method, 202

K

Karman vortices, 373

L

Labyrinth, steam turbine, 387
Lanchester, damper, 129
tourbillion, 372
Lissajous figures, 101
Locomotives, chattering slip, 355
nosing, 402
side-rod vibration, 413
Logarithmic decrement, 54
Lubrication, 364

M

Major critical speeds, 259
Mathieu's equation, 415

Membranes, 209
Metacenter, 133
Minor critical speeds, 259
Mohr's circle, 106
Motor supports, 96

N

Natural frequency formulas, centrifugal effect, 320
damped single degree, 53, 54
full rings, 205
gyroscopic effect, 323
lateral bending beams, 189–194
longitudinal beams, 172, 176
membranes, 209
organ pipes, 172, 176
part rings, 207
strings, 175
torsional beams, 173
undamped single degree, 45, 47
Neon lamps, 84, 87, 448
Newton's laws, 37, 214
Non-linear damping, 440
Non-linear mass, 426
Non-linear springs, 425
Normal functions, 198
Nosing locomotives, 402

O

Oil whip, 364
Organ pipe, 173, 176

P

Pendulum, coupled, 109
damper, 274
inverted, 422
variable length, 412
Penstocks, 8
Period, definition, 1
Phase-angle diagram, Coulomb damping, 438
viscous damping, 66
Phase-shift torsiograph, 88
Pilot, 143
Plates, 209
Primary unbalance, 226
Propeller, airplane, 327
ship, 262

Q

Quartic, stability criterion, 354

R

Rayleigh, method, 178
proof of theorem, 194
Relative motion, 61, 277
Relaxation oscillations, 444
Relaxation time, 56
Resonance diagrams, Coulomb damping, 438
single degree, 59, 61, 66, 77, 92
three degrees, 162
two degrees, 117
Riding quality, 147
Rings, full, 205
part, 207
Ritz method, 183

S

Saturation, magnetic, 399
Schlick, engine balancing, 227
ship gyroscope, 139
Secondary, critical speeds, 309
unbalance, 226
Seismic instruments, 75
Self-excited vibration, 346
Semicircular cylinder, 370
Series generator, 446
Ship propeller, 262
Ship stabilization, 133
Shock absorber, 145
Side-rod locomotive, 385
Singing propeller, 374
Single-phase machine, 93
Sleet, 368
Sound analyzer, 79
Southwell's theorem, 328
Sperry, 143
Spiral vibration, 308
Springs, series and parallel, 49
suspension, 90

Stability, criteria, 350
of speeds above critical, 288
Starting squeal, 355
Static balancing, 102, 293
Steam turbine (*see* Turbines)
Stodola's method, 194, 195
String, continuous, 170
with three masses, 157
with variable tension, 412
Stroboscope, 87
Subharmonic resonance, 448
Submarine motors, 325

T

Tachometer, Frahm, 75
Tanks, antirolling, 137
Teeth of electric machines, 324
Thearle balancing machine, 298
Torque, Diesel engine, 249
Torsiograph, 79, 86, 88
Torsional vibration, continuous shaft, 173, 177, 183
Diesel engine, 232–280
single degree of freedom, 38
Transients, 71
Transmission line, 367
Turbines, axial oscillation, 387
balancing, 293, 299, 309
disks and blades, 335
governors, 378
hydraulic, 8
Turbines, steam, 335, 387
Turbulence, 377

V

Vacuum tube, 350
Valve, Diesel fuel, 383
Valve springs (Prob. 71), 210
Variable cross section, 194
Variable elasticity, 408
Variable gravity, 423
Vector representation, 3
Vibrograph, 77, 81
Viscous damping, definition, 51

W

Wilberforce spring, 105
Wind, 370, 377, 395
Wing flutter, 392
Work performed, 19